Proposed Collaborative Research Center 1333

Molecular Heterogeneous Catalysis in Confined Geometries

University of Stuttgart

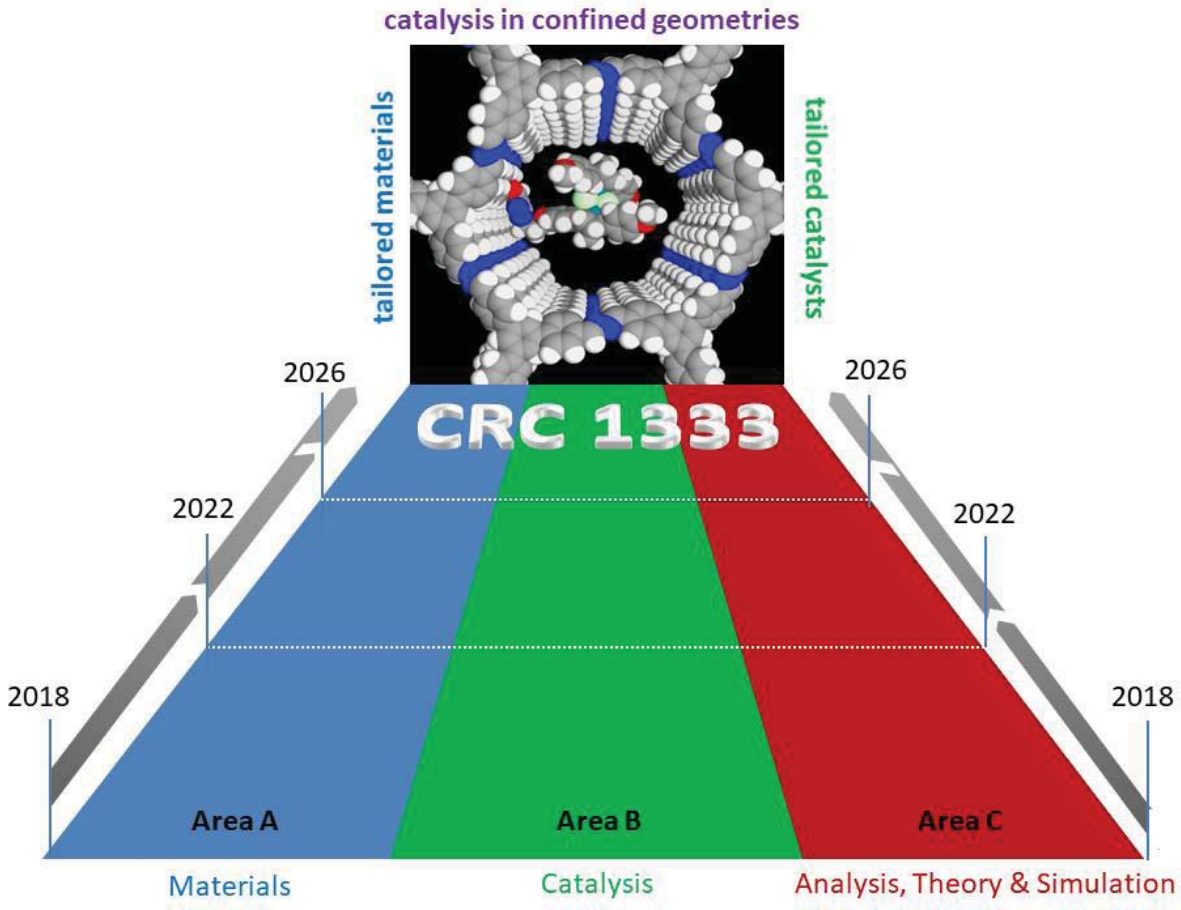

Funding Proposal
1st funding period
2018 - 2022

Proposal for the Establishment and Funding of
Collaborative Research Center 1333

Molecular Heterogeneous Catalysis in Confined Geometries

for
2018 – 2019 – 2020 – 2021 – 2022

Coordinating University:

University of Stuttgart

Spokesperson of the Collaborative Research Centre:
Prof. Dr. Michael R. Buchmeiser
Chair of Macromolecular Compounds and Fiber Chemistry
Institute of Polymer Chemistry
University of Stuttgart
Pfaffenwaldring 55, D-70569 Stuttgart
+49(0)711/685-64074
michael.buchmeiser@ipoc.uni-stuttgart.de

Management Office of the Collaborative Research Center:
Dr. Elisabeth Rüthlein
Chair of Macromolecular Compounds and Fiber Chemistry
Institute of Polymer Chemistry
University of Stuttgart
Pfaffenwaldring 55, D-70569 Stuttgart
+49(0)711/685-60799
elisabeth.ruethlein@ipoc.uni-stuttgart.de

Stuttgart, 20. 12. 2017

Univ.-Prof. Dr. rer. nat. Michael R. Buchmeiser
(Spokesman of CRC)

Stuttgart, 20. 12. 2017

Univ.-Prof. Dr.-Ing. Dr. h.c. Wolfram Ressel
(Rector of the University of Stuttgart)

Table of Contents

1 General information

1.1 Key data

1.1.1 Statutory bodies of the Collaborative Research Center (CRC)

Spokesperson of the Collaborative Research Centre:
Prof. Dr. Michael R. Buchmeiser
Chair of Macromolecular Compounds and Fiber Chemistry
Institute of Polymer Chemistry
University of Stuttgart
Pfaffenwaldring 55, D-70569 Stuttgart
+49(0)711/685-64074
michael.buchmeiser@ipoc.uni-stuttgart.de

Deputy Spokesman of the Collaborative Reserch Center
Prof. Dr. Bernd Plietker
Institute of Organic Chemistry
University of Stuttgart
Pfaffenwaldring 55, D-70569 Stuttgart
+49(0)711/685-64283
bernd.plietker@oc.uni-stuttgart.de

CRC Board:
Prof. Dr. Michael R. Buchmeiser
Prof. Dr. Bernd Plietker
Prof. Dr. Johannes Kästner
Prof. Dr. Bettina Lotsch
Prof. Dr. Joris van Slageren

1.1.2 Principal investigators

Principal investigators	Year of birth	Doctorate obtained in	Home institution, location	Project
apl. Prof. Dr. J. Bill	1962	1993	University of Stuttgart, Institute of Materials Science	A5
Prof. Dr. M. Bauer	1977	2008	University of Paderborn, Institute of Inorganic and Analytical Chemistry	S1
Prof. Dr. M. R. Buchmeiser	1967	1993	University of Stuttgart, Institute of Polymer Chemistry	A1, B2, Z1
Jun. Prof. Dr. M. Fyta	1976	2005	University of Stuttgart, Institute of Computer Physics	C6
Prof. Dr. F. Gießelmann	1963	1992	University of Stuttgart, Institute of Physical Chemistry	A4
Prof. Dr. J. Groß	1970	2001	University of Stuttgart, Institute of Technical Thermodynamics	C5
Jun. Prof. Dr. N. Hansen	1977	2010	University of Stuttgart, Institute of Technical Thermodynamics	C5
Prof. Dr. C. Holm	1960	1987	University of Stuttgart, Institute of Computer Physics	C6
apl. Prof. Dr. M. Hunger	1955	1984	University of Stuttgart, Institute of Chemical Technology	C1
Prof. Dr. J. Kästner	1978	2004	University of Stuttgart, Institute of Theoretical Chemistry	C4
Prof. Dr. S. Laschat	1963	1990	University of Stuttgart, Institute of Organic Chemistry	B3
Prof. Dr. B. V. Lotsch	1977	2006	MPI for Solid State Research, Stuttgart	A3
Prof. Dr. S. Ludwigs	1978	2004	University of Stuttgart, Institute of Polymer Chemistry	A2
Dr. S. Naumann	1986	2014	University of Stuttgart, Institute of Polymer Chemistry	A6
Prof. Dr. B. Plietker	1971	1999	University of Stuttgart, Institute of Organic Chemistry	B1, S1, Z1
Dr. M. Ringenberg	1984	2011	University of Stuttgart, Institute of Inorganic Chemistry	C2
Prof. Dr. G. Schmitz	1962	1994	University of Stuttgart, Institute of Materials Science	C3
Prof. Dr. J. van Slageren	1973	2000	University of Stuttgart, Institute of Physical Chemistry	C2
apl. Prof. Dr. T. Sottmann	1966	1997	University of Stuttgart, Institute of Physical Chemistry	A7
PD. Dr. Y. Traa	1969	1999	University of Stuttgart, Institute of Chemical Technology	A4

1.1.3 Participating institutions

University of Stuttgart:
Institut für Anorganische Chemie (Institute of Inorganic Chemistry, IAC, Fakultät Chemie)
Institut für Computerphysik (Institute of Computer Physics, ICP, Fakultät Physik und Mathematik)
Institut für Materialwissenschaften (Institute of Materials Science, IMW, Fakultät Chemie)
Institut für Organische Chemie (Institute of Organic Chemistry, IOC, Fakultät Chemie)
Institut für Physikalische Chemie (Institute of Physical Chemistry, IPC, Fakultät Chemie)
Institut für Polymerchemie (Institute of Polymer Chemistry, IPOC, Fakultät Chemie)
Institut für Technische Chemie (Institute of Chemical Technology, ITC, Fakultät Chemie)
Institut für Technische Thermodynamik und Thermische Verfahrenstechnik (Institute of Technical Thermodynamics, ITT, Fakultät Energie-, Verfahrens- und Biotechnik)
Institut für Theoretische Chemie (Institute of Theoretical Chemistry, TheoChem, Fakultät Chemie)

Max-Planck-Institute (MPI) for Solid State Research, MPI-FK, Stuttgart:
Nanochemistry Department

University of Paderborn:
Institute of Inorganic and Analytical Chemistry

1.1.4 Project groups and projects

Project	Title	Research area	Principal investigator(s), institute(s), location(s)
A1	Monolithic polymeric supports with uniform pore diameter and tailored functional groups	Polymer Chemistry, Preparative and Physical Chemistry of Polymers (306-01) Polymer Materials (306-03)	Prof. Dr. M. R. Buchmeiser Institute of Polymer Chemistry University of Stuttgart
A2	Tunable block copolymer templates for spatially controlled immobilization of molecular catalysts	Polymer Chemistry, Preparative and Physical Chemistry of Polymers (306-01)	Prof. Dr. S. Ludwigs Institute of Polymer Chemistry University of Stuttgart
A3	Covalent organic frameworks as tailored substrates with molecularly defined pores for molecular heterogeneous catalysis	Solid State and Surface Chemistry, Materials Synthesis (302-01)	Prof. Dr. B. V. Lotsch Nanochemistry Department MPI for Solid State Research Stuttgart
A4	Controlled synthesis of mesoporous silica materials	Solid State and Surface Chemistry, Materials Synthesis (302-01), Physical Chemistry of Solids and Surfaces, Materials Characterization (302-02)	PD Dr. Y. Traa/Prof. Dr. F. Gießelmann Institute of Chemical Technology University of Stuttgart/Institute of Physical Chemistry
A5	Organic/inorganic hybrid materials with tunable pore size as catalyst supports	Materials Science, Synthesis and Properties of Functional Materials (406-2), Structuring and Functionalization (406-4)	apl. Prof. Dr. J. Bill Institute of Materials Science University of Stuttgart
A6	Carbon materials with tailored, selectively functionalized mesopores using organocatalytically derived polyethers	Polymer Chemistry, Preparative and Physical Chemistry of Polymers (306-01) Polymer Materials (306-03)	Dr. S. Naumann Institute of Polymer Chemistry University of Stuttgart
A7	Nanoporous host materials with adjustable pore size, geometry and distribution: synthesis, functionalization and characterization	Polymer Chemistry, Preparative and Physical Chemistry of Polymers (306-01)	apl. Prof. Dr. T. Sottmann Institute of Physical Chemistry University of Stuttgart

Project groups and projects (ctd.)

Project	Title	Research area	Principal investigator(s), institute(s), location(s)
B1	„*Inner-pore*"-tethered tetraaza-ruthenium-complexes for the directed hydrogen-autotransfer catalysis	301-02 Organic Molecular Chemistry	Prof. Dr. B. Plietker Institute of Organic Chemistry University of Stuttgart
B2	Immobilized molybdenum imido, tungsten imido- and tungsten oxo alkylidene N-heterocyclic carbene complexes for olefin metathesis	Preparatory and Physical Chemistry of Polymers (306-01), Inorganic Molecular Chemistry (301-01), Organic Molecular Chemistry (301-02)	Prof. Dr. M. R. Buchmeiser Institute of Polymer Chemistry University of Stuttgart
B3	Asymmetric catalysis with supported chiral olefin-rhodium complexes in defined porous networks	301-02 Organic Molecular Chemistry	Prof. Dr. S. Laschat Institute of Organic Chemistry University of Stuttgart

Project groups and projects (ctd.)

Project	Title	Research area	Principal investigator(s), institute(s), location(s)
C1	Solid-state NMR methods for the study of the properties and spatial distribution of organo-metallic compounds anchored in porous solids	302-01 Solid State and Surface Chemistry, Material Synthesis 302-02 Physical Chemistry of Solids and Surfaces, Material Characterization	apl. Prof. Dr. M. Hunger Institute of Chemical Technology University of Stuttgart
C2	The static and dynamic electronic and geometric structure of catalysts in porous polymers	Inorganic Molecular Chemistry - Synthesis, Characterization (301-01) Theory, and Modeling (302-03)	Prof. Dr. J. van Slageren/Dr. M. Ringenberg Institute of Physical Chemistry/Institute of Inorganic Chemistry University of Stuttgart
C3	High resolution tomography of mesoscopic pore structures	406 Materials Science 406-4 Structuring and Functionalisation	Prof. Dr. G. Schmitz Institute of Materials Science University of Stuttgart
C4	Simulation of chemical reactivities	Theoretical Chemistry (303-02)	Prof. Dr. J. Kästner Institute of Theoretical Chemistry University of Stuttgart
C5	Atomistic and fluid-theoretical predictions of static and dynamic fluid properties in functionalized mesopores	Heat Energy Technology, Thermal Machines, Fluid Mechanics: Technical Thermodynamics (404-02) Process Engineering, Chemical Technology: Chemical and Thermal Process Engineering (403-01)	Prof. Dr. J. Groß/Jun.-Prof. N. Hansen Institute of Technical Thermodynamics University of Stuttgart
C6	A multi-scale simulation approach for optimizing molecular heterogeneous catalysis in confined geometries	Statistical Physics, Soft Matter, Biological Physics, Nonlinear Dynamics (310-01), Condensed Matter Physics (307-02)	Prof. Dr. C. Holm/Jun. Prof. Dr. M. Fyta Institute of Computer Physics University of Stuttgart

Project	Title	Research area	Principal investigator(s), institute(s), location(s)
S1	Service project	302-02 Physikalische Chemie von Festkörpern und Oberflächen, Materialcharakterisierung	Prof. Dr. B. Plietker/Prof. Dr. M. Bauer Institute of Organic Chemistry, University of Stuttgart/Institute of Inorganic and Analytical Chemistry, University of Paderborn
Z1	CRC central planning	-	Prof. Dr. M. R. Buchmeiser/Prof. Dr. B. Plietker Institute of Polymer Chemistry / Institute of Organic Chemistry, University of Stuttgart

1.2 Research profile of the Collaborative Research Centre

1.2.1 Summary of the research program

Compared to enzyme catalysis, organometallic catalysts are still often hampered by a lack of stereoselectivity and productivity. This is particularly true for organometallic catalysts immobilized on solid supports. Nonetheless, in view of dwindling resources and increasing environmental restrictions it is crucial that chemical production processes, including catalytic ones, offer optimum results. Timely progress in this research field is required to contribute to a more sustainable and energy-efficient production of industrially relevant chemical compounds. In view of this exigence, this collaborative research center (CRC) targets the rational development of hybrid, molecular, heterogenized organometallic catalyst systems, which are conceptually derived from biocatalysts (enzymes). To realize this goal, structurally defined organometallic catalysts will be introduced into highly defined, mesoporous support materials (pore sizes 2 – 50 nm) and anchored inside the pores of these materials. In analogy to three dimensional, highly defined enzyme structures, the bio-inspired approach presented here will exploit novel, well-defined catalyst-support hybrids, which cooperate synergistically. For such systems, we expect higher, or fundamentally different, chemo-, regio-, enantio-, or diastereoselectivities, resulting from the high level of order and the directing influence of the mesopores, compared to existing heterogeneous catalysts. We will explore the cooperative effects between support and organometallic catalyst, which must be understood to rationally access improved or even entirely new catalytic reactions and/or novel/better selectivities. Clearly, in such an approach, the role of the support is far beyond facilitating catalyst removal or ensuring longer lifetime. For quantification of these effects, the influence of pore size, pore polarity, tether length and rigidity on the catalytic reaction with a given catalyst will be studied and performance will be compared with that of the homogeneous analogue.

To reach this goal, the CRC will mobilize an extraordinary broad range of mesoporous support materials, including organic polymers, mesoporous oxides, covalent organic frameworks (COFs), carbon materials, polymer/inorganic hybrid materials and nano-foams, each giving access to different pore sizes in the mesoporous regime. Initially, these carrier materials will be loaded with well-established catalysts for transfer hydrogenation, olefin metathesis and asymmetric 1,4-addition reactions. Apart from fundamental catalyst parameters and characteristics such as productivity (expressed in turnover numbers, TONs), activity (expressed in turnover frequency, TOF), lifetime, etc., our interest will specifically focus on the interactions between the catalyst and the pore (wall). To understand these interactions in detail – and to exploit this knowledge to best effect – a range of experimental non-standard methods will be employed, but also high-level simulations on all relevant length scales. In summary, this interdisciplinary approach, characterized by its combination of broad scope and attention to detail, will reveal the synergistic interplay between mesoporous cavities and the catalysts confined in them. Timely progress in this research field is essential, since improved catalytic systems can ultimately contribute to a more sustainable and energy-efficient production of industrially relevant chemical compounds.

The insight gained from these investigations can be exploited to improve the properties of individual catalysts and chemical transformations. This will be rewarding and important by itself; however, based on current knowledge, even more fundamental advantages might be gained in the long term by using the catalysts' confinement to tap into novel reaction mechanisms and cascades. In this context, tailored pore systems with regard to size, shape and surface functionalization, will be crucial for success. This can open up access to challenging chemical transformations, including gas-liquid-solid reactions and catalysis with notoriously inert molecules such as dinitrogen or carbon dioxide.

1.2.2 Detailed presentation of the research program

Preamble

Catalytic reactions are, undisputedly, the backbone of modern chemical synthesis.[1-2] Compared to stoichiometric transformations, they save resources and energy, and are, by that virtue, much more sustainable. Nowadays, catalyzed reactions make up about 80% of all reactions in chemical and pharmaceutical industry and provide for savings of about 9 billion €/a.[3] Catalysis can take place in one or multiple phases, and it can be homogeneous or heterogeneous in nature. **Homogeneous organometallic catalysis** is solidly established in organic chemistry (Figure 1d) because it enables the

preparation of novel compounds in a highly specific, stereoselective manner, quite frequently also in high yields. However, under a wide range of experimental conditions, homogeneous catalysis is a process driven by chance encounters: the catalyst is free to move in all directions, usually molecularly dissolved and applied in high dilution. Likewise, the reactant is mobile and, albeit present in higher concentration than the catalyst, concentrations > 1 mol/L are rarely used. As a consequence, undesirable encounters between catalysts and other molecules, which cannot (or are not desired to) react, occur frequently. These include, among others, encounters with solvent, impurities or oxygen. In the best case this only results in slower conversion, but also a degradation of the homogeneous catalyst can occur, potentially resulting in lower TONs per catalytically active site compared to heterogeneous catalysis. These challenges are commonly met by skillful manipulation of the ligand sphere, to influence the catalysts' steric demand as well as its electronic properties.

In parallel, **biocatalysis** has developed rapidly,[4-6] where enzymes are optimized for the synthesis of specific target compounds. The main advantage of biocatalysis is typically seen in the directing influence of the three-dimensional enzyme structures, which commonly allow for impressive regio- and stereoselectivity, all under mild conditions. In the binding pockets, relatively high concentrations of (for example lipophilic) reactants can be accumulated, directed by the hydrophobicity of the binding pocket relative to the bulk medium surrounding the enzyme. Byproducts, like water, are removed continuously from the active site by polar channel structures. Also, intermediate compounds and states are able to react quickly because of the high reactant concentration, and the controlled geometry of the pocket ensures that this will proceed with high regio- and stereoselectivity. However, enzymes often suffer from limited pH stability, intolerance of organic solvents and frequently perform only within a rather limited temperature range.

Much in contrast to homogeneous catalysis, **heterogeneous catalysis** (Figure 1a) must be considered the fundamental base of technical large-scale processes.[7-12] Advances made during the last 25 years nowadays benefit numerous industrial applications.[2, 8, 13] Main reasons for this are high productivity, space-time yield and activity as well as innovative venues for process management such as continuous flow setups, gas-solid reactions or supported ionic liquid phase (SILP) technology. Additionally, it is easier to remove the catalyst and re-use it, which is obviously appealing given precious resources such as noble metals. Also, continuous biphasic reactions can be accomplished as impressively demonstrated e.g. in the Haber-Bosch process for NH_3 synthesis (gas/solid). These advantages commonly overcompensate for the reduced selectivity frequently encountered with heterogeneous catalysts.

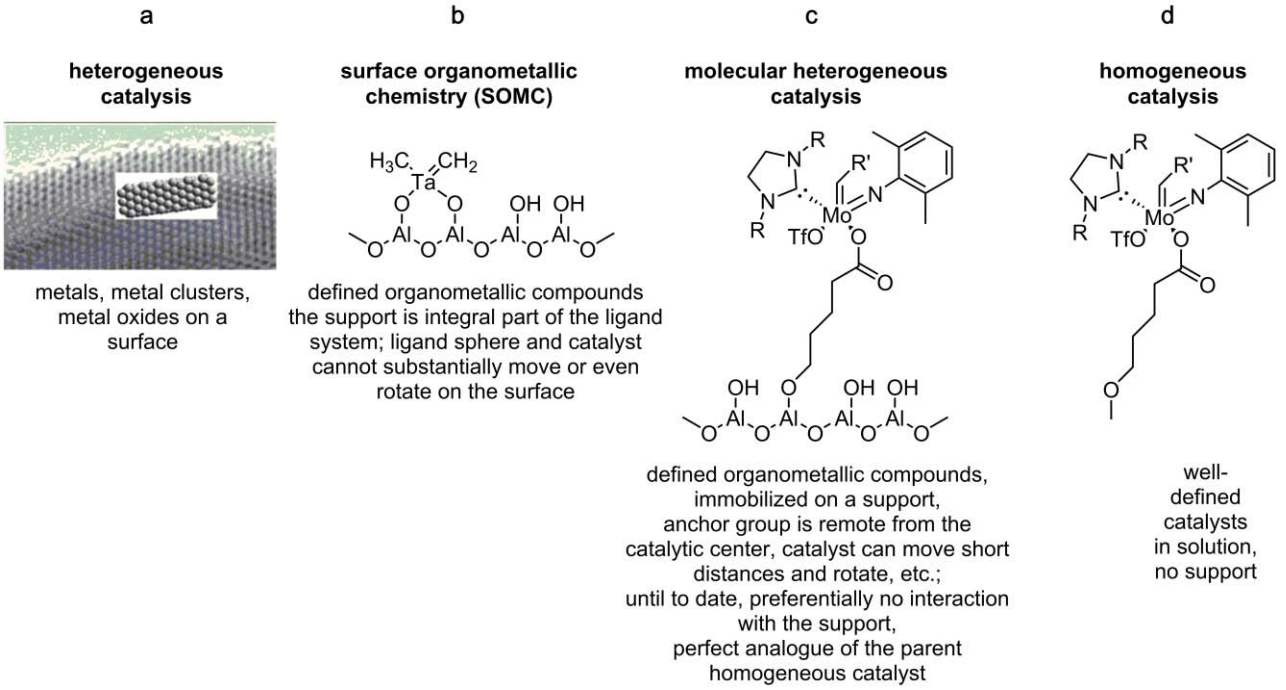

Figure 1. Subsections and features of heterogeneous (a-c) and homogeneous catalysis (d).

Closely related to heterogeneous catalysis is the so-called **surface organometallic chemistry** (SOMC, Figure 1b).[14-23] In SOMC, a geometrically defined, catalytically active organometallic compound is directly ligated to a support material. Consequently, the carrier material is also directly involved in the catalytic transformations since the support is part of the catalyst's ligand sphere. Disadvantages typically connected with SOMC are the comparatively low catalyst loadings to the material, restricted opportunities for ligand optimization, and most importantly a limited structural flexibility of the catalyst. The latter issue can however in some cases be advantageous, too. Despite other, obvious advantages of this concept (e.g., thermostability) the limited structural flexibility and a missing rationale for the influence of the support´s topology on a given catalytic transformation are somewhat disadvantageous. Also, the topology of the support has, to the best of our knowledge, so far not been employed in a rational manner.

Within recent years a new type of hybridization between a solid support and an organometallic catalyst has evolved - **molecular heterogeneous catalysis**[10, 24-29] **inside pores** (Figure 1c), where catalysts known from homogeneous settings are anchored in porous materials *via* a linker/spacer group. Here, porosity provides not only the cavities, but also the high surface area needed for sufficient catalyst loadings. Suitable supports include organic polymers, but also carbon materials and inorganic carriers (silicates, alumosilicates, etc.) as well as hybrid materials. In the simplest case, the catalysis itself is not influenced by the support material, which then solely provides high surface area and facile removal. As compared to SOMC, catalyst loadings can often be increased at least by a factor of two. If the method is refined by the use of polymeric grafting techniques, catalyst loadings up to 2 mmol/g can be achieved.[29-30] Finally, and most crucially, the catalyst reacts in the so-called **interphase** (provided that sufficiently long linkers or suitable grafting exists), which, in a simplified way, can be understood as a solution-like environment.[31-32] In this context, a layer of solvent molecules is relevant, which is no longer in direct contact (≥ 1 nm distance) with the support, and as such cannot be assigned unambiguously as part of the Nernst diffusion layer or, in the case of charged reactants, the Helmholtz layer. This has very recently been exemplified for water, whose spatial arrangement and structure inside pores is dramatically influenced by both the pore size and surface.[33] Thisclearly implies that in small pores of a few nanometers in diameter, the dielectric properties of the solvent can be expected to deviate strongly from the bulk, including a different charge distribution, significant concentration effects and special interactions between catalyst and pore wall such as hydrogen bridges, π–π interactions and dipolar interactions, to name just a few. This will, inevitably, impose changes on the local diffusion rate and the productivity (TON) as well as activity (TOF). Unfortunately, in the majority of cases the desired benefits (better stability, higher activity, etc.) were counteracted by secondary effects. These can include problematic issues like catalyst leaching or inhibition through interactions with the pore wall (in analogy to collapsing phases widespread observed in HPLC and referred to as "phase collapse"). Indeed, lower productivity than expected has led researchers to question the viability of the concept.[34]

Previous efforts, in our opinion, were unsuccessful because they were based rather on trial and error than on a comprehensive approach that fully considers the contributions of both the catalyst and the support. Therefore, instead, in this CRC we **specifically target the synergistic effects of enzyme-like catalysis by the skillful employment of directed, three-dimensional material synthesis and molecular heterogeneous catalysis (Figure 2)**. Within that context, especially the suitable manipulation of mass transport into mesoporous materials and the anchoring of the catalyst in such a cavity are central to the project. Conceptually, a support material is chosen to advantageously influence the catalytic reaction, although previously not much attention has been paid to this principle. Beneficial effects are composed of geometric factors, which can be understood as confinement-induced pre-orienting, and electronic factors, which include modified conditions on the pore surface (polarity, among others). Overall this will lead to a situation, very different from homogeneous catalytic reactions in solution (Figure 2). Indeed, as observed in a similar manner for enzymes or in micellar catalysis, an increased "hit rate" between catalyst and reactant, can be expected, as a consequence of the increased local concentration and pre-orientation[35] close to the catalytically active center.

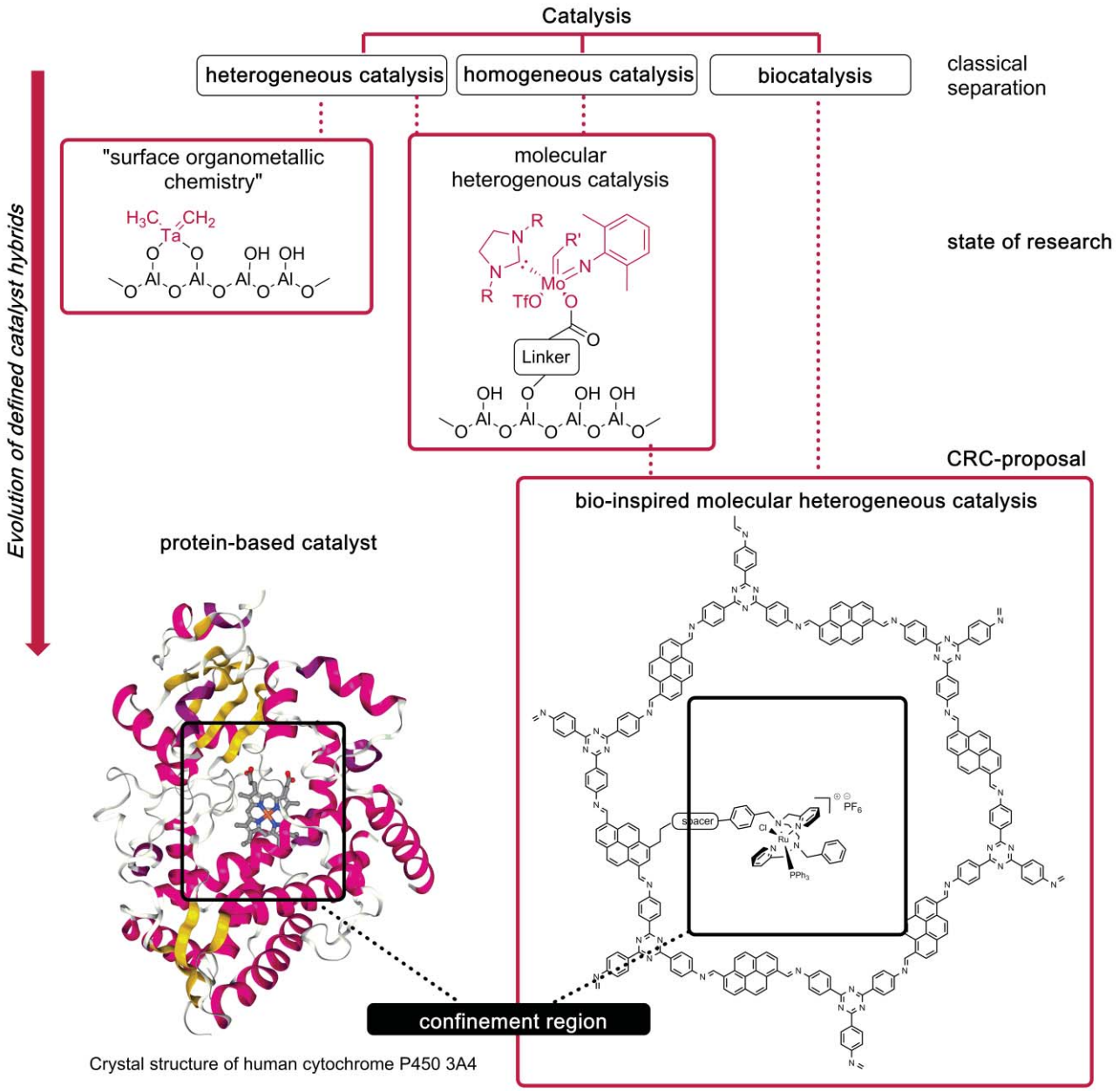

Figure 2. The evolution of bio-inspired molecular heterogeneous catalysis within this CRC – confinement as the key factor for selectivity.

Following from the dimensions of typical organometallic catalysts (ca. 1.5 nm), the use of **mesoporous materials** is evident: macroporous materials (> 50 nm) are too large to develop directing confinement effects,[36-39] while micropores (< 2 nm) are too small to accommodate the catalyst and to enable efficient mass transport. Ideally, a concept based on mesoporous materials retains the full flexibility of the catalyst but at the same time provides sufficient levels of confinement to generate the desired conditions. Although manifold positive effects of mesoporous supports on catalysis have been demonstrated, a deeper understanding of the synergistic interactions is lacking so far.[40] Currently, this frustrates any rational development and improvement of hybrid support-catalyst materials.

Enzymes can be viewed as a perfect fitting model system. Looking at this type of biocatalyst, it must be noted that the astounding selectivity of enzymes has not only evolved by fine-tuning of the catalytic center, but also by adaption of the three-dimensional topology as a whole. Different three-dimensional structures such as channels (“through pores”, which regulate the flow in one direction) but also blind pores including “ink bottles”, where only one opening is available, have been reported. More recent publications have even highlighted that more than one type of channel in an enzyme can be necessary to achieve the optimum “dosage” of different reagents or to maintain the ideal levels of removal of side

products. This perfect orchestration of specific diffusion processes to the catalytically active site is the prerequisite to sustain high selectivities and to perform reactions that would not be possible outside the protein core.[41]

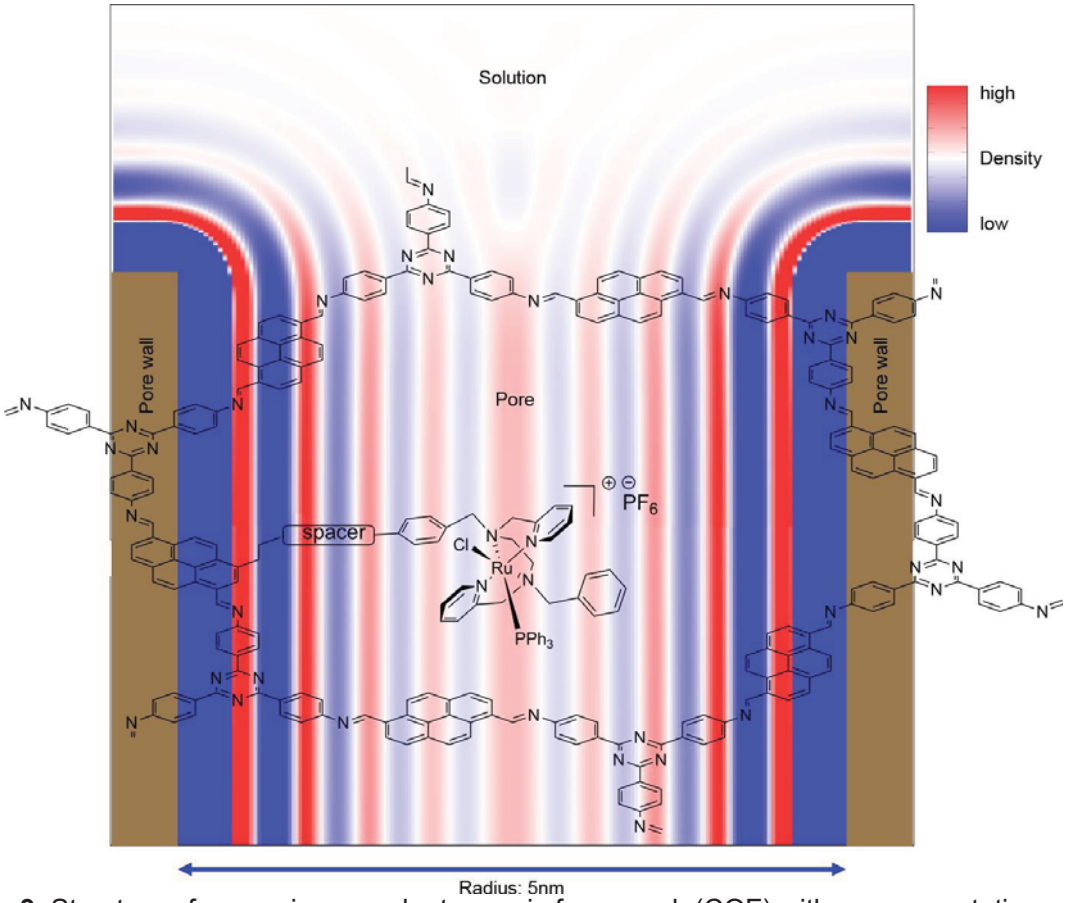

Figure 3. Structure of a pore in a covalent organic framework (COF) with a representative catalyst attached and the schematic distribution of solvent density fluctuations in the entry area of a cylindrical pore, calculated from classical density functional theory (classical DFT).

In the course of this CRC, defined, two- and three-dimensional structures containing open, continuous, tubular, channel-type or dead-end including ink-bottle-like pores will be prepared on the mesopore scale with nanosized pores, in the range of 2-20 nm. These support materials will be designed from a range of very different materials classes (**section A**), and will subsequently be equipped with suitable linker groups (**sections A and B**), which are designed to accommodate the special properties of both support and catalyst. The broad range of materials that are to be used during the course of this CRC entails polymeric, carbonaceous and inorganic materials including COFs. High-performance spectroscopy will be accompanied by quantum chemical (QC) calculations and modeling efforts on all relevant length scales (**section C**). In summary, a combination of all these approaches will result in a rational, but bio-inspired access to novel support-catalyst-hybrids.

Leading questions and long-term research goals

The planned CRC is dedicated to the investigation and understanding of catalytic reactions in defined and confined spaces. Once realized, this will allow for the optimization of catalytic reactions with the ultimate goal to establish both novel reaction pathways and even cascade reactions for catalytic reactions that have been only poorly realized or impossible to date. Such cascade reactions could consist of olefin metathesis/epoxidation or hydroxylation reactions, to name just a few. This is to be realized by the anchoring of well-defined organometallic catalysts inside pores with chemically defined surfaces based on the concept of combining the extraordinary selectivity of biological systems with the thermal and chemical stability of molecular heterogeneous catalysts. With this “confinement approach”,

which is ultimately bio-inspired in nature, we target the **rational development** of improved catalysts with the best possible parameters regarding activity, productivity and selectivity. **A comprehensive understanding, how a structurally well-defined pore geometry can, in analogy to enzymes, exert directing influence on the catalytic process, will be instrumental to success.** This directing influence comprises the orientation of the catalyst with respect to the inner pore surface, any pre-orientation of reactant(s), any concentration enhancement of reactant(s) and/or products at the pore wall or inside the pore, and selective transport phenomena into and out of the pore, to name a few. Only recently, some of these effects have been demonstrated, too, for metalloenzymes.[42] There, the manifold non-covalent interactions play a major role, which keep reactants in a specific pre-orientation.

The central and innovative approach to these fundamental questions will consist of a two-pronged strategy over all three funding periods. On the one hand, we will combine a rational (and broad) selection of support materials (**Section A**, Figure 4) with several well-defined catalysts (**Section B**). Initially, this will result in substantial necessary research effort, but will be much more rewarding than optimization of catalysts alone (without any support material). In other words: our combinatorial process will deliver synergistic results, which would be impossible to obtain otherwise. On the other hand, we take a detailed look at the interaction between catalyst, reactant(s) and product(s), both with each other and with the pore wall (**Section C**).

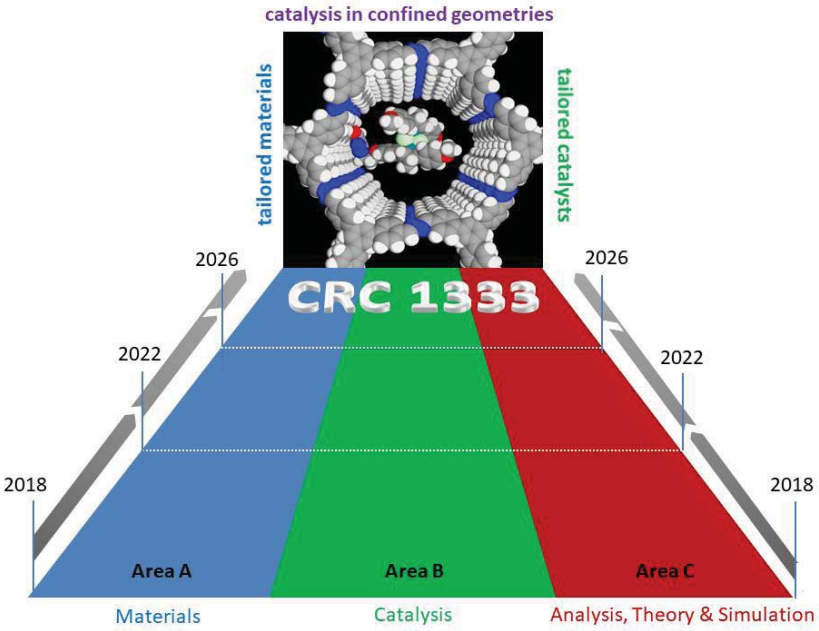

Figure 4. CRC-research cluster structure – interdisciplinary approach towards inner-pore molecular heterogenous catalysis.

To this end, we will apply a range of non-standard and partly custom-made characterization methods, such as modern NMR, EPR, Mössbauer and advanced X-ray measurements (**project S1**) such as XANES (X-ray absorption near-edge structure), EXAFS (extended X-ray absorption fine structure), HERFD-XANES (high energy resolution fluorescence detected XANES), vtc-XES (valence-to-core X-ray emission spectroscopy) and ctc-XES (core-to-core X-ray emission spectroscopy). Additionally, the hybrid catalyst/support systems will be modeled on **all** relevant length scales and the catalytic processes simulated accordingly. This again necessitates a range of methodologies, which entails highly accurate electronic structure calculations via molecular dynamics sampling as well as lattice-Boltzmann and fluid theoretical descriptions of mass transport phenomena. Reactivities will be calculated with density functional theory. The influence of the pore environment will be covered by QM/MM techniques. Molecular dynamics will provide information on diffusion rates and on the structural alignment of the catalyst and linker within the pore. Reactivities and diffusion constants will then be used in lattice-Boltzmann descriptions to estimate the mass flow within the pore towards the catalyst

and away from it. Fluid theoretical techniques, like classical density functional theory, will provide concentrations of the different components within the whole catalytic system.

Important sub-objectives and innovation
To realize the relevant research goals outlined above, the following sub-objectives have been identified:

1.) **Development of tailored mesoporous support materials.** This mainly concerns the controlled tuning of pore properties such as the nature, shape, topology, tortuosity and functionality, but also pore size distribution. Initially, our main focus will be on blind and channel-type pores. In addition, we aim to optimize the morphology of the materials (which can be powders, monoliths or films).
2.) **Development of suitable binding sites within the mesopores.** Functional groups, which will act as binding sites for the anchoring of the catalysts *via* a linker, will have to be compatible with both the material and the catalyst. Within that context, the chemistry for the selective generation of binding sites **inside** the pores, i.e. pore size-selective functionalization, has to be established, further improved and, if possible, extended.
3.) **Development of suitable linkers.** Linkers have the important role of connecting the catalyst to the corresponding support. Chemical reactivity of the binding site, and coupling of linker and catalyst, must display a high degree of orthogonality to ensure the selective formation of the target structures. Within that context, both the l**ength** and **stiffness** of the linker must be optimized.
4.) **Analysis of all processes relevant for the catalytic transformation on multiple length scales**, to be achieved by advanced physical characterization methods and theoretical modeling.
5.) **Quantification of the observed synergistic effects**, which will depend on pore dimensions, pore functionalization, length and flexibility of the linker and the type of reaction/catalyst. The influence imposed on activity, productivity and selectivity will be investigated and described quantitatively.

This CRC envisions a further development of initially won insights in a rational manner by specifically targeting synergistic interactions of support, reactant and catalyst, thereby generating new synergisms. Importantly, this also entails the tailoring of the pores with respect to geometry and tortuosity. This is expected to boost all relevant catalyst parameters, but will also enable new modes of reactivity. Finally, it is also evident that major findings of this CRC will be of highest interest for related research areas. On a longer time frame, the following aims can be defined:

1.) Extension of this concept from the relatively simple blind or channel-type pores to more complex, multimodal pore architectures.
2.) Development of multicomponent systems in mesoporous support materials (i.e., cascade reactions). This could, for instance, be olefin metathesis followed by hydroamination, hydroboration, etc.
3.) Extension of this concept to asymmetric catalysis, and generalization of the findings.
4.) Extension of this concept to other, related technologies, such as *supported ionic liquid phase*-(SILP)-processes or micellar catalysis (MC). Incorporation of these techniques into advanced material design. Developing “Catalysis 4.0”. After heterogeneous (Catalysis 1.0), homogeneous (Catalysis 2.0) and the “*in-silico*-catalysis” (Catalysis 3.0), now the merging of all available knowledge for a further step is required. Catalysis 4.0 is to be characterized by rational planning, using synthetic, analytical and theoretical tools to tailor both catalyst and support material (cf. Figure 2).

Some of the unique aspects of this CRC are summed up in the following:

1.) **Diverse set of support materials.** Typically, reports on molecular heterogeneous catalysis rely on the use of commercially available and consequently untailored and barely tunable oxidic materials such as silicates, aluminates and titanates or, typically, poly(styrene)-*co*-poly(divinylbenzene) (PS-DVB) resins as supports. In contrast, this CRC is based on a truly unique selection of very different materials, including tailored polymeric, inorganic, and carbonaceous, as well as crystalline and amorphous supports. The bandwidth of different material's properties (porosity, surface polarity, functionalizability etc.) allows for a systematic evaluation of the synergistic interaction between the type of material, pore characteristics, and a specific catalytic reaction. Developing an understanding of these interactions is a prerequisite for success and will lead to a much better understanding of factors relevant for catalysis. This also implies the possible discovery of surprising and novel reactivity.
2.) **Systematic investigations of interactions between pore (wall), reactants, products and catalysts**. This is considered the most crucial point since a comprehensive understanding of these issues is a prerequisite to utilize pore size, geometry and functionality as a directing tool that acts synergistically with the organometallic catalyst within the above-outlined bio-inspired approach. Previous work frequently disregarded any influence of the support material and solely focused on its role as solid anchor for the catalysts. Positive "pore effects" have been described in several cases, however, analysis of these has mostly been limited to reports on improved TONs. In line with that, correlation of factors such as pore geometry and selectivity of reactions are notably absent from the vast majority of publications. This is where this CRC is set to make a decisive difference.
3.) **Application of non-standard physical measurement methods.** This includes multi-frequency EPR, and pulsed field gradient NMR, Mössbauer spectroscopy and atom probe tomography, but also XANES, EXAFS, HERFD-XANES, vtc-XES and ctc-XES, in addition to conventional characterization methods. Combination of these methods will enable a comprehensive understanding of material and catalyst properties – both *ex* and *in situ* – and elucidate the interactions of pore and chemistry inside the pores.
4.) **Application of theoretical methods on all relevant length scales.** Calculation of the reactivity of a catalyst inside a pore is far from trivial. It is necessary to employ hybrid methods (QM/MM), whereby the catalytically active site is described quantum chemically (QM) and its surrounding is considered *via* classic force fields (MM), parts of which will have to be developed for our custom-made applications. Diffusion will be calculated using lattice-Boltzmann techniques and concentration profiles from classical DFT. Finally, simulation of transport processes within this outlined multi-scale calculation can be seen as a step in the direction of chemical and technical implementation of the catalysts, an aspect that has rarely been considered in this context.

Networking within this CRC and added value by cooperation
The individual scientists applying for this CRC are well renowned in their respective research areas. The groups of Bill, Buchmeiser, Gießelmann, Lotsch, Ludwigs, Sottmann and Traa are nationally and internationally highly recognized for their important contributions to the field of materials science, covering widely different subjects from polymers and foams to hybrid, biomimetic, nanostructured and oxide solid-state materials. The materials section is complemented by a high-potential young scientist – Dr. Naumann – whose group contributes organocatalytically-prepared polymers for mesoporous carbon materials. Furthermore, the groups of Buchmeiser, Laschat and Plietker have extensive and well-recognized expertise in catalysis. The Hunger and Van Slageren groups have special expertise in developing and adapting magnetic resonance and other spectroscopic methods critical for success of this CRC; their contribution is also enriched by the involvement of the young scientist Dr. Ringenberg and his experience in electrochemistry. Schmitz is an expert on electron microscopy methods and brings unrivalled experience in the novel method of atom probe tomography. Kästner has an impressive track record in the area of calculations for reaction mechanisms. The groups of Groß and young scientist Hansen work on aspects of technical thermodynamics including molecular dynamics for the quantification of diffusion rates. Finally, diffusion- and transport phenomena will be investigated by Holm and another young scientist, Jun. Prof. Fyta. Their expertise is augmented by advanced X-ray

spectroscopy, covered by a service project (**project S1**) in collaboration with Prof. M. Bauer, University of Paderborn.

None of these individual groups would be in a position to achieve the research goals of this CRC on their own, as an obvious consequence of the multi-faceted challenges of catalysis in confined spaces which include **material science** (**A**), **catalysis** (**B**), as well as **physical and theoretical investigations** (**C**). To make this CRC a success, a **cooperative approach** is clearly required (Figure 5).

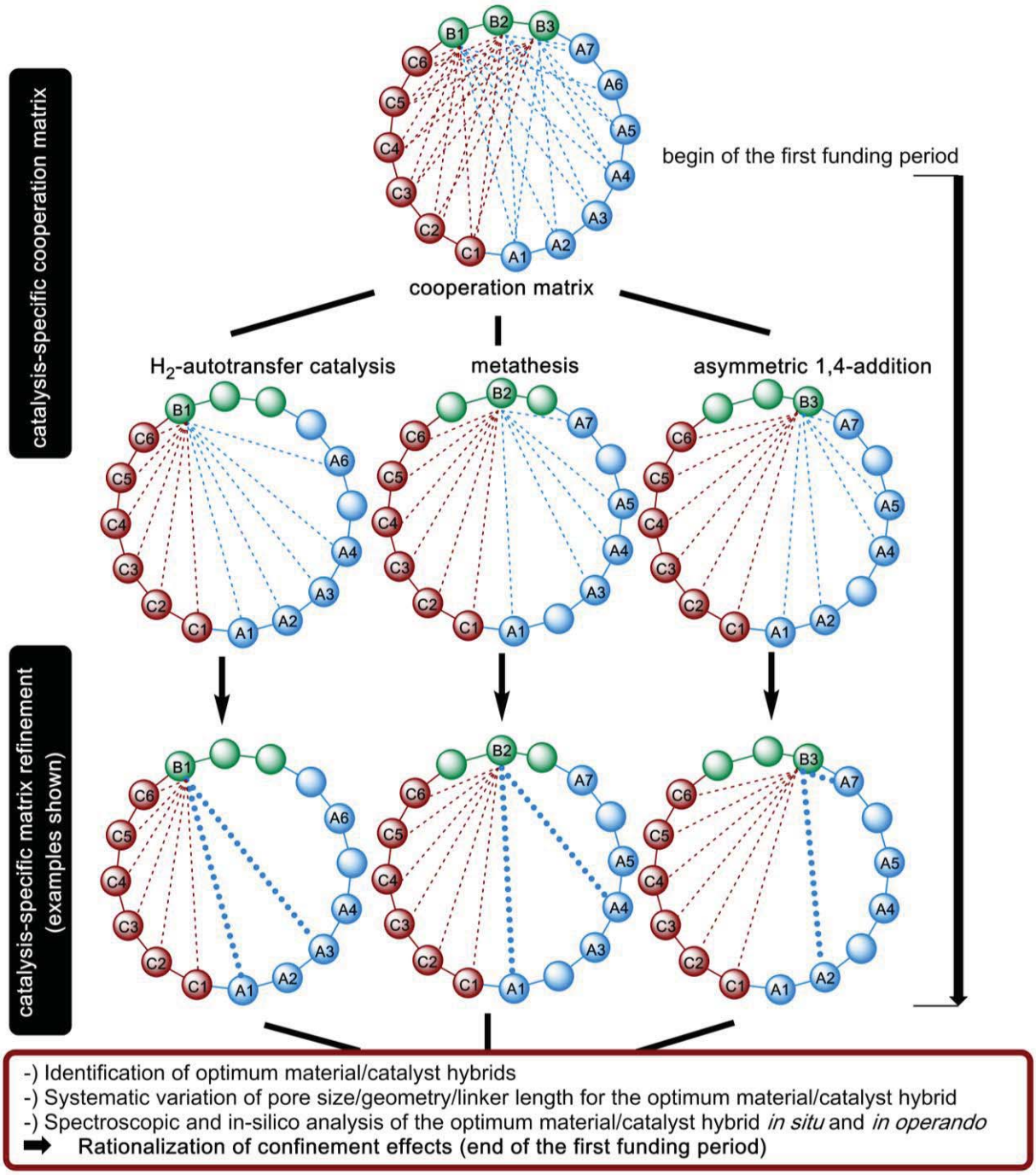

Figure 5. Cooperation within the CRC – catalysis as a bridging discipline (cooperations between areas A and C are not shown to improve clarity, the final cooperations between A and B at the end of the first funding period are examples).

The two main pillars of this CRC are formed by **Chemistry** (catalysis) and **Materials Science** (supports). At the University of Stuttgart both of these disciplines are embedded in the Faculty of Chemistry. As a result, close contact and connections already exist between the two disciplines. This gives Stuttgart a clear and decisive advantage over other universities as a location for the establishment of this CRC. In addition, there are strong links to the Max Planck Institute for Solid State Research and to the Faculty of Energy-, Process- and Biotechnology of the University of Stuttgart. The latter is already linked to the Faculty of Chemistry through the SimTech Cluster of Excellence.

Catalysis has a bridging function in this CRC. The pore-selective, defined positioning of the catalysts exclusively inside the cavities renders close cooperation between the individual groups and projects *de facto* mandatory (Figure 5). The development of suitable linkers and surface anchors is consequently equally important to other tasks. In close cooperation with the materials scientists, the teams from section **B** (catalysis) design the linker material and couple it to the ligand sphere. On the other hand, it must be ensured that the linkers find suitable binding sites, exclusively inside the pores, which is a challenging but rewarding task for groups from section **A**. Generally, such selectivity in immobilization can be achieved by differing the size of functionalities or linkers in case of hierarchical pore architectures, or by application of a polymeric reagent capable of pore size-selective "de-functionalization".[43-45] Alternatively, a templating approache will allow for a pore selective functionalization, too. Novel approaches may also be expected from this CRC. In principle and as the preferred approach, the anchoring step may either involve the catalyst as a whole, or as alternative, initially only the ligand system, which is then later provided with its metal center.

Quantum chemical calculations will increase our understanding of the catalytic mechanisms, but also allow for (time-resolved) simulations of dynamic processes inside pores, for example mapping diffusion processes or concentration gradients. It will be especially interesting to see wether these methods supporting the rational design of e.g. linker length or pore size for the experimental working groups.

Obviously, the complexity both in materials analysis and in the correlation of catalytic effects with materials properties sets high expectations on spectroscopy and requires powerful characterization methods. Synthesis, based on quantum chemical predictions, and the verification of the resulting structures by advanced spectroscopy is absolutely crucial for a deeper understanding, and thus for the CRC as a whole.

To reach these scientific goals the CRC is deliberately *not* sub-structured into bi- or trilateral cooperations but rather uses the three catalysis **projects B1** – **B3** as both the central and bridging projects. At the outset of the CRC, each of the B-projects cooperates with a selected and managable number of materials projects (A) to test the different materials in a systematic manner (Figure 5). **Project A4** (silica-based mesoporous materials) stands out in that it serves as a general model material on which immobilization strategies are tested and established. The resulting initial three silica-catalyst hybrids set the collaborators of area C in place to perform spectroscopic investigations and theoretical modelling studies. **Project A1** (monolithic supports) is positioned in a similar manner. Within the first funding period the catalysis-specific cooperation matrices will be refined to give at the very end a set of maximum of two successful catalyst-material hybrids per catalysis project. Bi- or even trilateral cooperation would result in only fragmental and relatively slow progress, because resources would still be too limited in view of the highly complex subject (i.e., investigation of the combination of *one* catalyst with *one* type of support is interesting, but insufficient to derive systematic conclusions and make rapid progress). Consequently, the level of cooperation provided by a CRC is not only the most suitable but also the most promising way to achieve the above-discussed aims in a sensible time frame: firstly, good inter-group communication is ensured by short distances (both geographically and by way of administration), which is always beneficial to any kind of cooperation. Secondly, this CRC is the only possibility to inspect the desired broad range of materials and catalysts in an efficient manner. Timely progress in this research field is certainly essential, since improved catalytic systems can ultimately contribute to a more sustainable and energy-efficient production of industrially relevant chemical compounds. We are convinced that one crucial advantage of this CRC will be its wide-ranging scope of both support materials and catalysts. To systematically extract potential effects of a given material/pore geometry/pore diameter on a catalytic reaction, we created a research structure in which three different catalytic reactions will be performed in five materials each. The added value that can be extracted from

these combinations will grow substantially with each catalyst/support hybrid investigated. It is also important to note that the physical/theoretical groups (section **C**) will provide their expertise to *all* projects of sections **A** and **B**.

State of the Art

The field of molecular heterogeneous catalysis has attracted a great deal of research efforts.[46] Numerous reactions based on organometallic catalysts have been investigated (i.e., C-C coupling, hydration reactions and others). It became clear from these investigations that the activity of a homogeneous catalyst upon immobilization is strongly dependent on the type of support, but also on the type of "immobilization chemistry" and the grafting density. However, these relatively diffuse findings have not yet been subjected to a fully systematic and thorough investigation to elucidate the origins of the observed effects. In consequence, there is currently little understanding at a fundamental level of the influence of a mesoporous environment on catalytic activity. Published reports suggest that apart from the chemical constitution of the support material (inorganic, polymeric, hybrid), the (Lewis-) acidity, the polarity or the functionalization of the surface and especially the fraction of mesopores and their size in relation to the organometallic catalyst, play a decisive role. Accordingly, several groups have reported a significant increase in activity,[47-50] productivity,[51-54] regio-, [55-56] enantio-[47-48, 51, 55, 57-66] or chemoselectivity[67] where catalysts were introduced into mesoporous materials. However, in this context, it is important to note that none of these groups have discriminated between organometallic catalysts immobilized either inside or outside pores. In view of the very different accessibility of the individual catalytic sites, this has to be looked at quite critically, since such a mixture of immobilization sites will only allow very limited, qualitative drawing of structure-activity correlations and inhibit quantitative considerations almost completely. It could be argued that **mesoporous materials** with pore sizes < 20 nm will have a massively increased inner surface, which marginalizes the number of catalysts that will be bound "outside". However, one could equally cite the possibly better accessibility of these "outside" catalysts, which would overall skew the results in a manner that makes clear deductions impossible. To receive unambiguous, reliable correlations in a manner suitable for this CRC, it is absolutely necessary to achieve **pore size-selective functionalization**. To this end, suitable synthetic concepts have to be employed or developed. Also, reports have pointed out the influence of the solvent in these systems, but again, no reliable and rationally justified correlations with pore porosity or polarity were revealed.[57] In other cases, adverse effects have been described when mesoporous systems were applied, for example a loss of enantioselectivity. Unfortunately, these findings were again not elaborated on and the underlying mechanisms remain unclear.[68] Lacking a profound understanding of the interplay of all factors involved, the majority of publications cite "*site isolation*" effects to explain the improved results found when catalysts were used with mesoporous supports. It is also argued that the homogeneous, spaced immobilization prevents detrimental bimetallic reactions between catalysts, hence the isolated sites gain productivity (or less deactivation occurs).[61, 67, 69-76] Such a crude assessment seems unsatisfactory since the same tendency should also appear in highly dilute catalyst solutions, but tellingly it is observed only very rarely. Also, the highly ordered nature of mesoporous MCM-41 systems[77] and the resulting decreased tortuosity[69] or improved diffusion phenomena[71, 77-79] have been proposed as explanation, again limited to qualitative statements without quantitative support. Furthermore, a possible analogy between micellar catalysis[80-81] and mesopores acting as microreactors[79] has been pointed out. Finally, rudimentary correlations of the properties of different support materials and catalytic activities were reported,[82-83] but these were limited to the comparison of obviously different average pore sizes, without considering the setup in a more complete manner.

Crosman and *Hölderich* invoked "*constraints*" as the reason for especially improved selectivity or productivity, but explicitly admitted that, so far, no clear understanding of this term exists.[84] *Ponchel* et al. remained similarly vague in a more recent work.[85] Overall, terms like "confinement effect", "cooperative effect" or "steric constraints" are only used sporadically in the context of organometallic catalysts in combination with mesoporous materials, and always without any specific or quantitative description.[47, 60, 86-88] Based on results for asymmetric catalysis,[51, 89-90] it was firstly J. M. Thomas who formulated a theory that the **confinement of reactants in mesoporous channels**, by exploiting the **cooperative action** of **chiral selector** and **pore wall**, could lead to an increased influence of the chiral selector on the orientation of the reactants relative to the catalytically active center.[64, 66, 91-93] Related effects are known for zeolites,[94-95] graphene[96-98] and even hollow polymeric networks[99] from conventional heterogeneous catalysis. Some early studies on *metal organic frameworks* (MOFs)[100]

and their use as biomimetics for synergies between structure and catalyst as well on carbon nanotube-immobilized catalysts[101] also exist. De Jong et al. were probably inspired by similar considerations when they described catalytic activity in a more recent work as a function of catalyst loading (active sites/100 nm^3) and pore opening ("*window size*").[102] Very recently, the impact of a confined geometry on the selectivity in cycloalkyne formation has been reported for the first time.[103]

The above remarks clearly imply that it is equally possible and necessary to correlate the influence of geometry, chemistry and physics imposed by the support material with key catalytic parameters. It is also clear that this is connected with a capacious work load. Even then, several factors remain largely unappreciated, including the polarity (functionality) of the pore wall (apolar, polar, protic, aprotic) and the prospective formation of single- or multiple layers of reactant(s), product(s) and solvent (Nernst, Helmholtz layers). Additionally, time-resolved change in concentration or composition during catalysis needs to be considered, especially the resulting "back coupling"-phenomena, which can for example exert considerable influence on selectivity. The latter effects seem all the more important since P. Wasserscheid and co-workers recently described the *in-situ* formation of a supported ionic liquid phase (SILP), which formed from hydroformylation products catalyzed by immobilized Rh compounds.[104] All the above gives direction to, but equally stresses the need for a concerted, systematic research effort in this field.

Own work, justification for choosing the University of Stuttgart as research location

At the University of Stuttgart both Chemistry and Materials Science are embedded in the Faculty of Chemistry. As a result, close contact and connections already exist between the two disciplines. Clearly, only an efficient interlocking of working groups from material science, catalysis, theory and spectroscopy can pave the way for successful realization of the CRC's strategic aims. All relevant scientific methods are solidly established in the involved teams. Stuttgart recommends itself as ideal environment for this CRC by its outstanding, internationally recognized materials science body, which is integrated within the Department of Chemistry, and also by the availability of special non-standard characterization methods and by the presence of renowned theoretical working groups. The interdisciplinarity within the CRC is obvious from the broad spectrum of expertise covered by the working groups involved, which encompasses chemistry in its full width as well as material science, analytics, physics and simulation. At the same time, the competence, the established collaborations and the computational infrastructure from the excellence cluster "*SimTech*" of the University of Stuttgart will be employed to the fullest extent. Consequently, engineers and physicists complete area C. Preparatory work for the single subprojects is outlined in the detailed project descriptions found in section 3.

Although a substantial number of project leaders (Profs. Ludwigs, Lotsch, Jun. Prof. Hansen, Jun. Prof. Fyta, Dr. Naumann, Dr. Ringenberg) have only recently arrived in Stuttgart or at the MPI-FKF, numerous collaborations and joint research proposals have already resulted. These joint proposals as well as joint publications are listed in the appendix.

Definition of the research field

In this CRC we will study homogeneous catalysts that are heterogenized by immobilization into porous materials. The environment (reaction space) is defined here as mesoporous inorganic/polymeric/hybrid materials, which include polymeric monoliths, crystalline porous polymers, mesoporous materials, and inorganic/polymeric/hybrid foams. Our self-imposed limitation to **mesoporous systems (2-50 nm)** is intentional and excludes micro- and macroporous setups. This limitation is based on simple fundamental assumptions, namely the fact that very small pores (< 2 nm, i.e. micropores) cannot physically accommodate organometallic catalysts with diameters typically around 1 nm *and* reactants at the same time. We expect the strongest effects to appear for pores of 3-20 nm in size, and accordingly the CRC focuses on mesopores, preferably with pore diameters in this range. We have limited the types of catalysis to those reactions outlined in the **section B** (**catalysis**) because these catalytic transformations are representative for important application fields in Organic Chemistry. Thus, dehydrogenation, hydrogenations as well as condensation reactions are the very heart of organic synthesis. Complementary, transition metal-catalyzed olefin metathesis has evolved as one of the most powerful strategies for C-C-bond formation. Finally, asymmetric catalysis is certainly the most challenging subdiscipline within the field of catalysis since only very subtle differences in energies can lead to high levels of stereoselectivity.

Confinement effects to be studied
The use of these mesoporous systems as supports for organometallic catalysts will answer the following exemplary questions central to this CRC:

(i) At what ratio of catalyst diameter: pore diameter do cooperative or directing effects appear? This issue will be addressed by systematic variations of the pore size as outlined in the projects of **section A** (**Materials**, *vide infra*), including for example the highly precise adjustment of pore sizes within a series of so-called isoreticular, pore-expanded COFs to study the influence of a confining reaction field on entropically challenging reactions such as acyclic diene metathesis (ADMET) polymerization and ring-closing metathesis (RCM).
(ii) How are these cooperative or directing effects influenced by the pre-orientation and/or complexation of reactants or the formation of product layers?
(iii) What is the role of pore size, geometry and tortuosity on the selectivity and productivity of the catalytic reactions to be investigated? Furthermore, at a later stage of the CRC, it will be interesting to study the influence of for example helically-structured or chiral mesoporous supports on enantioselectivity. Within that context, the use of chiral mesogens in templating will be addressed in later funding periods.
(iv) What is the mutual influence and synergism of the polarity of the pore wall, the solvent, the catalyst and the reactants/products?

In more detail, the following scientific questions will be addressed:

(i) Definition of the polarizability of a solvent and the dielectric constant of the pore fluid as a function of distance to the pore wall and the pore polarity. Thereby, interesting questions regarding the geometry of the mesopores will be highlighted (including channel- or dead-end structures and tortuosity).
(ii) Elaboration of a quantitative description of phenomena such as the prospective adsorption effects of one or more reactants (for example via capillary action). With respect to the second funding period, this might prove an elegant alternative to pressure in bringing reactants together.
(iii) Understanding the interactions between catalyst and/or reactants with the different mesoporous materials. This includes a systematic variation of the support materials and their properties (porosity, pore sizes, pore geometry, surface functionalities, topology and tortuosity), which will, together with selected catalysts and catalytic transformations, generate a comprehensive understanding of the interplay between organometallic catalyst, linker and support. This will also render the involvement of gaseous products such as ethylene in olefin metathesis reactions as well as asymmetric conversion necessary. The investigation of gaseous reactants will then be one of the central topics in the second funding period.
(iv) A unique feature of this CRC is the application of polymeric or hybrid support materials with a high degree of molecular definition and functionalization sites, which can potentially be complemented with the variation of electronic/optical properties in later stages of the CRC.
(v) Based on the findings outlined in (i) – (iv), multicomponent/cascade reactions will be investigated in the described mesoporous surroundings at a later stage of the CRC.

Notably, all projects will always focus on the understanding of catalytically relevant processes, underpinned by innovative physical analysis methods and theoretical modeling. In terms of theory and simulation, rate constants for the chemical step will be calculated in solution and compared to the values obtained in the pore, and simulations of the structure of the catalyst/linker within the pore will give profound insights into steric effects and the influence of solvent shells. Also, simple but most important questions, such as, whether a particular catalyst (including ligands) does actually fit in a specific pore, will be addressed.Questions regarding confinement effects based on linker packing on a pore surface and specifically the influence on linker/catalyst conformations will be addressed. Also, the question whether there is one generic catalytic site or several sites in a cylindrical or a slit pore of variable diameter will be addressed. Other important aspects are the influence of diffusion and reaction rate in confinement, transport issues concerning reactants and products in and out of pores, as well as the conformation of linker and spacer with an attached catalytic site in pores of variable geometry and with different wall interactions.

This CRC will rest on three subsections: **Materials** (A), **Catalysis** (B) and **Analysis, Theory & Simulation** (C), which will be interlinked by intensive interactions (Figure 4). The overall setup is such that all projects can start at the same time since at least supports from **projects A1**, **A4** and **A6** are available instantaneously; the overall synchronization and cornerstones of the CRC are shown in Figure 6.

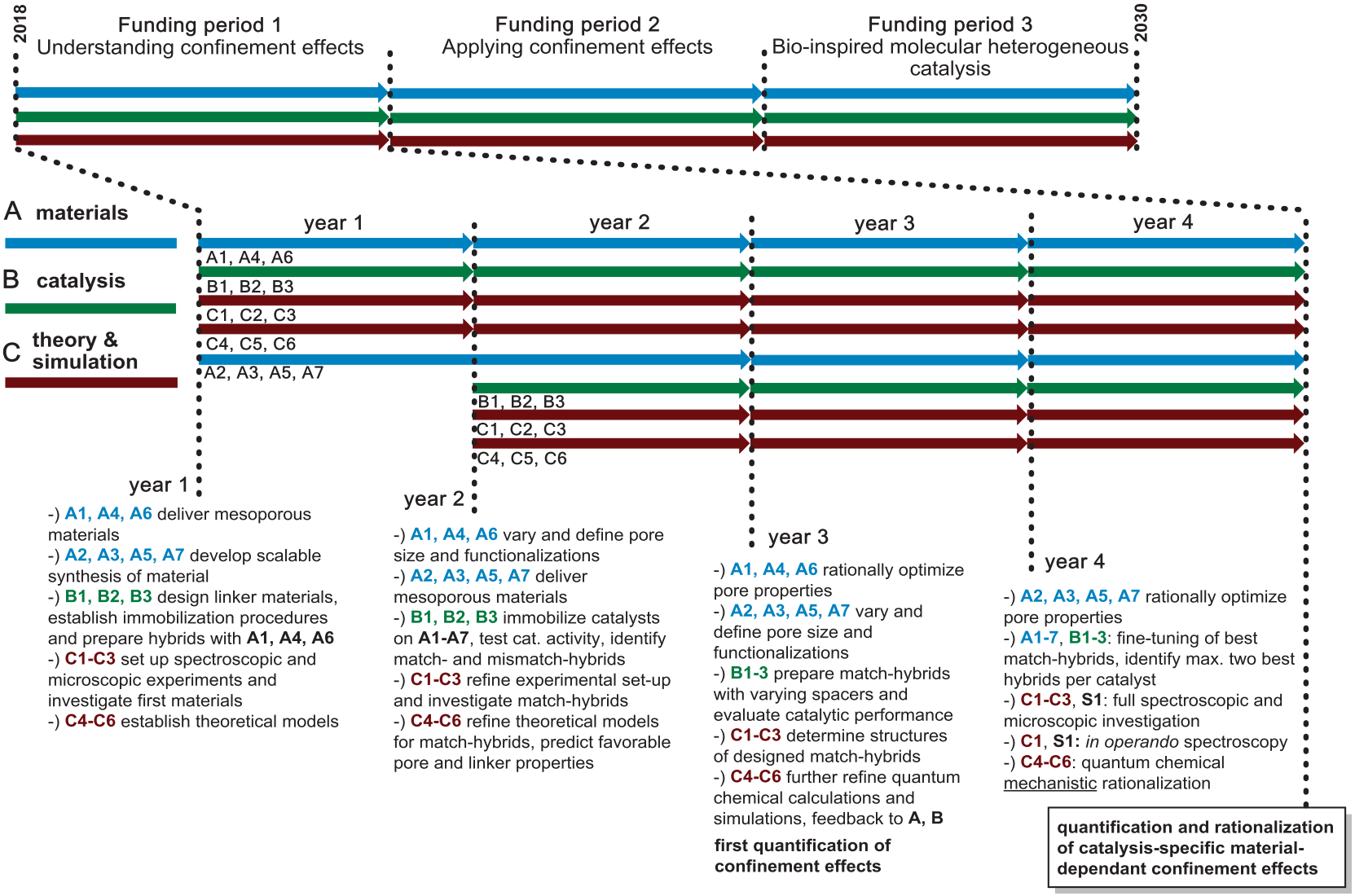

Figure 6. Conceptual cornerstones, synchronization of work-packages, and long-term research vision of the proposed CRC.

The above-discussed transfer of the mechanisms of biological reaction spaces to molecular heterogeneous catalysis in mesopores innovatively employs novel, tailored (hybrid-)support materials to gain synergetic effects from different factors (such as porosity, pore sizes, pore geometry, surface functionalities, solvents). To this end, directing surfaces and materials with multiple binding sites for preorganization, as well as modeling on all relevant length scales and innovative spectroscopic methods will be applied. The spectroscopic investigations will ensure three crucial key points: a) characterization of the material, b) spatially resolved catalyst concentration and c) time-resolved observation of reactions by way of *operando*-spectroscopy. As stated before, this routine will be applied to all different material/catalyst combinations.

Inner-pore immobilization of metal-catalysts using linker units of different flexibility as well as precisely tailored pore sizes allows for studying pure confinement effects as caused by the pore geometry, size and polarity. Moreover, it sets the stage for spectroscopic detection of a single-site catalyst in action. Although the inner-pore immobilization of enzymes appears to be of principle interest, too, the fact that the catalytic center in enzymes is shielded through a protein core that might overstir potential confinement effects created in a specific mesoporous material led us to exclude biocatalyst from this CRC.

Section A: Materials

A crucial task of this CRC is the generation of a hybrid unit consisting of pore and catalyst, whereby the pore itself has no direct catalytic role, but can influence catalytic reactions indirectly (e.g. by means of pore polarity) and functions as important synergist that brings reactants and catalyst together.

This CRC can draw upon a copious range of different materials that can act as supports, which will be partitioned in four groups. These are 1) polymeric support materials, 2) inorganic supports, 3) organic-inorganic hybrids and 4) carbonaceous materials. Together, they provide a comprehensive set of materials that allows for ample variations in pore type, size, size distribution, geometry and polarity. The individual advantages and properties of each type of support are outlined in **projects A1** – **A7**. Each type of material will be adapted to fit the desired catalyst system (size, charges, stability), the reaction conditions (temperature, solvent), the class of reaction and the type of reactant (aggregate state, dimensions). Apart from the chemical constitution, which obviously governs functionalization and surface chemistry of the support, morphology is one of the crucial properties. Especially the porosity (pore size, -volume, -shape and dimensionality), the size distribution of the pores (uni-, bi- or multimodal) as well as the accessible, catalytically relevant surface of the material must be characterized. Macroscopic appearance is a further degree of freedom, which may include powders (COFs, polymers, oxides, nanofoams), monoliths (polymers, oxides, nanofoams) or thin films (block-copolymers, COFs, oxides). Special attention must be paid to pore-selective functionalization, or the exclusive functionalization of pores of a desired size (for bi- or multimodal pore size distributions), in contrast to the “outside” surface of the support material.

Mesoporous Materials

(i) Polymeric/organic support materials: Polymeric monoliths are important examples for this type of support (Buchmeiser group, **project A1**).[24, 44, 105-126] These materials are synthesized by a solvent-induced phase separation (SIPS) process; importantly, their pore (size) distribution (and the specific surface) can be tailored to a high degree. However, monoliths with unimodal, defined pore diameter are not known yet and thus one aim of **project A1**. Functional monoliths can be easily obtained by using functionalized monomers. The Buchmeiser group frequently employs several relevant polymerization methods, including ring-opening metathesis polymerization (ROMP), electron-beam induced free radical polymerization, *reversible addition fragmentation transfer* (RAFT) polymerization and polyaddition (for poly(urethane)s). Using these techniques, polymeric monoliths can be synthesized in a broad variety of dimensions.

A large-pore alternative to monoliths is provided by the Sottmann group through their **polymeric nanofoams** (**project A7**), prepared via the NF-CID process (*Nanofoams by Continuity Inversion of Dispersions*). Starting from colloidal polymer crystals (based on PS or PMMA) NF-CID generates nanopores (>100 nm) by inclusion of gas from supercritical CO_2 in a highly viscous polymer matrix. An advantage of this support material is the easy scale-up of the synthesis to the kg scale. Average pore sizes down to 20 nm will be prepared by suitable adaptation of reaction parameters (pressure,

temperature, time) or by application of an inorganic oxide layer on the inner surface, a task that is to be accomplished in cooperation with **project A5**.

Block copolymers are used in the Ludwigs group (**project A2**) for preparation of oriented, mesoporous films with pore sizes between 10 and 20 nm. The formation of ordered mesopores is controlled by thermodynamic microphase separation of tailored, mainly non-polar AB- or ABC-block copolymers which are accessible by living anionic or radical polymerisation. The block copolymer thin film morphology can be tuned, depending on length and polarity of the single blocks and by post-synthetic temperature- or solvent-treatment, covering cylindrical and gyroid motifs. The mesopores are introduced by selective etching of the minority block and the pore wall chemistry functionality will be tuned in terms of hydrophilicity. Preparation of the templates on gold will be applied to allow thiol-anchor chemistry and make electrochemical probe techniques possible.

While the systems above use (living) polymerization methods followed by phase separation to generate pore size-variable material with amorphous walls, the so-called ***covalent organic frameworks***, **COFs**, **project A3**, constitute a relatively new, crystalline type of two- and three-dimensional polymers, which are *structurally* porous as opposed to porosity originating from a material's morphology. COFs are formed from building blocks in a *reversible* manner, along the lines of *dynamic covalent chemistry.* The Lotsch group exploits this principle to design topology, pore size and geometry of the networks by judicious choice of the building blocks; thereby, pores between 1 nm and 6 nm can be realized. Polarity and reactivity are influenced by the choice of monomers, which usually are di- tri- or tetratopic heteroaromatic alcohols, amines, aldehydes or boronic acids. Both their precisely defined pore size and high degree of order (Figure 7) render COFs complementary to the above described polymer classes.

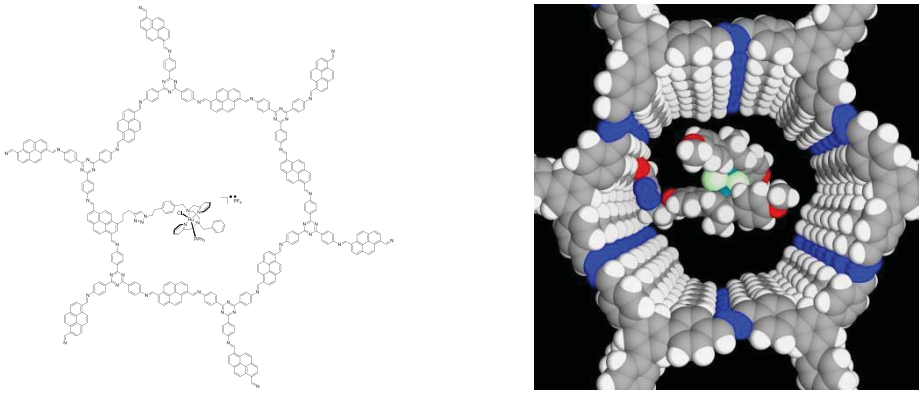

Figure 7. Left: Schematic sketches of a 2D-imine-COF (**project A3**) with immobilized Ru-catalyst (**project B1**). Right: Model of an azine-COF with immobilized Rh-catalyst (**project B3**). Both catalyst attachments are drawn based on an yne-azide click reaction.

(ii) Inorganic supports: Robust and easy-to-functionalize, **mesoporous SiO_2, SiO_2/Al_2O_3** or **TiO_2, oxide-materials** will be provided by the groups of Bill, Traa and Gießelmann (**projects A4, A5**); these partly well-established systems with variable surface chemistry can be delivered with different topologies (i.e., FDU-12, MCM-41, SBA-15, SBA-16), different degree of order (MCMs vs. *mesocellular foams*, MCF; amorphous (**project A4**) pore wall structures) and different pore sizes (2-20 nm). Oxidic mesoporous systems will be prepared by soft templating of lyotropic liquid crystals (**project A4**) and copolymers (**project A2**), the variation of which can be used to influence pore size and wall thicknesses. Apart from the lyotropic liquid crystals by the Gießelmann group (**project A4**), the block-copolymers employed by the Ludwigs group (**project A2**) may also be used to template inorganic oxides by electrodeposition. After the organic material is etched out (or burned off), films with ordered mesopores are obtained.

A further path to inorganic mesoporous structures in this CRC will be the **mineralization of organic nano-objects and their subsequent removal from the organic/inorganic hybrid** (Bill group, Sottman group, **projects A5** and **A7**).

(iii) Organic/inorganic hybrids: Apart from using the antipodes of purely organic or purely inorganic supports, the interplay of both components can be used to design hybrids with variable pore sizes, wall thicknesses and surface chemistry. The Bill group (**project A5**) follows a bio-inspired concept, whereby the organic parts serve to control the **mineralization of oxide layers** from suitable precursor solutions.

As organic components, nano-foams (**project A7**), block copolymer templates (**project A2**) and polymeric monoliths (**project A1**) are intended to be used. Layering these structures with inorganic material will allow for pore size selection within the limits of 2-50 nm. Alternatively, pores can be filled completely, and the organic component can be thermally removed afterwards (see also (ii)), which would equally introduce a defined porosity. By choice of different oxides (SiO_2, TiO_2, ZrO_2, ZnO, etc.) it is possible to take influence on the functionality and surface charges, which will serve as a highly promising method to **model the spatial arrangement of the catalyst (projects B1 - B3) by electrostatic forces** (Figure 8).

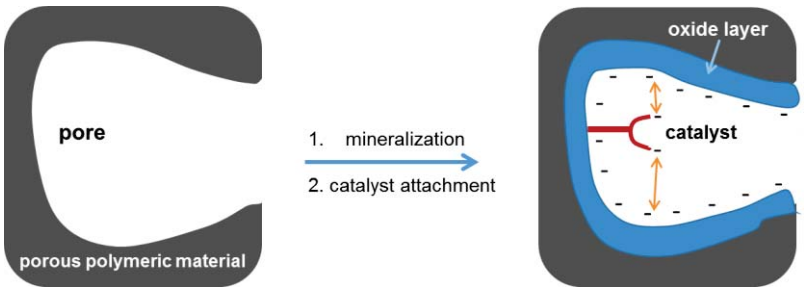

Figure 8. Process to generate a catalytically active organic/inorganic hybrid.

(iv) Carbonaceous materials: Copolymers play an important role for the preparation of **mesoporous carbonaceous materials** (**project A6**). For these materials, the template for a highly ordered pore structure is generated from the self-assembly of amphiphilic block-copolyethers; addition of thermally cross-linkable monomers immobilizes this structure. Subsequent calcination and carbonization then delivers the ordered mesoporous carbon material. Pore size and wall thickness can be directly influenced by the properties of the underlying polyether (block length of poly(ethylene oxide)/poly(propylene oxide)), which in **project A6** (Naumann group) will be achieved by way of an organocatalytic, highly controlled polymerization mechanism. Of these well-defined polymers, subtle variations will be synthesized to generate equally well-defined, subtly different carbon materials. Ease of functionalization, systematic pore size variation and chemical/thermal robustness render these materials a valuable extension of the support materials available for this CRC.

Functionalization of the support materials

(i) Pore-selective functionalization: For the concept of the CRC to be meaningful, catalysts have to be immobilized exclusively *inside* the pores. This aspect is of enormous importance since even small amounts of catalyst located outside the pores might substantially outperform the catalyst inside the pores because of a much better diffusion situationand will in turn render interpretation of the results difficult. Synthetically, this requires **pore-selective functionalization**. Several methods exist to realize such a targeted functionalization of mesopores. For example, polymeric, but also inorganic or carbonaceous materials can be chemically derivatized by epoxides and subsequently hydrolyzed with a macromolecular reagent; this reagent cannot migrate inside the pores - its solvodynamic radius is too large - and therefore only the functionalities inside pores with the desired size remain intact. The surviving epoxide moieties can then be used to anchor catalysts.[44, 114, 127] By way of similar measures, that is, passivation with sterically demanding reagents ensures that, with all the material systems contributing to this CRC, the inner surface (pore surface) can be addressed separately from the outer surface. Alternatively, all templating techniques, e.g., those used for the synthesis of tailored silica materials, benefit from the opportunity that the outer surface of the supports can be (de-) functionalized with simple reagents such as silanes prior to the removal of the template, followed by the functionalization of the pore.

(ii) Functionalization strategies and linker chemistry: Click chemistry has been chosen as the guiding method for the following reasons. First, this reaction has been demonstrated to proceed quantitatively even with polymeric materials. Second, the reaction as such tolerates numerous functional groups and under very mild conditions. Finally, the resulting 1,2,3-triazoles possess low basicity and low propensity to coordinate to a catalyst. The necessary alkyne and azide groups can be attached to the catalysts outlined in **projects B1** – **B3** and to all support materials. Details are found in **projects A1** – **A7** and **B1** – **B3**, respectively. Thus, **project A1** can provide, e.g., -OH,-NCO or –NH2

groups for further functionalization. The necessary groups for functionalization can also be introduced into, e.g., *block*-copolymer films by *soft-etching* (**project A2**) and -OH termini can be generated by hydrolysis of ester blocks. Also, the anchoring of catalysts at the bottom of a dead-end pore system can be envisioned; here, self-assembled-monolayer-(SAM-)specific surface functionalities constitute an interesting approach, especially when based on thiol chemistry.
Functionalization of covalent organic frameworks (**project A3**) can be achieved following two different strategies. One method with successful precedent is the direct introduction of a functionalized (and optionally also protected) linker (alkyne, etc.) during network formation. Attachment of the catalyst follows in a second step, for example aided by yne-azide click-chemistry or via nucleophilic substitution. Importantly, the density of functional groups (and thereby also of anchoring sites) can be controlled by the so-called mixed-linker-approach. With this technique, functionalized linkers are employed alongside non-functionalized ones. Alternatively, the post-synthetic attachment of a functionalized linker into a non-functionalized COF can be feasible in certain cases; this method takes advantage of the reversible condensation reactions during COF formation, which can be extended to post-synthetic linker exchange reactions.
The carbonaceous materials as investigated in **project A6** are functionalized by a sequence of surface oxidation (hydroxylation) and further reaction with epoxide-bearing reagents; the epoxides can be ring-opened to introduce “clickable” functionalities (azide, alkyne).
To immobilize catalysts on oxidic supports (SiO_2, Al_2O_3, TiO_2 etc., **projects A4**, **A5** and **A7**), a rich and versatile silane-chemistry can be employed, apart from the already considerable intrinsic reactivity of these surfaces (terminal OH-moieties), in order to achieve a tailored functionalization. Trialkoxysilanes are typical examples (X-$(CH_2)_n$-$Si(OR)_3$ (X = N_3, -CCH), but also sterically demanding silazanes such as 1,3-dimethyl-1,1,3,3-tetraphenyldisilazane und 1,1,3,3-tetramethyldisilazane. By chemical nature, size and concentration of the silane as well as by choice of the hydrolytic environment the surface functionalization and the respective reactivity can be designed (in addition to tailoring surface charge), notably a function of pore sizes. The polarity of the pores can be tuned by the use of functional trialkoxysilanes X-$(CH_2)_n$-$Si(OR)_3$ (X =OH, COOH, NH_2, NMe_2, etc.),

Section B: Catalysis
In the first funding period of this proposed CRC, the individual group leaders of Section B will employ robust, well defined and established catalysts from their previous research, which have so far been used under homogeneous conditions. It is important that for the selected catalysts/reactions, a fundamental mechanistic understanding already exists, in order to be able to compare results from conventional, homogeneous catalysis and molecular heterogeneous catalysis in mesopores. The synthesis of suitable linkers, which must provide a spatially resolved, selective functionalization of the support materials, efficient anchoring of the metal complexes and a tunable distance from the pore wall (while still maintaining some rigidity), will be a major task in this section. Previously published work frequently relied on aliphatic ethers as linkers, which are typically very flexible. This could potentially explain part of the frequently encountered problem of catalyst inhibition, by allowing the metal complex to react with or collapse onto the pore wall. This issue is to be addressed by designing stiffer linkers, for example using aromatic or cycloalkane moieties. Additionally, different “head”-motifs (where the linker is coupled to the ligand system of the catalyst) will be screened, which will include covalent, but also ionic binding strategies. The findings thus obtained will be accompanied and augmented by spectroscopy and quantum chemical calculations, which may also result in refined experimental procedures. In order to gain maximum insight in a reasonably short timeframe, the following catalyzed reactions, which are representatives for some of the most important transformations in Organic Chemistry, will be investigated in detail.

Transfer hydrogenation: The Plietker group (**project B1**), prepares transition metal-hydrogen complexes *in situ* as catalytically active intermediates. **Project B1** focuses on hydrogen auto transfer catalysis, using (NNNN)Ru-complexes. In such reactions, the active metal hydride species is formed by dehydrogenation of an alcohol. The carbonyl compound accessible in this way can be transformed through subsequent reaction steps (such as aldol condensation). In the final step of this intercepted catalytic cascade, a back-transfer of the H-atom from the catalyst to the organic intermediate occurs. This type of reaction is ideally suited for exploring the prospective advantages of confinement: (i) the metal hydride formed *in situ* should not react except to accommodate the hydrogen for a limited time before transferring it back, leading to increased catalyst lifetimes and TONs; (ii) the condensation

product may not move too far away from the metal hydride for successful H-transfer. It is exciting to imagine the multiple benefits (i.e. high local concentrations of intermediate dehydrogenation and condensation products at the catalytic center as well as defined diffusion kinetics of starting material (i.e. amine and alcohol), by-product (i.e. water) and product (i.e. secondary amine)) that could be derived from skillful confinement and cavity design. In line with this, the pore topology (ink-bottle type pores versus channels) is expected to have a direct influence on the catalytic performances. In **project B1** the removal of water, or its enrichment/depletion in the relevant solvent layers will be of high interest in this interplay of linker length, pore size- and surface, and entropy (two different reactants are brought together inside the pore). A similar interplay in a different setup can be observed in **project B3**, where an immobilized Rh-diene complex will be used for stereoselective 1,4-addition (*vide infra*). Water adsorption in the mesoporous support could increase the reaction rate. Here, it is a tantalizing prospect to be able to influence the enantioselectivity by the size and shape of the pore.

Olefin Metathesis: Olefin metathesis is especially well positioned for this CRC's goals. The Buchmeiser group (**project B2**) has a commanding array of active and functional-group tolerant Mo- and W-catalysts at their disposal.[128-130] These do not, in stark contrast to Ru-based Grubbs-type systems, display any inclination for olefin isomerization. Also, by deliberate variation of reactants (polar, non-polar, protic, aprotic) and type of reaction (ring-closing metathesis, ring-opening cross-metathesis, en-yne metathesis), reactions of first or second order can be conducted, and also the products can be either solvatized or gaseous. Of specific interest is the question how two competing olefin metathesis reactions, that is ring-closing metathesis (RCM) and acyclic diene metathesis (ADMET) polymerization, can be influenced such that selectivity is shifted towards RCM. This is of utmost interest in macrocyclization of complex, functional molecules. Also, issues of the *syn/anti* interconversion in Mo/W imido/oxo alkylidene N-heterocyclic carbene (NHC) complexes, their role in E/Z-selective olefin metathesis and the influence of pore confinements on such reactions will be studied. Together, such a variation allows for individual addressing of the scientific questions relevant to this CRC.

Enantioselective Catalysis: The foundation of enantioselective catalysis is the ability to achieve a defined, reactive and exclusive conformation in the reaction space. In enzymes, this exclusive conformation is realized by precise positioning and diffusion of reactants in the binding pocket. In conventional, homogeneous catalysis this pre-orientation is provided by chiral ligands, which generate a suitable three-dimensional space around the metal center. Decisive for a high degree of asymmetric induction is the adjustment of a preferential trajectory of the incoming substrate. In **project B3** (Laschat group) enantiomerically pure metal catalysts will be introduced in pores, and the influence of key parameters (geometry, size, etc.) on the enantioselectivity and overall activity will be analyzed. For these purposes, the Rh-diene complexes described above will be employed for the addition of aryl boronic acids to different Michael acceptor systems (both 1,4- and 1,2-addition). The interaction of pore geometry, position of the catalyst within the pore and analysis of steric demand will be supported by extensive spectroscopy and theoretical considerations with the overall aim of amplifying the typically subtle energy differences of diastereotopic transition states. In a similar manner, catalysts from **project B2** will be studied in enantioselective olefin metathesis reactions and desymmetrization reactions.

Section C: Analysis, Theory and Simulation

Analysis: In the literature, the influence of the support material on immobilized catalysts has so far, if at all, only been discussed in a largely qualitative manner. To grasp the quantitative relations between the mesopore structure and relevant catalytic parameters, the following steps are necessary: Firstthe support materials must be characterized comprehensively. Second, the binding of the catalyst and its static and dynamic orientation in the support must be determined. Subsequently, the activity of the immobilized catalyzed must be investigated. And as a final step, the influence of mass transport (from microscopic to macroscopic length scale) must be understood. Only then it will be possible to fully comprehend the proposed interactions of catalysis in confined spaces.
The first work package involves thorough characterization. Crystalline supports (for example COFs, **project A3**) will be subjected to X-ray powder diffraction. The specific surface will be obtained using common gas adsorption techniques; pore size and their distribution can be accessed best by this methodand by SAXS or SANS (the latter especially for light atoms). This CRC has special expertise in small angle scattering carried out in the Sottmann and Gießelmann group. These scattering methods,

however, only yield average values. Consequently, the detailed pore structure should also be analyzed with local spectroscopic (e.g. solid state NMR) and microscopic methods such as atomic-force microscopy (**project A2**) or transmission electron microscopy and scanning electron microscopy (**project A3** and **C3**). To complement these other techniques, extremely high resolved atom probe tomography will be adapted to porous (polymeric) materials for the first time, as a further unique characteristic of this CRC. Solid state NMR (**project C1**) and, for paramagnetic substances, also EPR (**project C2**) can help to characterize the structure and electronic properties of the close surrounding of individual catalyst sites inside the support materials. This CRC also involves Fe-based compounds (**projects B1**, **B2**, **B3**, and **C2**), and Mössbauer spectroscopy will provide a singular handle on those (**project C2**). By adsorption of probe molecules and their investigation *via* solid state NMR, information about nature, accessibility, orientation and chemical properties (Brønsted, Lewis) of the surface can be extracted. FT-IR and Raman spectroscopy will complete the range of characterization methods. Finally, **service project S1** offers access to advanced X-ray analysis comprising XANES (X-ray absorption near edge structure), EXAFS (extended X-ray absorption fine structure), HERFD-XANES (high energy resolution fluorescence-detected XANES), vtc-XES (valence-to-core X-ray emission spectroscopy) and ctc-XES (core-to-core X-ray emission spectroscopy) measurements. These methods will provide information about the oxidation state (XANES), local structural parameters around an X-ray absorbing metal center (EXAFS), the LUMO (HERF-XANES) and HOMO (vtc-XES) states of the complexes under investigation and their spin state (ctc-XES) *without* the need for any translational symmetry, i.e. crystallinity, and fully *independent* of the state of aggregation.

After successful anchoring of the catalyst in the support material, its position, mobility/flexibility and electronic ground-state structure will be investigated *in situ* through combined spectroscopic and theoretical analysis. This working package can be subdivided into several tasks.

- The binding site of the catalyst on the material must be characterized. Depending on the support, several methods can be applied to achieve this, including FT-IR, solid state NMR (Hunger group, dedicated **project C1**). For transparent materials, this list might be expanded to include Raman spectroscopy, time-resolved electron spectroscopy or (magnetic) circular dichroism ((M)CD, van Slageren, **project C2**).
- The geometric and electronic structure of the catalytic center will be elucidated. Information on local geometry and electronic configuration is accessible via X-ray spectroscopy (activation of inner-layer electrons, **project S1**) and Mössbauer-spectroscopy (activation of Fe-nuclei in ferrocenes, **project C2**). A state of the art variable temperature Mössbauer spectrometer will be developed for this CRC (**project C2**). Ferrocene moieties attached to the catalyst in such way that changes in the oxidation state and/or charge can be monitored by Mössbauer or MCD spectroscopies. For the analysis of the outer-layer electrons cyclovoltammetry, and, in case of paramagnetic catalysts, EPR-spectroscopy is employed (**project** C2). In addition, structural information will also be obtained from pulsed EPR measurements, relying on the dipolar interaction between spins on the catalytic species and the linker or pore wall. The local structural configuration of the immobilized metal-complex is analyzed through solid state NMR (**project C1**). The Schmitz group will focus on determining the catalysts' position using atom probe tomography inside the pore, for the first time ever (**project C3**). If successful, this will unlock a whole novel research area.
- The third task entails the identification of prospective interactions of the support surface and catalyst. For diamagnetic catalysts, solid state NMR is especially valuable in this context (after selective deuteration of support, linker or metal complex), providing access to orientation and dynamics *via* analysis of the ^{2}H-NMR signal shapes. Probe molecules will be used to identify differences in accessability of both unsupported and supported catalysts for different nucleophiles. The spatial environment of surface sites can be enlightened by the application of polarization transfer experiments (i.e., CP-solid state-NMR). Similarly, paramagnetic catalysts can be recorded by pulsed ENDOR (electron-nuclear double resonance, van Slageren group) and ELDOR (electron-electron double resonance).

Novel catalysts will be throughly characterized. We will apply conventional methods (IR, UV, MS, EA, XRD) for all catalysts. Redox-active catalysts will also be studied by (spectro-) electrochemistry (**project C2**). Paramagnetic species will be investigated by EPR techniques (**project C2**). The excited

state dynamics of potential photocatalysts will be determined by transient absorption and luminescence methods (**project A3**).
For benchmarking purposes, and to facilitate strictly systematic later comparisons, catalyst parameters (TON, TOF, etc.) under purely homogeneous conditions will be determined. Equally important, we will investigate the kinetics and thermodynamics of reactant/catalyst complexation. This will include conventional methods (IR, UV/Vis), but also more advanced technologies such as *in situ*-MAS NMR (Hunger group).
Interactions of reactant and support are most crucial to this CRC. Any such interactions will impact subsequent catalysis. Solid state NMR of isotopically enriched reactants will reveal the reactant's adsorption, orientation or catalytic transformation on active sites.
Finally, analysis of the actual catalysis will be central to this working package. Thermodynamics and kinetics of the immobilized catalysts will be investigated by varying concentrations and temperature. Direct comparison with conventional, homogeneously run reactions will reveal how confinement influences the catalysis. An important aspect will also be the analysis of catalyst degradation processes. These experimental catalysis screening processes will be supported by in-operando X-ray spectroscopy (**project S1**) to gain insight into potential catalytic intermediates and the microkinetics of the catalytic process.
The findings resulting from this comprehensive approach will allow for a much deeper understanding of the catalytic transformations. For productivity, however, mass transport is equally important. Interactions of reactant and support material can be judged by the respective retention time in flow-through reactors (equipped with *in situ* analytics). Pulsed field gradient NMR (**project C1**) can be employed for determination of the diffusion parameters of the reactants.

Theory and Simulation: Generally, modeling allows for the simulation of immobilized catalysts, reaction mechanisms, thermodynamics and kinetics of catalytic transformations and includes diffusion processes into and out of the pore.[131-132] The challenge in this context is the extent of time- and length scales that have to be integrated to achieve a comprehensive understanding of confinement effects. To make an accurate description of reactivity, the electronic structure must be considered quantum mechanically (about 1 nm or 100 atoms). The dynamics of the catalyst inside the cavity requires modeling of the whole pore (2-20 nm). This can be achieved by atomistic or coarse-grained force field methods. Simulation of diffusion of reactants and products, and their respective concentrations and affinity for the pore wall, requires mesoscopic and continuous models. An overall multiscale-bridging approach is necessary, which can be achieved by an interdisciplinary cooperation of engineers, physicists and chemists.
Compared to experiments, the simulation of catalyst activity (and stability) has the specific advantage of allowing simplified structural models. That means that individual parameters can be investigated and varied independently. As a first step, the mechanisms of the catalytic processes will be analyzed *ex situ* (that is, in solution) by the Kästner group (**project C4**). Reaction barriers and rate constants will be determined using *ab-initio* calculations/density functional theory in order to receive references for following in-pore simulations. Importantly, these results can also be directly compared to findings from spectroscopy. NMR shifts and electronic field gradients will be calculated and correlated with experimental data from solid state NMR.
While the simulation of reaction mechanisms in solution can be considered more or less a standard application, modeling of in-pore processes is more difficult and time consuming. For this, QM/MM-methods will be employed, that is, the combination of classic force fields (MM) with quantum chemical description (QM) of the active centers (**project C4**). This allows for an accurate simulation of the impact of the surroundings on the chemical transformation. Since the same QM-methods are used for simulation in solution, a direct comparison is possible and errors might be minimized. Such investigations will deliver rate constants for reactions on immobilized catalysts.
Force fields or potentials approximate interatomic interactions as parameterized functions of the atom coordinates. For some materials like silica, reliable and well-tested force fields are available, which are also compatible with commonly used force fields for water (i.e., TIP3P, SPC, etc). Novel mesoporous materials, such as COFs as well as linker molecules, however require the development of new force fields. These must reproduce parameters like density, polarity, vibration frequencies or structure. Moreover, they must also be compatible with simulation-derived properties, such as force constants or partial charges from *ab-initio*-calculations. Potentials specifically adapted to the pores used in this CRC will be developed. On the one hand, atomistic force fields will be parametrized (**projects C4**, **C6**) to

gather details on atomic scale, but also coarse-grained force fields are needed to cover larger time- and length scales (**project C6**). For this, 3-10 atoms are subsumed to one super atom. For parametrization of both approaches the experimental results will be indispensable. FT-IR and Raman spectroscopy will deliver vibrational frequencies; atom probe tomography (**project C3**) and EXAFS (**project S1**) will reveal the pore structure in a highly resolved manner. For catalyst description with force fields, however, *ab-initio* data will be necessary as a reference. This information as a whole will be employed to fit reliable potentials, which will enable predictive simulations of catalytic processes in pores.
Pores with different surface properties will interact differently with catalysts. The question whether the catalyst can move relatively freely inside the pore or whether it is adsorbed to the pore wall will depend significantly on the polarity of wall, catalyst and solvent. Diffusion and relaxation of the system as a whole is a slow process (nanosecond range), which requires simulation of molecular dynamics with force fields (Hansen, Groß, Holm, Fyta, **projects C5** and **C6**). Even slower processes will be approximated with coarse grained force fields (Holm, Fyta **project C6**). Such molecular dynamics simulations provide average geometries and time-resolved fluctuations, which can directly be correlated with experimental data. Depending on the catalyst, such verifications can also include solid state NMR (Hunger, **project C1**) or ENDOR/ELDOR spectroscopy (van Slageren, **project C2**). Reciprocally, simulated dynamics will reveal novel insights about the inner of the pore, which might inspire further opportunities for experimental investigations.
To generate macroscopic properties like TOF from rate constants, accurate descriptions of transport processes into and out of the pore are required.[133] These in turn are determined by polarity of pore surface and solvent, but also of reactants and products. Diffusion can be represented to a certain degree by use of atomistic molecular dynamics. Since relevant time scales, however, are often not accessible in this way, continuum models like the lattice-Boltzmann approach (**project C6**) and fluid theories like classical density functional theory are better suited (Groß group, **project C5**). While these ignore atomistic details, which are negligible on this scale anyway, they enable a competent prediction of concentrations and gradients, which in turn are necessary to determine a catalysts' efficiency.

In summary, all these targeted simulations will provide a consistent and reliable description of catalytic processes in mesopores. The applied models will be constructed in close collaboration with experimental working groups from Sections **A**, **B** and **C**, including rigorous verification. The insight gained and lessons learnt will inspire new experiments and allow for a novel, detailed multi-scale understanding of these processes.

References

[1] R. J. Wijngaarden, A. Kronberg, K. R. Westerterp, *Industrial Catalysis* In: (Ed.), Wiley-VCH, Weinheim, **1998**.
[2] R. Schlögl, *Angew. Chem.* **2015**, *127*, 3531–3589*; Angew. Chem. Int. Ed.* **2015**, 54, 3465-3520.
[3] M. Beller, *Evonik, Bonn, 7. 9. 2016.*
[4] C. J. Sih, S.-H. Wu, *Top. Stereochem.* **1989**, *19*, 63.
[5] K. U. Schöning, N. End, *Top. Curr. Chem.* **2004**, *242*, 273-317.
[6] K. Faber, H. Griengl, in *Chirality : from Weak Bosons to the Alpha - Helix* (Ed.: R. Janoschek), Springer, Berlin, **1991**, pp. 103-140..
[7] Y. I. Yermakov, *J. Mol. Catal.: A Chem.* **1983**, *21*, 35.
[8] J. M. Thomas, *ChemSusChem* **2014**, *7*, 1801-1832.
[9] K. Reuter, D. Frenkel, M. Scheffler, *Phys. Rev. Lett.* **2004**, *93*, 116105.
[10] R. A. van Santen, *J. Molec. Catal. A: Chem.* **1997**, *115*, 405-419.
[11] R. L. Burwell, Jr., *Chemtracts: Organic Chemistry* **1990**, *3*, 253.
[12] R. A. van Santen, P. W. N. M. van Leeuwen, J. A. Moulijn, B. A. Averill, *Catalysis: an integrated approach* In: Studies in Surface Science and Catalysis, (Ed.), *Vol. 123*, Elsevier, Amsteram, **2000**..
[13] A. J. Medford, A. Vojvodic, J. S. Hummelshøj, J. Voss, F. Abild-Pedersen, F. Studt, T. Bligaard, A. Nilsson, J. K. Nørskov, *J. Catal.* **2015**, *328*, 36-42.
[14] J. M. Basset, A. Choplin, *J. Mol. Catal: A Chemical* **1983**, *21*, 95-108.
[15] T. J. Marks, *Acc. Chem. Res.* **1992**, *25*, 57.
[16] P. Sautet, F. Delbecq, *Chem. Rev.* **2010**, *110*, 1788–1806.
[17] C. Copèret, M. Chabanas, R. P. Saint-Arroman, J.-M. Basset, *Angew. Chem.* **2003**, *115*, 164-191 *Angew. Chem. Int. Ed*. **2003**, *42*, 156-181.
[18] C. Copéret, A. Comas-Vives, M. P. Conley, D. P. Estes, A. Fedorov, V. Mougel, H. Nagae, F. Núñez-Zarur, P. A. Zhizhko, *Chem. Rev.* **2016**, *116*, 323–421.

[19] M. Valla, R. Wischert, A. Comas-Vives, M. P. Conley, R. Verel, C. Copéret, P. Sautet, *J. Am. Chem. Soc.* **2016**, *138*, 6774–6785.
[20] M. Pucino, V. Mougel, R. Schowner, A. Fedorov, M. R. Buchmeiser, C. Copéret, *Angew. Chem.* **2016**, *128*, 4372-4374*; Angew. Chem. Int. Ed.* **2016**, *55*, 4300-4302.
[21] V. Mougel, K.-W. Chan, G. Siddiqi, K. Kawakita, H. Nagae, H. Tsurugi, K. Mashima, O. Safonova, C. Copéret, *ACS Central* **2016**, *2*, 569–576.
[22] M. Valla, D. Stadler, V. Mougel, C. Copéret, *Angew. Chem.* **2015**, *128*, 1136–1139.
[23] M. P. Conley, C. Copéret, C. Thieuleux, *ACS Catal.* **2014**, 4, 1458-1469.
[24] E. B. Anderson, M. R. Buchmeiser, *ChemCatChem* **2012**, *4*, 30-44.
[25] A. Choplin, F. Quignard, *Coord. Chem. Rev.* **1998**, *178-180*, 1679–1702.
[26] P. W. Kletnieks, A. J. Liang, R. Craciun, J. O. Ehresmann, D. M. Marcus, V. a. Bhirud, M. M. Klaric, M. J. Hayman, D. R. Guenther, O. P. Bagatchenko, D. A. Dixon, B. C. Gates, J. F. Ha, *Chem. Eur. J.* **2014**, *13*, 7294–7304.
[27] G. A. Somorjai, *J. Mol. Struct. (Teochem)* **1998**, *424*, 101-117.
[28] M. R. Buchmeiser, *New J. Chem.* **2004**, *28*, 549-557.
[29] M. R. Buchmeiser, *Chem. Rev.* **2009**, *109*, 303-321.
[30] S. Lubbad, M. R. Buchmeiser, *Macromol. Rapid Commun.* **2003**, *24*, 580-584.
[31] E. Lindner, T. Schneller, F. Auer, H. A. Mayer, *Angew. Chem.* **1999**, *111*, 2288-2309; *Angew. Chem. Int. Ed*. **1999**, *38*, 2154-2174.
[32] E. Lindner, S. Brugger, S. Steinbrecher, E. Plies, M. Seiler, B. Bertagnolli, P. Wegner, H. A. Mayer, *Inorg. Chim. Acta* **2002**, *327*, 54-65.
[33] J. M. Mietner, F. J. Brieler, Y. J. Lee, M. Fröba, *Angew. Chem.* **2017**, *129*, 12519-12523*; Angew Chem. Int. Ed.* **2017**, *56*, 12348–12351.
[34] S. Hübner, J. G. de Vries, V. Farina, *Adv. Synth. Catal.* **2016**, *358*, 3–25.
[35] L. Yang, L. Zhao, Z. Zhou, C. He, H. Sun, C. Duan, *Dalton Trans.* **2017**, *46*, 4086-4092.
[36] G. Y. Yang, N. Tsubaki, J. Shamoto, Y. Yoneyama, Y. Zhang, *J. Am. Chem. Soc.* **2010**, *132*, 8129-8136.
[37] J. M. Thomas, R. Raja, *Acc. Chem. Res.* **2008**, *41*, 708–720.
[38] S. A. Miners, G. A. Rance, A. N. Khlobystov, *Chem. Soc. Rev.* **2016**, *45*, 4727-4746.
[39] J. Yuan, A. M. Fracaroli, W. G. Klemperer, *Organometallics* **2016**, *35*, 2149–2155.
[40] F. Hoffmann, M. Cornelius, J. Morell, M. Fröba, *Angew. Chem.* **2006**, *118*, 3290-3328; *Angew. Chem. Int. Ed*., **2006**, *45*, 3216–3251.
[41] L. Pravda, K. Berka, R. Svobodová Vařeková, D. Sehnal, P. Banáš, R. A. Laskowski, J. Koča, M. Otyepka, *BMC Bioinformatics* **2014**, *15*, 379-386.
[42] M. Jeschek, R. Reuter, T. Heinisch, C. Trindler, J. Klehr, S. Panke, T. R. Ward, *Nature* **2016**, *537*, 661-665.
[43] F. Švec, J. M. J. Fréchet, *Adv. Mater.* **1994**, *6*, 242-244.
[44] R. Bandari, T. Höche, A. Prager, K. Dirnberger, M. R. Buchmeiser, *Chem. Eur. J.* **2010**, *16*, 4650-4658.
[45] R. Bandari, A. Prager, T. Höche, M. R. Buchmeiser, *ARKIVOC* **2011**, *iv*, 54-70.
[46] A. Taguchi, F. Schüth, *Micropor. Mesopor. Mater.* **2005**, *77*, 1-45.
[47] A. Corma, M. Iglesias, C. del Pino, F. Sanchez, *J. Chem. Soc. Chem. Commun.* **1991**, 1253-1255.
[48] R. Augustine, S. Tanielyan, S. Anderson, H. Yang, *Chem. Commun.* **1999**, 1257-1258.
[49] S.-G. Shyu, S.-W. Cheng, D.-L. Tzou, *Chem. Commun.* **1999**, 2337-2338.
[50] P. Piaggio, P. McMorn, C. Langham, D. Bethell, P. C. Bulman-Page, F. E. Hancock, G. J. Hutchings, *New J. Chem.* **1998**, *22*, 1167-1169.
[51] S. A. Raynor, J. M. Thomas, R. Raja, B. F. G. Johnson, R. G. Bell, M. D. Mantle, *Chem. Commun.* **2000**, 1925-1926.
[52] S. S. Kim, W. Zhang, T. J. Pinnavaia, *Catal. Lett.* **1997**, *43*, 149-154.
[53] C. M. Crudden, D. Allen, M. D. Mikoluk, J. Sun, *Chem. Commun.* **2001**, 1154-1155.
[54] G. Gerstberger, C. Palm, R. Anwander, *Chem. Eur. J.* **1999**, *5*, 997-1005.
[55] H. M. Hultman, M. de LAng, M. Nowotny, I. W. C. E. Arends, U. Hanefeld, R. A. Sheldon, T. Machmyer, *Stud. Surf. Sci. Catal.* **2002**, *143*, 277-285.
[56] A. Marteel, J. A. Davies, M. R. Mason, T. Tack, S. Bektesevic, M. A. Abraham, *Catal. Commun.* **2003**, *4*, 309-314.
[57] H. Yang, L. Zhang, P. Wang, Q. Yang, C. Li, *Green Chem.* **2009**, *11*, 257-264.
[58] A. Kinting, H. Krause, M. Čapka, *J. Molec. Catal.* **1985**, *33*, 215-223.
[59] C. Pérez, S. Pérez, G. A. Fuentes, A. Corma, *J. Molec. Catal. A: Chem.* **2003**, *197*, 275-281.
[60] A. Corma, M. Iglesias, C. del Pino, F. Sánchez, *J. Organomet. Chem.* **1992**, *431*, 233-246.
[61] G. Liu, M. Yao, J. Wang, X. Lu, M. Liu, F. Zhang, H. Li, *Adv. Synth. Catal.* **2008**, *350*, 1464-1468.

[62] J. K. Park, S.-W. Kim, T. Hyeon, B. M. Kim, *Tetrahedron: Asymm.* **2001**, *12*, 2931-2935.
[63] C. Bianchini, V. Dal Santo, A. Meli, W. Oberhauser, R. Psaro, F. Vizza, *Organometallics* **2000**, *19*, 2433-2444.
[64] J. M. Thomas, R. Raja, *Stud. Surf. Sci. Catal.* **2004**, *148*, 163-211.
[65] A. Corma, H. Garcia, A. Moussaif, M. J. Sabater, R. Zniber, A. Redouane, *Chem. Commun.* **2002**, 1058-1059.
[66] M. D. Jones, R. Raja, J. M. Thomas, B. F. G. Johnson, D. W. Lewis, J. Rouzaud, K. D. M. Harris, *Angew. Chem.* **2003**, *115*, 4462–4467*; Angew. Chem. Int. Ed.* **2003**, *42*, 4326-4331.
[67] C. Bianchini, D. G. Burnaby, J. Evans, P. Frediani, A. Meli, W. Oberhauser, R. Psaro, L. Sordelli, F. Vizza, *J. Am. Chem. Soc.* **1999**, *121*, 5961-5971.
[68] P. Wang, J. Yang, J. Liu, L. Zhang, Q. Yang, *Micropor. Mesopor. Mater.* **2009**, *117*, 91-97.
[69] H. Li, H. Yin, F. Zhang, H. Li, Y. Huo, Y. Lu, *Environm. Sci. Technol.* **2009**, *43*, 188-194.
[70] H. Balcar, J. Čejka, *Coord. Chem. Rev.* **2013**, *257*, 3107-3124.
[71] H. Li, M. Xiong, F. Zhang, J. Huang, W. Chai, *J. Phys. Chem. C* **2008**, *112*, 6366-6371.
[72] G. Liu, Y. Sun, J. Wang, C. Sun, F. Zhang, H. Li, *Green Chem.* **2009**, *11*, 1477-1481.
[73] Y. Yang, S. Hao, Y. Zhang, Q. Kan, *Solid State Sci.* **2011**, *13*, 1938-1942.
[74] G. Liu, M. Liu, Y. Sun, J. Wang, C. Sun, H. Li, *Tetrahedron: Asymm.* **2009**, *20*, 240-246.
[75] B. Pugin, *J. Molec. Catal. A: Chem.* **1996**, *107*, 273-279.
[76] N. Anand, K. H. P. Reddy, V. Swapna, K. S. R. Rao, D. R. Burri, *Micropor. Mesopor. Mater.* **2011**, *143*, 132-140.
[77] H. Li, F. Zhang, Y. Wan, Y. Lu, *J. Phys. Chem. B* **2006**, *110*, 22942-22946.
[78] C. Kang, J. Huang, W. He, F. Zhang, *J. Organomet. Chem.* **2010**, *695*, 120-127.
[79] F. Zhang, C. Kang, Y. Wei, H. Li, *Adv. Funct. Mater.* **2011**, *21*, 3189-3197.
[80] Oehme G. Micellar Systems. In: B. Cornils, W. A. Herrmann, I. T. Horvath, editors. Multiphase Homogeneous Catalysis. Vol. 1. Weinheim, Germany: Wiley-VCH; 2005. pp. 132–136.
[81] O. Nuyken, R. Weberskirch, T. Kotre, D. Schoenfelder, A. Woerndle, *Polymers for micellar catalysis* In: Polymeric Materials in Organic Synthesis and Catalysis, M. R. Buchmeiser (Ed.), Weinheim, **2003**.
[82] T. Joseph, S. S. Deshpande, S. B. Halligudi, A. Vinu, S. Ernst, M. Hartmann, *J. Mol Catal. A: Chem.* **2003**, *206*, 13-21.
[83] Q. Sun, Z. Dai, X. Meng, L. Wang, F.-S. Xiao, *ACS Catal.* **2015**, *5*, 556–4567.
[84] A. Crosman, W. F. Hoelderich, *J. Catal.* **2005**, *232*, 43-50.
[85] N. Kania, N. Gokulakrishnan, B. Léger, S. Fourmentin, E. Monflier, A. Ponchel, *J. Catal.* **2011**, *278*, 208-218.
[86] F. Zhou, X. Hu, M. Gao, T. Cheng, G. Liu, *Green Chem.* **2016**, *18*, 5651-5657.
[87] W. Wang, C. Li, L. Yan, Y. Wang, M. Jiang, Y. Ding, *ACS Catal.* **2016**, *6*, 6091-6100.
[88] C. Li, W. Wang, Y. Li, Y. Wang, M. Jiang, Y. Ding, *J. Mater. Chem. A* **2016**, *4*, 16017-16027.
[89] B. F. G. Johnson, S. A. Raynor, D. S. Shephard, T. Mashmeyer, T. Mashmeyer, J. M. Thomas, G. Sankar, S. Bromley, R. Oldroyd, L. Gladden, M. D. Mantle, *Chem. Commun.* **1999**, 1167-1168.
[90] R. Raja, J. M. Thomas, M. D. Jones, B. F. G. Johnson, D. E. W. Vaughan, *J. Am. Chem. Soc.* **2003**, *125*, 14982-14983.
[91] M. D. Jones, R. Raja, M. J. Thomas, B. F. G. Johnson, *Topics Catal.* **2003**, *25*, 71-79.
[92] J. M. Thomas, T. Maschmeyer, B. F. G. Johnson, D. S. Shephard, *J. Molec. Catal. A: Chem.* **1999**, *141*, 139-144.
[93] J. M. Thomas, *Angew. Chem. Int. Ed.* **1999**, *38*, 3588-3628.
[94] S. Van de Vyver, Y. Román-Leshkov, *Angew. Chem. Int. Ed.* **2015**, *54*, 12554-12561.
[95] L. Vilella, F. Studt, *Eur. J. Inorg. Chem.* **2016**, 1514-1520.
[96] Y. Zhou, W. Chen, P. Cui, J. Zeng, Z. Lin, E. Kaxiras, Z. Zhang, *Nano Lett.* **2016**, *16*, 6058-6063.
[97] H. Li, J. Xiao, Q. Fu, X. Bao, *PNAS* **2017**, *114*, 5930-5934.
[98] W. Dai, C. Wang, B. Tang, G. Wu, N. Guan, Z. Xie, M. Hunger, L. Li, *ACS Catal.* **2016**, *6*, 2955-2964.
[99] N. A. Nemygina, L. Nikoshvili, V. Matveeva, M. G. Sulman, E. M. Sulman, L. Kiwi, *Top. Catal.* **2016**, *59*, 1185-1195.
[100] I. Nath, J. Chakraborty, F. Verpoort, *Chem. Soc. Rev.* **2016**, *45,* 4127-4170.
[101] M. Shaikh, K. K. Atyam, M. Sahu, K. V. S. Ranganath, *Chem. Commun.* **2017**, *53*, 6029-6032.
[102] M. Shakeri, R. J. M. Klein Gebbink, P. E. de Jongh, K. P. de Jong, *Angew. Chem.* **2013**, *125*, 11054–11057*; Angew. Chem. Int. Ed.*, **52**, 10854–10857.
[103] E. Pump, Z. Cao, M. K. Samataray, A. Bendjeriou-Sedjerari, L. Cavallo, J. M. Basset, *ACS Catal.* **2017**, *7*, 6581-6586.

[104] A. Kaftan, A. Schönweiz, I. Nikiforidis, W. Hieringer, K. M. Dyballa, R. Franke, A. Görling, J. Libuda, P. Wasserscheid, M. Laurin, M. Haumann, *J. Catal.* **2015**, *321*, 32-38.
[105] B. Autenrieth, W. Frey, M. R. Buchmeiser, *Chem. Eur. J.* **2012**, *18*, 14069-14078.
[106] R. Bandari, M. R. Buchmeiser, *Catal. Sci. Technol.* **2011**, *2*, 220-226.
[107] R. Bandari, M. R. Buchmeiser, *Macromol. Rapid Commun.* **2012**, *33*, 1399-1402.
[108] R. Bandari, M. R. Buchmeiser, *Analyst* **2012**, *137*, 3271-3277.
[109] R. Bandari, C. Elsner, W. Knolle, C. Kühnel, U. Decker, M. R. Buchmeiser, *J. Sep. Sci.* **2007**, *30*, 2821-2827.
[110] R. Bandari, W. Knolle, M. R. Buchmeiser, *J. Chromatogr. A.* **2008**, *1191*, 268-273.
[111] S. Beckert, F. Stallmach, R. Bandari, M. R. Buchmeiser, *Macromolecules* **2010**, *43*, 9441-9446.
[112] M. J. Beier, W. Knolle, A. Prager-Duschke, M. R. Buchmeiser, *Macromol. Rapid Commun.* **2008**, *29*, 904-908.
[113] M. R. Buchmeiser, *Polymer* **2007**, *48*, 2187-2198.
[114] M. R. Buchmeiser, R. Bandari, A. Prager-Duschke, A. Löber, W. Knolle, *Macromol. Symp.* **2010**, *287*, 107-110.
[115] C. Gatschelhofer, A. Mautner, F. Reiter, T. R. Pieber, M. R. Buchmeiser, F. M. Sinner, *J. Chromatogr. A* **2009**, *1216*, 2651-2657.
[116] S. H. Lubbad, R. Bandari, M. R. Buchmeiser, *J. Chromatogr. A* **2011**, *1218*, 8897-8902.
[117] S. H. Lubbad, M. R. Buchmeiser, *J. Chromatogr. A* **2010**, *1217*, 3223-3230.
[118] S. H. Lubbad, M. R. Buchmeiser, *J. Chromatogr. A* **2011**, *1218*, 2362-2367.
[119] S. Mavila, M. R. Buchmeiser, *Macromolecules* **2010**, *43*, 9601-9607.
[120] B. Sandig, L. Michalek, S. Vlahovic, M. Antonovici, B. Hauer, M. R. Buchmeiser, *Chem. Eur. J.* **2015**, *21*, 15835-15842.
[121] B. Scheibitz, A. Prager, M. R. Buchmeiser, *Macromolecules* **2009**, *42*, 3493-3499.
[122] B. Schlemmer, R. Bandari, L. Rosenkranz, M. R. Buchmeiser, *J. Chromatogr. A* **2009**, *1216*, 2664-2670.
[123] F. M. Sinner, C. Gatschelhofer, A. Mautner, C. Magnes, M. R. Buchmeiser, T. R. Pieber, *J. Chromatogr. A.* **2008**, *1191*, 274-281.
[124] V. P. Taori, R. Bandari, M. R. Buchmeiser, *Chem. Eur. J.* **2014**, *20*, 3292–3296.
[125] F. Weichelt, B. Frerich, S. Lenz, S. Tiede, M. R. Buchmeiser, *Macromol. Rapid Commun.* **2010**, *31*, 1540-1545.
[126] F. Weichelt, S. Lenz, S. Tiede, I. Reinhardt, B. Frerich, M. R. Buchmeiser, *Beilstein J. Org. Chem.* **2010**, *6*, 1199-1205.
[127] F. Švec, J. M. J. Fréchet, *Int. Lab.* **1997**, *5/97*, 12A.
[128] S. Sen, R. Schowner, D. A. Imbrich, W. Frey, M. R. Buchmeiser, *Chem. Eur. J.* **2015**, *21*, 13778-13787.
[129] S. Sen, J. Unold, W. Frey, M. R. Buchmeiser, *Angew. Chem.* **2014**, *126*, 9538-9542*; Angew. Chem. Int. Ed.* **2014**, *53*, 9384-9388.
[130] R. Schowner, W. Frey, M. R. Buchmeiser, *J. Am. Chem. Soc.* **2015**, *137*, 6188-6191.
[131] J. Kärger, D. M. Ruthven, *New J. Chem.* **2016**, *40*, 4027-4048.
[132] B. Coasne, *New J. Chem.* **2016**, *40*, 4078-4095.
[133] T. Müllner, K. K. Unger, U. Tallarek, *New J. Chem.* **2016**, *40*, 3993-4015.

1.2.4 Positioning of the Collaborative Research Centre within its general research area

As already outlined in the introduction, catalytic reactions are fundamental to uncountable chemical processes and form the basis for many industries relevant for our daily life. Notwithstanding the high technical standards and optimization of many catalytic reactions nowadays, the area is characterized by a very lively, global research community. Following efforts along the lines of "*altius, fortius, vitius*", *Web of Science* has counted more than 180,000 (as of 02.12.2017) peer-reviewed scientific publications on *catalysis*; however, from those merely 3,600 (2 %, Figure 9) were related to the "young" sector of *molecular heterogeneous catalysis*.

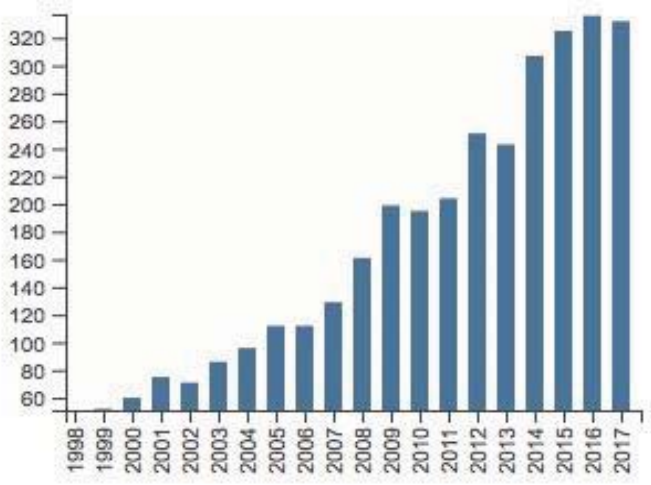

Figure 9. Publications (*peer reviewed*, *Web of Science*, as of 02. 12. 2017) on molecular heterogeneous catalysis.

This modest publishing activity can partly be explained by the lack of an integral, systematic approach to clarify the underlying questions. This alone urgently justifies a concentrated research effort as presented by this CRC. The complexity of this particular research field is undisputed and can only be overcome by close cooperation between experts from catalysis, material science, spectroscopy, theory and simulation. The latter has the equally difficult and rewarding task to describe the whole system on multiple scales, as discussed above, and to correlate their findings with experimental results. Hence, a concentration of all relevant expertise from chemistry, material science, theory, analysis and simulation is absolutely necessary; the resulting work packages can only possibly be managed in a powerful research initiative, such as this CRC. To meet these challenges, the described integral, multi-disciplinary approach will encompass all requirements from material science, (*in situ*) catalysis, analytics and theory.
In summary, catalytic transformations are undisputedly the most resource-protecting chemical reactions, because of their high inherent effectivity. In view of that, and based on the (long-term) goals as defined for this CRC, this research initiative will blend in perfectly with the current and future political focus on resource protection and sustainability.[123]

Existing Research Initiatives
Molecular heterogeneous catalysis is currently not the subject of any CRCs, priority programs, research networks or research training groups. In the wider sphere of catalysis, the **Leibniz Institut für Katalyse** (LIKAT) in Rostock, the **Fritz Haber Institute** in Berlin (MPI) as well as the **MPI für Kohlenforschung** conduct internationally recognized intense research on "classical" heterogeneous catalysis. In those institutions, molecular heterogeneous catalysis is not specifically targeted. Thus, if the CRC on "**Molecular Heterogeneous Catalysis in Confined Geometries**" would be established and a notable gap in the federal science landscape would be closed, further increasing the international importance of German research activities in the eminent field of catalysis.

The Excellence Cluster 314 "**Unifying Concepts in Catalysis**" (TU Berlin, Humboldt Universität, Freie Universität Berlin, Universität Potsdam, Fritz-Haber Institut, MPI für Kolloid- und Grenzflächenforschung) has defined its aims as follows: „[We...] *to unify concepts in catalysis by*

bridging the gaps between homogeneous, heterogeneous and biological catalysis, ranging from elementary gas-phase reactions to complex processes in highly organized biological systems, in fundamental as well as in applied catalysis research. Our research focuses on analyzing catalytic mechanisms, designing novel catalytic materials and strategies, and developing new catalytic processes on laboratory and mini-plant scales." There, emphasis is put on activation of CH_4, CO_2, C/O systems as well as cellular setups. Importantly, organometallic catalysis in mesoporous systems is not included in this Excellence Cluster. The CRC 858 (Universität Münster) **"Synergetic Effects in Chemistry - From Additivity towards Cooperativity"** focuses on cooperative effects in chemical, multi-component systems, but excludes porous supports or mesoporous cavities. The **Cat Center** (RWTH Aachen) equally does not look at this research field; the same largely holds for "**Munich Catalysis**" (TU München). There, apart from fundamental research, emphasis is on the development of novel, innovative catalysts to cope with the globally increasing demand for energy and chemicals.

Also internationally, for the moment at least, there appear to be no large research initiatives dedicated to this subject. At the **KAUST** (King Abdullah University of Science and Technology), classic heterogeneous catalysis and *Surface Organometallic Chemistry* (J.-M. Basset) are investigated. Similarly, *Surface Organometallic Chemistry* is also dealt with at the **ETH Zürich** (C. Copéret) and at the **CNRS in Lyon** (C. Thieuleux). Finally, in Amsterdam the group of J. N. H. Reek works on „*Catalysis in Confined Spaces*"; however, under this approach, the confined spaces are limited to supramolecular systems (i.e., cyclodextrines).

Progress beyond the current state of the art
The insights won from this CRC will create a new base for molecular heterogeneous catalysis, and thus for heterogeneous catalysis overall. For the first time, a comprehensive and reliable understanding for the cooperative interaction of organometallic catalyst and support would exist, in terms of „1+1 > 2". This would not only enable further optimization of existing processes, **but will also pave the way for completely new reactions or reaction cascades**. Especially access to difficult transformations like gas-liquid-solid-reactions would profit from this CRC, but also the catalysis with notoriously inert molecules such as methane, ethane, dinitrogen or carbon dioxide. For synthetic chemistry, industry and society the resulting added value is evident.

1.2.5 National and international cooperation and networking

All principal investigators have multiple and vivid cooperations, both with colleagues from national and international institutions. These are briefly summarized in the following:

Prof. Dr. M. Bauer:
Prof. Dr. M. Beller, LIKAT Rostock: XAS investigations of homogeneous catalyzed reactions
Prof. Dr. A. Brückner, LIKAT Rostock: XAS/XES/HERFD-XANES on chromium catalyzed reactions
Prof. Dr. P.-A. Carlsson, Chalmers University, Gotenburg: Development of X-ray methods for sustainable applications
Prof. Dr. W. Caseri, ETH Zurich: XAS investigations of polymeric SCO complexes
Dr. W. Gawela, Prof. Dr. C. Bressler, CUI Hamburg: fs-X-ray experiments
Prof. Dr. P. D. Gros, SCF Lorraine: Iron complexes for photocatalytic applications
Dr. S. Groß, University of Padua: Structural investigations of hybrid materials
Prof. Dr. K. Heinze, JGU Mainz: Photoactive iron complexes
Prof. Dr. S. Herres-Pawlis, RWTH Aachen: X-ray investgations of biomimetic copper complexes
Prof. Dr. T. Kühne, University of Paderborn: Theoretical X-ray spectroscopy
Prof. Dr. S. Kureti, TUBA Freiberg: New iron catalysts for CO oxidation
Prof. Dr. M. Muhler: XAS and XES measurements of water splitting reactions
Prof. Dr. R. Schlögl, FHI, Berlin and CEC, Mülheim: XAS investigations of heterogeneous catalyzed reactions
Prof. Dr. A. Jacobi von Wangelin, Hamburg University: XAS/XES/ HERFD-XANES investigations of iron catalysed reactions

Prof. Dr. J. Bill
Prof. Dr. Ute Kaiser, University of Ulm: Low-voltage TEM imaging of the organic/inorganic glue line in

tobacco mosaic virus-templated semiconductors
Prof. Dr. H. Cölfen, University of Constance: Mechanical characterization of bio-inspired materials
Prof. Dr. A. Fery, University of Bayreuth: Wrinkle-assisted virus alignment trough PDMS stamps
Prof. Dr. Christof Wöll, KIT Karlsruhe: IR characterization of SAM terminal groups on polymer substrates
Prof. Dr. Thomas Schimmel, KIT Karlsruhe: Piezoelectric bioinspired materials

Prof. Dr. M. R. Buchmeiser:
Prof. Dr. R. R. Schrock, MIT, Cambridge, USA: stereospecific ring opening metathesis polymerization
Prof. Dr. C. Coperét, ETH Zurich, CH: immobilization of Mo/W imido/oxo alkylidene NHC complexes on silica (SOMC)
Prof. Dr. K. Müllen, MPI-P, Mainz: carbon fibers from nitrogen free precursors
Prof. Dr. Y. Yagci, Technical University of Istanbul, Turkey: functional polyolefins
Prof. Dr. K. R. Liedl, University of Innsbruck, Austria: QM/DFT calculations on Mo/W imido/oxo alkylidene NHC complexes
Dr. A. Zielonka, FEM Schwäbisch Gmünd: recovery of rare earth elements via selective polymeric sorbents

Jun.-Prof. Dr. M. Fyta
Prof. Dr. R. Netz, FU-Berlin: development of ionic force fields
Prof. Dr. E. Kaxiras, Harvard, USA: coarse-grained potential for DNA from quantum-mechanical calculations
Prof. Dr. S. Meng, Chinese Academy of Sciences, China: N-heterocyclic carbene and diamondoids
Prof. B. Gorshunov, Russian Academy of Sciences, Russia: optical spectra of water in quasi-1D crystals
Prof. Dr. M. Prentiss, Harvard, USA: energetics in DNA
Prof. Dr. R. Scheicher, Uppsala University, Schweden: functionalized nanopores
Prof. Dr. U.M. Bettolo Marconi, University of Camerino, Italien: development of multiscale approach for molecular motion in solutions
Prof. Dr. R.G. Amorim, Universidade Federal Fluminense, Brazil: 2D materials for sensing
Prof. W.L. Scopel Universidade Federal do Espérito Santo-UFES, Brazil: MoS_2 heterostructures
Dr. S. Melchionna, CNR, Italy: DNA translocation through nanopores
Dr. J. Smiatek, Helmholtz Zentrum Münster: ionic liquids and additives
Dr. N. Schwierz-Neumann, Max-Planck Institute Frankfurt: development of coarse-grained potential for RNA
Dr. A. Vazquez-Mayagoitia, Argonne National Laboratory, USA: benchmarks for RNA potential
Dr. S. Mamatkulov, Uzbekistan Academy of Sciences, Uzbekistan: divalent cations and force fields
Dr. C. Mathioudakis, Cyprus University of Technology, Cyprus: nanocomposite carbon

Prof. Dr. F. Gießelmann
Prof. Dr. Rudolf Zentel, Johannes Gutenberg University Mainz: liquid-crystal elastomers and actuators
Prof. Dr. Garsten Tschierske, Martin Luther University Halle: self-assembly in soft matter, amphiphiles
Dr. Dirk Blunk, University of Cologne: surfactants, lyotropic liquid crystals
Prof. Dr. Per Rudquist, Chalmers University of Technology, Gothenburg, Sweden: chirality effects and topological defects in liquid crystals
Prof. Dr. Jan P. F. Lagerwall, Dept. of Physics, University of Luxembourg: lyotropic liquid crystals, carbon nanotube dispersions
Prof. Dr. Robert P. Lemieux, Queen 's University, Kingston, Canada: liquid crystal synthesis, chiral induction, de Vries-type smectics
Prof. Dr. Mikhail Osipov, University of Strathclyde, Glasgow, UK: phase transitions, theory and simulation of liquid crystals
Dr. Ingo Dierking, University of Manchester, UK: lyotropic liquid crystals, ferroelectric dispersions
Prof. Dr. Noel A. Clark, Prof. Dr. Joseph E. Maclennan, University of Colorado at Boulder, USA: chiral liquid crystals, bent-core mesogens, freeze-fracture electron microscopy, photoactive soft matter
Prof. Dr. David Walba, University of Colorado at Boulder, USA: liquid crystal synthesis
Dr. Milada Glogarova, Czech Academy of Sciences, Prague, Czech Republic: liquid crystal synthesis, ferroelectric liquid crystals

Prof. Dr.-Ing. J. Groß
Prof. Dr. A. Bardow, RWTH Aachen: Integrated Solvent and Process Design
Prof. Dr. D. Bedeaux, NTNU Trondheim, Norway: Nonequilibrium Thermodynamics, interfacial fluctuations
Prof. Dr. P. Colonna, Delft University of Technology, The Netherlands: Integrated Solvent and Apparatus Design
Prof. Dr. Th. W. de Loos, Delft University of Technology, The Netherlands: Experimental methods for phase equilibria
Dr. J. Hruby, The Czech Academy of Sciences, Prag, Czech Republic: Thermodynamics of fluid interfaces
Prof. Dr. S. Kjelstrup, NTNU Trondheim, Norway: Nonequilibrium Thermodynamics, interfacial transport properties
Jun. Prof. Dr.-Ing. K. Leonhard, RWTH Aachen: Entropy scaling of transport properties
Prof. Dr. A. Z. Panagiotopoulos, Princeton University, USA: Molecular Simulations of phase equilibrium properties
Jun. Prof. Dr. Markus Richter, Ruhr University Bochum: Measurements of physical properties

Jun. Prof. Dr.-Ing. N. Hansen
Dr.-Ing. S. Jakobtorweihen, TU Hamburg: Validation of force fields for cyclodextrins in solution
Prof. Dr. W. F. van Gunsteren, ETH Zürich: Development and testing of algorithms for protein structure refinement
Prof. Dr. L. Smith, University of Oxford, UK: Development and testing of algorithms for protein structure refinement
Prof. Dr. U. Tallarek, Philipps-Universität Marburg: Molecular dynamics simulations of complex fluids in mesoporous materials

Prof. Dr. C. Holm
Prof. Dr. R. Podgornik, Lubeljana, Slovenia: Polyelectrolytes
Dr. J. DeGraaf, Utrecht, Netherlands: Active Matter
Prof. Dr. U. Keyser, Cambridge, UK: Nanopore Translocation
Dr. Tyler N Shendruk, Oxford, UK: Active Matter
Dr. Arnold JTM Mathijssen, Oxford, UK: Active Matter
Dr. B Qiao, Argonne National Laboratory, Argonne, USA: ionic Liquids
Dr. M Sega, TU Wien, Austria: Dielectric spectroscopy
Dr. Pedro Sanchez, TU Wien, Austria: PE Multilayers
Dr. S. Kantorovich, TU Wien, Austria: Ferrofluids
Prof. Dr. W.C.K. Poon, Edinburgh, UK: Active Matter
Dr. A.T. Brown, Edinburgh, UK: Active Matter
Dr. P Košovan, Prag, CZ: Hydrogels
Prof. Dr. YL Raikher, Perm, Rus: Ferrogels
Dr. AV Ryzhkov, Perm, Rus: Ferrogels
Prof. Dr. G Fytas, FORTH, Heraklion, Greece: Polyelectrolytes and FCS
Dr. JJ Cerdà, Universitat de les Illes Balears. Palma de Mallorca, Spain.: Ferrofluids
Prof. Dr. T Sintes, Universitat de les Illes Balears. Palma de Mallorca, Spain: Ferrofluids
Dr. S Samin, Ben-Gurion University of the Negev, Beer-Sheva, Israel: Ionic Liquids
Prof. Dr. Y Tsori, Ben-Gurion University of the Negev, Beer-Sheva, Israel: Fluids in electric fields
Prof. S. Hardt, TU Darmstadt, Germany: Electrokinetics of Polymers
Prof. Dr. O. Borisov, Univ. Pau, France: Swelling of hydrogels
Prof. Dr. L. Schäfer, Uni Bochum: Martini-Force fields

apl. Prof. Dr. M. Hunger:
Prof. Dr. W. Dai, Prof. Dr. L. Li, Prof. Dr. G. Wu, Nankai University, Tianjin, People's Republic of China: Investigation of the catalytic cycles and deactivation mechanisms of the methanol-to-olefin conversion on zeolite catalysts
Prof. Dr. K. Sato, Tokyo Gakugei University, Tokyo, Japan: Methods for the decontamination of clays from the vicinity of Fukushima

DP Dr. H. Koller, Institute of Physical Chemistry, Universität Münster, Münster, Germany: Development of methods for the quantitative distance analysis by solid state NMR
Prof. Dr. Ch. Jäger, BAM, Berlin, Germany: Development of solid-state NMR methods for the differentiation of gels, zeolites, and water species in geopolymers
Prof. Dr. B. Sulikowski, Dr. M. Gackowski, Jerzy Haber Institute of Catalysis and Surface Chemistry, Polish Academy of Sciences, Kraków, Poland: Development of catalysts for the transformation of monoterpene hydrocarbons
Prof. Dr. L.T. Hoai Nam, Vietnam Academy of Science and Technology, Hanoi, Vietnam: Development of novel microporous/mesoporous composites for acid-catalyzed reactions

Prof. Dr. J. Kästner
Prof. Dr. Stephen K. Hashmi, Universität Heidelberg: Simulation of gold catalysis
Dr. S. Miranda-Rojas, Universidad Andres Bello, Santiago, Chile: QM/MM-simulation of enzymatic reactivity
Dr. G. Knizia, Penn State University, USA: intrinsic bond orbitals as a tool to understand catalysis
Prof. Dr. J. R. Flores, Universidad de Vigo, Spanien: atom tunneling
Prof. Dr. P. Sherwood, Dr. T. Keal, STFC Daresbury Lab, UK: ChemShell program development
Prof. Dr. B. Engels, Universität Würzburg: QM/MM and global optimization

Prof. Dr. S. Laschat
Prof. Dr. Thomas J. J. Müller, Universität Düsseldorf: mesoporous materials MCM-41
Prof. Dr. Yann Molard, University of Rennes, France: liquid crystals, hybrid materials
Prof. Dr. Rainer Schobert, Universität Bayreuth: organic synthesis, natural product chemistry
Prof. Dr. Patrick Huber, TU Hamburg-Harburg: liquid crystals confined in porous materials
Prof. Dr. Andreas Schönhals, BAM Berlin: liquid crystals confined in porous materials

Prof. Dr. Bettina Lotsch
Prof. Dr. Jürgen Senker, Universität Bayreuth: NMR spectroscopic characterization of photoactive metal-organic frameworks and carbon nitrides
Prof. Dr. Ram Seshadri, UC Santa Barbara, USA: electrochemical energy storage in covalent triazine frameworks
Prof. Dr. Brad Chmelka, UC Santa Barbara, USA: Dynamic nuclear polarization NMR spectroscopy of covalent organic frameworks
Prof. Dr. Anna Fontcuberta I Morral, EPF Lausanne: Photoelectrochemical water splitting by GaAs Nanowire Arrays on Si and CO_2 reduction
Prof. Dr. Dirk Johrendt, LMU München: Novel Na solid electrolytes in the system Si-P
Prof. Dr. Christina Scheu, MPI Düsseldorf/RWTH Aachen: TEM analysis of photoactive nanostructures
Prof. Dr. Christian Ochsenfeld, LMU München: Theoretical calculations of the structure and photoactivity of framework materials

Prof. Dr. S. Ludwigs
Prof. D. Neher, Universität Potsdam: photophysics of conducting polymers
Dr. D. Andrienko, Prof. K. Kremer, MPI-P, Mainz: modelling of crystallization of conducting polymers
Prof. A.H.E. Müller, Universität Mainz: block copolymer research
Dr. A. Kiriy, Leibniz-Institut für Polymerforschung, Dresden: Synthesis of n-type semiconducting polymers
Dr. M. Brinkmann, Institut Charles Sadron, Strasbourg: HR-TEM / ED characterization
Prof. C. Ruiz-Delgado, Prof. J. Lopez-Navarrete, University of Malaga, Spain: DFT-modelling of conjugated thiophene systems
Prof. F. Meldrum, University of Leeds, UK: biomineralization
Prof. A. Karim, University of Akron, USA: GISAXS and GIWAXS measurements
Prof. S. Haacke, Institut de Physique et Chimie des Matériaux de Strasbourg (IPCMS), France: femtosecond spectroscopy
Prof. Y. Bonassieux, Prof. G. Horowitz, Ecole Polytechnique Paris, France: electrolyte-gated transistors
Prof. T. Benincori, Prof. F. Sannicolo, Prof. P. Mussini, University of Milano, Italy: inherently chiral oligothiophenes
Prof. U. Steiner, Adolph Merkle Institut Fribourg, Switzerland: block copolymer research

Dr. S. Naumann
Prof. Dr. Andrew P. Dove, University of Warwick, UK: organopolymerization catalysis
Prof. Dr. Luigi Cavallo/Dr. Laura Falivene, KAUST, Saudi Arabia: NHOs as initiators for polymerization of acrylic monomers

Prof. Dr. B. Plietker
Prof. Dr. Werner Thiel, TU Kaiserslautern: homogenous hydrogenation of CO_2
Prof. Dr. M. Bauer, University of Paderborn: X-ray spectroscopic analysis of Fe-complexes
Prof. Dr. B. Sarkar, FU Berlin: Fe-triazolium-complexes for homogenous catalysis complexes
Prof. Dr. F. Götz, University of Tübingen: Bioactivity studies on polyprenylated polycyclic acylphloroglucines

Dr. Mark Ringenberg
Prof. Dr. Carsten Streb University of Ulm, EPR of low valent metals in polyoxometallate cages.
Jan Fiedler, Ing., CSc. J. Heyrovský Institute of Physical Chemistry, v.v.i., Academy of Sciences of the Czech Republic, spectroelectrochemistry of difficult electrochemical processes
Dr. Ulf-Peter Apfel, Ruhr-University Bochum, Mössbauer spectroscopy of (hetero)bimetallic iron complexes.

Prof. Dr. G. Schmitz
Prof. Dr. Zoltan Erdelyi, Debrecen, Hungary: Impact of stress on atomic transport
Prof. Dr. G. Gottstein, RWTH Aachen, Germany: Triple junction segregation
Prof. Dr. A. Gusak, National University of Cherkasy, Ukraine: Theory of diffusion
Prof. Dr. K. Hono, Tsukuba, Japan: Magnetic sensor layers
Prof. Dr. A. Hütten, Univ. Bielefeld, Germany: Magnetic sensor layers
Prof. Dr. Jacob, Univ. Ulm, Germany: atom probe instrumentation
Dr. L. Jeurgens, EMPA Zürich, Switzerland: APT of metal/nitride multilayers
Prof. Dr. M. Latroche, CNRS, Institute de Chimie et Materiaux, Paris-Est, France: hydrogen storage and thin film batteries
Dr. Angela Vella, Univ. Rouen, France: Laser-assisted field desorption
Prof. Dr. Francois Vurpillot, Univ. Rouen, France: APT reconstruction
Prof. Dr. C. Volkert, Univ. Göttingen, Germany: APT instrumentation
Dr. Nelia Wanderka, Helmholtz-Zentrum Berlin, Germany: APT of complex alloys
Prof. Dr. Weismüller, TH Hamburg, Germany: nanoporous metals

Prof. Dr. J. van Slageren
Prof. L. Chibotaru, Dr. L. Ungur, University of Leuven, Belgium, *ab initio* calculations of f-element complexes
Dr. M. Orlita, GHMFL, Grenoble, France, far-infrared measurements
Prof. R. Sessoli, University of Florence, Italy, cantilever torque magnetometry
Prof. R. Winpenny, Dr. F. Tuna, Prof. S. Liddle, University of Manchester, UK, synthesis and EPR of f-element complexes.
Prof. T. Sikola, Dr. J. Cechal, Dr. J. Novak, CEITEC, Brno, Czech, fabrication of nanostructures as well as surface deposition of molecular nanomagnets
Prof. R. Hillenbrand, Nanogune, San Sebastian, Spain, Terahertz near-field measurements
Dr. R Wylde, Thomas Keating Ltd., UK, Terahertz quasi optics
Prof. F. Neese, Dr. M. Atanasov, MPI Mülheim, *ab initio* calculations of transition metal complexes
Prof. R. Clérac, University of Bordeaux, France, synthesis of single molecule magnets and single chain magets
Prof. G. Aromí, University of Barcelona, synthesis of molecular quantum bits
Dr. I. Nemec, Dr. R. Herchel, University of Olomouc, synthesis of single ion magnets
Prof. S. Gao, Dr. S.D. Jiang, Beijing University, China, synthesis of single molecule magnets
Prof. B. Sarkar, FU Berlin, synthesis of transition metal complexes.

Apl. Prof. Dr. T. Sottmann
Prof. Dr. Simone Wiegand, Forschungszentrum Jülich GmbH: correlation between static and dynamic hydration shell and thermophoresis in micellar systems
Prof. J. Cabral, Imperial College, UK: microfluidic processing of model microemulsions
Dr. O. Holderer, Dr. H. Frielienghaus, Jülicher Zentrum für Forschung mit Neutronen (JCNS), Miunich: SANS and NSE on self-assembled nanostructured systems
Dr. R. Schweins, Dr. I. Hoffmann, Institut Laue Langevin, Grenoble, France: SANS and NSE on self-assembled nanostructured systems
Prof. T. Hellweg, University of Bielefeld: swelling/deswelling kinetics of *N*-*n*-propylacrylamide based microgels
Prof. U. Olsson, Lund University, Sweden: from regular solutions to microemulsions with a well-defined surfactant film
Prof. R. Schomäcker, TU Berlin: microemulsion based novel process concepts for the three step Boscalid® synthesis
Prof. R. Strey, University of Köln: from regular solutions to microemulsions with a well-defined surfactant film

PD Dr. Yvonne Traa
Prof. Dr. Thomas Hirth, KIT, Karlsruhe: Dehydration of lactic acid to acrylic acid on zeolite catalysts
Prof. Dr. Willi Kantlehner, Hochschule Aalen: Hydrogenation of lignin

1.3 Research profile of the applicant university

1.3.1 Strategy and planning

Integration of the proposed CRC with local structures. Currently, the following Institutes of the University of Stuttgart contribute to this research initiative:

Institute of Inorganic Chemistry (IAC, Faculty of Chemistry)
Institute of Computer Physics (ICP, Faculty of Physics and Mathematics)
Institute of Materials Science (IMW, Faculty of Chemistry)
Institute of Organic Chemistry (IOC, Faculty of Chemistry)
Institute of Physical Chemistry (IPC, Faculty of Chemistry)
Institute of Polymer Chemistry (IPOC, Faculty of Chemistry)
Institute of Chemical Technology (ITC, Faculty of Chemistry)
Institute of Technical Thermodynamics and Thermal Process Technology (ITT, Faculty of Energy-, Process- and Biotechnology)
Institute of Theoretical Chemistry (TheoChem, Faculty of Chemistry)

As non-university organization, the Max-Planck-Institute for Solid State Research (MPI-FKF), Stuttgart, participates.

The "*Struktur- und Entwicklungsplan der Universität Stuttgart*" (SEPUS) defines the research profiles for the Department of Chemistry, including "*Advanced Synthesis and Catalysis*" and "*Materials and Functional Molecules*" as well as "*Theory and Simulation*". The proposed CRC perfectly fits all of these research foci (Figure 10).

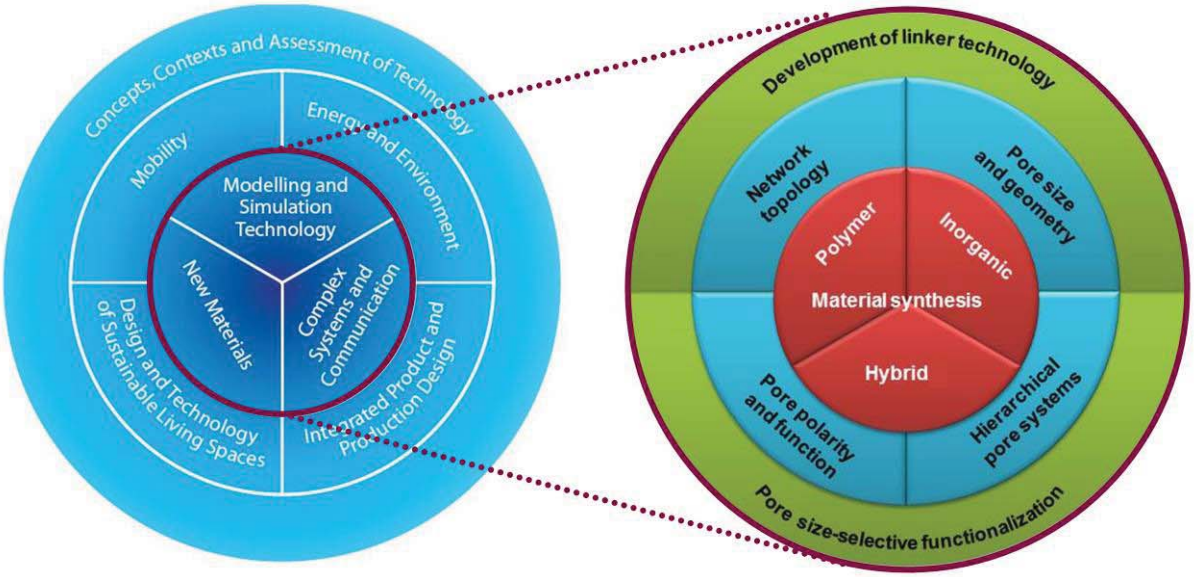

Figure 10. Incorporation of CRC 1333 (right circle) into SEPUS (left circle) (***S***truktur- und ***E***ntwicklungs***p***lan ***U***niversität ***S***tuttgart).

The close cooperation of chemistry and material science in Stuttgart is also supported by the fact that material science is integrated with the Department of Chemistry at this university, in contrast to the much more typical localization in engineering or physics. The interdisciplinary approach of this CRC bridges different research profiles of the Department of Chemistry and combines research fields from chemistry (materials, catalysis, theory and simulation) with those from material science. At the same time, theoretical/methodical subjects will be well integrated within the CRC structures. With this concept, a unique concentration of materials science, chemistry (notably involving all relevant disciplines!), physics and reaction process technology within the frame of a CRC will be focused on one single topic, which is of highest interest for both fundamental research as well as technical application. The University of Stuttgart together with its Faculty of Chemistry (which includes Materials Science), the Department of Physics and Mathematics, the Department of Energy-, Process- and Biotechnology and the Stuttgart-based Max Planck Institute for Solid State Research have all the expertise to successfully answer the scientific questions connected with this CRC. The working groups organized in sections A, B and C offer internationally recognized high-level research and broad experience, complemented by several (sub)projects led by young scientists. Additional preliminary works also originate from the successful research initiative “NanoBioMater”. Apart from numerous bilateral collaborations (including homogeneous/heterogeneous catalysis), especially the combined competence in the area of material science should be seen as exceptional (for example, bio-inspired mineralization or the Excellence Cluster Simulation Technologies “*SimTech*” which includes theoretical, physical and computational chemistry), recommending Stuttgart for installation of this CRC. Also worth to be mentioned is the initiative “*Windy Cities*” which entails a strong collaboration between groups working on Homogeneous Catalysis and Microreaction Technology. In the long run, this CRC will certainly contribute to a strengthening of these fruitful interconnections with natural science, and especially chemistry. This research initiative will profit the University of Stuttgart immensely, since it not only fits perfectly with the local research environment, but also sharpens the innovative profile of all contributing departments.

The advancement of interdisciplinary collaboration between scientists is also strongly endorsed by the University of Stuttgart. To this end, interdisciplinary councils have been established; they are intended to facilitate and deepen cooperation between different departments. Central to these councils are the so-called Research Centers, with the Excellence Cluster SimTech being its most prominent example. Several researchers of this CRC are also members of SimTech, namely: Prof. Dr. J. Kästner, Prof. Dr. J. Groß, Jun. Prof. Dr. N. Hansen, Prof. Dr. C. Holm, and Jun. Prof. M. Fyta.

The University of Stuttgart strongly supports this CRC and is willing to contribute 50% of the costs for the TEM (applied for in a separate grant proposal, *vide infra*). In addition to that, the University of

Stuttgart provides the necessary laboratory space as well as personel infrastructure. Finally, the spokesman of this CRC, Prof. Dr. M. R. Buchmeiser is offered a reduction in teaching duties of 2 hours/week.

1.3.2 Staff situation

In course of the first funding period, apl.-Prof. Dr. M. Hunger will retire. In order to close the gap, Dr. Michael Dyballa will take over his position at the Institute of Chemical Technology (ITC) at the University of Stuttgart. The Head of the ITC, Prof. Dr.-Ing. E. Klemm, guarantees for this substitution, which will ensure a continuous handling of the project goals and task in **project C1**. Dr. Dyballa finished his PhD in 2015 in the solid-state NMR Group of Prof. Michael Hunger, and since then stayed as a PostDoc at the University of Oslo in the catalysis group of Prof. Unni Olsbye and Prof. Karl Stian Svelle. He furthermore developed his knowledge and skills in characterizing heterogeneous catalysts using in particular solid-state NMR in collaboration with Dr. B. Arstad at SINTEF, Oslo. Dr. Dyballa will start on July 1st, 2018, more than 2 years before apl.-Prof. Dr. Michael Hunger will retire. This will allow Dr. Michael Dyballa to take over the position of the internationally reknown Prof. Michael Hunger in using probe molecules and sophisticated methods in solid-state NMR without loss of knowledge or experience. This is also true with regard to the project of Prof. Dr. Hunger in this CRC.

Interdisciplinary research is intended to support the university's research foci. The proposed CRC will in this regard be especially beneficial for Materials Science. By way of these interdisciplinary support structures and the active policy of the University of Stuttgart, this CRC allows for recruiting considerable number of renowned scientists who have already collaborated previously in research councils or other projects. CRC 706, CRC 1244 but foremost CRC 716 (“Dynamic simulation of systems with large particle numbers”) shall be named as examples in this respect. As a further supporting measure by the University, a junior professorship on the topic "Molecular heterogeneous catalysis/heterogeneous catalysis" is currently installed at the Institute of Chemical Technology (ITC) of the University of Stuttgart. This junior professorship will be integrated into the structure of this CRC and will lead its own projects in the second funding period. A major boon for the prospective CRC in this regard will be the special expertise of the ITC in the area of reaction engineering. This is why Prof. Dr.-Ing. E. Klemm is poised to join the CRC at the beginning of the second funding period. The broad interdisciplinary profile of the proposed CRC requires successful recruitment of young researchers. To facilitate this, the planned Summer Schools will be important tools, especially to attract PostDoc candidates with international perspectives. Presentations given by excellent female scientists, who are part of the CRC, are expected to gather interest specifically from female students, to further strengthen visibility and staffing.

1.3.3 Research infrastructure

All research outlined in this CRC can be carried out in the laboratories of the participating groups at the University of Stuttgart and the Max-Planck Institute for Solid State Research, Stuttgart. All necessary equipment is available with the following exceptions (requested equipment):

1. A transmission electron microscope (TEM), based at the University of Stuttgart, capable of analyzing both hard and soft matter samples will be applied for in a separate proposal for state-funded major instrumentation.
2. Advanced X-ray measurements such as XANES (X-ray absorption near-edge structure), EXAFS (extended X-ray absorption fine structure), HERFD-XANES (high energy resolution fluorescence detected XANES), vtc-XES (valence-to-core X-ray emission spectroscopy) and ctc-XES (core-to-core X-ray emission spectroscopy) will be carried out with the group of Prof. M. Bauer, University of Paderborn in a joint service project (**project S1**).

1.4 Support structures

1.4.1 Early career support

As evident by their respective publication lists, the early-career researchers involved in this project act autonomously and pursue independent scientific trajectories. This CRC initiative considers it an integral objective to further support young scientists in their career, including promotion and further career steps. A deeper catalytic understanding as well as the synthesis of functional, high-performance materials is pivotal for modern economies, and in this regard this CRC is perfectly positioned to provide such skills for students and young researchers involved in it. The interdisciplinary focus, the high scientific level as well as the obvious experimental and practical orientation will provide graduates with excellent access to the job market, both in industry and academia.
The early-career researchers involved in this CRC will be supported in the best possible way. This is expressed by the CRC's strategy to prominently include young researchers as independent project leaders, with all responsibilities. This is also intended to promote the team spirit amongst the scientific personnel of the CRC. Four out of 19 project leaders are early-career researchers:

Dr. M. Ringenberg, Institute of Inorganic Chemistry
Dr. S. Naumann, Institute of Polymer Chemistry
Jun. Prof. M. Fyta, Institute of Computer Physics
Jun. Prof. N. Hansen, Institute of Technical Thermodynamics

Additionally, Dr. Petia Atanasova, Institute of Materials Science, will contribute to **project A5**. All of the CRC's infrastructure may serve her further qualification. Her excellent abilities have already been demonstrated within the DFG-Priority Program 1569 (*Generation of multifunctional inorganic materials by molecular bionics*). She also has been engaged in teaching within the scope of the study program "Materials Science" at the University of Stuttgart. On the way to her own group and habilitation, her involvement in the CRC will certainly be very beneficial and promising.

During the first funding period, a concerted effort will try to attract young scientists as potential future project leaders for following funding periods with interesting research areas. For the career advancement of doctoral students the graduate school of the University of Stuttgart (GRAD*US*) will play a central role (which originated from the "*SimTech*" Cluster of Excellence). GRAD*US* itself is integral part of the doctoral degree regulation of the University of Stuttgart. To avoid duplication of educational structures, this CRC will join with these existing measures. Clear guidelines regarding generic and interdisciplinary education will be communicated.

Within the frame of this CRC, an advisory council for doctoral students will be installed, consisting of one professor from each of the four contributing departments (chemistry, mathematics, physics, as well as energy-, process- and bio-engineering). This council will consider the special requirements of a PhD process in the interdisciplinary CRC 1333. The council will especially look at the following two tasks:

- monitoring whether all aspects included in the promotion contracts are accounted for
- proposition of a defense committee in case the principal investigator (PI) is not entitled to lead the corresponding examinations. The final decision is with the Faculty of Chemistry.

1.4.1.1 Selection process for prospective PhD students

The announcement of open positions in CRC 1333 will be made via a specifically dedicated, own internet platform, via the online presence of university and contributing departments and via relevant job advertisement channels, such as internet job sites. New students will be recruited both nationally and internationally. Prospective students will apply directly to one of the PIs. The PI will in coordination with the CRC board invite suitable candidates for a presentation and interview. During the interview, the candidate will have the opportunity to visit labs and speak with PIs. In addition to the usual employment criteria, we will especially judge the candidate's identification with the multidisciplinary nature of the CRC. We will make a strong effort to recruit a high proportion of female candidates by explicitly asking female MSc students to apply and by contacting our scientific contacts specifically about potential female candidates. The CRC board will strongly encourage all PIs to keep contributing to this goal.

1.4.1.2 Support measures for PhD students

The major part of the scientific work will be conducted by PhD students. Consequently, CRC 1333 explicitly focuses on good support and excellent education of young, talented scientists. One of the key aspects for success of the CRC will be whether people with different backgrounds – such as natural sciences or engineering – can communicate effectively and productively. Therefore, clearly structured and regular exchange of people and ideas is mandatory. This way, the necessary communication is guaranteed and students are supported in their scientific work. On the level of the individual projects, such exchange is envisioned to take place every four weeks; on a higher level, colloquia and workshops will be organized in intervals of three months. PhD students will sign a mentoring contract with two professors, detailing their research topic, and they will take part in GRAD*US*. Within this scheme, scheduled review stages are agreed upon. Prior to finishing their respective dissertations, candidates will have highlighted the relevance of their work by having published in peer-reviewed, high-profile international journals.
In more detail, the qualification measures within CRC 1333 are organized as follows:

Mentoring (career counseling) of the doctoral thesis is organized to involve two teaching staff (supervisor and mentor). Special emphasis will be put on interdisciplinary learning. Especially the planned colloquia as well as the winter- and summer schools are well positioned for this (see below). GRAD*US* will complement this and provide lectures in topics well exceeding the subject of this CRC and also provide contacts into economy and academia. More specifically, the **individual development** and education of the PhD students is to be supported by several measures:

- Prospective PhD students will be recruited by the project leaders themselves *via* announcements of the single working groups.
- All students working on their PhD's will be mentored by an additional CRC co-supervisor as is currently already common practice in GRAD*US* and the graduate school SimTech. According to the current *Promotionsordnung*, a supervision agreement is mandatory.
- The students will have the opportunity to join qualification measures; this especially includes the university's broad program of project management, presentation techniques etc.
- Several scientific exchanges with foreign groups will be supported (duration 3-6 months) with the specific aim to strengthen scientific exchange and broaden PhD students' horizons.
- Participation in the prospective summer- and winter schools (organized by the students themselves) will be mandatory. Scientific questions and challenges regarding the CRC will be discussed there collectively. In this context, the students will be asked to take on responsibility for selected tasks, such as the organization of workshops or similar activities.
- To improve cooperation within the CRC, networking meetings will be held (in the follow-up to CRC-colloquia). These are to be organized by PhD students and PostDocs. To enable a free and non-formal exchange of questions and ideas, it is desired that no project leaders are present at these meetings. In these networking meetings, the students will elect a speaker team, invite external scientists for oral presentations and discuss specific questions arising from the CRC.

To provide the students with first experiences in organizing scientific projects, it is intended to let PhD students co-supervise, i.e. guide the daily work of a number of BSc and MSc students. The PhD students will also mentor the project students within the RISE framework (*Research Internships in Science and Engineering)*. PostDocs will take on more responsibilities and more complex issues, in order to provide them with a robust preparation for further scientific careers, by obtaining leading- and coordinating positions within the CRC. It is expected that PostDocs will play an inspiring role for PhD students, including the preparation of publications. In this context, habilitations are a distinct possibility for talented candidates and the CRC will strongly support such intentions. Young researchers will also be crucial to implement new insights won from the CRC into lectures and seminars ("research-directed education"), underlining their importance for high-quality education of future scientists.

Mentoring contract: The acceptance as PhD student is automatically connected with a mentoring contract, signed by both student and mentor(s). In this contract, the research topic and organization of the thesis work is detailed, as well as further modalities. Such a mentoring contract is also heavily endorsed by the Ministry for Science, Research and Art in the State of Baden-Württemberg, with the

overall aim of improving the quality of doctoral training. Indeed, the mentoring contract is part of the current *Promotionsordnung* of the University of Stuttgart. A copy of the mentoring contract will be deposited with the PhD committee and the advisory council for PhD students of this CRC. Importantly, specific qualification measures, which have to be completed by the student must be listed by the respective mentor in the written contract. To ensure an interdisciplinary training of the PhD students, each student should fulfill the following:

1. Successful participation in scientific, topic-related lectures/courses on a high level (with at least 12 credit points ensuing). Preferentially, complementary lectures will be chosen with regard to the students' own backgrounds. Suitable lectures (courses are recommended by mentors and students in accordance with the CRC advisory council).
2. Participation in non-specialist area lectures/courses on the PhD level to gain interdisciplinary qualifications (at least 3 credit points necessary). This includes subjects such as scientific work processes, time management, publishing or (oral) presentation techniques. This is part of the requirements for graduation within GRAD*US*.
3. Participation in two lectures/courses of GRAD*US* with interdisciplinary content (e.g., ethics in science, high-risk technologies,…). In well-founded exceptions, other achievements will be accepted as equally suitable by the PhD committee. All individual qualification measures should be completed until the first progress report is due and successful participation must be documented before defense (see PromO 2011, § 6)

Progress report: 18 months at the latest after acceptance as PhD student, the candidates will present the current state of their research. This milestone report will help to avoid disadvantageous developments early on and will allow both students and project leaders to fine-tune their research. The report will consist of a 30 minute oral presentation, followed by a 30-40 minunte open, scientific discussion. The report will be discussed with the mentor and an additional examiner (elected by the PhD committee). Successful participation must be documented prior to any application for a defense by the doctoral students.

Workshops: Every year, four workshops will take place. The departments involved with the CRC will organize these, in a rotating manner. These workshops will improve communication between the different scientific areas which are unified under the roof of the CRC. The PIs will thereby report about content, method and aims of their research area and project and will coordinate these with other projects. Additionally, PhD students will benefit from this forum as it allows them to address a larger audience at least once a year.

Colloquia: Presentations by the researchers of CRC 1333 will be integrated into group seminars already established in the individual working groups.

Status seminars: Every year, a two-day long status seminar will be held. These will be organized by the PIs with the help of PhD students and postdocs; they will also invite presenters from other academic institutions (both national and international). Students towards the end of their doctoral research will also have the possibility to show their work in this setup. In general, the participation of scientists in national and international conferences will be financially supported.

International scientific exchange: Especially well-performing young researchers will be supported with a three – six months long stay in a suitable foreign institution. This is considered helpful for fulfilling our scientific goals and for the comprehensive education of our PhD researchers. The number and quality of forein institutions are handpicked. Every stay aboard will be discussed with each supervisor according to the individual supervisor plan and the progress in the thesis. Notably, a quick adaption to the new environment and an extremely short process of arrival are required. Such exchange will also facilitate the uptake of novel working methods from the hosting institution, help finding valuable personal contacts and improve language. Nominations of suitable candidates will be agreed on by the advisory council for the PhD students. The necessary funds for travel and lodging are applied for in **project Z1** and will be distributed among the individual projects as outlined there.

1.4.1.3 Integration in GRAD*US*

To avoid duplication of educational structures, this CRC will integrate with the already existing graduate school of the University of Stuttgart (GRAD*US*). GRAD*US* itself is an integral part of the doctoral degree regulation of the University of Stuttgart. All techniques and methods relevant to this CRC will be central to teaching activities; a clear focus will be put on the **scientific quality** of all work conducted within the CRC (especially PhD).

Depending on their scientific background, doctoral students of natural sciences, engineering, biotechnology or other fields will have a different perception of methods, aims or criteria for judging successful scientific work. Thus, success of this CRC hinges to a large degree on proper communication between interdisciplinary teams; a common "language" must be established and furthered. Hence, a regular exchange on a *methodological* level must take place, not only the exchange of data or ideas. For such qualification, again GRAD*US* will be a valuable tool. GRAD*US* is approachable for anybody planning on doing doctoral work and offers interdisciplinary council on possibilities for this in the University of Stuttgart. GRAD*US* also helps with issues beyond the limits of individual projects. Explicitly, this institution supports interdisciplinary networking and is a platform for exchange and communication.

GRAD*US* in cooperation with the departments and already existing structures will guarantee a high-level education of PhD students in transdisciplinary areas; as such, this will increase the attraction of the University of Stuttgart as work place for excellent scientists from Germany and abroad. Notably, GRAD*US* also formulates minimum standards for the scientific qualification of doctoral students and defines the standards for good scientific practice; the trans/interdisciplinary requirements, which are so crucial for this CRC, will be best met with such a valuable institution. GRAD*US* furthermore can serve to give council independent from any CRCs.

1.4.1.4 Colloquium series

In addition to the activities outlined above, the CRC will also organize a series of high-level colloquia. Selected colloquia will be advertized to the general public, rendering them part of public relations activities. For these purposes, the CRC will install its own multi-disciplinary colloquium at the University of Stuttgart. These will consist of PhD reports and oral presentations of external scientists. Additional to this CRC colloquium, institutes will hold their own meetings with more specific thematic scopes, to which members of the CRC can be invited. Every year the progress of all projects will be presented. The CRC colloquia are intended to provide a forum on which existing cooperation can be deepened and adjusted. Clearly, the majority of these colloquia will serve for scientific exchange. It is intended to invite (foreign) guest scientists and researchers and to offer the colloquia as a platform to learn about the relevant latest results, as well as interact with leaders in the relevant fields. Importantly, this is also the forum where the most outstanding results of the CRC will be presented to best effect. This can also include progress reports by students. Research assistants and doctoral students close to finishing will be integrated, to offer a motivating experience; in general, it is desired that doctoral theses are presented to a larger audience in these colloquia, not only in institute seminars.

1.4.1.5 Summer school

An „International Summer School" will be established to address a new generation of scientists, and to interest them in the scientific scope of the CRC. The summer school includes lectures and seminars. An attractive idea is to invite guest lecturers who would present specifically selected aspects of interest to the CRC in the form of block courses. All such components – lectures, seminars, block courses – will be published online. As outlined before, molecular heterogeneous catalysis absolutely requires an interdisciplinary approach; this is all the more valid for students, since they have to adapt to such an environment in a short time, taking up new abilities from other fields of science – starting from their usually "monodisciplinary" master studies. Hence, careful selection and high-level education of young talent is one of the key features of this CRC. Especially the doctoral students must have the possibility to get into contact with all the tools, methods, aims and ethics of the different disciplines of this CRC during their work. This will increase understanding for concepts and thinking of other research areas – a most important requirement for good cooperation beyond the limits of their own subject areas. Hence, the PhD students will have access to a much broader working- and research environment than in a conventional PhD studies setting. Doctoral students within the CRC 1333 can therefore be expected to qualify for leading positions in economy and academia, where these abilities are necessary and highly sought after.

1.4.2 Gender equality and family-friendly policies

Gender equality is an ever more important aspect for universities competing for excellence. Therefore, the recruitment and support of talented and ambitious women is of self-evident interest for the university and a dedicated aim of this CRC. Apart from individual support, a number of projects and programs for women exist in Stuttgart. After a nation-wide auditing process, the University of Stuttgart has been labeled “family-friendly” by the Hertie Foundation GmbH (30.08.2012), thereby dedicating itself to measures, which improve the compatibility of career, studies and family matters. This is reflected in flexible working hours and recent improvement of child daycare infrastructure.

A successful inclusion of female scientists can be understood as a threefold challenge. Firstly, it is crucial to attract the interest of future scientists, especially for universities with a focus on natural science and technology/engineering, such as Stuttgart. Secondly, during the studies the university, and even more so this CRC, will present itself as supportive and attractive working environment. Finally, this also encompasses the provision of appealing prospects for female scientists to consider a future career in natural science or technology. This CRC regards gender equality as decisive factor for high-quality scientific performance.

The University of Stuttgart is dedicated to gender equality, successively realizes its guidelines on this subject and considers equality as beneficial for its innovative character and as an important key stone of quality management. With its distinct technical-scientific profile the University of Stuttgart must be considered to bear a special responsibility to increase the proportion of women in all areas of research, teaching and studies. Conceptually, this topic is addressed in the “*Struktur- und Entwicklungsplan of the University of Stuttgart (SEPUS)*” with far-reaching gender equality guidelines.
Since 2006, responsibility for gender equality is directly located with the university’s head office, and the equal opportunities officer participates in all strategically important committees and decisions. Overall, the university actively supports equal opportunities since the 1990s. Several projects aim to inspire school girls and win them over for technical or natural science subjects. These include, for example „*meccanica feminale*“ (Spring University for girls) or the „*Girls’ Day – Mädchen-Zukunftstag*“ as well as “*TryScience*”, which provides a survey over the MINT disciplines, as well as reporting on student role models (https://www.uni-stuttgart.de/studium/orientierung/try-science/).

Also, for the next qualification steps corresponding programs have been installed. Complementing the more general “*Femtec.Network*“, several mentoring schemes target specifically female students (“*StartScience*“), doctoral students (“*FeelScience*”), habilitands and PostDocs (“*DoScience*”), as well as female professors (“*BeScience*”) for career-building advice. The “*Service Gender Consulting*“ supports research applications. Additionally, the University of Stuttgart offers further measures to improve the compatibility of work and family. This includes short-notice child care, places for children aged 0-3 years, a holiday time care as well as e-work rules. Since 2011, counseling is offered for all questions regarding this topic by the “*Service Uni & Familie*”. All measures are continuously being developed and extended; consequently, re-auditioning was successfully completed in 2015. These activities highlight the ambitious targets the university has set itself regarding equal opportunities and gender equality and its resolve to further improve the working environment for all employees and students. Finally, we wish to refer at this point to the Charta of Diversity, which has been signed by the Rector of the University of Stuttgart, Prof. Dr.-Ing. W. Ressel and which contains a clear commitment to inclusion, participation and diversity (https://www.uni-stuttgart.de/universitaet/aktuelles/presseinfo/Diversity-als-Chance/).

Funding for quality measures:

To facilitate planning and to use the funding in the most effective manner, 50% of the funding for gender equality measures will be pooled together with funding from other existing CRCs at the University of Stuttgart. The pooled resources will be directly managed by the university administration. These funds are intended to support measures that can be employed by all research councils together; conception, selection and realization of such projects will be conducted in collaboration with all contributing research councils. The granting of funds from these pooled resources is overseen by an advisory council staffed by selected members from the respective research councils.

This proportional pooling will increase the visibility of all contributors, since individual projects of the respective research councils will be complemented by overarching, inclusive measures. The combination of individual projects and larger, synergistic measures will achieve an effective and pointed advancement of women in science and will help to focus resources and expertise. Also, the actual spending of funds will be facilitated by this pooling scheme to employ all DFG grants to their best extent.

Measures

Funding will be pooled (50%) and allocated to realize the following measures:

- organization of meetings (conferences, colloquia) with internationally renowned (female) researchers and other invited speakers, including topics such as *women in science* or *family-friendly university*.
- support of efforts to recruit female researchers prior to the start of projects
- mentoring for female PhD students, PostDocs and researchers
- coaching on career advancement for young female researchers, including information on funding schemes beyond the CRC.
- introduction of parent-child spaces (such as specially assigned rooms), potentially also the acquisition of mobile diaper changing tables
- childcare during meetings, conferences, workshops
- acquisition of day childcare slots specifically for members of the CRC
- setup of home-office work stations to increase flexibility and to attract more female scientists to work with the University of Stuttgart
- installation/upgrade of a job position monitoring the realization of these measures and projects (endorsed by the DFG, max. 50%).

The service institution "Gender Consulting" offers to speakers and applicants of CRCs detailed information and advice on this pooling scheme, including conception and coordination with the DFG (also cooperation contracts). All financial transactions will be managed and handled by the university administration.

Special CRC activities regarding equal opportunities and gender equality

Five projects of the CRC will be led or co-led by female scientists. Specifically, the female lead research groups are:

Prof. Dr. Bettina Lotsch, MPI-FKF (CRC board)
Prof. Dr. Sabine Ludwigs, Institute of Polymer Chemistry
Prof. Dr. Sabine Laschat, Institute of Organic Chemistry
Jun.-Prof. Maria Fyta, Institute of Computer Physics
PD. Dr. Yvonne Traa, Institute of Chemical Technology

In summary, one third of all research projects are led by female scientists. It is intended to further increase the proportion of women on all academic levels in the CRC and to support all female scientists involved. This support is to be steadily expended in sections **A** – **C**.

Attract Interest: As is the case already now in all participating institutes, every year's "*Girl's Day*" will get its own CRC presentation, designed to fit the age group of the visiting pupils. As these occasions are traditionally well frequented, this is a promising opportunity to inspire interest for catalysis in young

people. For those pupils that are old enough to take up studies in the near future, it is planned to increase the visibility of the CRC by tailored presentations held by the project leaders themselves, advisably by female project leaders.

Inclusion: The "*Struktur- und Entwicklungsplan 2013–2017*" clearly states that it is the aim of the university to further the cause of gender, and to expand its presence in teaching and education. To increase the CRC's attraction, a price will be raised for the best thesis of a female/male scientist within the CRC.

Further Measures: To advance international connections, and as role models for young scientists, the CRC wants to invite renowned international scientists for lectures and discussions. We aim to invite 40% female speakers for our colloquium series. A budget dedicated solely to childcare will be applied for. Also, a further university-owned child daycare institution is underway to be built, with a capacity of around 60 places, which should make life easier for scientists with family. With the same intention, CRC-related meetings, colloquia, presentations etc. will be terminated before 3 pm, so as to avoid collision with the closing time of child daycare institutions.

A. Research Staff

	First Funding Period intended female share [%]
Doctoral researchers	≥ 40
Postdoctoral researchers	≥ 40

B. Principal Investigators

Position	**First Funding Period**		
	Number of men/women		Proportion of women [%]
	m	w	
Postdoctoral researchers	0	0	
Group leaders, junior group leaders, junior professors	6	2	25.0
Professors C3/W2	3	0	0
Professors C4/W3	5	3	37.5
Total	14	5	26.3

1.4.3 Management of research data and knowledge

Scientific research generates, apart from the main findings published in journals, books or patent literature, significant amounts of raw data. This CRC will ensure to preserve these secondary data and render them accessible in order to enable future research based on this information. It should be noted, however, that the amounts of data referred to here will not amount to "Big Data", which simplifies the strategies necessary for efficient after-use and eliminates the need for dealing with meta data and similar resources. The University of Stuttgart supports its researchers to manage, save and share their research data. The research data policy of the University of Stuttgart provides guidelines for the handling of research data (http://www.ub.uni-stuttgart.de/forschen-publizieren/FoDa-Policy-English.pdf).

Overall, both the experiments and the numerical simulations performed within the proposed CRC 1333 will produce and use moderate amounts of research data. We will follow the "Principles for the Handling of Research Data" of the Alliance of German Science Organizations, as concretized by the DFG in its "Guidelines on the Handling of Research Data." Both simulations and measurements can produce large amounts of primary data (many GB to TB), of which in many cases only a fraction is relevant information. Wherever suitable, data will be archived after processing, which will reduce the required storage space.

Data will be exchanged directly between the projects wherever appropriate for the collaboration. The University of Stuttgart provides a file exchange service “Frams’ Fast File EXchange” for that purpose. For archiving and preservation including storage and backup of the data, we will collaborate with the Steinbuch Centre for Computing (SCC) at the Karlsruhe Institute of Technology (KIT) as well as with the FIZ Karlsruhe – Leibniz Institute for Information Infrastructure. In particular, the bwDataArchiv service, rda.kit.edu, of the SCC provides a reliable and sustainable infrastructure for long term data storage, which is especially well suited, technologically and economically, for storage and retrieval of very large but few individual files.
Data will generally be published as supporting information to the corresponding original publications. This ensures direct availability of background data to the scientific community.

In addition to that, we will implement the following specific strategies:

- **Publication of major findings.** As is good practice in natural sciences, we will publish all important research results in relevant, high-quality journals. Thereby, we will also use *Open Access* journals, or opt to make use of the respective choices in mixed journals (i.e., *Gold Open Access*). If this is not possible, we will provide the accepted version of the article free of charge via the CRC Website (institutional repository). Also, if applicable, general platforms may be used, for example *ArXiv* (physics), *ChemRxiv* (chemistry), *Research Gate* or *FigShare*.

- **Publication of raw data, synthetic procedures and analytical protocols.** There is a growing tendency to publish extensive data as part of the so-called “*Supplementary Information*” of journal articles. This usually contains additional information for better description of synthesis and analysis and may include different types of presentation, even including videos. We will make use of this possibility wherever possible and beneficial; also, the online platforms mentioned above may offer similar opportunities. Depending on their complexity, the raw data from computer-based simulations may encompass Terabytes, meaning they are too large to allow for long-term archiving. In these cases, only the source code of the used programs will be retained.

- **Exchange of data between the individual projects.** This is of vital importance for the CRC. For the whole duration of the CRC, the respective data of promising findings will be entered and organized on this platform (including key parameters such as development and anchoring of the catalyst, catalyst turn over numbers, characterization data, simulation results…). This exchange of data must include all levels, most notably also all the PhD students. This is necessary for efficient research, rational planning and successful publication, but also to generate a credible basis for future funding periods. To this end, a suitable database will be installed, which will enable swift access to relevant information. After the first funding period we will publish these data on a suitable platform (complete with DOI labelling). To realize this, the University of Stuttgart will provide the corresponding server access.

1.4.4 Knowledge transfer and public outreach

Knowledge transfer to industry is planned to occur mainly via the B-projects. In case the foundation of start-ups is envisaged, the existing initiative at the University of Stuttgart (TTI GmbH, https://www.tti-stuttgart.de) can be used. Public outreach at the University of Stuttgart is handled by the Team University Communications (https://www.uni-stuttgart.de/en/university/organization/administration/div1-universitycommunications/index.html). All activities of the CRC in that regards will be harmonized and coordinated with the Team University Communications. Press releases and newsletters are prepared by the CRC management on a regular basis and provide the desired and necessary visibility of both the University of Stuttgart and this CRC. A specifically dedicated home page will also be created.

1.5 Other sources of third-party funding for principal investigators

Principal investigator	Project	Project title	Funding period	Funding agency
Bauer	BA 4467/1-2	Time-resolved studies on the dynamics of electronic charge transfer processes in bioinorganic complexes – development of technological foundations	2015-2017	DFG
Bauer	BA 4467/2-2	Cu-S complexes in the heart of biological electron transfer: the homodinuclear CuA site of Cytochrome-c oxidases and N2O reductases	2015-2017	DFG
Bauer	BA 4467/3-1	Charge transfer Raman, XES and (HR)XAS studies on Type Zero model complexes	2015-2017	DFG
Bauer	BA 4467/4-1	Identifizierung der Natur aktiver Chromkatalysatoren in der Tetramerisierung von Ethylen durch (gekoppelte) operando-Spektroskopie	2016-2018	DFG
Bauer	BA 4467/5-1	Entwicklung von eisenbasierten Oxidationskatalysatoren für die Reinigung von Dieselabgasen	2017-2020	DFG
Bauer	BA 4467/6-1	Molekulares Design von und Röntgenspektroskopie an Nanocluster-Katalysatoren	2017-2020	DFG
Bauer	05K13UK1	Sustainable Chemistry by XES - SusXES	2014-2016	BMBF
Bauer	05K16PP1	TReXHigh	2016-2019	BMBF
Bauer	05K14PP1	Zeitaufgelöste in-situ Methoden zur Entwicklung katalytischer Zentren in der nachhaltigen Chemie - SusChEmX	2014-2017	BMBF
Bill	BI 469/19-3	Genetically optimized Tobacco mosaic viruses as scaffold for the in vitro generation of semicon-ductor bio/metal-oxide nanostructured architectures	2016-2018	DFG
Bill	BI 469/23-1	Erzeugung von lumineszierenden Materialien durch lebende Algen	2014-2018	DFG
Bill	BI 469/18-3	Coordination tasks within the Priority Programme SPP1569	2016-2018	DFG
Bill	BI 469/25-1	Hochauflösende Niederspannungstransmissions-elektronenmikroskopie	2016-2017	DFG
Bill	BioMatS-16	Selbstwachsende Nanopiezoaktorik - ein biologischer Ansatz	2014 -2018	Stiftung BW
Bill	BioMatS-10	Materialsynthese mit gesteuerten BioNanoreaktoren (Phagetools)	2014 -2018	Stiftung BW
Bill	-	Nanobiomaterialien - Projekthaus NanoBioMater	2014 - 2018	Carl Zeiss Stiftung
Bill	93-429	ROBOPHAGE	2017 - 2020	VW Stiftung
Buchmeiser	BU 2174/19-1	Mo-Imido Alkylidene NHC complexes	2015-2018	DFG

Buchmeiser	BU 2174/22-1	W-Imido Alkylidene NHC complexes	2016-2019	DFG
Buchmeiser	BU 2174/21-1	C/C-Si/C fiber-reinforced ceramics	2016-2019	DFG
Buchmeiser	CRC 1244		2017-2020	DFG
Buchmeiser	03ETE003D FiMaLis	FiMaLiS- Monolithic fiber-based hybrid cathode materials for lithium-sulfur high-performance batteries	2017-2020	BMWi
Buchmeiser	-	CORAL	2016-2019	BMBF
Buchmeiser	ARENA2016	Fiber- and textile-based integration of function	2013-2018	BMBF
Buchmeiser	031B0351A	PFIFF	1917-1920	BMBF
Buchmeiser	7-4332-62-FEM/37 SERec	Recovery of rare earth elements	2015-2018	MFW-BW
Buchmeiser	MAT0013	Bio-based acrylonitrile	2014-2018	BW Stiftung
Buchmeiser	-	Group 6 olefin and alkyne metathesis catalysts	2015-	XiMo AG, CH
Buchmeiser	-	NHC organocatalysis	2016-	Covestro
Buchmeiser	-	Li-S batteries	2012-	Daimler AG
Fyta	CRC 716	Diamondoid-functionalized nanopores as biosensors	2015-2018	DFG
Fyta	CRC 716	Structure and Stability of Carbon Nanoclusters	2015-2018	DFG
Fyta	EXC 310 SimTech	Machine learning and functionalized devices for DNA readout	2017-2018	DFG
Fyta	JPP-Programm	Properties of biomodified carbon nanomaterials	2015-2018	MWFK-BW, University of Stuttgart
Fyta	FIA	Nanoconfinement of Water in Quasi 1D Crystals	2017-2020	University of Stuttgart
Gießelmann	GI 243/8-1	Ionic Liquid Crystals	2015-2018	DFG
Gießelmann	GI 243/9-1	Lyotropic Gels	2016-2019	DFG
Groß	GR2948/2-2	„Methodik zum integrierten Entwurf von Fluiden und Prozessen mit PC-SAFT“	2017-2019	DFG
Groß	TRR 75/2-2017	Sub-project „Entwicklung und Anwendung von thermodynamischen Modellen für Grenzflächen mit der Dichtefunktionaltheorie“	2014-2017	DFG
Groß	SFB1313	Sub-project „Fluid- und Grenzflächeneigenschaften in porösen Medien aus der klassischen Dichtefunktionaltheorie und aus Molekularsimulationen“	2018-2021	DFG
Groß	FuE-Arbeiten	„Implementierungsarbeiten der PC-SAFT Zustandsgleichung“	2017 2018	BASF
Hansen	CRC 716	Modeling and prediction of supra-molecular complexes for the design of novel materials	2015-2018	DFG
Hansen	JPP-Programm	Development of efficient, robust and reproducible simulation protocols for the calculation of standard binding free enthalpies for cyclodextrin inclusion complexes	2016-2019	BW Stiftung

Hansen	Glykobiologie/ Glykobio-technologie	The molecular basis of chiral recognition in cyclodextrins and their derivatives	2017-2019	MWK
Hansen	DIPL-ING	Data management in infrastructures, processes and life cycles for engineering sciences	2017-2019	BMBF
Holm (Spokesman)	CRC 716	Dynamic Simulation of Systems with Large Particle Numbers	2009-2018	DFG
Holm	CRC 716	Macromolecular transport through nanoscaled pores	2009-2018	DFG
Holm	EXC 310 SimTech	Atomistic and mesoscopic simulations of polyelectrolytes and ionomeres	2010-2018	DFG
Holm; Hardt	HO 1108/22-1	Investigating the interaction of stretched, immobilized polyelectrolytes with external electric fields and fluid flows in presence of confined micro-geometries	2013-2018	DFG
Holm; Potts	HO 1108/25-1	Fast Fourier-based Coulomb solvers for partially periodic boundary conditions	2014-2019	DFG
Holm	AR 593/7-1	Simulations of weak polyelectrolytes: Interplay of acid-base equilibria, ion correlations and polymer topology	2015-2019	
Holm; de Graaf	SPP 1726 HO 1108/24-1 GR 4516/1-1	Cooperative motion of microswimmers: The role of shape anisotropy and hydrodynamic interactions	2016-2018	DFG
Holm	SPP 1681 HO 1108/23-2	Properties of magnetic hybrid materials – a microscopic simulational approach	2017-2018	DFG
Holm; Wilhelm	HO 1108/26-1	Distribution of low-molecular weight ions in charged hydrogels in equilibrium and under the application of external stimuli	2017-2020	DFG
Holm	SPP 1726 HO 1108/24-2	Cooperative Motion of Microswimmers: The Influence of Ionic and Reactive Screening on Hydrodynamic Interactions in Complex Fluids	2018-2020	DFG
Holm; Potts	AR 593/8-1	Fast Fourier-based Coulomb solvers for partially periodic boundary conditions	2017-2019	DFG
Hunger	HU533/13-1	Mechanismen heterogen katalysierter Hydrierreaktionen	2014-2017	DFG
Hunger	NMP4-LA-2013-604277	Fast industrialization by catalysts research and development	2013-2017	EU
Kästner	TUNNELCHEM	Atom-Tunneling in Chemistry	2015-2020	ERC

Kästner	CRC 716	TP C6: Pfade kleinster freier Energie berechnet mit Umbrella-Sampling-Simulationen TP C8: Molekular-Dynamik-Simulationen zur Bestimmung von Entfaltungspfaden und stabilen Konformationen von DNA G-Quadruplex-Strukturen	2015-2018	DFG
Kästner	EXC 310/2 Überbrückung	Interpolation of Potential Energy Surfaces using Gaussian Process Regression	2017-2018	DFG
Laschat	LA 907/17-1	Struktur und Dynamik ionischer Flüssigkristalle	2014-	DFG
Laschat	PLISE 57316794	Phosphorescent hybrid crystals using Supramolecular and Electrostatic interactions (PLISE)	2017-2018	DAAD
Laschat	BioMatS-011	Hydrogele mit optimierter Ladungsdichte (BIOGELplus)	2014-2017	BW Stiftung
Laschat	-	Projekthaus NanoBioMater	2014-2017	Carl-Zeiss-Stiftung
Ludwigs	1445/2-1, Emmy Noether group	Hierarchical nanostructure control of nanohybrid materials based on electroactive rod-coil block copolymers and inorganic nanoparticles	since 12/2008	DFG
Ludwigs	0563-2.8/707/1	Synthese n-halbleitender Polymere mit neuen Architekturen für thermoelektrische Anwendungen	2017 – 2019	Zeiss Foundation, PhD stipend
Ludwigs	P2017-0069	Poly-i-Skin - Bioinspirierte Schaltung von Polymeraktoren	2018 – 2019	Vektor-Stiftung
Lotsch	Projektnummer 639233	COFLeaf	2015-2020	ERC
Lotsch	FKZ: 03XP0030C	StickLis	2016-2018	BMBF
Lotsch	Projektnummer 316685525	SPP1928 (COORNETs)	2016-2019	DFG
Naumann	NA 1206/2-1	Dual Catalysis for Polymerizations	2016-2019	DFG
Plietker	PL 300/10-1	Development of Fe-catalyzed allylic and benzylic C-C-bond activations	2013-	DFG
Plietker	PL 300/11-1	Fe-catalyzed carbene insertions	2014-	DFG
Plietker	PL 300/12-1	Development of a selective hydroxylation, amination and alkylation of prochiral CH_2-groups through sequential Ru-catalysis	2014-	DFG
Plietker	-	Landesgraduiertenkolleg “WindyCities”	2016-	MWK-BW
Ringenberg	INST 40/467-1 FUGG	Calculations on Organometallic Complexes Containing Redox-Active Noninnocent Ligands	2016-2018	DFG
Schmitz	Grant Agreement No 607040	ITN “Novel complex metal hydrides for efficient and compact storage of renewable energy as hydrogen and electricity”	2014-17	EU

Schmitz	Schm1182/14	Solid state reactions, interfaces, and stress in core-shell nanostructures	2013-18	DFG
Schmitz	Schm1182/15	Reaktive Benetzung und Miniaturisierung von Lötverbindungen	2014-18	DFG
Schmitz	Schm1182/16	„Physikalische begründete Volumen-Rekonstruktion für die 3D-Atomsondentomographie	2016-18	DFG
Schmitz	Schm1182/18	„Reaktionskinetik von Autoabgaskatalysatoren unter Berücksichtigung der reversiblen Edelmetall-Oxidation“	2017-20	DFG
Van Slageren	SL104/3-2, SPP1601	Improving the sensitivity of THz frequency domain magnetic resonance	2015-2018	DFG
Van Slageren	SL104/5-1	Spektroskopische Untersuchungen an auf Lanthanoid-Ionen basierten Einzelmolekülmagneten	2015-2018	DFG
Van Slageren	2016-065	*Ab initio* Untersuchungen von auf *f*-Elementen basierenden molekularen Nanomagneten	2016-2018	Vector Stiftung
Van Slageren	–	Integration of Molecular Quantum Bits with Semiconductor Spintronics	2015-2018	IQ^{ST}
Van Slageren	767227	Plasmon Enhanced Terahertz Electron Paramagnetic Resonance	2018-2020	EU
Sottmann	03ET1409 PuNaMi	Polyurethan-Nanoschaum aus Treibmittel-basierten Mikroemulsionen zur Hochleistungswärmedämmung	2016-2019	BMWi
Sottmann	-	Investigations on surfactant aided gas flooding techniques for enhanced oil recovery application	2015-2018	Sasol Germany GmbH
Traa	TR 480/5-1	Maßgeschneiderte nukleophile und amphotere Zeolithe ohne große Hohlräume für die Dehydratisierung von Milchsäure zu Acrylsäure	2018-2020	DFG
Traa	FASTCARD	FAST industrialization by Catalysts Research and Development	2014-2017	EU

2 Existing funds and requested funds

2.1 Existing funds

2.1.1 Overview of direct costs available

Financial year	Core support provided by the University of Stuttgart	Core support provided by MPI-FK	Other funds	Total
2017	31,000.-	0.-	0.-	31,000.-
2018	62,000.-	0.-	0.-	62,000.-
2019	62,000.-	0.-	0.-	62,000.-
2020	62,000.-	0.-	0.-	62,000.-
2021	31,000.-	0.-	0.-	31,000.-
Total	248,000.-	0.-	0.-	248,000.-

(All figures in EUR)

2.1.2 Overview of existing staff

Category	Number of persons		
	University of Stuttgart	MPI-FK	University of Paderborn
Professors	10	1	1
Junior research group leaders	8	0	
Postdoctoral researchers	6	0	
Doctoral researchers	5	1	
Other research staff	0	0	
Non-research staff	17	2	
Student and graduate assistants	0	0	

2.1.3 List of existing instrumentation > € 10,000

Project	Description of instrumentation	Year of purchase	Cost of purchase (k€)	Source of funding
A1	Autosorb-1 (Quantachrom)	2006	96	loan from DFG
A1	ISEC	2010	56	Uni Stuttgart
A1, B2	400 MHz NMR	2010	349	DFG/Uni Stuttgart
A1, B2	ICP-OES	2011	72	Uni Stuttgart
A1, B2	5 Glove boxes + SPS	2010	393	Uni Stuttgart
A1, B2	IR	2013	22	Uni Stuttgart
A1, B2	GC-MS	2010	64	Uni Stuttgart
A1, B2	Microwave	2010	17	Uni Stuttgart
A2	NMR 250 MHz	1997	255	HBFG
A2	DSC/DMA	1998	190	HBFG
A2	FT-IR/MIR-Mikroskop/Raman	1997	265	HBFG
A2	GPC RI, UV-Vis, SLS	1998-2008	ca. 100	Uni Stuttgart
A2	Confocal LSM	2000	175	Uni Stuttgart
A2	Impedance spectrometer	2000	ca. 15	Uni Stuttgart
A2	Light microscope	2009	ca. 50	DFG-Emmy-Noether
A2	Glove box	2009	ca. 50	DFG-Emmy-Noether
A2	Transistor setup	2009	25	DFG
A2	Solvent vapor systems	2009	ca. 10	DFG-Emmy-Noether
A2	4 Potentiostates	2009-2014	32	DFG
A2	AFM	2011	236	HBFG
A2	Glove box system with sputter system	2011	252	HBFG
A2	SPS	2011	19	Uni Stuttgart
A2	Luminescence spectrometer	2011	23	Uni Stuttgart
A2	UV/Vis-spectrometer	2011	13	Uni Stuttgart
A2	Zeiss-spectrometer-system	2011	28	Uni Stuttgart
A2	Doctor blading system	2012	13	Uni Stuttgart

A2	Contact angle measurement system	2013	24	Uni Stuttgart
A2	Electrochemical quartz microbalance	2013	16	Uni Stuttgart
A2	Fluorescence spectrometer	2016	65	Uni Stuttgart
A3	Microwave with autosampler	2012	17	MPI-FKF
A3	IR	2011	18	MPI-FKF
A3	UV-Vis NIR	2013	59	MPI-FKF
A3	400 MHz NMR (solid und liquid state)	2015	230	MPI-FKF
A3	GC-MS	2009	85	MPI-FKF
A3	ICP	2004	79	MPI-FKF
A3	TEM	1993	683	MPI-FKF
A3	SEM + equipment	2001	90 + 11	MPI-FKF
A3	EDX	2001	61	MPI-FKF
A3	AFM	2011	138	MPI-FKF
A3	Cu XRD + monochromator	1989 + 1991	146 + 33	MPI-FKF
A3	Mo XRD	2001 + 2005	99 + 104	MPI-FKF
A3	Single crystal XRD + scintillation counter	2000	145 + 6	MPI-FKF
A3	Dynamic light scattering	2012	50	MPI-FKF
A3	Automated flash chromatography system	2012	26	MPI-FKF
A3	Photoluminescence spectrophotometer + flash lamp	2016 + 2017	140 + 11	MPI-FKF
A3	Physisorption (Autosorb-iQ MP2, Quantachrome)	2011	54	LMU München
A4	2D SAXS Bruker Nanostar	2006	250	BMBF/Uni
A4	2D VANTEC XRD Detector	2017	130	Schneider-Stiftung
A4, A7	1D SAXS, A. Paar	2010	371	Uni Stuttgart/DFG
A4	DSC, Perkin-Elmer Pyris	2013	53	Uni Stuttgart
A4	FT-IR with MCD, Bolometer	2016	240	Uni Stuttgart/DFG
A4	Polarisation microscope	2014	36	Uni Stuttgart

A4	Raman microscope	2007	223	Uni Stuttgart/DFG
A4	HPLC Agilent Ser. 1100	1996	80	Uni Stuttgart
A4	Quantachrome Autosorb 1	2009	60	Uni Stuttgart
A5	Fluorolog spectrophotometer	ca. 2005	60	MPI-IS/Uni Stuttgart
A5	UV-Vis spectrophotometer	ca. 2005	60	MPI-IS/Uni Stuttgart
A5	Malvern Zetasizer System	ca. 2000	60	MPI-IS/Uni Stuttgart
A5	Surpass zeta potential analyzer	ca. 1998	53	MPI-IS/Uni Stuttgart
A5	Spin-coater	2017	5	DFG
A5	Diproboter	ca. 2005	10	MPI-IS/Uni Stuttgart
A6	*dn/dc* increment device (620 nm)	2016	17	Leni Schöninger Foundation
A7	NMR probe DIFF/30 for NMR spectrometer pulsed-field gradient NMR experiments	2010	540	DFG/Uni Stuttgart
A7	3 High pressure cells	2006	15	loan (Uni Köln)
A7	1 Stroboscopic high-pressure SANS-cell	2011	15	loan (Uni Köln)
A7	4 Phase study equipment	2006	12	Uni Stuttgart
A7	3D-lioght scattering device	2010	220	DFG/Uni Stuttgart
B1	HPLC (Hewlett-Packard) PDA	2003	20	DFG
B1	HPLC (Hewlett-Packard) MWD	2005	20	DFG
B1	HPLC (Knauer) RI	2010	20	Uni Stuttgart
B1	HPLC Knauer (semipreparative) RI	2005	10	DFG
B1	HPLC Knauer (semipreparative) RI	2005	15	Dt. Krebshilfe
B1	HPLC Knauer (semipreparative) RI	2010	10	Uni Stuttgart
B1	Cyclovoltammetry (Metrohm)	2003	25	DFG
B1	Gas chromatography (Thermo Focus)	2003	25	DFG
B1	Gas chromatography (Thermo Focus)	2013	20	Uni Stuttgart
B1	Microwave CEM Explorer	2008	40	DFG
B1	*In-situ*-IR-Spectrometer mit ATR	2015	80	Uni Stuttgart
B1	GC-MS (Hewlett-Packard)	2007	20	Uni Stuttgart

B2	HPLC	2010	42	Uni Stuttgart
B3	FT-IR Bruker Alpha P	2013	19	Uni Stuttgart
B3	Finnigan MAT 95 GC-MS	1992	555	Uni Stuttgart
B3	Bruker Micro TOF LC-MS	2006	368	HBFG
B3	Shimadzu HPLC	2006	93	DFG
B3	Thermo Trace GC	2004	25	Uni Stuttgart
B3	Bruker 300 MHz	2004	170	HBFG
B3	Bruker 500 MHz NMR	2005	570	HBFG
B3	Bruker 400 MHz NMR	2014	540	HBFG
B3	Bruker 700 MHz NMR	2014	540	HBFG
B3	Bruker APEXII DuoDiffractometer	2010	420	HBFG
B3	Perkin Elmer Polarimeter	2008	20	Universität Stuttgart
C1	Bruker AvanceIII 400WB NMR spectrometer	1991 and 2010	1200	DFG
C1	2 vacuum lines for sample preparation	2017	40	Uni
C1	2 catalytic test equipments with on-line GC	1992 and 2007	80	DFG/Uni
C2	MCD-spectrometer	2012	233	DFG/Uni
C2	High-frequency EPR spectrometer	2012	300	DFG/Uni
C2	Frequency-domain EPR spectrometer	2009	220	EPSRC
C2	Q-band EPR spectrometer	2007	200	Uni
C2	Quantum design MPMS3 SQUID magnetometer	2014	530	DFG/Uni
C2	Bruker X-Band ESR spectrometer	1996	300	HBFG
C2	Network analyzer	2017	44	Uni
C3	UHV Ion beam sputter system	2007	80	Uni Stuttgart
C3	Reactive sputter deposition (Rau&Roth)	2012	110	Uni Stuttgart
C3	Magnetron sputter deposition (custom)	2015	30	Uni Stuttgart
C3	Laser-beam lithography (custom made)	2015	50	Uni Stuttgart
C3	Metallography-laboratory	2014	70	Uni Stuttgart

C3	Glove box (M. Braun)	2014	25	Uni Stuttgart
C3	2x Ball mills (Specs, Fritsch)	2005	30	Uni Stuttgart
C3	Ultramicrotome (Leica)	2009	60	Uni Stuttgart/DFG
C3	Dimple-grinder (Gatan)	2007	25	Uni Stuttgart/MPG
C3	Cryopreparation/transfer system (Leica)	2016	200	Uni Stuttgart /DFG
C3	Flash annealing oven (Riko)	2015	15	Uni Stuttgart
C3	White-light interferometer	2006	20	Uni Stuttgart
C3	Potentiostat/impedance spectrometer	2014	30	Uni Stuttgart
C3	X-ray diffractometer D 5000 (Siemens)	1995	60	Uni Stuttgart
C3	X-ray diffractometer X-pert (Philips)	2000	130	Uni Stuttgart
C3	X-ray diffractometer D8 (Bruker)	2008	250	Uni Stuttgart/MPG
C3	Environmental SEM Quanta 250 (FEI)	2016	200	Uni Stuttgart/DFG
C3	Dual Beam FIB Scios (FEI)	2016	1300	Uni Stuttgart/DFG
C3	TEM CM200 FEG (Philips)	1999	500	Uni Stuttgart
C3	Field-ion microscope (custom made)	2006	120	Uni Stuttgart/DFG
C3	Wide-angle atom probe (custom made)	2006	500	Uni Stuttgart /DFG
C3	Laser-assisted atom probe (custom made)	2010	500	Uni Stuttgart
C3	Cryo-transfer APT (custom made)	2016	900	BMBF
C3	Pico-flash laser (Coherent)	2016	180	BMBF
C3	Femto-second laser impulse (Clark)	2010	300	DFG
C5	PC cluster	2015	35	Uni Stuttgart
C5	4 GPU workstations	2016/17	10	DFG
C6	Cluster E5-2630v3 CPUs	2015	349	State of BW/DFG (1:1)
S1	Von Hamos spectrometer	2014	800	BMBF/Uni Paderborn
S1	Bruker Vertex-70	2014	80	BMBF
S1	Ocean Optics Raman spectrometer	2015	20	Uni Paderborn

2.2 Requested funds

2.2.1 Overview

Financial year	Funding for					Total
	Staff	Direct costs	Major research instrumentation	Fellowships	Global funds	
2018	712,500.-	158,000.-	558,000.-	0.-	85,000.-	**1,513,500.-**
2019	1,424,600.-	299,700.-	0.-	0.-	170,000.-	**1,894,300.-**
2020	1,424,600.-	291,700.-	0.-	0.-	170,000.-	**1,886,300.-**
2021	1,424,600.-	291,700.-	0.-	0.-	170,000.-	**1,886,300.-**
2022	712,500.-	146,000.-	0.-	0.-	85,000.-	**943,500.-**
Total	**5,698,800.-**	**1,187,100.-**	**558,000.-**	**0.-**	**680,000.-**	**8,123,900.-**

(All figures in EUR)

2.2.2 Overview of funds requested for staff

Project	2018					2019					2020					2021					2022				
	Postdocs	Doctoral researchers	Other research staff	Non-research staff	Research assistants	Postdocs	Doctoral researchers	Other research staff	Non-research staff	Research assistants	Postdocs	Doctoral researchers	Other research staff	Non-research staff	Research assistants	Postdocs	Doctoral researchers	Other research staff	Non-research staff	Research assistants	Postdocs	Doctoral researchers	Other research staff	Non-research staff	Research assistants
A1	-	2	-	-		-	2	-	-		-	2	-	-		-	2	-	-		-	2	-	-	
A2	-	2	-	-		-	2	-	-		-	2	-	-		-	2	-	-		-	2	-	-	
A3	-	1	-	-		-	1	-	-		-	1	-	-		-	1	-	-		-	1	-	-	
A4	-	2	-	-		-	2	-	-		-	2	-	-		-	2	-	-		-	2	-	-	
A5	1	-	-	-		1	-	-	-		1	-	-	-		1	-	-	-		1	-	-	-	
A6	-	1	-	-		-	1	-	-		-	1	-	-		-	1	-	-		-	1	-	-	
A7	-	1	-	-		-	1	-	-		-	1	-	-		-	1	-	-		-	1	-	-	
B1	-	2	-	-		-	2	-	-		-	2	-	-		-	2	-	-		-	2	-	-	
B2	-	2	-	-		-	2	-	-		-	2	-	-		-	2	-	-		-	2	-	-	
B3	-	1	-	-		-	1	-	-		-	1	-	-		-	1	-	-		-	1	-	-	
C1	-	2	-	-		-	2	-	-		-	2	-	-		-	2	-	-		-	2	-	-	
C2	1	1	-	-		1	1	-	-		1	1	-	-		1	1	-	-		1	1	-	-	
C3	-	2	-	-		-	2	-	-		-	2	-	-		-	2	-	-		-	2	-	-	
C4	-	2	-	-		-	2	-	-		-	2	-	-		-	2	-	-		-	2	-	-	
C5	-	1[1)]	-	-		-	1[1)]	-	-		-	1[1)]	-	-		-	1[1)]	-	-		-	1[1)]	-	-	
C6	-	2	-	-		-	2	-	-		-	2	-	-		-	2	-	-		-	2	-	-	
S1	-	1	-	-		-	1	-	-		-	1	-	-		-	1	-	-		-	1	-	-	
Z1	-	1[1)]	-	-	17	-	1[1)]	-	-	17	-	1[1)]	-	-	17	-	1[1)]	-	-	17	-	1[1)]	-	-	17
Total	2	26	-	-	17	2	26	-	-	17	2	26	-	-	17	2	26	-	-	17	2	26	-	-	17

In the individual projects, funding for doctoral researchers is requested for 67% positions with the exception of [1)] (**projects C5** and **Z1**), there we ask for 100% positions. Justifications are given in these projects. Funding for research assistants is incorporated into **project Z1** and thus into the global funds.

2.2.3 Overview of funds requested for major research instrumentation

Project	Description of instrumentation	Funds requested for				
		2018	2019	2020	2021	2022
A1	Gas adsorption apparatus	164,700.-	-	-	-	-
A2	Reactor anionic polymerization	25,000.-	-	-	-	-
A4	Autoclave	52,000.-	-	-	-	-
A7	Hydraulic pressure balance	10,900.-	-	-	-	-
B1	High-throughput equipment	10,600.-	-	-	-	-
B2	GC-MS	82,400.-	-	-	-	-
B2	High-throughput equipment	10,600.-	-	-	-	-
B3	High-throughput equipment	10,600.-	-	-	-	-
B3	chiral HPLC	27,500.-	-	-	-	-
C2	Mössbauer equipment	35,800.-	-	-	-	-
C2	Electrochem. equipment	19,000.-	-	-	-	-
C3	Optical parametric amplifier	88,500.-	-	-	-	-
C3	autocorrelator	20,400.-	-	-	-	-
Total		558,000.-	-	-	-	-

(All figures in EUR, including VAT, transportation, etc.)

3 Project details

3.1 Project A1

3.1.1 General information about Project A1

3.1.1.1 Monolithic polymeric supports with uniform pore diameter and tailored functional groups

3.1.1.2 Research Areas
Polymer Chemistry, Preparative and Physical Chemistry of Polymers (306-01)
Polymer Materials (306-03)

3.1.1.3 Principal Investigator
Buchmeiser, Michael R., Prof. Dr. born 08. 03. 1967, male, Austrian
Lehrstuhl für Makromolekulare Stoffe und Faserchemie, Institut für Polymerchemie
Universität Stuttgart, Pfaffenwaldring 55, 70569 Stuttgart
Tel.: 0711/685-64075
E-Mail: michael.buchmeiser@ipoc.uni-stuttgart.de
Tenured professor W3

3.1.1.4 Legal Issues
This project includes

1.	research on human subjects or human material.	no
2.	clinical trials.	no
3.	experiments involving vertebrates.	no
4.	experiments involving recombinant DNA.	no
5.	research involving human embryonic stem cells.	no
6.	research concerning the Convention on Biological Diversity.	no

3.1.2 Summary
For the first time, poly(urethane)- (PUR) based polymeric monolithic materials **with defined, narrow, unimodal, almost monodisperse porosity (*Đ* < 1.2) in the range of 2-20 nm, i.e. with mesopores, e.g., 5, 10, 15 or 20±1 nm in diameter**, will be generated. For these purposes, Janus-type nanoparticles equipped with one polymer-compatible and one polymer-incompatible hemisphere will be used in course of monolith synthesis such that they are finally located and half-embedded at the surface of the structure forming microglobules. Alternatively, polymeric monoliths with a defined pore-size distribution will be generated via solvent-induced phase separation. In parallel, in order to guarantee for a good permeability of the support and to make it suitable as catalytic support, transport pores in the micrometer range must be additionally generated in all monolithic structures. The monolithic materials' mesopores will be equipped with suitable **anchoring groups** for catalyst immobilization. As one guiding synthetic principle for the linker between the support and the catalyst, the Cu-catalyzed azide-alkyne Huisgen click chemistry is envisaged. In addition to the catalyst, tailored **functional groups** will be introduced into the pores, too, which will allow for tailoring the hydrophilic/hydrophobic and polar/non-polar character of the pore. In case of a Janus-type particle based approach, this is to be accomplished by a suitable reaction cascade. In case of monoliths with a defined pore size distribution, a pore size-selective functionalization approach will be employed to achieve a selective functionalization and catalyst immobilization inside the pores. The mespoporous monolithic materials will be used as supports for all catalytic reactions outlined in **projects B1** – **B3**. Catalytic reactions carried out in solution under similar (identical) conditions in terms of reactants, temperature, concentration, etc., using soluble catalysts structurally identical to the immobilized versions will be carried out to benchmark the supported catalyst versions. This will allow for studying the interplay between pore size (2-20 nm), pore shape (half sphere = "ink pot", cylinder), tortuosity, functionality (polar, non-polar, protic, non-protic), the chosen catalyst and its behavior in a given catalytic reaction.

3.1.3 Research rationale

3.1.3.1 Current state of understanding and preliminary work

Monolithic polymeric materials have gained a strong position in materials science, in particular in the areas of separation science and heterogeneous catalysis.[1-10] Interestingly, for both applications, supports are usually designed such that they display a very low micro-, meso- and macroporosity in order to reduce diffusion to a maximum extent, i.e. to limit it to Eddy-diffusion.[11] When used in heterogeneous catalysis, catalysts must be located at the surface of the structure-forming microglobules in order to be accessible for reactants. The necessary immobilization of the catalytic species can be accomplished by covalent binding of an organometallic complex. This, however, leads in view of the low specific surface areas of such monoliths (*vide infra*) to very low catalyst loadings, typically <0.01 mmol/g. Therefore, an alternative surface grafting approach using polymerizable organometallic complexes (catalysts) has been developed by our group allowing for catalyst loadings up to 1 mmol/g.[12-14] Apart from this tailored (non-) porosity, monoliths must possess large transport pores in the micrometer range (> 2 μm, Figure A1-1a), which guarantee for a good permeability of these materials. Under continuous conditions, these transport pores allow for high linear flow rates (≤ 20 mm/s) at low counter pressure (< 15 bar), even for solvents with viscosities up to ca. 500 mPa·s.[15] Following such a design, monolithic polymeric materials based on cross-linked polymers are typically characterized by a non-permanent, solvent swelling-induced porosity < 1 nm and by macropores >> 50 nm (500 Å, Figure A1-1b), which all together results in a very low specific surface area, in many cases < 10 m^2/g. While the pore size distribution of a polymeric monolithic support can be determined by N_2-adsorption, it is advisedly counterchecked by inverse-size exclusion chromatography (ISEC).[16-20] ISEC provides, in contrast to N_2-adsorption-derived values, the pore size distribution of the material *in the solvent swollen state* and thus in the state of operation. Depending on the material and degree of cross-linking, the individual values derived by these two entirely different techniques may differ significantly.

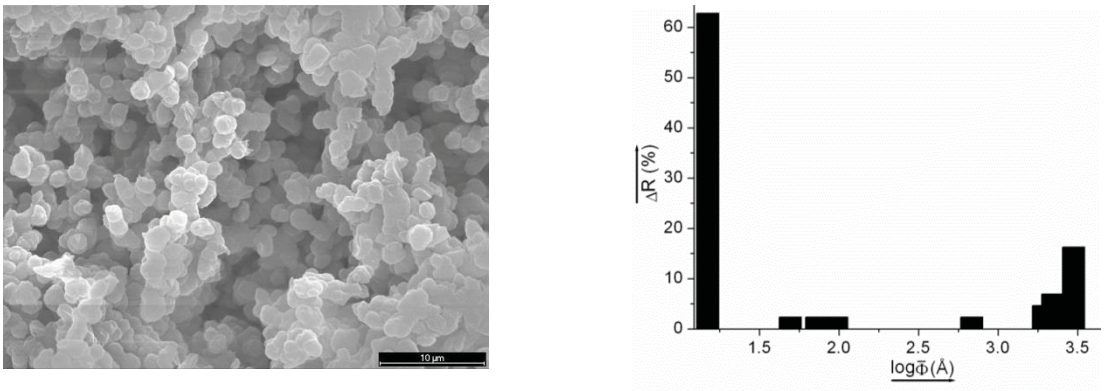

a) b)

Figure A1-1. a) Monolith structure; b) ISEC-derived distribution (relative abundance ΔR, %) of pore diameters (Φ, in Å) of monolithic supports. Pores < 1 nm (log(Φ =1.5)) are a result of a swelling-induced non-permanent porosity.

In terms of applicable types of polymerization, our group already successfully established synthetic routes to monolithic, polymeric separation materials with either continuous or discontinuous pore size distribution using ring-opening metathesis polymerization (ROMP), electron beam-, UV- or thermally induced free radical polymerization of (meth-)acrylates, as well as polyaddition.[1, 3, 12-13, 15, 21-79] The resulting polymeric monoliths have been successfully used for the separation of low molecular weight analytes,[53, 60] in proteomics and genomics,[13, 23, 26-27, 38, 41, 46, 50, 69-70, 75] in ultrafast size-exclusion chromatography of polymers,[25] in tissue engineering[48] and as support materials for nanoparticles,[58, 65-66, 77] organometallic catalysts and enzymes.[1, 14, 24, 29, 31-32, 34, 61, 71, 78-85] For the immobilization of organometallic catalysts and enzymes, both covalent binding and supported ionic liquid phase (SILP) technology[71, 78-79, 86] have been applied.

In terms of synthesis, several different approaches to polymeric, monolithic, porous supports exist. One is based on *solvent-induced phase separation (SIPS)*.[7] So far, this approach has been the method of choice in our group for the synthesis of monolithic supports. Its charming aspect is that the porosity of

the support can be determined by choosing the onset of phase separation together with the number of growing nuclei. An early onset of phase separation translates into (many) small nuclei while a late onset translates into (few) larger nuclei. Since these nuclei agglomerate and concomitantly swell to ultimately form the structure-forming microglobules (Scheme A1-1), the porosity of these microglobules strongly correlates with the packing density of the nuclei and, most important, with their size: the smaller the nuclei, the smaller the void volume between the resulting agglomerates and thus the lower the average pore diameter and the higher the pore volume is. The onset of phase separation as such is governed by temperature, the degree of cross-linking and the solvent mixture used. According to the Flory-Huggins equation,[87-88] it is, apart from temperature and the volume fractions of the solvents and the polymer, the Flory-Huggins interaction parameter χ and consequently the differences in the Hildebrand solubility parameters δ_i between polymer and solvent (mixtures) that govern this process. Generally, the situation with solubility parameters of solvent mixtures can be quite complex with polar (protic) solvent mixtures; however, here the non-solvent for polymers is usually a non-polar, aprotic one, which results in qualified average δ_i-values for the solvent mixture. Scheme A1-1 outlines the entire structure formation process in monolith synthesis and the genesis of microglobule porosity. It must be emphasized here that based on the above-outlined concept, both entirely non-porous monoliths with specific surface areas < 2 m^2/g and monoliths with a tailored porosity are accessible. Notably, both the size, i.e. the average diameter and volume fraction of the μm-sized *transport pores* is *not* affected by this process; these are solely governed by the monomer:solvent ratio, i.e. the volume fraction of monomers over the volume fraction of solvents.

An alternative, second approach, which is applicable in principle, too, utilizes the freezing of the solvent phase (cryogenic induced phase separation, CIPS) and might be applied if necessary. Finally, high-internal phase emulsion- (HIPE)[89-92] derived supports need to be mentioned. However, these will *not* be considered here since they possess a highly porous, open-pore microstructure[42] that is already provided by project **A7** (foams).

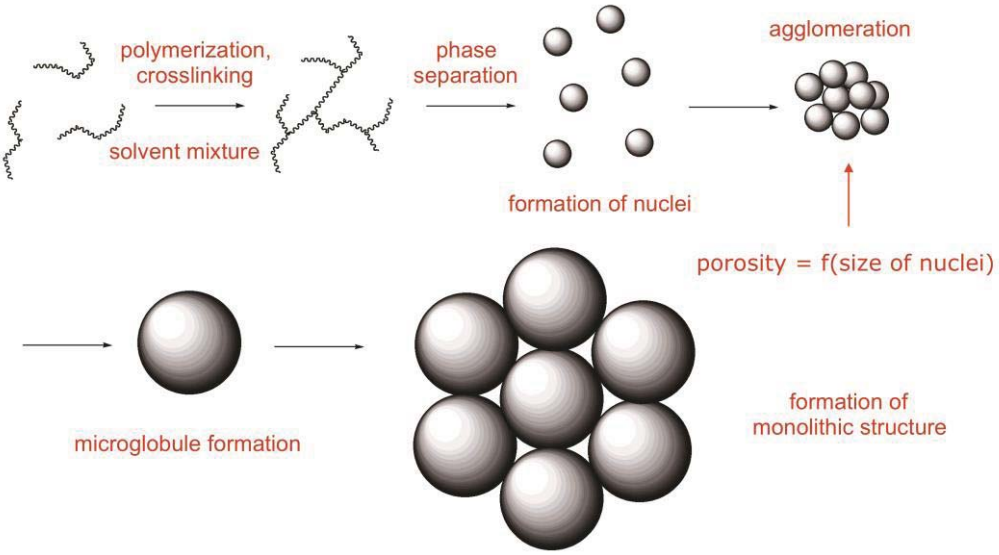

Scheme A1-1. Formation of a polymeric monolithic structure and tailoring of the porosity.

References

[1] E. B. Anderson, M. R. Buchmeiser, *ChemCatChem* **2012**, *4*, 30-44.
[2] R. D. Arrua, T. J. Causon, E. F. Hilder, *Analyst* **2012**, *137*, 5179-5189.
[3] M. R. Buchmeiser, *Macromol. Rapid. Commun.* **2001**, *22*, 1081-1094.
[4] M. R. Buchmeiser, *Angew. Chem.* **2001**, *113*, 3911-3913*; Angew. Chem. Int. Ed.* **2001**, *40*, 3795-3797.
[5] K. Cabrera, D. Lubda, H.-M. Eggenweiler, H. Minakuchi, K. Nakanishi, *J. High Resol. Chromatogr.* **2000**, *23*, 93-99.
[6] S. Eeltink, F. Švec, *Electrophoresis* **2007**, *28*, 137-114.

[7] F. Švec, T. B. Tennikova, Z. Deyl, *Monolithic Materials: Preparation, Properties and Application* In: J. Chromatogr. Libr., (Ed.), *Vol. 67*, Elsevier, Amsterdam, **2003**.
[8] F. Švec, *LC-GC Europe* **2005**, *18*, 17-20.
[9] E. C. Peters, F. Švec, J. M. J. Fréchet, *Adv. Mater.* **1999**, *11*, 1169-1181.
[10] T. B. Tennikova, B. G. Belenkii, F. Švec, *J. Liq. Chrom. & Rel. Technol.* **1990**, *13*, 63-70.
[11] A. A. Kalinske, C. L. Pien, *Ind. Eng. Chem.* **1944**, *36*, 220-223.
[12] S. Lubbad, M. R. Buchmeiser, *Macromol. Rapid Commun.* **2003**, *24*, 580-584.
[13] S. Lubbad, B. Mayr, M. Mayr, M. R. Buchmeiser, *Macromol. Symp.* **2004**, *210*, 1-9.
[14] M. R. Buchmeiser, *Chem. Rev.* **2009**, *109*, 303-321.
[15] R. Bandari, M. R. Buchmeiser, *Analyst* **2012**, *137*, 3271-3277.
[16] I. Halász, K. Martin, *Ber. Bunsenges. Phys. Chem.* **1975**, *79*, 731-732.
[17] I. Halász, K. Martin, *Angew. Chem.* **1978**, *90; Angew. Chem. Int. Ed*. **1978**, *17*, 901-909.
[18] M. Ousalem, X. X. Zhu , J. Hradil, *J. Chromatogr. A* **2000**, *903*, 13-19.
[19] Y. Yao, A. M. Lenhoff, *J. Chromatogr. A* **2004**, *1037*, 273-282.
[20] J. Urban, S. Eeltink, P. Jandera, P. J. Schoenmakers, *J. Chromatogr. A* **2008**, *1182*, 161-168.
[21] F. Sinner, M. R. Buchmeiser, *Angew. Chem.* **2000**, *112*, 1491-1494*; Angew. Chem. Int. Ed*. **2000**, *39*, 1433-1436.
[22] F. Sinner, M. R. Buchmeiser, *Macromolecules* **2000**, *33*, 5777-5786.
[23] B. Mayr, R. Tessadri, E. Post, M. R. Buchmeiser, *Anal. Chem.* **2001**, *73*, 4071-4078.
[24] M. Mayr, B. Mayr, M. R. Buchmeiser, *Angew. Chem.* **2001**, *113*, 3957-3960*; Angew. Chem. Int. Ed.* **2001**, *40*, 3839-3842.
[25] S. Lubbad, M. R. Buchmeiser, *Macromol. Rapid Commun.* **2002**, *23*, 617-621.
[26] S. Lubbad, B. Mayr, C. G. Huber, M. R. Buchmeiser, *J. Chromatogr. A* **2002**, *959*, 121-129.
[27] B. Mayr, G. Hölzl, K. Eder, M. R. Buchmeiser, C. G. Huber, *Anal. Chem.* **2002**, *74*, 6080-6087.
[28] M. R. Buchmeiser, *Metathesis Polymerization: A Versatile Tool for the Synthesis of Surface-Functionalized Supports and Monolithic Materials* In: Handbook of Metathesis, R. H. Grubbs (Ed), *Vol. 3*, Wiley-VCH, Weinheim, **2003**.
[29] M. R. Buchmeiser, S. Lubbad, M. Mayr, K. Wurst, *Inorg. Chim. Acta* **2003**, *345*, 145-153.
[30] J. O. Krause, S. Lubbad, M. Mayr, O. Nuyken, M. R. Buchmeiser, *Polym. Prepr. (Am. Chem. Soc., Div. Polym. Chem.)* **2003**, *44*, 790-791.
[31] J. O. Krause, S. Lubbad, O. Nuyken, M. R. Buchmeiser, *Adv. Synth. Catal.* **2003**, *345*, 996-1004.
[32] J. O. Krause, S. H. Lubbad, O. Nuyken, M. R. Buchmeiser, *Macromol. Rapid Commun.* **2003**, *24*, 875-878.
[33] C. Gatschelhofer, C. Magnes, T. R. Pieber, M. R. Buchmeiser, F. M. Sinner, *J. Chromatogr. A* **2005**, *1090*, 81-89.
[34] M. Mayr, D. Wang, R. Kröll, N. Schuler, S. Prühs, A. Fürstner, M. R. Buchmeiser, *Adv. Synth. Catal.* **2005**, *347*, 484-492.
[35] R. Bandari, A. Prager-Duschke, C. Kühnel, U. Decker, B. Schlemmer, M. R. Buchmeiser, *Macromolecules* **2006**, *39*, 5222-5229.
[36] S. Lubbad, S. A. Steiner, J. S. Fritz, M. R. Buchmeiser, *J. Chromatogr. A* **2006**, *1109*, 86-91.
[37] B. Schlemmer, G. Gatschelhofer, T. R. Pieber, F. M. Sinner, M. R. Buchmeiser, *J. Chromatogr. A* **2006**, *1132*, 124-131.
[38] R. Bandari, C. Elsner, W. Knolle, C. Kühnel, U. Decker, M. R. Buchmeiser, *J. Sep. Sci.* **2007**, *30*, 2821-2827.
[39] R. Bandari, W. Knolle, M. R. Buchmeiser, *Macromol. Rapid Commun.* **2007**, *28*, 2090-2094.
[40] R. Bandari, W. Knolle, M. R. Buchmeiser, *Macromol. Symp.* **2007**, *254*, 87-92.
[41] R. Bandari, W. Knolle, A. Prager-Duschke, M. R. Buchmeiser, *Macromol. Chem. Phys.* **2007**, *208*, 1428-1436.
[42] M. R. Buchmeiser, *Polymer* **2007**, *48*, 2187-2198.
[43] M. R. Buchmeiser, Monolithische Trägermaterialien für die Regenerativmedizin, DE 102007033078 A1, WO 2009010194 A1.
[44] K. Eder, C. G. Huber, M. R. Buchmeiser, *Macromol. Rapid Commun.* **2007**, *28*, 2029-2032.
[45] P. Sedláková, I. Miksik, C. Gatschelhofer, F. M. Sinner, M. R. Buchmeiser, *Electrophoresis* **2007**, *28*, 2219-2222.
[46] R. Bandari, W. Knolle, M. R. Buchmeiser, *J. Chromatogr. A.* **2008**, *1191*, 268-273.

[47] M. J. Beier, W. Knolle, A. Prager-Duschke, M. R. Buchmeiser, *Macromol. Rapid Commun.* **2008**, *29*, 904-908.
[48] A. Löber, A. Verch, B. Schlemmer, S. Höfer, B. Frerich, M. R. Buchmeiser, *Angew. Chem.* **2008**, *120*, 9279-9281*; Angew. Chem. Int. Ed.* **2008**, *47*, 9138-9141.
[49] F. M. Sinner, C. Gatschelhofer, A. Mautner, C. Magnes, M. R. Buchmeiser, T. R. Pieber, *J. Chromatogr. A.* **2008**, *1191*, 274-281.
[50] M. R. Buchmeiser, *ROMP-Derived Monoliths: Novel Materials for Separation Science, Heterogeneous Catalysis and Regenerative Medicine* In: NATO Science for Peace and Security Series A. Chemistry and Biology*,* E. Khosravi, Y. Yagci, Y. Savelyev, Klywer, Dordrecht, **2009**.
[51] M. R. Buchmeiser, *J. Polym. Sci. A: Polym. Chem.* **2009**, *27*, 2219-2227.
[52] C. Gatschelhofer, A. Mautner, F. Reiter, T. R. Pieber, M. R. Buchmeiser, F. M. Sinner, *J. Chromatogr. A* **2009**, *1216*, 2651-2657.
[53] S. H. Lubbad, M. R. Buchmeiser, *J. Sep. Sci.* **2009**, *32*, 2521-2529.
[54] B. Scheibitz, A. Prager, M. R. Buchmeiser, *Macromolecules* **2009**, *42*, 3493-3499.
[55] B. Schlemmer, R. Bandari, L. Rosenkranz, M. R. Buchmeiser, *J. Chromatogr. A* **2009**, *1216*, 2664-2670.
[56] R. Bandari, T. Höche, A. Prager, K. Dirnberger, M. R. Buchmeiser, *Chem. Eur. J.* **2010**, *16*, 4650-4658.
[57] S. Beckert, F. Stallmach, R. Bandari, M. R. Buchmeiser, *Macromolecules* **2010**, *43*, 9441-9446.
[58] M. R. Buchmeiser, R. Bandari, A. Prager-Duschke, A. Löber, W. Knolle, *Macromol. Symp.* **2010**, *287*, 107-110.
[59] A. Löber, B. Scheibitz, B. Frerich, M. R. Buchmeiser, *Macromol. Symp.* **2010**, *293*, 48-52.
[60] S. H. Lubbad, M. R. Buchmeiser, *J. Chromatogr. A* **2010**, *1217*, 3223-3230.
[61] S. Mavila, M. R. Buchmeiser, *Macromolecules* **2010**, *43*, 9601-9607.
[62] F. Weichelt, B. Frerich, S. Lenz, S. Tiede, M. R. Buchmeiser, *Macromol. Rapid Commun.* **2010**, *31*, 1540-1545.
[63] F. Weichelt, S. Lenz, S. Tiede, I. Reinhardt, B. Frerich, M. R. Buchmeiser, *Beilstein J. Org. Chem.* **2010**, *6*, 1199-1205.
[64] E. B. Anderson, B. Autenrieth, M. R. Buchmeiser, in *Stuttgarter Kunststoffkolloquium* (Eds.: C. Bonten, M. R. Buchmeiser), Stuttgart, **2011**.
[65] R. Bandari, M. R. Buchmeiser, *Catal. Sci. Technol.* **2011**, *2*, 220-226.
[66] R. Bandari, A. Prager, T. Höche, M. R. Buchmeiser, *ARKIVOC* **2011**, *iv*, 54-70.
[67] C. Elsner, C. Ernst, M. R. Buchmeiser, *J. Appl. Polym. Sci.* **2011**, *119*, 1450-1458.
[68] C. Ernst, C. Elsner, A. Prager, B. Scheibitz, M. R. Buchmeiser, *J. Appl. Polym. Sci.* **2011**, *121*, 2551-2558.
[69] S. H. Lubbad, R. Bandari, M. R. Buchmeiser, *J. Chromatogr. A* **2011**, *1218*, 8897-8902.
[70] S. H. Lubbad, M. R. Buchmeiser, *J. Chromatogr. A* **2011**, *1218*, 2362-2367.
[71] B. Autenrieth, W. Frey, M. R. Buchmeiser, *Chem. Eur. J.* **2012**, *18*, 14069-14078.
[72] R. Bandari, M. R. Buchmeiser, *Macromol. Rapid Commun.* **2012**, *33*, 1399-1402.
[73] C. Gatschelhofer, A. Prasch, M. R. Buchmeiser, A. Zimmer, K. Wernig, M. Griesbacher, T. R. Pieber, F. M. Sinner, *Anal. Chem.* **2012**, *84*, 7415-7421.
[74] S. Reichelt, C. Elsner, A. Prager, S. Naumov, J. Kuballa, M. R. Buchmeiser, *Analyst* **2012**, *137*, 2600-2607.
[75] R. Bandari, J. Kuballa, M. R. Buchmeiser, *J. Sep. Sci.* **2013**, *36*, 1169-1175.
[76] M. Sudheendran, S. H. Eitel, S. Naumann, M. R. Buchmeiser, R. Peters, *New. J. Chem.* **2014**, *38*, 5597-5607.
[77] V. P. Taori, R. Bandari, M. R. Buchmeiser, *Chem. Eur. J.* **2014**, *20*, 3292–3296.
[78] B. Sandig, L. Michalek, S. Vlahovic, M. Antonovici, B. Hauer, M. R. Buchmeiser, *Chem. Eur. J.* **2015**, *21*, 15835-15842.
[79] B. Sandig, M. R. Buchmeiser, *ChemSusChem* **2016**, *9*, 2917-2921.
[80] B. Bantu, K. Wurst, M. R. Buchmeiser, *Tetrahedron* **2005**, *61*, 12145-12152.
[81] T. S. Halbach, S. Mix, D. Fischer, S. Maechling, J. O. Krause, C. Sievers, S. Blechert, O. Nuyken, M. R. Buchmeiser, *J. Org. Chem.* **2005**, *70*, 4687-4694.
[82] N. Imlinger, K. Wurst, M. R. Buchmeiser, *Monatsh. Chem.* **2005**, *136*, 47-57.
[83] M. R. Buchmeiser, *Immobilization of Metathesis Catalysts* In: "Olefin Metathesis - Theory and Praxis*,* K. Grela, John Wiley & Sons, **2014**.
[84] M. R. Buchmeiser, *New J. Chem.* **2004**, *28*, 549-557.

[85] M. R. Buchmeiser, *Catal. Today* **2005**, *105*, 612-617.
[86] P. Lozano, E. García-Verdugo, R. Piamtongkam, N. Karbass, T. De Diego, M. I. Burguete, S. V. Luis, J. L. Iborra, *Adv. Synth. Catal.* **2007**, *349*, 1077-1084.
[87] P. J. Flory, *J. Chem. Phys.* **1942**, *10*, 51-61.
[88] P. J. Flory, *J. Chem. Phys.* **1949**, *17*, 223-240.
[89] H. Deleuze, R. Faivrea, V. Herroguez, *Chem. Commun.* **2002**, 2822-2823.
[90] P. Krajnc, J. F. Brown, N. R. Cameron, *Org. Lett.* **2002**, *4*, 2497-2500.
[91] P. Krajnc, D. Stefanec, I. Pulko, *Macromol. Rapid. Coomun.* **2005**, *26*, 1289-1293.
[92] N. R. Cameron, *Polymerized High Internal Phase Emulsion Monoliths* In: J. Chromatogr. Libr. "Monolithic Materials: Preparation, Properties and Application", F. Ŝvec, T. B. Tennikova, Z. Deyl (Ed), *Vol. 67*, Elsevier, Amsterdam, **2003**.

3.1.3.2 Project-related publications by participating researchers

[A1-1] F. Sinner, M. R. Buchmeiser, *Angew. Chem.* **2000**, *112*, 1491-1494*; Angew. Chem. Int. Ed*. **2000**, *39*, 1433-1436.
[A1-2] F. Sinner, M. R. Buchmeiser, *Macromolecules* **2000**, *33*, 5777-5786.
[A1-3] M. Mayr, B. Mayr, M. R. Buchmeiser, *Angew. Chem.* **2001**, *113*, 3957-3960*; Angew. Chem. Int. Ed.* **2001**, *40*, 3839-3842.
[A1-4] A. Löber, A. Verch, B. Schlemmer, S. Höfer, B. Frerich, M. R. Buchmeiser, *Angew. Chem.* **2008**, *120*, 9279-9281*; Angew. Chem. Int. Ed.* **2008**, *47*, 9138-9141.
[A1-5] R. Bandari, T. Höche, A. Prager, K. Dirnberger, M. R. Buchmeiser, *Chem. Eur. J.* **2010**, *16*, 4650-4658.
[A1-6] S. H. Lubbad, M. R. Buchmeiser, *J. Chromatogr. A* **2010**, *1217*, 3223-3230.
[A1-7] B. Autenrieth, W. Frey, M. R. Buchmeiser, *Chem. Eur. J.* **2012**, *18*, 14069-14078.
[A1-8] E. B. Anderson, M. R. Buchmeiser, *ChemCatChem* **2012**, *4*, 30-44.
[A1-9] B. Sandig, L. Michalek, S. Vlahovic, M. Antonovici, B. Hauer, M. R. Buchmeiser, *Chem. Eur J.* **2015**, *21*, 15835-15842.
[A1-10] B. Sandig, M. R. Buchmeiser, *ChemSusChem* **2016**, *9*, 2917-2921.

3.1.4 Project plan

The choice of the polymer system for this project obviously is crucial. With regards to the nature of the polymeric, monolithic matrix as such, a polymer system needs to be chosen that is dimensionally stable and does not swell in the solvents to be used in the envisaged catalytic reactions (e.g., 1,2-dichloroethane, toluene, THF, dioxane, THF/water, etc., c.f. **projects B1** – **B3**). This obviously requires a high degree of crosslinking. In addition to that, the polymer chemistry of choice should offer the possibility of post-synthesis functionalization in order to tailor the inner surface of a pore in terms of polarity and to facilitate other post-synthesis modifications such as mineralization (c.f. **project A-5**). Equally important, the final cross-linked polymer should display a polarity that allows for introducing both polar and non-polar solvents. In view of this general framework, poly(urethane)- (PUR) based monoliths, which have only recently been developed in our group,[78-79] appear suitable, the more since they also possess substantial stability versus acids. The general suitability of SIPS for the synthesis of polymeric monoliths in the presence of nanoparticles has already been demonstrated earlier[62-63] and will be applied here, too. Clearly, this “materials” project must provide polymeric monolithic supports that are suitable for studying the confinement effects outlined in the catalysis projects. With regards to that, the main goal is the realization of polymeric monolithic materials with **defined, unimodal, „monodisperse“ porosity in the range of 5-20 nm**. Notable, this induced mesoporosity will also enlarge the otherwise low specific surface area of polymeric monoliths (*vide supra*). In addition to this mesoporosity, **transport pores in the micrometer range** must be generated in order to realize their use as fully permeable catalytic supports for use in continuous catalytic reactions. Furthermore, suitable anchoring groups for the immobilization of the catalysts must be selectively allocated in a spatially defined way **inside** the pores. Pore diameter, pore functionality (polar, non-polar), aspect ratio of the pores (1, >>1) can be varied to study confinement effects. The corresponding work packages necessary to accomplish this goal are as follows:

- **WP 1: Generation of a tailored porosity via templating with Janus-type nanoparticles.** This work package entails the modification of both spherical and rod-like Janus nanoparticles in such way that they can be incorporated at the surface of the structure-forming microglobules of the monoliths such that upon removal defined pores are generated at the surface of the otherwise non-porous microglobules.
- **WP 2: Synthesis of surface-modified nanoparticles.** This WP entails the synthesis of bifunctional Janus nanoparticles and nano-rods. A biphasic mixture of a strongly hydrophilic (ionic) and a comparably hydrophobic reagent will be used for these purposes. Nanoparticles and rods will be chosen such that they can be removed by simple acid treatment to allow for the generation of well-defined pores.
- **WP 3: Generation of mesoporous PUR-based monolithic supports via SIPS.** This is the alternative approach to WP1, in which a certain mesoporosity is generated in monoliths using solvent-induced phase separation (SIPS). Pores with larger diameters can be rendered innocent using a pore-selective functionalization approach outlined in WP 5.
- **WP 4: Variation of pore diameter and pore geometry.** For these purposes, grafting-from techniques based on living or controlled polymerizations, surface functionalization with carboxylic acids followed by ion-pair formation with tertiary amines as well as a bio-inspired minearilzation approach are envisaged to study confinement effects.
- **WP 5: Functionalization of monoliths.** Functionalization of the monoliths and in particular of the monoliths pores is necessary to i) generate immobilization sites for the catalysts and ii) to vary the polarity of the pore to study confinement effects. Copper-catalyzed ene-yne click chemistry and surface silanization can be used to accomplish these goals.
- **WP 6: Pore size-selective functionalization of monoliths prepared via SIPS.** For these purposes, both a polymer- and a silane-based approach will be used. The first entails the per-epoxidation of the support followed by the selective hydrolysis of epoxides outside the pores using a polymer reagent. The remaining epoxies inside the pores can then be used for catalyst immobilization.
- **WP 7: Linker chemistry for the immobilization of catalysts.** This work package will allow for establishing all the necessary chemistry for catalyst immobilization and its spatially defined allocation. Actions include variations in the nature of the linker in terms of length and flexibility.

3.1.4.1 WP 1: Mesoporous polymeric monoliths with tailored porosity via templating with Janus-type nanoparticles

Irrespective of the method applied to monolith synthesis, i.e. whether it is to be based on SIPS or CIPS (see 3.1.3.1), at least two approaches can be envisaged for the generation of a tailored porosity. One suitable and straightforward method for generating a perfectly *unimodal* porosity in the range of 2-20 nm with a narrow pore size distribution is the *template approach*. For these purposes, nano-scaled, surface-modified Janus particles[93-96] with narrow particle diameter distribution are envisaged. For their realization refer to section 3.1.4.2. In order to keep the mass-fraction of nanoparticles, which must be predominantly located at the microglobules' surface of the structure-forming microglobules, as high as possible, the microglobules themselves must be small (ca. 1-2 µm, Scheme A1-1). This requires an early onset of phase separation (see section 3.1.3.1, which is in the case of PUR-based monoliths probably best accomplished by the use of a trifunctional isocyanate such as hexamethylenediisocyanate trimer and a multifunctional alcohol, e.g., poly(hydroxyethyl(meth)acrylate in combination with (low amounts of) 1,2-dichloromethane (δ_1 = 9.73 (cal/cm^3)$^{0.5}$) or THF (δ_1 = 9.49 (cal/cm^3)$^{0.5}$) as good and (large amounts of) heptane (δ_1 = 7.48 (cal/cm^3)$^{0.5}$) as poor polymer solvent (non-solvent). Apart from the large, micrometer-sized transport pores, the monoliths prepared by such an approach are expected to be virtually non-porous with some uncritical solvent swelling-induced microporosity in the <1 nm range. To accomplish an embedding of the nanoparticles at the microglobules' surface such that the nanoparticles are positioned half inside, half outside the polymeric matrix, functionalization of the nanoparticles must be accomplished according to a Janus-type[93-96] concept using one polymer-compatible and one polymer-incompatible functionalization, each selectively located either in the "northern" or "southern" hemisphere of the nanoparticles, respectively. One hemisphere of the Janus nanoparticles must be functionalized such that the corresponding half-sphere is fully compatible with the PUR-based polymeric matrix and the "good" polymer solvent. By contrast,

the second half-sphere must be totally incompatible with the polymer but compatible with the “poor” polymer solvent. This approach will allow for realizing a tailored penetration (Scheme A1-2) of the nanoparticles into the surface of the microglobules during monolith synthesis.

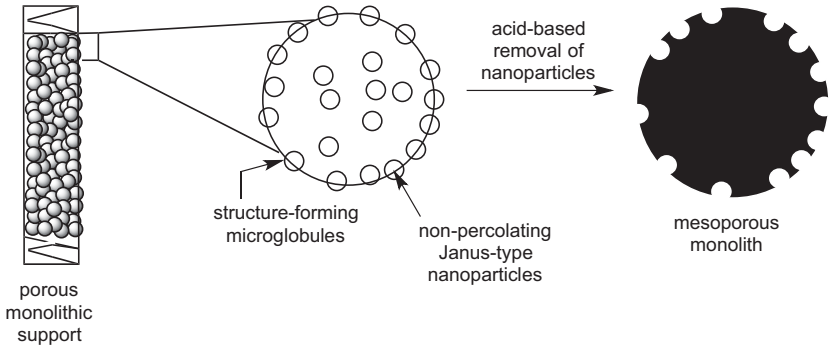

Scheme A1-2. Synthesis of mesoporous, polymeric monoliths with narrow (almost monodisperse) pore size distribution.

With the two types of functionalization present, the nanoparticles must be expected to concentrate at the phase border between the polymer, which is swollen by monomers and 1,2-dichloroethane and the second, heptane-rich phase such that they predominantly reside at the surface of the structure-forming microglobules, too. All this is proposed to proceed in analogy to ROMP-derived monoliths, were the polar Ru-based initiator is also mainly (>96%) located at the solid-liquid interface, i.e. at the microglobules’ surface.[21-22, 24] Finally, after monolith synthesis is complete, the templating Janus nanoparticles can be removed from the polymeric support via dissolution in dilute acid (HCl or acetic acid), leaving cup-type pores with an aspect ratio of roughly 1 behind. In order to obtain pores with an aspect ratio >>1, nanorods can be used, too, applying the same concept.

3.1.4.2 WP 2: Synthesis of surface-modified nanoparticles

A substantial variety of nanoparticles with narrow and defined particle size distributions is commercially available. The list includes but is not limited to metal oxides such as γ-Al_2O_3 (5, 10, 20 nm), ZnO (20 nm), $Mg(OH)_2$ (15 nm) and magnetic Fe_3O_4 (10 nm) or metals such as Ni (20 nm), Fe (25 nm) or Al (18 nm). All nanoparticles outlined here are acid soluble (acetic acid or HCl) and can thus be removed from the polymeric matrix at a later stage, provided they are embedded into the surface of the microglobules as outlined in section 3.1.4.1.2. Gratifyingly, any nanoparticles that become fully embedded in the polymeric matrix are “innocent” as such and must therefore not be removed. This half embedding into the monolithic, polymeric matrix requires the above-mentioned Janus-type concept that entails the synthesis of surface-modified, bifunctional nanoparticles with two different types of functional groups at the surface of the “northern” and “southern” hemisphere. Scheme A1-3 illustrates the concept for their synthesis that is based on the work of Andala et al.[97] Using a biphasic system based on toluene and water, nanoparticles are treated with a mixture of a strongly hydrophilic (ionic) and a comparably hydrophobic reagent, e.g. a hydroxylated alkane. The former dissolves in water while the latter dissolves in the organic phase. Upon addition of the parent nanoparticles, these accumulate at the phase border of the two solvent phases and react there with the individual reagents, thereby forming the bifunctional Janus-type nanoparticles.

As another fundamental requirement, surface functionalization of the nanoparticles must also be embellished in a way that percolation of these nanoparticles is effectively suppressed since this would unwantedly increase the final mean pore diameter in case entire agglomerates would allocate at the surface of the microglobules. This requires at least partially charged surfaces. Fortunately, the chosen approach according to ref.[97] does provide charged particles. As an example, Fe_3O_4 nanoparticles are treated with a mixture of a hydrophobic reagent, e.g. 1,2-dihydroxydecane, DHD, and a hydrophilic reagent, e.g., sodium dihydroxycinnamate, DHC, in a mixture of toluene and water (pH ≥ 10). Stable Janus-type nanoparticles form at the interface and can, in the case of Fe_3O_4 be easily separated by a magnet. These bifunctional nanoparticles will then used in monolith synthesis.[97]

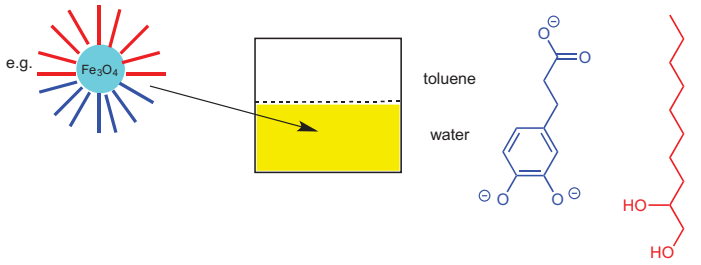

Scheme A1-3. Synthesis of bifunctional Janus-type particles acc. to ref. [97].

Depending on the type of nanoparticle used, different functional groups can be envisaged, which strongly bind or adsorb to the corresponding nanoparticles, thereby forming stable Janus-type nanoparticles:

Nanoparticle	**γ-Al_2O_3**	**Al**	**ZnO**	**$Mg(OH)_2$**	**Fe_3O_4**	**Fe**	**Ni**
Functional groups (selection)[98]	phenolates	phenolates	RCN RSCN	$RCOO^-$	RPO_3^-, 1,1-dipyridyl	RPO_3^-, 1,1-dipyridyl	RCN RSCN

In order to avoid cannibalistic replacement of one type of ligand, e.g., the less polar, non-ionic one, by the other type of ligand, e.g. the polar, ionic one, the chosen functional group or at least very similar ones have to be used for both types of ligands. Table 1 exemplifies potential combinations of compounds to be used for functionalization.

Table 1. Potential combinations for the polar, ionic and less polar, non-ionic derivatization agents for the preparation of Janus nanoparticles.

Type/compound	phenolate	RCN/RSCN	RPO_3^-	dipyridyl reagent
polar/ionic	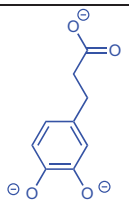	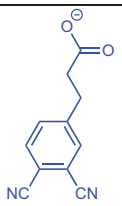		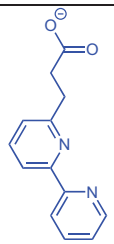
less-polar/non ionic				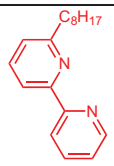

3.1.4.3 WP 3: Generation of mesoporous PUR-based monolithic supports via SIPS

Alternatively, monolithic supports with a designed, yet not monodisperse but still sufficiently narrow pore size distribution is accessible via SIPS. As already demonstrated for ROMP-derived, poly(norborn-2-ene)-[25] or poly(*cis*-cyclooctene)-[35, 37] based monoliths such an approach allows for a defined but more *continuous* pore size distribution covering pore diameters in a narrow *range*, e.g. 5 – 15 nm, see

Figure A1-1b. This can be accomplished via the tailoring of the onset of phase separation as outlined in section 3.1.3.1, again using hexamethylenediisocyanate trimer and a multifunctional alcohol, e.g., poly(hydroxyethyl(meth)acrylate). In order to access a pore range of 5 – 15 nm, the onset of phase separation must be somewhat delayed, which in turn translates into larger amounts of good polymer solvent (THF or 1,2-dichloroethane) and lower amounts of poor polymer solvent (heptane). Alternatively, poly(hydroxyethyl(meth)acrylate can be replaced by a simple triol such as 1,1,1-tris(hydroxymethyl)-propane, which lowers the degree of cross-linking compared to poly(hydroxyethyl(meth)acrylate. Any pores that are larger than those envisaged for catalyst immobilization can be rendered "innocent" via the pore-size selective functionalization approach outlined in section 3.1.4.6.

3.1.4.4 WP 4: Variation of pore diameter and pore geometry

Obviously, the pore diameters that can be realized via the templating approach using Janus-type nanoparticles are determined by the size of the nanoparticles chosen. Similar holds for the SIPS- (or CIPS-) based approach; with these techniques a certain range of pore diameters is accessible, however also with some limitation. In order to gain access to a more incremental variation of the pore diameter and thus to a higher degree of precision in the tuning of the average pore diameter, grafting-from approaches based on living polymerizations such as ROMP,[12, 99-100] atom-transfer radical polymerization (ATRP)[101-102] or reversible addition fragmentation transfer (RAFT)[103] polymerization can be applied (Scheme A1-4).

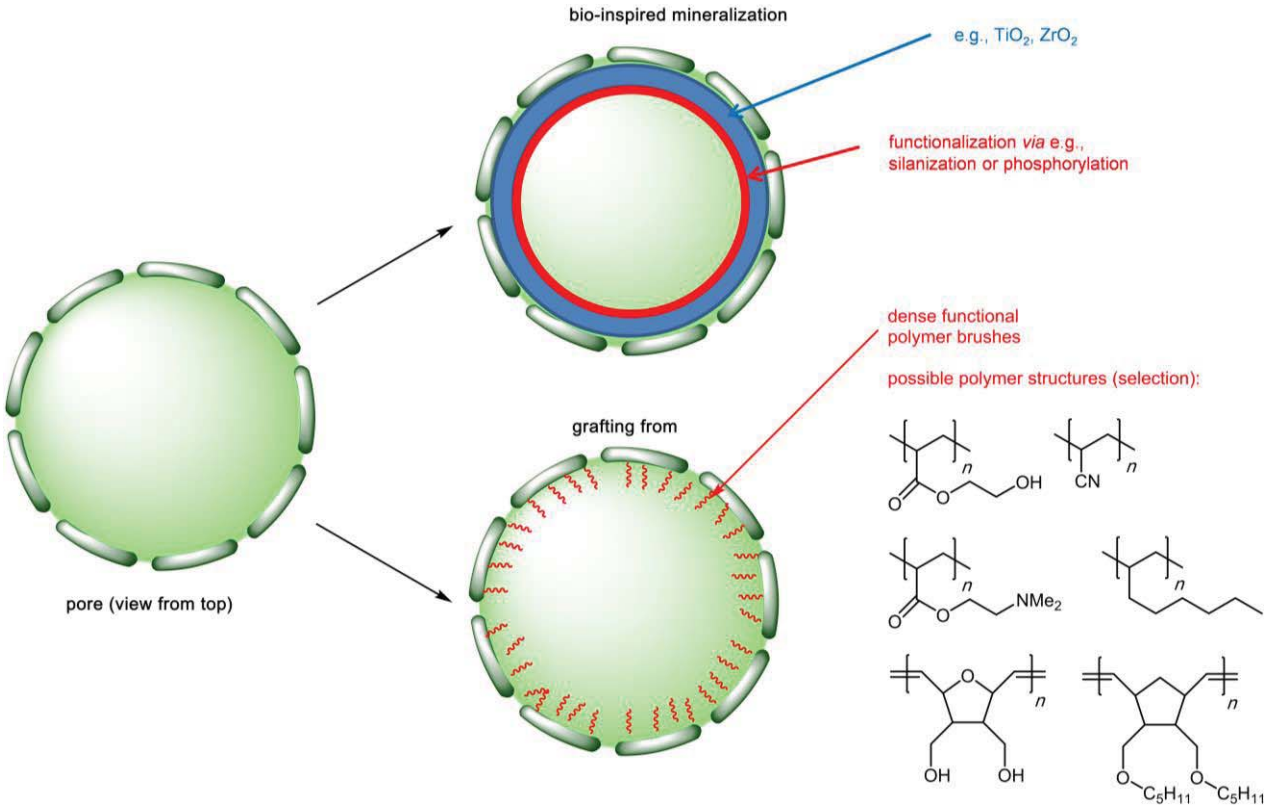

Scheme A1-4. Examples for the variation and functionalization of the inner pore diameter; top: via bio-inspired mineralization in cooperation with **project A5**; bottom: via grafting-from.

Such a grafting-from approach allows for realizing dense polymer brushes with very defined degrees of polymerization (Δ(DP) << 10%) and length and therefore for the desired fine-tuning of the pore diameter. In addition, these techniques allow for the use of functional monomers including polar and protic ones, too. Consequently, this offers also access to designed pores in terms of polarity (seen also section 3.1.4.4). Alternatively, free carboxylic acid groups can be introduced to the pore surface, e.g. via ring-opening of epoxy groups with sodium *N,N*-dimethylaminoethylcarboxylate. After reprotonation

of the carboxylic acid, reaction with tertiary amines of different size allows for the careful tuning of the pore diameter, too, though certainly to a limited extent. Thus, changes in pore diameter will be <2 nm.

Finally, mineralization of the pore allows for a reduction of the pore diameter (**project A5**, Scheme A1-4). Mineralized pores, e.g. using TiO_2, can then be further functionalized with, e.g., methoxysilanes. In such an approach, commercially available $C_{18}H_{37}$-, C_8H_{17}-, cyanopropyl-dimethylaminopropyltrimethoxysilanes, etc., can be used to generate the desired polar or non-polar and even ionic inner surfaces. Mineralized, ZrO_2-based surfaces can be functionalized using the corresponding phosphonates and phosphates, e.g. cyanoethylphosphate, naphthylphosphate, dibutylphosphite, etc. All these approaches serve the variation of the pore diameter and aspect ratio to study the confinement effects outlined in the catalysis projects.

3.1.4.5 WP 5: Functionalization of monoliths

Functionalization of PUR-based monoliths can be accomplished *in situ*.[8,9] Thus, the use of an excess of the alcohol component results in polar, OH-functionalized polymers, while an excess of isocyanate offers NCO- or, after hydrolysis of the isocyanates, polar NH_2- or, after protonation or peralkylation, polar, ionic ammonium-functionalized monoliths. Isocyanates can also be further derivatized with suitable amines or alcohols. Generally, hydroxyl groups can be further derivatized with silanes of the general formula $(MeO)_3SiR$ or $(EtO)_3SiR$ (R = alkyl, cyanoalkyl, PEG, dimethylaminopropyl, azidoalkyl, etc.). Depending on the silane used, either non-polar surfaces, e.g. via silanization with $(MeO)_3SiC_{18}H_3$, or polar surfaces, e.g. via use of *N*,*N*-dimethylaminopropyldimethylchlorosilane can be established. This way, confinement effects induced by a certain polarity can be studied (c.f. catalysis projects). It is worth pointing out that the functionalization cascades outlined here will also be used for the immobilization of the target catalysts see 3.1.4.6). Scheme A1-5 outlines the envisaged reaction cascades for functionalization.

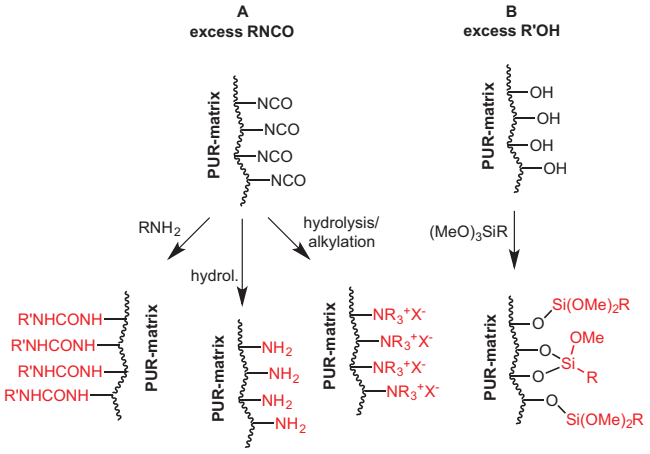

Scheme A1-5. Possibilities for derivatization (selection) relevant to surface functionalization and catalyst immobilization. R = e.g., $-C_8H_{17}$, $-C_{18}H_{37}$, $-(CH_2)_3$-CN, -PEG, $-(CH_2)_3NMe_2$, $-(CH_2)_n-N_3$ (n = 3, 11).

The approach outlined in Scheme A1-5A using monoliths prepared from excess isocyanate is particularly suited for the *templating approach* outlined in section 3.1.4.1.2. In this approach, the reaction sequence for functionalization is essential in order to avoid pore-selective functionalization. First, after monolith synthesis, the surface of the structure-forming microglobules, i.e. the monolith's surface is functionalized in the desired manner as described in Scheme A1-5A. The next step entails the removal of the templating, bifunctional Janus nanoparticles via acid treatment followed by the immobilization of the catalyst as outlined in section 3.1.4.6 and functionalization of the pores' surface (Scheme A1-6). Notably, this approach avoids any pore size-selective functionalization (see section 3.1.4.6).

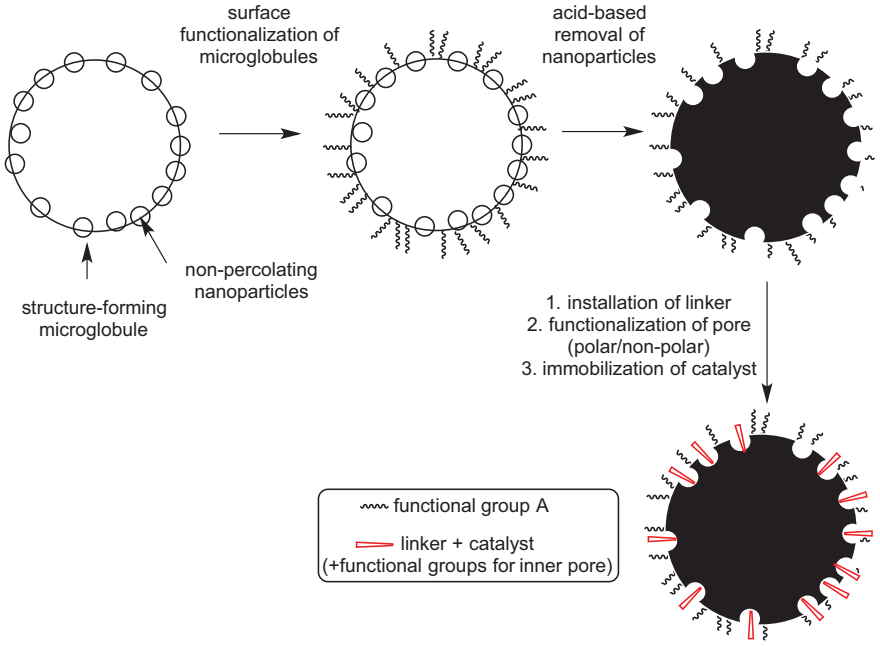

Scheme A1-6. Reaction cascade for surface modification and catalyst immobilization to be used in the *templating approach*.

3.1.4.6 WP 6: Pore size-selective functionalization of monoliths prepared via SIPS

In case the afore-mentioned, alternative approach based on monolithic supports with a designed pore size distribution with pore diameters predominantly in the range of 5 – 15 nm is to be used *en lieu* the Janus-particle-based approach, a *pore size-selective functionalization* is required. This can be realized through a per-epoxidation of hydroxyl-functionalized monoliths via reaction with epichlorohydrin, followed by selective hydrolysis of the oxirane outside the mesopores by a polymeric reagent with a radius of gyration 2.5 times the pore diameter following the rule of thumb that a pore must be ca. 2.5 times larger in diameter than the hydrodynamic radius of a compound/polymer that is to penetrate this pore. Consequently, polymers with a diameter >2.5 times the diameter of the pore cannot enter this pore (Scheme A1-7, **A**).[56, 58, 104] The remaining oxiranes inside the pores can then be used for catalyst immobilization and further polar/non-polar functionalization of the pore. In case of small mesopores < 5 nm, a hydroxyl-functionalized surface outside the pores can be excluded from reaction with catalyst via (acid or base-catalyzed) reaction with sterically demanding silanes such as (commercially available) heptakis(isobutyl)glycidoxypropylsilsesquioxane (pore diameter < 3 nm) or reaction with trimethoxysilyl-terminated polymers such as α-trimethyloxysilyl-poly(methyl methacrylate) or α-trimethyloxysilyl-poly(propylene oxide) (pore diameter < 5 nm). These telechelic polymers can be prepared by, e.g. living anionic polymerization in our laboratories. Molecular weights, radii of gyration and hydrodynamic radii in a given solvent can be determined by GPC-MALLS – viscosimetry - RI using the following equations:

$$[\eta]M = 10/3\Pi \cdot R_h^3 \text{ and } [\eta]M = 6^{1.5}\Phi_0 \cdot R_g^3.$$ [105]

For catalyst immobilization, isocyanate-functionalized catalysts can be directly reacted with the surface silanols or, alternatively, small but reactive silanes, e.g., trimethoxysilylpropylisocyanate are introduced into the pores and are then used for catalyst immobilization (Scheme A1-7, **B**). Finally, click-chemistry can be used for catalyst immobilization. Thus, either propargyl or azide-functionalized pores can be reacted with the corresponding counterparts, i.e. with azide or alkyne-functionalzed catalysts (Scheme A1-7B).

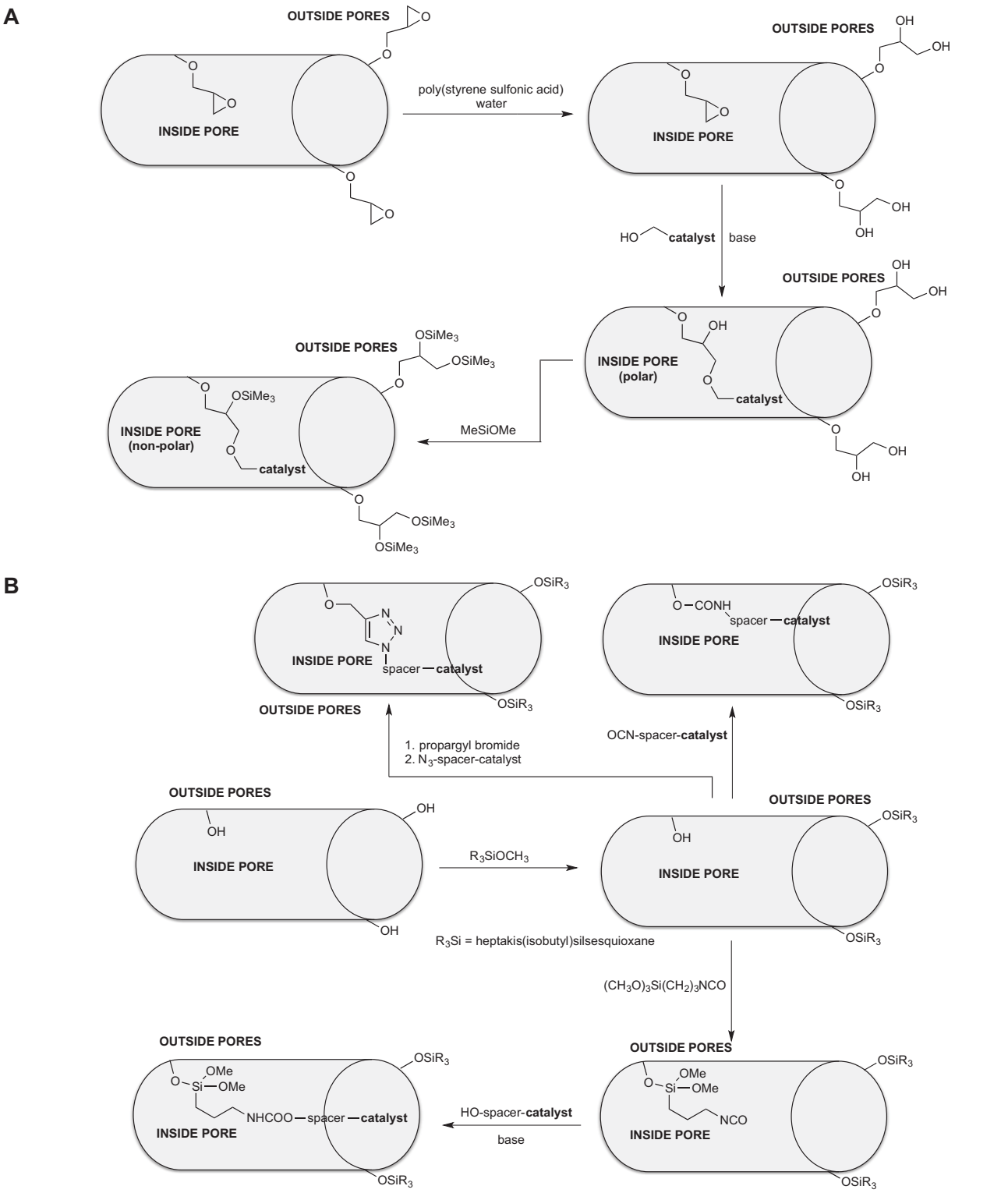

Scheme A1-7. Approaches to pore size-selective functionalization. Top (**A**): epoxy-based approach for small and large pores up to 20 nm. Bottom (**B**): reactive silane approach for small pores (< 5 nm). Base = 2,6-lutidine, 2,6-di(*t*-Bu)-pyridine.

3.1.4.7 WP 7: Linker chemistry for the immobilization of catalysts

The tailored polymeric monolithic materials prepared in course of this project will be used for the immobilization of catalysts prepared in **projects B1** – **B3**. Attachment of the linker to the individual catalysts is outlined in **projects B1** – **B3**. Generally, a tailored and spatially resolved catalyst immobilization inside *but not outside* the pores is a crucial point. Both the linker as such and the immobilization chemistry have to fulfill the following standards:

i) the linker may not interfere, i.e. react with or coordinate to the catalyst as such or even change the geometry of the catalyst, which is of particular importance for enantioselective reactions;

ii) the reactive group at the linker used for immobilization may not react with the catalyst. The same accounts for the functional group that results from the reaction of the linker's terminus with the support and, obviously, any functional group at the surface of the support including the functional groups located inside the pore;

ii) the nature of the linker in terms of length and flexibility should be adjustable.

In view of these requirements, the Cu-catalyzed azide-alkyne Huisgen click chemistry[106-107] is envisaged since this reaction has already proved to proceed quantitatively under mild conditions even with polymeric and heterogeneous systems.[108-111] Detailed information about the linkers and linker chemistry is provided in **projects B1** – **B3**.

3.1.4.8 Support-specific properties relevant to the catalytic reactions to be investigated

In principle, the tailored polymeric monolithic supports outlined in this proposal are considered suitable for all catalytic reactions outlined in the B-section (**projects B1** – **B3**) for the following reasons:

(i) The polymeric cross-linked matrix as such is chemically stable (urethane-based) and thermally stable up to at least 200°C, does not dissolve or swell in the solvents to be used in any of the catalytic reactions and has thus a stable pore geometry and size; it also does not interfere with the catalysts outlined in **projects B1** – **B3**.

(ii) With the tailored surface chemistry outlined in this proposal, one can address hydrogen transfer catalysis (**project B1**), since in principle polar surface that facilitate water transport along the pore wall or non-polar surfaces that guide the polar reactants to the polar catalyst are available.

(iii) Similar accounts for the olefin metathesis reactions outlined in **project B2**; in addition to its size the pore surface can be designed such that it fits the polarity of the reactants. Reactions can also be run neat, which omits the need for a solvent and significantly simplifies theoretical calculations. As for the asymmetric addition of boronic acids to α,β-unsaturated carbonyls, the influence of pore surface polarity on enantioslectivity will be studied.

(iv) As for the asymmetric addition of boronic acids to α,β-unsaturated carbonyls (**project B3**), the influence of confinement in terms of size and polarity in combination with solvent polarity on enantioselectivity will be studied as outlined for the olefin metathesis catalysts (**project B2**).

Chronological work plan:

	2018		2019				2020				2021				2022		
	Q3	Q4	Q1	Q2	Q3	Q4	Q1	Q2	Q3	Q4	Q1	Q2	Q3	Q4	Q1	Q2	
T1																	WP1: Generation of a tailored porosity via templating with Janus-type NPs (PhD1)
T2																	WP 2: Synthesis of surface-modified NPs (PhD1)
T3																	WP 3: Generation of mesoporous PUR-based monolithic supports via SIPS (PhD2)
T4																	WP 4: Variation of pore diameter and pore geometry (PhD1, PhD2)
T5																	WP 5: WP 6: Pore size-selective functionalization of monoliths prepared via SIPS (PhD2)
T6																	WP 6: Functionalization of monoliths (PhD1, PhD2)
T7																	WP 7: Linker chemistry for the immobilization of catalysts (PhD1, PhD2)

3.1.4.9 Methods applied

Besides of standard characterization techniques, inverse size-exclusion chromatography (ISEC) will be used to determine, respectively confirm the pore size distribution of the novel materials. These data will be correlated with those obtained from N_2- or, to reduce surface polarity effects, Ar-adsorption experiments, which will in turn allow for identifying any unwanted non-permanent porosity caused by swelling. Complementary, any swelling-derived porosity can also be identified by recording flow-pressure curves for different solvents and correlating these data with the viscosity of these solvents according to Darcy's law. In parallel, the permeability for different solvents is obtained. Electron microscopy in combination with EDX allows for identifying the existence and distribution of nanoparticles prior to and after acid treatment. Elemental analysis/inductively-coupled plasma-optical emission spectroscopy (ICP-OES) will allow for determining the grafting density of the corresponding catalyst. These data will be supplemented by TEM/EDX to receive spatial information as well as by high-resolution tomography (**project C3**). Experimental data on pore diameter and tailored hydrophilic/hydrophobic character of the pore will be correlated with the experimentally determined data on TON and TOF for every individual catalytic reaction (**projects B1** – **B3**) as well as with the results from theory and calculations (**project C6**). Calculations performed there will provide most relevant information on diffusivity, transport but also on the distribution of solvents, reactants and products inside a pore. In this context, the modeling of the pore entrance is of particular interest.

3.1.4.10 Vision

By the end of the first funding period, polymeric porous monoliths with tailored and defined mesoporosity in the range of 5 – 20 nm and volumes up to approx. 50 mL should be accessible. This would guarantee for a technically relevant scalability of this approach. There should be a clear picture on how linker length and rigidity in combination with pore size (diameter), pore form and pore polarity influences diffusion and catalytic activity of the reactions described in **projects B1** – **B3**. The same accounts for the interplay between catalyst, pore polarity, and polarity of the solvents and reactants to be used.

3.1.5 Role within the collaborative research center

This project is one out of seven different approaches to the creation of tailored pores. In case the approach based on Janus-type nanoparticles is used, it will provide access to half sphere-type pores with an aspect ratio of approximately one. Alternatively, using the approach based on a pore-selective functionalization starting from designed pore size distribution, cylinder-type pores with substantial tortuosity will be created. Since the matrix is based on PUR, we do not expect any negative interaction with the catalysts outlined in **projects B1** – **B3** and thus envisage their use as supports for all catalytic reactions outlined in these projects. Since the chemistry of the inner pore walls is well known, we can provide this information to the theory group of **project C6**. Together with the group of Prof. Hunger (**project C1**), transport issues related to pore geometry and polarity will be addressed. Finally, we will provide both materials and information to the group of Prof. Schmitz (**project C3**) working on high-resolution tomography. Because of their cross-linked, incompressible but porous nature, monolithic supports are considered particularly suited as supports for continuous flow applications. This will be addressed during the second funding period.

3.1.6 Differentiation from other funded projects

The work described in **project A1** is not subject or partly subject of any other research by the applicant.

3.1.7 Project funding

3.1.7.1 Previous funding

This project is currently not funded and no funding proposal has been submitted.

References (ctd.)

[93] M. Lattuada, T. A. Hatton, *Nano Today* **2011**, *6*, 286-308.
[94] J. Reguera, H. Kim, F. Stellacci, *Chimia* **2013**, *67*, 811-818.
[95] Y. Song, S. Chen, *Chem. Asian J.* **2014**, *9*, 418-430.
[96] A. Walther, A. H. E. Müller, *Chem. Rev.* **2013**, *113*, 5194-5261.
[97] D. M. Andala, S. H. R. Shin, H.-Y. Lee, K. J. M. Bishop, *ACS Nano* **2012**, *6*, 1044-1050.
[98] D. D. Perrin, *Masking and Demasking of Chemical Reactions* In: Chemical Analysis*,* P. J. Elving, I. M. Kolthoff (Ed.), *Vol. 33*, Wiley-Interscience, New York, London, Sydney, Toronto, **1970**.
[99] M. Ciftci, P. Batat, A. Demirel, G. Xu, M. R. Buchmeiser, Y. Yagci, *Macromolecules* **2013**, *46*, 6395–6401.
[100] M. R. Buchmeiser, F. Sinner, M. Mupa, K. Wurst, *Macromolecules* **2000**, *33*, 32-39.
[101] G. Xu, D. Wang, M. R. Buchmeiser, *Macromol. Rapid Commun.* **2012**, *33*, 1975-1979.
[102] K. Matyjaszewski, J. Xia, *Chem. Rev.* **2001**, *101*, 2921-2990.
[103] C. Barner-Kowollik, J. P. Blinco, M. Destarac, K. J. Thurecht, S. Perrier, *Reversible addition fragmentation chain transfer (RAFT) polymerization: mechanism, process and applications* In: Encyclopedia of Radicals in Chemistry, Biology and Materials*,* C. Chatgilialoglu, A. Studer (Eds.), *Vol. 4*, **2012**.
[104] F. Švec, J. M. J. Fréchet, *Adv. Mater.* **1994**, *6*, 242-244.
[105] M. Rubinstein, R. H. Colby, In: Polymer Physics*,* (Ed.), Oxford University Press, Oxford, UK, **2003**.
[106] R. Huisgen, *Angew. Chem.* **1968**, *80*, 329-337; An*gew. Chem., Int. Ed*. **1968**, *7*, 321-328.
[107] H. C. Kolb, M. G. Finn, K. B. Sharpless, *Angew. Chem.* **2001**, *113*, 2056-2075*; Angew. Chem. Int. Ed.,* **2001**, *40*, 2004-2021.
[108] W. H. Binder, C. Kluger, *Macromolecules* **2004**, *37*, 9321-9330.
[109] P. Wu, A. K. Feldman, A. K. Nugent, C. J. Hawker, A. Scheel, B. Voit, J. Pyun, J. M. J. Frechet, K. B. Sharpless, V. V. Fokin, *Angew. Chem.* **2004**, *116*, 4018-4022*; Angew. Chem. Int. Ed.,* **2004**, *43*, 3928-3932.
[110] G. Pawar, B. Bantu, J. Weckesser, S. Blechert, K. Wurst, M. R. Buchmeiser, *Dalton Trans.* **2009**, 9043-9051.
[111] M. Schaefer, N. Hanik, A. F. M. Kilbinger, *Macromolecules* **2012**, *45*, 6807–6818.

3.1.7.2 Requested funding

Funding for	2018		2019		2020		2021		2022		2018-2022	
Staff	Quantity	Sum	Quantity	Sum	Quantity	Sum	Quantity	Sum	Quantity	Sum	Quantity	Sum
PhD student, 67%	2	43,200.-	2	86,400.-	2	86,400.-	2	86,400.-	2	43,200.-	2	345,600.-
Total		43,200.-		86,400.-		86,400.-		86,400.-		43,200.-		345,600.-
Direct costs	Sum		Sum		Sum		Sum		Sum		Sum	
consumables	8,000.-		16,000.-		16,000.-		16,000.-		8,000.-		64,000.-	
Total	8,000.-		16,000.-		16,000.-		16,000.-		8,000.-		64,000.-	
Major research instrumentation	Sum		Sum		Sum		Sum		Sum		Sum	
Gas adsorption appartus	164,700.-		-		-		-		-		164,700.-	
Total	164,700.-		-		-		-		-		164,700.-	
Grand total	215,900.-		102,400.-		102,400.-		102,400.-		51,200.-		574,300.-	

(All figures in EUR)

3.1.7.3 Requested funding for staff

	Sequen-tial no.	Name, academic degree, position	Field of research	Department of university or non-university institution	Project commitment in hours per week	Category	Funding source
Existing staff							
Research staff	1	M. R. Buchmeiser, Dr., Full Prof.	Polymer Science, Catalysis, Organometallic Chemistry	Institute of Polymer Chem.	6		University
	2	D. Wang, Dr.	Polymer Science, Catalysis, Organometallic Chemistry	Institute of Polymer Chem.	6		University
Non-research staff	3	M. Wendel		Institute of Polymer Chem.	4		University
Non-research staff	4	R. Stiehle		Institute of Polymer Chem.	2		University
Requested staff							
Research staff	5	n.n. M.Sc.	Polym. Sci., Material Sci.	Institute of Polymer Chem.		PhD	
Research staff	6	n.n. M.Sc.	Polym. Sci., Material Sci.	Institute of Polymer Chem.		PhD	
Research staff	7	Research assistant	Polym. Sci., Material Sci.	Institute of Polymer Chem.			

Job description of staff (supported through existing funds):
1
Full Professor, Head of the Institute
2
Scientific coworker, in charge of (low/high-T) NMR, high-temperature GPC, ICP-OES, special syntheses
3
Technician, in charge of maintaining laboratories, laboratory equipment, management of chemicals, glove boxes
4
Secretary

Job description of staff (requested funds):
5
PhD student, work packages 1, 2, 4, 6 and 7
6
PhD student, work packages 3, 4, 5, 6 and 7
7
Research Assistants. **Justification:** The research assistants shall provide synthetic and analytical help for PhD 1 (WPs 1,2,4, 6, 7) and for PhD2 (WPs, 3, 4-7). This will allow them to pick up both non-standard synthetic and analytical techniques.

Research assistants and travel costs will be applied for collectively in the central administration propject Z1.

3.1.7.4 Requested funding of direct costs

	2018	2019	2020	2021	2022
Uni Stuttgart: existing funds from public budget	4,000.-	8,000.-	8000.-	8,000.-	4,000.-
Sum of existing funds	4,000.-	8,000.-	8000.-	8,000.-	4,000.-
Sum of requested funds	8,000.-	16,000.-	16,000.-	16,000.-	8,000.-

(All figures in EUR)

Consumables for financial year 2018

Chemicals, consumables, monomers, solvents, silica for columns, gases (Ar), NMR solvents	EUR	8,000.-

Consumables for financial year 2019

Chemicals, consumables, monomers, solvents, silica for columns, gases (Ar), NMR solvents	EUR	16,000.-

Consumables for financial year 2020

Chemicals, consumables, monomers, solvents, silica for columns, gases (Ar), NMR solvents	EUR	16,000.-

Consumables for financial year 2021

Chemicals, consumables, monomers, solvents, silica for columns, gases (Ar), NMR solvents	EUR	16,000.-

Consumables for financial year 2022

Chemicals, consumables, monomers, solvents, silica for columns, gases (Ar), NMR solvents	EUR	8,000.-

3.1.7.5 Requested funding for major research instrumentation

Equipment for financial year 2018

Gas physisorption apparatus. Justification: in course of this CRC, many materials will be developed in the A-section, including **project A1.** These new materials need to be characterized in terms of pore size distribution (and specific surface area). Apart from ISEC, the physisorption of gases such as N_2 or Ar is *the* method of choice, the more than it avoids in contrast to SEC the packing of columns. In view of the numerous materials and the time of measurement needed, we need to dispose over a device consisting of at least 3 simultaneous probes in order to accomplish measurements within reasonable times.	EUR	164,700.-

3.2 Project A2

3.2.1 General information about Project A2

3.2.1.1 Tunable Block Copolymer Templates for Spatially Controlled Immobilization of Molecular Catalysts

3.2.1.2 Research Areas
Polymer Chemistry, Preparative and Physical Chemistry of Polymers (306-01)

3.2.1.3 Principal Investigator
Ludwigs, Sabine, Prof. Dr. rer.nat. habil, born 19. 01. 1978, female, German
Lehrstuhl für Struktur und Eigenschaften polymerer Materialien, Institut für Polymerchemie
Universität Stuttgart, Pfaffenwaldring 55, 70569 Stuttgart
Tel.: 0711/685-64440
E-Mail: sabine.ludwigs@ipoc.uni-stuttgart.de
Tenured professor (W3)

3.2.1.4 Legal Issues
This project includes

1.	research on human subjects or human material.	no
2.	clinical trials.	no
3.	experiments involving vertebrates.	no
4.	experiments involving recombinant DNA.	no
5.	research involving human embryonic stem cells.	no
6.	research concerning the Convention on Biological Diversity.	no

3.2.2 Summary
The aim of **project A2** is the preparation of highly ordered tunable mesoporous templates based on block copolymer films which allow the specific immobilization and spatial positioning of molecular catalysts from project area **B** either at the pore bottom or at the pore walls.
Template creation in **A2** will combine synthesis of block copolymers by controlled polymerization techniques, structure formation into films and degradation of the minority block for mesopore formation. We will address pore hydrophilicity and stability of the templates with synthetic tools. Both standing cylindrical and cocontinuous morphologies (gyroids, perforated lamellae) with pores sizes between 20 and 10 nm are targeted which allow to directly compare tortuosity and interface effects of the templates. Further decrease of the pores will be achieved by inorganic replication and pore wall modification in close collaboration with **Bill (A5)**. As substrates mainly gold will be employed which i) allows to selectively attach the catalysts to the pore bottom and ii) can serve as electrode for electrochemical tests.

Electrochemical measurements will help to elucidate mesopore formation of the templates. The electrochemical activity of redox-active probes such as ferrocene within the templates will be studied by scan-rate dependent cyclic voltammetry. A close interconnection with **project C2 (van Slageren, Ringenberg)** is planned to study the spectroscopic and electrochemical behaviour of multifunctional redox probes under confinement.
From the catalytic projects from project area B, we will mainly work with molecular heterogeneous catalysts from **B3 (Laschat)**. Also the catalysts from **B1 (Plietker)** appear promising in connection with the proposed block copolymer templates. The confinement of the catalysts to either the pore bottom or the pore walls is expected to improve effects such as eduction of reaction couple products, increase selectivities and obtain high turn-over numbers.

3.2.3 Research rationale

3.2.3.1 Current state of understanding and preliminary work

The bottom-up self-assembly of block copolymer nanostructures still amazes scientists from different disciplines due to the beauty and functionality of the achievable structures making them highly attractive for application in nanoscience.[1] With controlled polymerization techniques well-defined block copolymers with tunable block chemistry, block lengths and molecular weights have become accessible. Typical domain sizes are in the range of 10 to 50 nm. Figure A2-1a highlights the phase diagram of diblock copolymers of polystyrene-*block*-polyisoprene which has been experimentally observed and fits to theoretical predictions by Bates and Fredrickson.[2] With introduction of a third block even more complex morphologies can be obtained.[3] Figure A2-1b shows a cocontinuous perforated lamella structure which is based on polystyrene-*block*-poly(2-vinylpyridine)-*block*-poly(tert-butylmethacrylate) (PS-*b*-P2VP-*b*-PtBMA) block copolymer thin films.[A2-1] While the first publications mainly dealt with the phase behavior and variety of morphologies, nowadays a huge number of applications have been realized. Especially film structures have been demonstrated for nanolithography, nanomembrane and nanotemplate applications.[4,5,6] Cylindrical and cocontinuous structures, such as perforated lamellae (Fig. A2-1b) and gyroids (Fig. A2-1c) are the most relevant here.

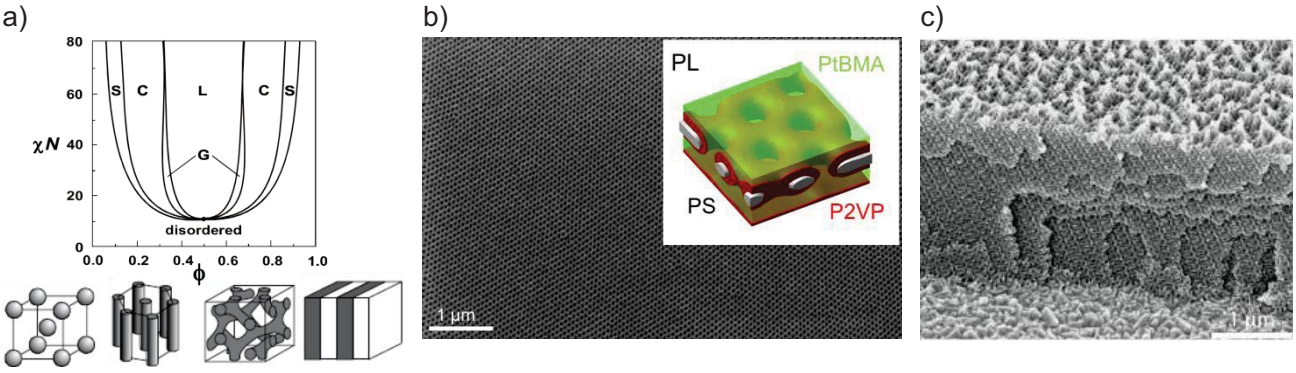

Figure A2-1. a) Theoretical phase diagram of diblock copolymers with sphere (S), cylinder (C), gyroid (G) and lamellar (L) bulk morphologies.[2] b) Film consisting of highly ordered perforated lamellae. Scanning electron microscope (SEM) image of a 40 nm thick film prepared from the triblock terpolymer PS-*b*-P2VP-*b*-PtBMA.[A2-1] c) Calcite single crystal replicated into a block copolymer template.[6] SEM image of a cross-section after degradation of the polymer template.

In the current proposal we want to build up on our own expertise on block copolymer structure formation in films (compare Figure A2-1b,c and preliminary work) and go beyond by tailor-making mesoporous templates with defined anchoring points for the immobilization of Rh- and Ru-based molecular catalysts. Key to success will be to make the block copolymer templates stable to catalytic reactions which can require rather harsh conditions. There is no literature on using block copolymer templates for molecular heterogeneous catalysis, but we can build upon existing chemistry and reactions within pores described in literature.

In general the strategy to obtain mesoporous templates is to introduce one block in the block copolymer which can be selectively degraded while the matrix is stable. As suitable blocks poly(methylmethacrylate) (PMMA), polyisoprene (PI), polybutadiene (PB), poly(4-vinylpyridine) (P4VP), polylactide (PLA) and polyethyleneoxide (PEO) have been identified because degradation can be achieved by photolysis, ozonolysis and reactive ion etching, aqueous base dissolution or water dissolution.[7] Other strategies include for example the use of supramolecular assembly of block copolymers and low molecular compounds into cylindrical structures and subsequent removal of the low molecular compound by dissolution.[8,9,10]

The working horse is still polystyrene-*block*-poly(methylmethacrylate) (PS-*b*-PMMA) where PMMA can be degraded after structure formation with UV-light and PS simultaneously gets crosslinked leading to rather stable templates. Russell and Thurn-Albrecht reported on high-density mesoporous arrays which were obtained by application of electric fields.[11] Alternative strategies to get standing cylindrical structures include the introduction of neutral surfaces based on statistical copolymers.[12] While the

electric field alignment can be applied up to 1 μm thick films, the use of neutral surfaces is typically limited to thinner films. Chemistry within these pores was successfully shown for vapor-phase and liquid-phase sol-gel reactions of tetraethoxy-silane.[13] Particularly straightforward is the use of electrodeposition within the mesopores if conducting substrates are provided beneath the cylindrical templates. This approach is motivated by earlier work of the C.R. Martin group on nanoelectrode arrays using polycarbonate membranes, track-etch membranes of colloidal self-assembled substrate.[14] Thurn-Albrecht and Russell electrodeposited Co nano-wires and used these arrays of wires for ultrahigh density storage media.[11] Jeoung et al. further demonstrated the use of block copolymer templates as nanoelectrode arrays using scan-rate dependent cyclic voltammetry with ferrocene as redox-active molecular probe in the electrolyte.[15]
The group of Ito reported on cylindrical PS-*b*-PMMA templates with film thickness and pore diameters around 30 nm, i.e. aspect ratios around 1. They used the carboxyl moieties at the pore walls which remain after UV-treatment for esterification and amidation reactions with ferrocene derivatives.[16,17] Varying lengths of the alkyl spacers allowed to vary the mobility of the ferrocene. The dependence of the spacer length within the pore and perpendicular to the substrate surface could be measured with cyclic voltammetry and electrochemical impedance spectroscopy. The use as electrochemical sensors was also demonstrated.[18]

Further chemistry in block copolymer pores includes influential work of Hillmyer and coworkers on block copolymers based on polylactide as soft-etchable polymer block.[19] The pore wall chemistry is more reliable than in the case of PS-*b*-PMMA since exclusively –OH functional groups are obtained after degradation of the PLA block. This was for example proven by reaction with trifluoroacetic anhydride and NMR /IR analysis.[20] The areal density of the hydroxyl groups was reported to roughly one –OH per 4 nm^2 for block copolymers with pores with 22 nm pore diameter.
To further modify the hydrophilicity of the pore templates, Rzayev and Hillmyer introduced a third middle block in the PS-*b*-PLA block copolymers.[21] Poly(dimethylacrylamide) (PDMA) remained after degradation of the PLA block as thin hydrophilic layer. Via hydrolysis the PDMA could be transformed into poly(acrylic acid). Polymer analogous reaction of the pore walls then allowed to introduce alkene, hydroxyl and pyridine functionalities.[22] An alternative strategy used blends of polystyrene-*b*-polyethyleneoxide (PS-*b*-PEO) and PS-*b*-PLA to modify the pore walls with PEO. The introduction of PEO resulted again in higher hydrophilicity of the pores. The more polar the pores, the better the infiltration with water due to capillary forces.[23]

As mentioned the choice of the solvents for catalysis might complicate the choice of the block copolymer templates. Different approaches have been performed in the past to increase the temperature and solvent resistance of mesoporous block copolymer templates.[24,25,26,27] One way is to improve the thermal pore stability by using alternative matrix blocks such as cyclohexylyethylene (CHE) in PCHE-*b*-PLA block copolymers.[26] The idea behind is to introduce matrix blocks with higher glass transition temperatures (136°C for PCHE vs. 94°C for PS).[26] SAXS measurements further showed that the PCHE mesoporous templates were more stable towards solvents such as pyridine and ethylacetate.[26] Other strategies include the mixture of the block copolymers with small crosslinker molecules such as dicumylperoxide[28] or tetramethoxymethylgly-couril with a photoacid generator[29], to crosslink the matrix after structure formation. This is however not so convenient because undesirable chemical functionality might be introduced.
A more elegant strategy is to introduce the crosslinkable unit as comonomer to the synthesis of the matrix block. Approaches remain rare in the literature. Hawker and coworkers introduced a thermal crosslinking strategy with 3-vinylbenzocyclobutene (VBCB) as comonomer for the PS block. Crosslinking at about 200°C resulted in significant higher template and pore stabilities both in modified PS-*b*-PMMA and PS-*b*-PLA block copolymer systems.[24,25] With AFM[24] and SAXS-measurements[25] the authors showed stability of the cylindrical morphology up to temperatures of 220°C. After hydrolysis of the PLA the mesoporous templates still revealed form stability towards THF at room temperature and benzene at the boiling point.[25] One has to mention however that AFM was used as method to prove this by measuring the surface morphology before and after exposure to the solvents.
In the current proposal we will elaborate on the crosslinking strategy with BCB and we will test electrochemical crosslinking as novel method, see below. Conditions needed for the catalysis will be used as benchmark conditions.

Preliminary work of the Ludwigs group

The project will combine the expertise of the Ludwigs group on polymer synthesis via controlled polymerization techniques, a strong track-record in morphology control in films and know-how on electrochemistry of redox-active molecules and polymers.

Ludwigs has started working on block copolymer structure formation and interfacial templating during her Diploma / PhD thesis in the groups of A.H.E. Müller and G. Krausch. This involved the synthesis of triblock terpolymers based on PS, P2VP and PtBMA by living anionic polymerization in different ratios and molecular weights. The block copolymers allowed for preparation of mesoporous perforated lamellae as well as for pH-switchable mesostructures in thin films.[A2-1] Ludwigs continued to work with U. Steiner, U. Wiesner and M. Hillmyer on soft-etchable block copolymer templates based on poly(fluorostyrene) (PFS) and poly(lactide) (PLA).[A2-2] Figure A2-2a shows the example of a standing cylindrical structure which was obtained by electric field alignment of films and subsequent soft-etching of the PLA phase with basic treatment. An in-situ electrochemical monitoring technique was established which allowed to determine morphology and thickness dependent etching rates, Figure A2-2b.[A2-3] The mesoporous templates were replicated with various inorganic materials to yield polymer-inorganic hybrid materials and – after degradation of the remaining PFS block – mesostructured inorganic materials. Electrodeposition was successfully applied to create mesostructured metals, e.g. gold, and semiconductors, such as TiO_2 and ZnO. The latter materials were extremely successful both in liquid-electrolyte and solid-state dye-sensitized solar cells. [A2-4] The replication of block copolymer gyroid structures into calcite single crystals has been shown above, Figure A2-1c, and was achieved by using the ammonium carbonate diffusion method, where the substrate was immersed in a solution of calcium chloride and exposed to ammonium carbonate vapor.[6] Preliminary experiments to mineralize block copolymer templates with inorganic precursors from the Bill group (**project A5**) are currently underway.

a) b)

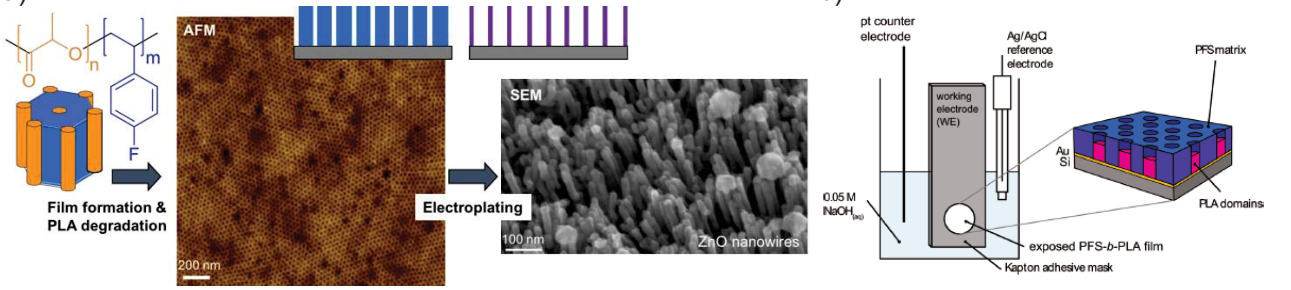

Figure A2-2. a) Sketch highlighting the preparation of highly ordered mesoporous cylindrical templates and the subsequent structure replication by electroplating.[A2-2] b) Electrochemical three-electrode-setup used for in-situ monitoring of the PLA degradation.[A2-3]

The soft-etch approach was further transferred to block copolymers which bear one conjugated or redox polymer block, e.g. triphenylamine-bearing polymers (VTPA).[A2-5] In this context the expertise of electrochemistry of conjugated monomers and polymers will be mentioned. In the case of TPA redox polymers electrochemical crosslinking by dimerization into tetraphenylbenzidine units is possible. [A2-6] Figure **A2-3** shows the cyclic voltammogram and the resulting dimerization reactions. This approach was also extended to conjugated redox polymers with polythiophene backbones and pendant TPA units. A recent publication highlights simultaneous crosslinking and doping of such polymer films by electrochemical means. [A2-7] The underlying mechanism is based on oxidative coupling which is also the key step in electropolymerizations. [A2-8] This crosslinking strategy will be implemented in the current DFG project to increase the stability of the polystyrene matrix phase towards solvents and temperature (compare WP2). We have recently synthesized a series of random copolymers consisting of styrene and VTPA by free radical polymerization where the film crosslinking could be successfully followed by absorption spectroscopy.

Other polymer-analogous reactions on polymer films included click chemistry and electroclick chemistry to modify electropolymerized polymer films based. [A2-9] Over the years various methods such as solvent vapor annealing or crystallization have been further developed for block copolymers and semicrystalline polymers. with the aim to induce long-range ordering and orientation in films. [A2-10]

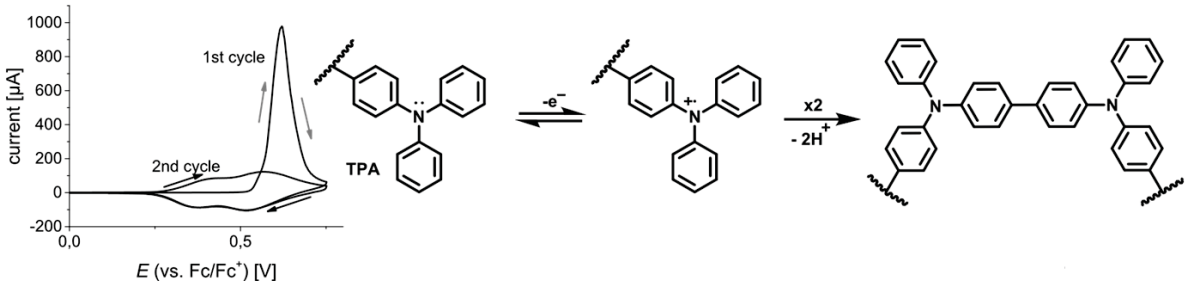

Figure A2-3. Cyclic voltammogram and schematic dimerization / crosslinking of TPA-containing polymer films. The first cycle involves the dimerization reaction into TPB units, the second cycle involves the reversible redox cycling of the TPB unit to its radical cation and dication.[A2-6]

References

[1] Blockcopolymers I & II, Editor V. Abetz, Springer-Verlag Berlin, Heidelberg, **2005**
[2] F. S. Bates, G. H. Fredrickson, *Phys. Today* **1999**, *52*, 32 –38
[3] U. Breiner, U. Krappe, V. Abetz, R. Stadler, *Macromol. Chem. Phys.* **1997**, 198, 1051-1083
[4] Nanolithography and patterning techniques in microelectronics, Editor D.G. Bucknall, CRC Press, Boston, New York, Washington DC, **2005**
[5] M. A. Hillmyer, *Adv. Polym. Sci.* **2005**, *190*, 137-181
[6] A. S. Finnemore, M. R. J. Scherer, R. Langford, S. Mahajan, S. Ludwigs, F. C. Meldrum, U. Steiner, *Adv. Mater.* **2009**, 21, 3928-3932
[7] E. L. Schwartz, C.K. Ober, in Advanced Nanomaterials, Editors K.E. Geckeler, H. Nishide, VCH-Wiley, **2010**, 1-66
[8] J. Ruokolainen, G. ten Brinke, O. Ikkala, *Adv. Mater.* **1999**, *11(9)*, 777-780
[9] B. K. Kuila, M. Stamm, *J. Mater. Chem.* **2011**, *21*, 14127-14134
[10] O. Ikkala, G. ten Brinke, *Science* **2002**, *295*, 2407-2409
[11] T. Thurn-Albrecht, J. Schotter, G. A. Kästle, N. Emley, T. Shibauchi, L. Krusin-Elbaum, K. Guarini, C.T. Black, M. T. Tuominen, T. P. Russell, *Science* **2000**, *290*, 2126-2129
[12] P. Mansky, Y. Liu, E. Huang, T.P. Russell, C. Hawker, *Science* **1997**, *275*, 1458-1460
[13] B. J. Melde, S. L. Burkett, T. Xu, J. T. Goldbach, T. P. Russell, *Chem. Mater.* **2005**, *17*, 4743-4749
[14] C.R. Martin, *Science* **1994**, *266*, 1961-1966
[15] E. Jeoung T. H. Galow, J. Schotter, M. Bal, A. Ursache, M. T. Tuominen, Ch. M. Stafford, T. P. Russel, V. M. Rotello, *Langmuir* **2001**, *17*, 6396-6398
[16] F. Li, B. Pandey, T. Ito, *Langmuir* **2012**, *28*, 16496-16500
[17] F. Li, R. Diaz, T. Ito, *RSC Advances* **2011**, *1*, 1732-1736
[18] T. Ito, *Chem. Asian J.* **2014**, *9*, 2708-2718
[19] A. Baruth, M. Seo, C. H. Lin, K. Walster, A. Shankar, M. A. Hillmyer, C. Leighton, *Appl. Mater. Inter.* **2014**, *6*, 13770-13781
[20] A. S. Zalusky, M. A. Hillmyer, *J. Am. Chem. Soc.* **2001**, *123*, 1519-1520
[21] J. Rzayev, M. A. Hillmyer, *Macromolecules* **2005**, *38*, 3-5
[22] J. Rzayev, M. A. Hillmyer, *J. Am. Chem. Soc.* **2005**, *127*, 13373-13379
[23] H. Mao, P. L. Arrechea, T. S. Bailey, B. J. S. Johnson, M. A. Hillmyer, *Faraday Discuss.* **2005**, *128*, 149-162
[24] E. Drockenmuller, L. Y. T. Li, D. Y. Ryu, E. Harth, T. Russell, I.-C. Kim, C. Hawker, *J. Poly. Sci.: Part A: Poly. Chem.* **2005**, *43*, 1028-1037
[25] J. M. Lesiton-Belanger, T. P. Russell, E. Drockenmuller, C. J. Hawker, *Macromolecules* **2005**, *38*, 7676-7683
[26] J. H. Wolf, M. A. Hillmyer, *Langmuir* **2003**, *19*, 6553-6560
[27] A. S. Zalusky, R. Olayo-Valles, J. H. Wolf, M. A. Hillmyer, *J. Am. Chem. Soc.* **2002**, *124*, 12761-12773
[28] K. A. Cavicchi, A. S. Zalusky, M. A. Hillmyer, T. P. Lodge, *Macromol. Rapid Commun.* **2004**, *25*, 704-709
[29] M. Li, K. Douki, K. Goto, X. Li, Ch. Coenjarts, D. M. Smilgies, Ch. K. Ober, *Chem. Mater.* **2004**, *16*, 3800-3808

3.2.3.2 Project-related publications by participating researchers

[A2-1] S. Ludwigs, A. Böker, A. Voronov, N. Rehse, R. Magerle, G. Krausch *Nature Mater.* **2003**, *2*, 744-747.
[A2-2] E.J.W. Crossland, S. Ludwigs, M. Hillmyer, U. Steiner, *Soft Matter* **2007**, *3*, 94-98.
[A2-3] E.J.W. Crossland, P. Cunha, S. Ludwigs, M. A. Hillmyer, U. Steiner, *Appl. Mater. Interf.* **2011,** *3*, 1375-1379.
[A2-4] a) E.J.W. Crossland, M. Kamperman, M. Nedelcu, C. Ducati, U. Wiesner, D.M. Smilgies, G.E.S. Toombes, M. Hillmyer, S. Ludwigs, U. Steiner, H. Snaith, *Nano Lett.* **2009**, *9*, 2807-2812. & b) *Nano Lett.* **2009**, *9*, 2813-2819.
[A2-5] E.J.W. Crossland, S. Scroggins, S. Moratti, O. Yurchenko, U. Steiner, M. Hillmyer, S. Ludwigs, *ACS Nano* **2010**, *4*, 962-966.
[A2-6] O. Yurchenko, D. Freytag, L. zur Borg, R. Zentel, J. Heinze, S. Ludwigs, *J. Phys. Chem. B*, **2012**, *116*, 30-39.
[A2-7] P. Reinold, K. Bruchlos, S. Ludwigs, *Polym. Chem.* **2017**, in press. DOI: 10.1039/C7PY01688C.
[A2-8] J. Heinze, B. Frontana-Uribe, S. Ludwigs, *Chemical Reviews* **2010,** *110*, 4724-4771.
[A2-9] M. Goll, A. Ruff, E. Muks, F. Goerigk, B. Omiecienski, I. Ruff, R.C. González-Cano, J.T. Lopez Navarrete, M.C. Ruiz Delgado, S. Ludwigs, *Beilstein J. Org. Chem*. **2015**, *11*, 335-347 & M. Goll, Dissertation, Uni Stuttgart **2017**.
[A2-10] G. Schulz, S. Ludwigs, *Adv. Funct. Mater.* **2017,** 27, 1603083.

3.2.4 Project plan

The overall aim of **project A2** is to generate highly defined *tunable block copolymer templates to spatially control the immobilization of molecular catalysts*, Figure A2-4. With our approach the role of pore width, length and tortuosity (cocontinuous vs. linear pores) and therefore interfacial area can be systematically varied and their influence on the molecular heterogeneous catalysis be screened and elucidated.

The project involves the synthesis of monodisperse block copolymers, structure formation in films and template formation by controlled pore formation upon etching of the minority block. Molecular heterogeneous catalysts from project area **B** and redox-active probes (in collaboration with **C2**) will be immobilized either on the pore bottom (**WP1**) or the pore walls (**WP2**) of the block copolymer templates. Click chemistry has been identified with the project partners from project area B as excellent tool to immobilize the catalysts. Together with **B1 (Plietker)** and **B3 (Laschat)** the chemistry of the linkers will be developed.

Electrochemistry with redox-active probes selectively attached to the pore bottom or pore will elucidate successful degradation of the minority block phases and reveal the nature of the nanoelectrode arrays. We will use well-defined ferrocene probes with different linker lengths. **Fyta (C6)** will integrate planar and beaker geometries for modelling studies of the immobilization of the ferrocence probe molecules on surfaces. We will closely work together with **project C2 (Ringenberg and van Slageren)** on advanced electrochemical and spectroscopic approaches to identify confinement effects. As multiprobe the 1,1'-bis(diphenylphosphino)ferrocene-tricarbonyliron scaffold (diFe) from **C2** is shown in Figure A2-4.

In terms of immobilization and testing of molecular heterogeneous catalysis under confinement we will have constant exchange with **project B3 (Laschat)** and **B1 (Plietker)**. A common task will be the identification of suitable reaction conditions. Currently the targeted block copolymer templates appear particularly compatible with **B3** since rather mild reaction conditions in methanol /water solvent mixtures and reaction times of 1 to 2 hours can be pursued. Figure A2-4 exemplarily shows the enanotioselective homogeneous Rh-catalyzed 1,4-addition of organobor reagents to enones. We expect the following advantages of performing the catalysis under confinement within the block copolymer templates: eduction of reaction couple products (boric acid) and water, high selectivities, high turn-over numbers, equilibrium towards active monomer species and cooperative effects.

The block copolymer templates from **WP2** will be further used for inorganic replication in **WP3** which will result in reduction of pore diameters. In particular the role of TiO_2 or ZnO walls on the immobilization of the molecular catalysts will be elucidated with **A5 (Bill)**. **Projects A4** and **C3** will be continuously involved for morphology characterization.

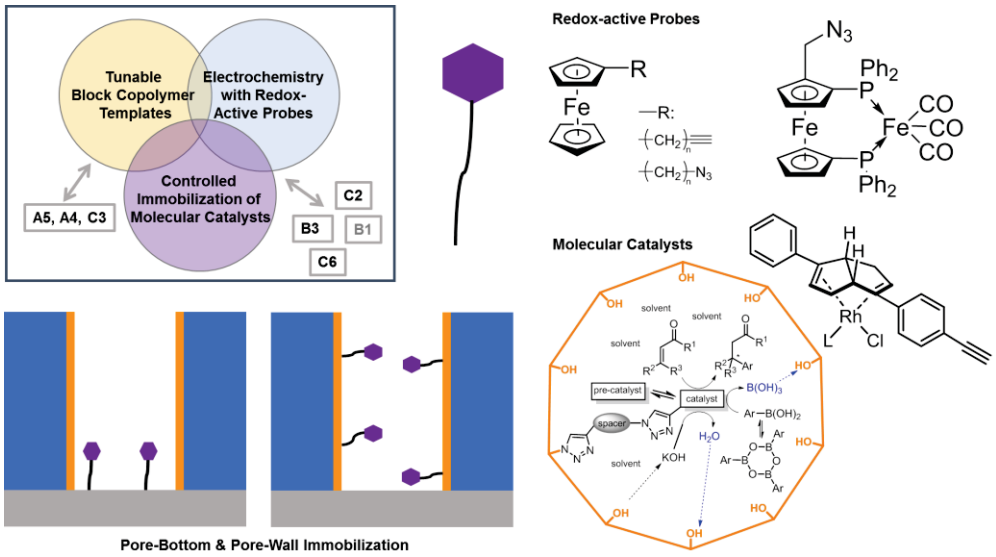

Figure A2-4. General strategy of A2.

In summary, the research goals are organized in work-packages as follows:

- **WP1: Confinement at pore bottom.** The approach is depicted in Figure A2-5. Planar electrodes will be compared to mesoporous block copolymer templates on top of electrodes. In case of PS-*b*-PMMA block copolymers the aspect ratio of the resulting beaker geometry will be tuned; film thicknesses between 30 nm and 1 μm and pore widths between 10 and 20 nm are targeted. SAMs with tailor-made anchor functionality and alkyne or azide headgroup will be attached to the pore bottom / electrode. Electrochemical activity of the nanoelectrode arrays will be studied in detail with scan-rate dependent cyclic voltammetry employing ferrocene probe molecules with varying linker lengths. Together with partners from C2, C6, B3 and B1 immobilization of catalysts at the pore bottom and catalysis under confinement will be studied.
- **WP2: Confinement at pore walls.** WP2 is a combination of synthesis, structure formation in films and pore generation by soft-etching. Synthetically, we will focus on the synthesis of block copolymers based on PS and PLA by controlled polymerization techniques. Main targets are: the variation of morphology and domain sizes of the resulting structures (cylinders, gyroids, perforated lamellae), the development of crosslinked PS matrix structures and the creation of polar pore walls upon degradation of the PLA phase with soft-etch methods. Figure A2-6 highlights synthetic routes to achieve the targeted block copolymers. After successful structure formation, mesoporous templates will be prepared, Figure A2-6. Electrochemical in-situ monitoring will help to control pore formation. PS-*b*-PLA templates have defined porous pore walls bearing OH-functionalities which can be reproducibly used for pore wall functionalization. Both linker chemistry and electrochemical probe techniques will be transferred from WP1 to WP2. Ultimate goal is to identify the role of confinement on the catalytic activities of pore wall immobilized catalysts.
- **WP3: Highly ordered mesostructured inorganic materials.** In WP3 the preparation of inorganic and inorganic/polymer hybrid structures by replication of block copolymer templates from WP2 will be conducted. On the one hand, full replication of the mesoporous structures will be achieved via electrodeposition of semiconductors, such as TiO_2 and ZnO and subsequent complete degradation of the polymer phase. On the other hand, the templates will be used by project A5 (Bill) to mineralize the porous polymer pore walls with inorganic layers based on TiO_2 or SiO_2. The idea behind both strategies is to decrease the mesopores below 10 nm. Together with B1 and B3 suitable linker chemistry and reactions conditions for the heterogeneous catalysis in inorganic templates will be identified.

3.2.4.1. WP 1: Confinement at pore bottom

Workpackage 1 is dedicated to the exclusive fixation of catalysts on the pore bottom. Gold will be mainly chosen as substrate because it is an electrode and allows for straightforward functionalization with thiol-bearing self-assembled monolayers. For ITO substrates phosphonic acid anchor chemistry will be applied. The chemistry of the SAMs can be altered in such a way that they bear either azide or alkyne headgroups which allows for a later click post-functionalization with the catalysts from **B3 / B1** and the multi-functional probes from **C2**. Mesoporous block copolymer films will be prepared on top of electrodes and compared to homogeneous planar naked electrodes. WP1 will focus on PS-*b*-PMMA cylindrical block copolymer templates giving beaker geometries. At a later stage of the project PS-*b*-PLA templates from WP2 will be transferred to WP1 and the influence of morphology and tortuosity will be studied.

Task 1.1: Functionalization of planar electrodes and establishment of electrochemical experiments

In a first step planar electrodes will be modified with thiol self-assembled monolayers which bear either azide- or alkyne-headgroups. In the literature SAM preparation of azido-undecanethiol on Au has been for example reported.[30] The number of functionalizable sites can be tuned by using mixed monolayers, e.g. upon deposition of azido-undecanethiol with undecanethiol. Via click chemistry alkyne/azide-terminated ferrocene probe molecules can be attached to the SAMs.[30] The ferrocene linker chemistry will be systematically modified with B1 and B3. The electrochemical behaviour of these surface-attached ferrocene probes will be compared to non-surface-bound ferrocene in the electrolyte. Scan-rate dependent cyclic voltammetry will be applied to study diffusion processes. Findings from Task 1.1. will directly flow in the following tasks. The experiments will be accompanied by modelling studies of Fyta (**C6**).

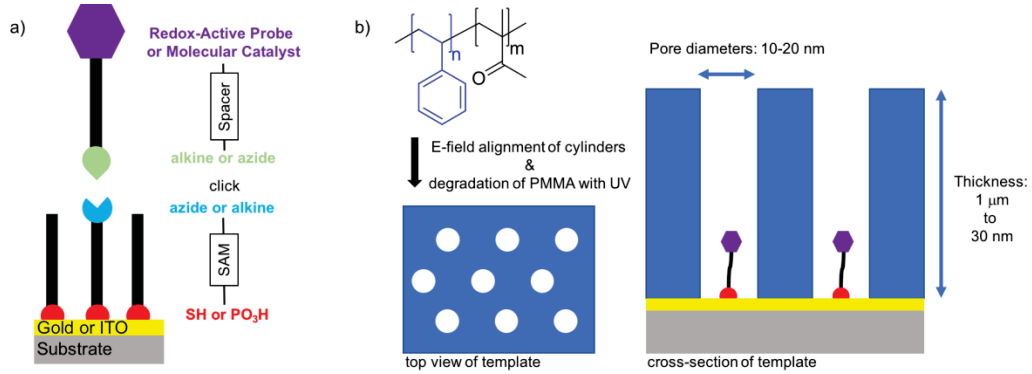

Figure A2-5. Approach for pore bottom functionalization in WP1. a) Self-assembled monolayers with azide or alkyne functionality will be deposited on Au or ITO electrodes. Electrochemical probes or molecular catalysts which are functionalized with the corresponding alkyne or azide functionality and tunable spacer can be attached to the SAMs via click chemistry. b) Schematic representation of the preparation of PS-*b*-PMMA cylindrical block copolymer templates on top of electrodes which can be modified according to a).

Task 1.2: Preparation of mesoporous templates and electrochemical probing

In order to create mesoporous arrays on top of the electrodes PS-*b*-PMMA cylindrical alignment will be performed by electric fields. This block copolymer is one of the most studied block copolymers for templating applications and is therefore an ideal model system for our project. Russell and Thurn-Albrecht could show that electric field alignment of cylinder-forming PS-*b*-PMMA can be used to generate mesoporous templates with varying aspect ratios and pore densities.[11] Upon exposure to UV-light PMMA is selectively degraded, while the PS becomes crosslinked. The crosslinking is advantageous because it increases the stability towards solvents and therefore solution chemistry within the pores. Problematic remains that mixtures of chemical functionalities in the pores are generated due to the UV-treatment. For WP1 this is however not an issue since the post-functionalization is tailored for the pore bottom which is based on gold or ITO. The pore wall chemistry is rather irrelevant in this approach. Well-defined PS-*b*-PMMA block copolymers prepared by living anionic polymerization will be purchased in block ratios 70:30 which show cylindrical bulk morphologies. Typical domain sizes of 10 to 20 nm are targeted. Recently we have set up an E-field alignment setup

in an oven in my laboratory: electric fields of around 40 V/μm can be achieved. First experiments for 500 nm thick films have been proven successful and shown successful degradation of the minority phase PMMA. In the project film thicknesses ranging from 30 nm to 1 μm will be systematically tailored to tune the aspect ratio of the highly ordered cylindrical pores. It is of utmost importance that the pores fully extend down to the electrode, i.e. there is no remaining PMMA at the pore bottom. Atomic force microscopy (AFM) and scanning electron microscopy (SEM) will be applied to check the quality of the templates both from the top surface as well as from cross-sections of the films. Similar to earlier research in the Ludwigs group electrodeposition of gold will be conducted within the pores. This method allows to prove the accessibility of the underlying electrode by replication of the pores and makes imaging of the obtained morphologies easier visible in microscopic techniques.

The resulting "nano-electrode" arrays will be subsequently modified with the same methodology as used for the planar electrodes with thiol self-assembled monolayers terminated with azide / alkyne groups. Alkyne- or azide-bearing ferrocene molecules will be attached to the respective SAMs by click chemistry. Scan-rate dependent CV will give information about diffusion processes and allow direct comparisons between non-surface bound ferrocene, ferrocenes bound to planar electrodes and ferrocenes confined to the pore bottom. These studies will be constantly compared to modelling studies of Fyta (**C6**) in a feedback loop.

At a later stage of the project pore bottom functionalization of more complex PS-*b*-PLA morphologies which are established in WP2 will be conducted. It is the aim to study the influence of i) hydrophilicity of the pores and ii) crosslinking of the PS matrix blocks on the conditions used for catalysis. Lessons learnt from Task 1.1. and Task 1.3 will flow into these experiments.

Task 1.3 Immobilization of multiprobe molecules from C2 and catalysts from B3/B1

Task 1.3 is a collaborative effort closely connected to **C2** and **B3/B1** and uses the SAM-modified electrodes and the mesoporous templates from Task 1.1 and 1.2.

In **C2** Ringenberg and van Slageren are interested in the static and dynamic electronic and geometric structure of multiprobe organometallic complexes in confinement. Starting from the ferrocene molecules more complex multiprobe redox-active systems will be explored (example given in Figure A2-4). In terms of electrochemical study, Ringenberg will apply advanced electrochemistry techniques such as rotating disc electrode experiments to study the performance of multiprobe molecules. As electrolytes acetonitrile is the solvent of choice. A constant feedback loop between the teams is envisaged.

Together with **projects B3** and **B1** the immobilization of the respective catalysts and the heterogeneous catalysis in confined block copolymer morphologies will be tested. The selective immobilization of the catalysts to the pore bottom in beaker geometries is a unique feature of **A2**. In addition to clicking the molecular catalysts to the pore bottom, catalytic reaction conditions have to be identified which are not detrimental for the block copolymer templates. In **project B3** this is for example straightforward since rather mild conditions, such as 50°C ,1-2 hour reaction times and solvent mixtures such as methanol / water can be applied. The compatibility of dioxane / water mixtures has to be explored, as well as more "harsh" reaction conditions necessary for **project B1**. Key to success will be a close interconnection with Laschat and Plietker to optimize the reaction conditions. The variation of the film thickness will allow to make statements about the confinement effects on the heterogeneous catalysis.

3.2.4.2 WP 2: Confinement at pore walls

The tasks of workpackage 2 are the synthesis and preparation of mesoporous block copolymer films based on PS and PLA as soft-etchable block and the controlled attachment of the organo-metallic molecules from **B3**, **C2** and **B1** at the pore walls. Both cylindrical and cocontinuous (gyroid and perforated lamellar) morphologies are tailored. The variation of the tortuosity and tunability of the interfacial area is expected to positively influence the targeted catalytic reactions. The synthesis of the block copolymers is designed in such a way that after successful formation of suitable templates –OH functionalities will be covering the pore walls. The OH-functionalized pore walls will be later on modified to azide functionalities to allow for click functionalization. Continuous pathways down to the pore bottom are of utmost importance which can be monitored by electrochemical measurements. Since solubility and degradation of the templates upon attachment of the molecular catalysts and catalysis itself might be an issue, routes to crosslink the PS matrix are proposed.

Task 2.1 Synthesis of stable PS-*b*-PLA block copolymers

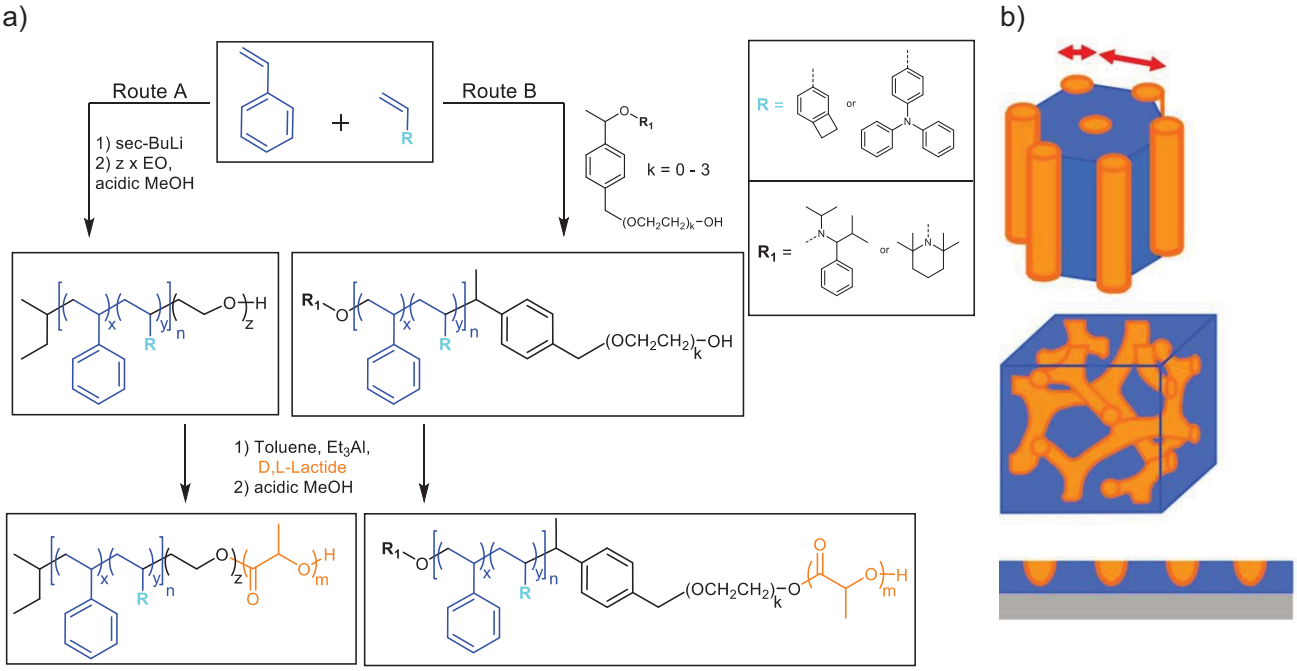

Figure A2-6. a) Synthetic routes towards PS-*b*-PLA block copolymers with potential copolymerization of the styrene with the crosslinkable units CH_2CHR being 3-vinylbenzocyclobutane and 4-vinyltriphenylamine. Route A: Living anionic polymerization of styrene and end-functionalization to a macroinitiator with OH-functionality. Route B: Controlled radical polymerization with tailor-made initiators also leading to OH-functionality of the first block. The OH-functionalization will be used for a ring opening polymerization of D,L-lactide. b) Targeted microdomain morphologies of block copolymers. In addition to standing cylindrical and gyroidal morphologies, very thin films further open up the possibility to generate surface-reconstructed structures.

Figure A2-6 gives an overview of the proposed polymerization routes. For the PS block both living anionic polymerization (Route A) and an NMRP controlled radical polymerization (Route B) are proposed. In terms of synthesis technology, first experiments will be done in standard glass equipment, but we will also set up a permanent glass reactor system for living anionic polymerization for scale-up reasons. For a later crosslinking of the PS phase both 3-vinylbenzocyclobutane (VBCB) and 4-vinyltriphenylamine (VTPA) can be introduced as comonomers which allow either temperature or electrochemical crosslinking of the PS phase after structure formation. For VBCB Hawker and coworkers could show successful thermal crosslinking of PS-*b*-PLA and PS-*b*-PMMA films at temperatures around 200°C.[24, 25]
As highlighted in the own preliminary work electrochemical crosslinking of TPA-units into dimers is another straightforward approach and only requires electrochemical oxidation as trigger.[A2-6] The PS matrix will be crosslinked this way, while the PLA can be degraded by soft-etch basic treatment. The crosslinking density can be tuned via the comonomer ratio in the PS matrix.
Both polymerization routes will guarantee –OH-functionalities at the junction between the two blocks after degradation of the PLA block. The OH-terminated PS blocks will then allow a ring-opening polymerization of D,L-lactide into polylactide.
To tune the hydrophilicity of the pore walls we propose to introduce different block lengths of ethylene oxide. Route A introduces ethyleneoxide oligomers / polymers as middle block. In Route B the number of ethyleneoxide units k can be varied between 0 and 3 as has been successfully shown.[31] Hydrophilic pore walls are important for the use and penetration of polar solvents (methanol/water, dioxane/water) as reaction medium in the planned catalytic reactions. Furthermore, we expect positive effects of the water-adsorption functionality of the PEO layer, e.g. with respect to eduction of water out of the equilibrium (compare **project B3**).
The block ratios and the molecular weights of the PS and PLA blocks will be targeted for cylindrical and gyroid morphologies in bulk. Microdomain spacings and later pore diameters between 10 and 20 nm will be reached. For chemical characterization mainly size exclusion chromatography and NMR-

spectroscopy will be used. For bulk domain characterization thick films will be formed and cross-sections will be studied both with TEM and SAXS.

Task 2.2 Preparation of mesoporous templates and electrochemical probing

First deposition of thin films with film thicknesses between 20 and 100 nm are planned to gain information about the thin film phase behaviour. Similar to WP1, in a first step, cylindrical structures are targeted which are varied in pore diameter, domain spacing and film thickness resulting in different aspect ratios, Figure A2-6b. Bicontinuous structures will further increase the tortuosity of the porous domains. In very thin films valley-like structures (Töpfchen) can be formed – note that this is the only thin film structure in the proposal which does not have continuous pores from the top of the films down to the substrate, Figure A2-6b. In very thin films other surface-reconstructed morphologies such as perforated lamellae also become accessible. All the other films will expose the underlying gold substrates after degradation of the minority block, which can be used as working electrode in the electrochemical experiments. Structure formation will be directed by interfacial templating, electric fields and solvent vapor atmospheres. Here the Ludwigs group has developed huge expertise in manipulation of films in the last years. Especially the use of solvent-vapor treatment and rational use of selective solvents seems particularly straightforward to reach the targeted morphologies.

After structure formation into the desired morphologies, the preparation of the pores by degradation of PLA in a basic etch solution or in an electrochemical bath will be conducted, Figure A2-7. The latter is based on the strategy shown in Figure A2-2b where in-situ electrochemical monitoring can be used to help identify pore generation and tortuosity. Statements on etching rate as function of the morphology can be drawn. It is of utmost importance that no continuous layer of PLA covers the substrates, otherwise the films will float off upon degradation.

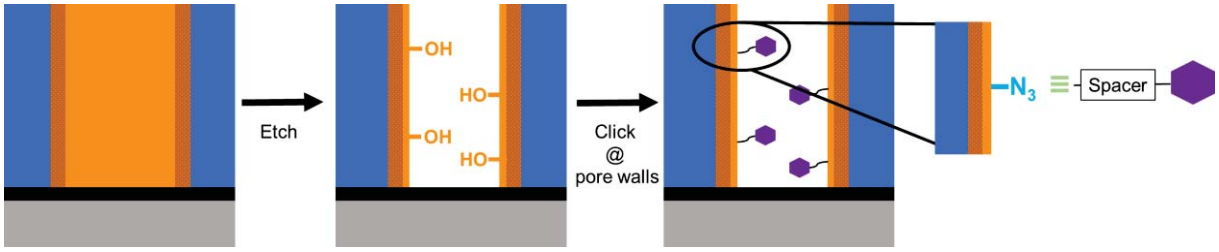

Figure A2-7. a) Sketch highlighting the etching of the PLA phase and exposure of OH-functionality at the pore walls. The OH-functionality will be chemically modified into azide groups which can be used to attach the organometallic molecules from B3/B1 and C2.

AFM and electron microscopy techniques are necessary to study the morphology of the resulting films. The electrodeposition of metals, e.g. gold, into the mesoporous templates will further help to better resolve the structures, estimate surface densities and test the accessibility of the whole pores.

Ultimate goal is to achieve mesoporous structures with crosslinked PS matrices to increase solvent and thermal resistance for the planned catalytic investigations. Studies by Drockenmüller et al.[24, 25] have shown that block copolymers consisting of styrene-co-VBCB blocks and PLA seem to follow the phase diagram of PS-*b*-PLA established by Hillmyer and coworkers. The crosslinking density of both comonomers VBCB and VTPA to the styrene block is expected to influence the thermal stability and solvent resistance of the later templates. Different tests on thermal and electrochemical crosslinking will be performed and the thermal resistance and the solvent stability will be screened. The choice of the solvent will be done in close collaboration with **projects B1** and **B3** to mimic the targeted conditions for the molecular heterogeneous catalysis.

Task 2.3 Heterogeneous catalysis in confinement

This task is directly correlated with WP3 from **project C2**, WP 7/ 8 from **B3** and WP3-B/ WP4-B from **B1**. Similar to Task 1.3 advanced electrochemical measurements and the immobilization and performance of the molecular catalysts will be tested. Further issues to be addressed will be:

a) which solvents are compatible for the block copolymer templates? The tunable crosslinking density of the PS phase will be highly relevant here.

b) how many catalysts will be attached to the pore walls? This is directly connected to the modification of the OH-groups into azide groups and subsequent click chemistry with the target molecules.

c) how does tortuosity influence the catalysis? Are the cocontinuous structures better for the catalytic applications?

3.2.4.3 WP3: Highly ordered mesostructured inorganic and inorganic hybrid materials

Task 3 deals with the preparation of mesostructured inorganic and inorganic / polymer hybrid scaffolds with pore diameters below 10 nm. This workpackage is a follow-up task of WP2. Simple PS-*b*-PLA morphologies will be used, the proposed thermal and electrochemical crosslinking strategies are not necessary here, since low-temperature protocols will be performed. Two main strategies are planned:

We have shown in the past (compare preliminary work) that electrodeposition of TiO_2 and ZnO into mesoporous templates is possible on conducting electrodes, such as gold and ITO. Here mainly the cocontinuous self-standing structures are of interest. Gyroidal structures prepared in WP2 will be replicated in electrochemical cells at room temperature conditions in electrolytes. For full exploitation of the inorganic materials the replication will be followed by an annealing step which leads to highly crystalline TiO_2 or ZnO mesostructures and simultaneously degrades the remaining PS phase. Due to volume shrinkage upon annealing even smaller mesopores are achievable with this approach, Figure A2-8a. Mesoporous networks with 4 to 8 nm pore diameter will be achieved here.

Together with Bill (**project A5**) the pore walls of OH-functionalized mesoporous PS-*b*-PLA templates will be mineralized with precursor solutions targeting for oxide layers consisting of ZnO, TiO_2, SiO_2, ZrO_2 or Al_2O_3. The Bill group has developed low temperature protocols, which are compatible with the block copolymer films. As shown in Figure A2-8b hybrid materials will be generated. The inorganic material projects from project area A – Bill (A5) and Traa / Gießelmann (**project A4**) – will establish suitable linker chemistry for the immobilization of the molecular catalysts from **projects B3** and **B1**. The role of confinement in different inorganic morphologies will be directly compared to the other projects.

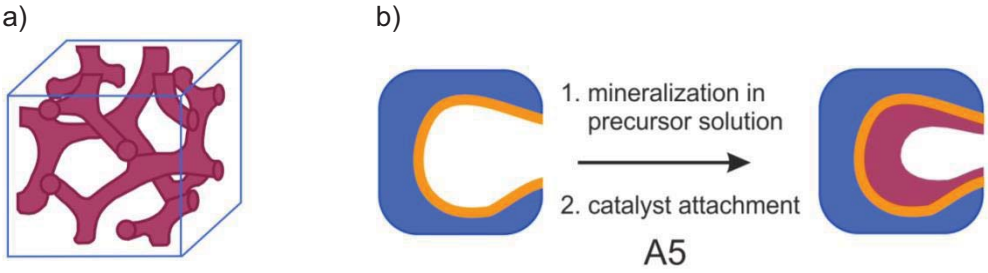

Figure A2-8. a) Sketch highlighting the replication of a cocontinuous morphology with an inorganic material. b) Approach of **project A5** to surface-functionalize mesopores with a mineralized inorganic layer.

Chronological work plan:

	2018 Q3 Q4	2019 Q1 Q2 Q3 Q4	2020 Q1 Q2 Q3 Q4	2021 Q1 Q2 Q3 Q4	2022 Q1 Q2	
						WP1: Confinement at pore bottom
T1.1						Functionalization of planar electrodes and establishment of electrochemical experiments (PhD1)
T1.2						Preparation of mesoporous templates and electrochemical probing (PhD1)
T1.3						Immobilization of multiprobe molecules from C2 and catalysts from B3/B1 (PhD1)
						WP 2: Confinement at pore walls
T2.1						Synthesis of stable PS-*b*-PLA block copolymers (PhD2)
T2.2						Preparation of mesoporous templates and electrochemical probing (PhD2 with PhD1)
T2.3						Heterogeneous catalysis in confinement (PhD2)
T3						**WP 3: Highly ordered mesostructured inorganic and inorganic hybrid materials (PhD1)**

3.2.4.5 Methods applied:
This project is a unique combination of polymer synthesis via controlled polymerization techniques, block copolymer self-assembly and interfacial templating in films, polymer-analogous reactions including click chemistry and molecular electrochemistry to test pore generation and functionalization. In addition to polymer synthesis and characterization techniques, the following methods will be applied:
- atomic force microscopy
- scanning electron microscopy
- transmission electron microscopy
- scan-rate dependent cyclic voltammetry

Click chemistry is chosen as method to attach the organo-metallic molecules from **projects B1, B3 and C2**.

3.2.4.6 Vision:
In terms of synthesis we will extend the diblock copolymer approach to triblock terpolymer systems which allow further fine-tuning of the matrix and pore-wall chemistry.
After successful crosslinking of the PS matrix phases in the block copolymer templates (WP2) we will also follow strategies to remove the templates from the underlying substrate or electrodes in order to obtain free-standing membranes. These channel-type architectures will help to perform the catalytic reaction in flow-through which might further improve turn-over numbers.
Ultimately the block copolymer templates will bear functionality as well, i.e. PS will be replaced by redox-active and electrocatalytically-active polymers. Here conducting polymers as matrix blocks appear particularly promising, because both electronic and energetic transfer from the confining matrix to the catalysts brings in novel phenomena.

3.2.5 Role within the collaborative research center:

Project A2 provides a unique toolbox of mesoporous templates with variable morphology, pore size and anchor functionalities. Selective modification of the pore bottom and the pore wall is unique in this project.

For the morphological characterization the project relies on collaboration with Schmitz (**C3**) and Gießelmann (**A4**). Schmitz' set of microscopy techniques comprising scanning and transmission electron microscopy, FIB tomography, and atom probe tomography will help to measure the 3D arrangement on the mesoscopic length scales. With Gießelmann SAXS experiments will be performed which give complementary structural information.

Electrochemistry is an excellent tool to replicate the structures by electrodeposition which makes morphology characterization easier and allows to identify successful attachment of organo-metallic molecules. As follow-up to experiments with ferrocene probe molecules, a close collaboration with van Slageren and Ringenberg (**C2**) will be established. Mesoporous templates from WP1 will be provided to **C2** to attach the multifunctional probes at the underlying electrode surfaces. In-depth characterization by Mössbauer, EPR, NMR, IR and in-situ spectroelectrochemistry will be performed. At a later stage of the project also the pore-wall functionalized block copolymer templates from WP2 will be studied together with **C2**.

In terms of immobilization with molecular catalysts from project area **B**, the Laschat systems from **B3** and the Plietker systems from **B1** have been identified. Tailor-made molecular catalysts bearing alkyne groups will be fixed to the pore bottom (WP1) or at the pore walls of the porous block copolymer templates (WP2). The confinement effect on the catalysis will be studied in detail with different morphologies and pore sizes.

In addition to manipulation of the microdomain spacing of the block copolymer templates, the OH-functionalized walls of the block copolymer templates in WP3 will be modified with SiO_2- or TiO_2-coatings by collaboration with Bill (**A5**). This way the pore diameter can be further decreased and the molecular catalysts can be attached in similar fashions as proposed in **A5**.

A constant feedback loop between experiments on the immobilization of the ferrocene probes on the SAMs is planned with modelling studies on different length scales with Fyta (**C6**).

3.2.6 Differentiation from other funded projects

The work described in **A2** is not subject or partly subject of other funded projects.

3.2.7 Project funding

3.2.7.1 Previous funding

This project is currently not funded and no funding proposal has been submitted.

References (ctd.)

[30] J. P. Collmann, N. K. Devaraj, T. P. A. Eberspacher, Ch. E. D. Chidsey, *Langmuir* **2006**, *22*, 2457-2464.

[31] E. Harth, B. Van Horn, V. Y. Lee, D. S. Germack, C. P. Gonzales, Robert D. Miller, C. J. Hawker, *J. Am. Chem. Soc.* **2002**, *124*, 8653-8660.

3.2.7.2 Requested funding

Funding for	2018		2019		2020		2021		2022		2018-2022	
Staff	Quantity	Sum	Quantity	Sum	Quantity	Sum	Quantity	Sum	Quantity	Sum	Quantity	Sum
PhD student, 67%	2	43,200.-	2	86,400.-	2	86,400.-	2	86,400.-	2	43,200.-	2	345,600.-
Total		43,200.-		86,400.-		86,400.-		86,400.-		43,200.-		345,600.-
Direct costs	Sum		Sum		Sum		Sum		Sum		Sum	
consumables	8,000.-		16,000.-		16,000.-		16,000.-		8,000.-		64,000.-	
Total	8,000.-		16,000.-		16,000.-		16,000.-		8,000.-		64,000.-	
Major research instrumentation	Sum		Sum		Sum		Sum		Sum		Sum	
Reactor for living anionic polymerization	25,000.-		-		-		-		-		25,000.-	
Total	25,000.-		-		-		-		-		25,000.-	
Grand total	76,200.-		102,400.-		102,400.-		102,400.-		51,200.-		434,600.-	

(All figures in EUR; staff funding according to DFG form 60.12)

3.2.7.3 Requested funding for staff

	Sequen-tial no.	Name, academic degree, position	Field of research	Department of university or non-university institution	Project commitment in hours per week	Category	Funding source
Existing staff							
Research staff	1	Sabine Ludwigs, Prof. Dr.	Polymer Science	Institute of Polymer Chemistry	4		University
	2	Klaus Dirnberger, Dr.	Polymer Science	Institute of Polymer Chemistry	4		University
Non-research staff	3	Beatrice Omiecinski		Institute of Polymer Chemistry	2		University
Requested staff							
Research staff	4	N. N.; M. Sc.	Polymer Physics, Electrochemistry	Institute of Polymer Chemistry		PhD	
Research staff	5	N. N.; M. Sc.	Polymer Synthesis & Self-Assembly	Institute of Polymer Chemistry		PhD	
Research staff	6	Research assistant	Polymer Synthesis & Self-Assembly	Institute of Polymer Chemistry			

Job description of staff (supported through existing funds):
1
Full professor, head of the institute
2
Academic director, permanent staff member, helping with administrative issues of the project. Furthermore Dr. Dirnberger has a synthetic polymer background and will help in synthetic questions regarding WP2.
3
Secretary
Job description of staff (requested funds):
4
PhD student 1 will ideally have a background in physics or physical chemistry of polymers. The thesis will be a combination between morphology tuning and electrochemistry. S/he will be mainly working on WP1. Electrochemical replication of the morphologies by metals and semiconductors will be also performed (WP 3). At a later stage of the project s/he will also work together with PhD student 2 on the pore wall functionalization (WP2).
5
PhD student 2 will have a strong polymer synthetic background and work on the controlled synthesis of PS-*b*-PLA block copolymers in WP2. S/he will set up the permanent reactor system for living anionic polymerization. Suitable block copolymers will be studied in terms of their structure formation in films. Together with PhD student 1 s/he will establish the pore wall chemistry.
6
Research assistents. **Justification:** The research assistant will assist PhD2 in the purification of monomers and solvents (for synthesis and electrolytes) and the polymerization of the block copolymers (WP2), and help in the upscaling to larger batches.

3.2.7.4 Requested funding of direct costs

	2018	2019	2020	2021	2022
Uni Stuttgart: existing funds from public budget	2,000.-	4,000.-	4,000.-	4,000.-	2,000.-
Sum of existing funds	2,000.-	4,000.-	4,000.-	4,000.-	2,000.-
Sum of requested funds	8,000.-	16,000.-	16,000.-	16,000.-	8,000.-

(All figures in EUR)

Consumables for financial year 2018

Chemicals, solvents p.a., glassware, substrates, gold, ITO electrodes for electrochemistry, commercial block copolymers	EUR	8,000.-

Consumables for financial year 2019

Chemicals, solvents p.a., glassware, substrates, gold, ITO electrodes for electrochemistry, self-assembled monolayers, AFM tips	EUR	16,000.-

Consumables for financial year 2020

Chemicals, solvents p.a., glassware, substrates, gold, electrodes for electrochemistry, AFM tips	EUR	16,000.-

Consumables for financial year 2021

Chemicals, solvents p.a., glassware, substrates, electrodes for electrochemistry, AFM tips	EUR	16,000.-

Consumables for financial year 2022

Chemicals, solvents p.a., glassware, substrates, electrodes for electrochemistry, AFM tips	EUR	8,000.-

3.2.7.5 Requested funding for major research instrumentation

Equipment for financial year 2018

Installation of a permanent reactor system for living anionic polymerization. Justification: in the course of **project A2**, living anionic polymerization will be one of the main synthetic tools for preparation of well-defined low polydispersity block copolymers. While first experiments can be performed with standard glass equipment, better reproducibility and scale-up of the products can be achieved with a permanently stirred glass reactor system. The reactor system shall allow the control of vacuum and inert atmosphere, temperature control and controlled supply of initiator, monomer (liquid and/ or gas, e.g. ethylene oxide) and solvents. The *Inertclave* from Buechi does fulfil all these requirements and does additionally meet the necessary safety requirements for use in a standard lab.	EUR	25,000.-

3.3 Project A3

3.3.1 General Information about Project A3

3.3.1.1 Covalent organic frameworks as tailored substrates with molecularly defined pores for molecular heterogeneous catalysis

3.3.1.2 Research Areas
Solid State and Surface Chemistry, Materials Synthesis (302-01)

3.3.1.3 Principal Investigator
Lotsch, Bettina Valeska, Prof. Dr., born 07.09.1977, female, German
Max Planck Institute for Solid State Research, Heisenbergstraße 1, 70569 Stuttgart
Tel: 0711/689-1610, E-Mail: b.lotsch@fkf.mpg.de
Tenured professor (W3)

3.3.1.4 Legal Issues
This project includes

1.	research on human subjects or human material.	no
2.	clinical trials.	no
3.	experiments involving vertebrates.	no
4.	experiments involving recombinant DNA.	no
5.	research involving human embryonic stem cells.	no
6.	research concerning the Convention on Biological Diversity.	no

3.3.2 Summary
Covalent organic frameworks (COFs), a new generation of crystalline porous organic polymers, will be explored as catalyst supports with molecular-level tunability and well-defined structural mesoporosity for molecular heterogeneous catalysis. The goal of this project will be the synthesis and post-synthetic modification of 2D and 3D COFs based on functional building blocks, which allow for the controlled tethering of molecular organometallic catalysts inside the pores by adjustable anchoring groups. Here, attachment schemes based on click chemistry will be tested to allow maximum compatibility with the molecular catalysts. Rigid and flexible linkers of different lengths will be employed to study the effect of catalyst immobilization at different distances from the pore wall. New linker and COF synthesis, with a focus on the generation of polar pore walls, will be developed as they are expected to be of most utility to alter the reaction equilibria in the case of the hydrogen auto transfer catalysis, to increase the pressure in microphase separated solvents in the pore for metathesis reactions and to enable the facile pre-orientation of the substrates. In the next step, pore size, geometry and network topology will be altered so as to optimize the catalyst – substrate interactions, as well as the development of multimodal pore systems with different functionalities that allow for tailored substrate delivery and product transfer to the tethered catalyst.
Due to the high level of control that can be exerted over both the molecular and long-range structure of COFs and the resulting accessibility of advanced analytical tools, COFs are ideal substrates for investigating the distribution, orientation, and mode of action of catalysts tethered to and confined by the pore walls. This does not only allow us to systematically and quantitatively study the influence of confinement effects in close collaboration with theory, but also to rationally tune such effects for maximizing catalyst efficiency.

3.3.3 Research Rationale

3.3.3.1 Current State of Understanding and Preliminary Work
The locally and chemically specific immobilization of molecular catalysts on high-surface area substrates forms the basis for directing substrate – catalyst interactions and provides one of the key strategies for controlling structure – property – activity relationships in heterogeneous catalysis. While oxide-based substrates such as silica, titania or alumina are used as ubiquitous support materials in

heterogeneous catalysis, the defined anchoring of a single-site catalyst is difficult due to their defective or often amorphous surface and bulk structures. In addition, such substrates are often used only to heterogenize the molecular catalyst without specifically taking advantage of possible confinement or surface-specific effects provided by porous structures to alter and influence catalytic activities.
In order to provide truly site-specific catalyst binding and maximize catalyst – support interactions, crystalline support materials with well-defined surface structures, high surface areas and chemically specific anchoring points for tethering molecular catalysts are desirable. In addition, substrates providing ordered porosity open up manifold degrees of freedom in directing and controlling the productivity and selectivity of catalytic reactions through pore size and confinement effects.[1] While along these lines, zeolites stand out as microporous, crystalline catalyst supports with acid, basic and redox functionalities, they suffer from significant mass transport limitations if large substrate molecules are involved.[2] On the other hand, mesoporous materials, prominently represented by the MCM family of compounds with pore sizes in the nanoscale range (and thus exceeding molecular dimensions), have been abundantly used as catalyst supports to circumvent diffusion limitations.[1] While chemically diverse and robust, most oxide, nitride and carbon-based mesoporous materials suffer from ill-defined surface or even bulk structures, which poses limitations to the site-specific anchoring of molecular catalysts to their pore walls.[3]
Covalent organic frameworks (COFs) form a new generation of micro- and mesoporous polymers, which distinguish themselves from classical polymers by three defining features: 2D or 3D (rather than 1D) network topologies, ordered porosity with surface areas in excess of 3000 m^2/g, and crystallinity. COFs are built up from rigid organic building blocks, which are linked under solvothermal conditions by reversible covalent bond formation reactions to ensure error correction and defect healing. The choice of organic building blocks significantly influences the chemical, electronic and optical properties of the resulting network and at the same time provides a large synthetic toolbox for introducing chemical functionalities at the backbone. The network topology and pore size can be designed by choice of the type and geometry of the building blocks to provide well-defined mesopores in the range between ≈ 1 and 5 nm.[4],[5],[6] Since COFs are synthesized by reversible bond formation reactions under relatively mild solvothermal conditions, integration of a myriad of functional groups is possible, but requires fine-tuning of the reaction conditions to maintain high reversibility leading to ordered but at the same time chemically stable systems.[7],[8],[9]
Since COFs have emerged as a new class of crystalline porous polymers only recently, their deployment as substrates in heterogeneous catalysis is naturally sparse. The seminal example by WANG *et al.* introduces an imine COF (COF-LZU1) with chelated metal ions as a potent catalyst system in the Suzuki-Miyaura coupling reaction.[10] The C-C coupling reaction is catalyzed by Pd(II) that is immobilized by complexation with the framework. Initial examples using COFs as catalyst supports are (i) limited to organocatalysis[11],[12],[13],[14] where COFs can also provide chirality[15],[16],[17] or act size- and/or shape-selectively,[18] or (ii) they utilize the COF linker as ligand system for the catalyst, akin to surface organometallic chemistry[19],[20],[21],[22], or (iii) they act as scaffold for catalytically active nanoparticles in COF-nanoparticle hybrid materials[23],[24]. Such catalyst systems are not in the focus of this CRC initiative. On the contrary, the tailored attachment of metal containing homogeneous catalysts to the pores of a COF *via* adjustable linking groups as proposed within the framework of this CRC has not yet been studied. More importantly though, the effects of pore size and topology, confinement, catalyst orientation and catalyst dynamics, as well as surface functionalization on the catalytic mechanism and efficiency of the above reactions are essentially unknown.
Besides their well-defined local and long-range structure, a key advantage of COFs is their tunability on the molecular building block level. A variety of “pre-“ or “post-synthetic” functionalization strategies exist which either take advantage of functionalized building blocks or modify pre-existing anchoring points after network formation, for example by means of Huisgen-type Click chemistry[15],[12],[25]. Such protocols will be used in the framework of this CRC to introduce anchoring points for tethering the catalyst to the pore wall, as they show high tolerance for a vast number of functional groups and low substrate dependence. At the same time, the mild reaction conditions and high regiocontrol in the system assures high yields and low amounts of side products.
Own work. The Lotsch group develops bottom-up chemical approaches to new materials ordered on multiple length scales by combining the tools of solid-state chemistry, molecular chemistry and nanochemistry. A main thrust of the group’s research is the development of crystalline porous organic and hybrid materials for photo(electro)catalysis, [A3-1]-[A3-6] electrochemical energy storage, sensing, gas

storage[A3-7] and drug delivery,[A3-8] with a focus on carbon nitrides, covalent organic frameworks (COFs) and metal-organic frameworks (MOFs).
Besides the development of nanoparticulate MOFs as stimuli-responsive materials for photonic crystal-based sensing devices, taking advantage of the size-, shape and chemically selective nature of the MOF pore cavities, we currently explore the use of photoactive MOF thin films as platforms for photoelectrocatalytic water splitting within the DFG priority program 1928.
COFs, including covalent triazine frameworks (CTFs) accessible through ionothermal trimerization of nitriles, have been extensively studied by us in terms of their formation mechanism, structure and nanoscale morphology, gas storage and separation capabilities, as well as optoelectronic and photocatalytic properties. Specifically, we have developed a series of nitrogen rich CTFs, which owing to their high nitrogen content and large surface areas show excellent hydrogen and CO_2 uptake as well as CO_2 over N_2 sorption selectivities relevant for applications in carbon capture and storage. Moreover, due to their thermal and chemical stability and nitrogen rich nature, CTFs and their oligomeric derivatives were established as potent photocatalysts for light induced hydrogen evolution[A3-4] and their electrochemical properties were evaluated in the context of lithium storage for battery applications.

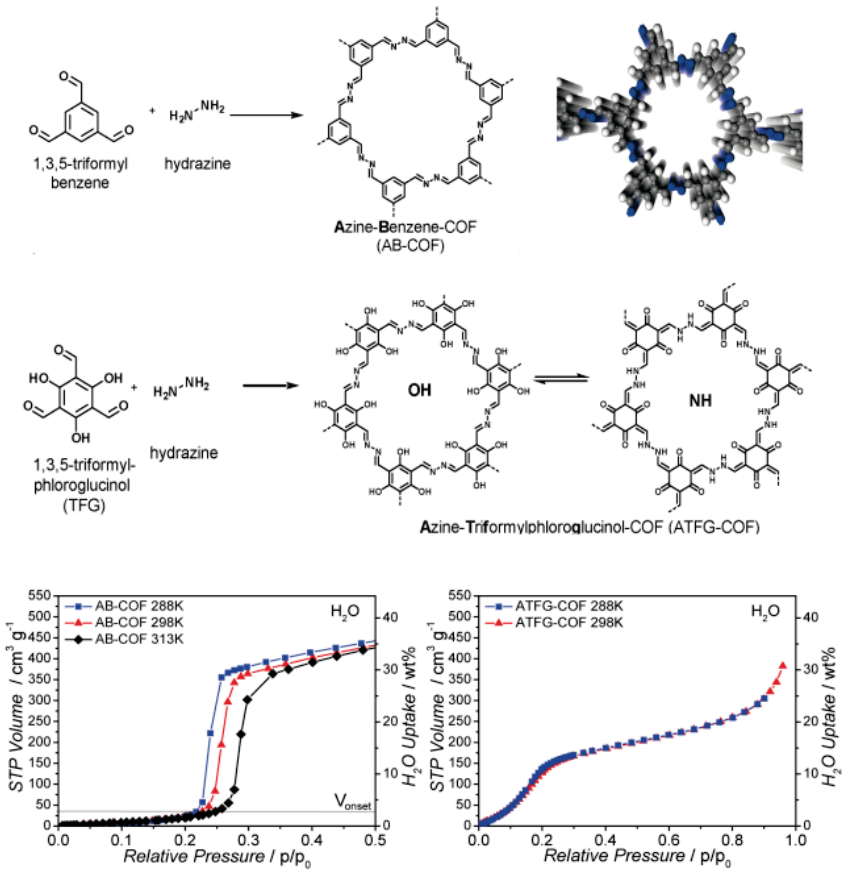

Figure A3-1: Introduction of hydroxyl groups to alter the polarity of the pore walls of COFs in a controlled fashion (top). Influence of the polarity on the water sorption properties of the isostructural azine linked COFs (bottom).

While CTFs rely on a relatively small portfolio of nitrile functionalized building blocks and are less tolerant to functional groups due to the harsh ionothermal synthesis conditions involved, COFs provide ample scope for molecular design and property tuning. An example is the modification of the CO_2 and water sorption properties of two isostructural azine COFs by selective introduction of hydroxyl groups into one of the building blocks (1,3,5-triformylbenzene vs 1,3,5-triformylphloroglucinol). Attachment of hydroxyl groups increases the polarity of the pore walls, leading to fundamental changes in the sorption behavior (Figure A3-1) – a feature that will be of key interest to this CRC.

The promise of COFs as molecular-based semiconductors with exceptional local and long-range definition forms the basis of our activities revolving around the synthesis, characterization and application of COFs as well defined model-systems for photocatalytic water splitting and, ultimately, CO_2 reduction. The bottom-up synthesis of such “molecular materials” provides a rich environment for the design of specific framework structures that can be tailored with a unique level of control.
We have exploited this concept extensively within the ERC Starting Grant “COFLeaf” to understand and control the structure – property – activity relationships of COFs for photocatalytic water splitting.

Specifically, our group has diversified the application of COFs in catalysis by establishing their use as versatile platforms for photocatalytic water splitting in conjunction with an electrocatalyst. Along these lines, we were the first to demonstrate that COFs can act as stable semiconductors for light induced hydrogen evolution in the presence of nanoparticulate Pt[A3-1],[A3-2] or molecular (e.g. cobaloximes) electrocatalysts.[A3-3] Taking advantage of the inherent molecular tunability of COFs, we were able to demonstrate that their hydrogen evolution activity can be gradually fine-tuned within a series of isoelectronic azine COFs by controlling the nitrogen content of their building blocks and, as a consequence, their electronic structure, crystallinity, porosity, and optoelectronic properties (Figure A3-1).[A3-2]

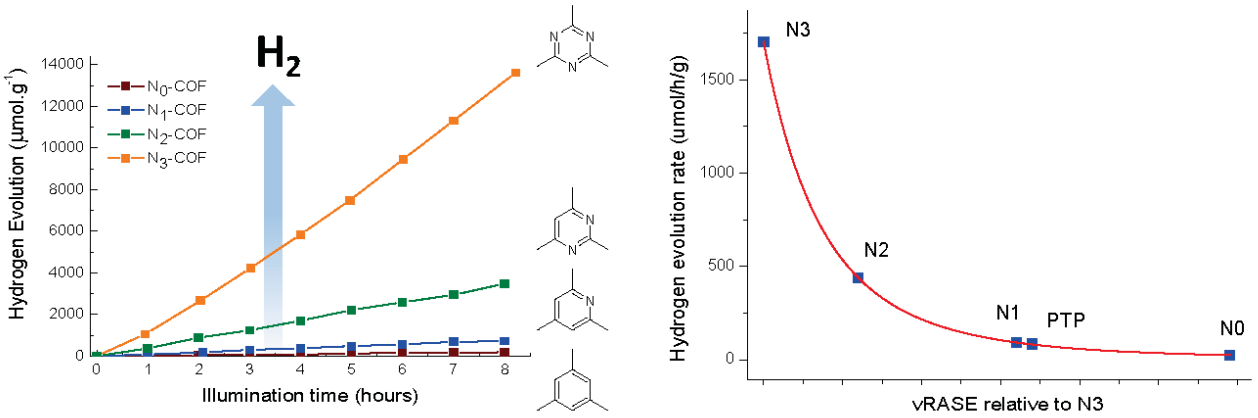

Figure A3-1: Photocatalytic hydrogen evolution in the Nx-COFs (left); Relation between the hydrogen evolution rates of triazryl-aryl azine COFs and the DFT based descriptor vertical radical anion stabilization energy, showing an exponential dependence (right).[A3-2]

Recent works elaborate on the impact of the multiscale structure of COFs (local structure, crystallinity and porosity / nanoscale morphology) on the photocatalytic hydrogen evolution activity of hydrazone, azine and imine COFs modified with molecular or nanoparticulate co-catalysts.[A3-9],[A3-10] In this context, special emphasis has been placed on elucidating subtle structural features of COFs including the nature of defects and stacking (dis)order, which we have successfully analyzed by a concerted approach based on powder X-ray diffraction analysis, transmission electron microscopy, solid-state NMR spectroscopy, Argon physisorption, and theoretical modeling (Figure A3-2). These studies not only reveal molecular features impacting the stacking order and formation of point and higher dimensional defects in 2D COFs, but furnish insights into the general mechanism of COF formation, vital to pinpoint strategies to further improve the crystallinity and stability of these materials. To enhance the stability of COFs without sacrificing their crystallinity, we have developed a route to lock imine-COFs into a stable configuration by post-synthetic treatment with sulfur (Figure A3-2B). This “lock-in” process points to a more general strategy that allows us to further reduce the sensitivity of certain COF systems to hydrolysis, especially under strongly acidic and basic conditions.

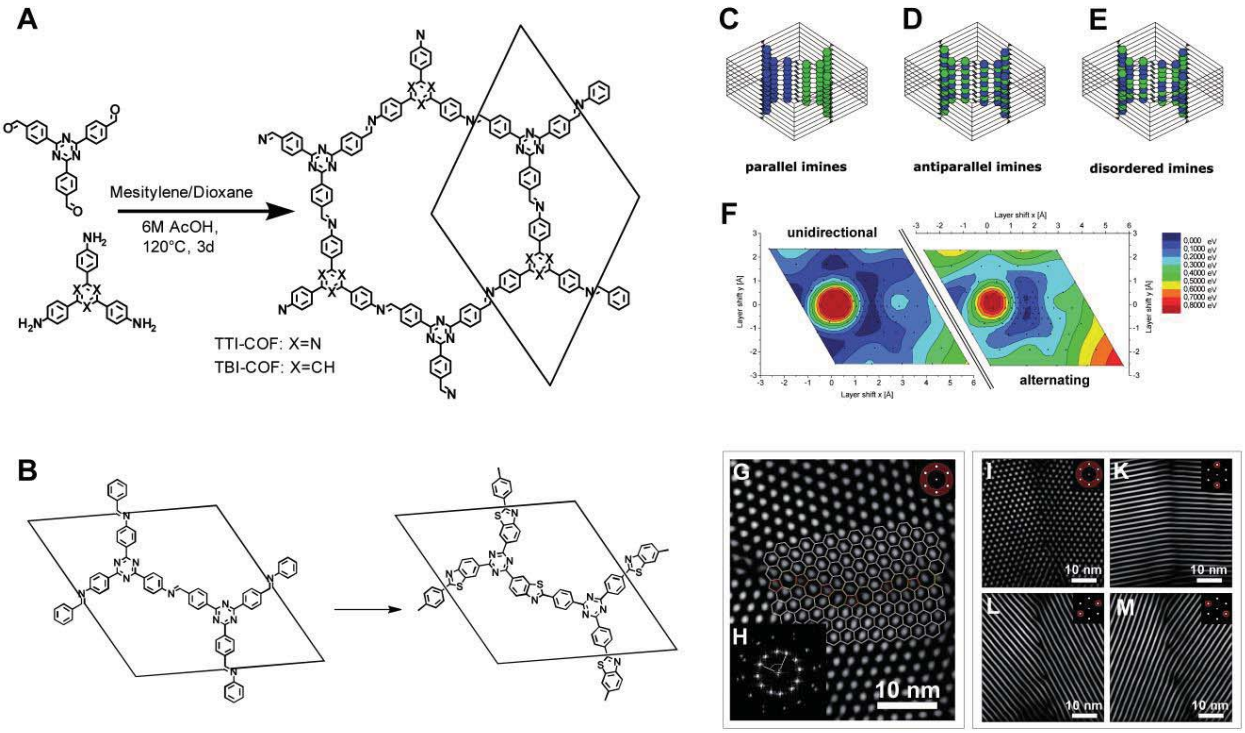

Figure A3-2: A: Schematic representation of the synthesis of TTI-COF and TBI-COF from a triamine and a trialdehyde. B: Schematic drawing of the sulfurization reaction of the TTI-COF to the S@TTI-COF. C-E: Three of the possible stacking motifs of the TTI-COF, where blue and green represent the amine and aldehyde building blocks, respectively. F: Energy landscape for slipping of the TTI-COF composed of two extended layers that are offset with respect to each other, while keeping the stacking distance constant. G: Grain boundaries of crystallites with co-aligned *c*-direction. To clarify the structure of the TEM images FFT-filters were applied, which are schematically indicated in the top right corner of each image. A: 94° grain boundary with a overlay indicating the five, six and seven membered rings. H: FFT of the image G showing the angle between grains close to 94°. I-M: small angle grain boundary with different Fourier filters applied, indicating the location of the edge dislocations.

Our work on the molecular tunability and structural engineering of COFs forms the basis for the design of COFs as scaffolds and nanoreactors for molecular heterogeneous catalysis. In preliminary work we have developed a hydrazone-linked COF platform composed of 2,5-diethoxyterephthalohydrazide (DETH) as C_2 building block and three different C_3 linkers, which give rise to COF-42[8], HTFG-COF, and TFPT-COF[A3-7] featuring different pore sizes (2.4 nm for COF-42 and HTFG-COF and 3.8 nm for TFPT-COF), surface areas (approx. 2000 $m^2 g^{-1}$ for COF-42, 1000 $m^2 g^{-1}$ for HTFG-COF, and 1600 $m^2 g^{-1}$ for TFPT-COF), and pore polarities (Figure A3-3). Organic modification of the ethoxy side chains of the DETH linker to form 2,5-di(prop-2-yn-1-yloxy)terephthalohydrazide (DPTH) allows us to introduce propargyloxy groups into the resulting COFs, which serve as anchoring points for click reaction to azide-modified catalyst linkers. Initial studies have shown that the modified linker can be doped into the COF systems by gradually replacing DETH for DPTH during solvothermal synthesis, nominally leading to one propargyl function per pore at a loading of 12.7 %.

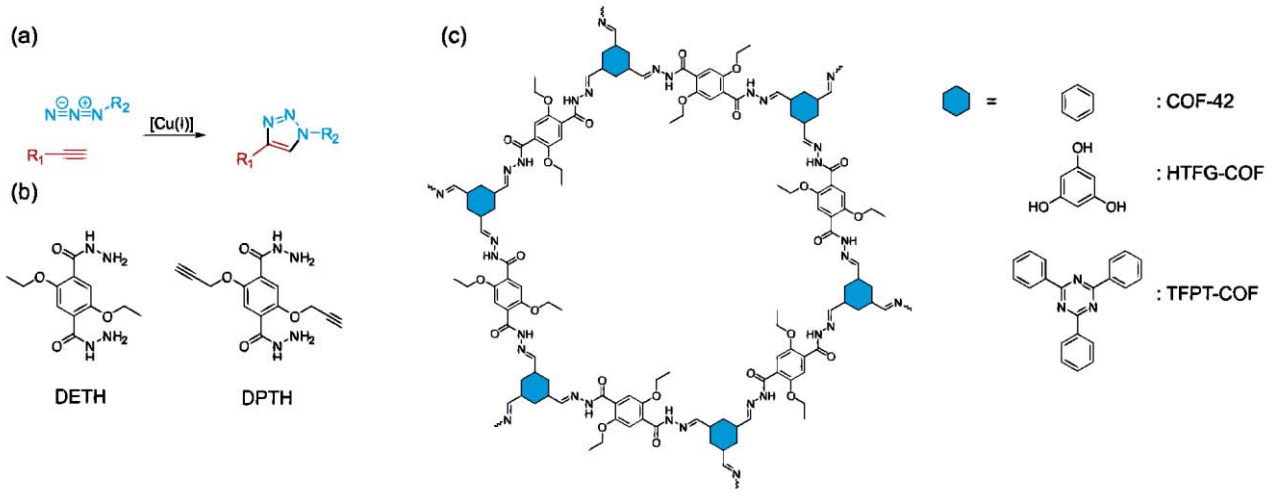

Figure A3-3: (a) 1,3 dipolar Huisgen cycloaddition reaction of an azide with a terminal alkyne. (b) Molecular structures of 2,5-diethoxyterephthalohydrazide (DETH) and 2,5-di(prop-2-yn-1-yloxy)terephthalohydrazide (DPTH). (c) Representation of the molecular structure of DETH-containing hydrazone COFs. The blue hexagon represents different node molecules (hexagon = benzene: COF-42, hexagon = benzene-1,3,5-triol: HTFG-COF, hexagon = 2,4,6-triphenyl-1,3,5-triazine: TFPT-COF).

References

[1] F. Hoffmann, M. Cornelius, J. Morell, M. Fröba, *Angew. Chem. Int. Ed.* **2006**, *45*, 3216-3251.

[2] T. Ennaert, J. Van Aelst, J. Dijkmans, R. De Clercq, W. Schutyser, M. Dusselier, D. Verboekend, B. F. Sels, *Chem. Soc. Rev.* **2016**, *45*, 584-611.

[3] A. Taguchi, F. Schüth, *Microporous Mesoporous Mat.* **2005**, *77*, 1-45.

[4] A. P. Côté, A. I. Benin, N. W. Ockwig, M. O'Keeffe, A. J. Matzger, O. M. Yaghi, *Science* **2005**, *310*, 1166-1170.

[5] E. L. Spitler, B. T. Koo, J. L. Novotney, J. W. Colson, F. J. Uribe-Romo, G. D. Gutierrez, P. Clancy, W. R. Dichtel, *J. Am. Chem. Soc.* **2011**, *133*, 19416-19421.

[6] A. P. Côté, H. M. El-Kaderi, H. Furukawa, J. R. Hunt, O. M. Yaghi, *J. Am. Chem. Soc.* **2007**, *129*, 12914-12915.

[7] A. Nagai, Z. Guo, X. Feng, S. Jin, X. Chen, X. Ding, D. Jiang, *Nat. Commun.* **2011**, *2*, 536.

[8] R. W. Tilford, S. J. Mugavero, P. J. Pellechia, J. J. Lavigne, *Adv. Mat.* **2008**, *20*, 2741-2746.

[9] M. S. Lohse, T. Stassin, G. Naudin, S. Wuttke, R. Ameloot, D. De Vos, D. D. Medina, T. Bein, *Chem. Mat.* **2016**, *28*, 626-631.

[10] S.-Y. Ding, J. Gao, Q. Wang, Y. Zhang, W.-G. Song, C.-Y. Su, W. Wang, *J. Am. Chem. Soc.* **2011**, *133*, 19816-19822.

[11] Y. Wu, H. Xu, X. Chen, J. Gao, D. Jiang, *Chem. Commun.* **2015**.

[12] H. Xu, X. Chen, J. Gao, J. Lin, M. Addicoat, S. Irle, D. Jiang, *Chem. Commun.* **2014**, *50*, 1292-1294.

[13] Y. Peng, Z. Hu, Y. Gao, D. Yuan, Z. Kang, Y. Qian, N. Yan, D. Zhao, *ChemSusChem* **2015**, *8*, 3208-3212.

[14] Y.-X. Ma, Z.-J. Li, L. Wei, S.-Y. Ding, Y.-B. Zhang, W. Wang, *J. Am. Chem. Soc.* **2017**, *139*, 4995-4998.

[15] H. Xu, J. Gao, D. Jiang, *Nat Chem* **2015**.

[16] H.-S. Xu, S.-Y. Ding, W.-K. An, H. Wu, W. Wang, *J. Am. Chem. Soc.* **2016**, *138*, 11489-11492.

[17] X. Wang, X. Han, J. Zhang, X. Wu, Y. Liu, Y. Cui, *J. Am. Chem. Soc.* **2016**, *138*, 12332-12335.

[18] Q. Fang, S. Gu, J. Zheng, Z. Zhuang, S. Qiu, Y. Yan, *Angew. Chem. Int. Ed.* **2014**, *53*, 2878-2882.

[19] X. Han, Q. Xia, J. Huang, Y. Liu, C. Tan, Y. Cui, *J. Am. Chem. Soc.* **2017**, *139*, 8693-8697.

[20] R. S. B. Goncalves, A. B. V. de Oliveira, H. C. Sindra, B. S. Archanjo, M. E. Mendoza, L. S. A. Carneiro, C. D. Buarque, P. M. Esteves, *Chemcatchem* **2016**, *8*, 743-750.

[21] S. Lin, Y. X. Hou, X. Deng, H. L. Wang, S. Z. Sun, X. M. Zhang, *RSC Advances* **2015**, *5*, 41017-41024.

[22] Q. Sun, B. Aguila, J. Perman, N. Nguyen, S. Ma, *J. Am. Chem. Soc.* **2016**, *138*, 15790-15796.
[23] P. Pachfule, M. K. Panda, S. Kandambeth, S. M. Shivaprasad, D. D. Diaz, R. Banerjee, *J. Mat. Chem. A* **2014**, *2*, 7944-7952.
[24] P. Pachfule, S. Kandambeth, D. Diaz Diaz, R. Banerjee, *Chem. Commun.* **2014**, *50*, 3169-3172.
[25] A. Nagai, Z. Guo, X. Feng, S. Jin, X. Chen, X. Ding, D. Jiang, *Nat. Commun.* **2011**, *2*, 536.

3.3.3.2 Project-related publications by participating researchers

[A3-1] L. Stegbauer, K. Schwinghammer, B.V. Lotsch, *Chem. Sci.* **2014**, *5*, 2789−2793.
[A3-2] V. S. Vyas, F. Haase, L. Stegbauer, G. Savasci, F. Podjaski, C. Ochsenfeld, B.V. Lotsch, *Nat. Commun.* **2015**, *6*, 8508.
[A3-3] T. Banerjee, F. Haase, G. Savasci, K. Gottschling, C. Ochsenfeld, B.V. Lotsch *J. Am. Chem. Soc.* **2017**, *139*, 16228-16234.
[A3-4] K. Schwinghammer, S. Hug, M.B. Mesch, J. Senker, B.V. Lotsch, *Energy Environ. Sci.* **2015**, *8*, 3345–3353.
[A3-5] V. W.-H. Lau, M. B. Mesch, V. Duppel, V. Blum J. Senker, B. V. Lotsch, *J. Am. Chem. Soc.* **2015**, *137*, 1064–1072.
[A3-6] K. Schwinghammer, M. B. Mesch, V. Duppel, C. Ziegler, J. Senker, B. V. Lotsch, *J. Am. Chem. Soc.* **2014**, *136*, 1730–1733.
[A3-7] L. Stegbauer, M. Hahn, A. Jentys, G. Savasci, C. Ochsenfeld, J. Lercher, B.V. Lotsch, *Chem. Mater.* **2015**, *27*, 7874–7881.
[A3-8] V. S. Vyas, M. Vishwakarma, I. Moudrakovski, F. Haase, G. Savasci, C. Ochsenfeld, J.P. Spatz, B.V. Lotsch, *Adv. Mater.* **2016**, *28*, 8749–8754.
[A3-9] F. Haase, T. Banerjee, G. Savasci, C. Ochsenfeld, B.V. Lotsch, *Faraday Discuss.* **2017**, *201*, 247–264.
[A3-10] F. Haase, K. Gottschling, L. Stegbauer, L.S. Germann, R. Gutzler, V. Duppel, V.S. Vyas, K. Kern, R.E. Dinnebier, B.V. Lotsch, *Mater. Chem. Front.* **2017**, *1*, 1354−1361.

3.3.4 Project Plan

The goal of this project is to develop a tailor-made nanoscale environment for two catalytic model reactions to be investigated in this CRC – hydrogen-autotransfer catalysis (**project B1**) and olefin metathesis (**project B2**) – based on mesoporous COFs. COFs stand out as porous 2D and 3D polymers providing both local and long-range order, which makes them particularly suitable as modular, molecularly defined heterogeneous reaction environments which allow for the precise tethering of molecular catalysts at spatially defined anchoring points within the COF pores. Key goals of this project are therefore the design of novel COFs based on functionalized building blocks which provide suitable surface functionalities and anchoring groups for introducing the catalyst **(WP1 & WP2**), the development of strategies for “pore-only” functionalization (**WP3**) and the controlled immobilization and in-depth characterization of catalysts and their model compounds inside the pores (**WP4**). To derive a comprehensive picture of the interplay between pore size, shape and polarity and their impact on the catalytic performance, the pore properties will be systematically varied by designing series of isoreticular COFs as well as COFs with different network topologies (2D and 3D), which will allow us to gauge whether surface polarity or confinement effects are operative (**WP5** & **WP6**), in close collaboration with **projects B1** and **B2**. By taking advantage of a closed feedback loop between materials design and characterization (**projects C1** and **C2**), catalysis screening (**projects B1** and **B2**) and theoretical modeling at multiple length scales (**projects C4**, **C5** and **C6**), we aim at establishing a tailor-made reaction environment leading to enhanced catalyst activity and selectivity.

Part A – COF level: Design of COFs with defined binding sites at the pore walls.

- **WP1: Design and synthesis of building blocks.** Functionalized building blocks for flexible and rigid linker attachment based on the orthogonal azide-alkyne click chemistry will be synthesized.
- **WP2: Synthesis** and characterization **of COFs with molecularly defined attachment points.** COFs with variable densities of attachment points will be synthesized by mixing functionalized and non-functionalized building blocks at varying ratios to probe and avoid potential steric crowding.
- **WP3: Development of pore-selective catalyst attachment strategies.** "Inner-pore" selective catalyst immobilization will be ensured by (i) the epitaxial growth of non-functionalized COF on top of functionalized COF particles, or (ii) by deactivation of surface functionalities by bulky reagents that cannot enter the pores.

Part B – Catalyst level: Anchor point distribution and selective placement of catalyst in the pores.

- **WP4: Catalyst tethering and distribution in the COF.** Diluted, homogeneous and site-selective catalyst immobilization will be pursued by optimizing the catalyst loading conditions; the density, orientation and interaction of the catalyst molecules will be optimized in collaboration with **projects B1** and **B2** and probed by spectroscopic and microscopic techniques in collaboration with **projects C1**, **C2** and **C4**.

Part C: Reaction level: Systematic studies.

- **WP5:** The chemical nature and polarity of the pore walls will be altered in order to gauge their influence on the catalyst's performance in **project B1** and **project B2**. Multiscale modelling of the solvent and reactant distribution and transport will be done in collaboration with **projects C4** – **C6**.
- **WP6:** Isoreticular COFs with gradually varying pore sizes as well as COFs with different network topologies and pore shapes will be developed to study the role of pore geometry and confinement effects on the catalytic model reactions (**project B2**) and mass transport in close collaboration with **projects C5** and **C6**.

3.3.4.1 WP1: Design and synthesis of building blocks.

In line with the molecular character of COFs, building block synthesis is the first and key step to design custom-made COFs. Already in this work package, several aspects of the catalyst attachment strategy as well as pore size and polarity variation (see WP5 and 6) will have to be considered.
The building blocks to be developed will mainly be functionalized by hydrazide, aldehyde and amide termini in order to provide access to hydrazone, azine, and imine COFs which have shown high levels of hydrolytic stability. Building blocks will be designed that provide both rigid and flexible attachment points for the unified linker/spacer concept based on the Cu-catalyzed alkyne-azide click chemistry developed in **project B1** and **project B2**. This will provide a maximum degree of freedom in positioning and arresting the catalyst in the pore by minimizing or amplifying the rigidity of the predefined spacer molecules provided by **project B1** and **project B2**. Flexible azide and alkinyl groups will be attached via literature-known protocols (Figure A3-4). So far, these strategies were exclusively based on aliphatic spacers between COF linker and functional group, which automatically causes significant flexibility for the catalyst placement in the pore. While this approach is synthetically straightforward, the exact catalyst position needs to be pinpointed by spectroscopic methods (see WP 4) and the reaction conditions tailored to avoid phase collapse, causing the catalyst to aggregate at the wall. The second, more robust approach poses bigger challenges as to the synthesis of the building blocks and the synthesis of the COF due to solubility issues and steric bulk. The rigid building blocks that will be investigated involve phenylene bridges based on T-shaped benzimidazole linkers (Figure A3-4). In addition to the design of the functionalized linkers, the unfunctionalized analogues need to be synthesized as well to dilute the functionalities and to avoid steric crowding of the catalyst. Therefore, the mixtures of linkers need to be compatible and mix freely to ensure dilute placement of the

attachment points. Further aspects that will be addressed already at the building block level include the polarity of the building blocks, which will be adjusted (i) by varying the nitrogen content and (ii) by introducing hydroxyl groups to the aromatic backbone (see WP 5), as well as the pore size and topology of the resulting COFs, which will be addressed by developing a series of isoreticular COFs as well as 3D COFs (see WP 6).

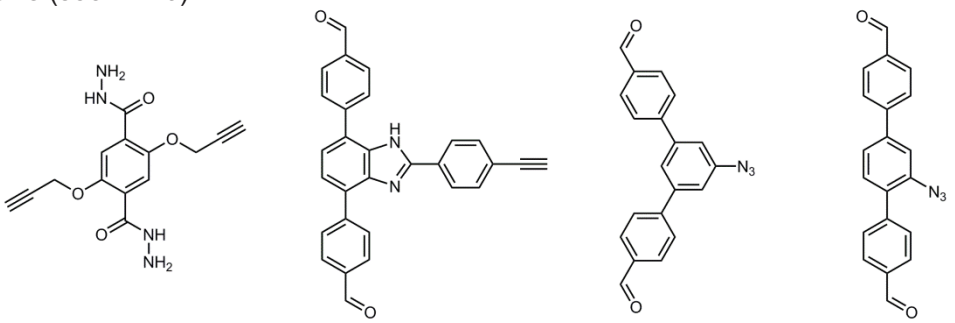

Figure A3-4: Examples of alkinyl (left) and azide (right) functionalized building blocks that will be investigated along with their non-functionalized counterparts. The propargyl functionalized building block (left) provides a flexible anchoring point, while the ethinyl-phenyl modified building block is rigid.

3.3.4.2 WP2: Synthesis and characterization of COFs with molecularly defined attachment points.

This WP addresses the synthesis and characterization of COFs with different degrees of dilution of the clickable catalyst attachment groups in the pores. To probe the catalytic activity as a function of catalyst density and interaction in the pore and to avoid steric crowding (see WP 4), solvothermal co-condensation of functionalized and non-functionalized building blocks will be explored. Synthetic challenges pertinent to COF synthesis, such as the control of crystallinity, stacking order and minimization of un-reacted “dangling bonds”, as well as the intactness of the attachment points after solvothermal synthesis will be addressed by varying the reaction conditions (solvent mixtures, reaction time and temperature etc). Special attention will be given to the development of scalable synthesis protocols that allow us to access COF on the scale of several hundred milligrams for a few batches. The resulting, partially functionalized COFs will be analyzed using spectroscopic (IR, solid-state NMR in collaboration with **project C1**) and microscopic probes (SEM and TEM), as well as powder X-ray diffraction/Rietveld analysis and physisorption.

3.3.4.3 WP3: Development of pore-selective catalyst attachment strategies.

Although the inner surface area of COFs significantly outweighs the outer surface area, catalyst attachment to the outer surface of the COFs needs to be avoided as the catalytic performance from different catalyst binding sites in (“inner-pore”) and external to the pores is difficult to disentangle. To derive meaningful insights into possible confinement effect by ensuring “inner-pore” immobilization only, two strategies will be pursued: (i), As unpublished results from the Dichtel group have shown, it is possible to epitaxially grow a COF particle on an underlying COF substrate. This approach will be adapted to passivate an azide/propargyl functionalized COF particle by homoepitaxial growth of isostructural, non-functionalized COF such that the catalyst will always be immobilized at sufficient distance from the surface (Figure A3-5). (ii) The second approach will follow the more traditional approach of using bulky, polymer based reagents to selectively “de-functionalize” the clickable azide/alkinyl groups hosted at the surface, for example through selective reduction of terminal azides to amines by using phosphine-modified poly(styrene) and water or the conversion of alkynes to di- or tetrabromoalkanes with polymer-bound pyridinium tribromide.

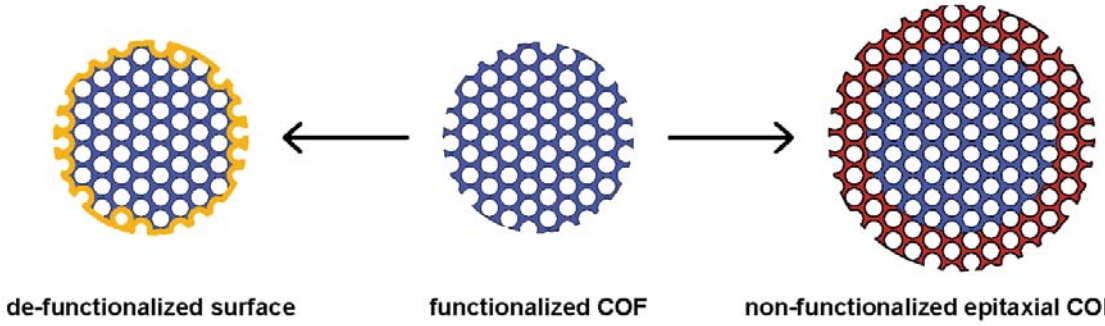

Figure A3-5: Schematic of the two passivation schemes that will be used to ensure inside-only functionalization. Blue: functionalized COF, orange: de-functionalized surface, red: epitaxial unfunctionalized COF-shell.

3.3.4.4 WP4: Catalyst tethering and distribution in the COF.

This WP will address the hybridization of the COF with the catalyst via click chemistry and the subsequent characterization of the density, orientation and dynamics of the tethered catalyst within the COF pore in close collaboration with **project C1**, **project C2** as well as insights from multiscale theoretical modeling of the COF - catalyst system by **project C4**. Key targets of this WP are (i) the controlled and uniform distribution of catalysts in the pores to avoid clustering and crowding (potentially leading to catalyst deactivation), and (ii) elucidation of the catalyst orientation and position and its interaction with other catalyst species and the pore walls.
Since the catalytic activity will be fundamentally dependent on the site-specific and quantitative attachment of the catalyst to the anchoring groups, catalyst immobilization strategies will be optimized in close collaboration with **project B1** and **project B2** and protocols for efficient infiltration, uniform distribution and quantitative removal of non-tethered catalyst in the pores will be elaborated to avoid pore blocking or trapping of excess catalyst.
Catalyst immobilization will first be analyzed with physisorption techniques (Ar and CO_2 sorption) to elucidate the effects of catalyst loading on surface area and accessible porosity. Homogeneous catalyst distribution in the pores will be probed with high-resolution TEM by using the heavy metal centers of the

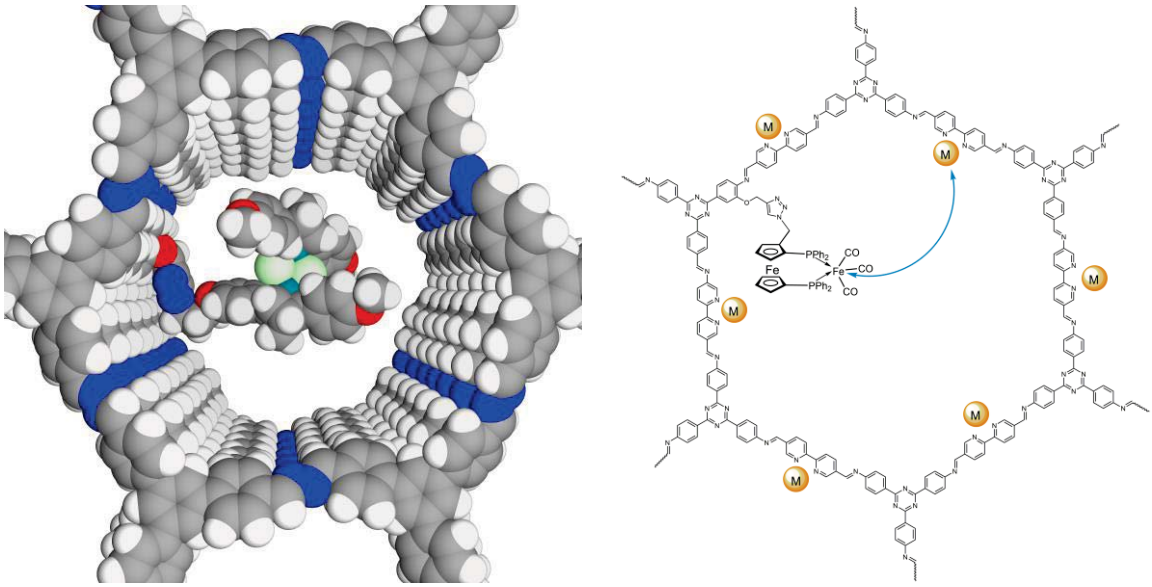

Figure A3-6: Left: Space-filling model of a homogeneous catalyst tethered to the pore wall of a COF that has been sparsely functionalized to avoid catalyst crowding in the pore. Right: A paramagnetically modified COF through chelation with a paramagnetic metal species by the bipyridine building blocks.

catalysts as probes. The spatial distribution and host – guest as well as guest – guest interactions will be studied by solid-state NMR spectroscopy in collaboration with **project C1** using specifically developed phosphine-based probe molecules in conjunction with polarization transfer techniques such as cross-polarization and double quantum experiments, if necessary with isotopically marked or enriched samples. In addition, the *dppf*-tricarbonyl-Fe model complex will be introduced into the COF pores and used as a multiprobe complex for in-depth Mössbauer, IR- and high frequency EPR spectroscopy carried out in **project C2**. Specifically, we will explore the dipolar couplings between this paramagnetic probe molecule and a paramagnetically functionalized / radical-bearing COF pore, which carries paramagnetic metal centers (M = Cu(II), Co(II) etc) immobilized within the linker as depicted in Figure A3-6 (right), to derive catalyst conformation, orientation and distance information. In perspective, such COFs hosting paramagnetic centers will be useful also for DNP NMR spectroscopic studies planned by **project C1**.

3.3.4.5 WP5: Polarity variation of the COF pore walls.

This WP is devoted to systematically studying possible effects of the surface functionalization and polarity of the COF pore wall on the catalytic performance and will rely on close feedback from selectivity and activity studies carried out in **project B1** and **project B2**.
Specifically, we will address the impact of pore polarity on the Ru-catalyzed hydrogen-autotransfer catalysis investigated in **project B1**. Here, alcohols are transformed into amines in a multi-step transformation of (catalytic) dehydrogenation – condensation – (catalytic) hydrogenation. Typically, the condensation agent (i.e. the amine) has to be used in large excess to shift the condensation equilibrium to the imine side, which severely reduces the efficiency of the reaction. The lipophilic (N,N,N,N)(P)Ru-complex developed in the Plietker group circumvents this shortcoming by enriching the ketone formed upon dehydrogenation in the ligand sphere of the catalyst whilst ensuring fast removal of the water formed during the condensation step (for details see **project B1**). It is envisaged that by enhancing the hydrophilicity of the pore walls, driving the water away from the catalyst to the pore surface, this process is made even more efficient. We will therefore aim at systematically studying the impact of varying pore polarity on the catalytic turnover by attaching polar and/or protic side groups to the pore walls, especially hydroxyl groups in order to increase polarity (Figure A3-7). Variation of the nitrogen content in the COF backbone will also be investigated as it is expected to impact the polarity of the pore walls further. These changes likely influence the substrate preorientation and the solvent distribution in the pores. To quantify the impact of pore wall functionalization and to obtain insights into the solvent distribution as a function of the distance from the pore wall as well as type of pore functionalization, molecular mechanics combined with quantum chemical calculations of the active center (QM/MM) will be carried out by **project C4**, and the spatio-temporal behavior of the fluid mixture, including the diffusional transport of the reactants and products in the COF pore systems, will be analyzed by **projects C5** and **C6** using atomistic molecular dynamics simulations, entropy scaling and classical DFT, or coarse-grained catalytic models, respectively. The goal is to obtain a range of COFs in which the used solvent mixtures form polarity gradients changing from hydrophobic at the pore center to hydrophilic at the pore wall within one system.
In a related approach, the impact of functional groups integrated into COFs (polar, non-polar, protic, aprotic) on the reactivity of immobilized N-heterocyclic carbene (NHC) complexes of Mo-imido-, W-imido- and W-oxo-alkylidenes for olefin metathesis will be studied in collaboration with **project B2**. Here, differently functionalized olefins (polar, non-polar, protic, aprotic) will be tested and their conversions in different types of ring-closing metathesis and macrocyclization reactions will be studied as a function of the nature of the COF pore walls.

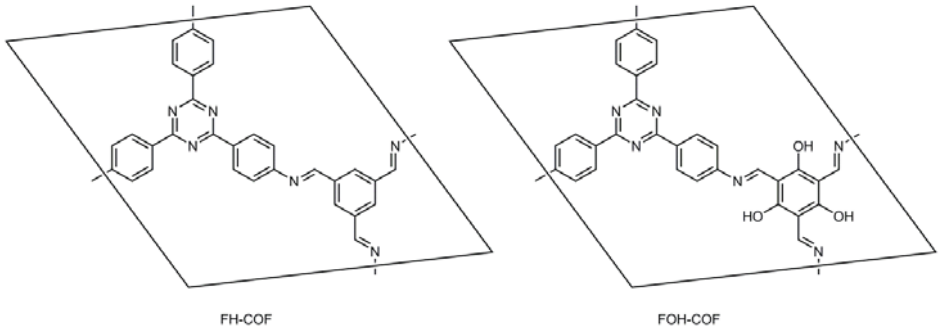

Figure A3-7: Isostructural COFs synthesized in the Lotsch group that show varying polarity.

3.3.4.6 WP6: Variation of pore size and network topology.

The impact of COF pore size will primarily be studied in the context of the metathesis reactions investigated in **project B2**. Due to the inherent reversibility of metathesis reactions, the final product distribution is expected to be influenced by a confining reaction field. This holds especially true for metathesis reactions with significant entropy contributions, such as the entropically challenged acyclic diene metathesis (ADMET) polymerization which entails significant changes in the number of reactants and their molecular weight. Specifically, the tendency of an acyclic diene substrate to undergo either cyclization or polymerization (ring-closing metathesis (RCM) vs. ADMET) will be monitored as a function of pore size, as confinement effects are expected to favour RCM over ADMET or drive ADMET towards short-chain oligomeric systems. Further confinement effects that will be addressed involve changes in product distribution in cross metathesis reactions as well as catalyst stability (for details see **project B2**).
The local densities of the reactants, as well as diffusive transport of substrates and products into and out of the pore will be studied and quantified in collaboration with **projects C5** and **C6** using atomistic molecular dynamics simulations and fluid-theoretical methods like classical DFT (**project C5**) or coarse-grained methods (**project C6**). To this end, we will provide precise structural parameters of COFs with different types of pore sizes, surface functionalizations and pore geometries (e.g. spherical pores vs. 1D channel-type pores) or multi-pore systems. A series of isoreticular, i.e. isostructural, pore expanded COFs will be designed by using isoreticular building blocks augmented by phenylene or alkyne units with a focus on two component COFs. Here, the clickable building block will be left unchanged and the other component expanded to keep the isoreticular COFs as similar to each other as possible (
Figure A3-8).

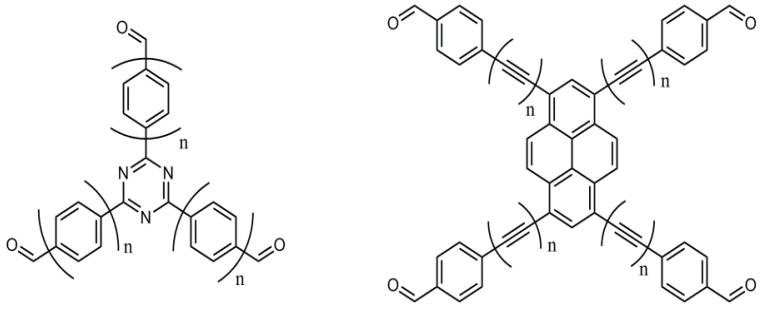

Figure A3-8: Two examples of building blocks for isoreticular COFs yielding systematically pore-expanded structures.

As the topology of the network and, hence, the geometry of the pores is expected to further influence the confinement effect for catalysis, we will replace the cylindrical pore systems of 2D COFs with non-cylindrical or spherical pores. Pronounced effects are expected specifically for the metathesis reactions studied in **project B2** were the pre-orientation of the catalyst and the olefin substrate, which are likely to influence catalyst activity and product distribution, will crucially depend on the pore size and shape. A change in pore topology will be effected by the synthesis of 3D instead of 2D COFs. These can be synthesized for example by the combination of tetrahedral C_4 building blocks (e.g. tetraphenylmethane)

with linear (C_2) ones, or by combining C_3 with C_4 symmetrical building blocks (Figure A3-9). The 3D COFs are more complex in their synthesis and often suffer from network interpenetration. This WP is therefore planned for the second half of this funding period.

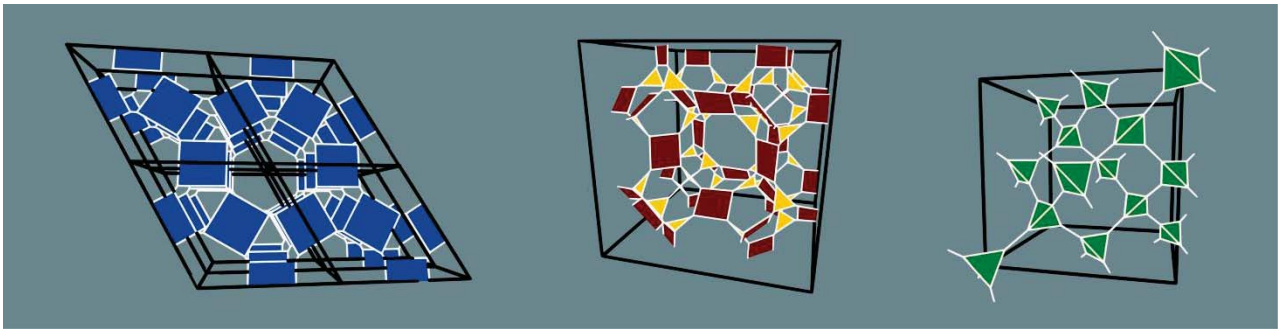

Figure A3-9: Examples of network topologies of 2D and 3D COFs demonstrating how the geometry of the building block and their combination determines the structure.

Chronological work plan:

	2018 Q3 Q4	2019 Q1 Q2 Q3 Q4	2020 Q1 Q2 Q3 Q4	2021 Q1 Q2 Q3 Q4	2022 Q1 Q2	
T1						WP1: Design and synthesis of building blocks (PhD1, PhD2, technician)
T2						WP 2: Synthesis and characterization of COFs with molecularly defined attachment points (PhD1, PhD2)
T3						WP 3: Development of pore-selective catalyst attachment strategies (PhD1, PhD2)
T4						WP 4: Catalyst/probe tethering and distribution in the COF (PhD1, PhD2)
T5						WP 5: Polarity variation of the COF pore walls (PhD1)
T6						WP 6: Variation of pore size and network topology (PhD2)

3.3.4.7 Methods applied

This project combines preparative methods from organic synthesis (linker design), “soft” chemistry and solid-state chemistry (COF synthesis) with spectroscopic (IR, solution and solid-state NMR spectroscopy, EELS, XPS), diffraction (PXRD), microscopic (SEM, TEM, AFM) and other techniques (physisorption) to arrive at a comprehensive picture of the local and long-range structure as well as nano and micron scale morphology of (functionalized) COFs.

3.3.4.8 Vision

By the end of the first funding period we expect to have access to a set of precisely defined and stable COF systems with site-specifically immobilized catalyst moieties that furnish detailed insights into the impact of pore size, geometry, polarity and network topology on the activity and selectivity of the catalytic model reactions. By virtue of the local and long-range definition, paired with the molecular tunability inherent to COFs, a comprehensive experimental and theoretical description of the COF –

catalyst hybrid system is realistic, which in turn should enable a detailed understanding of structure – property – activity relationships in the systems under study.

The synthetic achievements of the first funding period will form the basis for more complex COF topologies such as multipore COFs allowing for compartmentalized reaction spaces with different pore sizes and polarities within single COF scaffold, which could be interesting for multistep and multicomponent reactions (Figure A3-10). Another thrust will follow the development of hierarchical COF structures with communicating bi- or multimodal pore systems providing not only small mesopores as custom-made nanoreactors, but also larger transport pores which may be accessible by COF synthesis in the presence of soft templates. These architectural achievements will be used to enlarge the scope of catalytic reactions to be studied, including enantioselective and photo-redox catalysis.

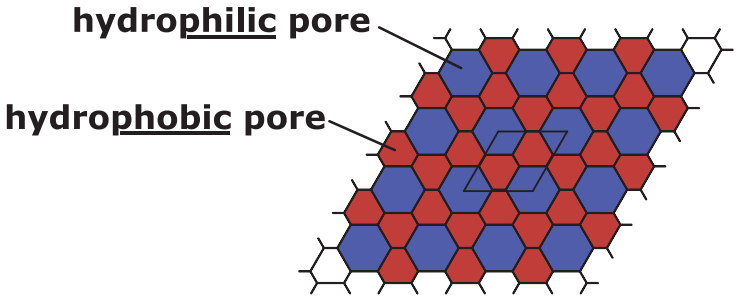

Figure A3-10: Schematic example of complex pore design by separation of pore channels to create separate reaction spaces with different polarities and pore sizes.

3.3.5 Role within the Collaborative Research Center

This project will deliver a modular polymeric materials platform for the defined attachment of different organometallic catalysts. Owing to the organic nature of COFs, paired with crystallinity, these materials provide a versatile basis for the study of heterogenized molecular catalysts in well-defined and geometrically confined spaces with precisely adjustable pore sizes, shapes, network topologies and variable surface chemistry. As such, COFs are complementary to both inorganic and other polymeric systems studied in the CRC.

By providing the substrate for the attachment of the catalyst systems studied in **project B1** and **project B2**, close interactions will naturally exist with Area B to study the catalytic performance of catalyst-substrate model systems. Likewise, details of the structure of the pristine and loaded COF as well as the arrangement and dynamics of the immobilized catalysts will be derived in close collaboration with Area C, specifically **project C1, project C2**, and **project C4**. For the simulation of the catalyst orientation and its chemical reactivity modified by the pores, COFs are particularly attractive systems owing to the molecularly defined nature and crystallinity of the backbone which enables the realistic modeling of the overall system at multiple length scales (including solvent distribution, substrate/product diffusion and transport, to be studied together with **projects C5** and **C6**), with minimal approximations and maximum precision.

3.3.6 Differentiation from Other Funded Projects

Project A3 has no direct topical overlap with other projects pursued in this PI's group:

BMBF project "StickLis" (FKZ: 03XP0030C), 1.1.2016-31.12.2018: Development of COFs as cathode materials for Lithium-Sulfur batteries; since the focus is on electrochemical properties of COFs there is no direct overlap with the current proposal.

ERC Starting Grant "COFLeaf" (grant number 639233), 1.9.2015-1.9.2020: Development of COFs as platforms for photocatalytic water splitting and CO_2 conversion. In this project, COFs are used as light absorbers hybridized with electrocatalysts. Since photoinduced reactions are exclusively targeted within this project and the electrocatalysts are either nanoparticulate metals or have no covalent connection with the COF, or the COF backbone is part of the catalyst's ligand system ("surface organometallic chemistry"), no direct overlap with the projects developed in this collaborative research program is given.

3.3.7 Project Funding

3.3.7.1 Previous Funding

This project is currently not funded and no funding proposal has been submitted.

3.3.7.2 Requested Funding

Funding for	2018		2019		2020		2021		2022		2018-2022	
Staff	Quantity	Sum	Quantity	Sum	Quantity	Sum	Quantity	Sum	Quantity	Sum	Quantity	Sum
PhD student, 67%	1	21,600.-	1	43,200.-	1	43,200.-	1	43,200.-	1	21,600.-	1	169,600.-
Total		21,600.-		43,200.-		43,200.-		43,200.-		21,600.-		169,600.-
Grand total	21,600.-		43,200.-		43,200.-		43,200.-		21,600.-		172,800.-	

No funding for direct costs is requested. (All figures in EUR; staff funding according to DFG form 60.12)

3.3.7.3 Requested Funding for Staff

	Sequen-tial no.	Name, academic degree, position	Field of research	Department of university or non-university institution	Project commit-ment in hours per week	Category	Funding source
Existing staff							
Research staff	1	Bettina, Lotsch, Prof. Dr.		Department Nanochemistry, MPI-FKF	4		MPI
Research Staff	2	M. Sc. Kerstin Gottschling	COF synthesis and character-ization	Department Nanochemistry, MPI-FKF	20		MPI
Non-Research Staff	3	Marie-Luise Schreiber	Synthesis of organic building blocks	Department Nanochemistry, MPI-FKF	8		MPI
Non-Research Staff	4	Sigrid Zehetleitner		Department Nanochemistry, MPI-FKF	2		MPI
Requested staff							
Research staff	5	M. Sc. Sebastian Hemmerling	COF synthesis and character-ization	Department Nanochemistry, MPI-FKF		PhD stu-dent, 67%	

Job description of staff (supported through existing funds):
1
Principal investigator for **project A3**
2
Kerstin Gottschling, PhD student, has carried out preliminary COF syntheses, characterization and functionalization with clickable anchoring groups. She will be involved in WP 1 – 3 as well as aspects of WP 4 – 6 dealing with metathesis reactions (**project B2**).
3
Marie-Luise Schreiber, chemical technical assistant, will assist the PhD students in all preparative aspects of building block synthesis and characterization
4
Secretary

Job description of research staff (requested funds):
5
One PhD Student E13 (67%) for 48 months is requested. The PhD student will be involved in WP 1 – 3 as well as aspects of WP 4 – 6 dealing with the hydrogen autotransfer catalysis (**project B1**). This work requires advanced synthetic expertise to produce and functionalize complex molecular building blocks and COF polymers. In addition, sound knowledge of solid-state chemistry and analytical skills are crucial for the in-depth structural characterization of COFs and their catalyst-modified derivatives. Hence, a chemist with a Master degree is required. An appropriately trained candidate – Mr. Sebastian Hemmerling – has already been identified.

3.3.1.4 Requested Funding of Direct Costs
No funding of direct costs is requested.

3.3.1.5 Requested Investments
No investments are requested.

3.4 Project A4

3.4.1 General information about project A4

3.4.1.1 Controlled synthesis of mesoporous silica materials

3.4.1.2 Research areas
Solid State and Surface Chemistry, Materials Synthesis (302-01), Physical Chemistry of Solids and Surfaces, Materials Characterization (302-02)

3.4.1.3 Principal investigators
Traa, Yvonne, PD Dr., born 10. 10. 1969, German, female
Institute of Chemical Technology
University of Stuttgart, Pfaffenwaldring 55, 70569 Stuttgart
Tel.: 0711/685-64061
E-Mail: yvonne.traa@itc.uni-stuttgart.de
Senior academic staff member

Gießelmann, Frank, Prof. Dr., born 01. 07. 1963, German, male
Institute of Physical Chemistry
University of Stuttgart, Pfaffenwaldring 55, 70569 Stuttgart
Tel.: 0711/685-64460
E-Mail: frank.giesselmann@ipc.uni-stuttgart.de
Tenured professor (W3)

3.4.1.4 Legal issues
This project includes

1.	research on human subjects or human material.	no
2.	clinical trials.	no
3.	experiments involving vertebrates.	no
4.	experiments involving recombinant DNA.	no
5.	research involving human embryonic stem cells.	no
6.	research concerning the Convention on Biological Diversity.	no

3.4.2 Summary
Since their discovery in 1992, ordered mesoporous silica materials (OMSMs) have received substantial scientific interest and set the benchmark for mesoporous materials. This project aims to push the limits of current OMSMs and extend their application to the field of molecular heterogeneous catalysis. This requires (i) an extension of the common pore diameter range from 2 – 8 nm in current OMSMs to a range from 8 – 20 nm, necessary for the attachment of bulky molecular catalytic systems to the inner pore surface, and (ii) the precise control of the mean pore diameter to enable conclusive studies of confinement effects. We suggest to meet these challenges by the so-called *true liquid crystal templating* of lyotropic liquid crystal phases, namely the 2D-hexagonal phases formed by amphiphilic block copolymers in water. Using the toolbox of surfactant liquid crystal chemistry, the diameter of rod-like micelles (and thus the pore diameter of the final OMSM) will be tailored by the composition of surfactants and cosurfactants, the final wall thickness is tuned by the water content of the liquid crystal template. To obtain detailed insights into the templating process, the structures of the initial liquid crystal templates, the as-synthesized hybrid materials thereof and the final OMSMs will be studied by small-angle X-ray scattering. The final OMSMs will be further characterized by standard nitrogen adsorption as well as by adsorption studies of probe molecules. Due to their superior thermal and chemical stability, the large pore OMSMs developed in this project will be applied in all three catalytic projects of this CRC. Silanol groups at the outer surface will be inertized *before* the organic templates are removed from the pores. After template removal, the inner pore surfaces will be selectively functionalized to enable the attachment of the molecular catalytic system by means of *click chemistry*. Finally, we will provide common SBA-type materials synthesized by proven recipes as reference standards for B and C projects and will explore OMSMs with new pore geometries, namely elliptical

pores as replica of rectangular ribbon phases or chirally structured pores as replica of lyotropic cellulose nanocrystal (CNC) phases.

3.4.3 Research rationale

3.4.3.1 Current state of understanding and preliminary work

Mesoporous silica materials

Only the discovery and application of micelles as templating agents has allowed the preparation of solids with constant pore sizes in the range of 2 to 10 nm. [1] Even though there had been some earlier reports, the actual breakthrough came with the first reports on the M41S family of ordered mesoporous silica materials at the beginning of the 1990s. [1,2] Thus, silica materials are the original mesoporous materials and are vital as support materials for this CRC. Later, a large number of materials with different compositions, symmetries and architectures have been developed. However, when looking at the most popular mesoporous silica materials, for which also verified synthesis recipes exist, the pore sizes range between 2 and 4 nm for MCM-41 and MCM-48 and between 4 and 8 nm for SBA-15 and SBA-16. Only for Al-SBA-15, pore diameters larger than 10 nm are reported in the verified synthesis recipes. [2] Thus, the range of accessible mesopore sizes is limited. In addition, the control of the pore size is difficult.

Due to the higher chemical, thermal and hydrothermal stability, which results from the thick microporous silica pore walls (3-6 nm), [2] the focus of the work for this CRC will be on SBA materials and related materials produced from non-ionic triblock copolymers ($EO_nPO_mEO_n$) with large polyethyleneoxide $(EO)_n$ and polypropyleneoxide $(PO)_m$ blocks in acidic conditions. Structures accessible with this synthesis technique are SBA-15 (2D pore system with hexagonally structured, curved parallel pores), PHTS (plugged hexagonal templated silica, derived from SBA-15 using microporous amorphous nanoparticle plugs resulting in inkbottle-like sections), SBA-16 (cubic phase consisting of two non-interpenetrating 3D channel systems with spherical cavities at the intersection of the channels) and MCF (mesostructured cellular foam, resulting by addition of a swelling agent such as mesitylene to the synthesis of SBA-15 causing an enlargement of the micelle resulting in a sponge-like foam with three dimensional structure and large open uniform spherical cells.). [2] In addition, FDU-12 (face-centered cubic packing of spherical cavities) is synthesized under similar conditions. [3]

Lyotropic liquid crystals (LLCs)

Lyotropic liquid crystals are long-range ordered fluid solutions of *e.g.* amphiphilic molecules (surfactants) in water.[4,5] Driven by the hydrophobic effect, amphiphilic molecules aggregate above a certain critical concentration into micelles, the shape and dimensions of which depend on the steric constraints of the surfactant molecule and the solvation state of its hydrophilic head group. At further increasing volume fraction of micelles, the micelles self-organize via inter-micellar interactions into liquid-crystalline structures, each of which exhibits specific degrees of long-range orientational and translational order (Fig. A4-1). In the hexagonal phase for instance, the principal axes of rod-shaped micelles are parallel to each other (long-range orientational order) and positionally arranged on a 2D hexagonal lattice (long-range 2D translational order). The hexagonal phase can thus be considered as a 2D “solid” in the directions along the 2D hexagonal lattice and a 1D fluid in the direction normal to the 2D lattice. The volume between the micelles is filled with water which enhances the fluidity of the phase.

Depending on the solvent concentration (and temperature), a single amphiphile can typically

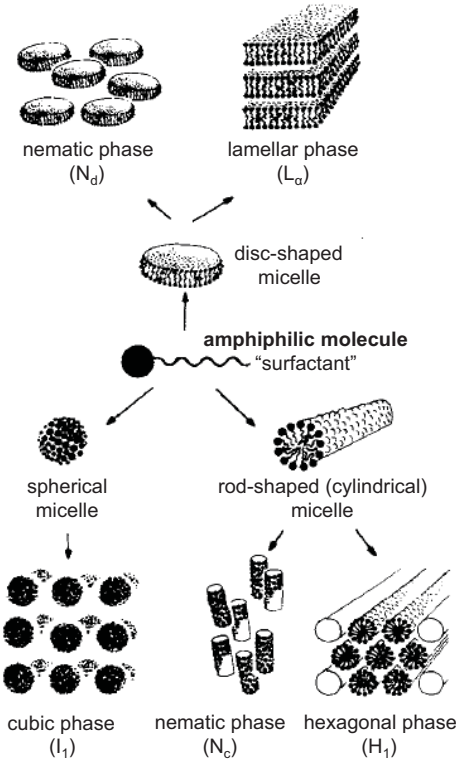

Fig. A4-1: Self-organization of amphiphilic molecules into micelles and lyotropic liquid crystal phases. Figure redrawn from Ref. [5].

form several LLC phases. A specific example is shown in Fig. A4-2: Below 60 wt-% of water (surfactant concentration > 40 wt-%) a hexagonal LLC phase of cylindrical micelles is formed. The further reduction of the water concentration leads to a more and more shrinking solvation sphere around the hydrophilic ethylene oxide head groups. This in turn reduces the mean curvature of the micellar aggregates and finally leads to a lamellar phase of flat amphiphile bilayers. The hexagonal and lamellar phases are separated from each other by an intermediate bi-continuous phase of cubic symmetry *Ia3d*.

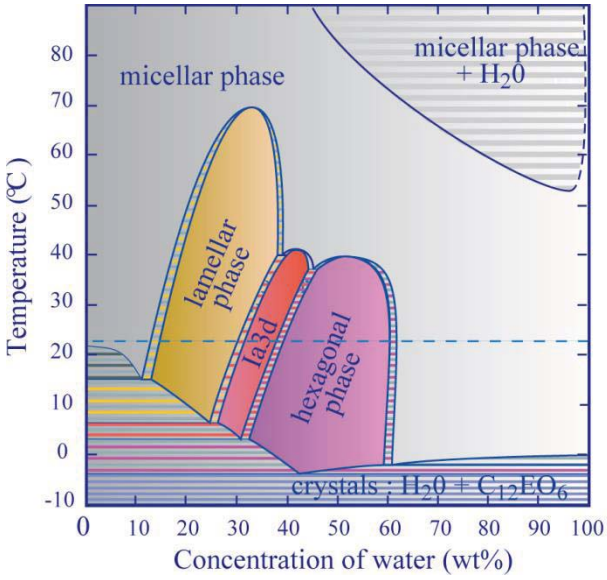

Fig. A4-2: Binary phase diagram of the non-ionic surfactant $C_{12}EO_6$ and water. [6]

For a given binary surfactant/water system the polymorphism of LLC phases can further be tuned by the addition of cosurfactants, namely long chain alcohols or fatty acids, which do not form micelles in water on their own. Instead, the cosurfactant molecules are incorporated into the surfactant micelles where they modify the shape, *i.e.* the mean curvature, as well as the volume of the micellar aggregates. This can dramatically change the LLC phase behavior and lead to rather complex ternary phase diagrams, even with LLC phases that do not exist in the binary phase diagram.
Today, soft matter science has achieved a substantial body of data and experience which allows – at least to a certain extent – to rationalize the appearance and the structure of LLC phases. This knowledge base opens a powerful toolbox for the design of LLC phases with tailored dimensions and arrangements of micellar structures.

True liquid crystal templating (TLCT)
With the groundbreaking work of Kresge *et al.*[7] in the beginning of the 1990ties, lyotropic liquid crystals received considerable relevance in the field of catalysis science and technology, since LLC phases – namely the hexagonal LLC phase – opened new and elegant synthetic routes to ordered mesoporous silica materials with narrow distributed pore diameters. These materials could now be synthesized via *soft templating* of either stable or intermediate lyotropic liquid crystals (LLCs) (Fig. A4-3).[2]
The so-called *true liquid crystal templating* (TLCT) route consists of three steps: In the first step the surfactants in highly concentrated aqueous solutions form a stable hexagonal LLC phase with cylindrical micelles. This phase can be considered as a periodic array of hydrophobic (the interior micelle volumes) and hydrophilic (the coherent water-rich intermicellar volume) regions. After addition of a silica source such as tetraethyl orthosilicate (TEOS, $Si(OEt)_4$) in the second step, the hydrolysis of $Si(OEt)_4$ and the subsequent condensation of the silanols will preferentially take place in the water-rich intermicellar volume. As a result, the water-rich regions of the former LLC phase will be replaced by an SiO_x structure, which encloses the cylindrical micelles. In the third step the micelle-forming organic surfactant is removed by calcination or extraction with organic solvents. The final mesoporous silica material is thus a more or less exact replica of the structure of the former LLC. Its structure (arrangement, diameter and shape of the pores) can thus be systematically controlled via formulation of proper LLC precursor phases. In particular, the diameter of the pores is related to the diameter of the cylindrical micelles which in turn can be precisely adjusted in the LLC formulation by the molecular length of the selected surfactant and the addition of cosurfactants. Another advantage of the TLCT route is the option to align the LLC phase before templating. As shown by Tolbert et al. [8] the templating of a magnetic-field aligned hexagonal LLC phase has led to mesoporous silica monoliths with pore directions parallel aligned over macroscopic dimensions (Fig. A4-4).

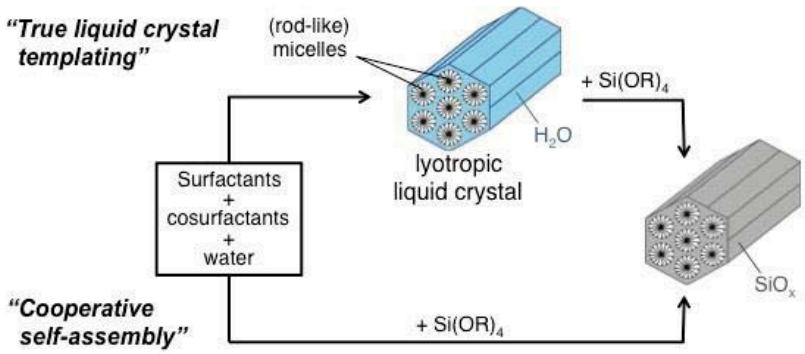

Fig. A4-3: Synthesis routes to mesoporous silica materials via *soft templating*.

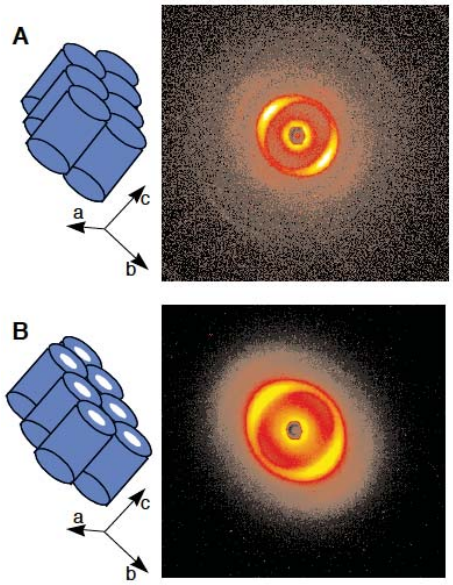

Fig. A4-4: 2D XRD patterns of mesoporous silica materials with aligned pore morphology before (A) and after (B) calcination. [8]

Via an alternative route, the silica source is directly added to a diluted aqueous micellar solution of surfactants, which can directly lead to an ordered hybride structure of SiO_x and surfactant micelles (Fig. A4-3). The precise mechanism of this so-called *cooperative self-assembly* route is still unexplained. Since this pathway is much easier in terms of handling and processing, it is frequently used in verified syntheses of mesoporous silica materials. [2] A rational and systematic control of the final mesoporous silica structures however is almost impossible and the design thus essentially relies on trial-and-error iterations.
Over the last 20 years the soft templating synthesis has developed to a very active and mature field of research where hundreds of new mesoporous silica materials were synthesized and investigated. [9,10] The vast majority of these materials however is limited to pore sizes below 10 nm (typically 2–8 nm). To the best of our knowledge there exist only very few examples of mesoporous silica materials with pore sizes in the range between 10 and 20 nm. [10] There is, e.g., only one reference for the synthesis of SBA-15 *via* TLCT. [11] The challenge for synthesis of large-pore ordered mesoporous materials was highlighted in a recent perspective article in JACS. [12] The so-far successful approaches use polyethylene oxide based amphiphilic block copolymers such as the commercial Pluronic polymers instead of low-molecular surfactants. Due to their high molecular volume, these block copolymers form micelles with larger diameter and thus lead to larger pores in the final silica replica. Further access to control the pore size is given by the addition of cosurfactants [13] or swelling agents such as *n*-dodecane or 1,3,5-trimethylbenzene [14] which are preferentially solubilized in the hydrophobic interior of the micelles and thereby enlarge the micelle diameter.
Since molecular heterogeneous catalysis in confined geometries requires larger pore diameters in the range from 5 to 20 nm, the rational design and controlled synthesis of large-pore mesoporous silica materials tailored for the needs of the catalytic projects of the CRC will be the foremost aim of this project throughout the first funding period.

Surface functionalization
Before focusing at functionalization of the mesoporous silica materials prepared, it is necessary to have a look at the surface properties: For the most frequently studied MCM-41 material, three different types of silanol groups can be observed, i.e., single, hydrogen-bonded and geminal silanol groups (Fig. A4-5). [15] Important is the fact that free silanol groups are highly accessible to silylating agents, whereas hydrogen-bonded ones are not. [15]

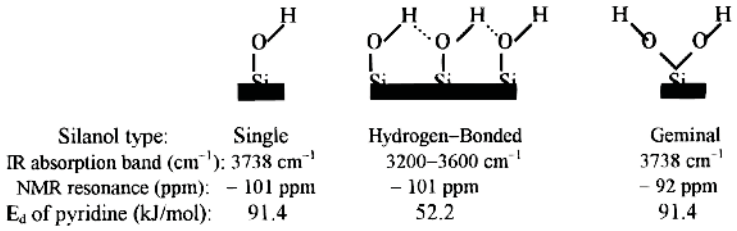

Figure A4-5: Schematic representation of the three types of silanol groups in siliceous MCM-41 and their characteristics. [15]

With increasing temperature, dehydroxylation of hydrogen-bonded and geminal SiOH groups leads to

siloxane bonds and more free SiOH groups. Whereas silica surfaces dispose of 5-8 SiOH groups per nm^2, the number is only 2.5-3 for MCM-41, since MCM-41 is better ordered than silica and, thus, the surface is more condensed with less SiOH groups. [15] The point of zero charge for silica and also mesoporous silica materials is around pH values of 2 or 3, which means that the surface is at neutral pH values negatively charged. [16] The hydrophilicity of the surface can be tuned by insertion of aluminum, and it has been shown for MCM-41 that the surface becomes less hydrophobic and more hydrophilic with increasing Al content as demonstrated by benzene and methanol adsorption. [17]
Silanization is a straightforward and well studied technique to functionalize the surface of silica. [18] This technique is obviously also useful for the functionalization of mesoporous silica materials. If the first silanization step is conducted *before* template removal, the external surface can easily be functionalized in a different way than the internal surface, which is then functionalized *after* template removal. [19] Another option is to use bulky silanes, which do not have access to the pore system, to functionalize the external surface and smaller silanes for the internal surface. A very elegant and economic way to functionalize the internal surface of mesoporous materials synthesized under acidic conditions is a direct exchange process with silanes replacing the surfactant (also called template displacement with organosilanes (TDS)). In this way, the weak hydrogen bondings between the surfactants and the silanol groups or the electrostatic interactions between the negatively charged deprotonated silanol groups and the positively charged surfactant cations are replaced by a strong chemical bond. Thus, the calcination step is avoided and the surfactant can be recovered. [20,21] The variation of the size of the side groups even renders a control of the coverage possible, since obviously higher densities of surface functionalities are possible with methoxy than with ethoxy groups. [20] In addition, the shrinkage of the structure as observed during calcination by condensation of neighboring surface silanols with formation of siloxane bonds is avoided, the structure is stabilized and higher silyl coverages are possible. It has also been demonstrated that TDS is possible for monoliths obtained via a TLCT approach. [22] Another option is even the direct co-condensation with the silane directly in the LLC phase during synthesis of the mesoporous material, which has been successfully applied for tetramethyl orthosilicate and 3-mercaptopropyltrimethoxysilane in the LLC phase of Brij 56 ($C_{16}EO_{10}$). [23]

Characterization of the pore size using molecular probes
For microporous zeolites, there are many methods for the characterization of the effective pore size: On the one hand, adsorption of probe molecules with different sizes is used to access the pore size. On the other hand, there are many different test reactions where the selectivity depends, in an unambiguous manner, on the pore width (so-called shape selectivity). These techniques are nowadays used as quick tests for probing the effective pore width under catalytically relevant conditions and/or for materials modified with post-synthesis methods. [24] However, these characterization methods are only available for microporous materials. Up to now, corresponding methods for the characterization of mesoporous materials have not been developed, and the literature is poor in this field. [25] The challenge is that the probe molecules have to be large enough to “feel” the presence of the pores for an assessment of the pore width, and this is not straightforward for mesopores with sizes between 2 and 50 nm.

References

[1] F. Di Renzo, A. Galarneau, P. Trens, F. Fajula, in: Handbook of Porous Solids (F. Schüth, K.S.W. Sing, J. Weitkamp, eds.), Vol. 3, Wiley-VCH, Weinheim, 2002, pp. 1311-1395.
[2] V. Meynen, P. Cool, E.F. Vansant, *Microporous Mesoporous Mater.* **2009**, *125*, 170-223.
[3] M. Kruk, C.M. Hui, *Microporous Mesoporous Mater.* **2008**, *114*, 64-73.
[4] C. Fairhust, S. Fuller, J. Gray, M. C. Holmes, G. J. T. Tiddy in: Handbook of Liquid Crystals (D. Demus, J. Goodby, G. W. Gray, H.-W. Spiess, V. Vill, eds.), Vol. 3, Wiley-VCH, Weinheim, 1998, pp. 341–392.
[5] H. Ringsdorf, B. Schlarb, J. Venzmer, *Angew. Chem. Int. Ed.* **1988**, *27*, 113-158.
[6] P. Pieranski, *Materials* **2014**, *7*, 3453-3469.
[7] C. T. Kresge, M. E. Leonowizc, W. J. Roth, J. C. Vartuli, J. S. Beck, *Nature* **1992**, *359*, 710-712.
[8] S. H. Tolbert, A. Firouzi, G. D. Stucky, B. F. Chmelka, *Science* **1997**, *278*, 264-268.
[9] A. Corma, *Chem. Rev.* **1997**, *97*, 2373-2419; Y. Yamauchi, N. Suzuki, L. Radhakrishnan, L. Wang, *Chem. Rec.* **2009**, *9*, 321-339; N. D. Petkovich, A. Stein, *Chem. Soc. Rev.* **2013**, *42*, 3721-3739.
[10] Y. Wan, D. Zhao, *Chem. Rev.* **2007**, *107*, 2821-2860.

[11] S.G. Wainwright, C.M.A. Parlett, R.A. Blackley, W. Zhou, A.F. Lee, K. Wilson, D.W. Bruce, *Microporous Mesoporous Mater.* **2013**, *172*, 112-117.
[12] J. Wei, Z. Sun, W. Luo, Y. Li, A. A. Elzatahry, A. M. Al-Enizi, Y. Deng, D. Zhao, *J. Am. Chem. Soc.* **2017**, *139*, 1706.
[13] P. Feng, X. Bu, D.J. Pine, *Langmuir* **2000**, *16*, 5304-5310.
[14] J. S. Lettow, Y. J. Han, P. Schmidt-Winkel, P. Yang, D. Zhao, G. D. Stucky, J. Y. Ying, *Langmuir* **2000**, *16*, 8291-8295.
[15] X.S. Zhao, G.Q. Lu, A.K. Whittaker, G.J. Milar, H.Y. Zhu, *J. Phys. Chem. B* **1997**, *101*, 6525-6531.
[16] A.J. O'Connor, A. Hokura, J.M. Kisler, S. Shimazu, G.W. Stevens, Y. Komatsu, *Separation Purification Technol.* **2006**, *48*, 197-201.
[17] H. Jing, Z. Guo, H. Ma, D.G. Evans, X. Duan, *J. Catal.* **2002**, *212*, 22-32.
[18] H. Engelhardt, P. Orth, *J. Liquid Chromatography* **1987**, *10*, 1999-2022.
[19] J. Sun, D. Ma, H. Zhang, X. Liu, X. Han, X. Bao, G. Weinberg, N. Pfänder, D. Su, *J. Am. Chem. Soc.* **2006**, *128*, 15756-15764.
[20] V. Antochshuk, M. Jaroniec, *Chem. Mater.* **2000**, *12*, 2496-2501.
[21] H.-P. Lin, L.-Y. Yang, C.-Y. Mou, S.-B. Liu, H.-K. Lee, *New J. Chem.* **2000**, *24*, 253-255.
[22] D. Brandhuber, H. Peterlik, N. Hüsing, *J. Mater. Chem.* **2005**, *15*, 3896-3902.
[23] D. Liu, J.-H. Lei, L.-P. Guo, X.-D. Du, K. Zeng, *Microporous Mesoporous Mater.* **2009**, *117*, 67-74.
[24] Y. Traa, S. Sealy, J. Weitkamp, in: Characterization II, Molecular Sieves – Science and Technology (H.G. Karge, J. Weitkamp, eds.), Vol. 5, Springer, Berlin, 2007, pp. 103-154.
[25] R. Denoyel, F. Rouquerol, in: Handbook of Porous Solids" (F. Schüth, K.S.W. Sing, J. Weitkamp, eds.), Vol. 1, WILEY-VCH, Weinheim, 2002, pp. 276-308.

3.4.3.2 Own work, project-related publications by participating researchers

The research group of Yvonne Traa has an extensive experience in the area of microporous materials, i.e., zeolite synthesis, characterization and catalysis. One example is the investigation into the influence of aluminum content, crystallinity and crystallite size of zeolite Pd/H-ZSM-5 on the catalytic performance in the dehydroalkylation of toluene with ethane to ethyltoluenes, including also the investigation of nanocrystalline zeolites.[A4-1] Another example is the finetuning of acidic and basic properties of zeolites for the concerted E2 elimination of water from lactic acid in order to avoid undesired side reactions.[A4-2] Co-operation with the Solid-State NMR spectroscopy group of Michael Hunger has been important for all this work.[A4-1,A4-2,A4-3] Early work in the group of Yvonne Traa also involved "pore size engineering" with tetraethylorthosilicate for tuning the pore size of the zeolite catalyst.[A4-4] Only later, the group extended its experience into the area of the mesoporous analoga of zeolites, the mesoporous SiO_2 and SiO_2/Al_2O_3 materials, for example synthesis, characterization and use of FDU-12 (Fig. A4-6).[A4-5] With regard to the characterization of the pore size of microporous zeolites using molecular probes, there is also ample experience available.[A4-6]

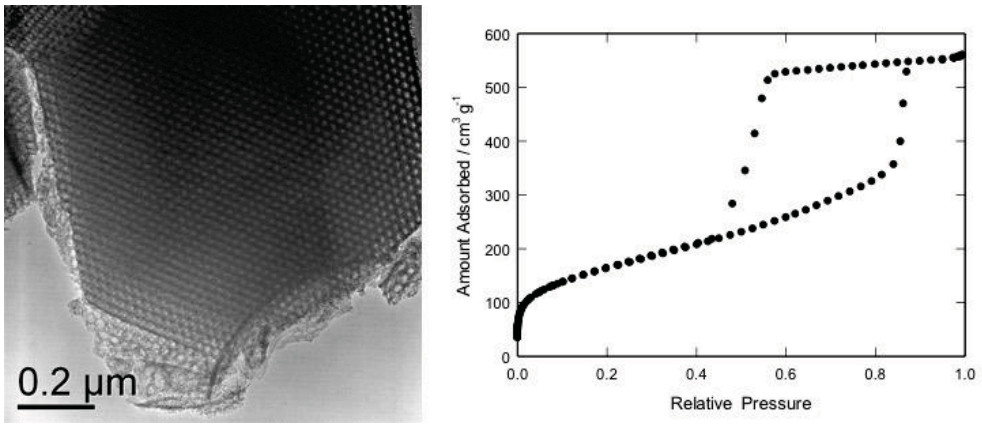

Figure A4-6: Left: TEM picture of FDU-12; right: nitrogen adsorption isotherm of FDU-12.[A4-5]

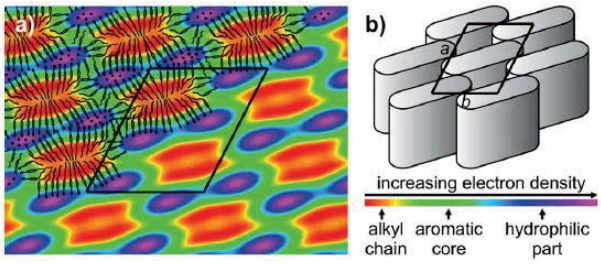

Fig. A4-7: Electron density map (a) reconstructed from the small-angle XRD pattern of a complex structured lyotropic liquid crystal phase ("ribbon phase") with inverse micelles and symmetry *p*2 (b). Cell parameters are 8 and 9 nm, respectively. The map visualizes the nano-segregation of water-rich hydrophilic and hydrophobic parts. [A4-10]

The *Liquid Crystals and Soft Matter* research group headed by Frank Gießelmann has a long-standing expertise in the field of liquid crystals, thermotropic as well as lyotropic and polymeric LCs. Beyond lyotropic liquid crystals, the group contributed to many aspects of liquid crystal research such as the understanding of phase transitions and chirality effects in liquid crystals, the electrical and optical properties of ferro- and antiferroelectric LCs, the connection between order and charge transport in LC semiconductors, the *stimuli* response of LC elastomers (with Rudolf Zentel, Mainz) and the self-organization principles in ionic LCs (with Sabine Laschat, Stuttgart). Since 2004 increasing activities in the field of lyotropic LCs – relevant to this project – have led to (i) the recognition of the simultaneous dispersion and alignment of carbon nanotubes in lyotropic LCs [A4-7], to the discovery of the first example of a new ferroelectric lyotropic LC phase – the lyotropic counterpart to the well-known ferroelectric chiral smectic C phase in thermotropics [A4-8] and to the recent discovery of the spontaneous formation of chiral structures in achiral micellar lyotropic liquid crystals under capillary confinement [A4-9]. The group is well experienced with the formulation, preparation, characterization and alignment of lyotropic liquid crystals as well as with the investigation of their phase diagrams and liquid-crystalline structures. Among other experimental techniques such as polarized optical microscopy (POM) and polarized vibrational spectroscopy (IR, Raman), differential scanning calorimetry (DSC), electro-optic studies and dielectric spectroscopy, the group has extensive expertise in various X-ray diffraction experiments by means of which new LC nanostructures can be elucidated [A4-10] and order parameters can be quantified (Fig. A4-7).

In this project, our two research groups will bring together their complementary expertise in mesoporous catalytic materials and lyotropic liquid crystals to undertake a joint research effort and explore the rational design and controlled synthesis of large-pore mesoporous silica materials by soft templating of tailored lyotropic liquid crystals. Right from the emergence of this CRC concept the two PIs started an informal collaboration and a few materials were synthesized via TLCT, where the lyotropic hexagonal LLC phase formed by hexadecyltrimethylammonium bromide and water was characterized. Afterwards, the phase was templated by the addition of tetramethylorthosilicate. After drying and calcination, a mesoporous silica material was obtained with short-range hexagonal order (Fig. A4-8). The pore-to-pore distance obtained in the SAXS measurements decreased from 4.68 nm in the LLC phase to 3.22 nm in the OMSM after calcination. Thus, the calcination step probably strongly reduces the order of the material, since it provokes significant shrinking.

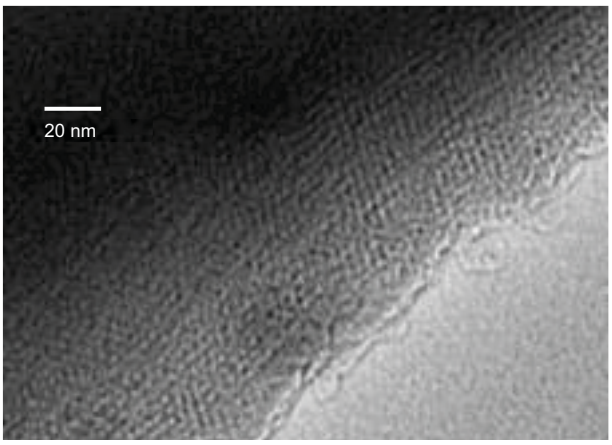

Figure A4-8: TEM picture of a mesoporous material synthesized *via* true liquid crystal templating from hexadecyltrimethylammonium bromide and tetramethylorthosilicate after calcination.

3.4.3.3 Project-related publications by participating researchers

[A4-1] A. Bressel, T. Donauer, S. Sealy, Y. Traa, *Microporous Mesoporous Mater.* **2008**, *109*, 278-286.

[A4-2] G. Näfe, M.-A. López-Martínez, M. Dyballa, M. Hunger, Y. Traa, T. Hirth, E. Klemm, *J. Catal.* **2015**, *329*, 413-424.

[A4-3] M. Dyballa, U. Obenaus, S. Lang, B. Gehring, Y. Traa, H. Koller, M. Hunger, *Microporous Mesoporous Mater.* **2015**, *212*, 110-116.

[A4-4] D. Singer, Y. Traa, *Chem.-Ing.-Tech.* **2007**, *79*, 878-882.

[A4-5] T. Montsch, M. Heuchel, Y. Traa, E. Klemm, C. Stubenrauch, *Appl. Catal. A* **2017**, *539*, 19-28.

[A4-6] Y. Traa, S. Sealy, J. Weitkamp, "Characterization of the Pore Size of Molecular Sieves Using Moleular Probes", in "Characterization II", Molecular Sieves – Science and Technology, Vol. 5, H.G. Karge, J. Weitkamp, Eds., pp. 103-154, Springer, Berlin (2007).

[A4-7] J. Lagerwall, G. Scalia, M. Haluska, U. Dettlaff-Weglikowska, S. Roth, F. Giesselmann, *Adv. Mater.* **2007**, *19*, 359-364.

[A4-8] J. R. Bruckner, J. H. Porada, C. F. Dietrich, I. Dierking, F. Giesselmann, *Angew. Chem. Int. Edit.* **2013**, *52*, 8934-8937.

[A4-9| C. F. Dietrich, P. Rudquist, K. Lorenz, F. Giesselmann, *Langmuir* **2017**, *33*, 5852-5862.

[A4-10] J. R. Bruckner, D. Krueerke, J. H. Porada, S. Jagiella, D. Blunk, F. Giesselmann, *J. Mater. Chem.* **2012**, *22*, 18198-18203.

3.4.4 Project plan

In summary, the research goals are organized in work packages as follows:

- **WP1: Synthesis of (Al-)SBA-15, PHTS, SBA-16, MCF and FDU-12** *(Traa):* These materials are all synthesized with pluronics P123 or F127 and TEOS in acidic solutions, are hydrothermally stable and have very different pore characteristics. Hence, the materials serve as test materials for adapting the characterization methods, the functionalization methods, the simulation methods, the linker chemistry and the catalytic reactions, which is vital for all B and C projects.
- **WP2: Tailored mesoporous silica materials via TLCT** *(Gießelmann, Traa):* Results from liquid crystal and surfactant chemistry are to be exploited to synthesize silica materials with defined pore structure in a controlled manner. First, silica materials with cylindrical pores will be synthesized as a replica of the columnar hexagonal liquid crystal phases of the system pluronic/water. Reliable methods for the precise control of the pore diameter in the range from 8 to 20 nm are to be developed by using appropriate cosurfactants. The correlations between the structures of the liquid crystal template phases and the pore structures of the thus received silica materials are to be thoroughly analyzed. Based on these results, pathways to silica materials with new pore geometries are to be opened, e.g., elliptical pores from lyotropic ribbon phases or chirally structured pores from chiral lyotropic phases. In addition, it will be investigated whether macroscopically aligned silica materials (monoliths) can be obtained by a pre-alignment (magnetic-field alignment, shear alignment) of the lyotropic liquid crystal templates.
- **WP3: X-ray diffraction investigations of ordered mesoporous materials** *(Gießelmann):* Small-angle X-ray scattering (SAXS) is widely known as a most powerful experimental tool to investigate nanoscale-structured materials. In this work package, we will systematically apply and advance the SAXS analysis of ordered mesoporous silica materials (OMSMs) including the reconstruction of electron density maps and the modelling of 2D SAXS patterns from cylindrical distribution functions. In combination with TEM and nitrogen absorption results, the advanced SAXS analysis will gain detailed insights into the nanostructure of OMSMs such as the cross-sectional shape and the orientational distribution of pores, which is important also for other A and C projects.
- **WP4: Functionalization** *(Traa):* The synthesized mesoporous materials are mainly SiO_2 but also SiO_2/Al_2O_3 materials, which have terminal OH groups. Hence, catalytically active species can be attached covalently via silanization. Silanol groups at the external surfaces will be inertized before removal of the organic template from the pores. Thus, it will be able to ensure that catalytic sites are only available in the confined space of the defined mesopores.
- **WP5: Characterization of the effective pore size of mesoporous materials using adsorption of molecular probes** *(Traa):* A technique to determine the accessible pore volume of mesoporous materials by adsorption of probe molecules of various sizes is to be developed. Up to now, such techniques are only available for microporous materials. The adsorption experiments will also be used to access the variation of the pore volume after functionalization and introduction of the catalytic complexes.

3.4.4.1 WP1: Synthesis of (Al-)SBA-15, PHTS, SBA-16, MCF and FDU-12 *(Traa)*. These materials are very versatile and hydrothermally stable, and already with verified synthesis recipes materials with largely different pore characteristics can be obtained:[2] (a) SBA-15 with a hexagonal, 2D pore system with parallel, channel-type, curved pores (diameter 5-8 nm; diameter of Al-SBA-15: 7-13 nm). The pore length can be varied, the pores can also be partially plugged as in PHTS with nanoparticles so that open and plugged sections coexist. (b) SBA-16 with a 3D cubic cage structure, where two 3D pore systems (diameter 4-6.5 nm) form spherical cavities. (c) Adding mesitylene gives MCF, a sponge-like foam with large open spherical cells (diameter 15-50 nm) (Fig. A4-9).[2] In addition, FDU-12 materials (cubic closest packing of spherical cavities connected with multi-directional cylindrical pores with amorphous wall structure, cf. Fig. A4-6) will be synthesized, which had been studied in the group before and allow cavity sizes between 10 and 26 nm.[A4-5]

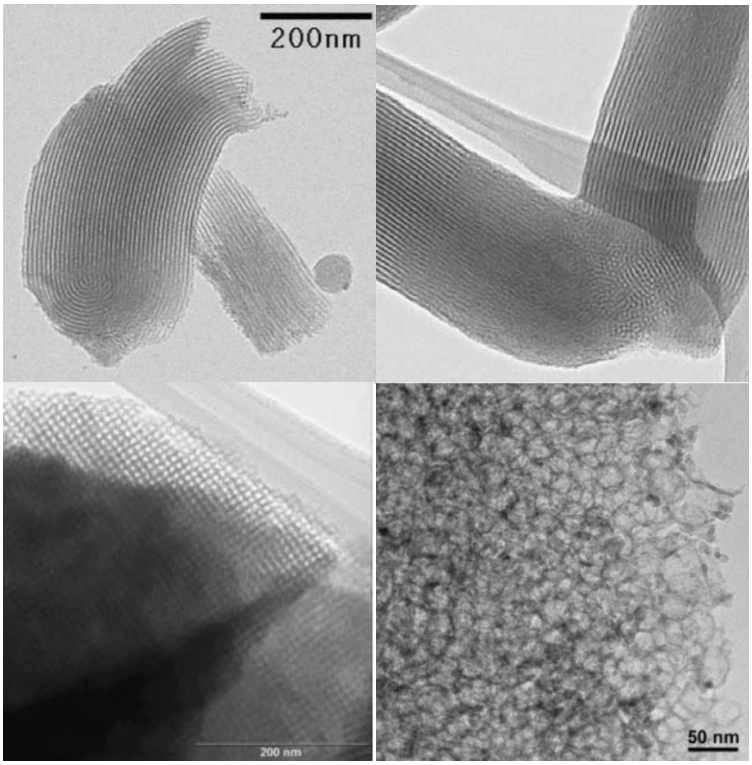

Figure A4-9: TEM pictures of different pore systems of mesoporous silica materials envisaged for this CRC: (top left) SBA-15 with a 2D pore system with hexagonally structured, channel-type, curved parallel pores, (top right) PHTS, derived from SBA-15 using microporous amorphous nanoparticle plugs resulting in coexistence of open and plugged pores, (bottom left) SBA-16 (cubic phase consisting of two non-interpenetrating 3D channel systems with spherical cavities at the intersection of the channels), (bottom right) MCF (sponge-like foam with 3D structure and large open uniform spherical cells (15-50 nm), accessible via large windows (5-20 nm). [2]

The big advantage of the materials chosen is the fact that all materials are synthesized from TEOS and the poloxamers from Sigma-Aldrich pluronic P123 $EO_{20}PO_{70}EO_{20}$ or pluronic F127 $EO_{106}PO_{70}EO_{106}$ in HCl-containing, acidic solutions. Since most recipes are verified, also larger batches of the materials can be prepared in the larger synthesis autoclave which is planned to be purchased. Such "standard batches" are vital for the establishment of powerful characterization methods in cooperation with **project C1, project C3** and the simulation **project C5**, of reliable silanization methods, of controlled linker chemistry (together with **projects B1, B2** and **B3**) and in preparation for the precise testing of confinement effects in catalytic reactions, for which solvent ratios and the like have to be adapted. The large variety of the materials allows for a first and rough testing of the influences of confinement by size (different pore sizes) and confinement by geometry (parallel pores, inkbottle-like sections, spherical cavities connected by pores and spherical cells) with the defined composition of SiO_2 materials. In addition, the influence of polarity can be tested by comparing SiO_2 materials with SiO_2/Al_2O_3 materials, where increasing Al content increases the hydrophilicity of the material. Thus, these materials are a vital starting point for all reactions studied in this CRC.

3.4.4.2 WP2: Tailored mesoporous silica materials via TLCT *(Gießelmann/Traa)*. This work package aims to explore, develop and apply a controlled synthesis procedure of large-pore ordered mesoporous silica materials (large-pore OMSMs) *via* true liquid crystal templating (TLCT) of the lyotropic hexagonal phases of amphiphilic EO-PO-EO tri-block co-polyethers and appropriate cosurfactants. Even though there is a number of large-pore OMSMs available *via* proven recipes – some of them will be produced as reference materials in WP1 – there is still an urgent need for the rational design and tailored synthesis of OMSMs with pore diameters ranging from 8 to 20 nm.[12] We aim to meet this challenge by using the more laborious and complex method of TLCT which, on the other hand, allows us to precisely formulate, characterize and tune the liquid-crystalline precursor, the structure of which will be extensively investigated by X-ray diffraction (XRD). Subsequent XRD studies

of the resulting hybrid material (the inorganic silica matrix enclosing the organic surfactant micelles, see Fig. A4-4) as well as the calcined OMSM and its particular correlation to the initial LLC precursor structure will lead to detailed insights into the soft-templating process and give us precise control over the pore diameter in the final OMSM. At the end, we aim to present a library of large-pore OMSMs with mean pore diameters ranging from 8 to 20 nm with 1 nm resolution. After proper functionalization in WP4, this library of OMSMs will meet the requirements of the catalytic projects **project B1, B2** and **B3** and – last but not least – the reliable and precise variation of the pore diameters will allow systematic studies of the confinement effects in molecular heterogeneous catalysis, mimicking the unprecedented catalytic performance of enzymes.

In more detail, this work package is divided into three successive sections:

(i) The initial work will be based on the approach of David Pine and co-workers [13] who successfully templated the lyotropic hexagonal phases of commercial Pluronic ABA tri-block polyethers, namely Pluronic P123 (approx. EO_{20}–PO_{70}–EO_{20}) and Pluronic F127 (approx. EO_{106}–PO_{70}–EO_{106}), and tuned the micelle diameter (and thus the resulting pore diameter) by various amounts of *n*-butanol, *n*-pentanol and *n*-hexanol as cosurfactants. In addition to what was reported in [13] we will systematically study the ternary phase diagrams of P123 with water and each of the three cosurfactants and undertake detailed small-angle X-ray scattering (SAXS) investigations into the nanoscale structures of the lyotropic liquid-crystalline precursors, the as-synthesized hybrid materials and the calcined OMSMs thereof. Even though these investigations are rather extensive and time consuming, we consider them as the essential step to a clear and predictive understanding of how the pore diameter of large pore OMSMs can be tailored by tuning the micelle diameter of the LLC precursor phases by cosurfactants. To access larger pore diameters up to 20 nm, we also plan to extend the choice of cosurfactants and perform similar investigations with longer chain alcohols such as *n*-octanol and *n*-decanol. Based on our extensive X-ray data, further attention will be paid to an optimization of the calcination process which is often observed to detrimentally reduce the diameter and the long-range ordering of the mesopores in the final OMSMs in comparison to their LLC precursors. In particular, we will study whether or not the calcination process can be replaced by a milder solvent extraction of the organic phase (e.g. by ethanol) followed by a thermal annealing treatment or by directly replacing the surfactant with silanes (TDS).

(ii) After gaining detailed control over the soft-templating process of Pluronic surfactants and the particular role of cosurfactants, the next important step will be the replacement of the commercial Pluronic surfactants with broader dispersity index by the tailored, well-defined amphiphilic block copolymers (dispersity index < 1.1), namely EO_{20}-PO_{70}-EO_{20}, EO_{20}-PO_{90}-EO_{20} and EO_{20}-PO_{120}-EO_{20} synthesized by **project A6**. The EO_{20}-PO_{70}-EO_{20} triblock copolymer comes close to the average composition of the commercial Pluronic P123. LLC phases of EO_{20}-PO_{70}-EO_{20} as well as the as-synthesized hybrid materials and calcined OMSMs thereof will be prepared and analyzed. The comparison to the analogous materials obtained from the commercial P123 in section (i) will give direct insights into the impact of polydispersity on the order and properties of OMSMs. On the other hand, the enlarged hypdrophobic PO blocks in EO_{20}-PO_{90}-EO_{20} and EO_{20}-PO_{120}-EO_{20} should give rise to larger micelle diameters and thus give access to larger pore diameters of the final OMSMs. In all cases, similar investigations (phase diagrams, SAXS investigations of LLC precursors, hybrid materials and OMSMs) as in section (i) are required.

(iii) The final section of this work package is devoted to more explorative aspects of soft templating including the fabrication of OMSM monoliths with pores aligned over macroscopic (millimeter) dimensions as well as the fabrication of OMSMs with elliptical pores and chiral OMSMs with helical-shaped pores. The so-far prime example of an OMSM with macroscopically aligned pores (see Fig. 4) was obtained via soft templating of a lyotropic hexagonal phase which was macroscopically aligned by the action of a strong magnetic field. The alignment was preserved during templating and led to a MCM-41 material with 2.2 nm thick pores, parallel aligned over millimeters.[8] Following these procedures, we will try to obtain macroscopically aligned LLC phases (“monodomains”) of our amphiphilic triblock copolymers and try to maintain the alignment during the templating which should lead to first examples of large-pore OMSMs. An alternative to the magnetic field alignment might be shear flow alignment which has been proven to be highly efficient in our previous work on LLCs. OMSMs with pores of elliptical cross section might be obtained by soft templating of the more exotic lyotropic ribbon phases, such as the aqueous ribbon phase of 5-[4-(5-n-heptylpyrimidine-2-yl)phenoxy] pentane-1,2-diol described in our previous work [A4-10] (see also Fig. A4-7). Finally, OMSMs with a helically structured inner surface of the pores might be obtained by soft templating of the lyotropic

liquid-crystalline phases formed by cellulose nanocrystals (CNCs) in water.[26] This attempt will be undertaken in close collaboration with Maria H. Godinho (New University of Lisbon) and Jan P. F. Lagerwall (University of Luxemburg), two leading groups in the field of CNC lyotropic liquid crystals. Chirally structured OMSMs might be most relevant for future approaches to stereoselective molecular heterogeneous catalysis.
The distribution of work over our two groups in this joint work package is planned as follows: Following our specific expertise, the Gießelmann group will be responsible for the formulation and characterization of all liquid crystal phases and the subsequent templating as well as for all X-ray investigations. The Traa group will be responsible for the calcination process and the further characterization of the final OMSMs by nitrogen adsorption and TEM.

3.4.4.3 WP 3: X-ray investigations of ordered mesoporous materials *(Gießelmann)*. Small-angle X-ray scattering (SAXS) is widely known to be among the most powerful experimental techniques to investigate nanoscale-structured materials such as (lyotropic) liquid crystals and ordered mesoporous materials. We thus consider extensive and detailed SAXS investigations as a key to the success of this **project A4** and of its WPs 1 and 2 in particular. This WP3 does not only comprise all SAXS measurements and analysis required in this **project A4** but will also provide necessary SAXS support to other **A** projects of this CRC. Particular support will be given to **project A6**. Since this project makes use of a very similar soft-templating approach to mesoporous carbon materials, SAXS investigations are expected to be of similar high importance as in this **project A4**; also, **projects A2** and **A7** will be supported.
Beyond standard SAXS analysis which provides exact information about the space group and the lattice parameters (or rather the pore-to-pore distance in the case of OMSMs) we plan to develop and apply advanced data analysis techniques, *i.e.* the reconstruction of electron density maps as shown in Fig. A4-7. These advanced analysis techniques provide additional insights into the structure of OMSMs such as the cross-sectional shape of the pores or the thickness of the silica walls. The reconstruction analysis will be supplemented by modelling techniques, assuming an adjustable form factor of the cylindrical pores, in this context the so-called cylindrical distribution function (CDF), and calculates the expected XRD pattern thereof. Iterative variations of the form factor parameters until the calculated XRD pattern fits the experimental data provide additional information about the density distribution around the pores and their mutual arrangement. 2D-SAXS measurements provide further information about *e.g.* the orientational distribution of cylindrical micelles or pores in LLCs and OMSMs, respectively. For all SAXS investigations, proper instruments are in-house available (Bruker NanoStar diffractometer with 2D VÅNTEC area detector, sample temperature control and magnetic-field alignment, Anton Paar SAXSess diffraction system with 1D CMOS detector and sample temperature control).

3.4.4.4 WP4: Functionalization *(Traa)*. Most of the mesoporous materials synthesized will be SiO_2 materials besides some SiO_2/Al_2O_3 materials, which all have terminal OH groups. With regard to silanol groups, it can be distinguished between single, hydrogen-bonded and geminal silanol groups. This is important since only free silanol groups are accessible to silylating agents. Thus, it is always necessary to characterize the materials after silanization for the degree of silanization.
In order to allow for an “inertization” of the external surface, the first silanization step will be carried out directly after synthesis of the materials before removal of the surfactant, i.e., when the pores are still filled with the surfactant. In this case, the silanization could be carried out with cheap trimethylchlorosilane, so that the external surface is inertized with $Si(CH_3)_3$, which is a common protecting group in organic chemistry. For materials, where this procedure is not possible, bulky molecules, such as 1,3-dimethyl-1,1,3,3-tetraphenyldisilazane, could be employed to remove the OH groups of the external surface. Afterwards, the internal surface of the materials can be functionalized by a direct exchange process, where silanes replace the surfactant (so-called template displacement with organosilanes (TDS)) (Equation 1). In this way, the calcination step, which has been shown to be problematic for the order of the

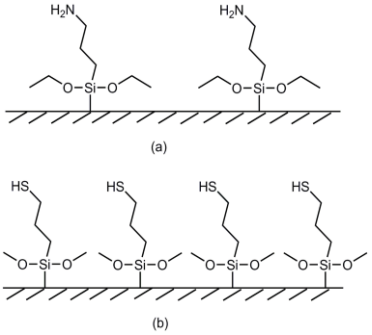

Figure A4-10: Side group effects on the bonding density in mesoporous materials functionalized with (a) 3-aminopropyldi***ethoxy***silyl and (b) 3-mercaptopropyldi***methoxy***silyl groups. [20]

materials, is avoided and the surfactant can be recovered. If high densities of functional groups are required, two methyl groups can be chosen as side groups. If low densities are desired, ethoxy groups or even bulkier side groups can be applied (Fig. A4-10). In order to make an azide functionalization available for attaching the catalytic function, first tests can be performed with 11-azidoundecyltriethoxysilane which is commercially available from AlfaAesar. Specially tailored materials can be functionalized with carefully prepared and adapted silanes.

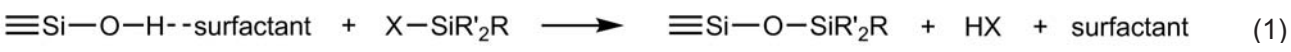

X = Cl or alkoxide; R' = alkyl or alkoxide

Another option for the functionalization is the direct co-condensation of the silane directly in the LLC phase during synthesis of the mesoporous material. However, the question here is, whether the silane also functionalizes the external surface of the material. Hence, all functionalized materials have to be carefully characterized with FTIR, ^{29}Si CP/MAS NMR (**project C1**) and elemental analysis. It is important to follow the degree of silylation. The total content of silyl groups can be assessed by NMR spectroscopy, whereas it is possible to determine the relative concentrations of two different silylation agents bonded to the surface by using a special FTIR method. [27]

3.4.4.5 WP5: Characterization of the effective pore size of mesoporous materials using adsorption of molecular probes *(Traa).* Techniques to determine the accessible surface area of *microporous* materials by adsorption of probe molecules of various sizes are nowadays used as quick tests for probing the effective pore width under catalytically relevant conditions and/or for materials modified with post-synthesis methods.[24] For the characterization of *mesoporous* materials, corresponding techniques are not available and have to be developed. The challenge is that the probe molecules have to be quite large and complex, and for such molecules, the sizes might also be changing depending on the environment. In addition, it is difficult and probably not possible to cover the whole range of mesopores between 2 and 50 nm. However, it should be possible to cover the range of about 4 to 10 nm, which is the range of SBA-15 and SBA-16 materials. Possible probe molecules envisaged are colecalciferol, the antibiotics cefuroxime and vancomycin as used in drug loading and release on FDU-12 and SBA-15, [28], the dyes Saframin O, Congo Red and Reactive Red 2 as used for the removal of dyes from wastewater with SBA-15, [29] the enzyme lysozyme with an average spherical diameter of about 3.2 nm used to examine the protein immobilization ability of FDU-12, [30] and other large probe molecules relevant for this CRC, e.g., metal complexes with and without tether from **projects B1, B2** and **B3**. The adsorption tests are planned to be performed in liquid phase under stirring until equilibrium is reached. Characterization of the probe molecule solutions before and after adsorption with HPLC and refractive index detector or diode array detector allows for a quantitative determination of the adsorbed probe molecule amount. The big advantage of the adsorption methods is, that it should be possible to determine the *accessible* surface area also of the functionalized materials and the catalytic system, whereas with the BET model used for nitrogen adsorption, higher values would be found due to the much smaller size of the nitrogen molecule.

3.4.4.6 Support-specific properties relevant to the catalytic reactions to be investigated

The SiO_2 and SiO_2/Al_2O_3 materials described in this project are suitable as support for all catalytic systems and reactions in this CRC (**projects B1, B2 and B3**) for the following reasons:

(i) The materials are chemically, thermally (up to at least 500 °C) and hydrothermally stable, do not dissolve or swell in the solvents to be used in any of the catalytic reactions and have, thus, a stable pore geometry and size.

(ii) With the surface properties of these materials, one can address hydrogen transfer catalysis (**project B1**) and the asymmetric addition of boronic acids to α,β-unsaturated carbonyls (**project B3**), since the polar surface can facilitate transport of water and boric acid along the pore wall, and the polarity can be tuned by going from SiO_2 to SiO_2/Al_2O_3 materials. By adjusting the pore size in the range from 8 to 20 nm, also diffusional effects and cooperative effects (can 2 catalytic systems close to each other cooperate or do they hinder each other?) can be studied. At a later stage of the CRC, it will be highly interesting to study the

influence of helically-structured mesoporous supports (cf. 3.4.4.8) on the enantioselectivity in **project B3**.

(iii) With regard to the olefin metathesis reactions studied in **project B2**, the fine-tuning of the polarity and the pore size (see above) allows to study the influence on cyclization versus polymerization activity of the catalytic systems involved.

Chronological work plan:

	2018 Q3 Q4	2019 Q1 Q2 Q3 Q4	2020 Q1 Q2 Q3 Q4	2021 Q1 Q2 Q3 Q4	2022 Q1 Q2	
T1						WP1: Synthesis of mesoporous reference materials via proven recipes (PhD1)
T2						WP2: Tailored mesoporous silica materials via TLCT (PhD2)
T3						WP3: X-ray diffraction investigations of ordered mesoporous materials (PhD2)
T4						WP4: Functionalization (PhD1)
T5						WP5: Adsorption of molecular probes (PhD1)

3.4.4.7 Methods applied: The identification and characterization of LLC phases as well as the investigation of their phase diagrams will be performed by polarized optical microscopy (POM), differential scanning calorimetry (DSC) and standard X-ray diffraction (XRD) measurements. Enhanced 1D- and 2D-SAXS experiments will be applied for detailed structural investigations of LLC precursor phases, as-synthesized hybrid structures and calcined OMSMs (see WP 3). Further characterization of OMSMs will be obtained from transmission electron microscopy (TEM) (**project C3**) and nitrogen adsorption measurements combined with simulation (**project C5**). The presence and spatial distribution of functional groups in the functionalized OMSMs will be investigated by means of solid-state NMR (**project C1**) and vibrational spectroscopy (FT-IR, Raman).

3.4.4.8 Vision: By the end of the first funding period we …

- have obtained detailed insights into and precise control of the soft templating process of lyotropic hexagonal phases of amphiphilic triblock polyethers, including the impact of cosurfactants and polydispersity on the pore diameter and the ordering of the resulting OMSMs.
- Based on this knowledge we will have provided a unique library of tailored hexagonally ordered mesoporous silica materials with mean pore diameters ranging from 8 to 20 nm with a resolution of 1 nm. This library enables systematic studies of the confinement effects in molecular heterogeneous catalysis.
- Last but not least, we found reliable methods to functionalize the inner surface of the OMSM pores according to the particular needs of the catalytic **projects B1, B2** and **B3**.

With the experience and knowledge obtained in the first funding period we envisage to develop more complex and exotic silica materials such OMSMs with macroscopically aligned, elliptically-shaped or helically-structured mesopores for the further advancement of molecular heterogeneous catalysis in the second funding period of our collaborative research center.

3.4.5 Role within the collaborative research center

In comparison to other materials, OMSMs constitute a rather far developed and established class of versatile support materials in (heterogeneous) catalysis. The design, fabrication and functionalization of OMSMs with larger pore diameters in the framework of this **project A4** is thus essential for the progress of molecular heterogeneous catalysis. According to this, the **project A4** closely collaborates with **A**, **B** and **C** projects of this CRC: **project A6** provides us with tailored amphiphilic triblock polyethers. On the other hand, we will take over the SAXS measurements and analysis required in **A6**.

In close collaboration with **projects B1, B2** and **B3,** we will functionalize the materials according to the needs of **projects B1, B2** and **B3** and provide sufficient amounts of support materials tailored for their use in the further catalytic studies and for the systematic studies of confinement effects. The spatial distribution of functional groups at the inner surface of the mesopores will be investigated together with **project C1**. Furthermore, our results of advanced SAXS analysis techniques (i.e., dimensions and form factors of pores) provide valuable input and refinement data for the computational **project C5**. The catalysis within silica pores will be simulated in **project C4**.

3.4.6 Differentiation from other funded projects

The work described in project A4 is not subject or partly subject of this research: DFG Gi 243/8-1 “Ionic Liquid Crystals” (with Sabine Laschat, Stuttgart) and DFG Gi 243/9-1 “Gelled lyotropic Liquid Crystals” (with Cosima Stubenrauch, Stuttgart).

3.4.7 Project funding

3.4.7.1 Previous funding

This project is currently not funded and no funding proposal has been submitted.

References (ctd.)

[26] J. P. F. Lagerwall, C. Schütz, M. Salajkova, J. Noh, J. H. Park, G. Scalia, L. Bergström, *NPG Asia Mater.* **2014**, *6*, e80.
[27] M. Mesa, A. Ramírez, J.-L. Guth, L. Sierra, *Studies in Surface Science and Catalysis* **2004**, *154*, 562-567.
[28] D. Carmona, F. Balas, J. Santamaria, *Materials Research Bulletin* **2014**, *59*, 311-322.
[29] H. Chaudhuri, S. Dash, A. Sarkar, *J. Environ. Chem. Eng.* **2015**, *3*, 2866-2874.
[30] J. Fan, C. Yu, F. Gao, J. Lei, B. Tian, L. Wang, Q. Luo, B. Tu, W. Zhou, D. Zhao, *Angew. Chem. Int. Ed.* **2003**, *42*, 3146-3150.

3.4.7.2 Requested funding

Funding for	2018		2019		2020		2021		2022		2018-2022	
Staff	Quantity	Sum	Quantity	Sum	Quantity	Sum	Quantity	Sum	Quantity	Sum	Quantity	Sum
PhD student, 67%	2	43,200.-	2	86,400.-	2	86,400.-	2	86,400.-	2	43,200.-	2	345,600.-
Total		43,200.-		86,400.-		86,400.-		86,400.-		43,200.-		345,600.-
Direct costs	Sum		Sum		Sum		Sum		Sum		Sum	
consumables	8,000.-		16,000.-		16,000.-		16,000.-		8,000.-		64,000.-	
Total	8,000.-		16,000.-		16,000.-		16,000.-		8,000.-		64,000.-	
Major research instrumentation	Sum		Sum		Sum		Sum		Sum		Sum	
Synthesis autoclave	52,000.-		-		-		-		-		-	
Total	52,000.-		-		-		-		-		-	
Grand total	103,200.-		102,400.-		102,400.-		102,400.-		51,200.-		461,600.-	

(All figures in EUR)

3.4.7.3 Requested funding for staff

	Sequential no.	Name, academic degree, position	Field of research	Department of university or non-university institution	Project commitment in hours per week	Category	Funding source
Existing staff							
Research staff	1	Yvonne Traa, PD Dr., senior academic staff member	Chemical Technology, Heterogeneous Catalysis, Nanoporous Materials	Institute of Chemical Technology	4		University
Research staff	2	Frank Gießelmann, Prof. Dr., tenured professor (W3)	Physical Chemistry, Liquid Crystals, Soft Matter	Institute of Physical Chemistry	4		University
Research staff	3	Dr. Nadia Kapernaum, Senior Scientist	Physical Chemistry, Liquid Crystals, XRD	Institute of Physical Chemistry	4		University
Non-research staff	4	Barbara Gehring; technical assistant	Nanoporous Materials	Institute of Chemical Technology	4		University
Non-research staff	5	Inge Blankenship		Institute of Physical Chemistry	2		University
Requested staff							
Research staff	6	N. N.; M. Sc.	Chemical Technology, Nanoporous Materials	Institute of Chemical Technology		PhD student, 67%	
Research staff	7	N. N.; M. Sc.	Physical Chemistry, Liquid Crystals	Institute of Physical Chemistry		PhD student, 67%	
Research Staff	8	Research assistant	Physical Chemistry, Liquid Crystals	Institute of Physical Chemistry			

Job description of staff (supported through existing funds):
1
Senior academic staff member, first principal investigator for **project A4**
2
Professor, second principal investigator for **project A4**
3
Senior academic staff member, work package 3
4
Technical assistant, work package 1
5
Secretary

Job description of staff (requested funds):
6
PhD student 1, work packages 1, 4, 5
7
PhD student 2, work packages 2, 3
8
Research Assistants. **Justification:** The research assistants will support the synthetic work of the PhD students in the synthesis of larger batches of materials for the other projects, as far as standard procedures are concerned.

3.4.7.4 Requested funding of direct costs

	2018	2019	2020	2021	2022
University of Stuttgart: existing funds from public budget	2,000.-	4,000.-	4,000.-	4,000.-	2,000.-
Sum of existing funds	2,000.-	4,000.-	4,000.-	4,000.-	2,000.-
Sum of requested funds	8,000.-	16,000.-	16,000.-	16,000.-	8,000.-

(All figures in EUR)

Consumables for financial year 2018

Chemicals, laboratory consumables, solvents, gases	EUR	8,000.-

Consumables for financial year 2019

Chemicals, laboratory consumables, solvents, gases	EUR	16,000.-

Consumables for financial year 2020

Chemicals, laboratory consumables, solvents, gases	EUR	16,000.-

Consumables for financial year 2021

Chemicals, laboratory consumables, solvents, gases	EUR	16,000.-

Consumables for financial year 2022

Chemicals, laboratory consumables, solvents, gases	EUR	8,000.-

3.4.7.5 Requested funding for major research instrumentation

Major research instrumentation for financial year 2019

Synthesis autoclave (volume: 1000 ml, from stainless steel with PTFE inlet, tantalum-coated parts to prevent corrosion in the acidic synthesis solutions) with temperature regulating system for larger batches of materials for catalysis groups. This synthesis autoclave is necessary for making larger batches of material which serve as reference standards for adapting the characterization methods, the functionalization methods, the simulation methods, the linker chemistry and the catalytic reactions. It is not an option to make these larger batches by combining several smaller batches, since the properties such as pore size and pore volume have to be as defined as possible, so that the different projects work with a uniform material and confinement effects are unambiguous	EUR	52,000.-

3.5 Project A5

3.5.1 General information about Project A5

3.5.1.1 Organic/inorganic hybrid materials with tunable pore size as catalyst supports

3.5.1.2 Research Areas
Materials Science, Synthesis and Properties of Functional Materials (406-2), Structuring and Functionalization (406-4)

3.5.1.3 Principal Investigator
Bill, Joachim, apl.-Prof. Dr., born 14. 12. 1962, male, German
Institut für Materialwissenschaft
Universität Stuttgart, Heisenbergstraße 3, 70569 Stuttgart
Tel.: 0711/685-61945
E-Mail: bill@imw.uni-stuttgart.de
Permanent contract

3.5.1.4 Legal Issues
This project includes

1.	research on human subjects or human material.	no
2.	clinical trials.	no
3.	experiments involving vertebrates.	no
4.	experiments involving recombinant DNA.	no
5.	research involving human embryonic stem cells.	no
6.	research concerning the Convention on Biological Diversity.	no

3.5.2 Summary
The goal of this project is to establish a template-based process for the formation of structured mesoporous organic/inorganic (hybrid) or pure inorganic materials with tunable pore diameter in the range of 5-20 nm. They will be used as a support for the specific attachment of catalyst molecules in the pores for studying molecular heterogeneous catalysis in confinements. To this aim, a bio-inspired method will be employed where polymer templates such as monoliths (**project A1**), block copolymers (**project A2**) and polymer foams (**project A7**) will be selectively mineralized with oxides like ZnO, TiO_2, SiO_2, ZrO_2 and Al_2O_3 under mild reaction conditions. This mineralization approach allows precise control over the thickness of the deposited inorganic layer varying from few nanometers up to several hundred nanometers. Thus, depositing thin oxide films on the pore walls, the pore size of the polymer templates will be precisely adjusted. This new class of tailor-made materials is considered to enhance the properties of polymer supports and hence to expand the spectrum of their application. Alternatively, pure inorganic mesoporous supports as inverse replica of polymer foams and colloidal crystals (**project A7**) with different pore geometry will be prepared. The surface properties of the deposited inorganic layers will be manipulated in order to tailor the polarity and wettability of the pore walls by varying the oxide type and/or by surface functionalization with self-assembled monolayers (SAMs) with appropriate terminal groups. The SAM formation will be supported by theoretical investigations in cooperation with **project C6**. Finally, catalyst molecules synthesized in **projects B2** and **B3** will be selectively attached to the pore surface of the hybrid and inorganic supports using “click” chemistry. For this purpose, linker molecules containing two terminal functional groups will be used. The first terminal group (e.g. alkoxysilane, carboxylate, phosphonate, thiol and sulfonate) serves to attach the linker molecule to the oxide pore walls, while the second anchoring group (e.g. azide or alkyne) will be coupled to the catalyst molecule. Further distance adjustment between the catalyst and the pore walls will be achieved through the length/polarity/rigidity of the linker and the polarity of the inorganic layer. Within this project, two confinement effects will be studied: i) the influence of the confinement on the mineralization mechanism as well as on the morphology and the structure of the deposited oxides and ii) the impact of the confined space (pore size, polarity and shape) on the investigated heterogeneous catalytic reactions. A cooperative work with **projects A1, A7**, **C1** and **C3** will assist the thorough characterization of the

synthesized support materials, while modelling of the mass transfer in a pore will be provided by **project C5**.

3.5.3 Research rationale

3.5.3.1 Current state of understanding and preliminary work

(Bio)organic/inorganic hybrid materials with their complex and oft unusual features have numerous advanced functional academic and industrial applications in fields like energy, health, microelectronics and optics, environment, etc.[1] The synthesis of such hybrids requires low-temperature methods especially when organic templates are used. These sensitive templates cannot withstand the harsh reaction conditions often used by conventional methods for the synthesis of functional inorganic materials. Alternatively, in living nature the organisms produce minerals at ambient conditions through biomineralization.[2] This process leads to formation of bio/inorganic composites. The formation of the inorganic components is usually controlled by biotemplates in localized volumes (e.g. in the case of the formation of nacre). Within these confinements, the organisms govern the mineralization process and hence the morphology and orientation of the minerals through control of the precursor ions and mineral phases.[3]

Inspired by biomineralization, the synthesis of organic/inorganic mesoporous hybrids as support materials for studying the molecular heterogeneous catalysis in confined spaces is envisaged in this project (Figure A5-1). The organic part of the hybrids, a porous polymeric material with different pore size and shape, serves as a template and defines the composite structure. The pore size and properties can be further precisely adjusted by the help of the inorganic phase, mineralized on the polymer pore walls. Additionally, the inorganic part is considered to enhance the mechanical and chemical stability of the hybrid materials, tune the polarity and wettability of the pore walls and offer anchor groups needed for coupling of the catalyst molecules. For this purpose, oxides like ZnO, TiO_2, SiO_2, ZrO_2 and Al_2O_3 are proposed to be deposited on the pore walls of the polymer templates. Owing to their numerous technological applications, the synthesis of these functional materials is well established. Methods like chemical bath deposition (CBD) and sol-gel processes, widely used for formation of functional oxide films and coatings, provide mild reaction conditions appropriate for the soft polymer templates. The samples are placed in a liquid deposition solution and mineralized at low temperatures below 100°C. Varying the mineralization conditions, oxides with different morphology, crystallinity and hence polarity and wettability can be achieved.

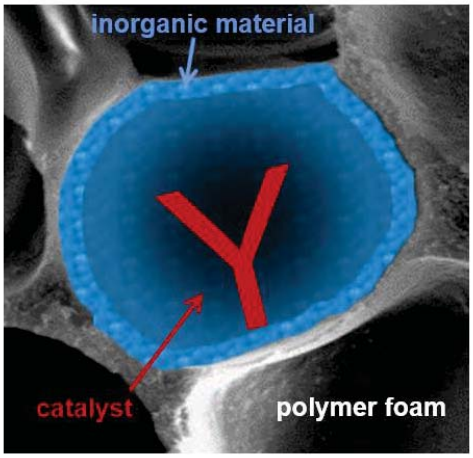

Figure A5-1. Schematic representation of a catalyst-activated pore in an organic/inorganic support material.

A prerequisite for successful infiltration and subsequent mineralization of the porous polymer is the presence of open cellular structure and hydrophilic pore walls. There are some examples for studies on the mineralization in confinements. For instance, controlled mineralization of $CaCO_3$ in confinements was investigated in a model system by C. J. Stephens *et al.*[3] and within collagen fibrils by H. Ping *et al.*[4] A difference in the morphology of the $CaCO_3$ in bulk and in confinement was observed, and a mineralization mechanism was proposed. The more technologically relevant ZnO has also been mineralized in confined space. However, except some reports on molecular simulation of ZnO nanostructures obtained in confinement,[5] there is only a limited number of publications. B. I. Seo *et al.* have fabricated ZnO nanotubes (around 200 nm in diameter) within the nanochannels of porous anodic alumina templates by a template wetting process.[6] ZnO species were hosted in the matrix of the mesoporous silicate MCM-48 by an organometallic route[7] while nanocrystalline, size-selected ZnO was deposited inside the pores of a “wormhole” mesoporous silica with pore diameter of 5 nm.[8] Although examples in the literature exist, there are no systematic studies on this process in small volumes, and if some structural/morphological changes of the inorganic material occur. Therefore, of special interest for our project is to gain insight on i) the mineralization mechanism of the investigated functional oxides in confinements, ii) the pore sizes and penetration depth in the support material which limits the deposition and iii) the role of other factors which might influence this process.

A further essential part of this project is functionalization of the oxide layers in the pores with SAMs. The SAMs consisting of bifunctional linker molecules should fix the catalyst molecules in the pores. Typical terminal groups reported in literature for SAM formation on oxide films are alkoxysilane, carboxylate, phosphonate, thiol and sulfonate groups. A study on the SAM formation process on Al_2O_3 using different models systems with various surface orientations and crystallinity has shown that the adsorption and stability of SAMs (in this case octadecylphosphonic acid) on the oxide surface is based on different types interfacial bonding.[9] It strongly depends on the Al_2O_3 surface orientation and local geometry,[9] while the surface coverage depends on the chain length.[10] Therefore, based on these factors the SAM formation on the oxides proposed in this project will be systematically studied. Furthermore, investigations on spherical silica particles and plane-crystal-shaped zirconia particles have shown that another important factor by SAM formation is the curvature of the surface.[11] Therefore, to exclude the influence of the curvature effect of the pore walls, first flat reference samples consisting of the corresponding polymer material and oxide film should be functionalized by self-assembly of linker molecules to find the best terminal groups and chain length for each oxide. The study will be accompanied by systematic characterization of the flat hybrids by means of surface coverage, adhesion and stability of the SAM layers in organic solvents used further for the catalytic reactions.

Parameters like polarity and wettability of the pore walls have a strong impact on the quality of the SAMs.[12] Basically, they also offer an opportunity to control the orientation and distance of the catalyst molecule to the pore walls (Figure A5-2). The pore wall polarity/wettability can be manipulated by the zeta potential of the oxide layer and SAMs, whereas the wettability can be further influenced by the roughness of the layer. The oxides, selected for the project, have different isoelectric points (IEP) as reported in the literature: SiO_2 (~2), TiO_2 (6-7), ZrO_2 (6.7-7.5), Al_2O_3 (>8) and ZnO (9-10)),[13,14] hence, their net charge at certain pH should differentiate from each other. However, the zeta potential and IEP, respectively, depend greatly on the synthesis conditions and solutions (e.g. ionic strength, aqueous or organic solutions) used for the measurement. The data reported in the literature are determined in an aqueous solution, while for the needs of the CRC the mesoporous organic/inorganic hybrids will be used as catalyst supports in organic solvents, which might cause much higher zeta potential values.[15] Therefore, information about the zeta potential of the studied oxide layers have to be collected.

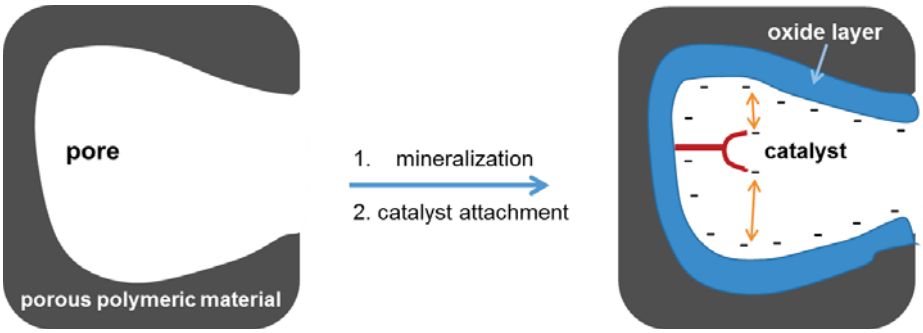

Figure A5-2. Schematic representation of electrostatic interactions between the catalyst molecule and oxide covered pore walls.

Finally, to enable a heterogeneous catalysis only in the confined spaces, the anchor groups for catalyst attachment have to be localized only in the pores but not on the support surface. Therefore, the inorganic layer and/or the attached SAMs have to be selectively removed/inactivated from the outer polymer surface. There are different options to perform this task such as chemical passivation of the oxide/SAM terminal groups, acid etching of the oxide film or mechanical removal in the case of microscopic support samples.

An alternative approach for building mesoporous support materials is the synthesis of hierarchical inorganic nanostructures based on polymer colloidal crystals (inverse opals)[16] or biological templates (biomorphic ceramics).[17] Colloidal crystals as templates have shown potential for preparation of highly ordered three-dimensional macroporous materials and inverse opals.[17-20] The latter represent three-dimensional periodic lattices consisting of closely packed air spheres interconnected to each other by small channels (Figure A5-3).

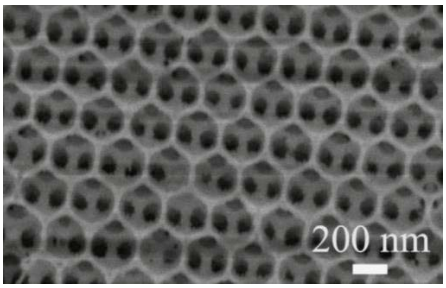

Figure A5-3. SEM image of a ZnO inverse opal prepared by L.Xia *et al.*[19] via sol-gel method using PMMA as a template.

They are prepared from monodispersed particles (e.g. polystyrene (PS), polymethyl-metacrylate (PMMA)) self-assembled into colloidal crystals. Then, different organic and inorganic materials can be infiltrated in the voids between the particles in the crystal and after treatment of the infiltrated materials (polymerization, curing, solidification), the template particles are removed and inverse opals are formed. Macroporous oxide inverse opals have been prepared.[19,20] Applying this approach, monodisperse PS nanoparticles with a mean diameter of 10-50 nm, synthesized in **project A7**, can be used to prepare mesoporous inverse opals with the oxides studied in our project in order to meet the target for the pore diameters, considered within the scope of this CRC.
Biological templates are abundant and in general inexpensive. Particularly interesting building blocks for synthesis of new composites are the viruses owed to their precisely defined size and shape (Figure A5-4). Among them, the tube-like tobacco mosaic virus (TMV) and bacteriophage (M13) attract attention due to their relative stability in a broad temperature and pH range, as well as in several organic solvents. The TMV has a length of about 300 nm, an outer and inner diameter of 18 nm and 4 nm, respectively, while the M13 particles are 900 nm long with diameter of only 6 nm. Based on their shape anisotropy, these virions exhibit advantageous interparticle interactions. TMV can arrange in micrometer long nanowires through head-to-tail assembly. Using different alignment techniques, mono and multilayers can be build.[21] The viruses have shown to be ideal scaffolds for deposition of inorganic materials such as metals, oxides and sulfides.[22,23] Therefore, they are promising template candidates for synthesis of biomorphic mesoporous oxides (Figure A5-4). Their robustness and properties might help to overcome the limits by formation of biomorphic mesoporous materials due to problems connected with incompatibility between the template and the inorganic precursor.[17]

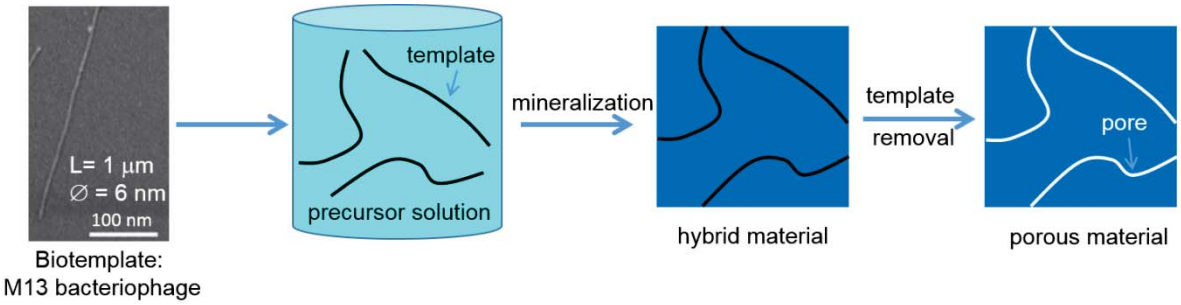

Figure A5-4. Formation of porous inorganic supports with defined porosity through mineralization and subsequent removal of the biotemplate from the inorganic matrix.

References

[1] C. Sanchez, P. Belleville, M. Popall, L. Nicole, Chem. *Soc. Rev.* **2011**, *40*, 696-753.
[2] S. Weiner, P. M. Dove, *Rev Mineral Geochem* **2003**, *54*, 1.
[3] C. J. Stephens, S. F. Ladden, F. C. Meldrum, H. K. Christenson, *Adv. Funct. Mater.* **2010**, *20*, 2108-2115.
[4] H. Ping, H. Xie, Y. M. Wan, Z. X. Zhang, J. Zhang, M. Y. Xiang, J. J. Xie, H. Wang, W. M. Wang, Z. Y. Fu, *J Mater Chem B* **2016**, *4*, 880-886.
[5] B. Coasne, A. Mezy, R. J. M. Pellenq, D. Ravot, J. C. Tedenac, *J. Am. Chem. Soc.* **2009**, *131*, 2185-2198.

[6] B. I. Seo, U. A. Shaislamov, M. H. Ha, S. W. Kim, H. K. Kim, B. Yang, *Physica E-Low-Dimensional Systems & Nanostructures* **2007**, *37*, 241-244.
[7] F. Schroder, S. Hermes, H. Parala, T. Hikov, M. Muhler, R. A. Fischer, *J. Mater. Chem.* **2006**, *16*, 3565-3574.
[8] S. Polarz, F. Neues, M. W. E. van den Berg, W. Grunert, L. Khodeir, *J. Am. Chem. Soc.* **2005**, *127*, 12028-12034.
[9] P. Thissen, M. Valtiner, G. Grundmeier, *Langmuir* **2010**, *26*, 156-164.
[10] A. G. Koutsioubas, N. Spiliopoulos, D. L. Anastassopoulos, A. A. Vradis, G. D. Priftis, *Surf. Interface Anal.* **2009**, *41*, 897-903.
[11] C. J. Lomoschitz, B. Feichtenschlager, N. Moszner, M. Puchberger, K. Muller, M. Abele, G. Kickelbick, *Langmuir* **2011**, *27*, 3534-3540.
[12] S. S. Kelkar, D. Chiavetta, C. A. Wolden, *Appl. Surf. Sci.* **2013**, *282*, 291-296.
[13] K. Kamada, M. Tokutomi, N. Enomoto, J. Hojo, *J. Mater. Chem.* **2005**, *15*, 3388-3394.
[14] S. E. Y. D. Gu, H. Baumgart, S. Qian, O. Baysal and A. Beskok, *ECS Transactions* **2010**, *33(2)*, 37-41.
[15] A. Kasseh, E. Keh, *J. Colloid Interface Sci.* **1998**, *197(2)*, 360-369.
[16] O. D. Velev, E. W. Kaler, *Adv. Mater.* **2000**, *12*, 531-534.
[17] P. Colombo, C. Vakifahmetoglu, S. Costacurta, *J Mater Sci* **2010**, *45*, 5425-5455.
[18] X. Li, J. G. Yu, M. Jaroniec, *Chem. Soc. Rev.* **2016**, *45*, 2603-2636.
[19] L. Xia, J. Song, R. Xu, D. L. Liu, B. Dong, L. Xu, H. W. Song, *Biosens Bioelectron* **2014**, *59*, 350-357;
[20] V. Abramova, A. Sinitskii, *Superlattices Microstruct.* **2009**, *45*, 624-629.
[21] P. Atanasova, N. Stitz, S. Sanctis, J. H. Maurer, R. C. Hoffmann, S. Eiben, H. Jeske, J. J. Schneider, J. Bill, *Langmuir* **2015**, *31*, 3897-3903.
[22] P. Atanasova, D. Rothenstein, J. J. Schneider, R. C. Hoffmann, S. Dilfer, S. Eiben, C. Wege, H. Jeske, J. Bill, *Adv Mater* **2011**, *23*, 4918-4922.
[23] P. Atanasova, I. Kim, B. Chen, S. Eiben, J. Bill, *Adv. Biosys*. **2017**, 1700106 (8pp).

3.5.3.2 Own work, project-related publications by participating researchers

Over the past decade, various oxide materials such as ZnO, ZrO_2, SnO_2, In_2O_3, TiO_2, and V_2O_5/TiO_2 were synthesized in our group via the CBD method.[A5-1 - A5-7] Additionally, a wide range of biomacromolecules such as peptides, proteins, DNA (Figure A5-5 (left)), and even bigger biological objects like viruses (Figure A5-5 (right)) and bacteria have been used as templates and scaffolds in the formation of new 1D and 2D hybrid bioorganic/inorganic nanostructures applying this technique.[A5-1 - A5-3] Further, nacre-like organic/inorganic multilayered structures (MLS) with highly sophisticated structural design have been synthesized.[A5-4] Here, polystyrene sulfonate, poly-L-glutamic acid and poly-L-lysine were used as organic template layers for the deposition of ZnO films in the MLSs.

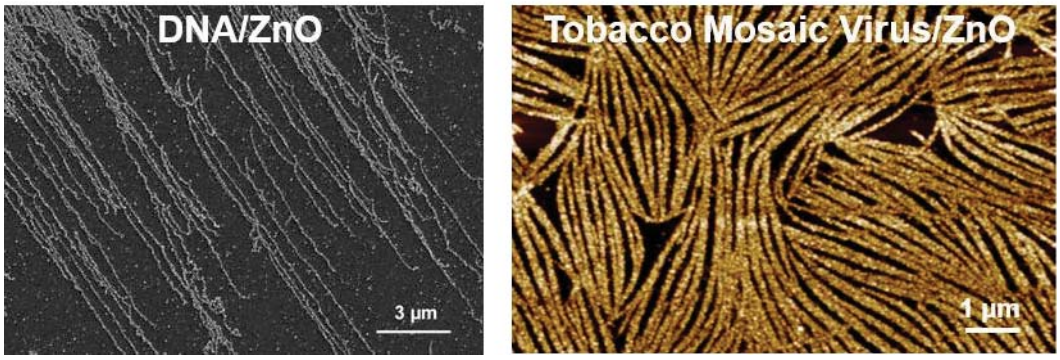

Figure A5-5. Nanostructured organic/inorganic hybrid materials: (left) stretched lambda-DNA and (right) monolayer of tube-like TMV selectively mineralized with nanocrystalline ZnO particles.

Controlling the mineralization conditions, the particle size and deposition rate can be influenced, and the thickness of the inorganic film on the template can be precisely tuned. Thus, layers from several nanometers up to micrometer range can be deposited (Figure A5-6).

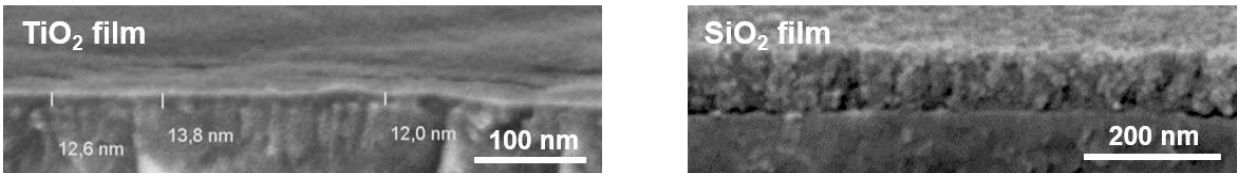

Figure A5-6. Cross-section SEM images of TiO_2 and SiO_2 thin films obtained via template-assisted synthesis.

The results of our first preliminary experiments conducted with the synthesized in **project A7** polymer foams based on PS and PMMA serve as proof of principle that the polymer surface can be mineralized. PS foams with pore diameter of several micrometers were mineralized in methanol-containing ZnO precursor solution at 60°C. As can be seen from the scanning electron microscopy (SEM) images in Figure A5-7, the PS pore walls of the foam (Figure A5-7a) are mineralized with thin inorganic film (Figure A5-7b). The energy-dispersive X-ray (EDX) spectroscopy confirmed the presence of Zn in the pores. A compression test analysis of foams with and without ZnO was performed. Although only the pores near to the foam surface were mineralized due to the close cellular structure of the PS foams, the results from stress/strain curves showed an enhancement of the elastic modulus of the foams in presence of ZnO. Furthermore, the latest experiments with PS in **project A7** confirmed formation of foams with open cellular structure as can be seen in Figure A7-6 (**project A7**) and next mineralization experiments are in the scope of our further joint work.

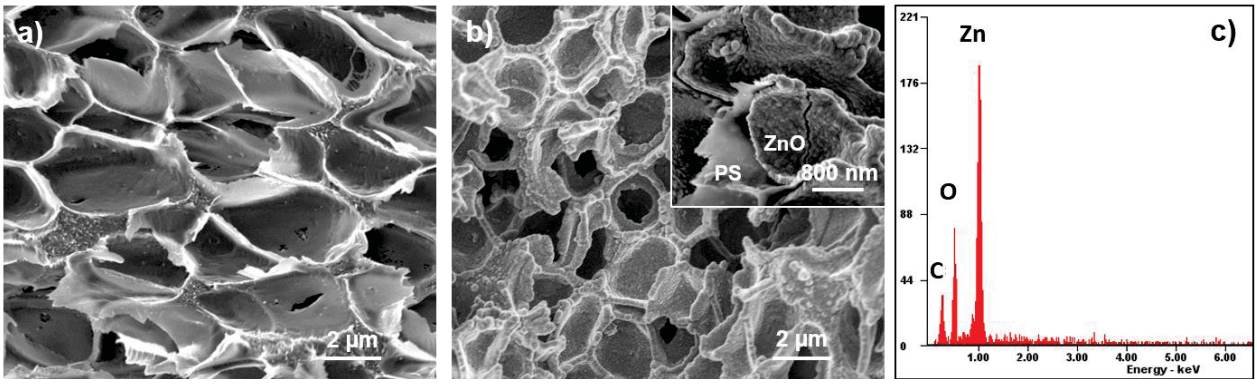

Figure A5-7. a) PS foam (delivered by **project A7**). b) ZnO mineralized PS foam. c) EDX spectrogram of ZnO mineralized PS foam.

PMMA foams with pore sizes of several micrometers and open cellular structurre were mineralized with a thin TiO_2 film at room temperature (Figure A5-8).

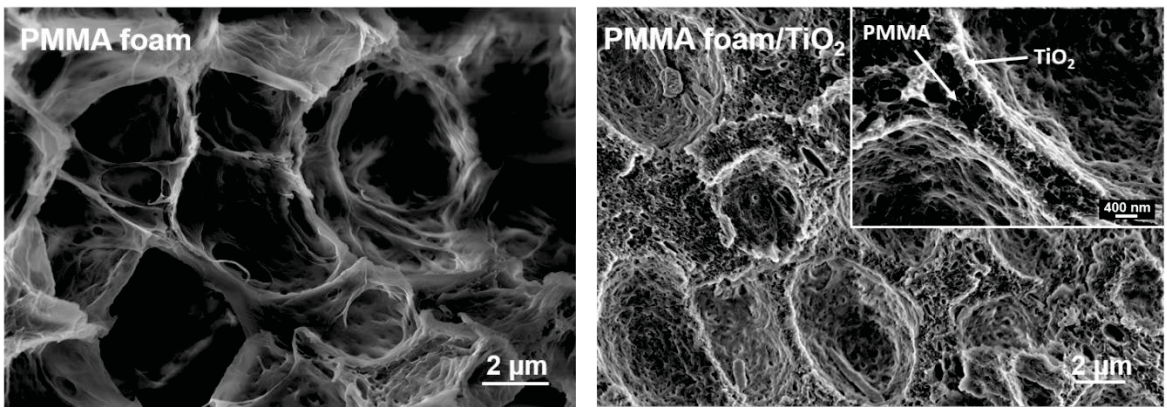

Figure A5-8. a) PMMA foam (delivered by **project A7**). b) TiO_2 mineralized PMMA foam.

In a first attempt to functionalize the inorganic surface with appropriate terminal groups and prepare it for further attachment of catalyst molecules, a model molecule was used to self-assemble on a ZnO film. For this purpose, propiolic acid, which has two terminal groups a carboxyl group needed for the

attachment to the ZnO surface and an alkyne group required for the coupling of the catalyst molecule was chosen. In Figure A5-9, the photoluminescence spectrum of a ZnO film with its characteristic sharp band gap (left) and broad defect peak (right) is shown. Washing with hexane used afterwards as solvent for the propiolic acid self-assembly, led to intensity reduction of the defect peak of ZnO. Further treatment of ZnO film with propiolic acid resulted in disappearance of the defect peak. This observation is in line with the attachment of the acid to the oxide surface, which eliminates the defects and causes loss of the defect peak giving a hint for the success of the SAM formation.

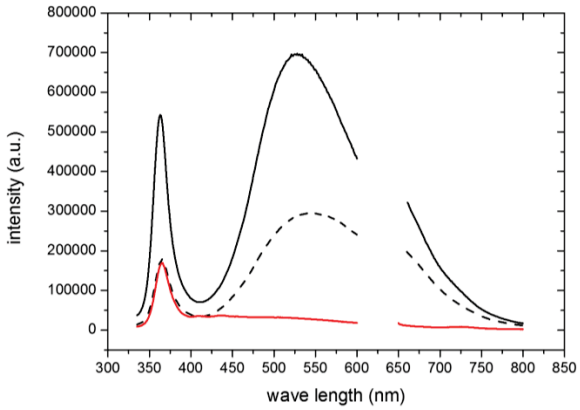

Figure A5-9. Photoluminescence spectra of a ZnO thin film (black curve), ZnO film placed in hexane (black dashed curve) and ZnO film self-assembled with propiolic acid from hexane solution. Excitation wave length 315 nm.

[A5-1] P. Atanasova, N. Stitz, S. Sanctis, J. H. M. Maurer, R. C. Hoffmann, S. Eiben, H. Jeske, J. J. Schneider, J. Bill, *Langmuir* **2015**, *31*, 3897-3903.

[A5-2] P. Atanasova, D. Rothenstein, J. J. Schneider, R. C. Hoffmann, S. Dilfer, S. Eiben, C. Wege, H. Jeske, J. Bill, *Adv. Mater.* **2011**, *23*, 4918-4922.

[A5-3] P. Atanasova, R. T. Weitz, P. Gerstel, V. Srot, P. Kopold, P. A. van Aken, M. Burghard, J. Bill, *Nanotechnol.* **2009**, *20*, 365302 (7pp).

[A5-4] P. Lipowsky, Z. Burghard, L. P. H. Jeurgens, J. Bill, F. Aldinger, *Nanotechnology* **2007**, *18*, 345707 (6pp).

[A5-5] D. Rothenstein, D. Shopova-Gospodinova, G. Bakradze, L. P. H. Jeurgens, J. Bill, *Crystengcomm* **2015**, *17*, 1783-1790.

[A5-6] D. Santhiya, Z. Burghard, C. Greiner, L. P. H. Jeurgens, T. Subkowski, J. Bill, *Langmuir* **2010,** *26*, 6494-6502.

[A5-7] P. Lipowsky, R. C. Hoffmann, J. Bill, F. Aldinger, *Adv. Funct. Mater.* **2007**, *17*, 2151-2156.

3.5.4 Project plan

The research goals of the proposed project are organized in work-packages as follows:

- **WP 1: Mineralization of polymer thin films.** Selective and controlled mineralization of polymer thin films with various oxides such as ZnO, TiO_2, SiO_2, ZrO_2 and Al_2O_3 applying mild reaction conditions. Optimization of the mineralization conditions and characterization of the obtained organic/inorganic hybrid films.
- **WP 2: Attachment of linker and catalyst molecules to organic/inorganic hybrid thin films.** SAMs made of bifunctional linker molecules on flat hybrid references prepared in WP1 will be generated. Additionally, to reduce the number of the coupling sides for the catalyst molecules, mixed SAMs will be examined. Thorough characterization of the functionalized hybrid thin films will be performed. The best terminal groups for coupling to each investigated oxide will be determined. The coupling of the catalyst molecules from **projects B2** and **B3** through "click" reaction will be tested and optimized.
- **WP 3: Mineralization in a confined model system.** A model system resembling confined space will be used to study the mineralization mechanism of the oxides synthesized at mild conditions excluding hindrances caused by infiltration and polymer permeability problems.
- **WP 4: Synthesis of inorganic mesoporous support materials** as an alternative way for synthesis of mesoporous catalyst supports: 1) Compete filling of the pores of the polymer foams (**project A7**) with inorganic phase and subsequent removal of the organic template. Formation of porous inorganic materials with adjustable pore size and shape (dependent on the thickness of the polymer pore walls) and density (dependent on the pore diameter of the organic template). 2) PS and PMMA nanoparticles (10-50 nm in diameter), synthesized in **project A7**, will be arranged in 3D colloidal crystals applying various assembly techniques. After infiltration of the voids between the polymer particles with precursor solution, inverse opals of the corresponding oxide will be prepared.
- **WP 5: Mineralization in the pores of polymer supports and functionalization with linker molecules.** Thin oxide films will be deposited on the pore walls of the porous polymeric templates from **projects A1**, **A2** and **A7** under optimal conditions identified in WP1. By varying the oxide type, the polarity of the pore walls will be adjusted. Mesoporous organic/inorganic hybrids with a pore diameter in the range of 5 - 20 nm have to be produced through precise control over the oxide film thickness on the pore walls. Thus, sustainable catalyst supports with preserved open porosity and good adhesion of the inorganic film to the polymer pore walls have to be achieved. The mechanical stability of the mesoporous hybrids will be determined via compression test analysis. Detailed characterization of the structure, morphology, composition and crystallinity of the deposited oxides in the pores (SEM, TEM (**project C3**), XRD, SANS and SAXS (**project A7**)) will provide information on the quality and properties of the hybrids, but also on the mineralization mechanism of different oxides in confinement. SAMs of linker molecules with the best terminal group for each oxide type will be formed within the pores of the organic/inorganic hybrids and the inorganic supports for further attachment of catalyst molecules and also for further adjustment of the pore wall polarity.
- **WP 6: Pore-selective functionalization.** To ensure the presence of anchoring groups for the catalyst attachment only in the pores but not on the outer side of the synthesized supports, different approaches will be tested depending on the characteristics of the polymers used as a template. According to the pore size achieved with the hybrids based on polymer monoliths (**project A1**) and block copolymers (**project A2**), either polymeric reagents with radius of gyration bigger than pore diameter or sterically demanding silanes, respectively, will be used to passivate the outer side of the support. Additionally, mechanical removal of the oxide layer from the outer surface of the block copolymer-based hybrids will be attempted with ion milling (**project C3**). Gentle oxide etching from the porous hybrids based on polymer foams (**project A7**) and the inorganic mesoporous supports (WP5) will be tested.

3.5.4.1 WP 1: Mineralization of polymer thin films

In the first work task of the proposal, the selective mineralization of oxides such as ZnO, TiO_2, SiO_2, ZrO_2 and Al_2O_3 on polymer materials in a controlled manner will be studied. Since the mineralization in the pores of the polymer matrix could be influenced by different factors like diffusion of the precursor, permeability of the polymer material and the curvature of the pore walls, the deposition of the inorganic material of choice will be investigated initially on polymer thin films. To do this, polymers selected for the synthesis of the polymer porous materials in **projects A1**, **A2** and **A7** and later taken for preparation of organic/inorganic hybrid catalyst supports (see WP5), will be used to prepare thin polymer films on a silicon substrates. These reference samples will be mineralized via mild CBD at room or slightly elevated temperature (60 – 70°C) using the corresponding oxide precursors. The presence of functional groups and surface charge on the polymer surface is crucial for the success of the mineralization. The solvent used for the preparation of the deposition solution should be adjusted according to the solvent resistivity properties of the corresponding polymer. Thus, inorganic thin films with different morphology (roughness) and surface functionality (zeta potential, surface functional groups) will be prepared. The growth rate of the inorganic films on the host polymer materials will be studied and evaluated by the use of AFM and SEM analysis. The surface morphology and crystallinity will be determined via SEM and XRD. The adhesion of the oxide film on the polymer surface, later very important for the sustainability of the hybrid support during the catalytic reaction, will also be assessed applying methods like ´scratch test´, ´peel test´ or ´pull test´. The zeta potential of the inorganic films, essential for the attachment, position and orientation of the catalyst molecules will be systematically determined for each oxide type in aqueous solutions but also in organic solvents used further for the catalytic reactions in **projects B2** and **B3**. For this purpose, a Zeta sizer or a SurPASS electrokinetic analyzer will be used. Here, reference experiments in cooperation with **projects B2** and **B3** should be conducted to exclude an effect of the oxides itself on the catalytic reactions. For this purpose, silicon substrates with polymer/oxide films will be used as additives in the investigated catalytic reactions.

3.5.4.2 WP 2: Attachment of linker and catalyst molecules to organic/inorganic hybrid thin films

The polymer/inorganic hybrid thin films, fabricated in WP1, will be used as a model system to study the SAM formation of linker molecules on the inorganic surface of the hybrids. These linker molecules (commercially available or synthesized in **B3**) serve to attach finally the catalyst molecules from **projects B2** and **B3,** to the catalyst support. They should possess two terminal functional groups (Figure A5-10). Thus, functional groups like alkoxysilane, carboxylate, phosphonate, thiol and sulfonate will be tested as a terminal group (TG1), which should attach the linker to the inorganic part of the hybrid. Further, azide or alkyne will be taken as a second anchoring group (TG2), which should conjugate the catalyst molecules using “click” reaction.

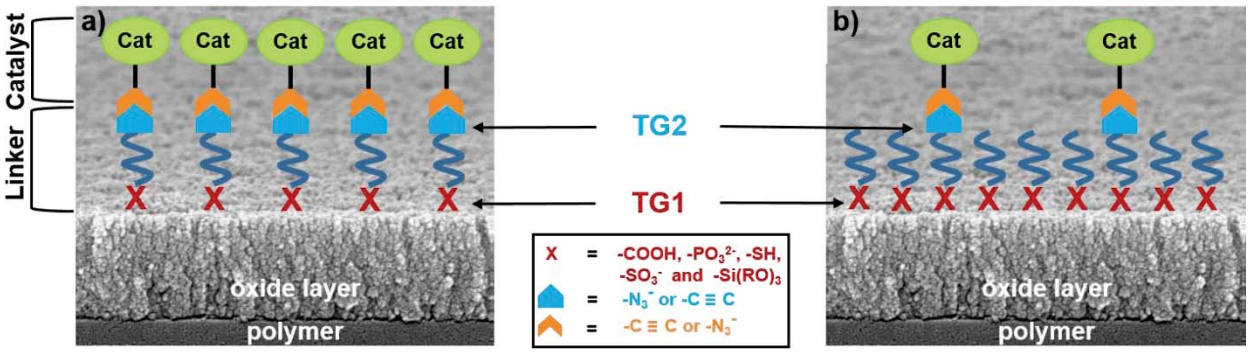

Figure A5-10. Schematic representation of catalyst coupling on the organic/inorganic catalyst support through linker molecules. a) SAM of linker with two terminal groups and b) mixed SAM of linkers with one and two functional groups to control the density of the attached catalyst molecules.

The SAM formation will be thoroughly characterized applying methods like contact angle goniometry, ellipsometry, FTIR, photoluminescence measurements, and XPS. In addition, in cooperation with **project C6** (**Fyta**) simulations studies should gain more insight into for the coupling mechanism of the

self-assembled linkers to the oxide films. The best TG1 for each oxide type by means of attachment stability and continuity of the SAMs should be found. Additionally, to enhance the SAM surface coverage and stability and for the needs of the catalytic studies, the length of the linker molecule will also be adjusted. If necessary, mixed SAMs consisting of linkers with and without TG2 will be examined in order to reduce the coupling sites and hence the number of the catalyst molecules attached on the catalyst support (Figure A5-10b).[24] Then, to accomplish the "click" reaction with the catalyst molecules equipped with the respective terminal functional group, samples will be provided to **projects B2** and **B3.** The obtained polymer/oxide hybrid thin films with immobilized linker and catalyst molecules should be examined in reference experiments. Here, important conclusions should be drawn: i) The results should serve to compare the heterogeneous catalysis on flat supports to those in confinements and ii) to figure out the critical linker length, where a transformation from heterogeneous to homogeneous catalysis occurs.

3.5.4.3 WP 3: Mineralization in a confined model system

To support our work in WP5, here we aim to gain more insight into the mineralization mechanism of the proposed oxides, synthesized at mild conditions, in confined spaces. To exclude the influence of side effects on the mineralization process, which might take place in the porous polymeric supports, a model system resembling confined space will be used. Inspired by the work of C. J. Stephens *et al*.[25] an analogous model consisting of two crossed half-cylinders forming an annular wedge around their contact points (Figure A5-11a) will be used. Such a model system will allow to study the confinement effect starting with surface separation from zero at the contact point and increasing the distance up to microscopic values (Figure A5-11b,c). The aim in this work task is to evaluate the influence of the confinement itself and also the interplay of the confined space with the template material on the mineralization behavior. The obtained products will be characterized via various spectroscopic methods.

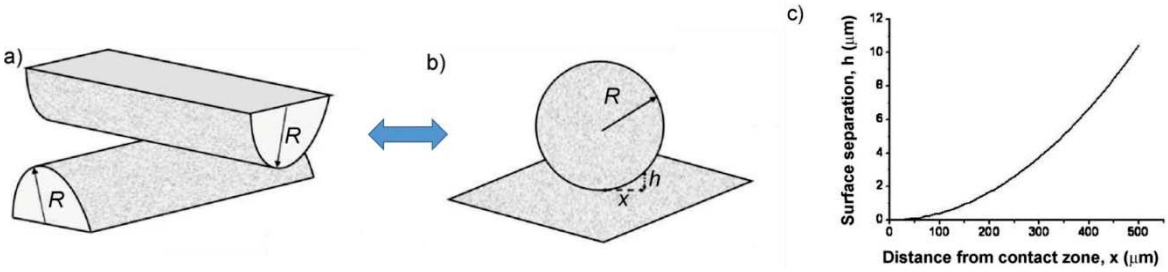

Figure A5-11. a) Schematic illustration of a crossed–cylinder configuration with radius of curvature R. b) The equivalent sphere-on-a-flat configuration with the surface separation h, related to the distance from contact x. c) The surface separation h plotted as a function of distance x to the contact point (modified).[25]

3.5.4.4 WP 4: Synthesis of inorganic mesoporous support materials

As an alternative for the preparation of mesoporous catalyst supports, pure inorganic porous materials will be synthesized applying two different approaches. According to the first one, the pores of the polymer foams provided by **project A7**, used also in WP5, will be mineralized with oxide until the pores are completely filled with inorganic phase. Then, the organic template will be removed with an appropriate organic solvent or removed by pyrolysis. In this way, the size and the shape (geometry) of the newly formed pores will depend on the thickness of the pore walls of the original organic porous material. Additionally, the distribution and density of the formed pores can be adjusted by the pore diameter of the organic template.
Colloidal crystals are going to be used as a second possibility to prepare template facilitated inorganic porous materials. As a result, oxide inverse opals with a target pore size of 10-50 nm have to be prepared. To this end, PS and PMMA nanoparticles (10-50 nm in diameter), synthesized through emulsion polymerization in **project A7** will be used as building blocks and assembled in 3D colloidal crystals (Figure A5-12). Beside the commonly used filtration, centrifugation or sedimentation methods, techniques like convective assembly, dip coating, spin coating and controlled evaporation, frequently

used in our group, will be tested here as well. Then, the voids between the polymer particles will be infiltrated with a precursor solution and mineralized to form the corresponding oxide inverse opal. In attempt to further decrease the pore diameter, the already used CBD method will be used. The synthesis of inorganic porous materials applying these approaches will be accompanied by a thorough characterization including SEM, TEM (**project C3**) and XRD analysis to determine the structure and composition of the materials, while Brunauer–Emmett–Teller (BET) analysis (**project A1**) will be used to assess the achieved porosity.

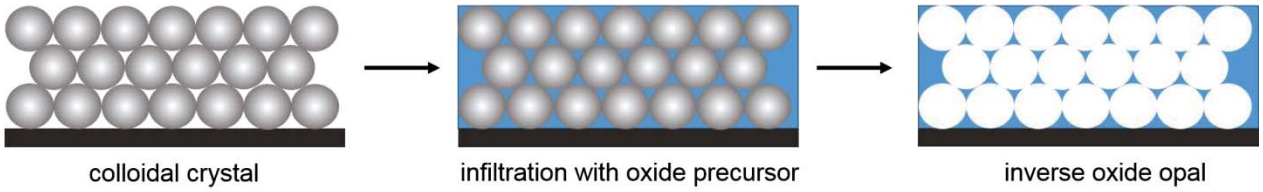

Figure A5-12. Schematic of the replication of a colloidal crystal structure into porous materials (inverse opals).

3.5.4.5 WP 5: Mineralization in the pores of polymer supports and functionalization with linker molecules

The intensive experimental work and systematic investigations in WP1 and WP2 on flat reference polymer surfaces should provide detailed information for i) the optimal deposition conditions for the proposed oxides and ii) the best terminal group and conditions for SAM formation for each oxide type. In this central WP, thin inorganic films will be deposited under optimized conditions on the pore walls of porous polymeric supports synthesized in **projects A1**, **A2** and **A7** (Figure A5-13). The monoliths from **project A1** will provide a bulk support material with narrow and almost monodisperse porosity on the surface of the microglobules surrounded by bigger voids for faster mass transport. The block copolymer supports delivered by **project A2** form structures with cocontinuous morphologies or thin films with single pores, which are perpendicularly oriented to the film surface. The pore diameter in the templates from **project A1** and **A2** should be in the range of 10-20 nm. The pore diameter in both template types should be in the range of 10-20 nm. The polymer foams in **project A7** are bulk support materials with isotropic distribution of pores with open cellular structure and diameter in the range of 50-250 nm. Applying a selective and precisely controlled deposition approach, the pore size will be finely tuned, which can be accomplished controlling the film thickness of the oxide layer mineralized on the pore walls. The obtained polymer/inorganic hybrid materials will be characterized with respect to control over the oxide film thickness, preserved open porosity of the hybrid support and good adhesion of the inorganic film to the polymer pore walls.

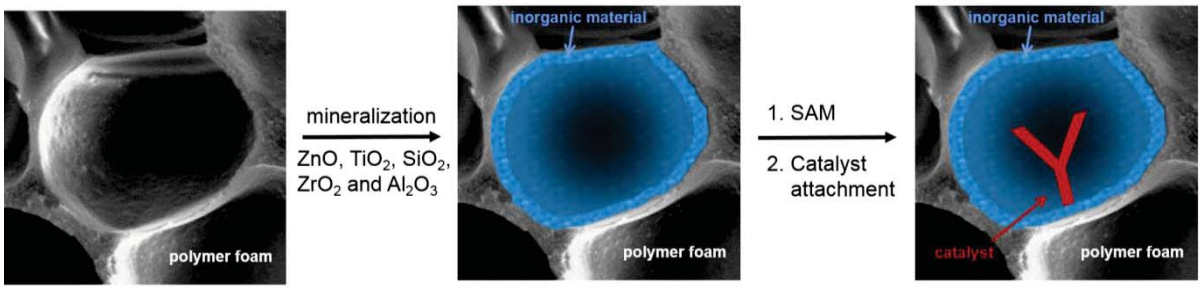

Figure A5-13. Schematic representation of the mineralization and subsequent functionalization of a pore in a polymer foam.

Next point in this WP is to shed light on the issue whether the findings in WP3 meet the results for mineralization of the inorganic material in the porous polymeric templates and whether they differentiate from those on flat surface in WP1. Therefore, the structure, morphology, composition and crystallinity of the oxides deposited in the porous polymers will be investigated. Additionally, the mechanical stability of the hybrids should be examined via compression test analysis.

Then, to enable attachment of the catalyst molecules from **project B2** and **B3** in the pores of the organic/inorganic hybrids, SAMs with free azide or alkyne groups for catalyst attachment will be formed on the oxide surface. Therefore, linkers with the best coupling terminal groups for each oxide will be assembled under optimized conditions (WP2), and the success of the coupling and the distribution of the linkers in the pores of hybrid materials will be investigated.
All products in this multiple step synthesis including mineralization of the porous polymeric supports, functionalization of the oxide pore walls and selective passivation/removal of the oxide layer with the SAM from the outer surface of the catalyst support (see 3.1.4.6. WP 6) will be systematically characterized by the help of techniques like SEM, TEM (**project C3**) solid-state NMR (**project C1**), atom probe tomography (**project C3**), SANS and SAXS (**project A7**). Further, modelling of the mass transfer in a pore to a catalyst molecule attached on a SiO_2 pore walls in **project C5** (**Hansen**) should give further input for interpretation of the obtained results. The diffusion within the synthesized porous support materials will be studied by fluorescence correlation microscopy in cooperation with Dr. K. Koynov, Max-Planck Institute for Polymer research, Mainz.[26,27] For this purpose, the diffusion of novel fluorescence merocyanine dyes from **project B3** in liquid filled mesoporous supports will be examined giving additional information for the permeability of the materials. In this regard, in cooperation with **projects B2** and **B3** homogeneous catalysis in mesoporous supports without catalyst functionalization will be performed as control experiments.

3.5.4.6 WP 6: Pore-selective functionalization

Before starting with the catalyst attachment in the pores, pore-selective functionalization of the support materials should be achieved. Depending on the individual characteristics of the obtained inorganic (WP4) and organic/inorganic (WP5) mesoporous support materials, different approaches for selective functionalization will be tested.

a) When monoliths from **project A1** are taken as polymer templates and mineralized, a thin oxide layer will be formed not only in the pores but also on the outer surface of the microglobules composing the monolith. In order to passivate the oxide surface outside the pores and to eliminate there the coupling sides for catalyst attachment, the method suggested in **project A1** for monoliths itself (see **project A1,** WP6) will be undertaken. The procedure includes the use of polymer reagents with radius of gyration 2.5 times larger than the pore size for bigger pores or sterically demanding silanes for smaller pores, synthesized in **project A1**.

b) In the case of porous templates based on block copolymers (**project A2**), the same approach can be used. In addition, making use here of the flat thin structure of the polymer/oxide hybrid with pores positioned perpendicular to the film plane, removal of the oxide layer can be attempted by applying ion-milling. This will be done in cooperation with **project C3**, where ion beam sputtering chambers (UHV vacuum 10^{-8} mbar) are available.

c) Finally, due to the isotropic pore distribution within the porous hybrids based on polymer foams (**project A7**) and the inorganic mesoporous supports (WP4), the oxide film mineralized on the support surface together with the functionalized SAM is planned to be selectively removed by gentle oxide etching either with acid or base depending on the oxide nature. Here, the concentration of the etching agent and the etching time will be varied to reach only partial oxide removal from the support outer surface.

3.5.4.8 Support-specific properties relevant to the catalytic reactions to be investigated

The synthesized organic/inorganic mesoporous materials are intended to provide enhanced mechanical stability. Additionally, the presence of rigid oxide film on the pore walls should ensure chemical stability against organic solvents, and thus, the pore size and shape of the hybrids should be retained. The polarity/wettability of the pore walls can be varied through the choice of the oxide and the assembled SAMs. These material properties make them suitable supports for catalyst molecules to study catalytic reactions like olefin metathesis (**project B2**) and asymmetric catalysis with chiral olefin-rhodium complexes (**project B3**). In respect to olefin metathesis, the impact of i) pore size, geometry and tortuosity of the mesoporous supports and ii) different functional groups at the pore walls (polar, non-polar, protic, aprotic) together with differently functionalized olefins (polar, non-polar, protic, aprotic) on the function of the organometallic catalyst will be investigated. In addition, a variation of the pore size and polarity will provide more insight into the influence of these factors on cyclization *vs*. polymerization

tendency (ring-closing metathesis (RCM) *vs*. acyclic diene metathesis (ADMET). For the asymmetric catalysis in **project B3** similarly, the influence of the pore size, pore wall polarity as well as the effect of the linker length, polarity and rigidity on the catalytic reaction will be studied.

Chronological work plan:

	2018	2019	2020	2021	2022	
	Q3 Q4	Q1 Q2 Q3 Q4	Q1 Q2 Q3 Q4	Q1 Q2 Q3 Q4	Q1 Q2	
T1						WP1: Mineralization of polymer thin films
T2						WP 2: Attachment of linker and catalyst molecules to organic/inorganic hybrid thin films
T3						WP 3: Mineralization in a confined model system
T4						WP 4: Synthesis of inorganic mesoporous support materials
T5						WP 5: Mineralization in the pores of polymer supports and functionalization with linker molecules
T6						WP 6: Pore-selective functionalization

3.5.4.9 Methods applied

CBD for synthesis of inorganic materials from liquid solutions is commonly used in our group and synthetic procedures for various oxides are already established. Methods like AFM, SEM, TEM (**project C3**) and XRD will be used for the thorough investigation of the structure, morphology and composition of products including thin oxide films (WP1 and WP3), inorganic porous materials (WP4) and mineralized polymer porous supports (WP5). Zeta potential measurements of solutions (Zeta sizer) and thin films (SurPASS electrokinetic analyzer) will be conducted to determine the surface charge of the hybrid materials. The success of SAM formation and attachment of linker molecules on thin films will be studied via contact angle measurements, ellipsomethry, FTIR, photoluminescence, and XPS. Qualitative proof for the SAM formation with linker molecules in the pores will be collected on powder samples via solid-state ^{13}C NMR (**project C1**). In regard to their distribution within the pores, atom probe tomography (**project C3**) will be used. SAXS und SANS (**project A7**) will be used to determine the pore size and distribution in the porous hybrids as well as to gain insight into the nucleation and growth of the mineralized oxides (reference thin films and in the pores). The porosity will be defined by BET (**project A1**) analysis. Compression test analysis will be used to examine the mechanical stability of the hybrid support materials. Along with the standard spin coating and dip coating techniques, home-made set-ups for convective assembly and controlled evaporation will be tested to produce 3D structures of colloidal crystals. Fluorescence correlation spectroscopy (cooperation with Dr. K. Koynov, Max-Planck Institute for Polymer Research, Mainz) will be performed to study the diffusion of fluorescence molecules in porous support materials. The experiments within our work program will be supported additionally by theoretical investigations concerning the coupling mechanism of the self-assembled linkers to the oxide films (**project C6**) and modelling of the mass transfer in a pore to a catalyst molecule attached on SiO_2 pore walls (**project C5**).

3.5.4.10 Vision

By the end of the first funding period, the results from the thorough investigations with the flat references will give deeper insight into the mineralization behavior of the studied oxides on polymer templates. The best terminal groups for each oxide type will be determined and homogeneous, dense and stable SAMs of linkers for catalyst attachment can be successfully produced. Mesoporous

organic/inorganic hybrids and inorganic materials with pore diameter in the range of 5-20 nm will be achieved through fine tuning the oxide film thickness on the pore walls. The polarity of the pore walls in the hybrids, important for the catalyst position, can be adjusted by mineralization with different oxide types and/or SAMs. Further, a deeper understanding of the mineralization of the studied oxides in confinement will give information about the opportunities of the corresponding mineralization approach. For later stages of the project, the synthesis of biomorphic mesoporous inorganic materials with channel-shaped pores is envisioned by making use of the anisotropic properties of biological objects like viruses with elongated geometry. Besides this, inorganic materials with catalytic properties (e.g. sulfides) and such, which would enhance the thermal stability of the mesoporous hybrids for high temperature catalytic reactions are intended.

3.5.5 Role within the collaborative research center

This project complements the group of mesoporous materials suggested to be used in this CRC and contributes with the proposed organic/inorganic hybrids and inorganic materials to provide a set of catalyst supports with diverse advantageous properties. Applying our synthesis approach, porous polymeric materials prepared in **projects A1**, **A2** and **A7** will be used as templates to obtain hybrid materials and inorganic inverse replica of polymer templates with enhanced stability, precisely controlled pore diameter and adjustable pore wall polarity/wettability. In intensive cooperation with projects from section A and C, a thorough characterization with solid-state NMR (**project C1**), high resolution tomography (**project C3**), SAXS and SANS (**project A7**) will accompany the preparation and functionalization of the mesoporous hybrids. The obtained hybrid supports will be provided to the research groups of **project B2** focused on the ring-closing metathesis at anchored molybdenum- and tungsten-complexes and **project B3** working on the asymmetric catalysis at anchored rhodium-complexes for further catalytic investigations. The organic/inorganic materials will be object of theoretical investigations in cooperation with **projects C5** and **C6**.

3.5.6 Differentiation from other funded projects

The work described in A5 is not subject or partly subject of other funding projects.

3.5.7 Project funding

3.5.7.1 Previous funding

This project is currently not funded and no funding proposal has been submitted.

References (ctd.)

[24] B. Feichtenschlager, C. J. Lornoschitz, G. Kickelbick, *J. Colloid Interface Sci.* **2011**, *360*, 15-25.
[25] C. J. Stephens, S. F. Ladden, F. C. Meldrum, H. K. Christenson, *Adv. Funct. Mater.* **2010**, 20, 2108 2115.
[26] T. Cherdhirankorn, M. Retsch, U. Jonas, H. J. Butt, K. Koynov *Langmuir* **2010**, *26(12)*, 10141-10146.
[27] R. Raccis, A. Nikoubashman, M. Retsch, U. Jonas, K. Koynov, H. J. Butt, C. N. Likos, G. Fytas *ACS Nano*. **2011**, 5(6), 4607-4616.

3.5.7.2 Requested funding

Funding for	2018		2019		2020		2021		2022		2018-2022	
Staff	Quantity	Sum	Quantity	Sum	Quantity	Sum	Quantity	Sum	Quantity	Sum	Quantity	Sum
PostDoc, 100%	1	35,000.-	1	69,900.-	1	69,900.-	1	69,900.-	1	35,000.-	1	279,700.-
Total		35,000.-		69,900.-		69,900.-		69,900.-		35,000.-		279,700.-
Direct costs	Sum		Sum		Sum		Sum		Sum		Sum	
consumables	4,000.-		8,000.-		8,000.-		8,000.-		4,000.-		32,000.-	
Total	4,000.-		8,000.-		8,000.-		8,000.-		4,000.-		32,000.-	
Major research instrumentation	Sum		Sum		Sum		Sum		Sum		Sum	
	-		-		-		-		-		-	
Total	-		-		-		-		-		-	
Grand total	39,000.-		77,900.-		77,900.-		77,900.-		39,000.-		311,700.-	

(All figures in EUR)

3.5.7.3 Requested funding for staff

	Sequential no.	Name, academic degree, position	Field of research	Department of university or non-university institution	Project commitment in hours per week	Category	Funding source
Existing staff							
Research staff	1	Joachim Bill, Prof. Dr., Research group leader	Organic/Inorganic Hybrids, Bio-Inspired Materials and Synthesis, Material Science	Institute for Materials Science	4		University
Requested staff							
Research staff	2	Petia Atanasova, Dr., Senior Researcher	Organic/Inorganic Hybrids, Bio-Inspired Materials and Synthesis, Material Science	Institute for Materials Science		PostDoc, 100%	
Research Staff	3	Research assistant	Organic/Inorganic Hybrids, Bio-Inspired Materials and Synthesis, Material Science	Institute for Materials Science			

The work program set out in **project A5** includes comprehensive research on the preparation of samples made of various polymer templates and metal oxides in order to establish template-based methods for the synthesis of structured mesoporous hybrid or pure inorganic materials with tunable pore diameter. A self-organization of polymer nanoparticles in colloidal crystals will be performed applying different assembly techniques. In addition, organic molecules have to be attached in controllable way on flat and porous materials. The realization of the work tasks and sample preparation will be accompanied by systematical characterization using diverse characterization techniques. The implementation of all these tasks shall be accomplished by Dr. Petia Atanasova as an expert in the field of nanostructuring of inorganic materials by making use of organic and bio-templates. She has comprehensive experience in chemical deposition techniques of inorganic materials, as well as fundamental knowledge in organic synthesis and surface structuring with organic templates. Furthermore, she was already involved in the DFG SPP 1569 (*Generation of multifunctional inorganic materials by molecular bionics*) and could demonstrate her outstanding scientific qualities and gained extensive experience in the field of hybrid materials.
Dr. Atanasova can profit from this CRC environment and is encouraged to develop her own research line, leading to scientific independence (for example through a potential Habilitation).

Job description of staff (supported through existing funds):
1
Research group leader, Principal investigator for **project A5**

Job description of staff (requested funds):
2
Senior Researcher, work packages 1-6
3
Research Assistants. **Justification:** A research assistant is required to support the lab work and to conduct already established mineralization reactions on flat and porous substrates for the systematical study of the mineralization behavior on the investigated polymer templates. Furthermore, the assistant shall be involved into the work on the assembly of polymer nanoparticles to colloidal crystals.

3.5.7.4 Requested funding of direct costs

	2018	2019	2020	2021	2022
Uni Stuttgart: existing funds from public budget	500.-	1,000.-	1,000.-	1,000.-	500.-
Sum of existing funds	500.-	1,000.-	1,000.-	1,000.-	500.-
Sum of requested funds	4,000.-	8,000.-	8,000.-	8,000.-	4,000.-

(All figures in EUR)

Consumables for financial year 2018

Chemicals, consumables, solvents, silicon wafers, AFM and SEM consumables	EUR	4,000.-

Consumables for financial year 2019

Chemicals, consumables, solvents, silicon wafers, AFM and SEM consumables	EUR	8,000.-

Consumables for financial year 2020

Chemicals, consumables, solvents, silicon wafers, AFM and SEM consumables	EUR	8,000.-

Consumables for financial year 2021

Chemicals, consumables, solvents, silicon wafers, AFM and SEM consumables	EUR	8,000.-

Consumables for financial year 2022

Chemicals, consumables, solvents, silicon wafers, AFM and SEM consumables	EUR	4,000.-

3.5.7.5 Requested funding for major research instrumentation
None

3.6 Project A6

3.6.1 General information about project A6

3.6.1.1 Carbon materials with tailored, selectively functionalized mesopores using organocatalytically derived polyethers

3.6.1.2 Research areas
Polymer Chemistry, Preparative and Physical Chemistry of Polymers (306-01)
Polymer Materials (306-03)

3.6.1.3 Principal investigator
Naumann, Stefan, Dr., born 16. 02. 1986, male, German
Institut für Polymerchemie
Universität Stuttgart, Pfaffenwaldring 55, 70569 Stuttgart
Tel.: 0711/685-64090
E-Mail: stefan.naumann@ipoc.uni-stuttgart.de
Habilitand, temporary contract (guaranteed for first funding period)

3.6.1.4 Legal issues
This project includes

1.	research on human subjects or human material.	no
2.	clinical trials.	no
3.	experiments involving vertebrates.	no
4.	experiments involving recombinant DNA.	no
5.	research involving human embryonic stem cells.	no
6.	research concerning the Convention on Biological Diversity.	no

3.6.2 Summary
Novel organocatalysts, so-called *N*-heterocyclic olefins (NHOs), will be employed for the highly controlled synthesis (polydispersity ($Đ_M$) <1.10) of ABA- and BAB-type block-*co*-polyethers (A = poly(ethylene oxide), B = poly(propylene oxide)), with preference for the latter ("*reverse Pluronics*"). This provides access to a library of defined, amphiphilic polymers with subtly different PPO-block length; systematically graded polyethers like these are not commercially available. By way of a fully organic self-assembly process with subsequent cross-linking and carbonization, mesoporous carbon materials will be received. Importantly, this project intends to tightly control the pore size by manipulation of a single parameter, namely the length of the lipophilic PPO block. Since metal-free, NHO-mediated polymerization of PO can be precisely tuned, it is desired to translate this control into the ability to tailor the mesopore size in an equally defined manner. Replications of the same carbon material with the same pore properties will then be functionalized (surface hydroxylation) to different degrees. This will change polarity and wettability in a systematic manner and allow for independent investigation of pore size and pore wall polarity; both parameters have been identified as crucial for this research initiative. For the first funding period, the targeted pore topology is to be long, cylindrical, isolated channels (hexagonal-columnar morphology, space group: *p6mm*) with uniform pore sizes in the range of 2-10 nm (diameter). As a final step, "clickable" functionalities will be selectively introduced inside the mesopores of the carbon material, following established procedures based on polymeric reagents.

3.6.3 Research rationale

3.6.3.1 Current state of understanding and preliminary work
Following a lively research activity, porous carbon materials nowadays have gained enormous importance for many applications and are considered to be central to a number of key technologies; especially *ordered mesoporous carbons* (OMC, pore size 2-50 nm) have shown their true potential in areas as different as sea water desalination, sensory applications, heavy metal adsorption, catalysts supports or electrode materials.[1-4] This broad applicability is the result of several beneficial properties

of OMCs, most prominently their low density in combination with a high surface area (500-1500 m^2/g), a tunable morphology, conductivity, manifold opportunities to functionalize the surface and, crucially, the possibility to prepare material with different pore sizes and –geometries.[5-6]
These fundamental characteristics evidently recommend OMCs as support materials for this CRC. In this context, it is of special relevance that (i) OMCs can be outfitted with different pore types (isolated cylindrical pores, interconnected channel networks, “ink bottles”, hierarchies), (ii) the very nature of the carbonaceous pore walls allows for many ways to functionalize them or change their polarity (hydroxylation in this project, but typical examples are also sulfonation, halogenation, N-, B-, P-doping…), (iii) they are inherently conductive (of interest for further funding periods) (iv) OMCs are tolerant to commonly employed solvents in catalysis and not prone to swelling, nor is there any thermal lability to be feared (in contrast to polymeric materials) (v) mechanic stability and a relative chemical inertness render OMCs suitable supports for a range of catalytic reactions. In the course of this project, these advantageous properties will be extended to also include (vi) a direct method to influence pore sizes (so far only indirect, process-related approaches exist) (vii) size and polarity of the pores can be investigated independently and (viii) the preparation of these OMC materials derived from tailor-made polyethers on the gram scale.
So-called “hard templating” has long been the dominant, most frequently applied method for structure-directed design of mesoporous carbon materials.[7-10] Typically, a mesoporous silica-based matrix first has to be constructed. Subsequently, this structure is filled with carbon precursor material, before this is being thermally polymerized and then carbonized. Finally, the silica is etched away (i.e., using hydrofluoric acid). Hard templating has been immensely successful and reliably delivers OMC. However, from above short description it is clear that up-scaling might be challenging, on account of the non-trivial multi-step setup and the unattractive etching process. Contrasting that, the relatively new “soft templating” (Fig. A6-1) approach according to Zhao and Dai,[11-14] exploits the self-organization of amphiphilic block-copolymers[15-16] in solution which results in supramolecular, ordered structures; these are infiltrated with cross-linkable monomers, which are subsequently thermally polymerized, followed by carbonization. Hence, this type of soft-templating employs established polymers plus a process cascade which essentially only depends on thermal steps, eliminates any etching and overall leads to a material with thicker pore wall (higher mechanic stability, less likelihood that micropores connect the cylindrical mesopores in the OMC with space group *p6mm*) and achieves an excellent degree of uniformity regarding pore properties.

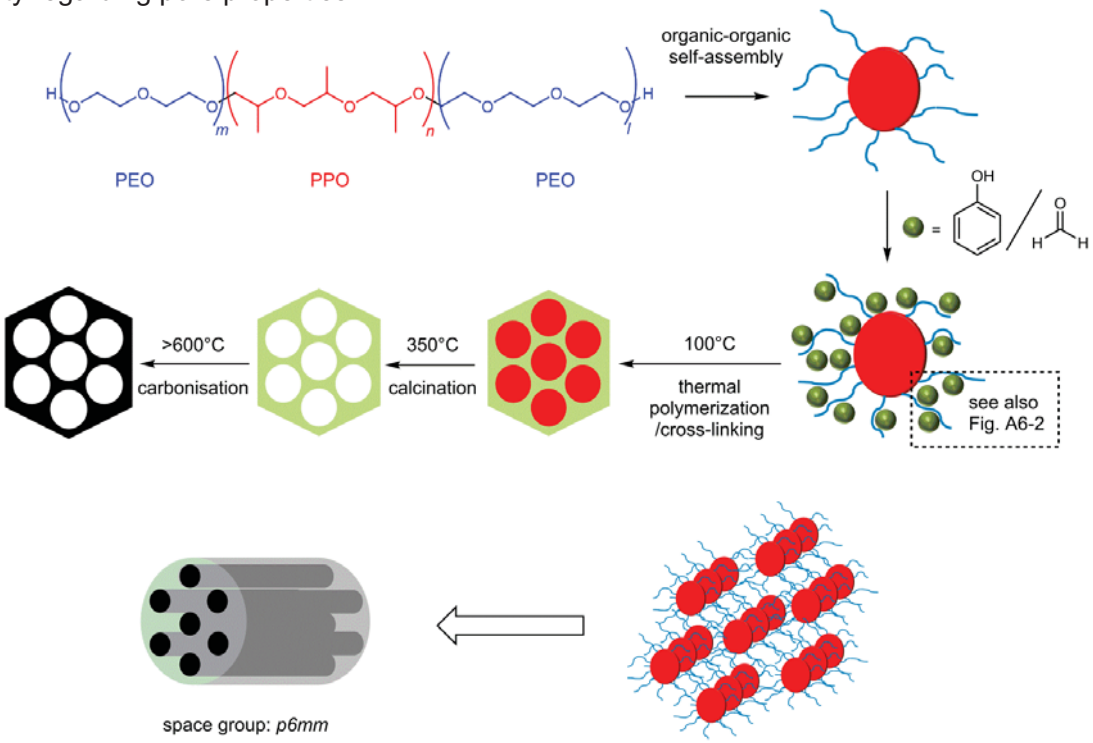

Figure A6-1. Schematic representation of the soft-templating approach based on ABA-type block-copolyethers and phenolic resins. Depending on a number of factors (size of the lipophilic PPO-unit, ratio of PO/EO, concentration,…), different pore sizes and morphologies (2D hexagonal in this case) can be realized.

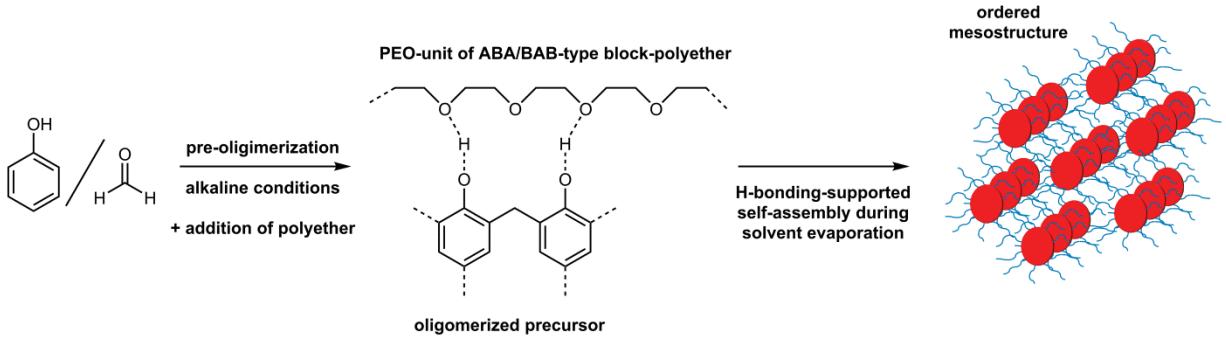

Figure A6-2. The self-assembly process of the amphiphilic polymer is both supported and influenced by H-bonding to the precursor. Thermosetting of the phenolic resin generates a robust matrix for carbonization.

Obviously, the structure-directing agent - in this case the amphiphilic polyether - is of crucial importance for the properties of the resultant OMC. One of the most user-friendly advantages of the block-copolyether-based templating strategies is that these polymers are well established: ethylene oxide/propylene oxide (EO/PO) triblock-copolymers can be used as lubricants or surfactants, the properties of which can be tuned by variation of the respective block sizes.[17] Consequently, commercially available (for example "*Pluronics*" by BASF: *F127* (*M*n = 12600 g/mol, PEO_{200}-PPO_{65}-PEO_{200}) or *L64* (*M*n = 2900 g/mol, PEO_{26}-PPO*30*-PEO_{26})) polymer can be employed as the base of OMC construction, further underlining the operationally simple and scalable character of this process. Depending on the ratio of hydrophilic EO and lipophilic PO in the macromolecule (and the ratio of template to crosslinking agents), different morphologies such as $Im\bar{3}m$ (body-centered cubic), $p6mm$ (2D-hexagonal) or $Ia\bar{3}d$ (3D-bicontinuous) can be generated.[5,18] These different pore topologies offer intriguing opportunities regarding the "enzyme-like" behavior that is envisioned for the interplay of catalysts and the mesoporous support in this CRC. For example, $Im\bar{3}m$ offers cage-like pores arranged in a body-centered cubic order, whereby the cages are connected by narrow mouths. $Ia\bar{3}d$, in contrast, contains congruent and interwoven but separate mesopore channel systems (gyroidal mesostructure). Hexagonal morphologies (Fig. A6-1) contain long, cylindrical pores which crucially are isolated and represent the simplest mesostructure for OMCs useful in this context. In the first funding period, this project will focus only on this latter topology; this should concentrate the work load on the primary goals during this phase, namely to gain full control over pore diameters and pore wall polarity as well as the subsequent pore-selective functionalization. Equally, for the initial phases of the catalytic transformations targeted in this CRC (B Section), the simpler pore types might be beneficial. Nonetheless, once all these parameters have been established, the vision to change catalytic profiles alongside the pore connectivity remains an appealing prospect for later funding periods and underlines the general suitability of OMCs for this kind of research.

Pore size control, in contrast, is much less straightforward. Apart from the polymer properties, the cross-linking conditions of the phenolic matrix and the thermal treatment (carbonization) all have impact on pore size and size distribution. Since the synthesis of polyethers is not trivial[17,19-20] (see discussion below) and further aggravated if narrow molecular weight distributions and more complex architectures, such as triblocks, are desired, the overwhelming majority of publications has resorted to the commercial polymer. Obviously, the different available polyethers can be converted into OMC with different pore sizes; but to gain a more subtle influence, which will be necessary to enable targeted pore design, so far only indirect measures have been employed with limited success. These approaches aim to impact pore generation indirectly by changing the reaction conditions or the subsequent heat treatment steps. This works, but only roughly. For example, it was reported that the carbonization temperature can be employed to manipulate the pore size.[5] Also, it was found that the pore size is influenced by the ratio of formaldehyde (cross-linking agent for the phenolic resin) to surfactant, as a consequence of the high degree of interaction of the polar reagents and the PEO-block (Fig. A6-2).[21] While both methods have their merits and again highlight that the resulting porosity of OMCs depends in principle on multiple parameters, they are also severely limited. While it is very challenging to control a carbonization process to such a degree that only a desired pore size results, extended heating times –especially at higher temperature – induce significant microporosity. And of course, pore sizes cannot be imposed at will; the range accessible by advanced carbonization setups is still pre-determined by the OMC precursor. Similarly, the approach to tailor the mesopores by variation of the cross-linker content (and

hence also the thermosetting kinetics) relies on capacious trial-and-error investigations; moreover, the parameters established would be different for each type of variation in polymer structure and thus not generally applicable. Physical and chemical constraints have to be considered too: the ratio of formaldehyde to block-copolymer cannot be varied freely, because this may change morphology rather than pore size (see above), or ensue incomplete cross-linking or different cross-linking densities (as a result of different aldehyde/phenol ratios). The application of swelling agents/co-surfactants (*n*-butanol, 1,3,5-trimethylbenzene, tetraethoxysilane, sodium dodecyl sulfate) is another way to influence pore evolution, though this is mainly used to alter morphology rather than specifically the pore sizes.[22-25]
In contrast, in this project it is proposed to tailor pore sizes more directly by rational design of the underlying block-copolyether structures. Specifically, exact control over the lipophilic (PO-derived) block sizes will be used to create a library of triblock-copolymers with systematic, finely graded variations (for example, PO_{35}-EO_{180}-PO_{35}, PO_{40}-EO_{180}-PO_{40}, PO_{45}-EO_{180}-PO_{45},…). During self-assembly, this will result in differently sized micellar structures (see Fig. A6-1), which will ultimately be translated into different pore sizes of the OMC. For this to succeed, a powerful catalytic system is needed, but also strictly uniform reaction conditions. The former requirement will be met with a novel organocatalytic concept developed by the applicant (see below), while the latter must ensure that all other parameters which can influence pore sizes (cross-linking setup, carbonization) are kept constant. **In the end, a system is envisioned where the desired pore size of the material can be rationally pre-determined simply by application of suitable polyethers, derived from a solvent- and metal-free catalytic process.** The detailed nature of the dependence of pore size on PPO-block size will be elucidated during these studies; one of the more obvious questions is whether a relatively "linear" correlation can be found, or whether other factors play a role.[18] The systematic variation of block sizes can be described by a change in the hydrophilic/hydrophobic volume ratio of the polymer (V_H/V_L), a well-known parameter that is usually employed for non-ionic surfactants to predict morphologies.[26] In general, more polar structure-directing block-copolymers (F108, F127) are able to realize structures with high curvature (cage-like cubic morphologies), while polymer with lower V_H/V_L-ratio (P123) entails the formation of phases with lower curvature (such as 2D hexagonal).[27] Equally, the hydrophilic-lipophilic-balance (HLB) is a similar tool frequently employed to characterize non-ionic surfactants.[28] It is readily calculated from the molar masses (eq. 1, ranging from 0-20 by definition, 0 = fully lipophilic, 20 = fully hydrophilic, M_H = molecular weight of the hydrophilic block(s)). Although it can be employed as a quick and convenient classification for the copolyethers used in this project, the parameter as such does not allow for predicting pore sizes or morphologies without further context (it disregards the overall molecular weight as well as polymer architecture for example).[29]

$$\mathrm{HLB} = 20 * \frac{M_\mathrm{H}}{M_\mathrm{total}} \qquad \text{(eq. 1)}$$

Although a deeper understanding is currently lacking, encouraging findings broadly support the emphasis of this project: it has been shown that for ABA-type polyethers the pore size of the resulting OMCs increases with the molecular weight of the lipophilic block (polybutylene oxide in this case), and *not* with the *overall* molecular weight of the copolymers.[30] In a broader picture, typical, spherical ABA-micelles contain 15-60 chains, resulting in diameters of 6-10 nm. Triblock-copolyether based precursor systems enable the preparation of OMCs with pore sizes between about 2-20 nm, with the majority of examples between 2-10 nm.[31]
Additionally, the above described method will enable a highly resolved understanding of just exactly where the limits of lipophilic/hydrophilic ratios are, at which changes in morphology occur (for example, transition from $p6mm$ to $Im\bar{3}m$ space group). As a final aspect, it will be possible to further elucidate the differences between ABA- and BAB-type copolyethers (A = PEO, B = PPO). Both will be part of the synthetic scheme (see work package 1, chapter 3.6.4.1), but preference will be given to BAB-type structures.[32-35] Albeit the majority of work on OMCs derived from soft-templating has focused on the more easily available ABA-type counterparts, BAB-type directing agents offer a number of interesting properties: (i) under the synthetic process proposed in this project, their preparation can be simplified to a convenient single-step procedure, covering the whole range of practicable EO/PO ratios; (ii) they offer access to morphologies which cannot be realized with the more common ABA-polymers (face-centered 3D-cubic $Fd\bar{3}m$);[36] (iii) they are typically considered to be chemically more stable (secondary alcohol as end group vs. primary alcohol). The main issue for application of BAB co-polyethers so far has been the formation of micellar networks, where the same polymer chain connects two micelles via its two PPO termini.[37] This obviously cannot happen for ABA-type polymer (compare Fig. A6-1) and

can prohibit the formation of ordered mesostructures. However, these difficulties can be circumvented by appropriate tailoring of the polymer structure; for PPO-PEO-PPO polymer with a long central PEO unit the generation of highly ordered structures such as $Fd\bar{3}m$ or $p6mm$ (hexagonal) is possible.[36] Consequently, well-defined OMCs on basis of these "reverse Pluronics" have been described recently, underlining the general feasibility of the proposed project.[21,38]
A subsequent, equally important part will be functionalization of the resulting OMC materials, with special emphasis on influencing the polarity/wettability in a systematic manner and secondly to achieve pore-selective functionalization (different functional groups within and outside the pores). Fortunately, carbon materials can be readily modified in a number of ways.[6] Most relevant here is hydroxylation of the surface, which can be realized by application of suitable oxidation agents. Excessive oxidation is to be avoided, since this usually leads to additional micropores, reduced mechanical stability and a mixture of different functional groups on the surface (-OH, -COOH, C=O, (C=O)OR,…). Apart from reaction conditions, also the type of oxidation agent controls the chemical nature of the oxidation products. Among the plethora of possible candidates for this, especially (diluted) hypochlorite solution seems promising, as the oxidative strength can be conveniently controlled by simple factors such as concentration, temperature and reaction time.[6, 39] Overall, mild conditions will be favored, which nonetheless requires a thorough characterization of the material before and after oxidation (pore size, total surface, density, type of functional groups and their concentration). If necessary, suitable post-treatment will be conducted to ensure that the introduced functional groups are selectively present as hydroxyl groups (see work package 3, chapter 3.6.4.3).[40] Taken together, the pore size control resulting from the triblock-copolyethers and a systematic variation of the degree of hydroxylation will allow for independent investigation of both parameters (Fig. A6-3); at the same time cooperative effects or "ideal" conditions may be revealed when these surface-functionalized OMCs are employed in the as catalyst support in **project B1** of this CRC.

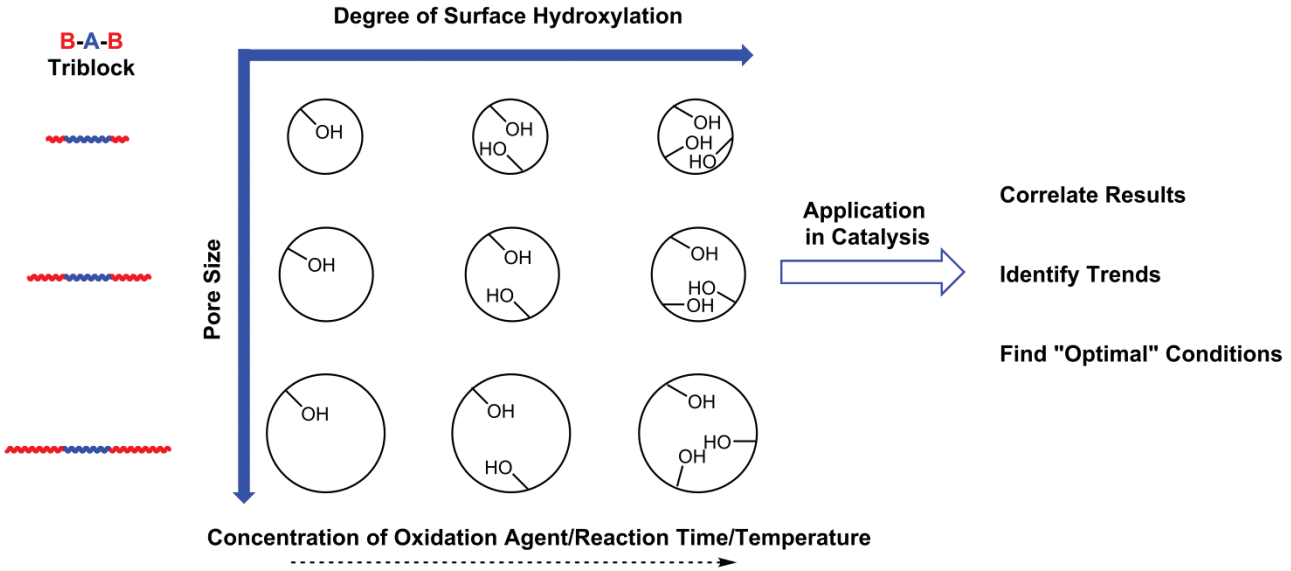

Figure A6-3. Simplified representation of the material matrix resulting from independent variation of the parameters "pore size" and "surface polarity". The different pore sizes are induced by application of suitably manipulated triblock-copolyethers, while the extent of hydroxylation is controlled by the nature of the oxidating agent and reaction conditions. After introduction of anchoring groups, these materials will be provided to **project B1** in order to to study the interplay of confinement and pore polarity. For catalytic reactions, it may well be expected that different combinations of size and surface properties will be best suited in each individual case; hence the access to such a modular OMC material will facilitate the identification of trends and optimized conditions.

As a final stage, pore-selective functionalization must be achieved, in order to provide anchoring sites for linker molecules; these will only be present inside the pores, but not outside. This is a necessary prerequisite if reliable investigation of confinement effects are intended, since even small amounts of "outside" catalysts may well distort the key parameters of a catalytic setup (TON, TOF, selectivity,…). Hydroxylation of the OMC in the previous step creates a surface which can be further modulated in manifold ways. One way to introduce anchoring sites is available by reaction with epoxide-bearing small organic molecules (i.e., epichlorohydrin). This will occur both on inner and outer surfaces, but subsequent treatment with a *macromolecular*[41-43] hydrolyzing agent as first described by Fréchet,[44] and since repeatedly applied successfully,[45] will ensure that the epoxide groups within the pores remain intact while those outside are hydrolyzed. The limiting physical property in this respect is the solvodynamic radius of the macromolecular reagent. If it is too large for pore penetration- which means, if polymer with suitably high molecular weight is employed- pore selective functionalization can succeed. The epoxides remaining inside the pores can then be ring-opened to provide the attachment sites for the linker chemistry. In this CRC, a modular concept based on Cu(I)-catalyzed click-chemistry has been developed, whereby the materials projects (Section A) provide suitable surface groups, while Section B attaches the catalysts and varies the linker length/stiffness. A convenient way to modify the OMCs in such a manner is to ring-open the epoxide using sodium azide or similar simple reagents. This final work package is discussed in section 3.6.4.4.

For preliminary work, the applicant recently established *N*-heterocyclic olefins (NHOs) as novel organocatalysts for polymerizations (DFG-funded, NA 1206-1).[A6-1,A6-2] NHOs contain a strongly polarized double bond which provides the exocyclic carbon with carbanion-like properties (Fig. A6-4). These characteristics have been shown to render NHOs stronger electron donors than *N*-heterocyclic carbenes (NHCs) and able to activate CO_2.[46-47] Additionally, NHOs possess excellent solubility and can be accessed in a modular and simple synthesis. The organocatalyst can be tailored by its ring structure and substituents, to specifically address desired polymerization pathways even for challenging monomer types. While saturated backbones decisively attenuate the reactivity, imidazolium-derived compounds display a remarkable activity. An illustrative example for this is provided by the metal-free polymerization of PO using NHOs. 2-Methylene-1,3,4,5-tetramethylimidazole (**1**), itself a very simple structure, can polymerize PO both along anionic and zwitterionic pathways (Fig. A6-5). By introduction of methyl groups on the exocyclic carbon (**2**), the zwitterionic mechanism is successfully suppressed and the polymerization proceeds exclusively via NHO-mediated anionic ROP. Importantly, this process is highly controlled, with end groups and molecular weights (1,000 – 12,000 g/mol) that are fully predictable ($Đ_M$ = 1.02-1.09), as attested by extensive NMR-, GPC- and MALDI-ToF MS-experiments. At the same time, the reaction is conducted under mild conditions (50°C) in a solvent- and metal-free manner, whereby transfer-to-monomer, one of the most frequent side reactions limiting the molecular weight of PPO, occurs only marginally. Hence, NHOs currently comprise the most effective organocatalytic system for the polymerization of the industrially relevant PO, to the best of the applicant's knowledge. Turn over numbers (TON) of > 2000 can be achieved with this setup, which constitutes a noteworthy performance for any organocatalytic system. Within this proposed project, these abilities will be employed to synthesize more complex polyethers, namely amphiphilic triblock-copolyethers for soft-templating to construct well-defined OMCs (see work packages). The properties of NHOs have recently been further elucidated by the applicant, which yielded deeper insight in their behavior regarding the polymerization of lactones, carbonates or acrylics, as well as their ligand properties.[A6-3, A6-4, A6-5, A6-6]

To be in optimal preparation for the CRC, direct preliminary work has also been conducted by the applicant. It was shown that by NHO catalysis BAB-type polyether could be prepared, forming varying lipophilic block lengths (PO_n-EO_{180}-PO_n, n = 20, 25, 40, 50, 66, 90…). Notably, the desired polymer was isolated without complicated work-up and received in high yield with excellent control (M_n up to 20 000 g/mol, $Đ_M \leq 1.03$). As proof of concept, these polymers were converted into mesoporous carbons using Zhao and Dai's[11-14] method. Characterization showed the material to be well-behaved with properties fully comparable to the literature (specific surface area up to 1000 m^2/g, 0.8 cm^3/g pore volume (N_2-sorption), average pore diameter in the range of 3-6 nm with monomodal and well-controlled size distribution, Fig. A6-6). Most notably, the size range for the PPO block length to result in *ordered* structures (under the given conditions) was also identified (ordered structure for n = 66, while for n = 50 or 90 disordered mesoporous carbons were formed).

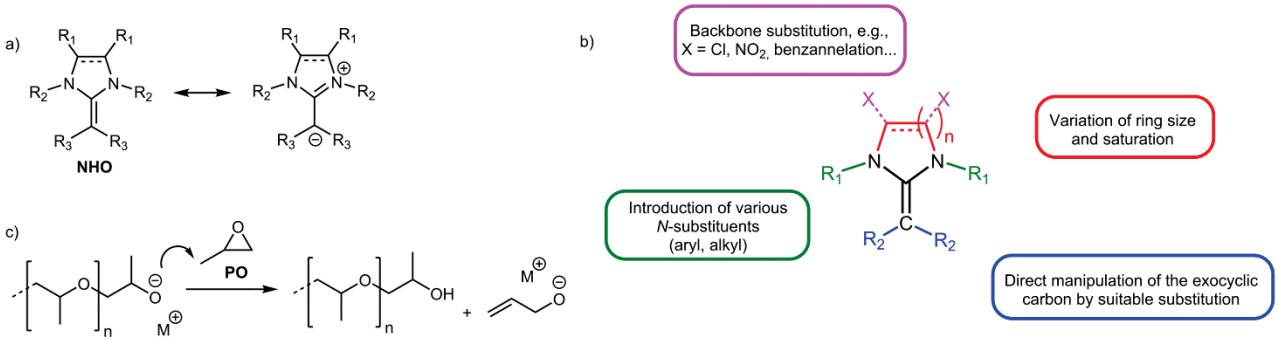

Figure A6-4. a) Mesomeric description of NHOs; b) modification strategies; c) transfer-to-monomer as major complication for PPO polymerization.

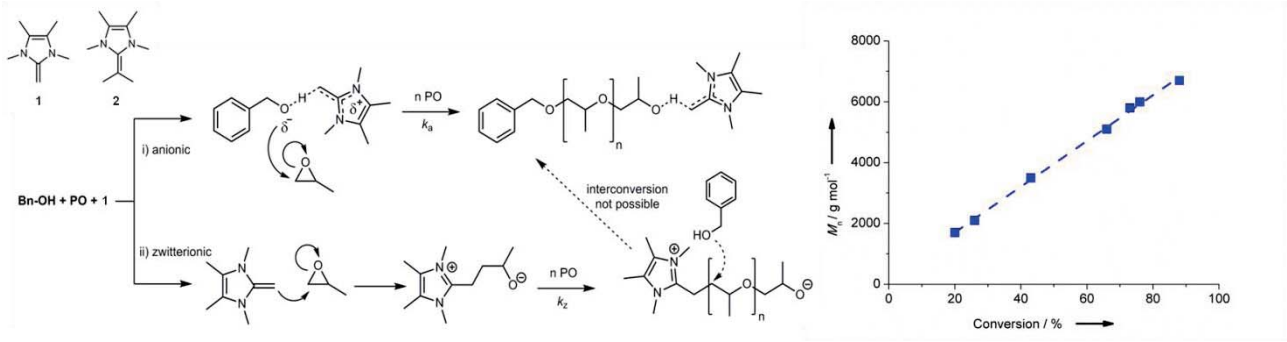

Figure A6-5. Metal- and solvent-free polymerization of PO by NHOs for well-defined polyether.

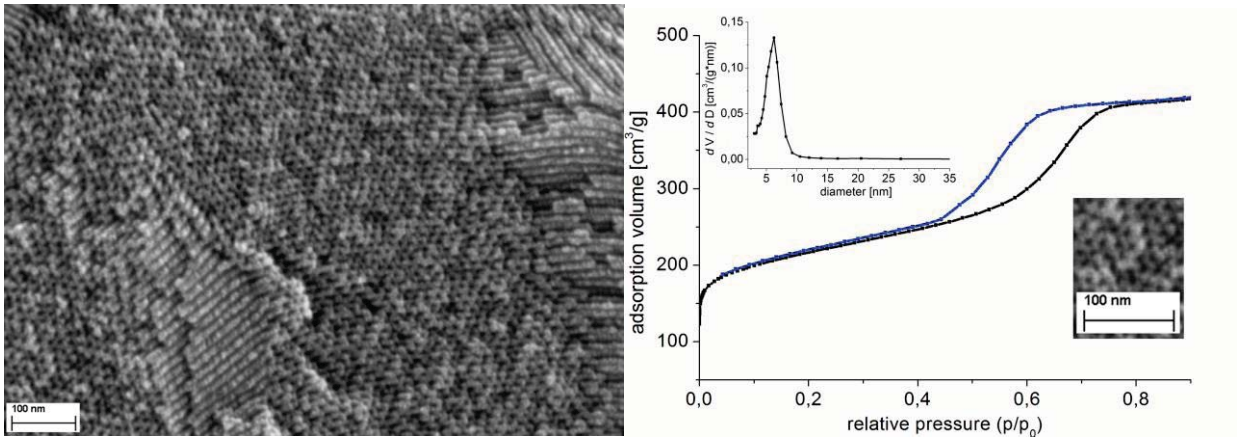

Figure A6-6. SEM recording of OMC based on PO_{66}-EO_{180}-PO_{66} and corresponding N_2 gas sorption results as prepared by the applicant's group.

References

[1] H. Chang, S. H. Joo, C. Pak, *J. Mater. Chem.* **2007**, *17*, 3078–3088.

[2] C. Liang, Z. Li, S. Dai, *Angew. Chem. Int. Ed.* **2008**, *47*, 3696–3717; *Angew. Chem.* **2008**, *120*, 3754-3776.

[3] T.-Y. Ma, L. Liu, Z.-Y. Yuan, *Chem. Soc. Rev.* **2013**, *42*, 3977–4003.

[4] W. Xin, Y. Song, *RSC Adv.* **2015**, *5*, 83239–83285.

[5] Y. Meng, D. Gu, F. Zhang, Y. Shi, L. Cheng, D. Feng, Z. Wu, Z. Chen, Y. Wan, A. Stein et al., *Chem. Mater.* **2006**, *18*, 4447-4464.

[6] A. Stein, Z. Wang, M. A. Fierke, *Adv. Mater.* **2009**, *21*, 265–293.

[7] N. D. Petkovich, A. Stein, *Chem. Soc. Rev.* **2013**, *42*, 3721–3739.

[8] J. Lee, J. Kim, T. Hyeon, *Adv. Mater.* **2006**, *18*, 2073-2094.

[9] Y. Xia, Z. Yang, R. Mokaya, *Nanoscale* **2010**, *2*, 639-659.
[10] W. Nickel, M. Oschatz, S. Rico-Francés, S. Klosz, T. Biemelt, G. Mondin, A. Eychmüller, J. Silvestre-Albero, S. Kaskel, *Chem. Eur. J.* **2015**, *21*, 14753-14757.
[11] F. Zhang, Y. Meng, D. Gu, Y. Yan, C. Yu, B. Tu, D. Zhao, *J. Am. Chem. Soc.* **2005**, *127*, 13508–13509.
[12] C. Liang, S. Dai, *J. Am. Chem. Soc.* **2006**, *128*, 5316–5317.
[13] X. Wang, C. Liang, S. Dai, *Langmuir* **2008**, *24*, 7500-7505.
[14] Y. Wan, Y. Shi, D. Zhao, *Chem. Mater.* **2008**, *20*, 932-945.
[15] S. Förster, M. Antonetti, *Adv. Mater.* **1998**, *10*, 195-217.
[16] N. Pal, A. Bhaumik, *Adv. Colloid Interface Sci.* **2013**, *189-190*, 21-41.
[17] J. Herzberger, K. Niederer, H. Pohlit, J. Seiwert, M. Worm, F. R. Wurm, H. Frey, *Chem. Rev.* **2016**, *116*, 2170–2243.
[18] See chapter 8.1 in D. Zhao, W. Zhou, Y. Wan, *Ordered Mesoporous Materials*, Wiley-VCH Verlag GmbH & Co. KGaA, Weinheim, **2013**.
[19] J. Raynaud, W. N. Ottou, Y. Gnanou, D. Taton, *Chem. Commun.* **2010**, *46*, 3203-3205.
[20] O. Rexin, R. Mülhaupt, *J. Polym. Sci. A Polym. Chem.* **2002**, *40*, 864-873.
[21] P. Li, Y. Song, Q. Guo, J. Shi, L. Liu, *Mat. Lett.* **2011**, *65*, 2130-2132.
[22] T.-W. Kim, F. Kleitz, B. Paul, R. Ryoo, *J. Am. Chem. Soc.* **2005**, *127*, 7601-7610.
[23] L. Wang, J. Fan, B. Tian, H. Yang, C. Yu, B. Tu, D. Zhao, *Microporous Mesoporous Mat.* **2004**, *67*, 135-141.
[24] Y. Q. Wang, C. M. Yang, B. Zibrowius, B. Spliethoff, M. Lindén, F. Schüth, *Chem. Mater.* **2003**, *15*, 5029-5035.
[25] D. Chen, Z. Li, C. Yu, Y. Shi, Z. Zhang, B. Tu, D. Zhao, *Chem. Mater.* **2005**, *17*, 3228-3234.
[26] J. M. Kim, Y. Sakamoto, Y. K. Hwang, Y.-U. Kwon, O. Terasaki, S.-E. Park, G. D. Stucky, *J. Phys. Chem. B* **2002**, *106*, 2552-2558.
[27] See chapter 3.3.4 in D. Zhao, W. Zhou, Y. Wan, *Ordered Mesoporous Materials*, Wiley-VCH Verlag GmbH & Co. KGaA, Weinheim, **2013**.
[28] W. C. Griffin, *J. Soc. Cosmetic Chem.* **1954**, *5*, 1-8.
[29] H. Schott, *J. Pharm. Sci.* **1995**, *84*, 1215-1222.
[30] C. Yu, J. Fan, B. Tian, G. D. Stucky, D. Zhao, *J. Phys. Chem. B* **2003**, *107*, 13368-13375.
[31] See chapter 2.9 in D. Zhao, W. Zhou, Y. Wan, *Ordered Mesoporous Materials*, Wiley-VCH Verlag GmbH & Co. KGaA, Weinheim, **2013**.
[32] J. Jang, J. Bae, *Chem. Commun.* **2005**, 1200-1202.
[33] Q. Wang, L. Li, S. Jiang, *Langmuir* **2005**, *21*, 9068-9075.
[34] Y. Huang, H. Cai, T. Yu, X. Sun, B. Tu, D. Zhao, *Chem. Asian J.* **2007**, *2*, 1282-1289.
[35] X. Qian, H. Li, Y. Wan, *Microporous Mesoporous Mat.* **2011**, *141*, 26-37.
[36] Y. Huang, H. Cai, T. Yu, F. Zhang, F. Zhang, Y. Meng, D. Gu, Y. Wan, X. Sun, B. Tu et al., *Angew. Chem. Int. Ed.* **2007**, *46*, 1089-1093; *Angew. Chem.* **2007**, *119*, 1107.
[37] K. Mortensen, W. Brown, E. Jorgensen, *Macromolecules* **1994**, *27*, 5654.
[38] P. Li, Y. Song, Q. Lin, J. Shi, L. Liu, L. He, H. Ye, Q. Guo, *Microporous Mesoporous Mat.* **2012**, *159*, 81.
[39] P. Vinke, M. van der Eijk, M. Verbree, A. F. Voskamp, H. van Bekkum, *Carbon* **1994**, *32*, 675–686.
[40] D. Yu, Z. Wang, N. S. Ergang, A. Stein, *Stud. Surf. Sci. Catal.* **2007**, *165*, 365.
[41] C. G. Overberger, K. N. Sannes, *Angew. Chem. Int. Ed.* **1974**, *13*, 99-104; *Angew. Chem.* **1974**, *86*, 139.
[42] P. H. Toy, K. D. Janda, *Acc. Chem. Res.* **2000**, *33*, 546-554.
[43] H. Salimi, A. Rahimi, A. Pourjavadi, *Monatsh. Chem.* **2007**, *138*, 363-379.
[44] V. Smigol, F. Svec, J. M. J. Fréchet, *Anal. Chem.* **1994**, *66*, 4308–4315.
[45] See for example: R. Bandari, T. Hoche, A. Prager, K. Dirnberger, M. R. Buchmeiser, *Chem. Eur. J.* **2010**, *16*, 4650–4658.
[46] A. Fürstner, M. Alcarazo, R. Goddard, C. W. Lehmann, *Angew. Chem. Int. Ed.* **2008**, *47*, 3210-3214; *Angew. Chem.* **2008**, *120*, 3254-3258.
[47] Y.-B. Wang, Y.-M. Wang, W.-Z. Zhang, X.-B. Lu, *J. Am. Chem. Soc.* **2013**, *135*, 11996-12003.

3.6.3.2 Project-related publications by participating researchers

[A6-1] S. Naumann*, A. W. Thomas, A. P. Dove*, *Angew. Chem. Int. Ed.* **2015**, *54*, 9550.

[A6-2] S. Naumann*, A. W. Thomas, A. P. Dove*, *ACS Macro Lett.* **2016**, *5*, 134.

[A6-3] S. Naumann*, D. Wang, *Macromolecules* **2016**, *49*, 8869.

[A6-4] D. A. Imbrich, W. Frey, S. Naumann*, M. R. Buchmeiser*, *Chem. Commun.* **2016**, *52*, 6099.

[A6-5] S. Naumann*, K. Mundsinger, L. Cavallo and L. Falivene*, *Polym. Chem.* **2017**, *8*, 5803.

[A6-6] P. Walther, S. Naumann*, *Macromolecules* **2017**, 50, 8406-8416.

3.6.4 Project plan

In summary, the research goals are organized in work-packages as follows:

- **WP1. Goal: Preparation of a library of ABA/BAB copolyethers using NHO organocatalysis.** The overall ratio of lipophilic/hydrophilic units as well as the block lengths will be varied in a systematic manner. Optimization of the polymerization conditions and characterization of the resulting polymer using standard techniques (NMR, MALDI-ToF MS, GPC). Investigation of micelle formation ((depolarized) dynamic light scattering, SAXS).
- **WP2. Goal: Synthesis of OMCs, based on the triblock copolymers as structure directing agents. The thus created set of carbon materials will display uniform, systematically varied pore sizes.** An organic **self-assembly process** will be used; depending on the desired macroscopic properties, the cross-linking and separation of mesostructured precursors will proceed via the **EISA-technique** (evaporation induced self-assembly, films) or by precipitation from watery solution (powder). Subsequent heat treatment (carbonization) will then deliver the OMC. Based on extensive characterization (especially N_2-adsoprtion, IR, advanced microscopy), it will then be possible to directly **correlate** the influence of the precursor polymer on the pore properties of the resulting carbon material. To limit the number of potentially interfering parameters, the synthesis route will be optimized and then be applied for all materials in strictly the same manner (especially the cross-linking process, but also the heating program, reagent concentration, reaction time).
- **WP3. Goal: Surface hydroxylation of the OMCs, with variations of the degree of functionalization.** The pristine OMCs, which have a largely (but not exclusively) non-polar, carbonaceous surface, will be functionalized by hydroxylation. This is to be achieved by relatively **mild oxidation agents** (diluted solutions of hypochlorite), whereby the degree of hydroxylation is to be controlled by simple factors like reaction time and reagent concentration. Here again, a systematic variation of this property is desired (compare Fig. A6-3). While it cannot be expected that central parameters of the mesoporous material will remain completely unchanged by this process, the surface modification must be conducted in a way which avoids the introduction of additional microporosity. To ensure that, again robust characterization is necessary, both to **quantify hydroxylation** (IR, solid state NMR) and to gauge the change in porosity (gas adsorption techniques -> pore volume, pore size, size distribution).
- **WP4. Goal: Introduction of anchoring sites exclusively inside the pores.** The functionality of choice will be the **epoxide group**; it can be ring-opened by nucleophilic linker molecules. Reaction of a suitable epoxy compound (epichlorohydrin or derivatives) with the hydroxylated surface will yield a non-discriminate distribution of epoxy groups on inner and outer surfaces. Subsequent application of a **macromolecular hydrolysis agent** (poly(styrene sulfonic acid)) then leaves only those epoxy groups intact which have been protected by being positioned inside a pore. The selectively positioned epoxides will subsequently be ring-opened in such as manner as to allow for click-chemistry (azide/alkyne). As with all steps before, a **thorough characterization** of the resulting material is crucial to verify the presence of epoxy groups specifically inside pores. This is best achieved by a combination of several methods, including gas adsorption, IR, solid state NMR, XRD or the more explorative characterization methods as envisioned in this CRC (such as **project C3**). The thus prepared materials will then be provided for catalysis experiments.

3.6.4.1 WP1: Preparation of a library of ABA/BAB copolyethers using NHO organocatalysis. In the initial phase of the proposed project, the required block-copolyethers will be synthesized. To achieve this, NHO-organocatalysis will be employed. After the synthesis of a suitable catalyst like compound **2**, which is accessible in few steps from simple starting chemicals, two parallel approaches will be evaluated (Fig. A6-7). On the one hand, this will encompass the preparation of ABA-type polymers; secondly, the reverse analogues with BAB-structure will be investigated. As briefly outlined above, there is a wealth of published data regarding the conversion of ABA polymers into OMC, but their synthesis will require two consecutive steps under the proposed scheme (Fig. A6-7b). Contrasting that, "reverse Pluronics" have been much less investigated but they will be accessible in a single, operationally simple process when NHO organocatalysis is used. Both types of structure-directing polymers will in the end deliver OMC, so in principle it would be justified to follow only one approach. However, if both pathways are focused on, this will not only act as a potential fail-safe, but also shed light on a number of interesting, as yet unanswered questions: the non-trivial differences of ABA/BAB structures with regard to their self-organization (micellar organization versus micellar networks, for example) will render a direct comparison of polymer structure and resulting OMC properties for both approaches highly interesting. Potentially, this could reveal what ratio of hydrophilic/hydrophobic units in both structures results in comparable pores size; how lipophilic PPO termini influence self-assembly compared to hydrophilic PEO termini for various sequence lengths; how relative block sizes exert their influence in both cases and whether molecular weight shows a different correlation with the resulting OMC porosity for ABA- or BAB-type, respectively.
Specifically, for PEO-terminated polymer (ABA), the preparation will start from a difunctional initiator (such as 1,4-butanediol), onto which PPO is grown. This process is critical, since for most types of anionic polymerization the reaction is prone to transfer-to-monomer as side reaction,[17,19-20,48] which not only broadens and severely limits the molecular weight, but also results in allyl-terminated PPO, which obviously cannot serve any more for further preparation of triblocks. It also cannot be separated from the desired α,ω-OH terminated material. Fortunately, NHO-mediated catalysis suppresses this side reaction satisfyingly and allows for molecular weights which are more than sufficient for suitable central PPO-units in the prospective ABA-polymer. Nonetheless, the prepared PPO will be thoroughly characterized by GPC, MALDI-ToF and NMR. In combination, these methods will reliably attest to the quality of the polymer and its end groups. The PPO will then be reacted with EO, a gaseous monomer at room temperature, using the same reaction conditions (NHO **2**, no solvent, slightly elevated temperature, pressure tubes). ABA polymers with subtly different chain lengths and block sizes, varied in a systematic manner, will be targeted. This will include variation of the PPO core while keeping the PEO termini constant, and vice versa. Conducting the polymerizations in a controlled manner is all important for success of this strategy, with a target dispersity of molecular weights (PDI) of < 1.1; the general feasibility of these ambitions via NHO catalysis and the preliminary work has already been described (chapter 3.6.3.1).

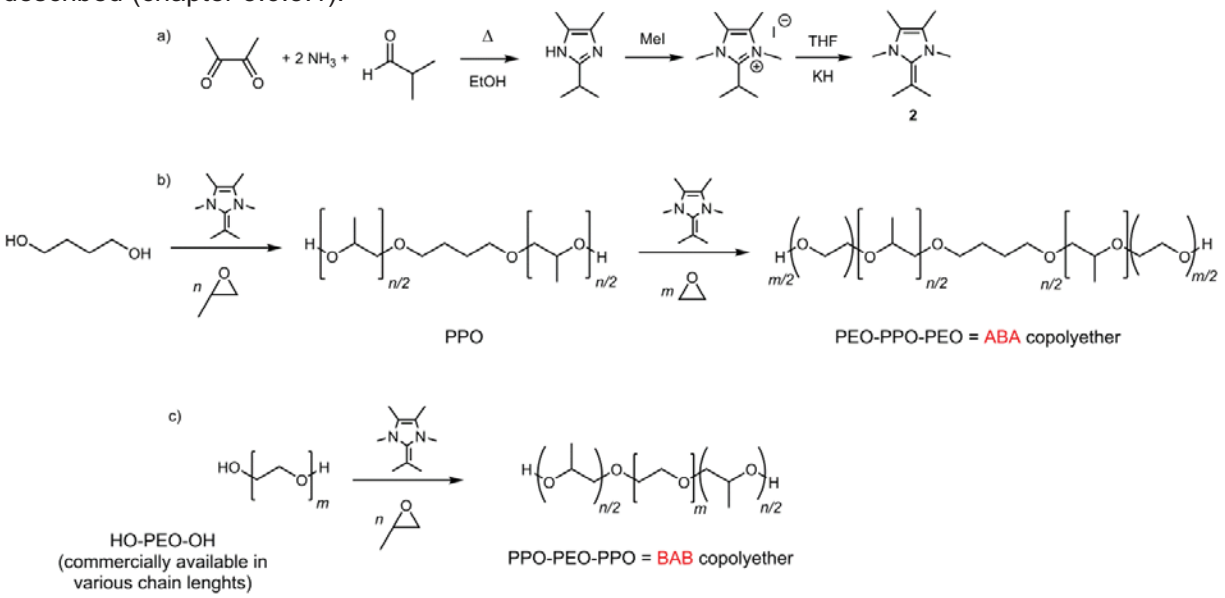

Figure A6-7. Schematic synthesis of a suitable NHO-catalyst for PPO preparation (a), and strategies for generation of ABA- (two steps, b) and BAB-triblocks (single step, c).

Complementing these efforts, the corresponding BAB structures will be prepared (Fig. A6-7c). In this case, readily available dihydroxy-terminated PEG (which is typically available in a range of 400 - 20 000 g/mol ($Đ_M$<1.1)) will be employed as macroinitiator. After scrupulous drying of the educt polymer (PEG is hygroscopic and must be expected to contain considerable amounts of water), it will be used with PO, again using similar reaction conditions and the same catalyst. While WP1 will remain active throughout the funding period, responding to insights won from WPs 2-4 and other projects of this research initiative, initial experiments will focus on BAB-type structures with relatively long central PEO blocks (150-250 repeating units; molecular weight roughly 6 000 – 12 000 g/mol). This reduces the curving energy for either backfolding of the chain to occur,[18] forming micelles when sufficiently dilute setups are employed, or to generate ordered micellar networks (two micelles connected by one polymer chain via its two PPO termini).[37]
Table A6-1 lists some examples for polymer constitutions that will be synthesized initially. These are based on successful precedence from literature, namely Pluronic P123 (EO_{20}-PO_{70}-EO_{20}, M_w = 5.8 kDa) and Pluronic F127 (EO_{106}-PO_{70}-EO_{106}, M_w = 12.6 kDa) for the ABA structures and PO_{97}-EO_{186}-PO_{97} (M_w = 19.5 kDa) for the BAB-type reverse analogues. Notably, under identical conditions (2D-hexagonal, 800°C carbonization) for the former two examples average pore sizes (N_2 sorption) of 3.1 nm and 2.6 nm have been found, clearly underlining that the correlation of polymer constitution with OMC properties urgently needs clarification.[5] The latter polymer has been converted into an OMC with 3.9 nm and 3.5 nm average pore size (2D-hexagonal, different polymer concentration), but also 3-12 nm ($Fd\bar{3}m$, multimodal).[38] The examples given in Table A6-1 illustrate the three systematic tuning approaches: Variation of the hydrophilic block(s) while the lipophilic one is kept constant and vice versa (for both ABA and BAB-type polymer), as well as a constant hydrophilic-lipophilic balance (HLB) while the overall molecular weight is varied. The latter is especially suited if a change in the micelle templates is to be avoided.
Micelle formation will be studied in cooperation with **project A7** using both static (SLS) and dynamic light scattering (DLS). This is not only intended to deliver basic information such as critical micelle concentration (CMC), critical micelle temperature (CMT) or the average size of the micelles in water (necessary for comparison with standard Pluronics), but also for more elaborate investigations regarding the self-assembly (formation of cylinder-like structures, see 3.6.5). This cooperation is important as it helps to clarify whether the structure of the OMC and the template correlates well, or whether pore formation is rather dominated by processing (polymerization, carbonization).

Table A6-1. Initially targeted library of copolymers (examples) for OMC generation, including molecular weights and HLB parameters.

ABA	Molecular weight [g/mol], HLB	BAB[a)]	Molecular weight [g/mol], HLB
EO_{20}-PO_{70}-EO_{20}	5 900, 6.1	PO_{60}-EO_{90}-PO_{60}	11 000, 7.3
EO_{30}-PO_{70}-EO_{30}	6 700, 7.9	PO_{100}-EO_{90}-PO_{100}	15 600, 5.1
EO_{40}-PO_{70}-EO_{40}	7 600, 9.3	PO_{130}-EO_{90}-PO_{130}	19 100, 4.2
…		…	
EO_{20}-PO_{60}-EO_{20}	5 300, 6.7	PO_{60}-EO_{180}-PO_{60}	14 900, 10.7
EO_{20}-PO_{90}-EO_{20}	7 000, 5.0	PO_{100}-EO_{180}-PO_{100}	19 600, 8.1
EO_{20}-PO_{120}-EO_{20}	8 800, 4.0	PO_{130}-EO_{180}-PO_{130}	23 100, 6.9
…		…	
EO_{100}-PO_{70}-EO_{100}	12 900, 13.7	PO_{55}-EO_{125}-PO_{55}	11 900, 9.3
EO_{110}-PO_{77}-EO_{110}	14 200, 13.7	PO_{100}-EO_{230}-PO_{100}	21 700, 9.3
EO_{130}-PO_{90}-EO_{130}	16 700, 13.7	PO_{135}-EO_{310}-PO_{135}	29 300, 9.3
…		…	

a) Central PEO blocks for BAB-type polymers: EO_{90} = PEG 4000, EO_{180} = PEG 8000, EO_{230} = PEG 10 000.

3.6.4.2 WP2: Synthesis of OMCs. With the amphiphilic block-copolymers as structure directing agents at hand, these are employed in a self-assembly process to generate mesoscale-ordered structures in solution. This process itself is well-described in literature;[11-14,49] the principal rationale behind this project is to find and use generally applicable, identical conditions for the synthesis of OMC

for the different grades of triblock co-polyethers to finally create a setup where the decisive property – pore size (diameter) – mainly depends on a single parameter, namely the chemical structure of the underlying polymers. To this end, all other influences have to be kept constant or minimized. This not only includes the thermal processing, but also the impact of the surface (glass plate), solvent and temperature as well as cross-linking agent (phenol, resorcinol, phloroglucinol).[3,13,33] Consequently, these parameters will not be varied in a major sense and successful precedence from published procedures will be employed.[11-14] All these efforts are necessary to limit the variables and parameters influencing the system and obtain a meaningful correlation of polymer and resultant OMC properties. Additionally, for initial experiments only a single morphology will be targeted (hexagonal, *p6mm*) to vary the pore sizes. Since a given mesostructure is only stable in a certain window defined by parameters such as the HLB and the ratio of polymer to cross-linking agent, it must be considered that the copolymer composition can only be adjusted in a range, the limits of which have to be found experimentally.

Two different, but established techniques will be used for the synthesis. This is firstly the so-called EISA-process (Evaporation Induced Self-Assembly).[2-3,16] Thereby, the copolymer is homogenized with phenolic resol (= oligomerized resin from phenol and formaldehyde) under alkaline conditions in ethanol. The solution is then applied to glass plates, from which the solvent slowly and gently evaporates. During this time, self-assembly takes place, driven also by the H-bond forming between resol and PEO block (see Fig. A6-1 and A6-2). A subsequent thermal curing step (100°C, polymerization/crosslinking of the phenolic resin) then stabilizes the ordered phase. The received polymer is then converted into OMC via carbonization at elevated temperature; again, this process must be led in a generally identical manner for all samples (oven time and temperature) to standardize the impact of carbonization on pore properties. Typical conditions would be 1-2 hours at 800°C under inert gas. At such a setting, the resulting OMCs will display a marked weight loss (70% or more) as the non-crosslinked regions are burned off and heteroatoms are removed. However, while highly ordered carbon materials with well-defined mesopores are received, in this temperature regime the carbon material will still contain some impurities (mainly oxygen) and the carbon matrix should not be seen as a perfect “graphene-like” structure. Preparation of mesoporous polymers (low-temperature treatment (calcination) < 350°C) will not be part of this project.

As an alternative to EISA, the “aqueous” route will be employed.[3] Here again, the copolymer is combined with phenol(-derivatives) and formaldehyde in an alkaline environment, but this time with water as solvent. Stirring at progressing temperature (20°C, 60°C, 70°C) leads over time to a precipitate; this solid results from partially polymerized template structures, which are not soluble in water any more. Thermal treatment likewise converts these materials into OMC. While EISA is especially well suited to prepare films, the “aqueous route” is easier to scale up and directly delivers mesoporous powders. EISA takes hours to complete, while the alternative process may take up to several days of reaction time.

Finally, these efforts are intended to provide a number of OMCs with uniform pore sizes, each material with finely graded differences to each other regarding pore size (while retaining the same 2D hexagonal morphology).

Once the OMCs have been prepared, a reliable and thorough characterization is of central importance (see also “Methods applied”, chapter 3.6.4.5). Special emphasis will be put on determination of pore sizes and their size distribution by N_2-adsorption isotherm measurements, flanked by additional data derived from elemental analysis, X-ray diffraction (XRD), infrared, optical investigation (electron microscopy with EDX) and conductivity measurements. XRD data will thereby reveal morphology and, less trivial, information on pore-to-pore distances. Electron microscopy can also yield details about structure, regularity and pore sizes. Elemental analysis and conductivity measurements provide a convenient handle to assess the degree of carbonization.

3.6.4.3 WP 3: Surface hydroxylation of the OMCs for systematically altered surface polarity. OMC can be functionalized in multiple ways; of these, oxidation is a rather fundamental, frequently applied operation.[6,50] A number of different functionalities can be introduced on the carbon surface, depending on the oxidation agent (air, oxygen, ozone, H_2O_2, hypochlorite solutions, nitric acid…). Also, the OMC received after the previous carbonization process must be expected to still contain considerable amounts of heteroatoms, mainly oxygen, since the heating program may not include very high temperatures and/or long oven times because of potential degradation and micropore generation. From this, three requirements follow: i) mild oxidation processes must be used; ii) reliable, detailed characterization is necessary; iii) post-treatment to convert all functionalities into hydroxyl groups may be beneficial.
As briefly outlined above, it is necessary to employ less aggressive oxidation settings and to control the degree of surface manipulation. This can be achieved by application of diluted hypochlorite solution and be systematically varied via reaction time. While the process can be lead in a way which strongly favors hydroxylation, non-desired functionalities (keto-, ester-, carboxyl-groups) must be spotted by suitable spectroscopy and eliminated. The preferred method to ensure this will be reduction with BH_3*THF, which back-converts overly oxidized sites into –OH (Fig. A6-8).[40,51] Obviously, again meaningful characterization is mandatory: a combination of methods (N_2-sorption, electron microscopy, IR, Raman) will show how oxidation has altered the material and surface properties and whether undesired degradation occurred. The chemical constitution of the external surface can be investigated with XPS analysis, for example to find oxygen. Electrochemical techniques will also be applicable in this case (cyclic voltammetry), especially since the redox properties of various oxygen surface species can be spotted and factors like the capacitance are markedly influenced by the presence of heteroatoms.[52] Another routinely employed method is TPD (temperature-programmed desorption, using a DSC-TGA MS setup), relying on the fact that different surface functional groups decompose in defined temperature ranges to produce volatile compounds as side products (H_2O, CO, CO_2). For example, carboxyl groups on a carbon surface decompose at much lower temperatures than hydroxyl groups, displaying a characteristic CO_2-peak.[6,48] Hence, by a combination of the methods mentioned above the purity and degree of hydroxylation can be verified. IR can be employed to quickly assess the degree of hydroxylation relative to the pristine OMC; for a more reliable *quantification* DSC-TGA MS and XPS are suitable. Notably, application of 2,2,2-trifluoroacetic anhydride (TFAA) allows for a selective and efficient chemical derivatization of hydroxyl groups on carbon black and carbon nanotubes.[53-54] This gives XPS analysis another handle to assess whether oxygen species are truly present as hydroxyl functionality. Furthermore, this way a highly NMR-sensitive nucleus is introduced, enabling the application of solid state NMR techniques (**project C1**) which would otherwise be hampered by a low signal-to-noise ratio (see also next work package). By combining DSC-TGA MS, XPS and, within limits, solid state NMR well-funded information about the –OH density (OH/nm^2) will be available.

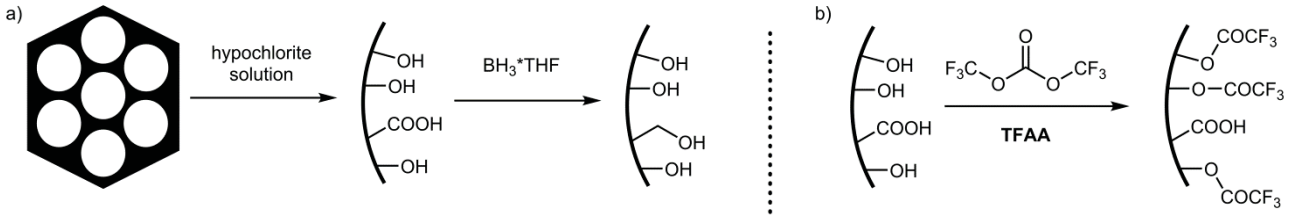

Figure A6-8. Left: Surface hydroxylation may be imperfect, resulting in “impurities” such as carboxylic acid groups. Reduction with BH3*THF leaves a uniformly –OH functionalized OMC. Right: TFAA selectively reacts only with carboxylic acids, thereby supporting detection of undesired functional groups and the quantification by XPS and MAS NMR spectroscopy.

The systematic hydroxylation of OMC materials with specific, uniform pore sizes will enable the independent investigation of both properties, and potential synergistic effects resulting from confinement in differently polar environments, when these materials are applied in catalysis (compare Fig. A6-3). An increase of polarity, introduced by a growing number of hydroxyl-groups on the surface, will improve wettability of the material and thereby impact the catalytic parameters when the OMCs are employed in the catalysis. It will also influence the adsorption of polar educts/byproducts (see **project B1**) and the concentration profile along the pores. It must also be considered that the presence of –OH is necessary for later attachment of epoxide groups and pore selective functionalization (next WP).

3.6.4.4 WP4: Pore-selective functionalization. As a final step, anchoring sites must be introduced into the material, where catalysts can be immobilized via linker molecules. Moreover, these sites have to be positioned *exclusively inside* the pores, otherwise no qualified statements will be possible regarding confinement effects. The ability to generate a different chemical environment on inner and outer surfaces can only be achieved in a limited number of ways. In this project, it is intended to employ reagents which, as a consequence of their size, cannot migrate into the pores, enabling selective functionalization. A well-established procedure – though not applied for carbon materials so far – is reacting of hydroxylated surfaces with epichlorohydrin, followed by hydrolysis with poly(styrenesulfonic acid) (Fig. A6-9).[44-45] This treatment will ensure that only epoxide groups within the pores remain intact. As a final preparation, these functionalities will be ring-opened to enable the Cu(I)-catalyzed click-chemistry-based approach that has been selected as universal linker strategy throughout this CRC.

The first step, reaction with epichlorohydrin, will define the density of epoxide groups within the pores, and simultaneously the position and concentration of potential catalyst sites for later application. It is thus neither necessary nor desired to obtain a quantitative conversion of the –OH groups into epoxide bearing ones; in contrast, a low concentration of epoxide groups on the carbon surface will be aimed for. Although it is obviously not yet clear what catalyst loading will deliver optimal results in the end, the catalyst concentration per pore will be low, both by intention and by physical demand, especially for the smaller mesopores: once a catalyst resides inside with full ligand sphere and spacer/linker set, the pore channel may well be blocked for further migration of large molecules such as catalysts in solution primed for immobilization.

For the second step, polymeric reagents are either commercially available or accessible by simple means (for example, ion exchange to prepare poly(styrenesulfonic acid) from sodium poly(styrenesulfonate). It is however important only to apply well-defined material with regard to molecular weight, as the limiting factor for pore-selectivity is the hydrodynamic radius of the reagent used for hydrolysis. The presence of short-chain oligomers will damage any pore-selectivity, especially for the larger mesopores. Relatively long reaction times (> 24 h) have to be accounted for, as the polymeric reagents are usually somewhat muted in their reactivity. This also has the added benefit that the pore “mouths” will be fully hydrolyzed, and the remaining epoxides are truly inside the pore and not near the opening.

The third and final step can be readily realized by application of commercially available reagents. For example, alkynes can be introduced by nucleophilic compounds such as 1-amino-3-butyne, while azides can be directly attached (Figure A6-9, bottom). Variations in linker length/stiffness will be conducted by the Section B groups to limit the amount of work for the materials projects.

As it was outlined for the previous work packages, a thorough characterization is required before the functionalized OMC is provided for catalysis experiments. On the one hand, this concerns changes in porosity. Epoxidation and hydrolysis of surplus epoxides on the outer surface may change average pore diameters, hence direct comparison with the hydroxylated (WP 3) and the pristine OMC (WP 2) will be enlightening. Also, while the degree of epoxidation is measureable by IR in combination with solid state NMR, it is especially the latter technique which will be useful to prove the in-pore positioning of functionalities. Interaction with **probe molecules** of variable size as outlined in **project C1** will provide detailed information on this end. It should be noted that solid state NMR spectroscopy of phenolic resins for activated carbon production,[55] as well as for mesoporous carbons and related compounds,[56-57] has already been reported, so even for this more advanced characterization there is data to draw upon. One of the difficulties in solid state NMR is the weak intensity of the signals to be observed and generally an obstructing “noise” in combination with broad signals. This will be mitigated by application of the above-mentioned probe molecules. However, should the potentially low concentration of epoxide functionalities aggravate observation, again the introduction of ^{19}F as sensitive nucleus will be useful. The chemical derivatization of oxygen functionalities on carbon surfaces has been well described,[58-59] employing diethylaminosulfur trifluoride as mild fluorination agent. This way, it is not only possible to differentiate between closely related functional groups by ^{19}F MAS NMR spectroscopy (such as aromatic/aliphatic carboxylic acid fluorides), but also to realize a “double probe” setup: upon interaction of the probe molecule with the fluorine-derivatized oxygen functionality, not only the probe molecule itself (^{31}P MAS NMR) but also the fluorine group will show a change in chemical shift, proving “contact”.

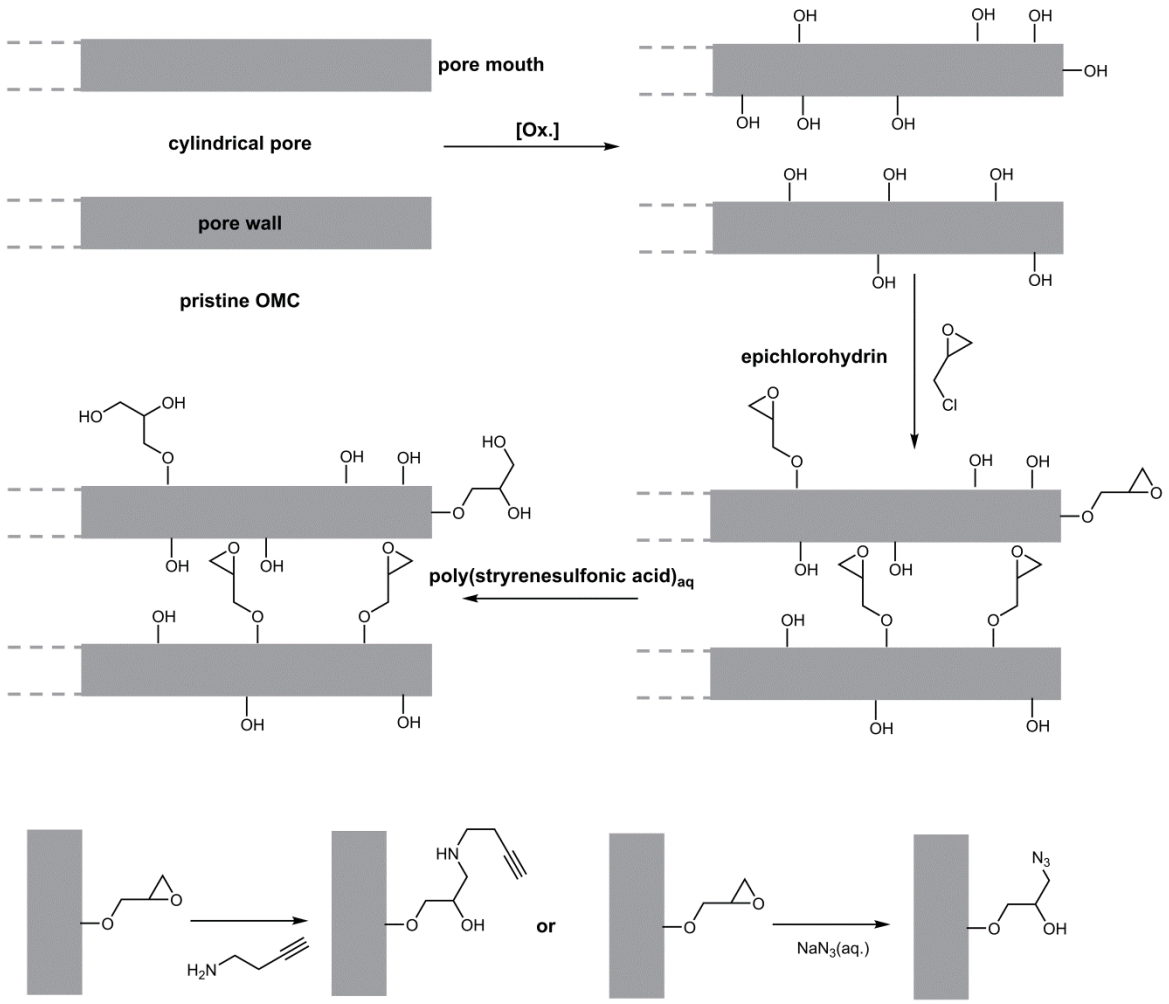

Figure A6-9. Schematic functionalization process for OMCs. Surface hydroxylation enables nucleophilic reaction with an epoxide-bearing reagent. Application of a polymeric acid only retains the epoxides inside the pores – the macromolecule is too large to migrate into these. Bottom: Examples for the introduction of "clickable" functionalities inside the mesopores (variations of linker length and stiffness will be conducted by the research groups of Section B).

Chronological work plan:

	2018	2019	2020	2021	2022	
	Q3 Q4	Q1 Q2 Q3 Q4	Q1 Q2 Q3 Q4	Q1 Q2 Q3 Q4	Q1 Q2	
T1						WP1: Synthesis of polyether library (PhD1)
T2						WP 2: preparation of OMC (PhD1)
T3						WP 3: Surface Hydroxylation (PhD1)
T4						WP 4: Pore-selective functionalization (PhD1)

For an optimal work flow, the work packages 1 and 2 will run in parallel; this ensures that the impact of structure-directing block-copolyether on pore properties is quickly identified and optimized. WPs 1 and 2 will remain active until the end of the first funding period, reacting to findings from other work

packages and cooperation partners, but with less intensity; the overall focus will shift from synthesis to characterization as the project develops. The work load is considered manageable as the synthesis of polymers and carbonization is operationally simple (no work-up for polymerizations, carbonization times 2 h and less). Hence, *pristine* OMCs will be provided for **B1** (and others) from the beginning of the CRC for pre-tests; *fully functionalized material* can be expected 1-1.5 years after start of the project. This ideally interlocks with **project A4**, which is scheduled to provide material to **B1** right from the beginning of the funding period.

3.6.4.5 Methods applied: Polymer synthesis and characterization will be achieved with methods well inside the standard repertoire. Simple glass reactors (pressure tubes) are sufficient for polyether synthesis and the modest pressures to be expected there. The relative block size of the copolyethers is conveniently determined by ^{1}H NMR. End groups are best assessed with MALDI-ToF MS and NMR analysis, which should be especially useful as the molecular weight distribution will be very defined and the molecular weights generally not too high (about 2-25 kDa). Common GPC analysis will reveal successful block-copolymer formation and can be used to spot side reactions (PPO from transfer-to-monomer, for example). All these methods are well established in the working group. Dynamic light-scattering (DLS) is a frequently employed method to gain information about micelle-formation, including "Pluronic"-type surfactants. For the more complex characterizations, it must be considered that cylinder-like micelles do not only show translation, but also rotation. This complicates data analysis; depolarized static LS (Sottmann, **A7**) will allow for qualitative information about the onset of the formation of cylinder/worm-like micelle structures.
On moving to OMC synthesis and functionalization, the required analytical tools are more advanced and call for cooperation between the working groups of this CRC. The carbonization process itself will be conducted in an oven with controlled atmosphere (N_2); the necessary heating equipment is accessible to the applicant. X-Ray techniques will also have a prominent place among characterization methods. XRD can be used to gain information about the periodicity and unit cell parameters of the OMC as well as its pore geometry and pore-to-pore distances. Analysis of the XRD pattern thus reliably allows for identification of the morphology of the carbon material, especially when combined with electron microscopy (see below); in general, the diffraction peaks mirror the regularity of the pores. Typical XRD patterns of OMCs show one dominant peak and only weak other signals, so for the most common morphologies "fingerprinting" can be applied. Interestingly, in a very limited sense XRD data can also yield information about the filling/functionalization of pores, because the presence of those reduces the contrast between the carbon walls and the pore (the electron densities have become more similar).[60] In this context, SAXS (Small-angle X-ray Scattering) is equally important, including also the determination of size and distribution of particles in liquid samples (aggregated micelles of the amphiphilic polyethers in solution, for example). As a powerful imaging technology, electron microscopy (EM) enables the investigation of the pore shape, periodicity and particle morphology of OMCs. The most capable instrument is high-resolution transmission EM (HR-TEM). Currently available to this project is also a scanning EM (SEM) with EDX (energy-dispersive X-ray spectroscopy) to gather information both about structure and chemical composition of the mesoporous material. For all EM methods, sample preparation is decisive and care must be taken when these images of ordered carbon materials are interpreted.[6,18] Solid state NMR analysis of the OMCs is a demanding process and requires a careful adaption of experimental conditions to the individual material to be investigated. One of the key advantages is that information about the degree of functionalization and placement of functionalities in carbon materials can be accessed. As briefly outlined above,[51-53] precedents exist for OMCs and much more so for carbon-rich material in general.[77] It must be considered that unclear chemical shifts, overlap, and broad signals are common, even for well-balanced experiments. Still, it can be expected that solid state NMR, and especially a combination of different measurement techniques, will deliver useful insights in the broadest sense (fraction of aromatic/aliphatic carbons, for example); for improved detection of functional groups a number of techniques exist, such as the fluorination of oxygen functional groups and/or the employment of probe molecules (**C1**).[61] One of the most versatile methods to gain knowledge about pore-related subjects is the interpretation of inert gas physical sorption isotherms. Typically (and also for the instrument accessible to the applicant), N_2 is employed and the Brunauer-Emmett-Teller-model (BET) is applied to calculate the surface area, while for pore size estimation a number of different methods can be employed. Again, great care has to be taken so as not to generate substantial artificial errors.[18] For example, for long cylindrical pores (such

as the ones targeted in this project), the BET approach is usually modified, taking into account the diameter of pores and adsorbate molecules. Pore size estimation itself must be adapted to the actual range of the mesopores in the material, as all models have limitations in this regard and may over- or underestimate pores sizes when these are outside their specific ranges. One of the most widely accepted models is the Barret-Joyner-Halenda (BJH) calculation, where it is assumed that cylindrical pores exist where multilayers of adsorbed nitrogen can form; this approach is therefore suitable for OMCs with 2D hexagonal morphology. Nonetheless, it must be kept in mind that errors of 10-20% can occur, especially for small (< 5 nm) and large (> 25 nm) mesopores. For mesoporous solids with cylindrical pores, further improvements of this model exist.[62] The total pore volume is accessible from single-point measurements.[6] Importantly, when a sample is directly compared before and after functionalization, the changes in pore properties potentially infer to the presence and placement of functional groups. For this information to be reliable, the combination with other characterization methods is indispensable, however, since degradation of the OMC during functionalization can deliver similar results. FT-IR is a simple, yet effective method to obtain general information about the degree and nature of functionalization of carbon materials,[63] readily achieved by direct comparison of modified and pristine material. Oxygen-related functional groups, the most relevant for this project, can be identified in a number of cases, including ethers, ketones, esters, phenolics or carboxyl groups. Although carbon materials can suffer from low transmission, some readily available techniques like Attenuated Total Reflectance (ATR-) IR can improve the quality of the spectra.[6]

3.6.4.6 Vision: By the end of the first funding period, a deepened understanding of the correlation between structure directing agent and resulting OMC properties will allow for rational and targeted pore size design, simply by choosing polyethers of appropriate chemical structure. The ability to pre-determine pore sizes with a resolution of < 1 nm, or potentially even better, is aimed for. A range of materials with monomodal and narrow pore size distribution will be at hand, where additionally the polarity of the surface is systematically altered, allowing for independent investigations of both properties. OMCs where pore size and pore polarity are fully controlled are expected to be of high interest for neighboring research fields, such as selective adsorption, water purification or battery electrodes. It will also be underlined that mesoporous carbon materials are excellently positioned for future funding periods: A change in *pore topology* from isolated pores to *channel networks or cage-like structures* is an obvious link from the first to the second funding period. This would allow deeper and potentially enlightening understanding of the connections between imposed geometry and catalytic performance. Further properties that are of interest for later stages of this proposed CRC include the inherent *electric conductivity* of carbon materials, which could be employed for redox-active catalysis, electrochemistry or externally triggered catalysis (“gate keeping”). Also, OMC can be prepared to display *hierarchical pore size distributions*,[36] a feature that might well prove to be necessary for the realization of complex cascade reactions or to achieve more “enzyme-like” individually tailored reaction zones inside different pores. An extension of the structure directing agents from triblocks to *high-molecular weight diblocks* might also be worthwhile, as this increases the window of accessible pore sizes towards larger ones. The application of *butylene oxide* instead of propylene oxide might likewise help to increase the volume of the lipophilic part of the structure-directing polymer and strengthen the contrast to hydrophilic PEO-repeating units.

3.6.5 Role within the collaborative research center

This project represents an important addition to the range of mesoporous materials available to this research initiative. Several key points recommend the application of OMC as described above for this CRC. The inherent properties of the material – low density, high surface area, scalable preparation, conductivity, mesoporous order and chemical, thermal as well as mechanical stability – certainly justify its investigation along with the perhaps more traditional mesoscale materials in this CRC. However, apart from these benefits, the most relevant aspect of this work will be its adaptability and modularity. Investigation of confinement effects obviously requires a defined mesoscale environment; deeper understanding can however only evolve once it is also possible to systematically alter the confinement and evaluate the resulting changes in catalytic transformations. Together with the conveniently manipulated surface polarity, from non-polar (pristine carbon) to polar (densely hydroxyl-functionalized), OMCs are well positioned to contribute to the scientific agenda of the research initiative.

It should also be noted that the key advance for OMC synthesis envisioned by this project, namely full control of pore sizes by convenient means and the ability to tailor pore functionalities and pore sizes, has also been identified in related fields as crucial factors for future progress: the application of OMCs as battery electrodes is a notable example. It can therefore be expected that findings from this project and this CRC will be of interest to a much wider audience.
The functionalized OMC will be provided for **project B1** and will be part of advanced spectroscopic and theoretical investigations (Section C). Being chemically relatively inert and thermally robust, the carbon materials will be in principle applicable for most types of catalysis. The following projects will be most intensively cooperated with:
- A4 (Gießelmann, Traa). This project aims to prepare well-defined mesoporous silica materials by use of commercially available amphiphilic block-copolymers ("Pluronics") and suitable co-surfactants. To complement this setup, and to create an interesting juxtaposition of both approaches, the custom-synthesized polyethers prepared in **project A6** will be provided also for application in **project A4**. This will enable a direct comparison of both methods regarding their consequences for pore size (distribution). In return, the expertise in the Gießelmann/Traa groups for X-ray characterization will be made available for **project A6**. This will not only encompass standard observations (morphology) but also less trivial, important aspects of the OMCs (such as pore-to-pore distance). An ambitious aim is to achieve in-situ characterization of a liquid, self-organizing sample by SAXS measurement.
- A7 (Sottmann). For characterization of the direct OMC precursors, namely the well-defined polyethers targeted in **project A6**, static and dynamic light-scattering will be an indispensable tool. This expertise is given in the Sottmann group, regarding both the analysis of scattering data of both spherical (diluted conditions) and worm-like/cylindrical micelles (concentrated solutions). Depolarized dynamic light scattering can qualitatively assess the onset of the latter. Time-resolved investigation of micelle formation might reveal more details about how evaporation influences the self-assembly.
- B1 (Plietker). This project is dedicated to hydrogen-autotransfer catalysis using (*N*,*N*,*N*,*N*)(*P*)Ru-complexes (average diameter: 1.3 nm), whereby in a visionary concept the pore properties are employed in a manner that is not conceivable for even the most sophisticated ligand systems in homogeneous catalysis: by the interplay of (hydrophilic) pore walls and the solvent, concentration gradients will be introduced. This may help to adjust the complex kinetics of this reaction (with overall conversion of primary alcohols into secondary amines via a carbonyl intermediate generated by dehydrogenation), for example by transporting polar products (or side-products, such as water) away along the polar pore walls, while less polar starting compounds can concentrate in the center of the pore (where the catalysts is). Potentially, this enhances transformation rates while reducing side reactions at the same time. These requirements clearly recommend OMCs as described above; the graded polarity of the pore walls by hydroxylation, in combination with adjustable pore size, should provide ideal experimental conditions for **project B1**. Also, typical reaction conditions (toluene, 100°C, catalytic amounts of base) are easily tolerated by the carbonized materials. For initial experiments, **project B1** will be provided with graded OMCs displaying pore sizes in the range of of 4-8 nm and a narrow pore size distribution individually. These requirements are full in the range of accessible structures for OMCs derived from organic self-assembly (2-10 nm range, whereby each gradual step in size can be addressed with high control, i.e., delivering materials with monomodal and small pore size distributions). Moreover, the targeted 2D hexagonal morphology will enable a direct comparison to other materials applied in **project B1**, such as the silica-based SBA-15 (provided by **project A4**).
- **C1 (Hunger).** In this project, probe molecules (based for example on phosphorus) will be employed to detect metal catalysts/functional sites of the mesoporous supports (including spatial distribution). OMCs are among the materials proposed by **project C1** to be investigated by 1D and 2D solid state NMR. As outlined above, this specialized NMR technique could play a role to characterize the carbons after hydroxylation (WP 3) and again after (pore selective) epoxidation (WP 4). Fluorination of functional groups is a useful method to introduce a highly NMR-susceptible nucleus. This will simplify detection by solid state NMR, both in the presence and absence of further interactions with probe molecules. All NMR experiments will be conducted by **C1** personnel, while the optional fluorine-based labelling is part of **project A6**.
Finally, it should also be noted that the long, cylindrical pores targeted in **project A6** are one of the structures which are investigated by **project C6**, regarding their diffusion properties (multipore system, inlet/outlet flow). With this knowledge it might be possible in a later stage of the first funding period of this proposed CRC to select a tailored pore size, optimized for its diffusion properties. In turn, this will be of central importance to the catalytic **project B1**, which employs OMCs as support material.

3.6.6 Differentiation from other funded projects

The work described in **project A6** is not subject or partly subject of other funded projects.

3.6.7 Project funding

3.6.7.1 Previous funding

This project is currently not funded and no funding proposal has been submitted. The other DFG project led by the applicant, NA-1206-2 "*Advancing Polymerization Catalysis by Cooperativity: Dual Catalysis as a Tool to Achieve High Performance at Maximum Simplicity*" has no topical connection to **project A6**.

References (ctd.)

[48] See chapter 7-2a in G. Odian, *Principles of Polymerization (Fourth Edition)*, Wiley-Interscience, S.l., **2004**.
[49] C. Liu, L. Li, H. Song, X. Chen, *Chem. Commun.* **2007**, 757-759.
[50] Z. Wu, P. A. Webley, D. Zhao, *Langmuir* **2010**, *26*, 10277-10286.
[51] D. Yu, Z. Wang, N. S. Ergang, A. Stein in *Studies in Surface Science and Catalysis*, Elsevier, **2007**, pp. 365–368.
[52] M. J. Bleda-Martínez, D. Lozano-Castelló, E. Morallón, D. Cazorla-Amorós, A. Linares-Solano, *Carbon* **2006**, *44*, 2642-2651.
[53] L. A. Langley, D. E. Villanueva, D. H. Fairbrother, *Chem. Mater.* **2006**, *18*, 169-178.
[54] K. A. Wepasnick, B. A. Smith, K. E. Schrote, H. K. Wilson, S. R. Diegelmann, D. H. Fairbrother, *Carbon* **2011**, *49*, 24-36.
[55] C.-C. Lin, H. Teng, *Ind. Eng. Chem. Res.* **2002**, *41*, 1986-1992.
[56] R. Xing, Y. Liu, Y. Wang, L. Chen, H. Wu, Y. Jiang, M. He, P. Wu, *Microporous Mesoporous Mat.* **2007**, *105*, 41-48.
[57] Y. Wang, D. Nepal, K. E. Geckeler, *J. Mater. Chem.* **2005**, *15*, 1049-1054.
[58] E. W. Hagaman, S. K. Lee, *Energy Fuels* **1995**, *9*, 727-734.
[59] M. Hudlicky, *J. Fluorine Chem.* **1987**, *36*, 373-384.
[60] M. H. Lim, C. F. Blanford, A. Stein, *Chem. Mater.* **1998**, *10*, 467-470.
[61] J. Z. Hu, M. S. Solum, C. M. V. Taylor, R. J. Pugmire, D. M. Grant, *Energy Fuels* **2001**, *15*, 14-22.
[62] M. Kruk, M. Jaroniec, A. Sayari, *Langmuir* **1997**, *13*, 6267-6273.
[63] Z. Wang, N. S. Ergang, M. A. Al-Daous, A. Stein, *Chem. Mater.* **2005**, *17*, 6805-6813.

3.6.7.2 Requested funding

Funding for	2/2018		2019		2020		2021		1/2022		2018-2022	
Staff	Quantity	Sum	Quantity	Sum	Quantity	Sum	Quantity	Sum	Quantity	Sum	Quantity	Sum
PhD student, 67%	1	21,600.-	1	43,200.-	1	43,200.-	1	43,200.-	1	21,600.-	1	172,800.-
Total		21,600.-		43,200.-		43,200.-		43,200.-		21,600.-		172,800.-
Direct costs	Sum		Sum		Sum		Sum		Sum		Sum	
consumables	4,000.-		8,000.-		8,000.-		8,000.-		4,000.-		32,000.-	
Total	4,000.-		8,000.-		8,000.-		8,000.-		4,000.-		32,000.-	
Major research instrumentation	-		-		-		-		-		-	
	-		-		-		-		-		-	
Total	-		-		-		-		-		-	
Grand total	25,600.-		51,200.-		51,200.-		51,200.-		25,600.-		204,800.-	

(All figures in EUR; staff funding according to DFG form 60.12)

3.6.7.3 Requested funding for staff

	Sequential no.	Name, academic degree, position	Field of research	Department of university or non-university institution	Project commitment in hours per week	Category	Funding source
Existing staff							
Research staff	1	Stefan Naumann, Dr., Habilitand.	Polymer Science, Catalysis, Organocatalysis, Material Science	Institute of Polymer Chemistry	8		University
Requested staff							
Research staff	2	N. N.; M. Sc.	Polymer Science, Material Science	Institute of Polymer Chemistry		PhD	
Research staff	3	Research assistant	Polymer Science, Material Science	Institute of Polymer Chemistry			

Job description of staff (supported through existing funds):
1
Habilitand, principal investigator for **project A6**

Job description of staff (requested funds):
2
PhD student, work packages 1-4
3
Research assistants. **Justification:** The research assistants will be employed to work both on synthetic as well as analytic tasks. This may include scale-up experiments, GPC analysis, NMR investigations, MALDI-ToF MS or N_2 physical sorption. This serves to reduce the work-load for the PhD student (repetitive work) and will familiarize the research assistants with scientif lab work.

3.6.7.4 Requested funding of direct costs

	2018	2019	2020	2021	2022
Uni Stuttgart: existing funds from public budget	0.-	0.-	0.-	0.-	0.-
Sum of existing funds	0.-	0.-	0.-	0.-	0.-
Sum of requested funds	4,000.-	8,000.-	8,000.-	8,000.-	4,000.-

(All figures in EUR)
Consumables for financial year 2018

Chemicals (monomers, catalyst synthesis, PEG...), solvents, GPC consumables	EUR	4,000.-

Consumables for financial year 2019

Chemicals (monomers, catalyst synthesis, PEG...), solvents, GPC consumables	EUR	8,000.-

Consumables for financial year 2020

Chemicals (monomers, catalyst synthesis, PEG...), solvents, GPC consumables	EUR	8,000.-

Consumables for financial year 2021

Chemicals (monomers, catalyst synthesis, PEG...), solvents, GPC consumables	EUR	8,000.-

Consumables for financial year 2022

Chemicals (monomers, catalyst synthesis, PEG...), solvents, GPC consumables	EUR	4,000.-

3.6.7.5 Requested funding for major research instrumentation

none

3.7 Project A7

3.7.1 General information about Project A7

3.7.1.1 Nanoporous host materials with adjustable pore size, geometry and distribution: Synthesis, functionalization and characterization

3.7.1.2 Research Areas
Polymer Chemistry, Preparative and Physical Chemistry of Polymers (306-01)

3.7.1.3 Principal Investigator
Sottmann, Thomas, apl. Prof. Dr. born 15.03.1966, male, German
Institut für Physikalische Chemie
Universität Stuttgart, Pfaffenwaldring 55, 70569 Stuttgart
Tel.: 0711/685-64494
E-Mail: thomas.sottmann@ipc.uni-stuttgart.de
Team leader, permanent position

3.7.1.4 Legal Issues
This project includes

1.	research on human subjects or human material.	no
2.	clinical trials.	no
3.	experiments involving vertebrates.	no
4.	experiments involving recombinant DNA.	no
5.	research involving human embryonic stem cells.	no
6.	research concerning the Convention on Biological Diversity.	no

3.7.2 Summary
Polystyrene (PS) or poly methyl methacrylate (PMMA)) nanofoams will be prepared as tailor made substrates for molecular catalysis following the *NanoFoam Continuity Inversion of Dispersions* (NF-CID) principle. This principle provides access to a mesoporous bulk material with adjustable pore size, geometry and homogeneity. We therefore propose a systematic study of the influence of size and properties of the used polymeric nanoparticles, and the foaming process parameters on the size, distribution and morphology of the pores in the formed nanofoam. We expect that this systematic study will allow us to reduce the pore diameter to below 50 nm at the end of first funding period of the project. The pore surface will be functionalized by hydroxylation, e.g. using dilute solutions of hypochlorite or appropriate co-monomers (hydroxyl methyl styrene for PS) in the synthesis of the polymeric nanoparticles. Adjusting the degree of hydroxylation will allow us to change polarity and wettability of the pore surface in a systematic way. Epoxide groups will be pore-selectively introduced which will then serve as anchoring sites for linker molecules or linker group-bearing Rh-catalysts for the catalyzed 1,4-addition of boronic acids to enones (**project B3**). Potential weaknesses of the polymeric nanofoams are the instability with respect to hydrophobic solvents and high temperature as well as the limited pore size. To overcome these weaknesses the polymeric nanofoams will be further processed in **project A5** preparing organic/inorganic hybrid materials. Via the stepwise deposition of layers of metal oxides such as ZnO, TiO_2, SiO_2, ZrO_2 and Al_2O_3 through a mineralization reaction process, the pore diameter will be reduced to d_{pore}≥25 nm through a precise control over the oxide film thickness and hence a fine tuning of the pore size. Furthermore, the stability with respect to solvents and temperature can be further increased removing the polymeric foam template with an appropriate organic solvent or by pyrolysis. The characterization of the prepared polymeric nanoparticles, nanofoams and organic/inorganic hybrid materials as well as their functionalization will be performed in close cooperation with the project areas A and C using SEM, SANS, SAXS, PFG-NMR, BET, as well as IR- und solid state-NMR-spectroscopy. Last but not least, it should be mentioned, that because of the expected very low thermal conductivity (10-15 mW/mK) and the associated optical transparency, polymeric nanofoams with a pore diameter of the order of 50 nm bear also a high potential for application as highly efficient insulation materials.

3.7.3 Research rationale

3.7.3.1 Current state of understanding and preliminary work

Nanofoams

Polymeric nanofoams with adjustable pore size, geometry and homogeneity are a new promising class of tailor made substrates to study the influence of the confinement of molecular heterogeneous catalysts on the productivity and selectivity of catalytic reactions. Compared to other mesoporous materials, polymeric nanofoams appeal through their easy production allowing large quantities (m^3/day). Furthermore, the foam morphology can be easily varied adjusting the degree of open foam cells.

While it is to our knowledge the first time that polymeric nanofoams will be used as tailor made substrates for molecular heterogeneous catalysts, polymeric nanofoams are also considered to be the insulation materials of the future[1]. Here the exploited property is the gaseous thermal conductivity, which, according to the Knudsen effect, can be lowered enormously, if the pore size of the foam is reduced to the mean free path length l_{mean} of the enclosed cell gas[2]. Compared to aerogels that are produced using a sol-gel-process which was first published by Kistler[3], but suffer from the unavoidable time-consuming supercritical drying step[4], the production of polymeric nanofoams is expected to be easy. Such polymeric nanoporous materials with a pore size below 100 nm could be produced by a sudden expansion of thin films of thermo-responsive polymers such as polyetherimide, polysulfone[5] or PMMA[6] saturated with supercritical CO_2 ($scCO_2$). However, as such films of a few millimeters thickness require saturation times of several hours and high expansion rates, this approach is inappropriate for an efficient production of nanomaterials. Template strategies are the most promising approach to prepare such materials. Formulating a $scCO_2$-in-water (c/w) emulsion at high pressure as template, a microcellular foam could be obtained via a sudden pressure release, while a polar monomer is polymerized at the same time[7].

About 10 years ago we suggested that microemulsions, which are thermodynamically stable, nanostructured mixtures of at least a hydrophilic, hydrophobic and an amphiphilic components[8], seem to be perfect templates for polymeric nanofoams. In the Principle of Supercritical Microemulsion Expansion[A7-1,A7-2] (POSME) a microemulsion is expanded, which consist of CO_2-swollen micelles in a continuous matrix. The latter is selected such it can be solidified either by cooling below the glass temperature or polymerizing a hydrophilic monomer. In order to avoid a nucleation step, which would most probably destroy the template structure, the expansion is performed above the critical temperature of CO_2. In contrast to conventional foaming procedures the high density of the blowing agent in the microemulsion droplets and its supercritical state allow for the unhindered formation and growth of bubbles without mass transport. In order to study the properties of CO_2-microemulsions, a variety of high pressure cells was developed[A7-3,A7-4,A7-5], which will be used in this collaborative research center. However, the synthesis of polymeric nanofoams with the POSME principle struggles with the coarsening of the microemulsion structure during polymerization and expansion. Recently, we were able to study the coarsening kinetics using time-resolved small angle neutron scattering (SANS)[A7-6].

Nanofoams by Continuity Inversion of Dispersion (NF-CID) Principle

In this study the template strategy developed by *Strey* and *Müller* in 2010[9] will be used to prepare nanofoams as tailor made substrates for molecular catalysis. This procedure is called nanofoams by continuity inversion of dispersion (NF-CID) and is based on randomly dispersed fluid inclusions of nanometer size in a highly viscous polymer matrix. The main advantages of the NF-CID procedure, which is schematically shown in Fig.1, are the rapid saturation of the polymer with supercritical blowing agent and the high number density of CO_2 pools, both obtained by the use of polymeric nanoparticles. The principle can be divided in 5 steps:

Firstly, thermoplastic polymer nanoparticles of adjustable size ($d_{part} \geq 10$ nm) and narrow size distribution, are synthesized by emulsion[10], miniemulsion[11] or microemulsion[12,A7-7] polymerization. Hereafter the nanoparticle dispersion is dried by evaporation of the solvent (step 2). Eventually, a colloidal crystal consisting of close-packed nanoparticles is formed. In step 3 the voids between the particles are filled with a super-critical fluid (sc-fluid) at an adjustable temperature and pressure. As a result of the small size of the nanoparticles and the huge surface of the colloidal crystal, the sc-fluid, which later on acts as blowing agent, is transported almost instantaneously into the polymer nanoparticles. Time-resolved SANS measurements showed that saturation times of the order of only 30 s are required[A7-8]. Due to the saturation of the polymer nanoparticles with the sc-fluid the glass temperature T_g is considerably reduced. Thereby the glass temperature T_g^* depends strongly on the

solubility of a given sc-fluid in a polymer, which is a function of temperature and pressure[13]. E.g. PMMA which exhibits a glass temperature of T_g=105 °C transfers to the rubbery state already at T = 40 °C, if it is exposed to CO_2 adjusting a pressure of $p \geq 60$ bar[14].

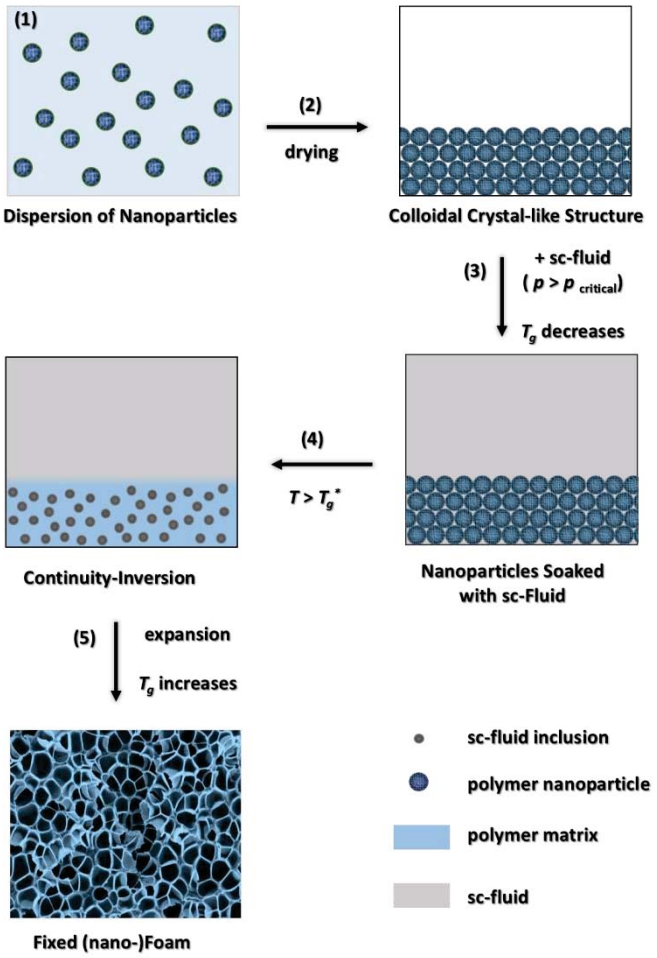

Figure A7-1: Scheme of the NF-CID principle. (1) Thermoplastic nanoparticles are synthesized by emulsion, miniemulsion or microemulsion polymerization. (2) Drying the dispersion results in closed packed nanoparticles, which are in step (3) filled with a supercritical fluid, decreasing the T_g of the polymer. (4) Increasing the temperature above the lowered T_g, the octahedral and tetrahedral voids (ideal packing) filled with the sc-fluid transform into spherical nano-droplets in the highly viscous polymer matrix. (5) Expanding the system leads to both foaming and fixation of the polymer. Redrawn from[9].

In step 4 (continuity inversion) the temperature is increased above the T_g^* of the polymer nanoparticles saturated with the sc-fluid at the respective pressure. Thus, the polymer particles lose their spherical shape and form a connected polymer matrix. Due to the high interfacial tension between the sc-fluid and the saturated nanoparticles, the octahedral and tetrahedral voids (ideal packing) filled with sc-fluid transform to spherical nanodroplets in the highly viscous polymer matrix to minimize the interfacial energy. In the last step, the pressure is released to 1 bar. Thereby, the density of the sc-fluid changes gently from the liquid-like to a gas-like state. Accordingly, each spherical nanodroplet transforms gradually into a foam bubble. At the same time the polymer matrix solidifies due to a rapid increase of T_g of the polymer to its original value caused by the diffusion of sc-fluid molecules out of the polymer.

Assuming spherical geometry, the diameter d_{scfluid} of the spherical nanodroplets in the highly viscous matrix is directly related to the diameter d_{part} of the polymeric nanoparticles, according to

$$d_{\mathrm{scfluid}} = d_{\mathrm{part}} \sqrt[3]{\frac{N_{\mathrm{part}} \phi_{\mathrm{scfluid}}}{N_{\mathrm{scfluid}} (1-\phi_{\mathrm{scfluid}})}}. \quad (1)$$

Here, ϕ_{scfluid} is the volume faction of the sc-fluid and N_{part} and N_{scfluid} are the number of particles and spherical nanodroplets, respectively. The volume of the spherical nanodroplets and foam pores depends on the density of the sc-fluid at high and low pressure (1 bar), i.e. $\rho_{\mathrm{scfluid,liquid\text{-}like}}$ and $\rho_{\mathrm{scfluid,gas\text{-}like}}$. Thus, the diameter d_{pore} of a pore is given by

$$d_{\mathrm{pore}} = d_{\mathrm{scfluid}} \sqrt[3]{\frac{\rho_{\mathrm{scfluid,liquid-like}}}{\rho_{\mathrm{scfluid,gas-like}}}} = d_{\mathrm{part}} \sqrt[3]{\frac{\rho_{\mathrm{scfluid,liquid-like}} N_{\mathrm{part}} \phi_{\mathrm{scfluid}}}{\rho_{\mathrm{scfluid,gas-like}} N_{\mathrm{scfluid}} (1-\phi_{\mathrm{scfluid}})}}. \quad (2)$$

Altogether, this leads to the conclusion that the pore size in the foam is predictable and directly adjustable by the diameter of the used polymer nanoparticles. Assuming that the particles are ideally close-packed and that the octahedral and tetrahedral spaces are so close together that they build one inclusion when the polymer becomes ductile, $N_{\mathrm{part}}/N_{\mathrm{scfluid}}=1$ and $\phi_{\mathrm{scfluid}} \approx 0.26$. Calculating the diameter of a pore using CO_2 as sc-fluid and an expansion from p = 250 bar to 1 bar at 80°C results in

$$d_{\mathrm{pore}} \approx 5.4 \cdot d_{\mathrm{part}}. \quad (3)$$

According to this relation, the synthesis of nanofoams with an adjustable pore diameter $d_{\mathrm{pore}} \geq 50$ nm should be possible using polymer particles with the respective diameters of $d_{\mathrm{part}} > 10$ nm. Note, that furthermore a smaller Δp decrease the pre-factor in eq. 3. Thus, also mesoporous nanofoams with pore diameter below 50 nm for the study of the confinement of molecular heterogeneous catalysts on the productivity and selectivity of catalytic reactions should be possible.
From the above it is obvious, that the diameter d_{part} of the polymeric nanoparticles is one important parameter to adjust the pore size d_{pore} of the nanofoam. Besides d_{part}, the course of the NF-CID procedure has a comparable impact on the pore size, geometry and homogeneity of the nanofoam[A7-8]. Particularly the formation of sc-fluid filled nanodroplets in the highly viscous polymer matrix, i.e. continuity inversion (step 4), and the pressure release (step 5) are crucial steps for the procedure. Both are sensible to aging effects which are triggered by the minimization of the interfacial energy via a reduction of the interfacial area. In both steps the aging phenomena depend strongly on the viscosity of the polymer matrix, which is controlled by the glass temperature T_g^* of the polymer saturated with the sc-fluid (it's solubility), temperature, pressure, saturation and expansion time.

Aging Phenomena
Two mechanisms are responsible for the aging of structures: *Ostwald* ripening[15,16] and coagulation followed by coalescence[17,18]. The *Ostwald* ripening describes the growth of larger droplets on the expense of the smaller ones. The driving force of this process is explained by the *Young-Laplace* equation

$$\Delta p = p_{\mathrm{inside}} - p_{\mathrm{outside}} = \frac{4\sigma}{d_{\mathrm{scfluid}}}, \quad (4)$$

with the *Laplace* pressure Δp, p_{inside} and p_{outside} the pressure inside and outside the droplet, σ the interfacial tension between sc-fluid and polymer. Figure A7-2, left illustrates the ripening mechanism exemplarily for CO_2-droplet in a molten polymer matrix. As can be seen, the molecular diffusion of the CO_2-molecules from the smaller to the larger droplets is driven by the larger *Laplace* pressure in the smaller droplets. Thus, the ripening processes can be slowed-down by decreasing the droplet polydispersity and the solubility of $scCO_2$ in the polymer.

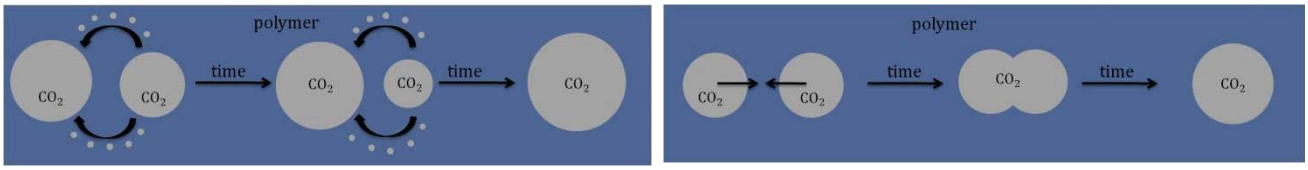

Figure A7-2: Left: Schematic drawing of *Ostwald* ripening:[15,16] larger droplets grow at the expense of smaller ones. Right: Illustration of the process of coagulation followed by coalescence. The coagulation rate depends mainly on the diffusion coefficient of the fluid containing droplets. The coalescence on the interfacial tension and the rigidity of the interface.[17,18]

The coagulation of droplets is primarily determined by the diffusion,[17,18] which mainly depends on the temperature, the droplet size and the viscosity of molten polymer matrix and thus on the distance to the glass temperature T_g^* of the polymer saturated with the sc-fluid. Whether the coagulation of two droplets is followed by their coalescence (Figure A7-2, right), depends mainly on the interfacial tension between sc-fluid (here CO_2) and polymer and the rigidity of the interface. Thus, the rate of coagulation followed by coalescence should be reduced, by increasing the viscosity of the molten polymer matrix, the rigidity of the interface and decreasing the interfacial tension.

i) Preliminary work: Time-resolved SANS and SEM study of the NF-CID procedure

A deep knowledge in the processes taking place in the course of the NF-CID procedure will allow for the identification of the most prominent parameters which determine the size, geometry and homogeneity of the nanofoam. Thus, we recently studied the structural transitions occurring during the NF-CID procedure by DLS, SEM and time-resolved SANS.[19] Drying a PMMA nanoparticle (diameter d_{part}=28 nm ($d_{part,hyd}$=35 nm)) dispersion the formation of a colloidal crystal-like structure exhibiting some defects could be proven by SEM (Figure A7-3, left) and SANS (Figure A7-3, center, t=0 s). Time-resolved SANS was then used to study the structural changes induced by the addition of CO_2 (T=25°C and p=70 bar). With time the scattering peaks disappear (at t≈30s) and the intensity increase caused by the packing defects disappear. Furthermore, the scattering intensity at intermediate q-values increases, leading to the formation of a shoulder at low q (scattering vector). These results suggest that the addition of CO_2 induces a disordering of the colloidal crystal. The PMMA particles swell with CO_2 until the polymer particles contact each other. Furthermore, the addition of CO_2 reduces the glass temperature so that the polymer reaches its rubbery state forming an inverted bicontinuous polymer/CO_2-matrix. Figure A7-3, right illustrate the proposed intermediate structures extracted from the quantitative analysis of the scattering curves. Thereby, the structure of the inverted bicontinuous polymer/CO_2-matrix formed at t = 50 s could be proven recording a SEM image of the sample after releasing the pressure (and therewith removing CO_2). Looking closely, the structure seems to consist of remnants of the PMMA particles which are melted together.

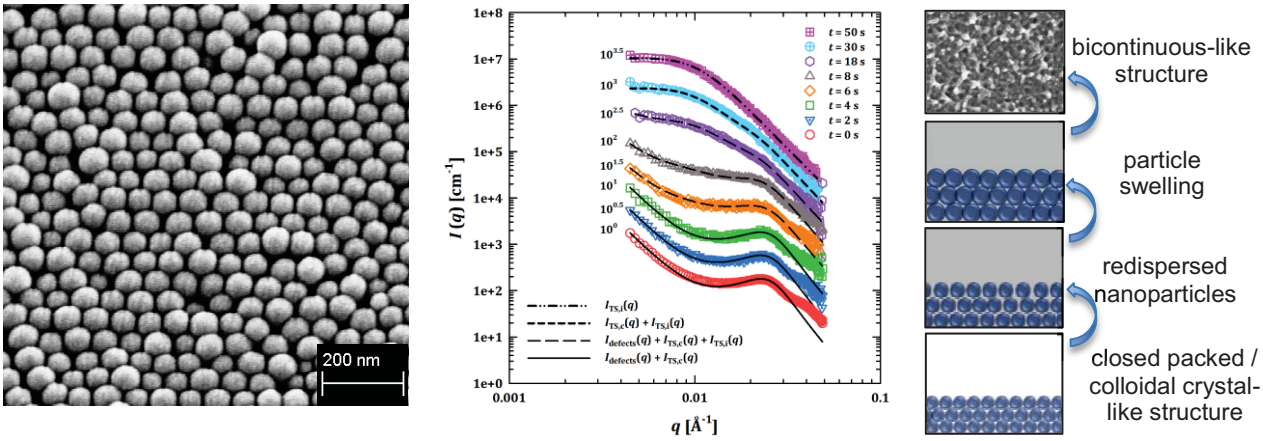

Figure A7-3: Left: SEM-picture of the closed packed/colloidal crystal-like PMMA nanoparticles. Center: Scattering curves after the addition of CO_2 to the colloidal crystal at T_0=25°C and p_0=70 bar. The data are described by a linear combination of scattering models: At t=0 s by the weighted sum of a Teubner-Strey structure factor $I_{TS,c}(q)$[20] and a q^{-4}-decay[21], for t≥50 s solely with the Teubner-Strey model $I_{TS,i}(q)$

describing the structure of the inverted bicontinuous PMMA/CO_2-matrix. Right: Schematic representation of the proposed intermediate structures.

In the next step (4) of the NF-CID – procedure the temperature is increased above the T_g^* of the CO_2-saturated polymer nanoparticles to induce the formation of CO_2 nanodroplets in a molten PMMA matrix. To follow the structural transitions SANS curves were recorded when the inverted bicontinuous PMMA/CO_2-matrix was heated to T = 55 °C causing an increase of the pressure to p = 165 bar (Figure 4, left). Then, at t=3000 s the pressure was increased to p = 250 bar. Analyzing the individual scattering curves, it became obvious that the scattering curves recorded at temperatures T≤50°C can be quantitatively described by the *Teubner-Strey* structure factor[20] indicating that the structure of the PMMA/CO_2 system is still bicontinuous-like. However, the formation of the envisaged CO_2 nanodroplets can be observed, when the temperature is increased to T=55°C (and afterwards the pressure to p = 250 bar). Due to the appearance of slight oscillations in the intermediate q-range, the scattering curves could only be quantitatively described by a polydisperse droplet form factor $P(q)$ with a diffuse interface[A7-8] combined with the *Percus-Yevick* structure factor $S_{PY}(q)$[22].

The aging of the CO_2-nanodroplets in the molten PMMA-matrix at T = 55 °C and p = 250 bar becomes obvious considering the scattering curves recorded as a function of the saturation time t_{sat} (Figure A7-4, right). As can be seen, the characteristic oscillation of the scattering intensity, which becomes clearly visible after t_{sat}=5 min, shifts to smaller q-values with increasing saturation time, indicating the growth of the CO_2-nanodroplets due to *Ostwald* ripening or coagulation followed by coalescence, which are discussed in 3.7.3.1. The quantitative analysis of the SANS data revealed that the diameter $d_{scfluid}$ of the CO_2-nanodroplets increases from 47 nm to 70 nm and that the number density of the droplets decreases accordingly from 10^{16} cm^{-3} to 10^{15} cm^{-3}.

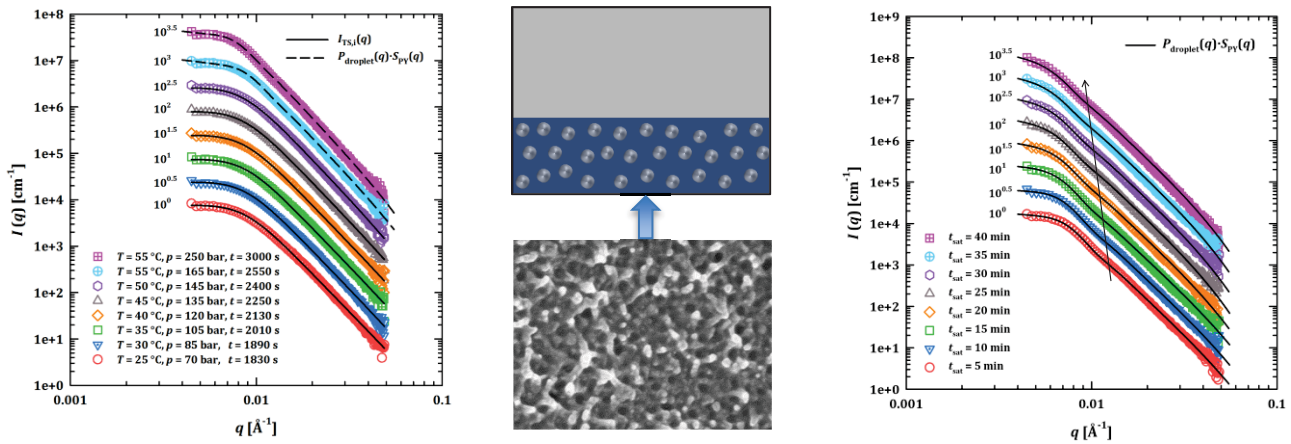

Figure A7-4: SANS curves of the PMMA/CO_2-matrix during the heating process from T=25°C and p=70 bar to T=55°C and p=250 bar (left) and after different saturation time's t_{sat} (right). While for T≤50°C the scattering data are better described by the Teubner-Strey model $I_{TS,i}(q)$[20], the form factor $P_{droplet}(q)$ of polydisperse spheres[A7-8] and the Percus-Yevick structure factor $S_{PY}(q)$[22] provides a better description for T>50°C. Center: Heating and pressure induced transition from the inverted bicontinuous PMMA/CO_2-matrix (SEM-picture) to the spherical CO_2-nanodroplets (schematic representation).

Figure A7-5 shows the SEM image of a PMMA nanofoam that was obtained releasing the pressure to p = 1 bar starting from T = 55 °C and p = 250 bar after a saturation time of t_{sat}=30min. Due to the decreasing density of CO_2, the spherical nanodroplets transform gradually into foam bubbles foaming the PMMA matrix, which is almost simultaneously stabilized by two effects. The *Joule-Thomson* effect leads to a temperature decrease of around ΔT = 30 °C. Furthermore, the glass temperature T_g^* of the polymer increases rapidly to its original value T_g due to the strongly decreasing CO_2 solubility in PMMA. The kinetic of the expansion process was also studied by SANS recording the integrated detector intensity during the pressure release. We found that the detector intensity increases considerably because of the growth of the structure but stays constant after 4 s indicating that foaming process is completed. Recording the scattering curve of the obtained PMMA nanofoam, unfortunately, only a q^{-4}-decrease of the scattering intensity could be detected due to the limited q-range. However, analyzing

the SEM-picture a mean pore diameter d_{pore} = 280 nm is obtained, which is in almost quantitative agreement, if $d_{scfluid}$=70 nm is used in Eq. 3.

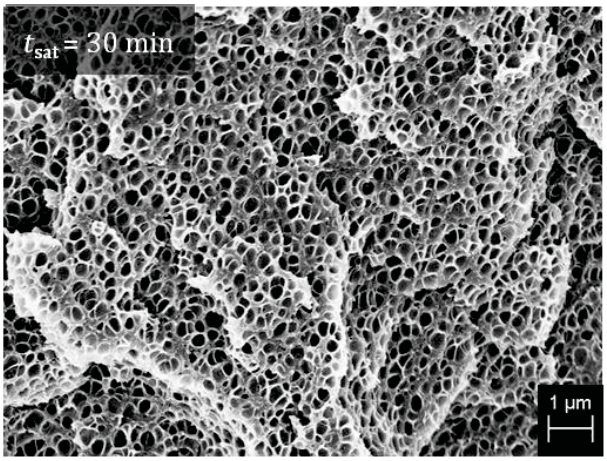

Figure A7-5: SEM image of a PMMA nanofoam that was obtained releasing the pressure to p = 1 bar starting from T = 55 °C and p = 250 bar after a saturation time of t_{sat}=30min. The nanofoam shows a monomodal size distribution with a mean pore diameter d_{pore} = 280 nm.

ii) Preliminary work: Influence of the course of the expansion process (Δ*p*, d*p*/d*t*, and d*T*/d*t*)
The time-resolved SANS and SEM study of the NF-CID principle has shown that the diameter d_{part}, temperature, pressure and saturation time are important parameters that determine not only the size d_{pore}, shape and polydispersity of the pores but also the overall structure of the nanofoam (open- versus closed-cellular). With the goal to identify other important parameters of the principle we studied the influence of the course of the expansion process by means of polystyrene nanofoams generated from PS nanoparticles of the diameter d_{Part}=48 nm. In a preliminary experiment we started at T = 80 °C and p = 250 bar after a saturation time of t_{sat}=10 min and decreased the temperature to T = 25 °C before the expansion. Due to the fact that the volume is kept constant, the pressure decreases to p = 75 bar. Subsequently the pressure is released to p = 1 bar. The SEM images shown in Figure A7-6 show the obtained PS nanofoam, which seems to have an open-cellular structure exhibiting a mean pore diameter of d_{pore} = 65 nm. One may speculate that the structure of the nanofoam is mainly formed and stabilized during the cooling step. In order to confirm this hypothesis a time-resolved SANS-study is planned.

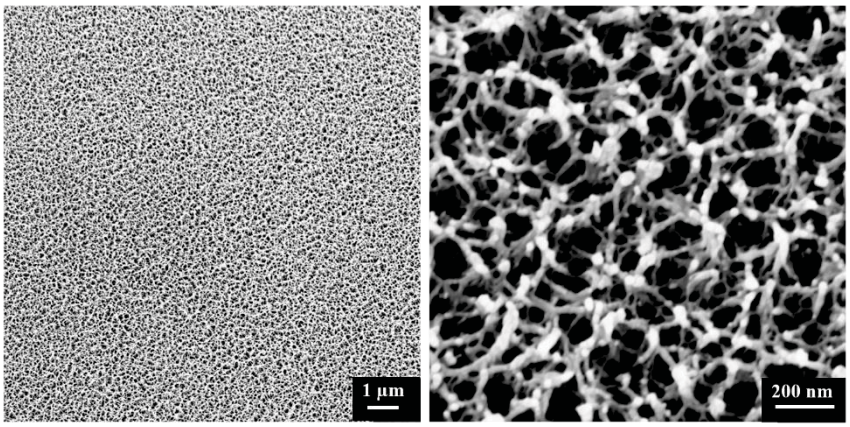

Figure A7-6: SEM image of a PS nanofoam that was obtained decreasing the temperature from T = 80 °C to T = 25 °C after a saturation time of t_{sat}=10 min. Due to the fact that the volume is kept constant, the pressure decreases from p = 250 bar to p = 75 bar. Subsequently the pressure is released to p = 1 bar obtaining an open-cellular foam exhibiting a mean pore diameter of d_{pore} = 65 nm.

iii) Preliminary work: Synthesis of nanoporous PS/ZnO hybrid materials

In cooperation with the **project A5** a nanoporous organic/inorganic material was produced as a proof of principle, which represent another promising class of tailor made substrates to study the influence of the confinement of molecular heterogeneous catalysts on the productivity and selectivity of catalytic reactions. In this smart approach we propose to use open-cellular polymeric nanofoams as template and adjusting the pore size (d_{pore}≥25 nm) by the stepwise deposition of layers of metal oxide on the pore walls of these nanoporous materials through a mild mineralization reaction[23]. Herewith we bypass potential weaknesses of the polymeric nanofoams, i.e. their instability with respect to hydrophobic solvents and high temperature as well as the limited pore size.

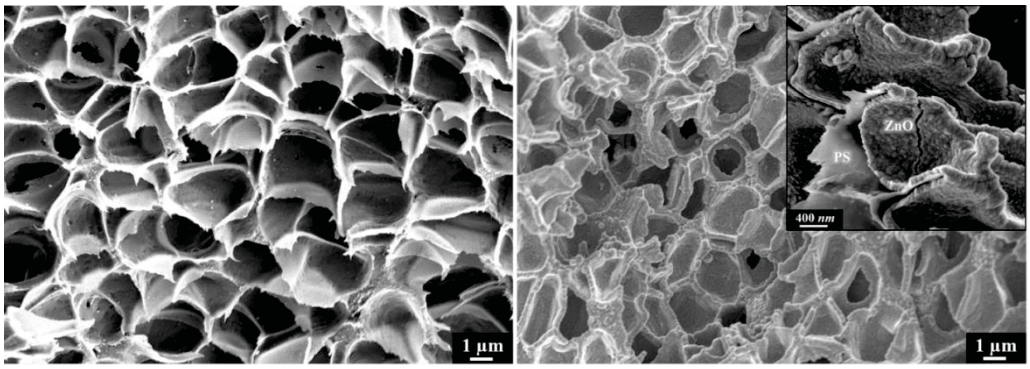

Figure A7-7: SEM images of a polystyrene foam (left) and polystyrene foam/ZnO hybrid material (right) after 10 deposition cycles. The inset clearly shows the existence of a thin ZnO-layer which is by chance detached from the PS pore at one position.

First experiments were performed by **project A5** using a polystyrene foam produced according to the NF-CID principle. For this proof of principle a foam with large mean pore diameter of $d_{pore} \approx 2$ µm was used to facilitate the infiltration of methanol solution of zinc acetate dihydrate, tetraethylammonium hydroxide (TEAOH) and polyvinyl pyrrolidone. Figure A7-7 shows the SEM images of a polystyrene foam (left) and polystyrene foam/ZnO hybrid material (right) after 10 deposition cycles performed at T=60°C. Comparing the two images it seems, that the diameter of the pore decreases as a consequence of the deposition of ZnO on the pore walls. Furthermore, the inset clearly shows the existence of a thin ZnO-layer which is by chance detached from the PS pore at one position. These experiments show, that the PS-foam is resistant to the methanol solution which indeed mineralizes the foam pores. The next series experiments will be performed studying the influence of the pore size of PS foam and its morphology, which can be easily varied adjusting the degree of open foam cells, on the mineralization process.

References

[1] B.P. Jelle, A. Gustavsen, R. Baetens, *J. Buld. Phys.* **2010**, *34*, 99-123.
[2] M. Knudsen, *Ann. Phys.* **1909**, *336*, 205–229.
[3] S. Kistler, *Nature* **1931,** *127*, 741.
[4] G. Reichenauer, U. Heinemann, H. Ebert, *Colloids and Surfaces A: Physicochem. Eng. Aspects* **2007**, *300*, 204–210.
[5] B. Krause, H.J.P Sijbesma, P. Mu, *Macromolecules* **2001**, *34*, 8792–8801.
[6] S. Siripurapu, J. Coughlan, R.J. Spontak, S. Khan, *Macromolecules* **2004**, *37*, 9872–9879.
[7] R. Butler, C.M. Davies, I. Cooper, *Adv. Mater.* **2001**, *13*, 1459–1463.
[8] T. Sottmann and R. Strey in *Fundamentals of Interface and Colloid Science* **2005**, Volume V, ed. J. Lyklema, Academic Press.
[9] R. Strey, A. Müller, Deutsche Patentanmeldung **2010**, *DE102010053064A1*.
[10] F. K. Hansen, J. Ugelstad, "Emulsion Polymerization" *Academic*; **1982**.
[11] K. Landfester, *Angew. Chem. Int. Ed.* **2009**, *48*, 4488.
[12] M. Antonietti, H.-P. Hentze, *Chem. Ing. Tech.* **1997**, *69*, 369.
[13] Y. Shieh, K. Liu, *J. Polym. Res.* **2002**, *9*, 107.
[14] P.D. Condo, K.P. Johnston, *J. Polym. Sci., Part B: Polym. Phys.* **1994**, *32*, 523.
[15] W. Ostwald, *Zeitschrift Für Physikalische Chemie* **1900**, *34*, 495–503.
[16] S. Egelhaaf, U. Olsson, P. Schurtenberger, J. Morris, H. Wennerström, *Physical Review. E* **1999**, *60*,5681–5684.
[17] M. von Smoluchowski, *Zeitschrift Für Physikalische Chemie* **1916**, *19*,129-135.
[18] P. Meakin, *Physica A*, **1991**, *171*, 1–18.
[19] L. Grassberger, PhD-Thesis *University of Cologne* **2016**, ISBN: 978-3-8439-2623-2.
[20] M. Teubner, R. Strey, *J. Chem. Phys.* **1987**, *87*, 3195-3200.
[21] G. Porod, “Small Angle X-ray Scattering“, O. Glatter, O. Kratky, **1982,** ISBN: 0-12-286280-5.
[22] J. Percus, G. Yevick, *Phys. Rev.* **1958,** *110*, 1-13.
[23] P. Atanasova, N. Stitz, S. Sanctis, J. H. M. Maurer, R. C. Hoffmann, S. Eiben, H. Jeske, J. Schneider, J. Bill, *Langmuir* **2015**, *31*, 3897–3903.

3.7.3.2 Project-related publications by participating researchers

[A7-1] R. Strey, T. Sottmann, M. Schwan, *German Patent* **2008,** 102 60 815.
[A7-2] M. Schwan, L. G. A. Kramer, T. Sottmann, R. Strey, *Phys. Chem. Chem. Phys*. **2010**, 12, 6247.
[A7-3] O. Holderer, M. Klostermann, M. Monkenbusch, R. Schweins, P. Lindner, R. Strey, D. Richter, T.Sottmann, *Phys.Chem.Chem.Phys.* **2011**, *13*, 3022.
[A7-4] M. Klostermann, T. Foster, R. Schwein, P. Lindner, O. Glatter, R. Strey, T. Sottmann, *Phys. Chem. Chem. Phys.* **2011**, *13*, 20289-20301.
[A7-5] M. Klostermann, R. Strey, T. Sottmann, R. Schweins, P. Lindner, O. Holderer, M. Monkenbusch, D. Richter, *Soft Matter* **2012**, *8*, 797-807.
[A7-6] A. Müller, Y. Pütz, R. Oberhoffer, N. Becker, R. Strey, A. Wiedenmann, T. Sottmann, *Phys. Chem. Chem. Phys.* **2014**, *16*, 18092−18097.
[A7-7] R. Schwering, L. Belkoura, R. Strey, T. Sottmann, X. Gong, H.-T. Davis, *SÖFW-Journal* **2009***, 135*, 43.
[A7-8] T. Foster, T. Sottmann, R. Schweins, R. Strey, *J. Chem. Phys.* **2008,** *128*, 054502.

3.7.4 Project plan

In summary, the research goals are organized in work-packages as follows:

- **WP1: Formations of colloidal crystals made of PS and PMMA nanoparticles of adjustable size**. The diameter d_{part} of polymeric nanoparticles is one important parameter to adjust the pore size d_{pore} of the nanofoam (Eq. 7). Thus, PS and PMMA particles with defined diameter d_{part} in the range from **$10 \leq d_{part}/nm \leq 50$** will be synthesized using emulsion, miniemulsion or microemulsion polymerization. In order to facilitate the formation of a colloidal crystal structure with only a small number of defects, special attention will be paid to the synthesis of monodisperse nanoparticles. As the colloidal crystal structure is obtained by a gentle drying of the nanoparticle dispersion evaporating the solvent, the influence of the drying procedure on the number of defects will be studied. The structure of nanoparticles and the colloidal crystal structure will be studied by **GPC, DLS, SAXS/SANS and SEM**.
- **WP2: Synthesis of PS and PMMA nanofoams with adjustable pore diameter $40 \leq d_{part}/nm \leq 250$.** In order to achieve this objective, the influence of important parameters of the NF-CID principle on the size d_{pore}, shape and polydispersity of the pores but also the morphology of the nanofoam (adjusting the degree of open foam cells) will be systematically studied. These parameters are the nanoparticle diameter d_{part}, the temperature, pressure and saturation time of the NF-CID principle as well as the exact procedure of the expansion step. Furthermore, in order to bypass potential weaknesses of the polymeric nanofoams, i.e. their instability with respect to hydrophobic solvents and high temperature as well as the limited pore size, the polymeric nanofoams will be further processed in **project A5** preparing mesoporous organic/inorganic hybrid materials with adjustable pore size ($d_{pore} \geq 25$ nm).
- **WP3: Structural characterization of nanoporous polymeric and organic/inorganic materials.** In order to use these two promising classes of tailor made substrates for the study of the effect of confined heterogeneous catalysts on the productivity and selectivity of catalytic reactions, the structure of the substrates has to be determined quantitatively. While the overall structure of the materials can be studied by SEM, inverse GPC and NMR-self-diffusion, detailed information will be obtained by neutron scattering, which allows for **highlighting different structural items by adjusting the contrast (scattering length densities)** accordingly. SANS and time-resolved SANS will be used to characterize the nanoporous structure of the substrates as well as the structural evolution during the NF-CID principle. Furthermore, we propose to study the **formation of the metal oxide layer** on a **flat polymeric substrate** and **on the pore walls of the nanofoam** by systematic **time-resolved *Grazing Incidence* (GI)SANS and SANS experiments**, respectively
- **WP4: Pore-selective epoxide functionalization of the polymeric nanofoams.** The pore surface will be functionalized in a first step by **hydroxylation**, e.g. using dilute solutions of hypochlorite or appropriate co-monomers (hydroxyl methyl styrene for PS). The degree of hydroxylation can be controlled by reaction time, reagent and co-monomer concentration, respectively. **Epoxide groups** will be introduced as **anchoring sites** via the reaction of a suitable epoxy compound with the hydroxylated surface. Polystyrene sulfonic acid will be used to ensure the presence of **anchoring sites only inside the pores**. To ensure that the polymeric nanofoam remains unchanged during both steps, SEM, SANS, inverse GPC, NMR-self-diffusion, and BET will be used. To quantify hydroxylation as well as the number of epoxy groups (inside the pores), solid state NMR and IR will be used. After that the functionalized materials will be provided for catalysis experiments.

3.7.4.1 WP1: Formations of colloidal crystals made of PS and PMMA nanoparticles of adjustable size.

In the initial phase of the proposed project, PS and PMMA particles with defined diameter d_{part} in the range from **$10 \leq d_{part}/nm \leq 50$** will be synthesized using emulsion, miniemulsion or microemulsion polymerization. In all NF-CID studies performed so far, nanoparticles are used, which were synthesized using emulsion polymerization. In order to synthesize smaller nanoparticles we will apply microemulsion polymerization. In a previous study[A7-7] we could synthesize small polyhexylmethacrylate (PHMA) nanoparticles exhibiting a small polydispersity (Figure A7-8, left) using a microemulsion consisting of H_2O/(sucrose/trehalose), HMA/EGDMA (ethylene glycol dimethacrylate) and the non-ionic surfactant

mixture of Lutensol XL 70 and Agnique PG 8105-G. The sugar solution was used to increase the viscosity and therewith decelerating diffusion dominated aging phenomena during the polymerization. Figure A7-8, right shows that the synthesis of polymeric particles with adjustable size between 10 ≤ d_{part}/nm ≤ 50 should be feasible simply by adjusting the mass fraction w_B of monomer (HMA) and performing the polymerization at the respective temperature of the emulsification failure boundary.

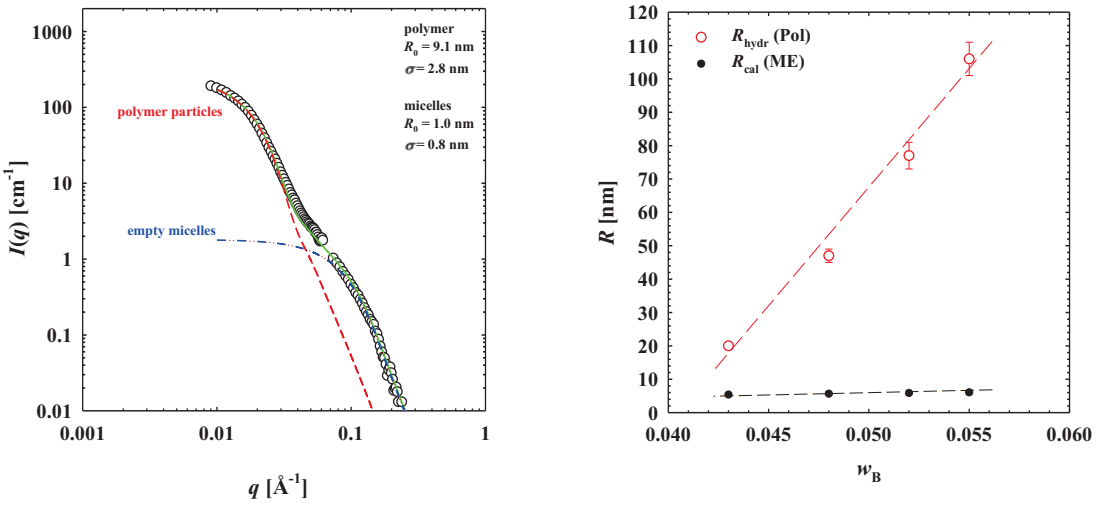

Figure A7-8: Left: SANS curve of a polymerized (using UV-light (λ = 370 nm) and the initiator Irgacure 819) microemulsion consisting of H_2O/(sucrose/trehalose), HMA/EGDMA (ethylene glycol dimethacrylate) and the non-ionic surfactant mixture Lutensol XL 70 and Agnique PG 8105-G. The analysis reveals the synthesis of polyhexylmethacrylate (PHMA) nanoparticles with a radius of R_0=9.1±2.8 nm which coexist with empty micelles. Right: Hydrodynamic radius R_{hyd}(pol) of the PHMA nanoparticles and the calculated radius R_{calc}(ME) of the HMA swollen micelles as a function of the mass fraction w_B of HMA at constant surfactant mass fraction. The linear dependence of R_{hyd}(pol) on w_B indicates, that the synthesis of polymeric particles with adjustable size should be feasible.

Thus, the studies of WP1 can start using the results obtained in [A7-7]. However, compared to emulsion polymerization, large amounts of surfactant are used which have to be removed before the formation of the colloidal crystal structure. In order to increase the amount of nanoparticles, the influence of the mass fraction w_B of monomer on the particle diameter should be studied at constant monomer/surfactant ratio. Furthermore, the synthesis is performed using 15wt% of the cross-linker EGDMA in the mixture of monomer and cross-linker. As preliminary experiments have shown, that the foaming of a highly cross-linked polymer melt is difficult, the influence of the amount of cross-linker on the particle diameter has also to be studied. Last but not least, the results on the synthesis of PHMA nanoparticle using microemulsion polymerization have to be transferred to PMMA and PS nanoparticles. Having synthesized polymeric nanoparticles of different size and polydispersity the influence of polydispersity and drying procedure on the colloidal crystal structure (number of defects) will be studied. In order to study the influence of the diameter of the polymeric nanoparticles and polydispersity on both the structure of the colloidal crystals as well as the polymeric nanofoams, selected experiments will be performed using commercially available nanoparticles. However, aside from the fact that these particles are very expensive, particles with diameter d_{part} smaller 20nm seem to be not available.
The nanoparticles and colloidal crystals will be characterized by **GPC, DLS, SAXS/SANS and SEM.** The synthesized polymeric nanoparticles and colloidal crystals produced in this work package will also be used in **project A5** to synthesize mesoporous oxides inverse opals.

3.7.4.2 WP2: Synthesis of PS and PMMA nanofoams with adjustable pore diameter 40 ≤ d_{part}/nm ≤ 250.

In order to ensure a reproducible synthesis of PS and PMMA nanofoams with a defined size d_{pore} (±5-10 nm) and polydispersity of the pores controlling also the morphology (adjusting the degree of open foam cells) a systematic study of the influence of the important parameters of the NF-CID principle on

the structural parameters of the nanofoam is indispensable. In table 1 the dependencies expected on the basis of preliminary studies including a recently performed time-resolved SANS experiments are compiled. However, up to now, a systematic study of the influence of the nanoparticle diameter d_{part}, the parameters temperature, pressure and saturation time which play a major role in the different steps of the NF-CID principle is not conducted. Furthermore, the influence of the nanoparticle properties itself, as the degree of crosslinking (which determines the foamability and chemical stability of the foam) and the polymerization co-monomers to functionalize the particle/foam weren't conducted.
In more detail, this work package is divided into two parallel sections: On the one hand, the colloidal crystals formed by the PS and PMMA particles synthesized in WP1 will be used to study the influence of particle properties (d_{part}, polydispersity, degree of crosslinking) on the pore diameter, polydispersity and morphology of the foam. On the other hand, selected colloidal crystals with similar structure will be used to study the influence of the process parameters temperature, pressure and saturation time. Furthermore, it will be investigated to which extent the exact procedure of the expansion step have an influence on the nanofoam structure (see Figure A7-6). The polymeric nanofoams will be characterized by **SEM, SANS, inverse GPC, NMR-self-diffusion, and BET.**

Table 1: Expected influence of the so-far[9,A7-8] identified important parameters particle diameter d_{part}, temperature T, pressure p, saturation time t_{sat} and rate of expansion $\Delta p/\Delta t$ of the NF-CID principle on the solubility of CO_2 in the PS and PMMA nanoparticles, the glass temperature T_g^*, the ratio N_{part}/N_{CO2} of the number of particles and CO_2-nanodroplets, the diameter d_{CO2} of the latter, their diffusion coeffecient D_{CO2} and on the diameter d_{pore} of the pore.

	$\phi_{CO_2,\,mon}$	T_g^*	$\frac{N_{part}}{N_{CO_2}}$	d_{CO_2}	D_{CO_2}	d_{pore}
↑ d_{part}	—	—	↓	↑	↓	↑
↑ $T > T_g^*$	↑	↓	↑	↑	↑	↑
↑ p	↑	↓	↑	↑	↑	↑
↑ $t_{sat} > t_{sat}^*$	—	—	↑	↑	—	↑
↑ $\Delta p / \Delta t$						↓

The PS and PMMA nanofoams synthesized within this work-package will be used twofold: After proper functionalization in WP4 the polymeric nanofoams will be used in the catalytic **project B3.** In order to bypass potential weaknesses of the polymeric nanofoams, i.e. their instability with respect to hydrophobic solvents and high temperature as well as the limited pore size, the polymeric nanofoams will be further processed in **project A5** preparing mesoporous organic/inorganic hybrid materials with adjustable pore size (d_{pore}≥25 nm). Therefore, the open-cellular polymeric nanofoams will be used as template, adjusting the pore size by the stepwise deposition of layers of metal oxide on the pore walls. After proper functionalization of these nanoporous organic/inorganic hybrid materials will be used in **projects B2** and **B3.** The reliable and precise variation of the pore diameters will allow systematic studies of the confinement effects in molecular heterogeneous catalysis, mimicking the unprecedented catalytic performance of enzymes.

3.7.4.3 WP 3: Structural characterization of nanoporous polymeric and organic-inorganic materials. While the overall structure of the two classes of nanoporous materials can be studied by SEM, inverse GPC and NMR-self-diffusion, detailed structural information can be obtained by neutron scattering, which allows for highlighting different structural items by adjusting the scattering length densities of the components accordingly (Figure A7-9, left). Thus, this work package deals with elaborate time-resolved *Grazing Incidence* (GI) SANS (Figure A7-9, right) and SANS experiments. Therefore we will apply for beamtime at the neutron facilities *Institut Laue Langevin* (ILL, Grenoble) and *FRM2* (Munich).
In more detail, we will further elucidate the structural transitions occurring during the NF-CID principle. Here we will concentrate on the formation of selected highly porous polymeric materials (nanofoams, exhibiting small pore diameter and nanofoams, which are produced using different expansion procedures). However, the central task of this work package is the investigation of the formation of organic-inorganic hybrid materials produced in **project A5**. In order to study whether the formation of the metal oxide layer depends on the geometry or is confinement dependent, time-resolved SANS

experiments will be performed on flat polymeric substrates and polymeric nanofoams. The results will be valuable input for the simulation of the metal oxide layers on polymer surfaces. **Project C6** which will begin in the first funding period and should deliver in the second funding period whether the nucleation depends on the geometry or is confinement dependent.

Figure A7-9: Left: Contrast variation of enabling to record the formation of the metal oxide layer on a flat polymeric substrate and on the pore walls of the nanofoam. Of particular interest is the "Shell" contrast highlighting the ZnO layer (ρ(ZnO)=4.77·10^{10} cm^{-2}). It can be easily adjusted matching the scattering length densities of the polymer (ρ(PS)=1.41·10^{10} cm^{-2}) and the methanol solution using a mixture of protonated (ρ(CH_3OH)=-0.37·10^{10} cm^{-2}) and deuterated (ρ(CD_3OD)=-5.81·10^{10} cm^{-2}). Right: Schematic representation of Gracing Incidence (GI)-SANS setup allowing for recording the formation of the metal oxide layer on a flat polymeric substrate.

3.7.4.4 WP4: Pore-selective epoxide functionalization of the polymeric nanofoams.

The pore surface will be functionalized by hydroxylation, e.g. using dilute solutions of hypochlorite or appropriate co-monomers (hydroxyl methyl styrene for PS). The degree of hydroxylation can be controlled by reaction time, reagent and the co-monomer concentration, respectively. Following the route used in **project A6**, epoxide groups will be introduced as anchoring sites via the reaction of a suitable epoxy compound (epichlorohydrin) with the hydroxylated surface. Polystyrene sulfonic acid, which can't enter the pores, but will react with those epoxy groups being positioned at the macroscopic surfaces of the nanofoam, will be used to ensure the presence of anchoring sites only inside the pores. To ensure that the polymeric nanofoam remains unchanged during both steps, SEM, SANS, inverse GPC, NMR-self-diffusion, and BET will be used. To quantify hydroxylation as well as the number of epoxy groups (inside the pores), solid state NMR and IR will be applied. After that the epoxy groups serve as anchoring sites for linker molecules or linker group-bearing Rh-catalysts. Thereby, for selected systems small angle neutron scattering (SANS) will be performed to elucidate the structure of the catalyst system, e.g. linker or Rh center and its location with respect to the pore surface via contrast matching experiments. First proof of principle Rh-catalyzed 1,4-additions of boronic acids to enones will be performed using polymeric nanofoams exhibiting a pore diameter d_{pore} smaller than 50 nm (**project B3)**. Furthermore, the use of tailor-made microemulsions is envisaged to avoid a demixing of the reaction mixture inside the pores.

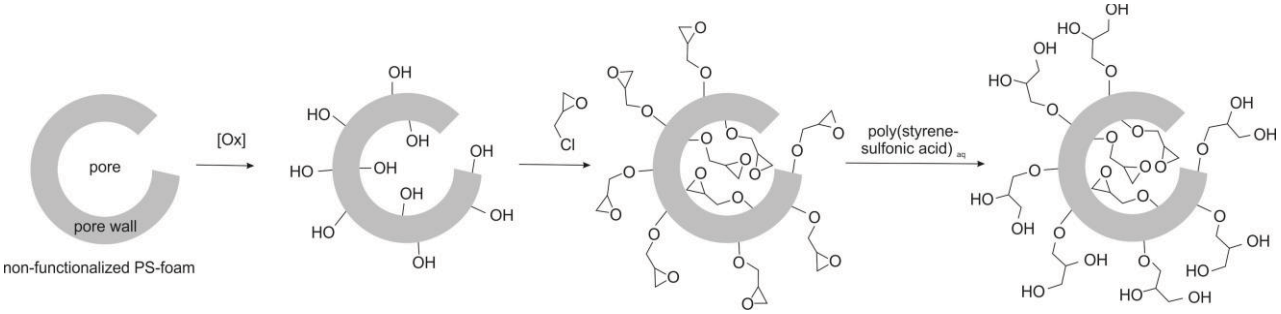

Figure A7-10: Schematic functionalization process of the PS nanofoams. Surface hydroxylation enables nucleophilic reaction with an epoxide-bearing reagent. Application of a polymeric acid only retains the epoxides inside the pores – the macromolecule is too large to migrate into these.

Time Schedule:

	2018		2019				2020				2021				2022		
	Q3	Q4	Q1	Q2	Q3	Q4	Q1	Q2	Q3	Q4	Q1	Q2	Q3	Q4	Q1	Q2	
T1 A																	Synthesis & characterization of mono-disperse PS & PMMA nanoparticles of defined size $10 \leq d_{part}/nm \leq 50$ and polydispersity – transfer to **project A5**
T1 B																	Formation of colloidal crystals: Influence of polydispersity & drying – transfer to **project A5**
T2 A																	Synthesis of nanofoams I: Influence of temperature, pressure & saturation time – transfer to **project A5**
T2 B																	Synthesis of nanofoams II: Influence of the exact procedure of the expansion step – transfer to **project A5**
T2 C																	Synthesis of nanofoams III: Influence of particle diameter – transfer to **project A5**
T3																	Structural characterization of nanoporous polymeric and organic-inorganic materials: SANS/GISANS – cooperation with **projects A5, C6 and B3**
T4																	Pore-selective epoxide functionalization of the polymer-ric nanofoams – cooperation & transfer to **project B3**

3.7.4.5 Methods applied:

The diameter of the polymeric nanoparticles and their polydispersity will be studied mainly by DLS, for selected samples by SAXS/SANS. The synthesis of the PS and PMMA nanofoams (steps 3-5 of the NF-CID principle) will be performed in specially developed high-pressure cells. The morphology of the colloid crystal structure as well as of the synthesized nanofoams and organic-inorganic hybrid materials will be determined in cooperation with **project C3** using SEM. The quantitative determination of the pore diameter and polydispersity will be achieved for selected samples using SANS and for materials with small pore diameter in cooperation with **project A4** using SAXS. The porosity of the materials will be determined by gas adsorption (BET), as outlined in **project A6**. In order to determine the morphology of the nanofoam, i.e. to determine the connectivity of the nanofoams PFG-NMR will be used in cooperation with **project C1**. Time-resolved SANS (specially developed high-pressure SANS cell) will be used to elucidate the structural transitions during the NF-CID procedure. Contrast variation SANS experiments will be performed to characterize the structure of the organic-inorganic hybrid materials synthesized by **project A5**. In order to study whether the formation of the metal oxide layer depends on the geometry or is confinement dependent, time-resolved SANS experiments will be performed on flat polymeric substrates and polymeric nanofoams. The results will be valuable input for the simulation of the metal oxide layers on polymer surfaces which will be performed by **Project C6**. Proposals for SANS/GISANS-beamtime will be submitted to the neutron facilities *Institut Laue Langevin* (Grenoble) and *FRM2* (Munich). IR/Raman will quantify the introduction of functional groups, while solid state NMR (**project C1)** will differentiate between inside/outside pore functionalization.

3.7.4.6 Vision:

By the end of the first funding period we have obtained detailed insights into the role of the different parameters (d_{part}, T, p, t_{sat}, $\Delta p/\Delta t$) of the NF-CID principle. Based on this knowledge we will be able to provide a unique library of tailored PS and PMMA nanofoams with adjustable pore diameter $40 \leq d_{part}/nm \leq 250$ with a resolution of 5-10 nm and adjustable morphology. We will have provided tailored open-cellular PS and PMMA as templates to the **project A5**, where the pore size is adjusted to $d_{pore} \geq 25$ nm by the stepwise deposition of layers of metal oxide on the pore walls with an accuracy of ± 3 nm. Last but not least, we will have found reliable methods to functionalize the inner surface of the pores of the nanofoam according to the particular needs of the catalytic **projects B2** and **B3**.

With the experience and knowledge obtained in the first funding period we envisage to further optimize or adapt the NF-CID principle to reduce both the pore diameter and the resolution towards 20 nm and 2nm, respectively. Furthermore, we plan to identify the parameters, which allow for the synthesis of a bimodal foam structures, the large ones (several μm) being responsible for the transport of linker, catalyst, reactants and products into and out the small mesopores.

3.7.5 Role within the collaborative research center

In comparison to the other materials synthesized in this research center, polymeric nanofoams provide prominent properties, as a low density, high surface area and easily up-scalable preparation (up to m^3 per day). Furthermore, the foam morphology can be easily varied adjusting the degree of open foam cells. Thus, functionalized polymeric nanofoams with adjustable pore diameters, polydispersity and morphology are expected to complement other materials and thus will provide additional structural features to study the influence of the confinement of molecular heterogeneous catalysts on the productivity and selectivity of catalytic reactions. This subproject collaborates with all three projects areas of this research center.

The **project A5** will use our tailored open-cellular PS and PMMA as templates to synthesize nanoporous organic/inorganic hybrid materials with a pore diameter of $d_{pore} \geq 25$ nm and an accuracy of ± 3nm. We will functionalize the materials according to the needs of the **project B3** and provide sufficient amounts of support materials tailored for their use in the catalytic studies and for the systematic studies of confinement effects. The spatial distribution of functional groups at the inner surface of the mesopores will be investigated together with **project C1**. Furthermore, our results of advanced SANS studies and analysis techniques (i.e., dimensions and form factors of pores as well as metal oxide films) provide valuable input for the simulation study whether the nucleation and formation of the metal oxide layers on polymer surfaces depends on the geometry or is confinement dependent **(Project C6).** Furthermore, dynamic and static light scattering (DLS &SLS) will be used to characterize the structure and structural transitions of triblockcopolymer micelles used in **project A6** as direct precursors of ordered mesoporous carbons (OMC).

3.7.6 Differentiation from other funded projects

The work described in A7 is not subject or partly subject of this research

3.7.7 Project funding

3.7.7.1 Previous funding

This project is currently not funded and no funding proposal has been submitted.

3.7.7.2 Requested funding

Funding for	2018		2019		2020		2021		2022		2018-2022	
Staff	Quantity	Sum	Quantity	Sum	Quantity	Sum	Quantity	Sum	Quantity	Sum	Quantity	Sum
PhD student, 67%	1	21,600.-	1	43,200.-	1	43,200.-	1	43,200.-	1	21,600.-	1	172,800.-
Total		21,600.-		43,200.-		43,200.-		43,200.-		21,600.-		172,800.-
Direct costs	Sum		Sum		Sum		Sum		Sum		Sum	
consumables	6,000.-		12,000.-		12,000.-		12,000.-		6,000.-		48,000.-	
Total	6,000.-		12,000.-		12,000.-		12,000.-		6,000.-		48,000.-	
Major research instrumentation	Sum		Sum		Sum		Sum		Sum		Sum	
Hydraulic pressure balance CPB5800 (WIKA)	10,900.-		-		-		-		-		10,900.-	
Total	10,900.-		-		-		-		-		10,900.-	
Grand total	38,500.-		55,200.-		55,200.-		55,200.-		27,600.-		231,700.-	

(All figures in EUR)

3.7.7.3 Requested funding for staff

	Sequential no.	Name, academic degree, position	Field of research	Department of university or non-university institution	Project commitment in hours per week	Category	Funding source
Existing staff							
Research staff	1	Thomas Sottmann, apl.-Prof. Dr., Team Leader	Physical Chemistry, Scattering Techniques,	Institute of Physical Chemistry	8		University
Requested staff							
Research staff	2	N. N.; M. Sc.	Physical Chemistry, Scattering Techniques	Institute of Physical Chemistry		PhD student, 67%	
Research staff	3	Research assistant	Physical Chemistry, Scattering Techniques	Institute of Physical Chemistry			

Job description of staff (supported through existing funds):
1
Apl. Professor, Team leader of the group “Self-Assembly at the Nanoscale”, permanent contract

Job description of staff (requested funds):
2
PhD student, work packages 1-4
3
Research assistants. **Justification:** The research assistants are supposed to support the PhD-student in the synthesis and characterization of PS and PMMA nanoparticles with defined diameter applying emulsion and microemulsion polymerization (WP1). Furthermore, it is planned that the research assistants contribute to the study of the influence of the NF-CID process parameters on the size, shape and polydispersity of the pores as well as the morphology of the nanofoams (WP2). Finally, the research assistants are supposed to support the PhD-student in the pore selective functionalization of the nano-foams with epoxide (WP4).

3.7.7.4 Requested funding of direct costs

	2018	2019	2020	2021	2022
Uni Stuttgart: existing funds from public budget	0.-	0.-	0.-	0.-	0.-
Sum of existing funds	0.-	0.-	0.-	0.-	0.-
Sum of requested funds	6,000.-	12,000.-	12,000.-	12,000.-	6,000.-

(All figures in EUR)

Consumables for financial year 2018

Chemicals, consumables, monomers, polymeric nanoparticles, membranes and seals for pressure cells, solvents, gases (N_2, CO_2)	EUR	6,000.-

Consumables for financial year 2019

Chemicals, consumables, monomers, polymeric nanoparticles, membranes and seals for pressure cells, solvents, gases (N_2, CO_2), deuterated monomers	EUR	12,000.-

Consumables for financial year 2020

Chemicals, consumables, monomers, membranes and seals for pressure cells, solvents, gases (N_2, CO_2), deuterated monomers	EUR	12,000.-

Consumables for financial year 2021

Chemicals, consumables, monomers, membranes and seals for pressure cells, solvents, gases (N_2, CO_2), deuterated monomers	EUR	12,000.-

Consumables for financial year 2022

Chemicals, consumables, monomers, membranes and seals for pressure cells, solvents, gases (N_2, CO_2), deuterated monomers	EUR	6,000.-

3.7.7.5 Requested funding for major research instrumentation

Equipment for financial year 2018

Hydraulic pressure balance CPB5800 (WIKA) to calibrate the pressure probes of the four pressure cells essential for **project A7**. Three pressure cells (sample volume 3 ml) will be used in WP2 to synthesize the polymeric nanofoams as well as studying the influence of the process parameters of the NF-CID principle on the size, shape and polydispersity of the pores but also the morphology of the nanofoams. Using the high pressure SANS cell we will elucidate the structural transitions occurring during the NF-CID principle by time-resolved SANS measurements (WP4). So far the pressure probes of all four pressure cells are calibrated every three to four month at the University of Cologne (Prof. R. Strey, Department Chemistry). Due to the time-consuming and costly transport as well as the retirement of Prof. Strey at the end of 2015 the access of the Cologne pressure balance becomes increasingly difficult. Thus, the acquisition of a pressure balance is indispensable to ensure a correct pressure measurement.	EUR	10.900.-

3.8 Project B1

3.8.1 General Information about Project B1

3.8.1.1 „*Inner-pore*“-tethered tetraaza-ruthenium-complexes for the directed hydrogen-autotransfer catalysis

3.8.1.2 Research Areas
301-02 Organic Molecular Chemistry

3.8.1.3 Principal Investigator
Plietker, Bernd J., Prof. Dr., born 22. 01. 1971, male, German
Professor für Organische Chemie, Institut für Organische Chemie
Universität Stuttgart, Pfaffenwaldring 55, 70569 Stuttgart
Tel.: 0711/685-64283
E-Mail: bernd.plietker@oc.uni-stuttgart.de
Tenured professor W3

3.8.1.4 Legal Issues
This project includes

1.	research on human subjects or human material.	no
2.	clinical trials	no
3.	experiments involving vertebrates.	no
4.	experiments involving recombinant DNA.	no
5.	research involving human embryonic stem cells.	no
6.	research concerning the Convention on Biological Diversity.	no

3.8.2 Summary
The H_2-autotransfer catalysis (also termed “borrowing hydrogen”) has attracted considerable interest within the field of homogenous catalysis. The in-situ formation of a ketone/aldehyde through catalytic dehydrogenation of a secondary/primary alcohol, its subsequent use in condensation chemistry, and the “re-transfer” of the catalyst-bound hydrogen to the organic condensation product leads to products that are commonly obtained through the application of classical substitution reactions using pre-activated alcohols. Water is formed as the only by-product, which makes this type of catalytic transformation particularly attractive. The reversibitly of the condensation reaction has been recognized as one of the major issues connected with the degree of product formation. This is due to the fact that the conversion of the alcohol to the final product goes hand in hand with the formation of water, which acts as a competing nucleophile in the condensation step. In order to avoid these problems, an excess of the active nucleophile is usually added, however, this strategy limits the practicabilty of this catalytic concept. Within the context of this research collaboration we consider this mutistep process to be an interesting model reaction to study potential confinement effects. Through the use of polar-protic pores of different diameters and immobilized (N,N,N,N)(P)-Ru-catalysts and an aprotic solvent we aim to study the influence of (water) diffusion from the reactive (aprotic) catalyst and the aprotic intermediates to the pore surface. In an ideal case diffusion is faster than the dehydrogenation/hydrogenation reactions rendering the condensation reaction to be irreversible which should result in a clean reaction devoid of excess of any reagent at signifcantly lower temperature. Different materials with different pore geometries/porosities/hydrophilicities will be employed. The solvent polarity within the pore will be analyzed through combined use of quantumchemical simulation and spectroscopy. These results will be alligned with the experimental outcome of the catalytic transformations and lead to a mechanistic model for the influence of confinement effects on H2-autotransfer catalysis.

3.8.3 Research rationale

3.8.3.1 Current state of understanding and preliminary work

Within the past 10 years the concept of H_2-autotransfer catalysis has been applied to a range of organic transformations.[1] The in-situ activation of an alcohol via catalytic dehydrogenation to provide small quantities of a carbonyl compound sets the stage for adapting the plethora of known carbonyl chemistry.[2] Methods for the direct transformation of the carbonyl group via condensation reaction with nucleophiles or pronucleophiles (amines, malonic acid derivatives, ylides (Wittig reagents), etc.) were shown to be applicable for a fast in-situ transformation of the intermediate aldehyde/ketone. Moreover, in-situ deprotonation at the α-carbon of the intermediate ketone/aldehyde set the stage for atom-bond formations adjacent to the reactive carbonyl group (e.g. aldol condensation, etc.).[3]

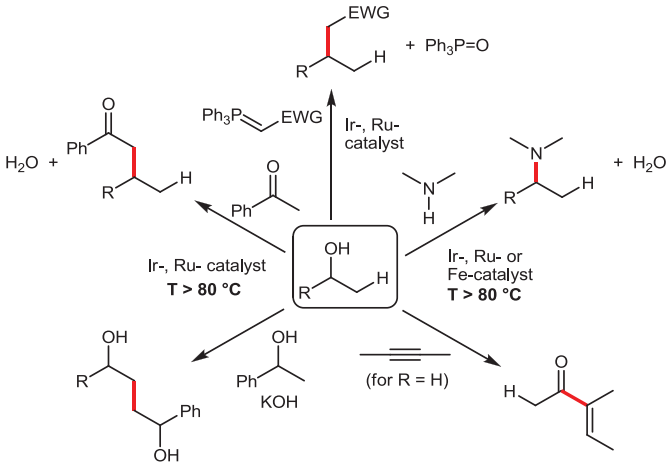

Figure B1-1. H_2-autotransfer catalysis – representative examples.

In the fast majority, Ir-based complexes were shown to be the most active catalysts.[4-8] Within recent years however, Ru-[9-12] and, most recently, also Fe-based catalysts[13-16] were reported to be efficient in this type of catalysis. Independent on the type of catalyst employed in these studies, in the vast majority of reports an excess of the condensation reagent appeared to be necessary in order to obtain high chemical yields.

In 2013 the group of Gao and Hou reported an interesting catalyst system, in which an Ir-NHC-complex was immobilized on SBA-15 (a mesoporous silica material with a pore size of 5-8 nm).[17,18] This system was employed in H_2-autortransfer catalysis using different amines and alcohols. Excellent catalytic turnover numbers and chemical yields were reported. The catalyst system was used up to twelve times without significant loss of activity. However, the authors did not report a inner-pore functionalization, but rather immobilized the catalyst in an ill-defined way both outside and inside the pores. Moreover, the study of confinement effects was not part of this report. Nevertheless, the material is compatible with the reaction conditions, the multifold use of the catalyst system underlines the preparative use of heterogenous molecular catalysis, and most importantly, different from most literature reports equimolar amounts of the substrates were employed. As compared to the corresponding transformation using the homogenous molecular Ir-complex about 10 – 15 % higher yields were obtained with the Ir-SBA-15 hybride catalyst.

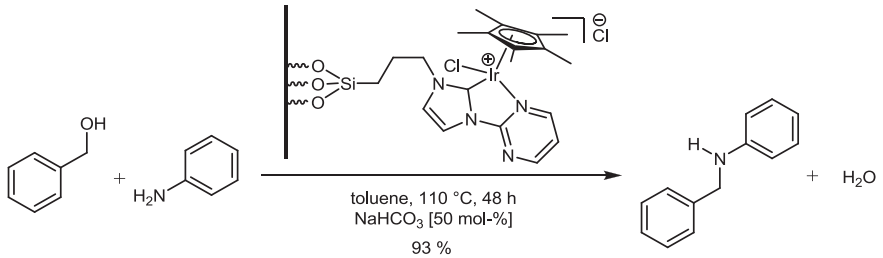

Figure B1-2. H_2-autotransfer catalysis in an Ir-SBA-15-catalyst system.

Research in the Plietker-group focusses on the development of Ru-[B1-1,B1-2] or Fe-based catalytic systems[B1-3,B1-4,B1-5] and their application in total synthesis[B1-6]. Apart from our intense research activities in the field of Fe-catalysis methods for Ru-catalyzed C-H-activations and dehydrogenations and hydrogenations using a tetradentate (PNNP)-ligand scaffold were developed.[B1-7,B1-8] In line with the afore mentioned resarch activities, we developed recently a novel type of cationic (N,N,N,N)(P)Ru-complexes for the H_2-autotransfer catalysis[B1-9,B1-10]. The underlying idea of the catalyst design was the creation of very lipophilic monodentate metal complex able to efficiently dehydrogenate alcohols allows to effectively remove water (from the condensation step) and to shift the equilibrium between aldehyde and imine towards the imine. Indeed, this idea proved successful. A set of different (N,N,N,N)(P)Ru-complexes was synthesized and tested for their activity. Moreover, through the use of quantumchemical methods the HOMO-LUMO-gaps of these complexes were calculated and shown to are proportional to the experimentally derived redox potential. Furthermore, it was shown that there is an optimum redox potential at 0.4 – 0.45 V (vs. $FcH^{0/+}$), a result that defines the starting point for a rational in-silico design of catalysts (Figure B1-3).

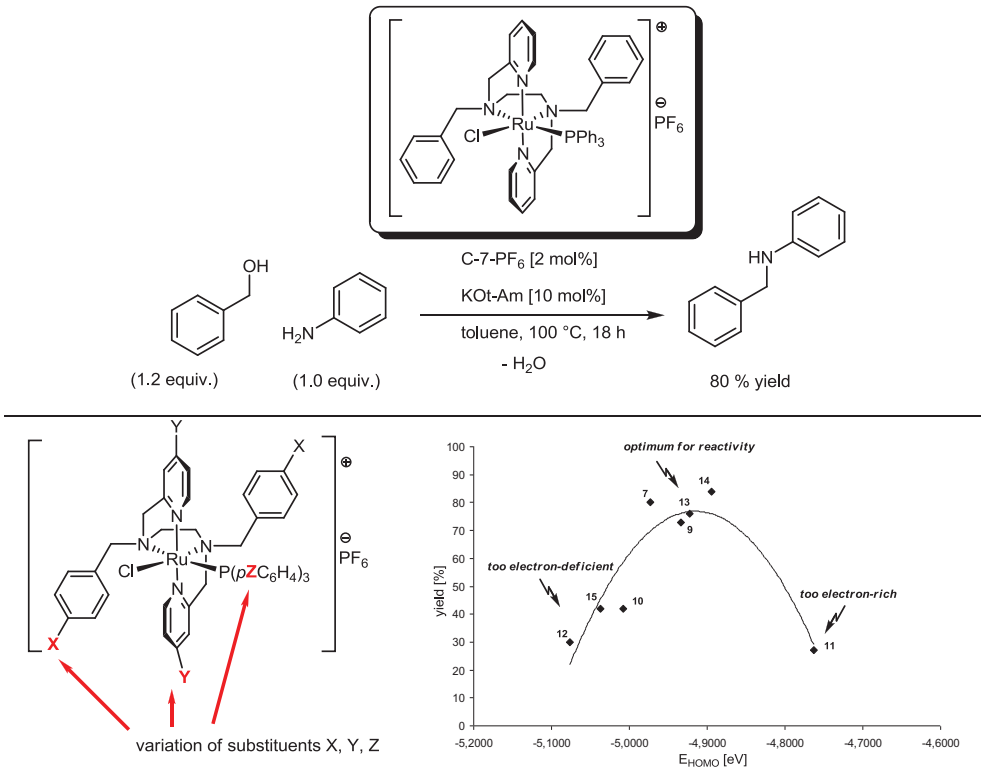

Figure B1-3. H_2-autotransfer catalysis by (N,N,N,N)(P)Ru-complexes.

References

[1] G. E. Dobereiner, R. H. Crabtree, *Chem. Rev.* **2010,** *110,* 681 – 703.
[2] M. H. S. A. Hamid, P. A. Slatford, J. M. J. Williams, *Adv. Synth. Catal.* **2007**, *349*, 1555 – 1575.
[3] F. Huang, Z. Liu, Z. Yu, *Angew. Chem. Int. Ed.* **2016**, *55*, 862 - 875.
[4] P. J. Black, G. Cami-Kobeci, M. G. Edwards, P. A. Slatford, M. K. Whittlesey, J. M. J. Williams, *Org. Biomol. Chem.*, **2006**, *4*, 116 – 125.
[5] O. Saidi, A. J. Blacker, M. M. Farah, S. P. Marsden, J. M. J. Williams, *Angew. Chem. Int. Ed.* **2009**, *48*, 7375 – 7378.
[6] L. K. M. Chan, D. L. Poole, D. Shen, M. P. Healy, T. J. Donohoe, *Angew. Chem. Int. Ed.* **2014**, *53*, 761 – 765.
[7] X. Quan, S. Kerdphon, P. G. Andersson, *Chem. Eur. J.* **2015**, *21*, 3576 – 3579.
[8] B. Blank, R. Kempe, *J. Am. Chem. Soc.* **2010**, *132*, 924.
[9] M. H. S. A. Hamid, C. L. Allen, G. W. Lamb, A. C. Maxwell, H. C. Maytum, A. J. A. Watson, J. M. J. Williams, *J. Am. Chem. Soc.* **2009**, *131*, 1766 - 1774.
[10] N. J. Oldenhuis, V. M. Dong, Z. Guan, *J. Am. Chem. Soc.* **2014**, *136*, 12548 - 12551.
[11] K. O. Marichev, J. M. Takacs, *ACS Catal.* **2016**, *6*, 2205 - 2210.

[12] M. L. Buil, M. A. Esteruelas, J. Herrero, S. Izquierdo, I. M. Pastor, M. Yus, *ACS Catal.* **2013**, *3*, 2072 - 2075.
[13] Y. Zhao, S. W. Food, S. Saito, *Angew. Chem. Int. Ed.* **2011**, *50*, 3006 – 3009.
[14] A. Pagnoux-Ozherelyeva, N. Pannetier, M. D. Mbaye, S. Gaillard, J.-L. Renaud, *Angew. Chem. Int. Ed.* **2012**, *51*, 4976 – 4980.
[15] T. Yan, B. L. Ferringa, K. Barta, *Nat. Commun.* **2014**, *5*, 5602 (doi: 10.1038/ncomms6602).
[16] K. P. J. Gustafson, A. Guđmundsson, K. Lewis, J.-E. Bäckvall, *Chem. Eur.J.* **2017**, *23*, 1048 – 1051.
[17] D. Wang, X.-Q. Guo, C.-X. Wang, Y.-N. Wang, R. Zhong, X.-H. Zhu, L.-H. Cai, Z.-W. Gao, X.-F. Hou, *Adv. Synth. Catal.* **2013**, *355*, 1117 - 1125.
[18] This system was most recently investigated using advanced ^{15}N NMR-spectroscopy: K. V. Kovtunov, L. M. Kovtunova, M. E. Gemeinhardt, A. V. Bukhtiyarov, J. Gesiorski, V. I. Bukhtiyarov, E. Y. Chekmenev, I. V. Koptyug, B. M. Goodson, *Angew. Chem. Int. Ed.* **2017**, *56*,10433 – 10437.

3.8.3.2 Project-related publications by participating researchers

[B1-1] M. Neisius, B. Plietker, *Angew. Chem. Int. Ed.* **2009**, 48, 5752 – 5755.
[B1-2] T. Schabel, B. Plietker, *Chem. Eur. J.* **2013**, *19*, 6938 - 6941.
[B1-3] J. E. M. N. Klein, B. Miehlich, M. S. Holzwarth, **M. Bauer**, M. Milek, M. M. Khusniyarov, G. Knizia, H.-J. Werner, B. Plietker, *Angew. Chem. Int. Ed.* **2014**, *53*, 1790 - 1794.
[B1-4] J. E. M. N. Klein, G. Knizia, B. Miehlich, **J. Kästner**, B. Plietker, *Chem. Eur. J.* **2014**, *20*, 7254 - 7257.
[B1-5] I. Alt, B. Plietker, *Angew. Chem. Int. Ed.* **2016**, *55*, 1519 – 1522.
[B1-6] N. Biber, K. Möws, B. Plietker, *Nature Chemistry* **2011**, *3*, 938 - 942.
[B1-7] S.-F. Hsu, B. Plietker, *ChemCatChem* **2013**, *5*, 126 - 129.
[B1-8] S.-F. Hsu, S. Rommel, P. Eversfield, K. Muller, E. Klemm, W. R. Thiel, B. Plietker, *Angew. Chem. Int. Ed.* **2014**, *53*, 7074 – 7078.
[B1-9] D. Weickmann, W. Frey, B. Plietker, *Chem. Eur. J.* **2013**, *19*, 2741 - 2748.
[B1-10] D. Weickmann, B. Plietker, *ChemCatChem* **2013**, *5*, 2170 - 2173.

3.8.4 Project plan

The H_2-autotransfer catalysis is a multi-step transformation of catalytic dehydrogenation-condensation-hydrogenation, in which alcohols are directly transformed into e.g. amines without the use of preactivating steps. The underlying vision of **project B1** is sketched in Figure B1-4.

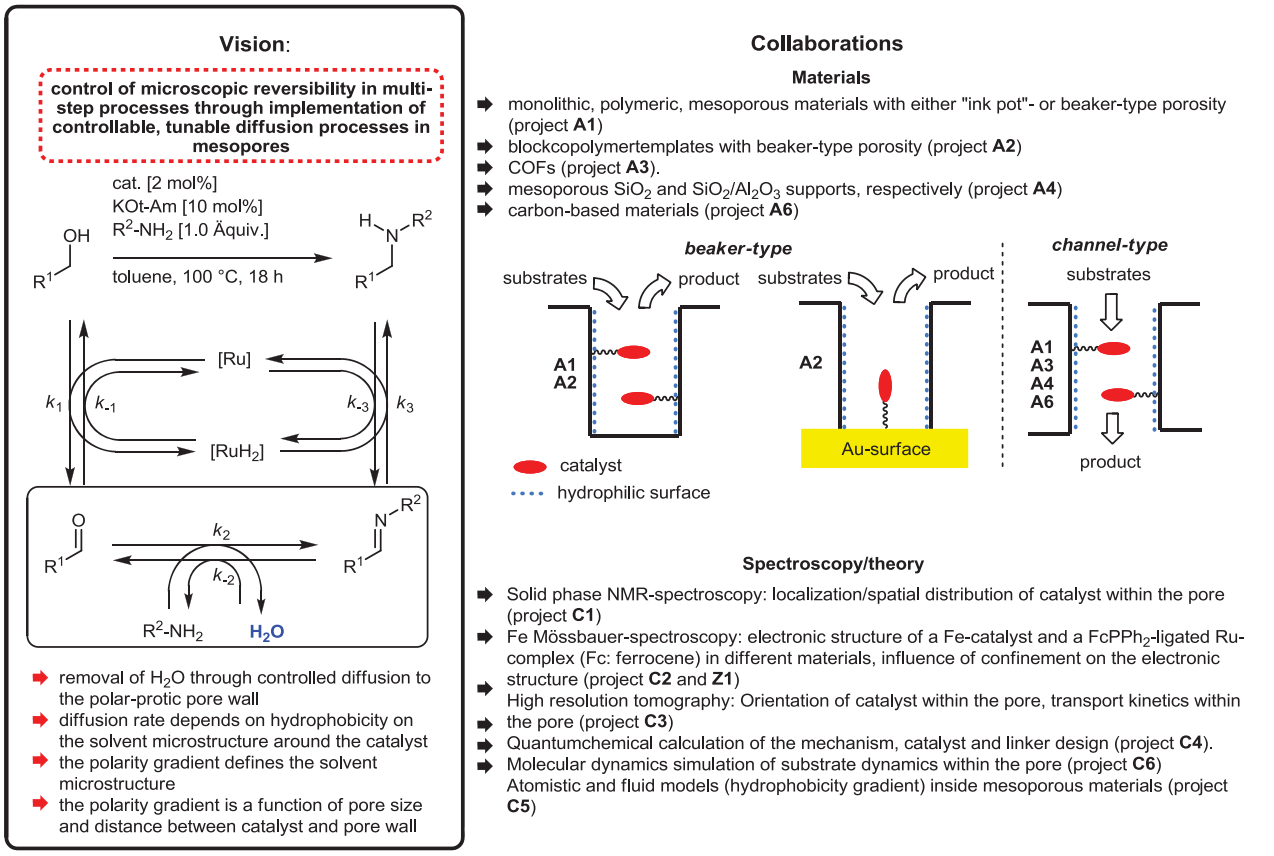

Figure B1-4. Research vision and collaborations.

The initial catalytic dehydrogenation leads to the formation of small (equimolar to catalyst) quantities of an aldehyde/ketone. This intermediate product reacts with e.g. an amine in an condensation reaction to give water and an imine. The latter compound is hydrogenated by the metal-hydride catalyst in solution. In the majority of reported cases this multi-step transformation performs well unless an excess of the condensating reagent (e.g. the amine) is present. The excess of amine is a pre-requisite to get satisfying yields and turnover numbers. However, if equimolar amounts of amine (equimolar to the starting material) are used, the condensation reaction reaches an equilibrium resulting in a formal stop of the reaction. As a consequence, a plethora of methods are reported in which the condensating agent (e.g. the amine) is used in a multi-fold excess to ensure a fast and irreversible condensation reaction. The (N,N,N,N)(P)Ru-complex developed in our group has an octahedral configuration and is ligated by five very lipophilic ligands (bep (bis-benzyl-bis-picolyl-ethylenediamine) and triarylphopshine). The ketone formed in the first step does not leave the catalyst environment, thus the condensation reaction takes place within the ligand sphere of the catalyst (maybe even catalyzed by the Ru-complex). This lipophilic microenvironment created by the ligand sphere around the catalytic center guarantees a fast removal of water molecules. This catalyst design allowed the use of equimolar amounts of both starting materials (alcohol and amine).

Within **project B1** we would like to accelerate the fast diffusion of water from the metal center by hybridizing the molecular catalyst into a mesopore with polar-protic pore walls (Figures B1-4 and B1-5). Diffusion of water is a function of hydrophobicity created at the catalytic center and its direct microenvironment (solvent cage). The hydrophilicity of the material is a function of pore size, pore geometry, and hydroylation of the inner pore-wall. *Connecting both modules (material plus catalytic complex) using defined spacers and different pore geometries (channels vs. beakers) would allow to control the water diffusion process in such a way that the diffusion rate is becoming part of the overall kinetic orchestration in H_2-autotransfer processes*.

Depending on the material different pore diameters and pore geometries are accessible. As pointed out above, hydrophilicity of the pore wall is expected to be a key factor in H_2-autotransfer catalysis in this particular set-up. Smaller pores (< 10 nm) will have a steeper solvent-to-water gradient which might be beneficial for the water diffusion process, however these pores add significant steric constraints to the catalyst/substrate and alter their mobility/electronic configuration. The effect of these constraints and (water) diffusion lengths will be studied systematically both in experiment (TON, TOF), spectroscopy and theory. Different pore geometries (beaker, and channel) will be tested (Figure B1-4). Whereas the 2D-structure of the pore is important in order to tune steric constraints, solvent gradients, etc. the 3D-structure offers opportunities with respect to a controlled diffusion of substrates/products. Enzymes are highly selective catalytic machineries, in which both 2D- and 3D-parameters are finetuned for a given specific organic transformation. Both beaker(and ink-pot)- and channel-type structures are found in nature and are key-factors for the high degree of selectivity. In the case of *beaker(and also the ink-pot-)type structures* both the substrates and one of the products (i.e. the secondary amine or water) have to either enter or leave the pore. The control of these diffusion processes is possible through variation of hydrophilicity/-phobicity of the inner pore wall, the diameter of the pore and the length of the pore.

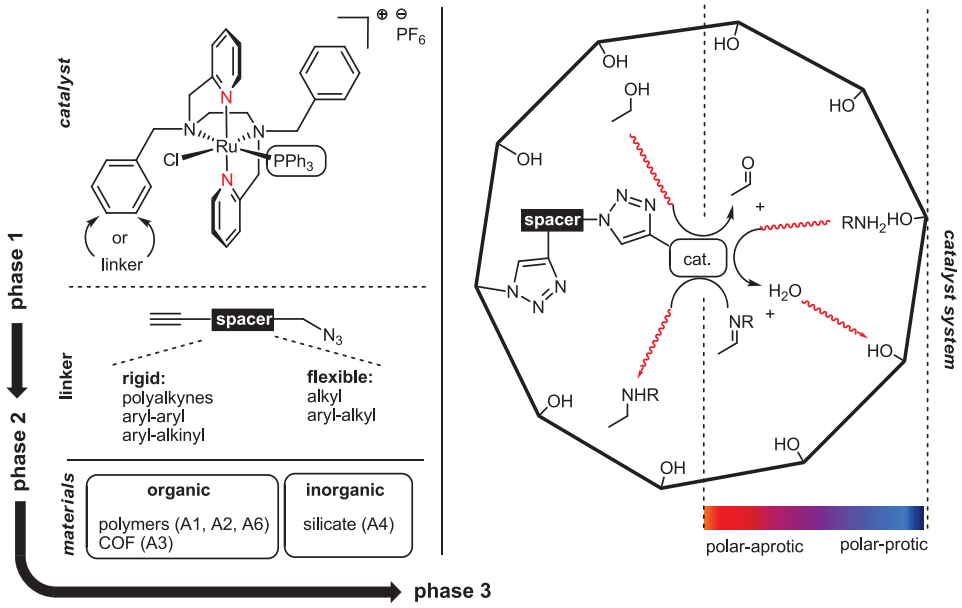

Figure B1-5. Work-flow for the development of material-catalyst hybride systems within **project B1**.

By adjusting the position of the catalyst within the pore (immobilization at the pore wall or the bottom) these parameters can be varied (**A1**, **A2**). Channel-type structures have the advantage of a defined substrate-product diffusion direction. These open structures allow for an efficient mass-transfer (also of the by-product water) and for an efficient recycling of the catalyst (**A1**, **A3**, **A4**, and **A6**). With respect to H_2-autotransfer catalysis however, the mass-flow within the pore is an important feature, since the dehydrogenation of the substrate (alcohol) leads to the formation of an aldehyde/ketone and a hydrogenated catalyst species (Figure B1-5). The subsequent condensation should occurr preferentially in the direct coordination sphere of the catalyst to ensure a fast hydrogenation of the condensation product (e.g. the imine). These transport events will be analyzed both by means of spectroscopy (**C1**) but also using theoretical methods (**C5**, **C6**) in order to shed light into the interaction of pore geometry and size vs. solvent polarity vs. pore wall polarity vs linker length on a particular chemical transformation (i.e. dehydrogenation, condensatioin, hydrogenation). The in-depth understanding will provide the base to a material specific confinement model (Figure B1-5). *It is important to not that the (N,N,N,N)(P)Ru-complex used in this study has an average diameter of 13 A or 1.3 nm (values derived from X-ray structure analysis).*

To streamline this complex multifacet chemical investigation the present project consists of two parts. Part A (**PhD 1**) will focus on the development of a rigid-linker synthesis, immobilization of the catalyst inside the pore of inorganic silica-based materials, and the synthesis of molecular probe complexes for spectroscopic investigations.

Part A: (N,N,N,N)(P)Ru-catalyzed H_2-autotransfer catalysis in inorganic materials.

- **WP1-A: Development of a unified linker concept – synthesis of rigid spacer molecules.** Development of a common linker stragy based on a double-Click approach. Synthesis of rigid spacer molecules.
- **WP2-A: Preparation of alkyne- or triazole-modified (N,N,N,N,N)(P)Ru-complexes.** Synthesis of alkynyl-(N,N,N,N)(P)Ru-complex. Establishment of the Click-transformation using alkyl azides. Analysis of alkynyl- and triazolidinyl-Ru-complexes by means of electrochemistry and quantumchemical calculations (HOMO-LUMO gap vs. redox potential).
- **WP3-A: Investigations on the influence of linker-attached (N,N,N,N)(P)Ru-complexes in homogenous H_2-autotransfer catalysis.** Testing of the new Ru-complexes in homogenous H_2-autotransfer catalysis.
- **WP4-A: Immobilization of (N,N,N,N)(P)Ru-complexes in inorganic materials.** Immobilization of the alkynyl-substituted (N,N,N,N)(P)Ru-complex inside silica-based inorganic materials (SBA-15, -16). Development of a "inner-pore"- versus "outer-pore"-anchor attachment strategy.
- **WP5-A: Catalytic investigations of SBA-15- and -16-based catalyst systems.** Evaluation of the new catalyst hybride systems for their catalytic activity in H_2-autotransfer catalysis (benzyl alcohol plus aniline or piperidine). Evaluation and comparison of experimental data, preparation of other silica-based catalyst materials with increased pore-sizes.
- **WP6-A: Preparation of probe molecules.** Preparation of organometallic probe complexes that allow to measure the pore influence onto the catalytic center, and the localization of the catalytic complex.

Part B (**PhD 2**) will start with the development of a flexible-linker synthesis, will perform detailed kinetic investigation in solution, and performs the immobilization of the catalyst in four different organic materials. In depth studies on catalytic activities following the algorithm developed in part A on silica-based inorganic materials will be applied.

Part B: (N,N,N,N)(P)Ru-catalyzed H_2-autotransfer catalysis in organic materials.

- **WP1-B: Development of a unified linker concept – synthesis of flexible spacer molecules.** An analogy to WP1 in Part A, WP1 in Part B will focus on the preparation of flexible spacer units.
- **WP2-B: Kinetic investigations of triazol-modified (N,N,N,N)(P)Ru-complex in homogenous H_2-autotransfer catalysis.** Detailed kinetic studies are a pre-requisite to analyze the effect of pore-size/-geometry on H_2-autotransfer catalysis. The kinetics of dehydrogenation, condensation and hydrogenation will be analyzed through use of in-situ IR- and NMR- spectroscopy.
- **WP3-B: Immobilization of (N,N,N,N)(P)Ru-complexes in organic materials.** Immobilization of the alkynyl-substituted (N,N,N,N)(P)Ru-complex inside the pores of organic materials will be investigated. In order to assure a "inner-pore"-connectivity of the catalyst, a strategy for blocking "outer-pore"-anchor groups through click-chemistry using bulky alkynes needs to be developed.
- **WP4-B: Organic material-catalyst systems: Investigation of catalytic activities**

Both parts will perform a catalyst screening using parallel solid phase reactors in order to ensure a maximum degree of comparability and reproducibilty. In summary, the research goals of the two parts A and B of this project are organized in following work-packages

3.8.4.1 Part A: (N,N,N,N)(P)Ru-catalyzed H_2-autotransfer catalysis in *inorganic materials*.

3.8.4.1.1 WP1-A: Development of a unified linker concept – synthesis of rigid spacer molecules.

The "hybridization" of different materials with a molecular catalyst within a mesopore is certainly at the center of this collaborative research initiative. By definition the material is meant to be catalytically inactive and to provide a uniform reaction environment (cavity) that allows to assemble catalyst and substrate/reagent in a defined spatial manner. The molecular catalyst needs to be active even after immobilization and a strategy needs to be developed to ensure that the catalyst is linked with high site selectivity (inside and not outside the pore). In order to compare catalyst activities within different materials we must ensure that effects that are measured are solely a function of confinement. In order

to reach this goal we propose the following strategy, which relies on the use of the Cu-catalyzed Huisgen 1,3-dipolar azide-to-alkyne cycloaddition (Click-chemistry) approach (Figure B1-6).

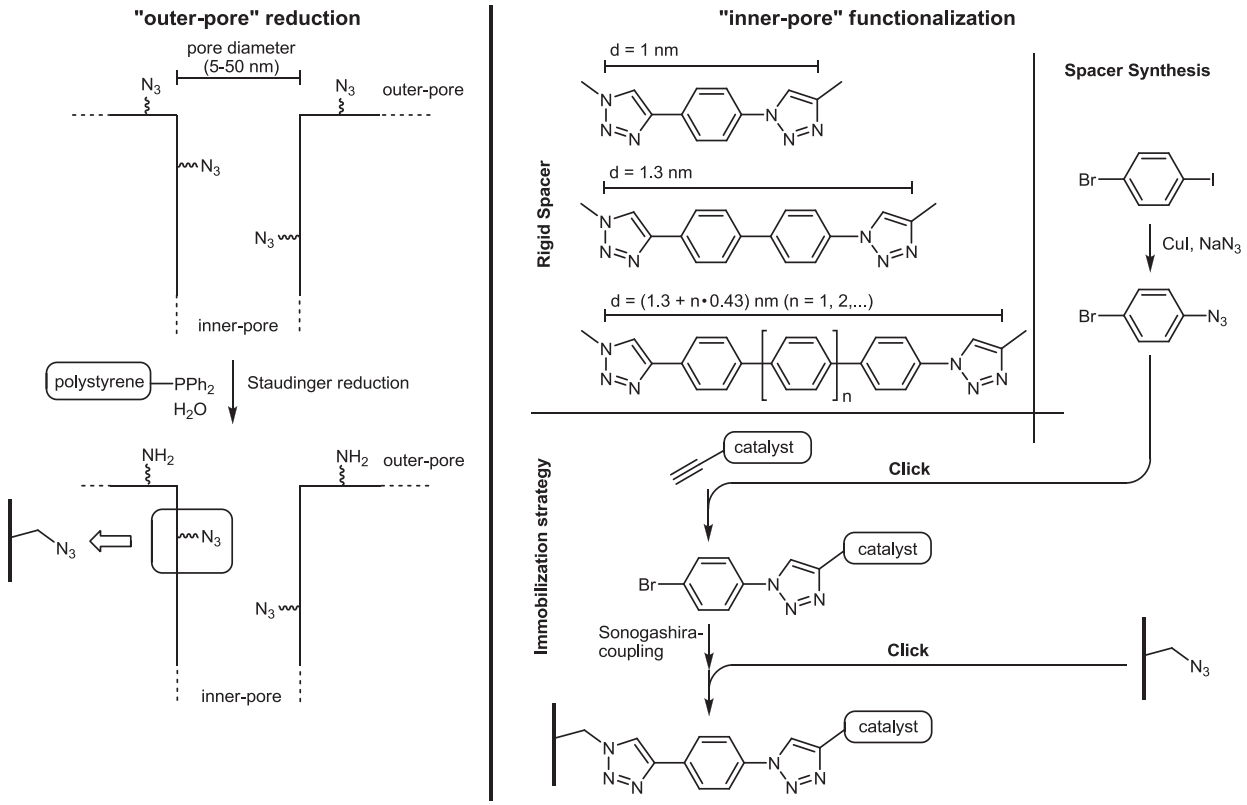

Figure B1-6. Linker-concept,and inner-pore immobilization strategy.

p,p´-Substituted (poly)arenes are transferred into the corresponding aryl azide using established cross-coupling methods. The first Click-reaction with the alkinyl-modified catalyst generates the first triazole motif. Subsequent Sonogashira-reaction establishes the alkyne moiety which sets the stage for the inner-pore functionalization. Various spacer molecules with different length will be prepared. Before immobilizing the the catalyst inside the pore, azido groups exposed outside the pore will be reduced to the corresponding amine through Staudinger reduction using polystyrene modified phosphine and water (Figure B1-6). Alternatively, a heterogenous catalyzed hydrogenation using Pd/C will also be tested. After reduction of the external azide moieties, the material will be treated with the catalyst solution. After equilibration over night the material and catalyst will be joined via Cu-catalyzed Click-reaction. In addition, building blocks for the modular linker strategy will be exchanged with **project B3**.

3.8.4.1.2 WP2-A: Preparation of alkyne- or triazole-modified (N,N,N,N,N)(P)Ru-complexes.

In preliminary studies we were able to show that the analysis of the HOMO-LUMO-gap within different (N,N,N,N)(P)Ru-complexes correlates with the redox potential of these complexes. A close analysis of the correlation between conversion in H_2-autotransfercatalysis and redox potential revealed that subtle effects within the ligand core can lead to significantly decreased conversion rates. Based on these results we will use an in-silico analysis for the identification of the optimum connectivity point (triazole unit) between ligand and spacer molecule. The optimum redox potential would be in a range between 0.4 – 0.45 V (vs. $FcH^{0/+}$). With the proposed optimum ligand structure in hand the corresponding alkyne-modified ligand will be prepared, and coupled to the corresponding spacer molecule using the Cu-catalyzed Click-reaction conditions (Figure B1-6).

3.8.4.1.3 WP3-A: Investigations on the influence of linker-attached (N,N,N,N)(P)Ru-complexes in homogenous H_2-autotransfer catalysis.

A set of (N,N,N,N)(P)Ru-complexes will be prepared through Huisgen 1,2-dipolar azide-alkyne cycloadditions using spacer molecules of *three different lengths and rigidity* (**WP1-A**: aryl-, biaryl- and triaryl-linker; **WP1-B**: propyl-, pentyl- and heptyl-linker). These six complexes will be analyzed

spectroscopically and by means of cyclovoltammetry (**projects A2** and **C2**). The isolated complexes will be employed in H_2-autotransfer catalysis between benzylalcohol and aniline as our reference reaction under the reaction conditions developed in our previous work in order to investigate the influence of the linker unit on the catalytic performance. The complexes will be calculated using quantumchemical methods in order to understand the effect of the linker unit on the catalytic performance (**project C4**). In the same line silica-based materials will be employed as additives (see also: **WP3-B**). These results might be regarded as background informations that are necessary in order to clearly identify the influence of the inner-pore immobilization on the H_2-autotransfer catalysis.

3.8.4.1.4 WP4-A: Immobilization of (N,N,N,N)(P)Ru-complexes in inorganic materials.

Project A4 and the established materials (Al-)SBA-15 and SBA-16 will serve as a suitable starting point to hybridize material and catalysis science within **project B1**. The materials in detail:

> **A4**: monolithic, polymeric, mesoporous silica-based materials with channel-type porosity and different Al-content (variation of hydrophilicity)

These materials are accessible in bigger quantities, they possess defined pore sizes, are thermally stable, and methods to functionalize these materials inside and outside the pores are literature known. In particular SBA-15 (pore size: 5-8 nm) and SBA-16 (pore size: 4.5-6 nm) are of interest, incorporation of Al into the SBA-material increases the hydrophilicity, a factor that is of particular importance for this project. Adding commercially available azidopropyltriethoxysilane to the SBA-synthesis following a landmark report by Stack for the preparation of SBA-15 with site-isolated azidofunctionalization.[19] Treatment of this material with PS-PPh_2 would result in a site selective reduction of the outer pore azido moieties in SBA-15 or -16. Alternatively, a selective reduction using a heterogenous Pd/C-catalyst and H_2-gas could would react the azide groups exposed outside the pore into amino groups. Subsequent incorporation of the six Ru-complexes (three complexes with rigid (**WP1-A**) and three with flexible (**WP1-B**) linker units) will be employed in this WP by treatment of the material with a solution of the complex, equilibration overnight and subsequent inner-pore Click-reaction. This procedure would generate a first [2x6]-catalyst system matrix.

3.8.4.1.5 WP5-A: Catalytic investigations of SBA-15- and -16-based catalyst systems.

The twelve SBA-15- and -16-based protype catalyst systems will be employed in our model transformation (i.e. the amination of benzylalcohol by aniline) in order to identify the most active catalyst-spacer-material combination. Turnover number and frequency will be measured and referenced to the homogenous catalyzed reaction. The most active material-catalyst combination will be selected and both linker length and pore size will systematically be altered. The resulting catalyst systems will be screened in a second iteration using our model reaction. *A schematic represention of the screening process and the attempted development of a structure-activity model is shown in Figure B1-10*.

To analyze the data of this iterative catalyst screening, kinetic measurements will be performed both on the first generation hybride catalyst as well as on the optimum catalyst system. Two different in-operando methods will be applied, i.e. solid-state NMR-spectroscopy (**project C1**) and IR-spectroscopy. The comparision of kinetics between the homogenously catalyzed process (->**WP2-B**), two medium active systems (one with a flexible, one with a rigid linker) relative to the best catalyst system will provide insight into the influence of material and linker-type/-rigidity onto the cataytst performance in a given material. The kinetic data obtained both for the homogenous as well as for the heterogenous catalytic system are a fundamental data set that will be interpreted on a molecular level in terms of diffusion processes, polarity gradients, and spatial distributions of solvent, reactant and product molecules within the pore and around the catalyst as obtained from atomistic molecular dynamics simulations (**project C5**).

3.8.4.1.6 WP6-A: Preparation of probe molecules

In order to identify potential confinement effects and to rationalize the data obtained in **WB5-A** (and **WB4-B** and **WP5-A**) a set of Ru-complexes having different phosphine ligands will be prepared and immobilized into the respective material (inorganic materials and organic materials (->**WP4-B**) (Figure B1-7). The phosphine ligands will be substituted either with fluorine atoms (e.g. (*p*-FC_6H_4)3P) or with a ferrocenyl unit ($FcPPh_2$).

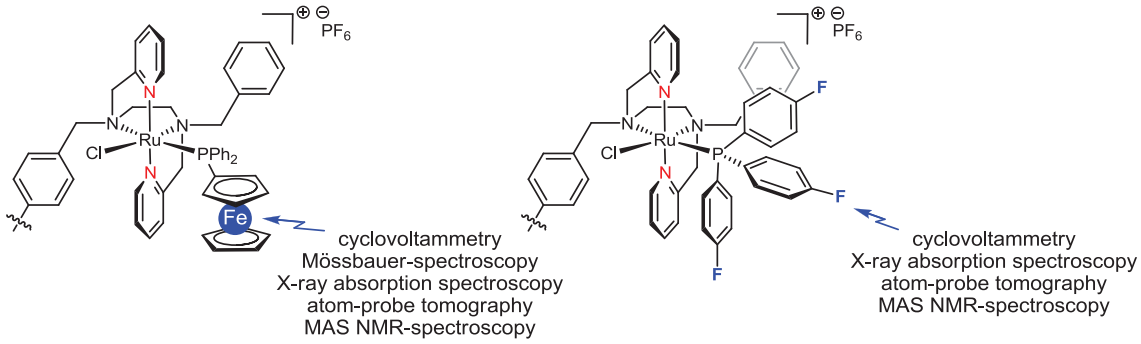

Figure B1-7. Organometallic probes.

Both ligands are not actively involved into the catalytic cycle (but do of course influence catalytic performance, which will be checked for the homogenously catalyzed process), but allow to use CP-MAS NMR-spectroscopy to perform in-operando mechanistic investigations and to identify potential catalytic intermediates (**project C1**). Of particular importance is the identification of a potential Ru-H-intermediate. The PHIP (p-hydrogen induced polarization)-technology developed in the Hunger group allows through polarization transfer to the P-atom of the phosphine ligand (via H-Ru-P) to also enhance the selectivity of the ^{31}P signals. At the same time, important information on the H-Ru-P bond angle can be derived from the coupling constants. Any changes to the geometry of this bond angle due to steric constraints etc. will become visible through this particular NMR-technique (**project C1**). A similar effect is expected from the corresponding ferrocenyl-substitued Ru-complex. Ferrocene acts as a probe that allows to measure the influence of pore size / geometry, linker-length and linker rigidity on redox properties of the respective Ru-complex by means of cyclovoltammetric measurements (**project C2**, Ringenberg). At the same time Fe-Mössbauer spectroscopic measurements on these complexes will be performed (**project C2**, van Slaggeren) to quantify the influence of inner-pore immobilization onto the electronic ground-state structure of the catalytic center. This data set will be complemented by the data obtained via multi-dimensional in-operando X-ray absorption spectroscopy (**project S1**, EXAFS, XANES, RIXXS, V2C, etc.) on non-modified Ru-complexes. For the interpretation of these experimental spectroscopic data a close collaboration with **project C4** is required. Moreover, the presence of a second heavy atom increases the contrast in atom-probe tomography and will improve the sensitivity (**project C3**) allowing to localize the catalytic center and to extract information regarding the spatial distribution of the catalytic centers within the pore. The relative orientation and flexibility of the catalyst-system inside the pore will be analyzed and simulated using Molecular Dynamics simulations in **project C6** (Fyta), while the mass transport will be modeled through a lattice Boltzmann approach in **project C6** (Holm).

3.8.4.2 Part B: (N,N,N,N)(P)Ru-catalyzed H_2-autotransfer catalysis in ***organic materials***.

3.8.4.2.1 WP1-B: Development of a unified linker concept – synthesis of flexible spacer molecules.

In analogy to **WP1-A** flexible spacer molecules will be prepared in **WP1-B**. Instead of using rigid aryl-aryl-linker units, more flexible aliphatic spacer units will be prepared. A possible synthetic route involves azidation via nucleophilic substitution, deprotection of the acetal to give an aldehyde, which will be transformed into an alkyne using established methodology (e.g. Ohira-Bestmann, Corey-Fuchs, etc.). If the Ru-complex proves to be incompatible with these organic reactions, the introduction of the spacer unit prior to the ligation to the transition metal is envisioned as a backup strategy (Figure B1-8, see also Figure B1-6). In addition, building blocks for the modular linker strategy will be exchanged with **project B3**.

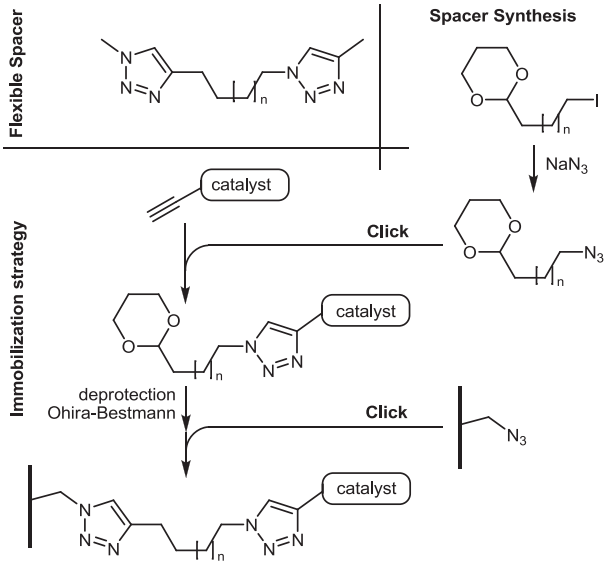

Figure B1-8. Synthesis of flexible spacer units and immobilization strategy.

3.8.4.2.2 WP2-A: Kinetic investigations of triazole-modified (N,N,N,N)(P)Ru-complex in homogenous H_2-autotransfer catalysis.

It is the vision of this project to use confinement effects to manipulate a catalytic system such that microscopic reversibility of each step is influenced through subtle effects like e.g. diffusion or steric constraints. In line with these ideas it is important to understand the kinetics of each separate transformation, i.e. the catalytic dehydrogenation of benzylalkohol (as model substrate) to benzaldehyde, the condensation of benzaldehyde with aniline to the corresponding imine, and the hydrogenation of the imine to the amine (Figure B1-9).

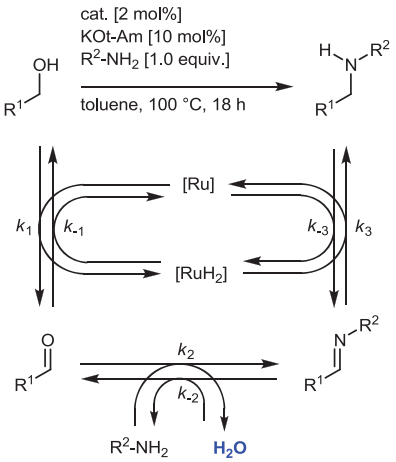

Figure B1-9. Kinetic parameters within the H_2-autotransfer catalysis.

Only if $\boldsymbol{k_2 >> k_1}$ and if $\boldsymbol{k_1 \approx k_3}$ a clean formation of the desired secondary amine will be observed. *If however k_2 is not significantly faster than k_1 the hydrogenation of the aldehyde (backreaction of the first step) will become an emerging problem.* The overall kinetics of the condensation step will solely be a function of the primary amine concentration. However, if diffusion of water from the catalytic center to the pore wall is tuned in such a way that it become the fastest processes within this entire reaction setup, the condensation kinetics will not be decisive anymore. Tuning of the diffusion kinetics is possible through proper adjustment of spacer length and rigitiy, pore size and geometry and the hydrophilicity gradient. In order to fully understand the influence of confinement on the catalytic turnover a detialed kinetic analysis of the homogenous Ru-mediated H_2-autotransfer catalysis will be performed using NMR- and IR-spectroscopy. The data will be cross-checked with the results obtained by quantumchemical calculations (**project C4**). Catalytic intermediates will be analyzed through *in*

operando NMR-spectroscopy (**project C1**) and X-ray absorption spectroscopy (**project S1**). The kinetic data will be transferred to **project C6** in order to generate a model of diffusion processes/mass transport within the pore.

3.8.4.2.3 WP3-B: Immobilization of (N,N,N,N)(P)Ru-complexes in organic materials.

In order to have a defined starting point and to compare the catalysis results obtained by using organic porous materials with the established SBA-15 and -16-systems developed in **WP4-A** *materials with a pore size of 4-8 nm* will be employed for these initial experiments. The materials in detail:

A1: monolithic, polymeric, mesoporous materials with channel-type porosity

A2: blockcopolymertemplates with beaker-type porosity

A3: COFs with channel-type porosity

A6: OCM (ordered carbon-based mesoporous materials) with channel-type porosity

Before immobilization the four materials will be added to a homogenous H_2-autotransfer catalysis using benzylalcohol and aniline to ensure compatibility with the reaction conditions. In every case the materials will be filtered and analyzed to make sure that pore size and geometry are not affected by the organic solvent/organic substrates/catalyst/base. In particular the materials of **project A2** might encounter problems (polymer swelling in toluene at 100 °C, leaching of polymer phase from the substrae, etc.). Moreover, a synthesis of materials within **project A3** needs to be developed. Hence, a simultaneous testing of all three materials will not be possible from the very beginning. *Priorization* will be on **project A1** and **A6** within the first half of the funding period, **project** A3 will join as soon as the materials are available and **project A2** will be tested upon development of a more cross-linked polymer film or, if the confinement effects in the materials of **projects A4, A1, A3**, and **A6** result in an overall reduction of reaction time and temperature, at reduced temperatures. With the compatibility test results in hand the six linker-modified (N,N,N,N)(P)Ru-complexes prepared in **WP2-A** will be “clicked” into the different porous organic materials following the conditions established in **WP4-A** to give in summ a [4X6]-matrix of catalyst hybrides which will be characterized as described in **WP4-A** and **WP5-A**.

3.8.4.2.5 WP4-B: Organic material-catalyst systems: Investigation of catalytic activities

The catalyst system matrix will be simultaneously employed to the standard reaction conditions (1 equiv. benzylalcohol, 1 equiv. aniline, 10 mol-% KO*t*-amyl, toluene, 100 °C, 18 h) to guarantee a maximum degree of comparability between the different systems.

Catalytic performance will be analyzed after 12 h using gas chromatography. The results of this first catalyst screening will allow to get a first priorization of material, pore geometry (channel vs. beaker) and linker unit (rigid vs. flexible). With this first selection the optimum combination of material plus linker will be further studied through variation of linker length and pore diameter. With regard to the molecular dimensions of catalyst, substrate and product relative to pore diameter materials with bigger pore diameter will be screened systematically with different linker lengths. These materials will be tested in a parallel fashion.

The most active catalyst systems will be analyzed using the spectroscopic and theoretical tool-box developed in **WP5-A** and **WP6-A** (cooperation with **C1**-**C6**). In order to extract potential confinement effects generated through alteration of pore size and linker length the second most reactive catalst systems for a given material will also be analyzed. Comparision of the results from both spectroscopy and theory for the most and second most active materials will lead to a first confinement model (Figure B1-10).

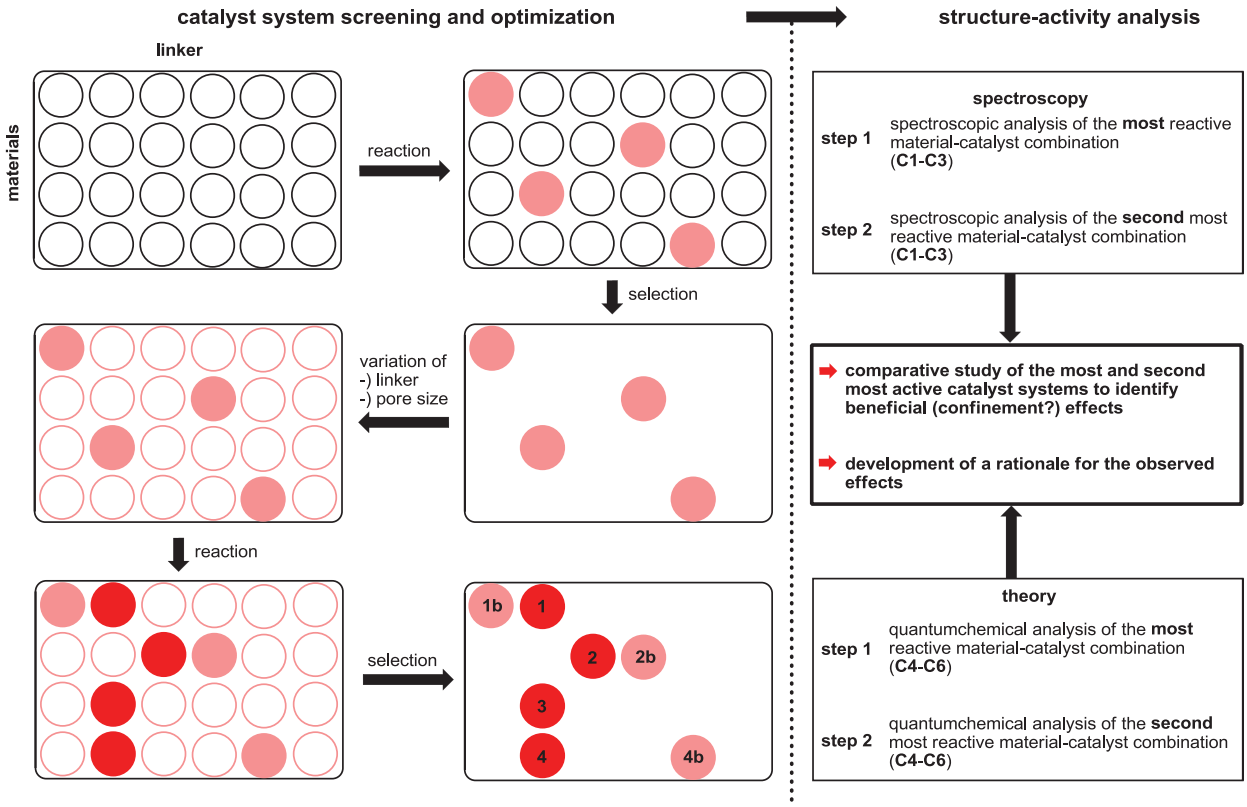

Figure B1-10. Screening algorithm and comparative analysis.

3.8.4.3 Selection criteria for the chosen materials

The H_2-autotransfer catalysis requires organic solvents at temperatures around 100 °C and long reaction times. These reaction conditions reflect the coexistency of three different reactions (dehydrogenation, condensation, and hydrogenation). The materials selected for **project B1** are, apart from **project A2**, tolerant towards these reaction conditions. Furthermore, a fast diffusion of water as a byproduct to the inner pore wall is considered to be a key factor to accelerate the intermediate condensation step. It is for these reasons that small pore diameters (5 – 10 nm) are considered to be good starting diameters. These pore sized are found in the afore mentioned projects. **Project A2** is an exception, but it allows to selectively immobilize the catalyst at the bottom of the beaker-type polymer structure. Material synthesis toward more cross-linked polymeric structures will be developed in this funding period and hopefully allow to use these materials in H2-autotransfer catalysis.

Chronological work plan:

	2018	2019			2020				2021				2022		
	Q3	Q4	Q1	Q2	Q3	Q4	Q1	Q2	Q3	Q4	Q1	Q2	Q3	Q4	
T1															WP1-A: Development of a unified linker concept – synthesis of rigid spacer molecules (PhD1).
T2															WP2-A: Preparation of alkyne- or triazole-modified (N,N,N,N,N)(P)Ru-complexes(PhD1).
T3															WP3-A: Investigations on the influence of linker-attached (N,N,N,N)(P)Ru-complexes in homogenous H_2-autotransfer catalysis (PhD1).
T4															WP4-A: Immobilization of (N,N,N,N)(P)Ru-complexes in inorganic materials (PhD1).
T5															WP5-A: Catalytic investigations of SBA-15- and -16-based catalyst systems(PhD1).
T6															WP6-A: Preparation of probe molecules (PhD1).
T7															WP1-B: Development of a unified linker concept – synthesis of flexible spacer molecules (PhD2).
T8															WP2-B: Kinetic investigations of triazol-modified (N,N,N,N)(P)Ru-complex in homogenous H_2-autotransfer catalysis (PhD2).
T9															WP3-B: Immobilization of (N,N,N,N)(P)Ru-complexes in organic materials (PhD2).
T10															WP4-B: Organic material-catalyst systems: Investigation of catalytic activities (PhD2).

3.8.4.4 Methods Applied

Project B1 is one out of three catalysis projects and will use all standard spectroscopy tools (^{1}H, ^{19}F, ^{13}C and ^{31}P NMR, IR, UV) to analyze the structures of the homogenous catalysts in solution. For characterization of the immobilized complexes EPR, CP MAS NMR-spectroscopy (**project C1**), X-ray absorption spectroscopy (**project S1**), and Moessbauer spectroscopy (**project C2**) will be employed. Measurement of reaction kinetics will be done by GC-MS, ^{1}H NMR, and in-situ FT-IR (ATR-technology). Spatial resolution of the catalyst inside the pore will be done by atom probe tomography (**project C3**).

3.8.4.5 Vision

By the end of the first fundig period a selection of new tailored mesoporous materials for Ru-catalyzed H2-autotransfer catalysis will be accessible. Through interdisciplinary collaborations with material scientists, physical chemists and theoreticians the subtle influences of pore size and geometry on H2-autotransfer catalysis will be analyzed and developed into a model showcasing confinement effects. In an ideal scenario the fast confinement-controlled diffusion of water will allow to control the unfavorable microscopic reversibility of the condensation reaction which results in an overall reduction of temperature and reaction time plus an increase in catalyst stabililty (as reflected through turnover frequency and numbers).

3.8.5 Role within the collaborative research center

Project B1 is one out of three different types of catalysis in this collaborative research proposal. The (N,N,N,N)(P)Ru-catalysts were developed in the group of the principal investigator, are stable and fully characterized by experimental, electrochemical (CV) and theoretical methods. The complexes are accessible in gram-quantities, are air and moisture stable and hence define a perfect catalyst material to be used for the type of investigations presented in this project. This preliminary work defines a perfect starting point for joint research projects in combination with material **projects A1**-**A4**, **A6** and spectroscopy/theory **projects S1**, **C1**-**C6**. **Projects A1-4**, **A6** will provide materials exposing azide functionalities within the pore, immobilization and catalytic testings will be performed in B1. The hybride materials will be analyzed through spectroscopy (**projects C1-C3**), if necessary specific probe molecules for e.g. NMR-, or Mössbauer-spectroscopy and atom-probe tomography will be synthesized within **project B1**. The results of our kinetic measurements build the base for calculations on various scales (QM/MM for mechanistic investigations: **project C4**; DFT to visualize mobility of the catalyst within the pore: **project C6**; force-field to create fluid models: **project C5**).

3.8.6 Delineation from other funded projects

Projects related to Ru-catalyze H_2-autotransfer catalysis are currently not funded. No funding proposal has been submitted or is under revision.

3.8.7 Project funding

3.8.7.1 Previous funding

This project is currently not funded and no funding proposal has been submitted.

References (ctd)

[19] J. Nakazwa, B. J. Smith, T. D. P. Stack, *J. Am. Chem. Soc.* **2012**, *134*, 2750-2759.

3.8.7.2 Requested funding

Funding for	2018		2019		2020		2021		2022		2018-2022	
Staff	Quantity	Sum	Quantity	Sum	Quantity	Sum	Quantity	Sum	Quantity	Sum	Quantity	Sum
PhD student, 67%	2	43,200.-	2	86,400.-	2	86,400.-	2	86,400.-	2	43,200.-	2	345,600.-
Total		43,200.-		86,400.-		86,400.-		86,400.-		43,200.-		345,600.-
Direct costs	Sum		Sum		Sum		Sum		Sum		Sum	
consumables	8,000.-		16,000.-		16,000.-		16,000.-		8,000.-		64,000.-	
Total	8,000.-		16,000.-		16,000.-		16,000.-		8,000.-		64,000.-	
Major research instrumentation	Sum		Sum		Sum		Sum		Sum		Sum	
High throughput equipment	10,600.-		-		-		-		-		10,600.-	
Total	10,600.-		-		-		-		-		10,600.-	
Grand total	61,800.-		102,400.-		102,400.-		102,400.-		51,200.-		420,200.-	

(All figures in EUR)

3.8.7.3 Requested funding for staff

	Sequential no.	Name, academic degree, position	Field of research	Department of university or non-university institution	Project commitment in hours per week	Category	Funding source
Existing staff							
Research staff	1	B. J. Plietker, Dr., Prof.	Organic Chemistry, Catalysis, Organometallic Chemistry	Institute of Organic Chemistry	6		University
Requested staff							
Research staff	2	N.N M.Sc.	Organic Chemistry, Catalysis, Organometallic Chemistry	Institute of Organic Chemistry		PhD	
Research staff	3	N.N M.Sc.	Organic Chemistry, Catalysis, Organometallic Chemistry	Institute of Organic Chemistry		PhD	
Research staff	4	Research assistant	Organic Chemistry, Catalysis, Organometallic Chemistry	Institute of Organic Chemistry			

Job description of staff (supported through existing funds):
1
Professor
Job description of staff (requested funds):
2
PhD student, working packages WP1-6, part A
3
PhD student, working packages WP1-4, part B
4
Research assistants. **Justification:** The research assistants will be employed for synthetic and analytical work, supporting the PhD students. Their tasks will include linker and catalysts synthesis (and scale-up thereof) as well as the recording of spectroscopic or kinetic data.

3.8.7.4 Requested funding of direct costs

	2018	2019	2020	2021	2022
Uni Stuttgart: existing funds from public budget	1,000.-	2,000.-	2,000.-	2,000.-	1,000.-
Sum of existing funds	1,000.-	2,000.-	2,000.-	2,000.-	1,000.-
Sum of requested funds	8,000.-	16,000.-	16,000.-	16,000.-	8,000.-

(All figures in EUR)

Consumables for financial year 2018

Chemicals, consumables, monomers, solvents, silica for columns, gases (Ar), NMR solvents	EUR	8,000.-

Consumables for financial year 2019

Chemicals, consumables, monomers, solvents, silica for columns, gases (Ar), NMR solvents	EUR	16,000.-

Consumables for financial year 2020

Chemicals, consumables, monomers, solvents, silica for columns, gases (Ar), NMR solvents	EUR	16,000.-

Consumables for financial year 2021

Chemicals, consumables, monomers, solvents, silica for columns, gases (Ar), NMR solvents	EUR	16,000.-

Consumables for financial year 2022

Chemicals, consumables, monomers, solvents, silica for columns, gases (Ar), NMR solvents	EUR	8,000.-

3.8.7.5 Requested funding for major research instrumentation

Equipment for financial year 2018

catalyst-screening-block. Justification: In order to avoid destruction of the porous materials and the resulting catalyst systems due to mechanical stress induced by stirring, classical magnetic stirrers can not be used. Therefore, the mechanical workshop will build a catalyst screening block for the parallel screening of different catalyst systems consisting of an IKA shaker 260 control (3.560.- €), a cryostat Julabo, model: Corio CD-200F cooling circulation thermostat -20 to +150°C (3.370.- €), 2 aluminium heating blocks with sockets for the cryostat (3 x 24 Schlenk tubes D10 mm, 3 x 12 Schlenk tubes D20 mm), 6 aluminium condenser units for the heating device made by mechanical workshop, estimated 2.000 €), 30 pressure Schlenk vials D10 mm, 20 pressure Schlenk vials D20 mm (made by glass blowers, estimated 1670.- €).	EUR	10,600.-

3.9 Project B2

3.9.1 General Information about Project B2

3.9.1.1 Immobilized Molybdenum Imido, Tungsten Imido- and Tungsten Oxo Alkylidene N-Heterocyclic Carbene Complexes for Olefin Metathesis

3.9.1.2 Research Areas
Preparatory and Physical Chemistry of Polymers (306-01), Inorganic Molecular Chemistry (301-01), Organic Molecular Chemistry (301-02)

3.9.1.3 Principal Investigator
Buchmeiser, Michael R., Prof. Dr., born 08. 03. 1967, male, Austrian
Lehrstuhl für Makromolekulare Stoffe und Faserchemie, Institut für Polymerchemie
Universität Stuttgart, Pfaffenwaldring 55, 70569 Stuttgart
Tel.: 0711/685-64075
E-Mail: michael.buchmeiser@ipoc.uni-stuttgart.de
Tenured professor W3

3.9.1.4 Legal Issues
This project includes

1.	research on human subjects or human material.	no
2.	clinical trials	no
3.	experiments involving vertebrates.	no
4.	experiments involving recombinant DNA.	no
5.	research involving human embryonic stem cells.	no
6.	research concerning the Convention on Biological Diversity.	no

3.9.2 Summary
Selected olefin metathesis reactions that are expected to be particularly susceptible to confinement effects will be studied. In course of these investigations, we wish to scrutinize both the influence of the pore surface (polar, non-polar, protic, aprotic) and the pore size, geometry and tortuosity of various mesoporous systems in combination with differently functionalized olefins (polar, non-polar, protic, aprotic) on the reactivity of organometallic catalysts immobilized in these mesoporous systems. As catalysts, *N*-heterocyclic carbene (NHC) complexes of Mo-imido-, W-imido- and W-oxo-alkylidenes, representatives of a new class of highly active, partially functional group tolerant olefin metathesis catalysts, will be used. Olefin metathesis reactions will comprise of ring-closing metathesis (RCM), in particular macrocyclization, as well as of ethenolysis and homometathesis (HM) reactions. In course of macrocyclizations, the influence of surface polarity and pore size on cyclization *vs*. polymerization propensity (i.e. RCM *vs*. acyclic diene metathesis (ADMET) polymerization) will be studied. In ethenolysis and HM, which are based on the same reaction, though in opposite direction, the influence of ethylene concentration (pressure) on reactivity with regard to pore polarity will be studied. Once established, the concept will be extended to other olefin metathesis reactions including en-yne metathesis and stereoselective olefin metathesis. For the latter, the influence of pore diameter/form and pore polarity in combination with the polarity of the solvents used on stereoselectivity is of utmost interest. Finally, another central question, i.e. whether and if yes, under which conditions pore size and/or polarity of a Mo/W oxo/imido alkylidene NHC catalyst influences the *syn*/*anti*-ratio in a metal alkylidene and thus reactivity, *E*/*Z*-selectivity and regioselectivity of the [2+2] cycloaddition, will be addressed.

3.9.3 Research rationale

3.9.3.1 Current state of understanding and preliminary work
Generally, the immobilization of well-defined organometallic catalysts on different supports is state of the art.[1-2] The same accounts for well-defined olefin metathesis catalysts based on Mo, W or Ru.[3-11]

Representatives of supported catalysts, i.e. immobilized (chiral) Schrock-, Grubbs and Grubbs-Hoveyda-type systems, have been realized to a significant extent by our group.[12-28] So far, we predominantly used polymeric (monolithic or beaded) but also silica-based supports.

More recently, in an effort to create equally reactive and stable cationic metal alkylidenes, our group reported on the first cationic NHC complexes of Mo-imido-, W-imido- and W-oxo-alkylidenes (Figure B2-1).[16, 28-39] Using a surface organometallic chemistry approach, the first representatives of this novel class of olefin metathesis catalysts have been immobilized on silica and allowed for unusually high productivity in cross-metathesis (turn over numbers, TONs) exceeding 10^6.[28]

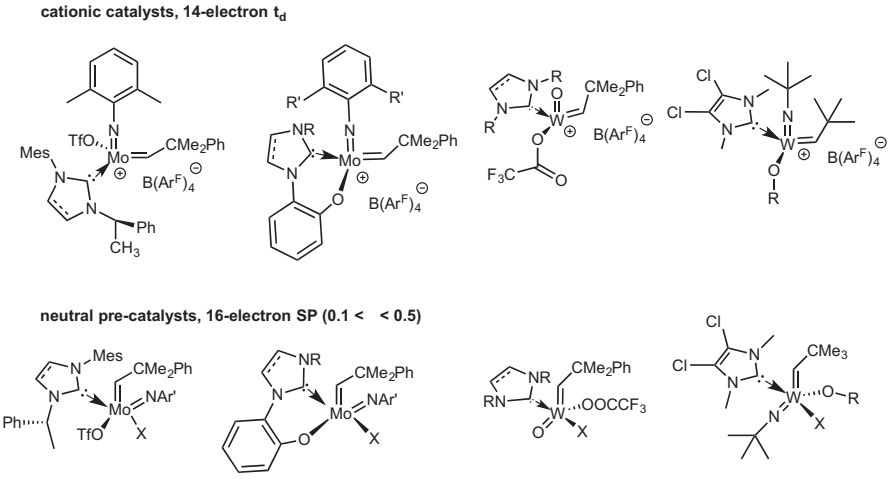

Figure B2-1: Selection of cationic, 14-electron Mo-imido, W-imido and W-oxo alkylidene NHC complexes and their neutral 16-electron progenitors. Note that all catalysts are chiral at the metal. t-factor was calculated acc. to ref. [40]. t_d = tetrahedral, SP = square planar.

Despite the impressive number of immobilized well-defined olefin metathesis catalysts that exists,[13] until now, no systematic investigations on the influence of pore size, geometry, functionality, tortuosity or polarity on the outcome of an olefin metathesis reaction, which ever, exists. By contrast, all immobilizations carried out so far are based on the unuttered mutual understanding that the support used, which ever, only acts as the carrier material and is entirely innocent in any of the reactions investigated. This might be the case for non-porous polymeric monolithic supports with grafted, catalyst-containing polymer chains acting in the interphase, which give productivities, selectivities and activities very similar to the parent, homogeneous systems.[24, 27, 41-45] However, this is most probably not true for all other supports described including silica. In fact, in many cases silica-based materials with immobilized Ru-alkylidenes very often display a much lower productivity than is observed for the homogeneous counterparts, which strongly suggests an influence of the support on catalyst performance, which ever.[24, 46-51]

In this project, we therefore wish to address this influence of the confinement of different support materials on catalytic performance. Both in view of their reactivity and functional group tolerance, the above-mentioned Mo-imido-, W-imido- and W-oxo-alkylidene NHC complexes seem particularly suited for these purposes, the more since they are available with almost unlimited structural variability. Equally important, if necessary, they can also be immobilized in their stable, neutral, five-coordinate 16-electron pre-catalyst configuration.[16] Finally, the linker can conveniently be attached at the remote 4- or 5-position of the NHC, e.g., imidazol-2-ylidenes or in form of azido-alcoholates, -thiolates or-carboxylates. Since either the NHC or the anionic ligand is the last ligand to be introduced into the metal complex, this does neither impede catalyst variability nor increase synthetic complexity.

References

[1] C. V. Pittman Jr., *Polymer Supported Catalysts* In: Comprehensive Organometallic Chemistry, G. Wilkinson, F. G. A. Stone, E. Abel (Ed), *Vol. 8*, Pergamon, Oxford, **1982**.
[2] F. R. Hartley, in *The Use of Organometallic Compound Organic in Synthesis., Vol. 4* (Ed.: F. R. Hartley), Wiley, Chichester, **1987**, pp. 1163-1225.
[3] S. Nguyen, R. H. Grubbs, *J. Organomet. Chem.* **1995**, *497*, 195-200.
[4] B. Rhers, A. Salameh, A. Baudouin, E. A. Quadrelli, M. Taoufik, C. Copéret, F. Lefebvre, J.-M. Basset, X. Solans-Monfort, O. Eisenstein, W. W. Lukens, L. P. H. Lopez, A. Sinha, R. R. Schrock, *Organometallics* **2006**, *25*, 3554-3557.
[5] C. Copéret, J.-M. Basset, *Adv. Synth. Catal.* **2007**.
[6] V. Mougel, M. Pucino, C. Copéret, *Organometallics* **2015**, *34*, 551–554.
[7] D. Grekov, Y. Bouhoute, K. C. Szeto, N. Merle, A. De Mallmann, F. Lefebvre, C. Lucas, I. Del Rosal, L. Maron, R. M. Gauvin, L. Delevoye, M. Taoufik, *Organometallics* **2016**, *35*, 2188–2196.
[8] J. Yuan, A. M. Fracaroli, W. G. Klemperer, *Organometallics* **2016**, *35*, 2149–2155.
[9] N. Merle, F. Le Quéméner, Y. Bouhoute, K. Szeto, C., A. De Mallmann, S. Barman, M. K. Samantaray, L. Delevoye, R. M. Gauvin, M. Taoufik, J.-M. Basset, *J. Am. Chem. Soc.* **2017**, *139*, 2144-2147.
[10] K. C. Hultzsch, J. A. Jernelius, A. H. Hoveyda, R. R. Schrock, *Angew. Chem.* **2002**, *114*, 609-611; *Angew. Chem. Int. Ed.* **2002**, *41*, 589-593.
[11] S. J. Dolman, K. C. Hultzsch, F. Pezet, X. Teng, A. H. Hoveyda, R. R. Schrock, *J. Am. Chem. Soc.* **2004**, *126*, 10945-10953.
[12] E. B. Anderson, M. R. Buchmeiser, *ChemCatChem* **2012**, *4*, 30-44.
[13] M. R. Buchmeiser, *Immobilization of Metathesis Catalysts* In: "Olefin Metathesis - Theory and Praxis, K. Grela, John Wiley & Sons, **2014**.
[14] T. S. Halbach, S. Mix, D. Fischer, S. Maechling, J. O. Krause, C. Sievers, S. Blechert, O. Nuyken, M. R. Buchmeiser, *J. Org. Chem.* **2005**, *70*, 4687-4694.
[15] S. Mavila, M. R. Buchmeiser, *Macromolecules* **2010**, *43*, 9601-9607.
[16] S. Sen, R. Schowner, D. A. Imbrich, W. Frey, M. R. Buchmeiser, *Chem. Eur. J.* **2015**, *21*, 13778-13787.
[17] D. Wang, R. Kröll, M. Mayr, K. Wurst, M. R. Buchmeiser, *Adv. Synth. Catal.* **2006**, *348*, 1567-1579.
[18] L. Yang, M. Mayr, K. Wurst, M. R. Buchmeiser, *Chem. Eur. J.* **2004**, *10*, 5761-5770.
[19] B. Autenrieth, W. Frey, M. R. Buchmeiser, *Chem. Eur. J.* **2012**, *18*, 14069-14078.
[20] M. R. Buchmeiser, *New J. Chem.* **2004**, *28*, 549-557.
[21] M. R. Buchmeiser, *Catal. Today* **2005**, *105*, 612-617.
[22] M. R. Buchmeiser, *Chem. Rev.* **2009**, *109*, 303-321.
[23] M. R. Buchmeiser, S. Lubbad, M. Mayr, K. Wurst, *Inorg. Chim. Acta* **2003**, *345*, 145-153.
[24] J. O. Krause, S. Lubbad, O. Nuyken, M. R. Buchmeiser, *Adv. Synth. Catal.* **2003**, *345*, 996-1004.
[25] R. M. Kröll, N. Schuler, S. Lubbad, M. R. Buchmeiser, *Chem. Commun.* **2003**, 2742-2743.
[26] M. Mayr, M. R. Buchmeiser, *Macromol. Rapid. Commun.* **2004**, *25*, 231-236.
[27] M. Mayr, D. Wang, R. Kröll, N. Schuler, S. Prühs, A. Fürstner, M. R. Buchmeiser, *Adv. Synth. Catal.* **2005**, *347*, 484-492.
[28] M. Pucino, V. Mougel, R. Schowner, A. Fedorov, M. R. Buchmeiser, C. Copéret, *Angew. Chem.* **2016**, *128*, 4372-4374*; Angew. Chem. Int. Ed.* **2016**, *55*, 4300-4302.
[29] J. Beerhues, S. Sen, R. Schowner, M. R. Buchmeiser, *J. Polym. Sci. A: Polym. Chem.* **2017**, *55*, 3028-3033.
[30] M. R. Buchmeiser, *Polym. Rev.* **2017**, *57*, 15-30.
[31] M. R. Buchmeiser, S. Sen, C. Lienert, L. Widmann, R. Schowner, K. Herz, P. Hauser, W. Frey, D. Wang, *ChemCatChem* **2016**, *8*, 2710-2723.
[32] I. Elser, W. Frey, K. Wurst, M. R. Buchmeiser, *Organometallics* **2016**, *35*, 4106-4111.
[33] I. Elser, R. Schowner, W. Frey, M. R. Buchmeiser, *Chem. Eur. J.* **2017**, *23*, 6398-6405.
[34] K. Herz, J. Unold, J. Hänle, W. Frey, M. R. Buchmeiser, *Macromolecules* **2015**, *48*, 4768-4778.
[35] D. A. Imbrich, I. Elser, W. Frey, M. R. Buchmeiser, *ChemCatChem* **2017**, *9*, 2996-3002.
[36] D. A. Imbrich, W. Frey, S. Naumann, M. R. Buchmeiser, *Chem. Commun.* **2016**, *52*, 6099-6102.
[37] C. Lienert, W. Frey, M. R. Buchmeiser, *Macromolecules* **2017**, *50*, 5701-5710.
[38] R. Schowner, W. Frey, M. R. Buchmeiser, *J. Am. Chem. Soc.* **2015**, *137*, 6188-6191.

[39] S. Sen, J. Unold, W. Frey, M. R. Buchmeiser, *Angew. Chem.* **2014**, *126*, 9538-9542*; Angew. Chem. Int. Ed.* **2014**, *53*, 9384-9388.
[40] A. W. Addison, T. N. Rao, J. Reedijk, J. van Rijn, G. C. Verschoor, *J. Chem. Soc. Dalton Trans.* **1984**, 1349-1356.
[41] F. Sinner, M. R. Buchmeiser, *Macromolecules* **2000**, *33*, 5777-5786.
[42] M. R. Buchmeiser, *Macromol. Rapid. Commun.* **2001**, *22*, 1081-1094.
[43] M. R. Buchmeiser, *Metathesis Polymerization: A Versatile Tool for the Synthesis of Surface-Functionalized Supports and Monolithic Materials* In: Handbook of Metathesis*,* R. H. Grubbs (Ed), *Vol. 3*, Wiley-VCH, Weinheim, **2003**.
[44] J. O. Krause, S. Lubbad, M. Mayr, O. Nuyken, M. R. Buchmeiser, *Polym. Prepr. (Am. Chem. Soc., Div. Polym. Chem.)* **2003**, *44*, 790-791.
[45] E. B. Anderson, B. Autenrieth, M. R. Buchmeiser, in *Stuttgarter Kunststoffkolloquium* (Eds.: C. Bonten, M. R. Buchmeiser), Stuttgart, **2011**.
[46] J. Lim, S. S. Lee, J. Y. Ying, *Chem. Commun.* **2008**, 4312-4314.
[47] D. P. Allen, M. Van Wingerden, R. H. Grubbs, *Org. Lett.* **2009**, *11*, 1261–1264.
[48] A. Keraani, C. Fischmeister, T. Renouard, M. Le Floch, A. Baudry, C. Bruneau, M. Rabiller-Baudry, *J. Molec. Catal. A: Chem.* **2012**, *357*, 73-80.
[49] H. Balcar, J. Čejka, *Coord. Chem. Rev.* **2013**, *257*, 3107-3124.
[50] M. Bru, R. Dehn, J. H. Teles, S. Deuerlein, M. Danz, I. B. Müller, M. Limbach, *Chem. Eur. J.* **2013**, *19*, 11661–11671.
[51] Y. Cui, N. Liu, Y. Xia, J. Lv, S. Zheng, N. Xue, L. Peng, X. Guo, W. Ding, *J. Molec. Catal. A: Chem.* **2014**, *394*, 1-9.

3.9.3.2 Project-related publications by participating researchers

[B2-1] M. Mayr, M. R. Buchmeiser, K. Wurst, *Adv. Synth. Catal.* **2002**, *344*, 712.
[B2-2] J. O. Krause, M. T. Zarka, U. Anders, R. Weberskirch, O. Nuyken, M. R. Buchmeiser, *Angew. Chem.* **2003**, *115*, 6147-6151; *Angew. Chem. Int. Ed*. **2003**, *42*, 5965.
[B2-3] J. O. Krause, K. Wurst, O. Nuyken, M. R. Buchmeiser, *Chem. Eur. J.* **2004**, *10*, 777.
[B2-4] L. Yang, M. Mayr, K. Wurst, M. R. Buchmeiser, *Chem. Eur. J.* **2004**, *10*, 5761.
[B2-5] M. R. Buchmeiser, *Chem. Rev.* **2009**, *109*, 303.
[B2-6] E. B. Anderson, M. R. Buchmeiser, *ChemCatChem* **2012**, *4*, 30.
[B2-7] S. Sen, J. Unold, W. Frey, M. R. Buchmeiser, *Angew. Chem.* **2014**, *126*, 9538-9542*; Angew. Chem. Int. Ed.* **2014**, *53*, 9384.
[B2-8] S. Sen, R. Schowner, D. A. Imbrich, W. Frey, M. R. Buchmeiser, *Chem. Eur. J.* **2015**, *21*, 13778.
[B2-9] R. Schowner, W. Frey, M. R. Buchmeiser, *J. Am. Chem. Soc.* **2015**, *137*, 6188.
[B2-10] M. Pucino, V. Mougel, R. Schowner, A. Fedorov, M. R. Buchmeiser, C. Copéret, *Angew. Chem.* **2016**, *128*, 4372-4374*; Angew. Chem. Int. Ed.* **2016**, *55*, 4300.

3.9.4 Project plan

The main purpose of this catalysis project is to provide suitable group 6 metal alkylidene olefin metathesis catalysts and olefin metathesis reactions to study confinement effects with the materials chosen. In summary, the work packages are as follows:

- **WP 1: Selection of catalysts, tethering and immobilization on tailored mesoporous supports.** Both neutral 16-electron and cationic 14-electron catalysts based on Mo/W-imido and W-oxo alkylidene NHC complexes will be used. Tethering will be accomplished via the NHC and the alkoxides using both ene-yne click and silane chemistry. Flexible and chain-stiff tethers will be used. Finally, ferrocene-modified catalysts will be used to allow for measuring confinement effects on the metal center via Moessbauer spectroscopy.
- **WP 2. Selection of supports.** The following supports are envisaged: monolithic, polymeric, mesoporous materials with either "ink pot" or "cylinder" type porosity (**project A1**), COFs (**project A3**), mesoporous SiO_2 and SiO_2/Al_2O_3 supports, respectively (**project A4**), hybrid materials (**project A5**) and mineralized foams (**project A7**).
- **WP 3. SILP-technology.** Supported ionic liquid phase (SILP) technology will be applied to retrieve a comprehensive picture on confinement effects.
- **WP 4. Olefin metathesis reactions.** The selection of olefin metathesis reactions is such that the envisaged confinement effects can be studied and reaction kinetics can be measured, respectively confinement-induced changes therein can be identified.
- **WP 5: Confinement effects to be studied.** The following confinement effects will be studied (i) confinement by size, (ii) confinement by geometry/tortuosity/aspect ratio, (iii) confinement by polarity.

3.9.4.1 WP 1: Selection of catalysts, tethering and immobilization on tailored mesoporous supports

Owing to their substantial stability and functional group tolerance,[16, 31, 39] the neutral progenitors rather than the cationic Mo- and W-based olefin metathesis catalysts shown in Figure B2-1 will be modified such that they contain, e.g., an ω-azido-tether, which allows for their immobilization via click-chemistry. In principle, the immobilization of the catalysts outlined in Figure B2-2 can be accomplished either via the NHC or an anionic ligand. For the latter, azido-alcoholates, -thiolates but also –carboxylates can be envisaged (Figure B2-2).

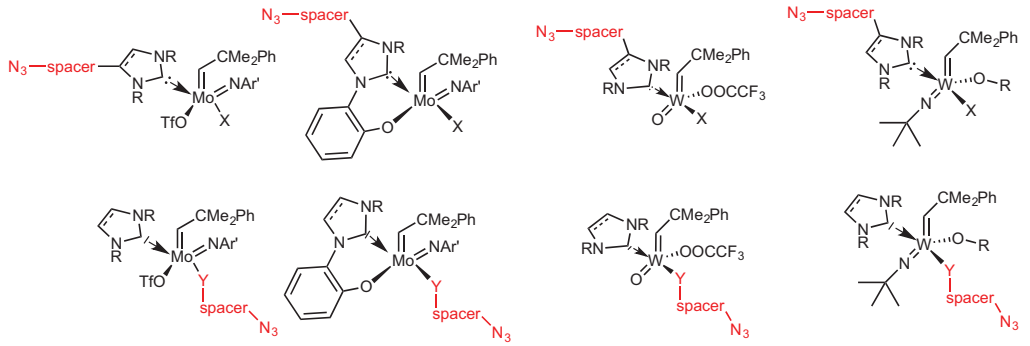

Figure B2-2. Tethered Mo-imido, W-imido and W-oxo alkylidenes. X = fluorinated alcoholate, triflate; Y = O, S, COO.

Reaction of these tethered pre-catalysts with surface alkyne groups in the presence of catalytic amounts of copper will lead to the immobilization of these catalysts (Scheme B2-1). It is important to underline that the 1,2,3-triazines created in course of this reaction combine rigidity with low basicity (pK_a values of 1,4-R,R'-1,2,3-triazinium salts are around 1.25).

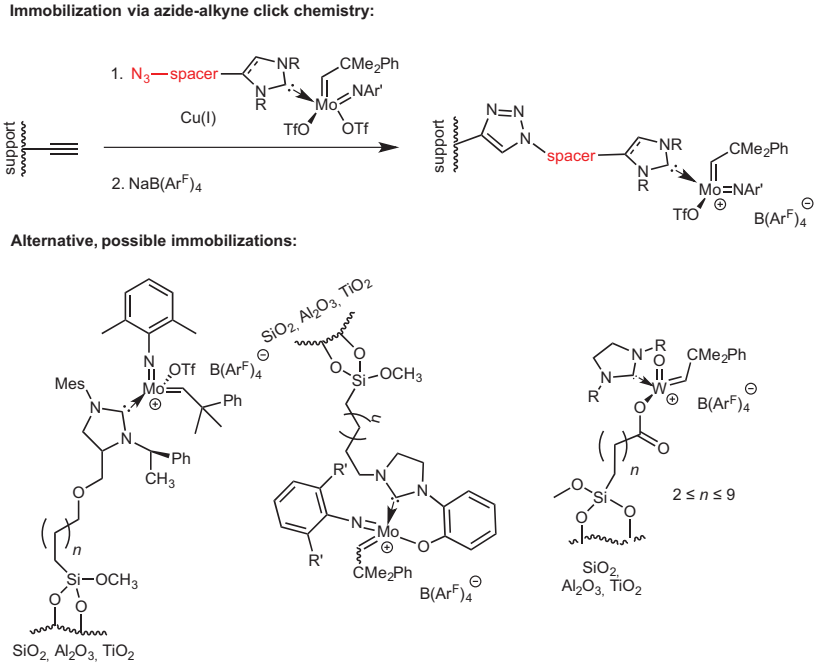

Scheme B2-1. Immobilization of the pre-catalyst and generation of the active species, exemplified for a Mo-imido NHC bistriflate complex.

Finally, reaction with either *N*,*N*-Me$_2$-anilinium B(Ar^F)$_4^-$ (X = fluorinated alcoholate) or Na$^+$B(Ar^F)$_4^-$ (X = triflate) will generate the active catalyst (Scheme B2-2). Notably, both the azide-alkyne click reaction and the generation of the cationic species are quantitative reactions. Alternatively, immobilization can be accomplished via the NHC, either using the corresponding azide-click chemistry or trialkoxysilanes, which allow for a straightforward reaction with most inorganic supports (Scheme B2-1). Trialkoxysilane chemistry obviously also qualifies for immobilization via the anionic ligand. It is important to stress that, despite (deceptive) reports on the "*boomerang*" – type behavior of olefin metathesis catalysts immobilized via the metal alkylidene,[52-56] any such immobilization is strictly excluded here. In principle, the length of the spacers can be freely chosen, depending on the dimensions of the pore. Short-chain, flexible alkylenes (≤C$_6$) and short-chain, chain-stiff perfluoroalkylenes (≤C$_6$) are envisaged. Further functionalization of all inorganic surfaces can be accomplished via silanization. With the use of either C$_{18}$H$_{37}$-, C$_8$H$_{17}$-, cyanopropyl- dimethylaminopropyltrimethoxysilanes, etc., can be used to generate the desired polar or non-polar and even ionic inner surfaces. Mineralized surfaces, e.g., ZrO$_2$-based, can be functionalized using the corresponding phosphonates and phosphates, e.g. cyanoethylphosphate, naphthylphosphate, dibutylphosphite, etc. (c.f. **project A1**). Most conveniently, the corresponding trialkoxysilyl-based reagents can be used for the binding to TiO$_2$, Al$_2$O$_3$ or SiO$_2$ surfaces. Alternatively, phosphonates can be used for bonding to ZrO$_2$ surfaces. Compatibility checks can be quickly carried out on flat model surfaces. For the immobilization to polymeric, poly(urethane) monolithic surfaces (supports), both the hydroxyl and isocyanate groups can be used to introduce alkyne groups (c.f. **project A1**).[2, 9, 10]

We also plan to introduce metals that can be addressed by Moessbauer spectroscopy (**project C2**). This will allow studying subtle changes in the electronic structure at the catalytic center. For these purposes, ferrocene moieties will be introduced in the imido and NHC ligand, respectively Figure B2-3). Since in both cases the ferrocene (iron) is in conjugation with the group 6 metal, the iron will experience changes in electron density at the metal, e.g. a switch from the neutral pre-catalysts (not shown) to the cationic Mo or W catalysts.[57-58] Similarly changes in the electronic structure of the catalysts provoked by, e.g. changes in polarity of the surrounding environment (solvent, olefin(s), product(s), pore wall) must also be expected to lead to small but detectable changes in both the isomeric shift and quadrupole splitting (IS, QS) of the iron as well as in its temperature-dependent values (d*IS*/d*T*, d*QS*/d*T*).

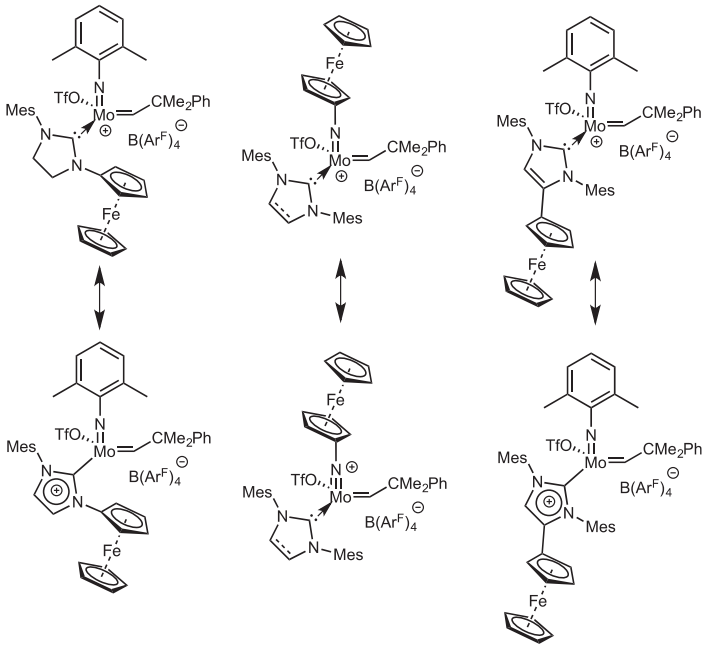

Figure B2-3. Ferrocene-containing catalysts and mesomeric structures that illustrate the involvement of the ferrocene moiety.

3.9.4.2 WP 2. Selection of supports

The following supports will be used:

- monolithic, polymeric, mesoporous materials with either “ink pot” or “cylinder” type porosity (**project A1**)
- COFs (**project A3**).
- mesoporous SiO_2 and SiO_2/Al_2O_3 supports, respectively (**project A4**).
- hybrid materials (**project A5**).
- mineralized foams (**project A7**)

At least the materials provided by **projects A1, A3** and **A4** can immediately be used under **continuous conditions**, too, and thus represent **key materials** as they allow for checking the **influence of processing parameters on catalytic performance** at an early stage of the CRC. Table B2-1 provides a survey over the supports to be used and the corresponding functionalization chemistry. Obviously, the linker chemistry must be adopted to every support material used.

3.9.4.3 WP 3. SILP-technology

Alternatively, olefin metathesis catalysts can be incorporated inside pores *without* the use of any linker applying *supported ionic liquid phase* (SILP) technology.[19, 59-64] For these purposes, the pores are filled with an ionic liquid (IL) solution of the cationic catalyst. Capillary forces retain the catalyst-containing IL inside the pore, which can additionally be functionalized such that there is a strong interaction with the IL, which in turn efficiently suppresses leaching of the IL. This can be achieved by, e.g., introduction of ionic groups at the inner surface of the pore (Figure B2-4). Concerning the synthesis of ammonium-functionalized pores, refer to **project A1**. Once the catalyst-containing IL is brought into contact with a solution of olefin(s), which is immiscible with the IL, one gains access to a *supported liquid-liquid reaction*.[19, 63-64] This approach is complementary to all other aforementioned variations in that it is entirely linker free and consequently guarantees full mobility and flexibility of the catalyst inside the pores. For implications concerning correlations between catalytic activity and e.g., diffusivity, *vide infra.* In terms of supports, those outlined in section 3.9.4.2 will be used in order to ensure full comparability with the results obtained with tethered catalysts.

Table B2-1. Survey over the supports to be used in combination with **project B2** and envisaged functionalization chemistry.

Project	Type of material	Functionalization
A1	PUR-based polymeric monolith	H_2N-C_6H_4-CCH, H_2N-$(CH_2)_4$-CCH, $ClCH_2$-C_6H_4-N_3,…
A3	COF	propargyl, generally terminal –CCH groups
A4	SiO_2, alumosilicates	$(MeO)_3Si$-$(CH_2)_n$-CCH, $(MeO)_3Si$-$(CH_2)_n$-N_3,…
A5	Hybrid (ZnO, TiO_2, SiO_2, ZrO_2, Al_2O_3) and replica materials (TiO_2, SiO_2, ZrO_2)	$(MeO)_3Si$-$(CH_2)_n$-CCH, HO_3P-$(CH_2)_3$-CCH, …..
A7	Mineralized foams	$(MeO)_3Si$-$(CH_2)_n$-CCH, HO_3P-$(CH_2)_3$-CCH, …..

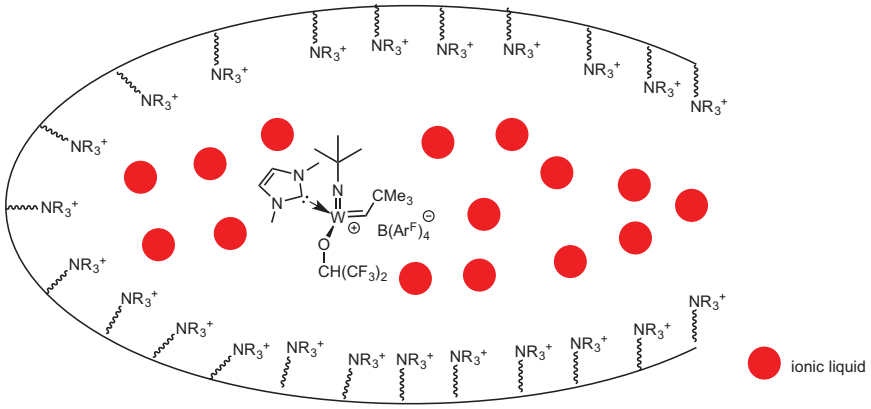

Figure B2-4. SILP approach to biphasic catalysis.

3.9.4.4 WP 4. Olefin metathesis reactions

In terms of catalytic reactions, homometathesis (HM) and ring-closing metathesis (RCM), in particular macrocyclization (MC) reactions will be investigated. RCM and MC, respectively, are of particular importance, since they allow investigating the influence of pore size on two competing reactions: MC and acyclic diene metathesis (ADMET) polymerization. Particularly with dienes that form larger rings >C_6, upon cyclization, ring strain gains increasing influence and the linear, oligomeric products form first.[65] Driven by further release of small olefins, e.g., ethylene, these can form the desired products, too, however, usually in low yields. This issue is of enormous importance in the synthesis of cyclic natural products and drugs. Since these compounds are usually prepared via multi-step syntheses, it is simply inacceptable to loose major amounts of compounds during cyclization at a comparably late stage of synthesis. Also, in collaboration with the Laschat group,[66] issues regarding the ring size of the resulting macrocycles will be addressed. Current approaches to overcome this problem entail reactive distillation, which, however, requires volatile products, and high dilution (<0.05 M in olefin), which is cost intensive and results in low space-time yields. Now, running macrocyclizations in constrained geometries, *intramolecular* olefin metathesis must be expected to dominate over *intermolecular* olefin metathesis, simply because approach of a second diene to the catalytic centers sterically blocked (Scheme B2-2). In other words, RCM should dominate over ADMET polymerization for simple steric reasons. One can now with all the different types of materials provided in course of this collaborative research project address this confinement effect as outlined in section 3.10.4.4. Usually, product analysis in RCM or MC is best accomplished by GC-MS. With concurring ADMET, however, NMR is the preferred method. In case of overlapping signals, quantitative product analysis may become complex but manageable.

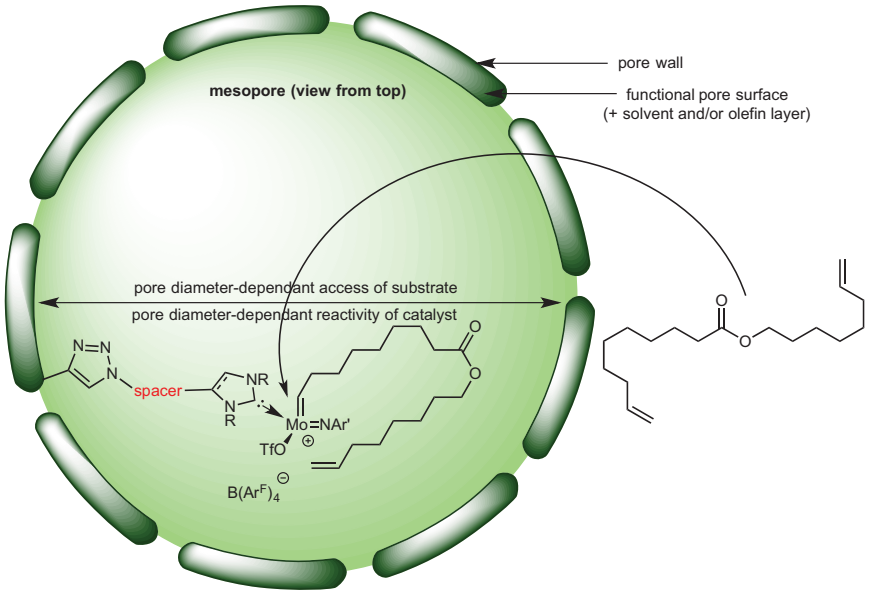

Scheme B2-2. MC *vs.* ADMET polymerization inside tailored mesopores.

One complementary approach, that helps quantifying the observed concurrent reactions, is measuring reaction kinetics. Both RCM and MC are 1st-order in olefin,[67-68] while concurrent ADMET, formally a polycondensation, and homometathesis reactions are 2nd-order in olefin. Thus, without analyzing the products, one can identify which reaction to which extent occurs by determining the exponential factor *a* in $\frac{-d[olefin]}{dt} = k[catalyst][olefin]^a$.

Also, for a given olefin, immobilized catalyst and support, kinetic measurements should allow for identifying enrichment effects of either the product or the reactant inside the pores such as formation of multi-layers of olefin or product(s) by simply comparing the (apparent) rate constants, $k_{app.}$, of a reaction. Within that context, the intermediary, instable metal alkylidenes, which usually decompose 1st order, are indirectly but particularly suited to investigate and quantify differences in olefin diffusivity, enrichment effects of products and/or olefins in pores in dependence of pore size and pore functionality.

Complementary, ethenolysis reactions of fatty acid esters will be investigated. Apart from being of technical relevance, these reactions are special in that they represent the back reaction of an RCM or MC reaction and even an ADMET polymerization. It is therefore of utmost interest, how pores must be designed with respect to polarity, form and size to guarantee for a perfect introduction of ethylene, to suppress outgassing and bubble formation and to optimize reaction rates. We expect non-polar pore walls to give the best results; this, however is to be demonstrated.

Another very important feature of the catalytic system to be used here, i.e. of Mo/W imido and W-oxo alkylidenen NHC complexes is related to the fact that all these catalysts exist in a *syn*- and *anti*-form, with the R-group at the alkylidene (CMe_2Ph or *t*-Bu) either pointing towards the imido or oxo ligand (*syn*) or pointing away from it (*anti*). These two *syn/anti* forms interconvert at interconversion rates $k_{a/s}$ and $k_{s/a}$, respectively, and with $K = k_{a/s}/k_{s/a}$, that are specific for a given catalyst (Scheme B2-3). It is well known that *syn*/*anti* interconversion rates are also strongly solvent dependent because of coordination of a donor solvent such as THF or acetonitrile to the (distorted) tetrahedral 14-electron complex and formation of a five-coordinate, 16-electron species.[69] It is also well known that the reactivity of an *anti*-isomer can be orders of magnitude higher than the one of the *syn*-isomer.[70] Upon [2+2] cycloaddition of the olefin to the metal alkylidene, the stereochemistry of the progenitor complex prevails in this pericyclic reaction. Consequently, depending on the addition of the olefin to the metal alkylidene, stereospecific reactions can be carried out leading to either high *Z*- or high *E*-olefins. We very recently demonstrated[37] that it is the ratio of the apparent rate constant of polymerization over the apparent rate constant of *syn/anti* interconversion that determines the *E*- or *Z*-content of a polymer.[37] Now, the same must apply to HM: if the HM reaction is fast with respect to $k_{s/a}$ ($k_r >> k_{s/a}$) then high Z-olefins are obtained in combination with a bulky alkoxide (phenolate). Vice versa, if $k_r << k_{s/a}$, high E-olefins are obtained (Scheme B2-3). We could also show that complexes based on O-chelating NHCs (top right,

Scheme B2-3) experience a very slow interconversion, which is related to the sterically overloaded ligand sphere.[37] Together, the very special features make Mo/W imido/oxo alkylidene NHC complexes perfect probes for olefin/product enrichment inside the pores since this will change *syn/anti* interconversion. Also, any steric constraints can be detected, since this will most probably mimic the steric congestion provided by, e.g. O-chelating NHCs and should thus influence *syn/anti* interconversion, too, and thus change the *E/Z* ratio even in simple HM reactions.

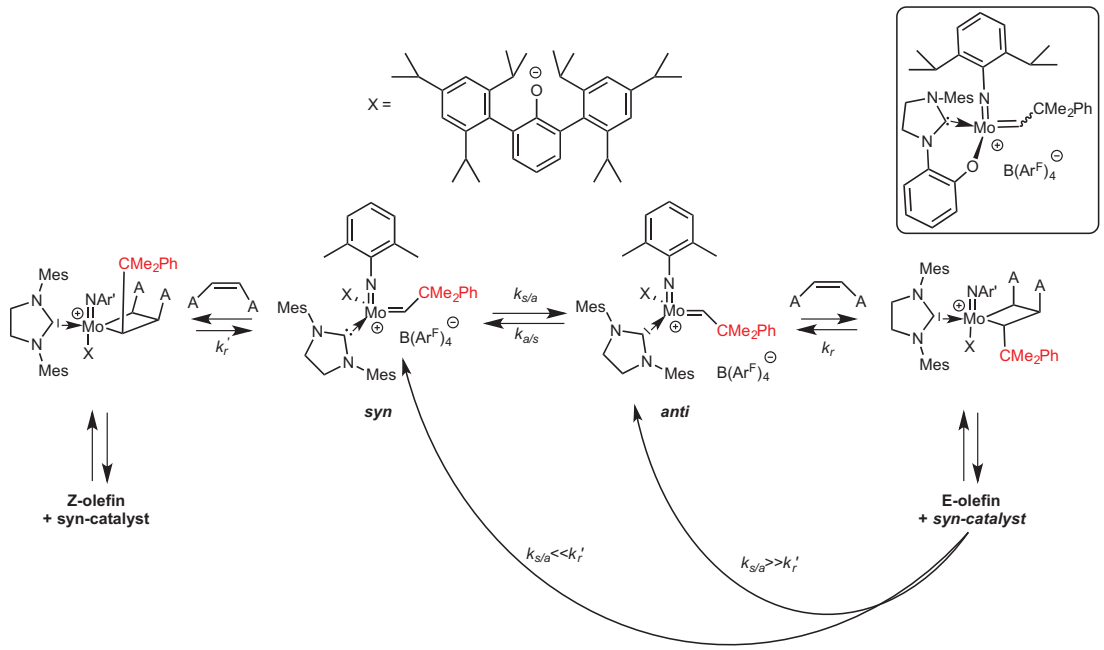

Scheme B2-3. Bottom: *syn*- and *anti*-isomer of a cationic Mo-imidoalkylidene NHC complex with a bulky alkoxide (X) and reaction with a *Z*-olefin to yield an *Z*- or *E*-olefin. Top, right: cationic Mo-imido alkylidene containing an O-chelating NHC.

Finally, chiral catalysts, either based on axially chiral alkoxides or onaxially chiral bidentate ligands as shown in Figure B2-4, will be used to study confinement effects. The enantioselectivity of the catalysts shown there strongly depends on the ligand geometry around the metal center. When moving from catalysis in solution to molecular heterogeneous catalysis in confined geometries, additional interactions between the catalyst and the pore wall, respectively the functional groups located there, may become part of the game. This obviously depends on the pore size, the tether length and rigidity, the functional groups inside the pore and the solvent used. Now, for a given experimental setup, one should be able to determine the critical pore diameter by simply monitoring the *ee*-values of a reaction in dependence of the pore diameter. Staying slightly above this critical pore diameter, one can then vary solvents and concentrations of reactants to determine enrichment or competitive or synergistic effects on the reaction. Backed up by calculations (**projects C5 and C6**), this is proposed to provide substantial insight into various confinement effects, whether based on size or on polarity. Since **project B3** addresses similar issues in the asymmetric 1,4-addition reactions, results from both projects (**B2**, **B3**) will be correlated. Untethered catalysts as shown in Figure B2-5 can be directly used suing SILP technology as outlined in section 3.9.4.3; for the tethering of these catalysts via the NHC the principles outlined in section 3.9.4.1 can be applied.

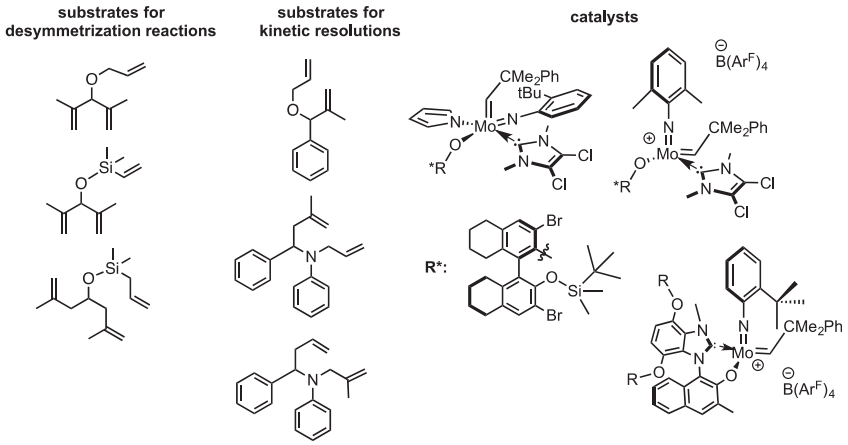

Figure B2-5. Benchmark olefins and catalysts for desymmetrization reactions and for kinetic resolutions for probing confinement effects.

3.9.4.5 WP 5: Confinement effects to be studied

As already outlined, we first generally wish to scrutinize both the influence of different functional surface groups (polar, non-polar, protic, aprotic) and the size, geometry and tortuosity of various mesoporous systems in combination with differently functionalized olefins (polar, non-polar, protic, aprotic) on the reactivity of Mo/W imido/oxo alkylidene NHC catalysts immobilized inside these mesoporous systems in MC and CM reactions. Once established, the concept will be extended to other olefin metathesis reactions including en-yne metathesis and stereoselective olefin metathesis. Using the support materials outlined in section 3.9.4.2, the following confinement effects will be investigated:

A) Confinement by size:

Depending on the **pore diameter**, the pore walls (+ solvent molecules in the solvent layer + olefins + products) will add additional **steric constraints** to the catalyst. As already sketched above, this is expected to result in

a) a different mobility of the catalyst including the alkylidene ligand. This is proposed to result in different *syn/anti* interconversion rates compared to the parent catalyst in solution. This will influence reactivity but also regio- and stereoselectivity of the [2+2] cycloaddition, i.e. *E/Z* ratios in HM reactions but also the *ee*-values in desymmetrization reactions as outlined in Figure B2-4. The thickness of the Solvent/olefin layer in dependence of the olefins and solvents and the concentration profiles are to be calculated by **project C5**.

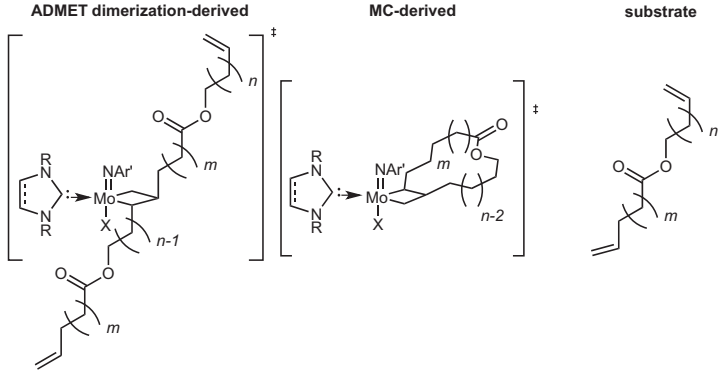

Figure B2-6. Transition states in ADMET polymerization (left) and MC (right).

c) a suppression of side reactions and consequently an increased chemoselectivity in the macrocyclization of dienes to form large rings (typically 12-18 membered). This effect is proposed to strongly correlate with both the size of reactants *and* the ring size of the product. Decisive for a selective MC over ADMET polymerization are the sizes of the corresponding transition states (Figure B2-6, only formation of a dimer is shown, higher oligomers obviously require even more space). Clearly, the transition state of the road to the MC product is sterically significantly less demanding.

B) Confinement by geometry/tortuosity/aspect ratio:

a) a higher tortuosity decreases diffusion[71] and thus activity, usually expressed as turn-over frequency, TOF, and eventually, productivity, expressed on turn-over numbers, TONs, because the envisaged Mo and W based catalysts decompose 1st order in analogy to their Ru-alkylidene counterparts[67-68] in the absence of olefin. Clearly, COF-based materials (**project A3**) have a low tortuosity and must therefore behave differently (better?) than materials with higher tortuosity as prepared, e.g., in **projects A1** (polymeric monoliths with continuous porosity) and in **project A4** (SiO_2, alumosilicate materials).
b) Ink pot *vs*. tubes: the Janus-type approach to polymeric, monolithic, mesoporous materials as described in **project A1** yields ink pot-type pores with an aspect ratio of approximately 1. Similar accounts for pores prepared in **project A7** and modified via bio-inspired mineralization as outlined in **project A5**. By contrast, the supports prepared in **projects A1** using a continuous pore distribution, and in **projects A3** and **A4** contain open tube- (cylinder) type mesopores with very high, almost infinite aspect ratio. Under stirred batch conditions, low aspect ratio pores are proposed to experience less diffusion problems and thus better activity and productivity in CM reactions.

C) Confinement by polarity:

Depending on the polarity of the inner surface of a pore (polar/non-polar, protic, aprotic), the polarity of the solvent and the polarity of the product(s), different situations can be generated. These can in turn be used to study the influence of polarity on the catalytic behavior. Both ethenolysis and HM reactions, which describe the same reaction, though in opposite direction, will be studied. Of particular interest is the influence of ethylene concentration (pressure) on reactivity with regard to pore polarity. In detail, the following variations will be carried out to shed light on the influence of both the polarity of the pore's inner surface and the interplay between olefin/pore wall/solvent:

a) A non-polar, aprotic surface, e.g. C_{18}-alkyl derivatized, in combination with non-polar, aprotic olefins, e.g., pure hydrocarbon dienes and thus products, a polar solvent with low solvent strength, e.g. *t*-butyl methyl ether, and a polar cationic catalyst are proposed to lead to a situation, in which, irrespective of its location, the catalyst will move away from the surface. Consequently, there is a comparably weak influence of both linker rigidity but proposedly a strong influence of linker length on both TOF and TON. By contrast, olefins and or products will interact with the non-polar surface and eventually even form an olefin layer. This results in a comparably low concentration of olefins at the catalyst, at least at the beginning of the reaction. In case of solvent-free (neat) reactions, this might result in a drowning of the catalyst in product, eventually leading to a shut down in catalytic activity. Recording of the reaction kinetics will reveal such effects; even Michaelis Menten kinetics[72] could occur. Since the solvent/olefin layer is expected to be comparably thick, the apparent pore diameter might be smaller than the one determined by, e.g., N_2-adsorption. This effect can be studied by carrying out MC experiments. In comparison to b) – d) (*vide infra*), the ratio of MC over ADMET oligomerization products will be used as a direct measure for the *effective* pore size and influence of surface polarity on this reaction. This is to be experimentally determined and corroborated with theoretical calculations (**projects C4 – C6**).
b) By contrast, a polar, protic or even ionic surface in combination with polar, protic olefins and products and a polar (protic) solvent will, together with a polar, cationic catalyst probably result in rather homogeneous reactions conditions. Both the reactant(s) and product(s) dissolve well in the solvent of choice and will be transported away from the catalyst. The solvent layer is probably thin

and the apparent pore diameter correlates well with the experimentally determined one. There is a flat concentration profile for both the reactant(s) and product(s) between pore wall and the catalyst. The cationic catalysts do not experience any spatial restriction in terms of polarity; consequently, there is strong influence of both linker length and rigidity on TOF and TON.

c) A polar, eventually protic or ionic surface in combination with non-polar, aprotic olefins and products and a non-polar (aprotic) solvent together with a non-polar catalyst probably represent the most intriguing combination. For this special setup, the neutral 16-electron pre-catalyst outlined in Figure B2-1 will be used. In this a setup, neither the solvent nor the olefins will substantially interact with the solvent/reactant layer. The catalyst will also try to move away from the surface. This will result in a very poor interaction of the catalytic system as such with the pore wall and concentration of both the reactants and the products in the solvent phase. Whether this will result in higher TOFs and TONs compared to the situation described in a) and b) is to be investigated. Such an approach can also potentially be used to increase chemoselectivity in CM. Thus, the CM of two olefins with different reactivity such as hexadiene and acrylonitrile is always thwarted by HM. By artificially increasing the concentration of the less reactive partner, i.e. of acrylonitrile inside a pore, one can potentially shift selectivity to the target reaction. The situation created here is somewhat similar to the one in micellar catalysis[73-75] where enrichment effects but also competitive inhibition have been observed. The latter can be circumvented by applying continuous flow.[63] Additional effects such as phase collapse or dewetting,[76] as observed in chromatography, have to be kept in mind, too.
d) A polar, protic or ionic surface together with non-polar, aprotic olefins and products, a polar solvent and a non-polar catalyst is proposed to result in a situation where the polar solvent will together with the surface-functional groups of the pore eventually exclusively form a solvent layer. The non-polar olefins will concentrate at the non-polar catalyst and not at the pore wall. This should lead to higher (initial) TOFs and, eventually, to higher TONs, at least under continuous conditions, which can at least be realized with polymeric, monolithic PUR-based monoliths (**project A1**) but most probably also with silica- (**project A4**) and COF-based materials (**project A3**).
e) The SILP-based approach outlined in section 3.9.4.3 is also special in that the ionic catalyst can move freely inside the pore. The pore surface, the solvent and the catalyst are highly polar. Since the second, transport phase needs to be immiscible with the IL phase, it is preferably non polar or has low polarity. Typically, *n*-heptane or *t*-butyl methyl ether is used for these purposes. This restricts olefin metathesis reactions to non-polar olefins or reactants with low polarity such as olefins or fatty acid esters, however, does not reduce the quality of the conclusions that can be drawn in terms of confinement effect(s).

Obviously, the individual confinement effects outlined in 3.9.4.4 A) – C) might occur simultaneously, though to different extent. Therefore, experimental results need to be thoroughly backed up by quantitative descriptions (calculations) on the nature and thickness of the solvent layer, potential concentration profiles and implications on spacer length and rigidity as well as polarity of the outer ligand sphere of the catalysts. This will be addressed by **projects C4 – C6**.

In cooperation with the group of Prof. Hunger (**project C1**), probe molecules such as alkyl aryl phosphines, PAr_xR_y (x+y=3), will be used to identify differences in accessability of both unsupported and supported catalysts for different nucleophiles. For these purposes, solid-state ^{31}P NMR will be used. Together with changes in pore diameter and geometry, this will allow for identifying the determining parameters for reactant accessibility. Using simple model reactions such as the RCM of diethyl diallyl malonate (DEDAM), solid-state ^{1}H NMR will allow for identifying differences in reaction kinetics with different linkers and pore size/geometries. Since the olefins can be injected in situ into the spinning sample, highly reactive cationic catalysts outlined in Figure B2-1 will be used for these purposes. The use of chiral alkoxides in conjunction with prochiral olefins is envisaged, too.

The spatial distribution of catalysts inside the pores will be addressed by a complementary set of microscopic techniques comprising of scanning and transmission electron microscopy, FIB tomography, and atom probe tomography to capture the 3D arrangement on all relevant length scales (**project C3**).

The experiments outlined above will be supported by theoretical investigations. **Project C4** (Prof. Kästner) will focus on calculating electronic structures, reaction pathways, barrier heights ($\Delta G^{\ddagger}$), reactivities, rate constants and catalyst geometries that are not accessible by single-crystal X-ray

structure analysis, e.g., transition states, using DFT and QM/MM methods. Comparisons between the gas phase and the reactivity in solution will provide information on the influence of solvent and olefin/product polarity on reactivity. Together with **projects C5** and **C6**, information on the steric design of pores and an estimation of the confinement, which will in turn allow for a redesign of the ligands, is envisaged. **Projects C5** and **C6** will focus both on fast (ps/ns) diffusion processes using molecular dynamics (MD, Jun.-Prof. Hansen, Jun.-Prof. Fyta), on a continuous description of concentration profiles as well as on slow diffusion processes on the base of polarity and hydrophilicity (Prof. Groß, ms to s range). This will allow studying the role of the confinement on dynamic processes. Also, concentration profiles of polar/non polar solvents/reactants/products in a pore with a given dimension and polarity can be predicted. Finally, **project C6** (Prof. Holm) will provide most essential information on effective catalyst and, most important olefin and product size and diffusivity, respectively, whether neat or in solution, based on parameterized force fields and coarse-grained MD, respectively. Also, the optimum geometry and polarity of a pore can be predicted for a given reaction/catalyst. Equally important, a pressure-induced flow can be simulated, which will be of utmost relevance for continuous reactions as envisaged in the 2nd funding period. Experimentally determined values for TON and TOF will be correlated with the results from simulation on diffusion, olefin entry and exit rates, concentration profiles and chemical reactivity (**projects C4 - C6**). All together, the resulting multi-scale approach will provide the necessary information to both facilitate material design and devise catalyst immobilization strategies.

Chronological work plan:

	2018	2019	2020	2021	2022	
	Q3 Q4	Q1 Q2 Q3 Q4	Q1 Q2 Q3 Q4	Q1 Q2 Q3 Q4	Q1 Q2	
T1.1						WP 1: Selection of catalysts (Mo-based), tethering and immobilization on mesoporous supports (PhD1)
T1.2						WP 1: Selection of catalysts (W-based), tethering and immobilization on mesoporous supports (PhD2)
T2						WP 2: Selection of supports (PhD1)
T3						WP 3: SILP-technology (PhD2)
T4.1						WP 4: Olefin metathesis reactions (HM, MC, PhD1)
T4.2						WP 4: Olefin metathesis reactions (E/Z, PhD2)
T5						WP 5: Confinement effects (PhD1, PhD2)

3.9.4.6 Methods Applied

This is clearly a catalysis project and thus uses all methods and techniques usually associated with such projects. These include solution and solid-state ^{1}H, ^{19}F, ^{13}C and ^{31}P NMR, measurement of reaction kinetics by GC-MS and, where necessary, by ^{1}H NMR. Also chiral HPLC and chiral GC, single-crystal X-ray analysis will be used. Other important features include Moessbauer spectroscopy on the catalysts (**project C2**) and spatial resolution of the catalytic sites (**project C3**).

3.9.4.7 Vision

By the end of the first funding period, there should be a clear concept on how linker length and rigidity in combination with pore size (diameter), pore form and pore polarity influences catalytic activity in olefin metathesis. The same accounts for the catalysts to be used: here the most appropriate systems, both in terms of metal, ligand sphere and electron count, must be identified. There should also be a first picture on the interplay between stereoselectivity of the catalyst, material used, pore polarity, and polarity of the solvents and olefins to be used. As of materials, a set of materials most appropriate for this type of catalysis must have been identified (max. 2-3).

3.9.5 Role within the collaborative research center

This project is one of the three catalysis projects. It uses an important, maybe the most important catalytic C-C bond forming reaction, i.e. olefin metathesis. The catalysts presented in this proposal represent a novel and still quite unexplored class of metal alkylidenes that are sufficiently stable to explore not only olefins with different functional groups and polarity but also substantially different pore polarities, functionalities and even acidities. The ligands at the metal (imido, oxo, alkylidene, NHC and anionic groups) are sensitive towards both Brønstedt and Lewis acidic groups such that these groups do not destroy the catalyst but affect its reactivity. Also worth to be mentioned, Mo and W as group 6 metals are distinct enough from the Ru- and Rh-catalysts outlined in **projects B1** and **B3** in that they are more oxophilic. However, in contrast to catalysts based on group 4 and 5 metals, the corresponding catalysts are sufficiently stable to be used in the outlined studies. In that regards, the catalysts chosen here represent most suitable probes to study the confinement effects outlined in this CRC proposal. As one of the catalysis projects, the data acquired here will be of utmost significance for all theoretical calculations (**projects C4-C6**).

3.9.6 Differentiation from other funded projects

Fundamental research on Mo and W imido/oxo alkylidene NHC complexes is currently funded by the DFG (BU 2174/19-1, BU 2174/22-1). The work described in B2 is *not* subject or partly subject of this ongoing research.

3.9.7 Project funding

3.9.7.1 Previous funding

This project is currently not funded and no funding proposal has been submitted.

References (ctd.)

[52] M. Ahmed, A. G. M. Barrett, D. C. Braddock, S. M. Cramp, P. A. Procopiou, *Tetrahedron Lett.* **1999**, *40*, 8657-8662.

[53] M. Ahmed, T. Arnauld, A. G. M. Barrett, D. C. Braddock, P. A. Procopiou, *Synlett* **2000**, 1007-1009.

[54] D. Rix, F. Caïjo, I. Laurent, L. Gulajski, G. K., M. Mauduit, *Chem. Commun.* **2006**, 3771-3773.

[55] H. Clavier, S. P. Nolan, M. Mauduit, *Organometallics* **2008**, *27*, 2287-2292.

[56] H. Clavier, F. Caijo, E. Borré, D. Rix, F. Boeda, S. P. Nolan, M. Mauduit, *Eur. J. Org. Chem.* **2009**, 4254-4265.

[57] H. Schottenberger, M. R. Buchmeiser, R. Herber, *J. Organomet. Chem.* **2000**, *612*, 1-8.

[58] H. Schottenberger, M. Buchmeiser, H. Angleitner, K. Wurst, R. Herber, *J. Organomet. Chem.* **2000**, *605*, 174-183.

[59] B. Autenrieth, F. Willig, D. Pursley, S. Naumann, M. R. Buchmeiser, *ChemCatChem* **2013**, *5*, 3033–3040.

[60] C. P. Ferraz, B. Autenrieth, W. Frey, M. R. Buchmeiser, *ChemCatChem* **2014**, *6*, 191-198.
[61] M. Koy, H. J. Altmann, B. Autenrieth, W. Frey, M. R. Buchmeiser, *Beilstein J. Org. Chem.* **2015**, *11*, 1632-1638.
[62] J. Zhao, D. Wang, B. Autenrieth, M. R. Buchmeiser, *Macromol. Rapid Commun.* **2015**, *36*, 190-194.
[63] B. Sandig, M. R. Buchmeiser, *ChemSusChem* **2016**, *9*, 2917-2921.
[64] B. Sandig, L. Michalek, S. Vlahovic, M. Antonovici, B. Hauer, M. R. Buchmeiser, *Chem. Eur. J.* **2015**, *21*, 15835-15842.
[65] J. C. Conrad, M. D. Eelman, J. A. Duarte Silva, S. Monfette, H. H. Parnas, J. L. Snelgrove, D. E. Fogg, *J. Am. Chem. Soc.* **2007**, *129*, 1024-1025.
[66] T. Heidt, A. Baro, A. Köhn, S. Laschat, *Chem. Eur. J.* **2015**, *21*, 12396-12404.
[67] M. Ulman, R. H. Grubbs, *J. Org. Chem.* **1999**, *64*, 7202-7207.
[68] M. Ulman, R. H. Grubbs, *Organometallics* **1996**, *17*, 2484-2489.
[69] R. R. Schrock, J.-K. Lee, R. O'Dell, J. H. Oskam, *Macromolecules* **1995**, *28*, 5933-5940.
[70] J. H. Oskam, R. R. Schrock, *J. Am. Chem. Soc.* **1992**, *114*, 7588-7590.
[71] S. Beckert, F. Stallmach, R. Bandari, M. R. Buchmeiser, *Macromolecules* **2010**, *43*, 9441-9446.
[72] E. Seibert, T. S. Tracy, *Methods Molec. Biol.* **2014**, *1113 (Enzyme Kinetics in Drug Metabolism)*, 23-35.
[73] T. Kotre, M. T. Zarka, J. O. Krause, M. R. Buchmeiser, R. Weberskirch, O. Nuyken, *Macromol. Symp.* **2004**, *217*, 203-214.
[74] G. Pawar, B. Bantu, J. Weckesser, S. Blechert, K. Wurst, M. R. Buchmeiser, *Dalton Trans.* **2009**, 9043-9051.
[75] G. M. Pawar, M. R. Buchmeiser, *Beilstein J. Org. Chem.* **2010**, *6*, doi:10.3762/bjoc.3766.3728.
[76] M. Przybyciel, R. E. Majors, *LC-GC Europe* **2002**, 1-5.

3.9.7.2 Requested funding

Funding for	2018		2019		2020		2021		2022		2018-2022	
Staff	Quantity	Sum	Quantity	Sum	Quantity	Sum	Quantity	Sum	Quantity	Sum	Quantity	Sum
PhD student, 67%	2	43,200.-	2	86,400.-	2	86,400.-	2	86,400.-	2	43,200.-	2	345,600.-
Total		43,200.-		86,400.-		86,400.-		86,400.-		43,200.-		345,600.-
Direct costs	Sum		Sum		Sum		Sum		Sum		Sum	
consumables	8,000.-		16,000.-		16,000.-		16,000.-		8,000.-		64,000.-	
Total	8,000.-		16,000.-		16,000.-		16,000.-		8,000.-		64,000.-	
Major research instrumentation	Sum		Sum		Sum		Sum		Sum		Sum	
GC-MS	82,400.-		-		-		-		-		82,400.-	
High throughput equipment	10,600.-		-		-		-		-		10,600.-	
Total	93,000.-		-		-		-		-		93,400.-	
Grand total	144,200.-		102,400.-		102,400.-		102,400.-		51,200.-		502,600.-	

(All figures in EUR)

3.9.7.3 Requested funding for staff

	Sequential no.	Name, academic degree, position	Field of research	Department of university or non-university institution	Project commitment in hours per week	Category	Funding source
Existing staff							
Research staff	1	M. R. Buchmeiser, Dr., Full Prof.	Polymer Science, Catalysis, Organometallic Chemistry	Institute of Polym. Chem.	6		University
	2	D. Wang, Dr.	Polymer Science, Catalysis, Organometallic Chemistry	Institute of Polym. Chem.	6		University
Non-research staff	3	M. Wendel		Institute of Polym. Chem.	6		University
Non-research staff	4	R. Stiehle		Institute of Polym. Chem.	2		University
Requested staff							
Research staff	5	N.N. M.Sc.	Polymer Science, Organometallics	Institute of Polym. Chem.		PhD	
Research staff	6	N.N. M.Sc.	Polymer Science, Organometallics	Institute of Polym. Chem.		PhD	
Research staff	7	Research assistant	Polymer Science, Organometallics	Institute of Polym. Chem.			

Job description of staff (supported through existing funds):
1
Full Professor, Head of the Institute
2
Scientific coworker, in charge of (low/high-T) NMR, high-temperature GPC, ICP-OES, special syntheses,
3
Technician, in charge of maintaining laboratories, laboratory equipment, management of chemicals, glove boxes
4
Secretary

Job description of staff (requested funds):
5
PhD student, work packages 1 (Mo), 2, 4 (HM, MC) and 5
6
PhD student, work packages 1 (W), 3, 4 (*syn/anti* interconversion, E/Z-selectivity, asymmetric catalysis) and 5
7
Research assistants. **Justification:** The research assistants shall provide synthetic and analytical help for PhD 1 (WPs 1, 2, 4, 5) and for PhD2 (WPs, 1, 3, 4, 5). This will allow them to pick up both non-standard synthetic and analytical techniques.

3.9.7.4 Requested funding of direct costs

	2018	2019	2020	2021	2022
Uni Stuttgart: existing funds from public budget	4,000.-	8,000.-	8000.-	8,000.-	4,000.-
Sum of existing funds	4,000.-	8,000.-	8000.-	8,000.-	4,000.-
Sum of requested funds	8,000.-	16,000.-	16,000.-	16,000.-	8,000.-

(All figures in EUR)

Consumables for financial year 2018

Chemicals, consumables, monomers, solvents, silica for columns, gases (Ar), NMR solvents	EUR	8,000.-

Consumables for financial year 2019

Chemicals, consumables, monomers, solvents, silica for columns, gases (Ar), NMR solvents	EUR	16,000.-

Consumables for financial year 2020

Chemicals, consumables, monomers, solvents, silica for columns, gases (Ar), NMR solvents	EUR	16,000.-

Consumables for financial year 2021

Chemicals, consumables, monomers, solvents, silica for columns, gases (Ar), NMR solvents	EUR	16,000.-

Consumables for financial year 2022

Chemicals, consumables, monomers, solvents, silica for columns, gases (Ar), NMR solvents	EUR	8,000.-

3.9.7.5 Requested funding for major research instrumentation

Equipment for financial year 2018

GC-MS (Agilent 7890/5977B) with autosampler. Justification: GC-MS allows for the fast and cheap analysis of complex reactant/product mixtures, including the analysis of mixtures of enantiomers in case chiral columns, e.g. ß-cyclodextrin-based, are used. In view of the large numbers of experiments that are to be carried out, a high sample throughput must be guaranteed in order to have the necessary progress in research.	EUR	82,400.-
catalyst-screening-block. Justification: In order to avoid destruction of the porous materials and the resulting catalyst systems due to mechanical stress induced by stirring, classical magnetic stirrers can not be used. Therefore, the mechanical workshop will build a catalyst screening block for the parallel screening of different catalyst systems consisting of an IKA shaker 260 control (3.560.- €), a cryostat Julabo, model: Corio CD-200F cooling circulation thermostat -20 to +150°C (3.370.- €), 2 aluminium heating blocks with sockets for the cryostat (3 x 24 Schlenk tubes D10 mm, 3 x 12 Schlenk tubes D20 mm), 6 aluminium condenser units for the heating device made by mechanical workshop, estimated 2.000 €), 30 pressure Schlenk vials D10 mm, 20 pressure Schlenk vials D20 mm (made by glass blowers, estimated 1670.- €).	EUR	10,600.-

3.10 Project B3

3.10.1 General information about Project B3

3.10.1.1 Asymmetric catalysis with supported chiral olefin-rhodium complexes in defined porous networks

3.10.1.2 Research Areas
301-02 Organic Molecular Chemistry

3.10.1.3 Principal Investigator
Laschat, Sabine, Prof. Dr., born 20.08.1963, female, German
Institut für Organische Chemie
Universität Stuttgart, Pfaffenwaldring 55, 70569 Stuttgart
Tel.: 0711/685-64565
E-Mail: sabine.laschat@oc.uni-stuttgart.de
Tenured Professor C4

3.10.1.4 Legal Issues
This project includes

1.	research on human subjects or human material.	no
2.	clinical trials.	no
3.	experiments involving vertebrates.	no
4.	experiments involving recombinant DNA.	no
5.	research involving human embryonic stem cells.	no
6.	research concerning the Convention on Biological Diversity.	no

3.10.2 Summary
The aim is to investigate the interplay between soft confinement, i.e. a chiral solvation shell around a covalently tethered metal diene catalyst, and hard confinement, i.e. a porous material in asymmetric catalysis. This unique arrangement and the presence of a polarity gradient between the inner pore surface and the catalyst in the center of the pore enables directed diffusion which will be probed experimentally and theoretically employing the Rh-catalyzed 1,4-addition of boronic acids to enones as a benchmark system. The homogeneous process is known including our own previous work, but has several drawbacks such as competing pre-equilibria, the presence of reactants of different polarity in a biphasic solution and poor reactant conversion by many catalysts, which requires tedious optimization of catalysts and reaction conditions for each reactant class. In a novel approach chiral olefin-Rh complexes will be confined and preorganized by tailor-made covalent anchoring via organic linkers inside mesoporous materials from **projects A2, A4, A5, A7**. By using materials with polar (e.g. hydroxy) groups at the inner pore and non-polar or dipolar aprotic solvent, a polarity gradient is generated between the polar protic inner pore wall and the dipolar aprotic center, where the catalyst is located. This polarity gradient should a) enhance transport of byproducts (water, boric acid) from the catalyst to the pore surface, b) shift the boronic acid/boroxine equilibrium together with H-bonding interactions of the pore wall in favour of the boronic acid and c) favour the formation of the catalytically active monomeric hydroxo-Rh-olefin complex versus non-polar dimeric Rh-olefin precursor. Microscopic reversibility via directed fast diffusion of the enone from the pore wall to the catalyst in the center will further increase the reaction rate. The steric confinement should enable synergic interactions between monomeric active catalysts resulting in improved enantioselectivities. Moreover, due to the chiral olefin ligands the catalyst is encapsulated by a chiral solvation shell inside the pore, providing a chiral confinement, which contributes to the asymmetric induction. Thus, even subtle energetic differences regarding the catalyst / reactant / solvent cage / pore interactions can be probed by simply measuring the enantiomeric excess of the 1,4-addition product. Synthetic variation of linker lengths, polarity, flexibility and terminal anchor groups will be tested in order to obtain reproducible catalyst loading of the pores, stable and positionally well defined surface anchoring and prevent leaching of the immobilized metal. Spectroscopic, analytical and theoretical studies of these catalysts in asymmetric 1,4-additions in collaboration with **projects C1** – **C6** will give insight into the chirality transfer and molecular mechanism

in confined systems.

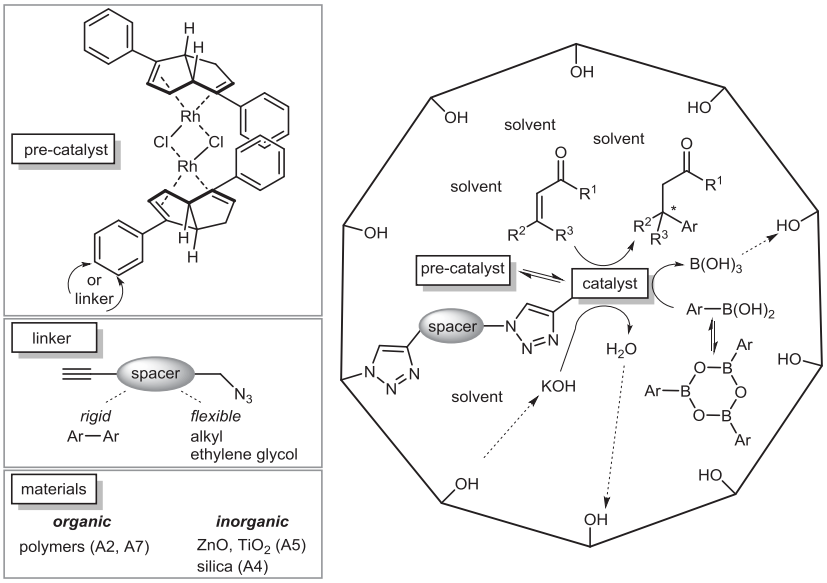

Figure B3-1 Summary of the proposed project.

3.10.3 Research rationale

3.10.3.1 Current state of understanding and preliminary work

The asymmetric heterogeneous catalysis with supported transition metal complexes has been extensively studied over the last decades.[1-7] In particular, there is a growing interest in asymmetric molecular heterogeneous catalysis, where the catalyst is covalently anchored in a porous material, such as meso-porous silica, metal-organic frameworks (MOFs), nanoparticles or polymers etc.[1] The porous confinement of such immobilized catalyst not only results in increased catalyst lifetime, durability and better recycling.[8] Moreover, depending on the type of porous material the confinement generates synergic effects between two anchored transition metal complexes within the same pore, and/or between an anchored transition metal complex and hydroxyl groups on the inner pore wall, resulting in increased activity and enantioselectivity by bringing catalyst, reactant and further additives in close proximity and overcoming rate-limiting diffusion processes.[9]

A remarkable enhancement of the enantioselectivity was observed for catalytic asymmetric Diels-Alder reactions employing chiral Cu-bisoxazoline (BOX) complexes tethered to SiO_2 surfaces, when the remaining "free" SiO_2 surface was functionalized with achiral 3-methacryloxypropyl-trimethoxysilane (Figure B3-2).[10] Based on solid state NMR experiments the results were rationalized by hydrogen bonding between the chiral BOX ligands and the achiral methacrylate on the SiO_2, which suppressed rotation of the tethered catalyst and "glued" a new chiral assembly together, which is not possible in solution. Indeed, upon addition of the achiral silane reagent to the reaction solution containing Cu(BOX)-supported SiO_2, the enantioselectivity did not change. It is expected that this confinement effect on the enantioselectivity should be even more pronounced when the catalyst is anchored inside a pore rather than on a flat surface. Surprisingly, this confinement effect has neither been investigated for catalysts tethered inside pores nor explored for other catalytic transformations. Therefore this literature precedence is particularly relevant for the proposed work in **project B3**.

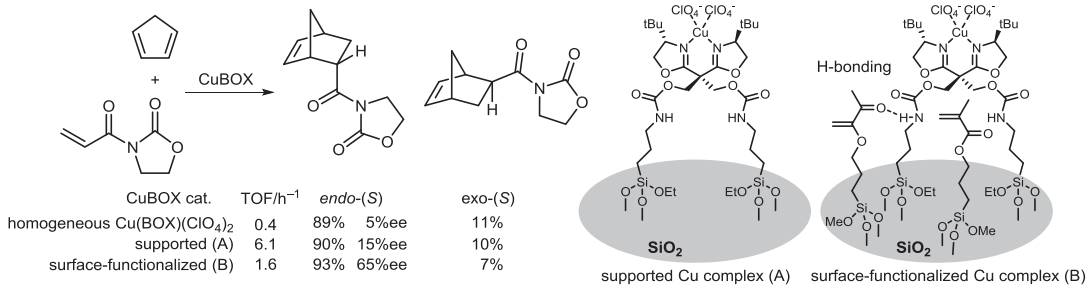

CuBOX cat.	TOF/h^{-1}	*endo*-(*S*)	exo-(*S*)
homogeneous Cu(BOX)$(ClO_4)_2$	0.4	89% 5%ee	11%
supported (A)	6.1	90% 15%ee	10%
surface-functionalized (B)	1.6	93% 65%ee	7%

supported Cu complex (A) surface-functionalized Cu complex (B)

Figure B3-2 Catalytic asymmetric Diels-Alder reaction with supported (A) and surface-functionalized Cu complexes (B). In the latter case a significant increase of the enantioselectivity was observed, presumably due to conformational fixation via H-bonds. Figure was modified according to ref.[10]

With respect to the chiral ligands used in asymmetric heterogeneous catalysis most work has been devoted to phosphanes, ligands with N- and O-donor atoms as well as N-heterocyclic carbenes (NHCs).[1-7] In contrast, chiral diene ligands were only rarely employed for this purpose. Based on the seminal discoveries by Hayashi,[11] Carreira,[12] and Grützmacher[13] that chiral alkene and diene ligands exert efficient stereocontrol in homogeneous asymmetric transition-metal-catalyzed reactions, many groups worldwide have contributed to this field (for reviews see ref.[14-19]). Most previous work has been focused on the development of novel diene or alkene ligands (Figure B3-3) and their use in homogeneous Rh-catalyzed asymmetric 1,4-addition of organoboron reagents to Michael acceptors (e.g. enones, α,β-unsaturated esters and amides, maleimides), and 1,2-additions to carbonyl derivatives. Other catalytic reactions such as 1,6-additions, [4+2]- and [3+2]-cycloadditions, C-H-alkylations, carbene insertions in B-H or Si-H bonds, arylative cyclizations, cyclopropanations and hydrogenations employing Rh-, Ir- and Pd-diene complexes have been reported as well.

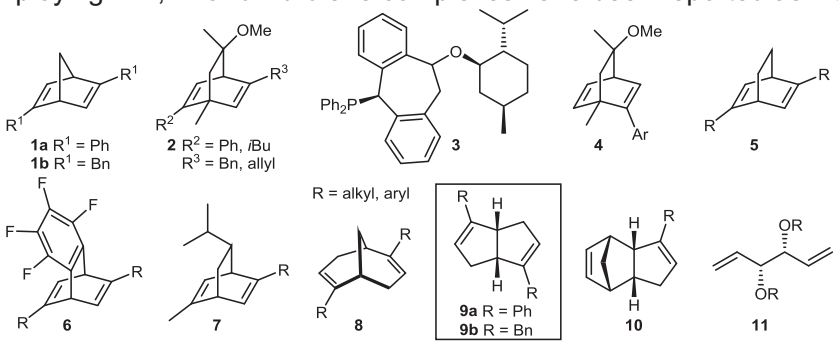

Figure B3-3 Selected examples of chiral diene and alkene ligands **1** – **11** from the literature.[14-19] Bicyclo[3.3.0]octa-2,5-dienes **9a**,**b** were independently developed by Lin[20] and us (see below chapter 3.10.3.2).

Typical experimental conditions for the homogeneous Rh-catalyzed 1,4-addition of organoboronic acids (e.g. **13**) to enones (e.g. cyclohexenone **12a**) are shown in Figure B3-4.[11] Instead of the phenylboronic acid **13**, the corresponding triphenylboroxine **15**, i.e. the cyclic anhydride, or other organoboron species can be used as C-nucleophiles. Usually the homogeneous catalytic 1,4-addition is carried out in polar solvents (e.g. dioxane/H_2O or THF/H_2O mixtures) and sometimes extensive optimizations of solvent and base are required.[21,22]

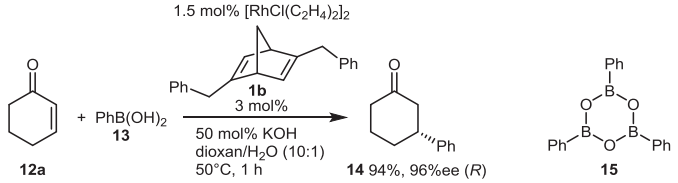

Figure B3-4 Enantioselective homogeneous Rh-catalyzed 1,4-addition of phenylboronic acid **13** to cyclohexenone **12a** in the presence of chiral diene ligand **1b** as reported by Hayashi.[11]

Based on X-ray crystal structure analyses of Rh-diene complexes (summarized in ref.[14]; for selected examples see ref.[23-25]), ^{1}H NMR studies of Rh-diene complexes in solution,[23] comparison with mechanistic data from the corresponding Rh-bisphosphine complexes (e.g. [Rh(acac)(*S*)-BINAP])[26] and theoretical calculations,[27-31] the following catalytic cycle was proposed (Figure B3-5).

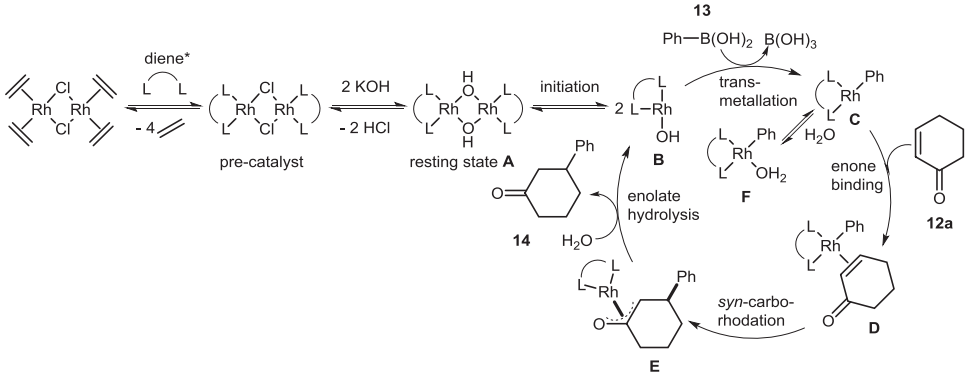

Figure B3-5 Proposed catalytic cycle for the enantioselective homogeneous Rh-catalyzed 1,4-addition of phenylboronic acid **13** to cyclohexenone **12a** in the presence of chiral dienes.[14, 27-31]

The dimeric catalyst precursor $[Rh(CH_2{=}CH_2)_2Cl]_2$ reacts with the chiral diene* to the dimeric chloro-bridged Rh-diene* complex $[Rh(diene^*)Cl]_2$, which is then converted in the presence of aqueous base to the hydroxo-bridged Rh-diene* complex $[Rh(diene^*)(OH)]_2$ (resting state **A**), followed by splitting into the active monomeric hydroxo-Rh-diene* complex **B**. Subsequent transmetallation with phenylboronic acid results in the formation of the phenyl-Rh-diene* complex **C** and simultaneously delivers boric acid. Then the C=C unit of enone **12a** is η^2–bound to the vacant coordination site of complex **C** resulting in the formation of tetracoordinated Rh-(η^2–enone) complex **D**, which undergoes *syn*-carborhodation to the corresponding Rh-(η^3-oxyallyl) complex **E** followed by enolate hydrolysis to the 4-phenylcyclohexanone **14** and recovery of the active catalyst.

The stereochemical outcome of the homogeneous Rh-catalyzed 1,4-addition to enones is explained by the model outlined in Figure B3-6, which was proposed by Hayashi.[11] Theoretical studies indicate that the enthalpy-driven enantioselection takes place during the carborhodation rather than the enone binding step.[28, 31]

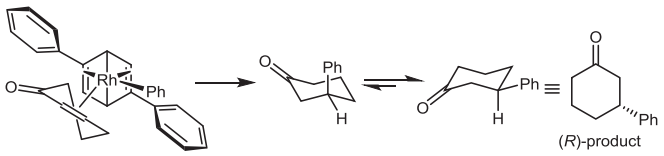

Figure B3-6 Proposed stereochemical model for the enantioselective homogeneous Rh-catalyzed 1,4-addition of phenylboronic acid **13** to cyclohexenone **12a** in the presence of chiral dienes.[14, 31]

However, recent DFT calculations on the homogeneous Rh-catalyzed 1,2-addition to N-tosylimines in the presence of bicyclo[3.3.0]octa-2,5-diene ligand **9a** revealed[32] that the mechanistic picture is more complicated. It was proposed that the equilibrium between phenylboronic acid **13** and its cyclic anhydride, i.e. triphenylboroxine **15** interfer with the catalytic cycle by forming a variety of Rh-boronato complexes. Thus, with respect to the proposed **project B3**, the mechanistic details of the Rh-catalyzed 1,4-addition to enones are still not fully solved.

Despite the above mentioned previous experimental and theoretical investigations of the homogeneous Rh-catalyzed 1,4-addition to enones, immobilization of the Rh-complexes has only been very little studied. Stabilized Rh/Ag bimetallic nanoparticles based on polystyrene-based copolymers with cross-linking moieties, carbon black and chiral dienes carrying an amide moiety were employed for the catalytic 1,4-addition to enones.[33,34] These heterogeneous catalysts allowed expansion of reactant scope towards enoates, which are difficult reactants under homogeneous conditions. More recently,

cellulose-supported chiral Rh-nanoparticles were developed, which gave 1,4-addition products in high yields and enantioselectivities without metal leaching.[35]

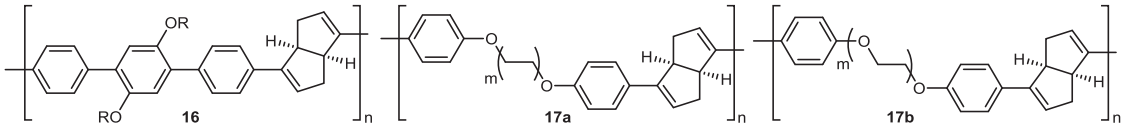

Figure B3-7 Main chain polymers **16**, **17a**,**b** carrying chiral diene units were used as ligands for Rh-catalyzed 1,2-addition to imines.[36]

Stereoregular chiral diene copolymers **16**, **17** based either on rigid terphenyl linkers or flexible oligoethyleneglycol linkers which connected the 2,5-diphenyl-bicyclo[3.3.0]octa-1,5-diene units in the main chain of the polymer were developed (Figure B3-7).[36] Their use in Rh-catalyzed 1,2-additions produced high yields and enantioselectivities in up to three cycles. However, the polymeric materials were not characterized.

Thus to the best of our knowledge, enantioselective molecular heterogeneous catalysis with chiral diene ligands tethered inside mesoporous materials is virtually unexplored. In particular, detailed experimental and theoretical studies to obtain structural information on the supported catalysts, their position inside pores, differentiation between surface bound catalysts and inner-pore bound catalysts, reaction kinetics and diffusion processes towards a complete mechanistic understanding are missing.

Own work. During the total synthesis of the natural product cylindramide[B3-1] we developed a gram-scale synthesis of the enantiomerically pure diketone (*3aS,6aS*)-**18** (Figure B3-8) and its optical antipode, which served as valuable building blocks for the novel bicyclo[3.3.0]octa-2,5-dienes **9a**,**b** in 2 steps and 52% and 44% overall yield, respectively.[B3-2] Diene ligands **9a**,**b** were employed in the homogeneous Rh-catalyzed 1,4-addition of arylboronic acid to various cyclic and acyclic enones.The examples in Figure B3-8 illustrate the complementary behavior of the ligands. Whereas phenyl-substituted diene **9a** worked best for cyclic enones, providing 3-phenylcyclopentenone **20** in 74 %, 95 %ee (*R*), it was inactive for acyclic enones. In contrast, benzyl-substituted diene **9b** gave 4-phenyl-2-pentanone **21** in 71 %, 91 %ee (*R*). The scope of the boronic acids could be further extended to (*Z*)-propenylboronic acids and (*E*)-2-phenylethenyl boronic acids.[B3-3] A recent study on regioisomeric dienes yielded high enantioselectivities in 1,2-additions to *N*-tosyl-imines (up to 99 %ee) and provided theoretical insight into a Rh-catalyzed double bond isomerization.[B3-4]

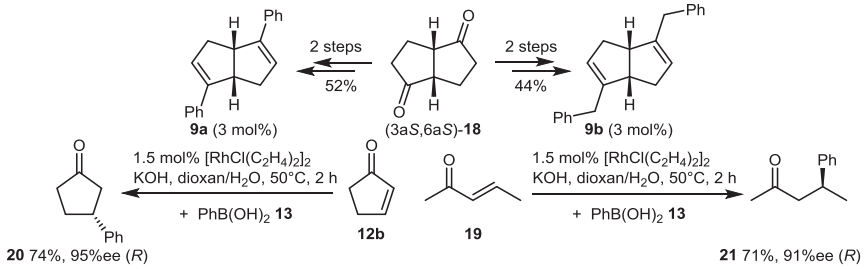

Figure B3-8 Chiral diene ligands **9a**,**b** developed by our group and their complementary performance in homogeneous Rh-catalyzed 1,4-additions.[B3-2]

In order to probe *exo*- and *endo*-coordination modes of Rh, a series of chiral alkene/P-ligands **25**–**30** based on the tropane scaffold **22** was developed (Figure B3-9).[B3-5] Catalytic 1,4-additions to cyclohexenone revealed that *exo*-ligands **25**, **27** gave better yields and enantioselectivities than the *endo*-ligands **26**, **28**, while the presence of phosphorus and diene moiety (e.g. **29**, **30**) deteriorated catalytic activity and/or enantioselectivity.

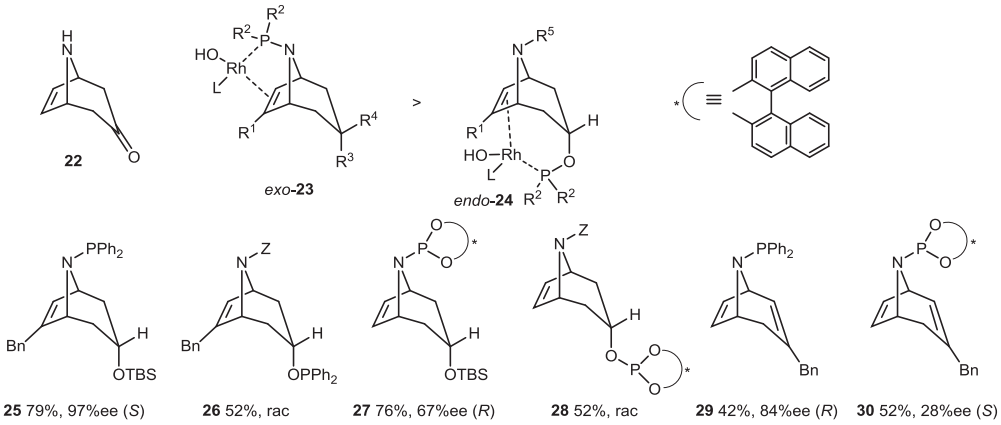

Figure B3-9 Chiral alkene/P-ligands **25** – **30** probing *exo*- and *endo*-coordination of Rh and the resulting yields and enantioselectivities of the homogeneous Rh-catalyzed 1,4-addition of phenylboronic acid to cyclohexenone using these ligands.[B3-5]

Our group has a long-standing experience regarding the synthesis of liquid crystals and their characterization particularly by X-ray diffraction, i.e. wide angle and small angle X-ray scattering (WAXS, SAXS). Along these lines, the equilibria between arylboronic acids and their cyclic anhydrides were studied, which led to the discovery of novel discotic triarylboroxines.[B3-6]

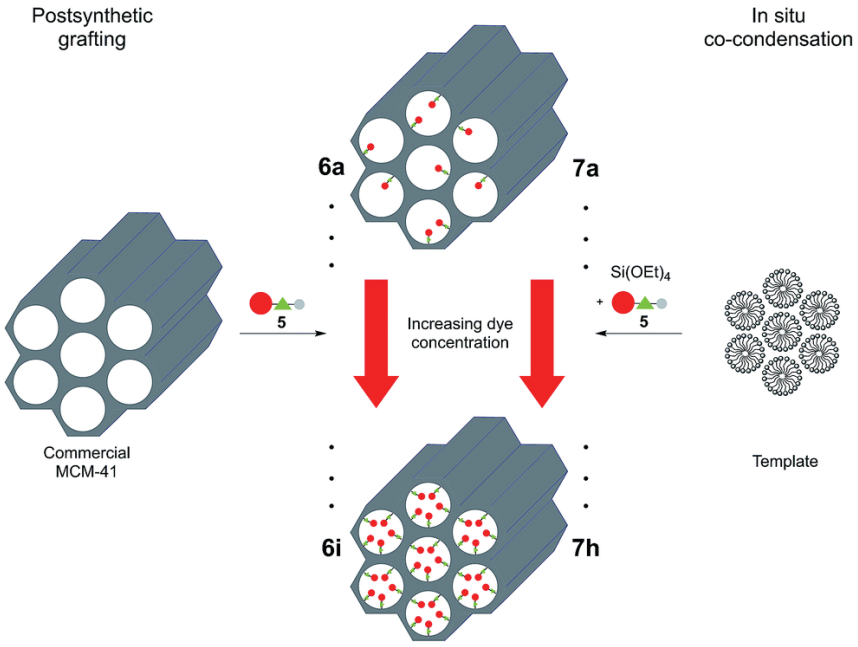

Figure B3-10 Synthesis of grafted (**6a-i**) and co-condensed (**7a-h**) MCM-41 hybrid materials with different loadings of Nile red dye. The figure was taken from ref.[B3-7]

In collaboration with T. J. J. Müller (Univ. Düsseldorf), the distribution of covalently bound Nile red dyes immobilized in mesoporous silica MCM-41 was studied by SAXS,[B3-7] which revealed a 2D hexagonal ordered mesoporous structure which is not affected by the functionalization with the Nile red dye (Figure B3-10). It was also shown that the co-condensed materials possess a predominant functionalization inside the pores.
During our previous work on heterocyclic crosslinkers for bio-inspired hydrogels, click reactions were employed for the synthesis of triazole crosslinkers.[B3-8,B3-9]

References

[1] M. W. A. MacLean, L. M. Reid, X. Wu, C. M. Crudden, *Chem. Asian J.* **2015**, *10*, 70-82.
[2] C. J. Baddeley, in *Heterogeneous Catalysts for Clean Technology*, K. Wilson, A. F. Lee (eds.), **2014**, 103-124.
[3] T. Tsubogo, T. Ishiwata, S. Kobayashi, *Angew. Chem. Int. Ed.* **2013**, *52*, 6590-6604.
[4] R. Sebesta (ed.), *Enantioselective Homogeneous Supported Catalysis*, RSC, Cambridge, **2011**.
[5] H.-U. Blaser, B. Pugin, in *Handbook of Asymmetric Heterogeneous Catalysis*, K. Ding, Y. Uozumi (eds.), **2008**, 413-437.
[6] C. Bianchini, P. Barbaro, *Topics Catal.* **2002**, *19*, 17-32.
[7] K. Fodor, S. G. A. Kolmschot, R. A. Sheldon, *Enantiomer* **1999**, *4*, 497-511.
[8] Recent example: Q. Sun, Z. Dai, X. Meng, F.-S. Xiao, *Chem. Mater.* **2017**, *29*, 5720-5726.
[9] C. Yu, J. He, *Chem. Commun.* **2012**, *48*, 4933-4940.
[10] K. Motokura, M. Tada, Y. Iwasawa, *Catal. Today* **2009**, *147*, 203-210.
[11] T. Hayashi, K. Ueyama, N. Tokunaga, K. Yoshida, *J. Am. Chem. Soc.* **2003**, *125*, 11508-11509.
[12] C. Fischer, C. Defieber, T. Suzuki, E. M. Carreira, *J. Am. Chem. Soc.* **2004**, *126*, 1628-1629.
[13] P. Maire, S. Deblon, F. Breher, J. Geier, C. Böhler, H. Rüegger, H. Schönberg, H. Grützmacher, *Chem. Eur. J.* **2004**, *10*, 4198-4205.
[14] C. Defieber, H. Grützmacher, E. M. Carreira, *Angew. Chem. Int. Ed.* **2008**, *47*, 4482-4502.
[15] J. B. Johnson, T. Rovis, *Angew. Chem. Int. Ed.* **2008**, *47*, 840-871.
[16] D. Müller, A. Alexakis, A. *Chem. Commun.* **2012**, *48*, 12037-12049.
[17] X. Feng, H. Du, *Asian J. Org. Chem.* **2012**, *1*, 204-213.
[18] R. M. Maksymowicz, A. J. Bissette, S. P. Fletcher, *Chem. Eur. J.* **2015**, *21*, 5668-5678.
[19] M. Nagamoto, T. Nishimura, *ACS Catal.* **2017**, *7*, 833-847.
[20] Z.-Q. Wang, C.-G. Feng, M.-H. Xu, G.-Q. Lin, *J. Am. Chem. Soc.* **2007**, *129*, 5336-5337.
[21] B. M. Trost, A. C. Burns, T. Tautz, *Org. Lett.* **2011**, *13*, 4566-4569.
[22] H.-J. Yu, C. Shao, Z. Cui, C.-G. Feng, G.-Q. Lin, *Chem. Eur. J.* **2012**, *18*, 13274-13278.
[23] Y. Otomaru, A. Kina, R. Shintani, T. Hayashi, *Tetrahedron: Asymmetry* **2005**, *16*, 1673-1679.
[24] R. Shintani, Y. Ichikawa, K. Takatsu, F.-X. Chen, T. Hayashi, *J. Org. Chem.* **2009**, *74*, 869-873.
[25] S.-S. Zhang, Z.-Q. Wang, M.-H. Xu, G.-Q. Lin, *Org. Lett.* **2010**, *12*, 5546-5549.
[26] T. Hayashi, M. Takahashi, Y. Takaya, M. Ogasawara, *J. Am. Chem. Soc.* **2002**, *124*, 5052-5058.
[27] H. L. Qin, X.-Q. Chen, Z.-P. Shang, E. A. B. Kantchev, *Chem. Eur. J.* **2015**, *21*, 3079-3086.
[28] E. A. B. Kantchev, *Chem. Commun.* **2011**, *47*, 10969-10971.
[29] E. A. B. Kantchev, *Chem. Sci.* **2013**, *4*, 1864-1875.
[30] H.-L. Qin, X.-Q. Chen, Z.-P. Shang, E. A. B. Kantchev, *Chem. Eur. J.* **2015**, *21*, 3079-3086.
[31] S. Gosiewska, J. A. Raskatov, R. Shintani, T. Hayashi, J. M. Brown, *Chem. Eur. J.* **2012**, *18*, 80-84.
[32] Theoretical studies of the 1,2-addition to imines with ligand **9a**: N. Sieffert, J. Boisson, S. Py, *Chem. Eur. J.* **2015**, *21*, 9753-9768.
[33] T. Yasukawa, H. Miyamura, S. Kobayashi, *J. Am. Chem. Soc.* **2012**, *134*, 16963-16966.
[34] T. Yasukawa, A. Suzuki, H. Miyamura, K. Nishino, S. Kobayashi, *J. Am. Chem. Soc.* **2015**, *137*, 6616-6224.
[35] T. Yasukawa, H. Miyamura, S. Kobayashi, *Chem. Sci.* **2015**, *6*, 6224-6229.
[36] H. Yang, M. Xu, *Chin. J. Chem.* **2013**, *31*, 119-122.

3.10.3.2 Project-related publications by participating researchers

[B3-1] N. Cramer, S. Laschat, A. Baro, H. Schwalbe, C. Richter, *Angew. Chem. Int. Ed.* **2005**, *44*, 820-822.
[B3-2] S. Helbig, S. Sauer, N. Cramer, S. Laschat, A. Baro, W. Frey, *Adv. Synth. Catal.* **2007**, *349*, 2331-2337.
[B3-3] S. Helbig, K.V. Axenov, S. Tussetschläger, W. Frey, S. Laschat, *Tetrahedron Lett.* **2012**, *53*, 3506-3509.
[B3-4] T. Mühlhäuser, A. Savin, W. Frey, A. Baro, A. J. Schneider, H.-G. Döteberg, F. Bauer, A. Köhn, S. Laschat, J. Org. Chem. 2017, DOI: 10.1021/acs.joc.7b02601.
[B3-5] S. Vlahovic, N. Schädel, S. Tussetschläger, S. Laschat, *Eur. J. Org. Chem.* **2013**, *8*, 1580-1590.
[B3-6] T. Wöhrle, A. Baro, S. Laschat, *Materials* **2014**, *7*, 4045-4056.
[B3-7] M. Börgardts, K. Verlinden, M. Neidhardt, T. Wöhrle, A. Herbst, S. Laschat, C. Janiak, T. J. J. Müller, *RSC Adv.* **2016**, *6*, 6209-6222.
[B3-8] M. Martini, P. S. Hegger, N. Schädel, B. B. Minsky, M. Kirchhoff, S. Scholl, A. Southan, G. E. M. Tovar, H. Boehm, S. Laschat, *Materials* **2016**, *9*, 810.
[B3-9] P. S. Hegger, J. Kupka, B. B. Minsky, N. Schädel, N. Petri, S. Laschat, H. Boehm, *Chem. Select* **2017**, *2*, 7701-7705.

3.10.4 Project plan

In summary, the research goals are organized in work-packages as follows:

- **WP1: Synthesis of chiral diene ligands for click anchoring of spacers.** For an efficient linking strategy chiral diene ligands will be synthesized either stepwise or via a one-pot statistic route using chiral bis-enoltriflates as common intermediates. The position and type of substituent at the diene will be varied to tailor the steric and electronic environment in close proximity to the Rh center. The ligands will be employed in **WP2**.
- **WP2: Synthesis and characterization of alkyne- and triazole-modified Rh-diene* complexes.** Chiral diene ligands from **WP1** will be converted into alkyne-modified Rh-diene*-complexes to tailor the distance between the Rh pre-catalyst and the inner pore wall, spacers with different lengths, polarity and flexibility will be attached to the alkyne-modified Rh-diene*-complexes via click reaction. For this purpose a modular spacer concept will be developed.
- **WP3: Investigations on the influence of linker-attached Rh-diene* complexes in homogeneous catalytic 1,4-addition.** Homogeneous Rh-catalyzed 1,4-addition of phenylboronic acid to cyclohexenone employing soluble Rh complexes prepared in **WP2** will provide information whether the linker exerts already in solution effects on the catalytic turnover, enantioselectivity and catalyst lifetime, e.g. due to restricted conformational mobility or steric hindrance. The experimental and theoretical results will serve as a necessary background information for the heterogeneous catalysis studies in **WP5**.
- **WP4: Immobilization of Rh-diene* complexes in inorganic materials using a modular linker concept.** The linker-attached Rh-diene* complexes prepared in **WP2** will be immobilized in inside-pore-functionalized mesoporous inorganic materials ((Al-)SBA-15, SiO_2, ZnO, TiO_2, Al_2O_3) and hybrid polystyrene foam/ZnO via click reaction. Experimental and theoretical studies will probe the immobilized catalytic systems on different length scales to gain insight regarding the location of the Rh pre-catalyst inside the pores and the interactions between the Rh pre-catalyst with the linker and the inner pore wall. The distribution of Rh-diene*-complexes inside the pores will be investigated spectroscopically (e.g. via SAXS) and theoretically.
- **WP5: Catalytic investigations on inorganic materials.** The immobilized Rh-diene* complexes prepared in **WP4** will be evaluated for their catalytic activity and enantioselectivity in the 1,4-addition of phenylboronic acid to cyclohexenone. Experimental results will be complemented by spectroscopic and theoretical methods to gain insight how the confinement affects the reaction kinetics, pre-equilibria and catalytic cycle as well as chirality transfer.
- **WP6: Synthesis of heteroleptic Rh-diene* complexes and Rh-diene* complexes with ancillary ligands, immobilization on SBA-15 and catalytic investigations.** In order to distinguish between catalyst systems containing one Rh center per pore and those containing two Rh centers inside the pore and to suppress competing homogeneous catalysis, well defined heteroleptic dimeric Rh-diene* complexes and monomeric Rh-diene* complexes with ancillary ligands (phosphanes, acetylpyridine, NHCs) will be prepared, immobilized and studied in the benchmark 1,4-addition. The experimental and theoretical studies should reveal, whether the catalytic cycle and reaction mechanism in the confined system is different from the traditional homogeneous catalysis.
- **WP7: Immobilization of Rh-diene* complexes in organic materials using a modular linker concept.** The linker-attached Rh-diene* complexes prepared in **WP2** will be immobilized in inside-pore-functionalized mesoporous organic materials (block copolymer templates and polystyrene foams) via click reaction. Experimental and theoretical studies will probe the immobilized catalytic systems on different length scales to gain insight regarding the location of the Rh catalyst inside the pores and the interactions between the Rh catalyst with the linker and the inner pore wall.
- **WP8: Catalytic investigations on organic materials.** The immobilized Rh-diene* complexes prepared in **WP7** will be evaluated for their catalytic activity and enantioselectivity in the 1,4-addition of phenylboronic acid to cyclohexenone. Experimental results will be complemented by spectroscopic and theoretical methods. Comparison with the results from **WP5** should provide structure-property relationships, insight into the chirality transfer in confined systems and allow the design of novel catalyst systems with high activity and enantioselectivity.

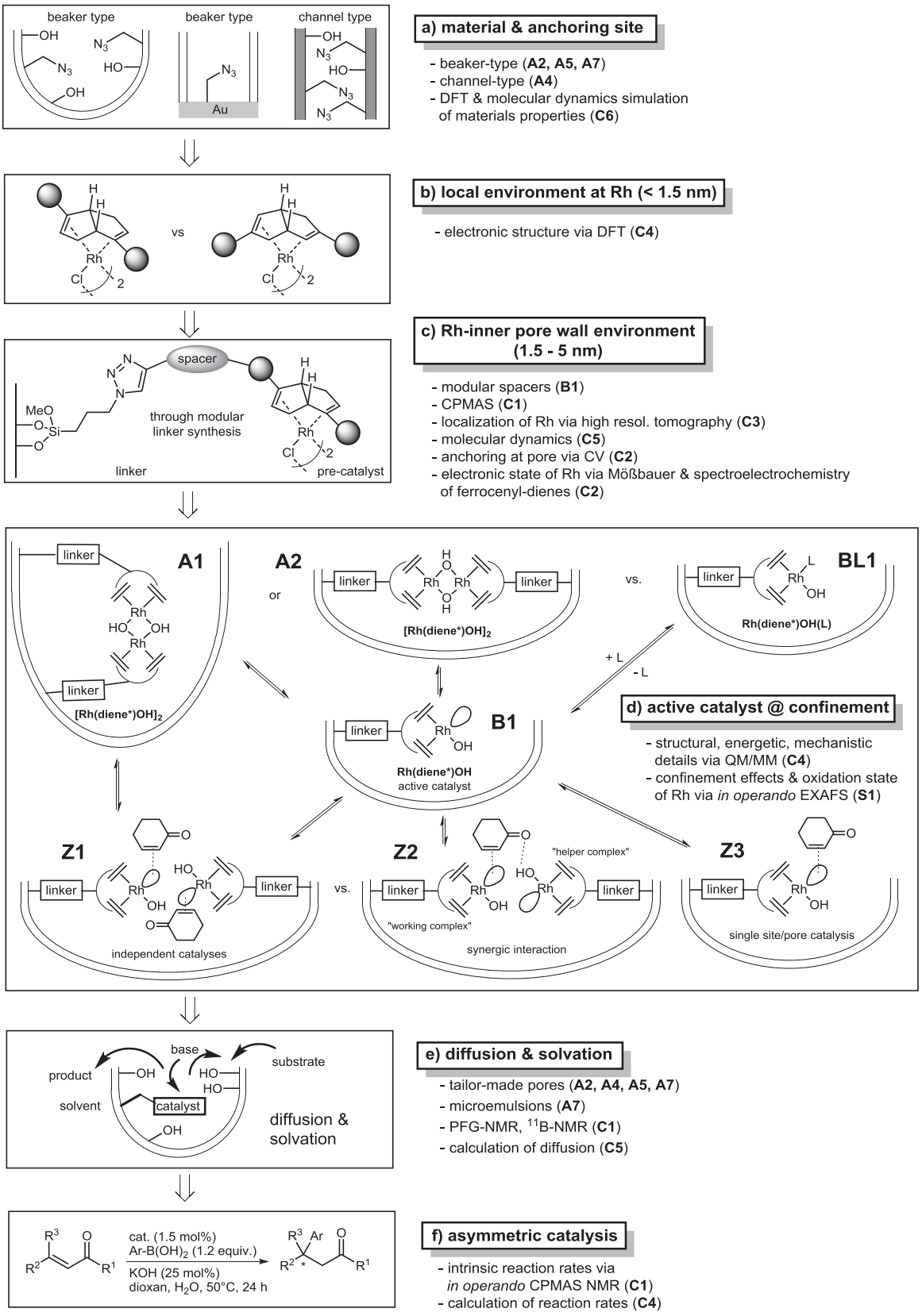

Figure B3-11 Workflow of the B3 project and collaborations with other projects.

The workflow of the B3 project consists of six major topics outlined in Figure B3-11, which are relevant for work packages **WP1** – **WP8** detailed in chapters 3.10.4.1 – 3.10.4.8:

a) **Selection of materials** with suitable pore size, polarity and **anchoring site** (**WP4**, **WP7**).

b) The **local environment at the Rh** center will be controlled by tailor-made ligand architecture and synthesis (**WP1**).

c) In order to control the **environment between Rh complex and inner pore wall**, a modular linker concept will be developed and immobilized Rh complexes synthesized (**WP2**).

d) Generation of the monomeric **active catalyst** from the dimeric pre-catalyst **in the confinement** (**WP5**, **WP6**, **WP8**) and comparison with the homogeneous catalysis (**WP3**) will be performed, in order to identify steric and synergy effects of the confinement.

e) **Diffusion and solvation** processes during catalysis will be analyzed experimentally and theoretically (**WP5**, **WP6**, **WP8**).

f) The performance of the catalytic systems in **asymmetric catalysis**, i.e. 1,4-additions of boronic acids to enones, will be studied experimentally and theoretically in inorganic materials (**WP5**), in the presence of ancillary ligands (**WP6**), in organic materials (**WP8**) and for comparison in homogeneous solution (**WP3**).

3.10.4.1 WP1: Synthesis of chiral diene ligands for click anchoring of spacers. In order to obtain diene ligands which can be attached to the inner pore wall by a modular linker strategy using click chemistry, i.e. Cu-catalyzed Huisgen 1,3-dipolar azide-alkyne cycloaddition to the corresponding triazoles, bicyclo[3.3.0]octa-2,5-dienes with one terminal alkyne unit will be synthesized (Figure B3-12). The ligands **31**, **32** and **38**, **39** were chosen, because they enable the control of the electronic (phenyl vs. benzyl) and/or steric environment (**31** vs. **38** and **32** vs. **39**) around the Rh center.

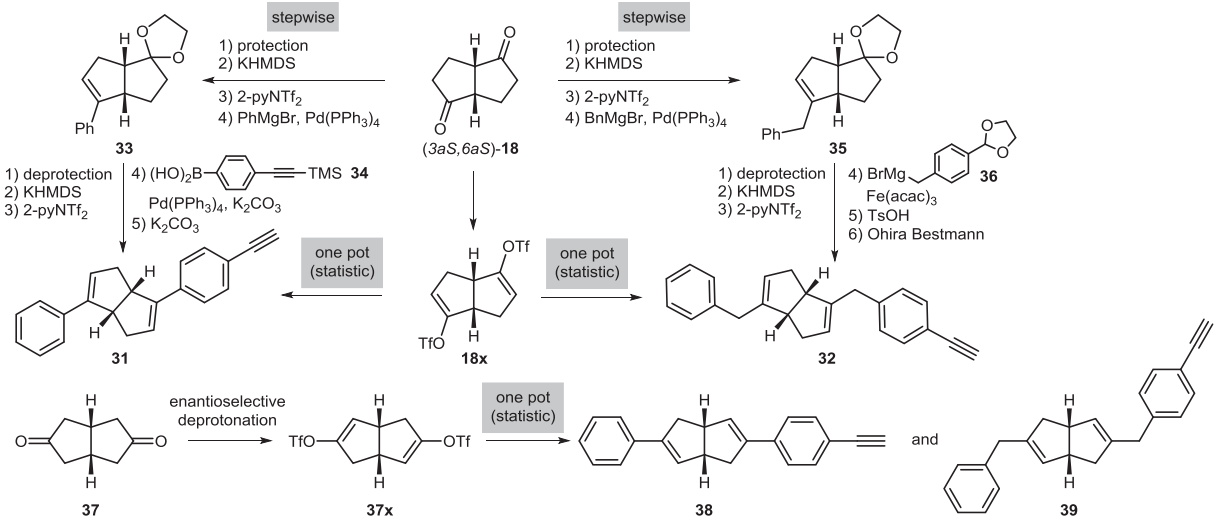

Figure B3-12 Synthesis of diene ligands **31**, **32** and **38**, **39** with one terminal alkyne unit.

A stepwise procedure is planned for ligands **31**, **32**. According to our previously reported procedure,[B3-2] chiral diketone **18** can be obtained from 1,5-cyclooctadiene in 4 steps on a gram scale. Diketone **18** will be converted to the mono-acetal,[37] followed by generation of the enoltriflate and Negishi cross coupling with phenyl Grignard to the corresponding alkene **33**. Subsequent deprotection, formation of the enoltriflate followed by Suzuki cross coupling with the commercially available trimethylsilyl-alkynylphenylboronic acid **34** and basic removal of the TMS group will then deliver diene **31**. An analogous stepwise procedure will yield the benzyl-substituted intermediate **35**, which will then be converted in 3 steps into the enoltriflate, followed by Negishi cross coupling with the Grignard reagent **36**. Acidic acetal cleavage and subsequent Ohira-Bestmann reaction[38,39] will deliver the diene ligand **32**. Alternatively, for both ligands **31**, **32** a statistic synthesis is envisaged. For example, conversion of the diketone **18** to the bis-enoltriflate **18x** and subsequent simultaneous Suzuki cross coupling with 1 equiv. of phenylboronic acid and 1 equiv. of boronic acid **34** should yield the unsymmetric product **31**.

Although this more direct route bears the risk that symmetric cross coupling products are formed as well, they can either be used as reference compounds in homogeneous catalysis or immobilized via double click reaction in case of the bis-alkynyl-terminated symmetric diene.
To access the ligands **38**, **39** the commercially available Weiss diketone **37** can be converted into the chiral bis-enoltriflate **37x** via an enantioselective deprotonation developed previously by us,[40,41] and subsequent statistic Suzuki cross coupling as described above.

3.10.4.2 WP2: Synthesis and characterization of alkyne- and triazole-modified Rh-diene* complexes. Starting from dimeric precursor complex $[Rh(ethene)_2Cl]_2$ and chiral diene ligand **31** prepared in **WP1** a series of alkyne- and triazole-modified chiral dimeric Rh-diene* complexes **40**, **44**, **45** will be synthesized according to our previously established procedure.[B3-2] The strategy is illustrated in Figure B3-13 (left side) for diene ligand **31**, which is converted to Rh-diene* complex **40**. Subsequent click reaction with flexible azido-functionalized spacer **43** will provide triazole-modified Rh-diene* complex **44**.[42] Deprotection and Ohira-Bestmann reaction will then yield the alkyne-modified Rh-diene* complex **45**.
By employing spacers **43** of different lengths (butyl-, hexyl-, octyl-, decyl-) and polarity (diethylene glycol-, triethyleneglycol-linker) the size and flexibility of the spacer-modified Rh complexes can be adjusted. Further variation of rigidity will be achieved by using rigid aryl-, and biaryl-linker units developed in **project B1** (see also Figure B3-14 regarding the modular linker concept).
In an analogous fashion other chiral dienes with terminal alkyne unit from **WP1** (e.g. **32**, **38**, **39**) will be converted to the corresponding alkyne- and triazole-modified Rh-diene complexes.
The Rh complexes will be characterized by solution NMR, ESI-MS and X-ray crystal structure analysis. These crystallographic data will be used by **project C4** for force field parameters in order to calculate the interactions of the Rh-complexes with reactants, solvents and pores by QM/MM. DFT calculations of the Rh complexes derived from diene ligands **31**, **32**, **38**, **39** varying in the position and type of substituent will provide insight into the steric and electronic microenvironment around the Rh center. Crystallographic data will also aid **projects A2**, **A4**, **A5** and **A7** in designing materials with suitable pore size.

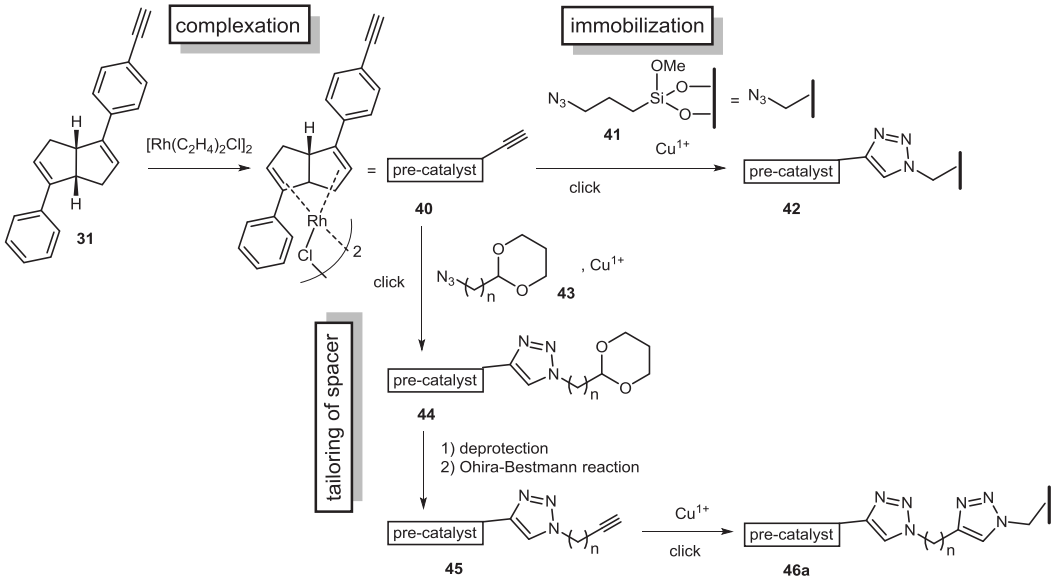

Figure B3-13 Preparation of pre-catalysts and immobilization strategy via a modular linker concept. The alkyne-modified pre-catalysts **40**, **45** will be immobilized to the mesoporous materials carrying the azidopropylsiloxane anchoring group (**41**) via Cu-catalyzed click reaction.

3.10.4.3 WP3: Investigations on the influence of linker-attached Rh-diene* complexes in homogeneous catalytic 1,4-addition. The soluble Rh-diene* complexes **40**, **44**, **45** prepared in **WP2** will be employed in Rh-catalyzed 1,4-additions of phenylboronic acid to cyclohexenone as benchmark reactant following our standard protocol.[B3-2] Known phenyl- and benzyl-substituted dienes **9a**,**b** will be used as reference ligands. Enantioselectivities will be determined by GC and HPLC using a chiral stationary phase. These experiments will allow to separate linker effects from confinement effects observed on immobilized catalysts regarding catalytic activity and enantioselectivity. At a later stage soluble Rh-diene* complexes derived from ligands **32**, **38**, **39** (from **WP1**) will be studied as well.

The catalytic studies will be complemented by quantum chemical calculations of the Rh complexes in **project C4** to gain insight regarding the steric and electronic influence of the linker on the catalytic performance of the diene ligands.
In order to differentiate between effects of the inner pore-bound catalysts and surface effects of the material, reference experiments are required. For example, adsorption of enones, boronic acid or catalyst on the surface might compromise activity and/or enantioselectivity. Therefore inorganic materials provided by **projects A4** and **A5** as well as organic materials provided by **projects A2** and **A7** will be used as additives in homogeneous catalytic 1,4-additions.

3.10.4.4 WP4: Immobilization of Rh-diene* complexes in inorganic materials using a modular linker concept. As discussed in chapter 3.10.3.1 the catalytic 1,4-addition requires solvent mixtures, such as dioxane/water or THF/water and the presence of a base (e.g. KOH). Therefore, robust materials with a polar inner pore surface will be used as powder samples:
Mesoporous silica (Al-)SBA-15 delivered by **project A4** will be investigated. Initial immobilization experiments will start with SBA-15 with hexagonal channel-type pores (pore size: 5 – 8 nm) due to their reliable accessability, thermal stability and the possibility to selectively functionalize these mesoporous materials inside the pores, e.g. via site-isolated azidofunctionalization with azidopropyltriethoxysilane during the SBA synthesis,[42,43] while the outer pore surface can be blocked. In addition, the hydrophilicity of the SBA-material can be increased by incorporation of Al and the pore size can be adjusted between 5 – 15 nm through the choice of pluronic surfactants used for preparation of the silica materials.
At a later stage azido-functionalized mesoporous SiO_2, ZnO, TiO_2, Al_2O_3 materials (pore size 10 – 20 nm) prepared by **project A5** will be employed for immobilization. For comparison Rh-diene* complexes will also be immobilized on flat surfaces (e.g. SiO_2, ZnO) provided by **project A5**.
In addition, organic/inorganic hybride materials consisting of polystyrene foams (from **project A7**), whose pores (50 nm ≤ pore size ≤ 250 nm) are covered with a ZnO layer (**project A5**) will be used for immobilization. Through tailored deposition of the ZnO layer (**project A5**), the effective pore size can be adjusted.

As shown in Figure B3-13 (right side), the alkyne-modified Rh-diene* complexes **40**, **45** will be immobilized at the azido-functionalized inner-pore surface via click reaction to provide the catalytic systems **42**, **46**.

By a modular linker concept utilizing flexible alkyl spacers of different lengths (butyl-, hexyl-, octyl-, decyl-) and polarity (diethyleneglycol-, triethyleneglycol-linker) as well as rigid aryl- and biaryl-spacers, the distance of the Rh center to the inner pore wall can be adjusted (Figure B3-14). Taking the size of the central dimeric Rh-diene* unit (1.3 – 1.5 nm) and the linker lengths for **42** (0.2 nm) and **46a**-**c** (0.9 – 1.8 nm, fully extended conformations) respectively into consideration, minimum pore sizes of 2 nm (**42**) and 3 – 4 nm (**46a**-**c**) are required. Special care must be taken for the immobilized Rh-diene* complex **42** with the shortest linker, because strong interactions between the metal center and the inner pore wall are expected. Catalytic systems carrying the diphenyl-diene scaffold **31** with different linkers will be submitted for the initial catalysis experiments in **WP5**.

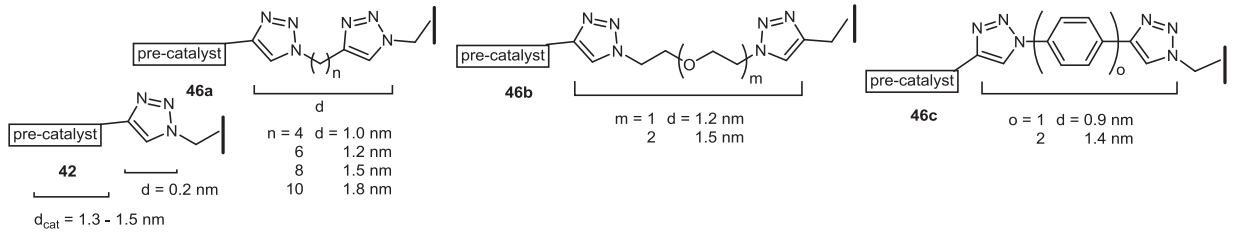

Figure B3-14 Modular linker concept for immobilized Rh-diene* complexes **42**, **46a**-**c** with spacers of different lengths, polarity and flexibility. For the immobilization strategy see Figure B3-13.

The immobilization of the dimeric Rh-diene* pre-catalyst, e.g **40** in Figure B3-13 bears the potential risk that only one Rh-diene* unit of the dimer is covalently attached to the solid support, while the linker of the second Rh-diene* unit remains unreacted in solution. Upon dissociation into the two active monomeric hydroxo-Rh-diene* complexes this might lead to a competition between heterogeneous and homogeneous catalysis in the same pore. Thus repetitive washing cycles and careful trace analysis of

the washing and reaction solutions by ICP-OES (**project A1**) to detect any Rh leaching are of utmost importance (for an alternative strategy see **WP6**).
The porosity and the ratio of pores filled with Rh-complexes and "empty" pores will be determined by gas adsorption (BET) (**project A4**, Traa). Inner-pore and outer-pore surfaces show different adsorption enthalpies and thus can be distinguished. The introduction of the spacer-modified Rh-complexes in the pores will be identified and quantified by IR and Raman spectroscopy. Optical methods (REM) will reveal the morphology of the porous catalyst systems. The lengths and diameters of the pores are known from TEM measurements in **project A4** (Traa).
By using our previous method[B3-7] SAXS experiments will provide information, whether the Rh complexes are located preferably inside or outside pores and whether the geometry of the mesoporous material has changed during the immobilization. Difficult cases will be analyzed together with **project A4** (Gießelmann). For selected catalyst systems small angle neutron scattering (SANS) will be performed (**project A7**). Parts of the catalyst system, e.g. linker or Rh center can be highlighted via partial deuteration and contrast matching experiments.
These informations will be combined with solid state NMR experiments to differentiate between inside/outside pore functionalization and to probe the position of the Rh complex in the pore (**project C1**). While the solid support in SBA-15, SiO_2 and Al_2O_3-derived catalyst systems can be studied directly by solid state NMR, this is difficult (or impossible) for ZnO and TiO_2 due to inaccessible resonance frequencies or long acquisition times. However, tailored probe molecules enable indirect observation via solid state NMR. For example, spatially resolved localization of the immobilized Rh-complexes at the inner-pore walls will be performed by CPMAS NMR with phosphane probe molecules developed by **project C1** and in selected cases by high resolution tomography (**project C3**).
The dynamic behavior of the immobilized Rh-complexes inside the pores (with and without solvents) will be studied by molecular dynamics simulations (**project C5**, Hansen) and compared with the dynamics of the linker-attached Rh-diene* complexes from **WP2**. The structural and energetic consequences of the different linker types (Figure B3-13) on the immobilized Rh complexes and their interactions with the inner pore wall will be investigated by QM/MM methods (**project C4**).

3.10.4.5 WP5: Catalytic investigations on inorganic materials. The inorganic and hybrid organic/ inorganic catalytic systems from **WP4** will be employed in benchmark 1,4-addition of phenylboronic acid to cyclohexenone **12a** in order to identify the most active catalyst-linker-material combination.
A set of 27 catalytic systems carrying the diphenyl-diene scaffold **31** (9 SBA-15, 9 x mesoporous SiO_2, 9 x flat SiO_2) will be submitted for the initial catalysis experiments. Comparison of the results from mesoporous and flat SiO_2 will allow to differentiate between spatial confinement effects and immobilization effects. The latter should decrease with increasing linker lengths, while spatial confinement effects are expected even for long flexible linkers as long as the catalyst is located inside the pore.
Turnover number and frequency and the enantioselectivity will be measured, using the homogeneous catalyzed reaction in **WP3** as reference. The most active material-catalyst combination giving the highest ee-values will be selected and linker lengths, polarity and rigidity will be systematically varied using the immobilization concept described in **WP4**. The resulting catalyst systems will be screened in a second iteration. In a third iteration step catalyst systems with different pore radii will be examined.
At a later stage of the project 9 catalytic systems carrying the diphenyl-diene scaffold **31** and selected linkers (3 x ZnO, 3 x TiO_2 and 3 x polystyrene foam/ZnO hybrid) will be tested, followed by a final round with the remaining solid supports from **WP4**.

Spectroscopic and analytic methods will provide insight into the catalysis. Pore diffusion of reactants into the pore and products out of the pore will be probed by PFG-NMR (**project C1**). The fate of the Rh complexes during catalysis and the reaction kinetics will be studied by *in operando*-CPMAS-NMR (**project C1**). The different B species (boronic acids, triphenylboroxines, boric acid) will be analyzed by ^{11}B-NMR giving insight into the reaction kinetics (**project C1**). Utilizing a recently reported method by Fröba,[44] the mobility of water inside the pores will be probed by solid state NMR (**project C1**).
Due to the fact, that the solvent shell affects the coordination chemistry of the Rh complex, confinement effects during the catalysis and changes of the oxidation state can be studied by *in operando* EXAFS and XANES (**project S1**).
Atomistic simulations of the confined catalyst systems using force field methods will deliver diffusion constants (**project C5**, Hansen). Force field parameters for the respective solvent system will be developed by **project C5** (Hansen) and used by **project C4** as input for the QM/MM calculations of

interaction energies between solvent and catalyst as well as reaction pathways in the confined systems. The conformational aspects of the confined catalyst systems and the structuring of the solvent around these systems for the ZnO- and TiO_2-based materials will be calculated in **project C6** (Fyta) using molecular dynamics simulations. These theoretical methods will deliver guidelines to improve catalytic turnover and identify rate-limiting steps of the confined systems.
Solvent effects are of utmost importance of the asymmetric catalysis in **project B3** not only with regard to diffusion processes. In the presence of a solvent (or solvent mixture) the chiral ligand generates a chiral solvation shell around the tethered Rh-diene* complex inside the pore in a similar fashion as soluble Rh-diene* complexes carry a chiral solvation shell during homogeneous catalysis. However, in the mesopore (diameter < 5 nm), the maximum distance between the "first" chiral solvation shell directly surrounding the ligand sphere of the tethered Rh-diene* complex and the inner pore wall is < 3.5 nm. Thus, it is expected that the pore wall (solvated or unsolvated) strongly influences the chiral solvation shell around the Rh catalyst in contrast to a free, i.e. non-immobilized Rh-diene* complex in solution in the absence of any confinement. In other words, with increasing pore size and increasing linker lengths this "chiral solvation shell effect" should decrease, which can be probed experimentally by determining the enantioselectivities via GC or HPLC on chiral stationary phases. By taking inspiration from previous work on carbon nanotubes dissolved in ionic liquids,[45,46,47] calculations of the chiral solvation shell via QM/MM methods in **project C4** and molecular dynamics methods in **project C5** (Hansen) will provide insight, how the confinement contributes to chirality transfer and helps **projects A4** and **A5** to tailor the pore size of the materials.
In order to clarify, whether the spatial distribution of the Rh catalysts in the pore and their linkage to the inner-pore wall changes during catalysis, selected post-catalysis samples will be investigated via high resolution tomography in **project C3**.

3.10.4.6 WP6: Synthesis of heteroleptic Rh-diene* complexes and monomeric Rh-diene* complexes with ancillary ligands, immobilization on SBA-15 and catalytic investigations. As discussed in Figure B3-5 the homogeneous catalytic 1,4-addition involves a series of pre-equilibria leading to the catalytically active monomeric hydroxo-Rh-diene* complex **B**, while the resting state is the corresponding dimer **A**. For an immobilized Rh-diene* catalyst in the mesopore, this should lead to a complex situation illustrated in Figure B3-11 (4th block). Ideally, in each pore only one monomeric hydroxo-Rh-diene* active catalyst **B1** is immobilized, resulting in a single site/pore catalysis (**Z3**). Alternatively, the immobilized resting states **A1** or **A2** dissociates into two monomeric hydroxo-Rh-diene* catalysts running independent catalytic cycles (**Z1**). In a sterically confined mesopore unfavorable steric interactions between the two catalysts and/or reactants and reagents are anticipated. Alternatively, a synergic interaction is conceivable (**Z2**), where one active catalyst is "working", while the other hydroxo-Rh-diene* complex acts as a "helper complex", e.g. by binding the enone through H-bonding.
Another problem might arise, when immobilization of the dimeric Rh-diene* pre-catalyst only takes place at one Rh center, while the other Rh center is not covalently bound. Upon dissociation of the dimeric resting state to the monomeric active catalyst, the "free" Rh unit undergoes competing homogeneous catalysis interfering with heterogeneous catalysis of the immobilized Rh unit.
In order to circumvent these difficulties, three different approaches outlined in Figure B3-15 will be investigated.

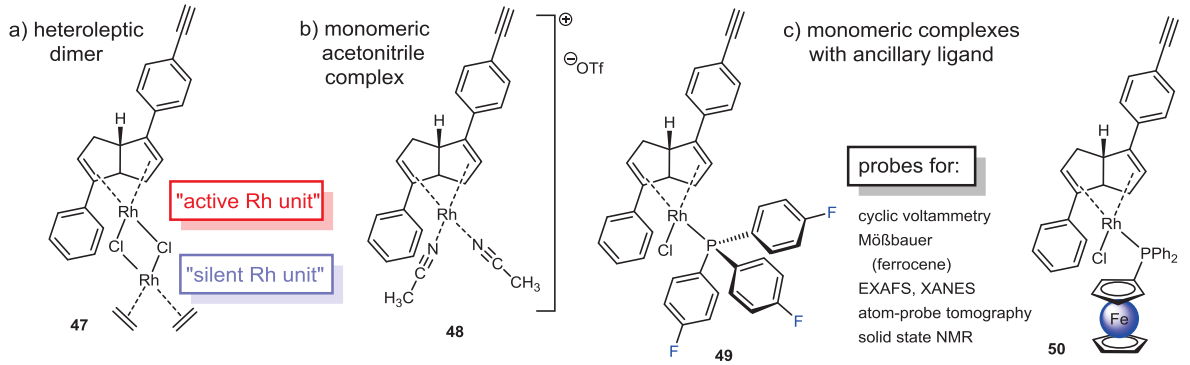

Figure B3-15 Three different approaches to circumvent competitive heterogeneous and homogeneous catalysis inside the pores by using a) heteroleptic dimer **47**, b) monomeric acetonitrile complex **48** and c) monomeric complexes **49**, **50** with ancillary ligands for immobilization via click reaction.

a) Heteroleptic dimeric Rh-diene* complexes **47** consisting of one “catalytically silent” Rh-bisethene unit and one “catalytically active” Rh-diene* unit through reaction of 1 equiv. of dimeric $[Rh(ethene)_2Cl]_2$ with 1 equiv. of diene*. The active Rh center carries the alkyne unit for the click immobilization, so that only heterogeneous catalysis should be possible through this immobilized Rh center.[48]
b) Monomeric Rh-diene* complexes **48** carrying labile acetonitrile ligands, which will be prepared from the diene* ligand, $[Rh(CO)_2Cl]_2$ and AgOTf in acetonitrile according to a method by Grützmacher.[49]
c) Monomeric Rh-diene* complexes with ancillary ligands L will be prepared. Following previous methods by Nishimura[50,51] and Buchmeiser (**project B2**), phosphanes (e.g. tricyclohexylphosphane, dimethylphenylphosphane) will be used as ancillary ligands. In addition N-acetyl-N,N-dipyridine[52,53] and NHC-ligands[54,55] from the Buchmeiser group will be tested. We will particular focus on Rh-diene* complexes **49**, **50** carrying tris(4-fluorophenyl)phosphane and ferrocenylphosphane respectively, because phophanes are suitable probes for solid state NMR (**project C1**), providing insight into catalyst-reactant and catalyst-confinement interactions due to the close proximity of the phosphane relative to the Rh center. Fluorinated compounds result in improved resolution of atom-probe tomography (**project C3**). The presence of the ferrocene unit in the ancillary ligand enables the use of Mößbauer spectroscopy (**project C2**, van Slageren) and spectroelectrochemistry (**project C2**, Ringenberg) to gain insight into the electronic state of the Rh center during the catalysis.

The above described Rh complexes will be immobilized in SBA-15 materials according to the methods described in **WP4** and tested in catalytic 1,4-additions.
Spectroscopic and theoretical analysis of the immobilized catalyst systems and catalytic reactions will be performed as described in **WP5** for the SBA-15-derived materials.

3.10.4.7 WP7: Immobilization of Rh-diene* complexes in organic materials using a modular linker concept. The organic mesoporous materials were selected according to the size requirements of the chiral Rh-diene* catalysts and the compatibility with the solvents, base and reagents of the catalytic 1,4-addition. The following materials will be used for immobilization:
Polystyrene-*b*-polymethylmethacrylate (PS-*b*-PMMA) and polystyrene-*b*-polylactide (PS-*b*-PLA) blockcopolymer templates with beaker-type porosity (pore size 10 – 20 nm) will be provided by **project A2**. Both the pore bottom and the pore walls can be selectively used for immobilization of the chiral Rh-diene* complex via click reaction. For pore bottom functionalization Au substrates can be modified with azido-alkylthiols[56] (compare WP1 in **A2**). In case of PS-*b*-PLA the pore etching process leads to materials with polar inner-pore walls, which can be modified with azide chemistry. The provided materials are stable against methanol/water/KOH. Crosslinking of the materials will also make the use of dioxane/water/KOH possible.[57]
Polystyrene foams with beaker-type porosity (pore size ≤ 50 nm) provided by **project A7** will be employed at a later stage of the project. These polystyrene foams are relatively hydrophobic mesoporous materials. This may lead to different ratios of the solvent mixtures inside and outside the pores. In order to avoid this “demixing” and polarity gradient with a lower polarity inside, tailor-made microemulsions will be tested by **project A7** based on their previously developed method for Mn-catalyzed epoxidations.[58] Immobilization will be performed as described in WP4 by using the click reaction on azido-functionalized polystyrene foams (Figure B3-13, right side).

Porosity of these materials will be determined by gas adsorption (BET) in **project A4** (Traa). Spatial distribution of Rh complexes will be analysed by SAXS in collaboration with **project A4** (Gießelmann) and for selected cases by SANS (**project A7**) and high resolution tomography (**project C3**).
The conformational aspects of the block-copolymer catalyst systems and the structuring of the solvent around these systems will be calculated in **project C6** (Fyta) using molecular dynamics simulations.

3.10.4.8 WP8: Catalytic investigations on organic materials. The polystyrene-foam- and block-copolymer-based catalyst systems from **WP7** will be employed in benchmark 1,4-addition of phenylboronic acid to cyclohexenone **12a** in order to identify the most active catalyst-spacer-material combination. A set of 18 catalytic systems carrying the diphenyl-diene scaffold **31** (9 x polystyrene-foam, 9 x block-copolymer) will be submitted for the initial catalysis experiments.

Turnover number and frequency and the enantioselectivity will be measured, using the homogeneous catalyzed reaction as reference. The most active material-catalyst combination giving the highest ee-

values will be selected and linker lengths, polarity and rigidity will be systematically varied using the immobilization concept described in **WP4**. The resulting catalyst systems will be screened in a second iteration. In a third iteration step catalyst systems with different pore sizes will be examined.

The most active catalyst systems with the highest ee-values will be analyzed by the spectroscopic, analytic and theoretical methods outlined in **WP5** in cooperation with **projects C3** – **C6**. In order to develop structure-property relationships for the catalyst systems, the second most active and enantioselective catalyst systems for a given material will be also analyzed. This should lead to design principles for new catalyst systems.

3.10.4.9 Chronological work plan:

	2018		2019				2020				2021				2022		
	Q3	Q4	Q1	Q2	Q3	Q4	Q1	Q2	Q3	Q4	Q1	Q2	Q3	Q4	Q1	Q2	
T1																	WP1: Synthesis of chiral diene ligands for click anchoring of spacers
T2																	WP2: Synthesis and characterization of alkyne- and triazole-modified Rh-diene* complexes
T3																	WP3: Investigations on the influence of linker-attached Rh-diene* complexes in homogeneous catalytic 1,4-addition
T4																	WP4: Immobilization of Rh-diene* complexes in inorganic materials using a modular linker concept.
T5																	WP5: Catalytic investigations on inorganic materials
T6																	WP6: Synthesis of heteroleptic Rh-diene* complexes and Rh-diene* complexes with ancillary ligands, immobilization on SBA-15 and catalytic investigations
T7																	WP7: Immobilization of Rh-diene* complexes in organic materials using a modular linker concept
T8																	WP8: Catalytic investigations on organic materials

3.10.4.10 Methods applied

B3 is a clear catalysis project using therefore all methods and techniques associated with such projects. These includes solution ^{1}H-, ^{13}C-NMR, ESI-MS, IR, UV/Vis and X-ray crystal structure analysis as well as GC and chiral HPLC. Other tools include measurement of complex distribution inside the pores by SAXS (**project A4**), of reaction kinetics by *in operando*-CPMAS-NMR and ^{11}B-NMR (**project C1**), of complex location in the pores by IR and Raman spectroscopy. Mößbauer spectroscopy and spectroelectrochemistry will be used to identify the electronic state of the metal during catalysis (**project C3**).

3.11.4.10 Vision

By the end of the first funding period we aim to understand the structural and molecular details, elementary steps and kinetics of the enantioselective molecular heterogeneous catalysis with metal-diene complexes using the Rh-catalyzed 1,4-addition of boronic acids to enones as a case study. It is a long-term goal to control diffusion processes and synergetic interaction of metal complexes in confined spaces through well-defined pore size, geometry, polarity, inner-pore functionalization and linker design in order to achieve high catalytic activity, enantioselectivity and catalyst lifetime. By tailoring the interaction between the chiral solvation shell around the immobilized Rh catalyst and the pore wall insight into chirality transfer in confined systems will be gained. In the second funding period, we aim at catalyst systems prepared from achiral metal complexes confined in chiral porous materials, e.g. containing helical channel-type pores. This knowledge should enable the use of diene and alkene ligands in new catalytic applications such as enantioselective oxidations and broaden the scope of enantioselective molecular heterogeneous catalysis towards new ligand, reactants and reaction classes.

3.10.5 Role within the collaborative research center

Project B3 is one out of three different types of catalysis in this collaborative research proposal. The chiral Rh-diene* complexes were developed in our group. They are stable and fully characterized by experimental and theoretical methods. The complexes are preparative accessible, are air and moisture stable and hence define a perfect catalyst material to be used for the type of investigations presented in this project. The preliminary work defines a good starting point for joint research projects in combination with **projects A2**, **A4** – **A5**, **A7**, which provide azide-functionalized mesoporous materials (SBA-15, mesoporous SiO_2, TiO_2, ZnO, Al_2O_3, PS-foam/ZnO, PS-foam, PS/PMMA-block-copolymers) and dedicated analytic and spectroscopic tools (BET, ICP-OES, SANS). **Project B3** will perform the immobilization of the catalysts and the catalyst testing as well as SAXS experiments. Collaborations with spectroscopy and theory **projects C1** – **C6**, **S1** provide insights into the potential role of confinement effects in the catalytic transformation, allowing for a feedback-loop into material synthesis. Transfer of knowledge regarding catalysis and exchange of linker building blocks and ligands with catalysis groups **B1**, **B2** will broaden the scope of molecular heterogeneous catalysis. An overview of the collaboration with other projects within CRC 1333 is given in the workflow diagram (Figure B3-11).

3.10.6 Differentiation from other funded projects

Projects related to Rh-catalyzed 1,4-addition are currently not funded. No funding proposal has been submitted or is under revision.

References

[37] N. Cramer, M. Buchweitz, S. Laschat, W. Frey, A. Baro, D. Mathieu, C. Richter, H. Schwalbe, *Chem. Eur. J.* **2006**, *12*, 2488-2503.
[38] S. Ohira, *Synth. Commun.* **1989**, *19*, 561-564.
[39] G. J. Roth, B. Liepold, S. G. Müller, H. J. Bestmann, *Synthesis* **2004**, 59-62.
[40] V. Lutz, N. Park, C. Rothe, C. Krüger, A. Baro, S. Laschat, *Eur. J. Org. Chem.* **2013**, 761-771.
[41] For a stepwise approach see: V. Lutz, A. Baro, P. Fischer, S. Laschat, *Eur. J. Org. Chem.* **2010**, 1149-1157.
[42] (3-Azidopropyl)triethoxysilane has been recently used for click immobilization of *cis*-platin and titanocene in mesoporous silica microspheres for drug delivery. For details see: I. del Hierro, Y. Perez, P. Cruz, R. Juarez, *Eur. J. Inorg. Chem.* **2017**, 3030-3039.
[43] J. Nakazawa, B. J. Smith, T. D. P. Stack, *J. Am. Chem. Soc.* **2012**, *134*, 2750-2759.
[44] J. B. Mietner, F. J. Brieler, Y. J. Lee, M. Fröba, *Angew. Chem. Int. Ed.* **2017**, *56*, 12348-12351.
[45] Y. Shim, H. J. Kim, *ACS Nano* **2009**, *3*, 1693-1702.
[46] S. Wang, N. M. Cann, *J. Chem. Phys.* **2008**, *129*, 054507/1.
[47] J. Neugebauer, *Angew. Chem. Int. Ed.* **2007**, *46*, 7738-7740.
[48] Heteroleptic Ru arene complexes have been prepared to obtain water-soluble catalysts for asymmetric transfer hydrogenations. For details see: M. A. N. Virboul, R. J. M. Klein Gebbink, *Organometallics* **2012**, *31*, 85-91.
[49] F. Lang, F. Breher, D. Stein, H. Grützmacher, *Organometallics* **2005**, *24*, 2997-3007.
[50] T. Nishimura, T. Kawamoto, M. Nagaosa, H. Kumamoto, T. Hayashi, *Angew. Chem. Int. Ed.* **2010**, *49*, 1638-1640.

[51] T. Nishimura, Y. Takiguchi, Y. Maeda, T. Hayashi, *Adv. Synth. Catal.* **2013**, *355*, 1374-1382.
[52] B. Bantu, K. Wurst, M. R. Buchmeiser, *J. Organomet. Chem.* **2007**, *692*, 5272-5278.
[53] G. M. Pawar, J. Weckesser, S. Blechert, M. R. Buchmeiser, *Beilstein J. Org. Chem.* **2010**, *6*, 28. doi: 10.3762/bjoc.6.28.
[54] Y. Zhang, D. Wang, K. Wurst, M. R. Buchmeiser, *J. Organomet. Chem.* **2005**, *690*, 5728-5735.
[55] N. Imlinger, M. Mayr, D. Wang, K. Wurst, M. R. Buchmeiser, *Adv. Synth. Catal.* **2004**, *346*, 1836-1843.
[56] N. K. Devaray, P. H. Dinolfo, C. E. D. Chidsey, J. P. Collman, *J. Am. Chem. Soc.* **2006**, *128*, 1794-1795.
[57] E. J. W. Crossland, P. Cunha, S. Ludwigs, M. A. Hillmeyer, U. Steiner, *ACS Appl. Mater. Interfaces* **2011**, *3*, 1375-1379.
[58] S. Sottmann, A. Berkessel, A. Griesbeck, *Tenside Surf. Det.* **2002**, *39*, 17-22.

3.10.7 Project funding

3.10.7.1 Previous funding

This project is currently not funded and no funding proposal has been submitted.

3.10.7.2 Requested funding

Funding for	2018		2019		2020		2021		2022		2018-2022	
Staff	Quantity	Sum	Quantity	Sum	Quantity	Sum	Quantity	Sum	Quantity	Sum	Quantity	Sum
PhD student, 67%	1	21,600.-	1	43,200.-	1	43,200.-	1	43,200.-	1	21,600.-	1	172,800.-
Total		21,600.-		43,200.-		43,200.-		43,200.-		21,600.-		172,800.-
Direct costs	Sum		Sum		Sum		Sum		Sum		Sum	
consumables	4,000.-		8,000.-		8,000.-		8,000.-		4,000.-		32,000.-	
Total	4,000.-		8,000.-		8,000.-		8,000.-		4,000.-		32,000.-	
Major research instrumentation	Sum		Sum		Sum		Sum		Sum		Sum	
high throughput instrumentation	10,600.-		-		-		-		-		10,600.-	
chiral preparative HPLC	27,500.-		-		-		-		-		27,500.-	
Total	38,100.-		-		-		-		-		38,100.-	
Grand total	63,700.-		51,200.-		51,200.-		51,200.-		25,600.-		242,900.-	

(All figures in EUR)

3.10.7.3 Requested funding for staff

	Sequential no.	Name, academic degree, position	Field of research	Department of university or non-university institution	Project commitment in hours per week	Category	Funding source
Existing staff							
Research staff	1	S. Laschat, Dr., Prof.	Organic chemistry, Catalysis	Institute of Organic Chemistry	4		University
	2	A. Baro, Dr.	Organic chemistry, Catalysis	Institute of Organic Chemistry	2		University
Non-research staff	3	U. Henn		Institute of Organic Chemistry	2		University
Requested staff							
Research staff	4	N.N., M. Sc.	Organic chemistry, Catalysis	Institute of Organic Chemistry		PhD	
Research staff	5	Research assistant	Organic chemistry, Catalysis	Institute of Organic Chemistry			

Job description of staff (supported through existing funds):
1
Full Professor, principal investigator
2
Senior Scientist (Akademische Rätin), in charge of writing publications and reports, transfer of knowledge with other projects of CRC 1333
3
secretary
Job description of staff (requested funds):
4
PhD student, working packages WP1-8
5
Research assistant. **Justification:** The research assistants will perform the syntheses of linkers with different lengths, polarity and rigidity according to the modular linker concept as described in WP 4.

3.10.7.4 Requested funding of direct costs

	2018	2019	2020	2021	2022
Uni Stuttgart: existing funds from public budget	2,000.-	4,000.-	4,000.-	4,000.-	2,000.-
Sum of existing funds	2,000.-	4,000.-	4,000.-	4,000.-	2,000.-
Sum of requested funds	4,000.-	8,000.-	8,000.-	8,000.-	4,000.-

(All figures in EUR)

Consumables for financial year 2018

Chemicals, consumables, Rh precursors, solvents, silica for columns, gases (Ar), NMR solvents, HPLC-grade solvents, analytical HPLC- and GC-columns	EUR	4,000.-

Consumables for financial year 2019

Chemicals, consumables, Rh precursors, solvents, silica for columns, gases (Ar), NMR solvents, HPLC-grade solvents, analytical HPLC- and GC-columns	EUR	8,000.-

Consumables for financial year 2020

Chemicals, consumables, Rh precursors, solvents, silica for columns, gases (Ar), NMR solvents, HPLC-grade solvents, analytical HPLC- and GC-columns	EUR	8,000.-

Consumables for financial year 2021

Chemicals, consumables, Rh precursors, solvents, silica for columns, gases (Ar), NMR solvents, HPLC-grade solvents, analytical HPLC- and GC-columns	EUR	8,000.-

Consumables for financial year 2022

Chemicals, consumables, Rh precursors, solvents, silica for columns, gases (Ar), NMR solvents, HPLC-grade solvents, analytical HPLC- and GC-columns	EUR	4,000.-

3.10.7.5 Requested funding for major research instrumentation

Equipment for financial year 2018

catalyst-screening-block. Justification: In order to avoid destruction of the porous materials and the resulting catalyst systems due to mechanical stress induced by stirring, classical magnetic stirrers cannot be used. Therefore, the mechanical workshop will build a catalyst screening block for the parallel screening of different catalyst systems consisting of an IKA shaker 260 control (3.560.- €), a cryostat Julabo, model: Corio CD-200F cooling circulation thermostat -20 to +150°C (3.370.- €), 2 aluminium heating blocks with sockets for the cryostat (3 x 24 Schlenk tubes D10 mm, 3 x 12 Schlenk tubes D20 mm), 6 aluminium condenser units for the heating device made by mechanical workshop, estimated 2.000 €), 30 pressure Schlenk vials D10 mm, 20 pressure Schlenk vials D20 mm (made by glass blowers, estimated 1670.- €).	EUR	10,600.-
preparative HPLC column with chiral stationary phase & equipment for incorporation into existing HPLC device. Justification: The synthesis of enantiomerically pure diene ligands requires preparative HPLC with chiral stationary phases (Chiralcel-OJH and Chiralcel-OD columns) as the final purification step, which have shown reliable performance and gave reproducible results in previous work.[B3-4] For both preparative Chiralcel-OJH and Chiralcel-OD column an analytical column with the same stationary phase is required. In order to achieve a maximum lifetime of these columns pre-columns are required (see quotation # 2027300688-AN from 30.10.2017 by MZ-Analysentechnik GmbH).	EUR	27,500.-

3.11 Project C1

3.11.1 General information about project C1

3.11.1.1 Solid-state NMR methods for the study of the properties and spatial distribution of anchored metal complexes in porous solids

3.11.1.2 Research areas

302-01 Solid State and Surface Chemistry, Material Synthesis

302-02 Physical Chemistry of Solids and Surfaces, Material Characterization

3.11.1.3 Principal investigator

Hunger, Michael, apl.-Prof. Dr., born 23. 04. 1955, Leipzig, male, German
Institut für Technische Chemie
Universität Stuttgart, Pfaffenwaldring 55, 70569 Stuttgart
Tel.: 0711/685-64079
E-Mail: michael.hunger@itc.uni-stuttgart.de
Permanent position

3.11.1.4 Legal issues

This project includes

1.	research on human subjects or human material.	no
2.	clinical trials.	no
3.	experiments involving vertebrates.	no
4.	experiments involving recombinant DNA.	no
5.	research involving human embryonic stem cells.	no
6.	research concerning the Convention on Biological Diversity.	no

3.11.2 Summary

This project C1 will contribute to the success of the collaborative research center by the development and application of novel solid-state NMR methods for characterizing the properties of molecular metal-organic catalysts anchored inside the pores of three-dimensional support materials. The two parts of this project will focus on (i) the development of novel NMR probe molecules for the determination of the spatial distribution of metal sites and on (ii) the determination of intermediates, reaction mechanisms, and reaction kinetics at immobilized molecular catalysts and of the transport properties of model reactants inside the porous supports.

For topic (i), modern methods of one- and two-dimensional solid-state NMR spectroscopy will be utilized for the characterization of porous support materials including polymeric monoliths, covalent organic frameworks, mesoporous silicas, organic/inorganic hybrids, polymeric nanofoams and ordered mesoporous carbons, and of their surface sites, utilized for the anchoring of molecular catalysts. These investigations will be an important prerequisite for optimizing the preparation methods required for obtaining highly active and selective catalyst systems. For the solid-state NMR characterization of the chemical properties and spatial distribution of catalytically active metal sites of anchored complexes, novel probe molecules will be prepared and tested. These probe molecules will be applied since direct solid-state NMR spectroscopy of the metals (Ru, Mo, W, and Rh) of the anchored complexes is not possible due to their low resonance frequencies and low NMR sensitivities. By utilizing solid-state NMR probe molecules with different molecular diameters, the location of anchored metal complexes inside the pores and at the outer particle surface of the support materials will be distinguished. Suitable candidates are alkyl phosphine oxides (POR_y), alkyl aryl phosphine oxides ($POAr_xR_y$), alkyl phosphines (PR_y), and alkyl aryl phosphines (PAr_xR_y) with systematically increasing numbers of aryl groups and with alkyl chains of different length. By the preparation and application of series of probe molecules with two interaction centers in a well-defined distance, a novel solid-state NMR tool for investigating site distances beyond the range of dipolar interactions (< 0.5 nm) will be developed.

In part (ii) of this project, in situ solid-state NMR spectroscopy will be utilized for investigating the interactions of model reactants with the catalytically active metal sites, the formation of reaction

intermediates, and for determining reaction kinetics. Furthermore, pulsed-field gradient NMR spectroscopy (PFG NMR) will be applied for characterizing the molecular transport properties of model reactants and solvent molecules inside the pores of support materials. These studies will deliver data for quantum-chemical calculations of chemical reactivities and molecular-dynamics simulations, respectively, carried out by other groups of the CRC. For studying the interactions of model reactants in the hydrogen-autotransfer catalysis (piperidine/benzylalcohol or aniline/benzylalcohol), ring-closing metathesis (diethyl diallyl malonate), and asymmetric catalysis (boronic acids) at anchored metal complexes, suitable methods for the reproducible preparation of NMR samples must be developed and tested. In a second step, the interactions of the model reactants with the anchored metal complexes, studied by in situ solid-state NMR spectroscopy, will be compared with those of metal complexes in solution, which will be investigated by liquid NMR spectroscopy. Furthermore, the formation of intermediates at anchored metal complexes, reaction mechanisms, and reaction kinetics will be investigated. The results of these in situ solid-state NMR studies and of the PFG NMR measurements, in connection with theoretical simulations performed by other groups of the CRC, will significantly support the development of highly active and selective catalyst systems and the modelling of the reaction systems under study.

3.11.3 Research rationale

3.11.3.1 Current state of understanding and preliminary work

During the past decades, solid-state NMR spectroscopy has become an important analytical research tool in the field of heterogeneous catalysis. The applications of this spectroscopic method have focused on the characterization of catalyst frameworks and their active surface sites and the investigation of the mechanisms of heterogeneously catalyzed reactions, including the identification of intermediates, which are not observable by complementary methods, such as gas chromatography and mass spectrometry.[1, 2]

An important advantage of solid-state NMR spectroscopy, e.g. in comparison with diffraction methods, is the sensitivity of this method for the local structure of solids. Common applications are, therefore, the investigation of framework atoms, their coordination, and the nature of neighboring atoms. By one- and two-dimensional cross polarization (CP) experiments,[3, 4] atoms in the vicinity of the catalyst surface, e.g. framework atoms in the local structure of surface OH groups, strongly adsorbed solvent molecules and surface complexes, can be selectivity characterized. In these cases, the hydroxyl protons or the H atoms (*I*-spins) of adsorbate molecules and complexes are excited by a radio frequency $\pi/2$ pulse. Subsequent irradiation of well-adjusted long contact pulses (τ) at these H atoms (*I*-spins) and, simultaneously, at neighboring framework atoms (*S*-spins), e.g. ^{29}Si or ^{13}C nuclei, causes a polarization transfer from the *I*-spins to dipolar coupled *S*-spins (see Figure C1-1). In many cases, however, the catalytically active sites at catalyst surfaces cannot be directly observed by solid-state NMR spectroscopy. Reasons for this limitation are, e.g., their low isotopic abundance or low gyromagnetic ratio, which is accompanied by a low resonance frequency and a low NMR sensitivity. A suitable approach in this situation is the use of probe molecules, which are NMR sensitive in their interactions with the surface sites under study. In the past decades, numerous solid-state NMR probe molecules were introduced and utilized for the investigation and characterization of surface sites on solid catalysts (see e.g. Table C1-1).[4] Until now, the focus for the application of solid-state NMR probe molecules has been on the characterization of Brønsted (BAC) and Lewis acid sites (LAC) (see Figure C1-2).[5] However, a gap exists for the solid-state NMR characterization of metal sites by probe molecules. Furthermore, most of the probe molecules applied in the field of heterogeneous catalysis can distinguish the chemical nature of surface site (e.g. Brønsted and Lewis acidic properties), are used for determining their surface densities, can evidence their accessibility, or are utilized to measure the strength of acid sites. However, no probe molecules with different molecular diameters for distinguishing the location of surface sites at the outer surface and inside the pores of support materials by solid-state NMR investigations were introduced. Similarly, no two-center probe molecules for the determination of surface site distances by solid-state NMR were described in literature until now. In this connection, it must be mentioned that only very few research groups worldwide are able to combine application of probe molecules with their solid-state NMR spectroscopic investigation.

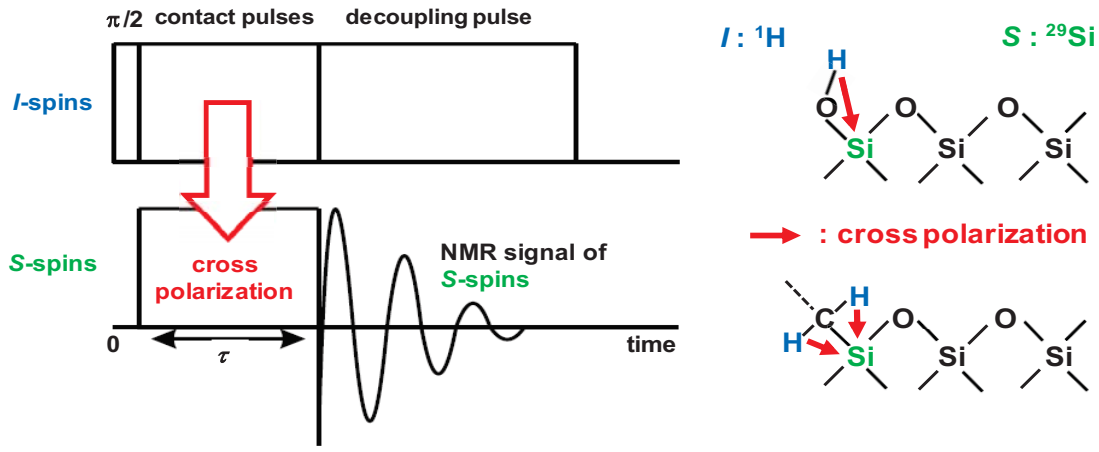

Figure C1-1. Scheme of a Cross Polarization (CP) experiment (left-hand side) and examples for polarization transfer routes between *I*- and *S*-spins (right-hand side) on the surface of a pure (top) and modified (bottom) silicate.

Table C1-1. Survey on solid-state NMR probe molecules for the characterization of Brønsted (BAC) and Lewis acid sites (LAC). The ^{1}H and ^{13}C NMR shifts are referenced to tetramethylsilane (δ_{1H} and δ_{13C} = 0 ppm), while the ^{15}N and ^{31}P NMR shifts are referenced to $^{15}NH_3$ (δ_{15N} = 0 ppm) and H_3PO_4 (δ_{31P} = 0 ppm), respectively.[4]

Probe molecule	Resonance and effect
ammonia	BAC: δ_{1H} = 6.5-7.0 ppm for ammonium ions at former acidic OH groups LAC: δ_{1H} = -0.5 to 3.0 ppm for NH_3 coordinated at γ-Al_2O_3, anatase, and Li-exchanged zeolite Y
^{13}C-2-acetone	BAC: δ_{13C} = 216-225 ppm for H-bonded acetone at acidic OH groups LAC: δ_{13C} = 233 to 245 ppm for acetone at extra-framework aluminum species in zeolite USY, on $AlCl_3$/MCM-41, and pure $AlCl_3$
^{15}N-pyridine [a)]	BAC: δ_{15N} = 295 ppm for pyridinium ions protonated by strongly acidic OH groups LAC: δ_{15N} = 265 ppm for pyridine at Lewis acid sites of silica-alumina and γ-Al_2O_3
trimethylphosphine	BAC: δ_{31P} = 11.1-14.8 ppm for TMP ions protonated by strongly acidic OH groups LAC: δ_{31P} = -32 to -67 ppm for TMP at dealuminated zeolite Y
trimethylphosphine oxide	BAC: δ_{31P} = 46 ppm for TMPO for TMPO at acidic OH groups LAC: δ_{31P} = 48 to 51 ppm for TMPO coordinated at γ-Al_2O_3, anatase, and Li-exchanged zeolite Y

While numerous publications describe liquid-state NMR investigations of homogeneously catalyzed reactions at metal complexes in solution (see e.g. [6, 7]), solid-state NMR spectroscopic studies are rare. One of the reasons is the strong broadening of NMR signals due to solid-state spin interactions for metal complexes rigidly anchored on solid supports. In the case of homogeneous catalysis at metal complexes in solution, these spin interactions are averaged due to the high mobility of the complexes and molecules under study. In solids, however, these spin interactions must be averaged, or at least strongly decreased, by application of sophisticated solid-state NMR methods.[2] The application of these methods is accompanied by demanding procedures for the sample preparation, e.g. in the case of rapid sample spinning around an axis in the magic angle (MAS: Magic Angle Spinning). In the past decades, various techniques of in situ MAS NMR spectroscopy were developed and utilized for the investigation

of heterogeneously catalyzed reactions.[3] An often used approach of in situ MAS NMR spectroscopy is the study under batch conditions. In this case, the activated catalyst, loaded with reactant molecules, is sealed in an MAS NMR rotor with gas tight rotor cap or in a symmetric glass ampoule being inserted into a rotor. Subsequently, the reactant conversion is measured after step-wise increase of the reaction temperature. In the case of in situ solid-state NMR studies under flow conditions, the MAS NNR rotor is utilized as a fixed-bed microreactor with a cylindrical catalyst bed (see Figure C1-3).[8]

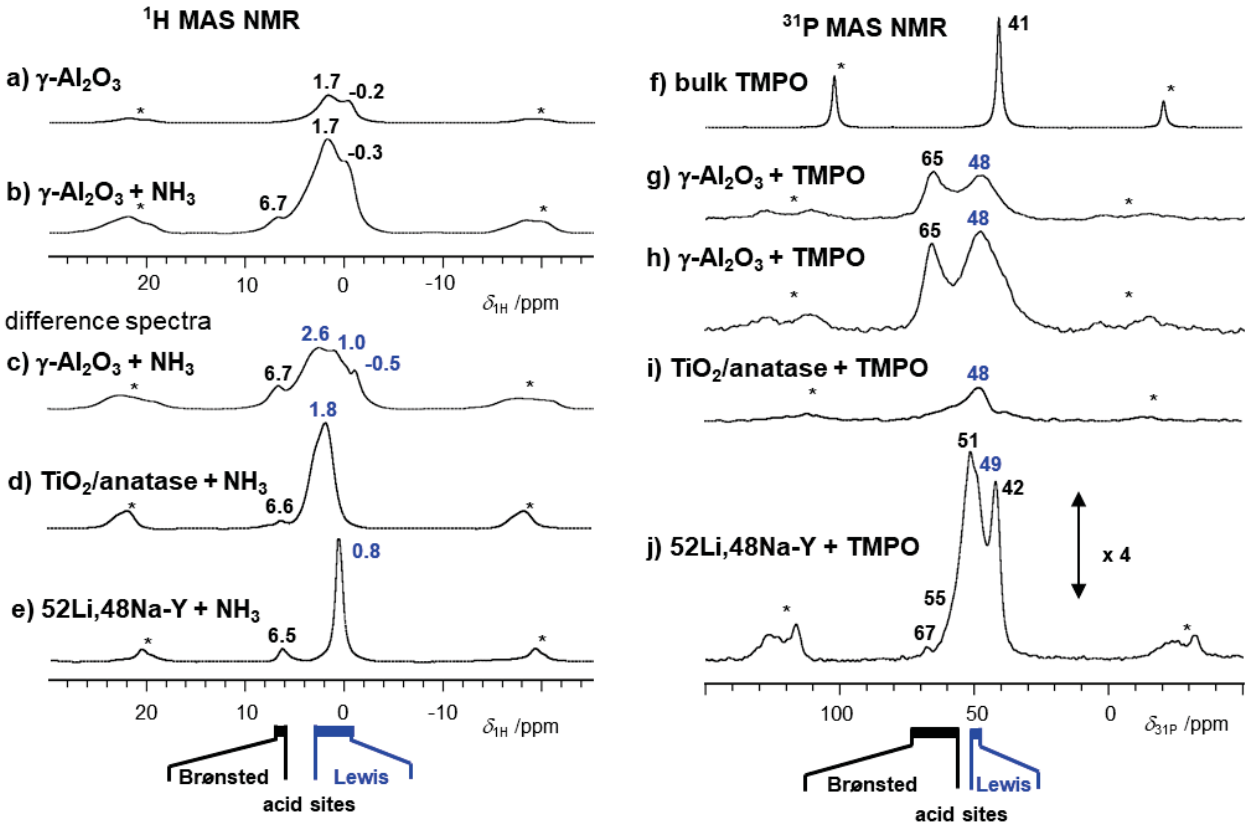

Figure C1-2. The ^{1}H MAS NMR spectra on the left-hand side (a to e) were recorded before (a) and after (b) adsorption of ammonia on dehydrated (vacuum, 623 K) samples, while c to e were obtained by subtracting spectra recorded before from those recorded after ammonia adsorption. The ^{31}P MAS NMR spectra on the right-hand side were obtained for pure TMPO (f) and for TPMO adsorbed on dehydrated (vacuum, 623 K) samples (g to j).[5]

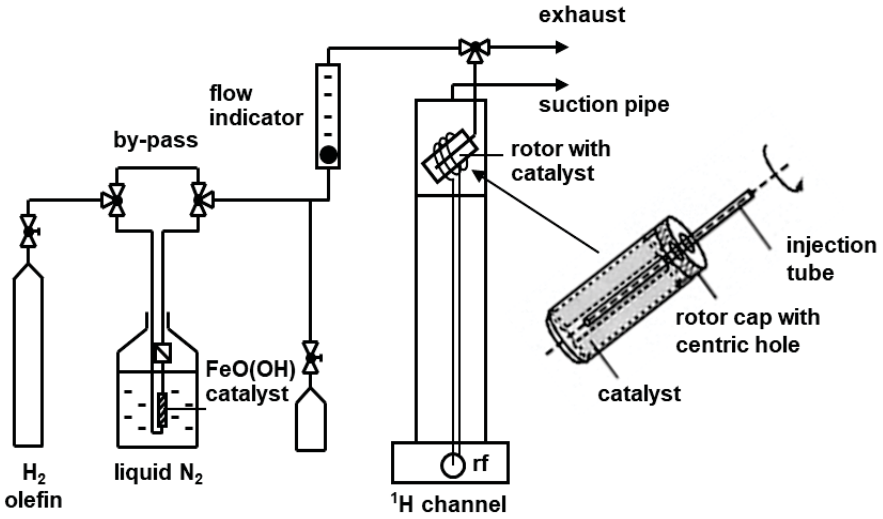

Figure C1-3. Set-up for in situ MAS NMR experiments for the heterogeneously catalyzed hydrogenation of olefins with parahydrogen (p-H_2) under continuous-flow conditions. The FeO(OH) catalyst is used for the para-enrichment of the hydrogen gas at the temperature of liquid nitrogen.[8]

The reactants are injected into this spinning microreactor via an injection tube inserted into the empty part of a hollow cylinder inside the catalyst bed. With this experimental set-up, in situ solid-state NMR studies under similar conditions like in a standard fixed-bed reactor can be performed. Additional experimental approaches are a combination of the former two set-ups, e.g., for stopped-flow and semi-batch experiments. In the case of stopped-flow experiments, the formation of intermediates is studied after stopping a continuous reactant flow. In semi-batch experiments, one reactant is preloaded on the activated catalyst, while the other reactant is continuously injected into the MAS NMR rotor during the in situ study.[9]

References

[1] M. Hunger, W. Wang, *Adv. Catal.* **2006**, *50*, 149-225.
[2] W. Dai, C. Wang, M. Dyballa, G. Wu, N. Guan, L. Li, Z. Xie, M. Hunger, *ACS Catal.* **2015**, *5*, 317-326.
[3] Y. Jiang, J. Huang, W. Dai, M. Hunger, *Solid State Nucl. Magn. Reson.* **2011**, *39*, 116-141.
[4] J.B. Mietner, F.J. Brieler, Y.J. Lee, M. Froeba, *Angew. Chem.* **2017**, *129*, 12519-12523.
[5] S. Lang, M. Benz, U. Obenaus, R. Himmelmann, M. Hunger, *ChemCatChem* **2016**, *8*, 2031-2036.
[6] M.R. Buchmeiser, S. Sen, J. Unold, W. Frey, *Angew. Chem. Int. Ed.* **2014**, *126*, 9584-9388.
[7] G. Floros, N. Saragas, P. Paraskevopoulou, N. Psaroudakis, S. Koinis, M. Pitsikalis, N. Hadjichristidis,K. Mertis, *Polymers* **2012**, *4*, 1657-1673.
[8] H. Henning, M. Dyballa, M. Scheibe, E. Klemm, M. Hunger, *Chem. Phys. Lett.* **2013**, *555*, 258-262.
[9] M. Hunger, *Prog. Nucl. Magn. Reson. Spectrosc.* **2008**, *53*, 105-127.

3.11.3.2 Own work, project-related publications by participating researchers

During the past decades, the Hunger group focused on the preparation and solid-state NMR characterization of novel porous catalysts for applications in heterogeneous catalysis (see e.g. Refs. [C1-1, C1-2]) and on in situ solid-state NMR studies of heterogeneously catalyzed reactions (see e.g. Refs. [C1-3, C1-4]). An important content of this work was the development of novel tools and methods for solid-state NMR studies in the field of heterogeneous catalysis. These tools and methods are based, e.g., on the preparation of solid catalyst samples under well-defined conditions for solid-state NMR studies, the investigation of new probe molecules for the characterization of specific surface sites at solid catalysts,[C1-5] and the development of novel in situ solid-state NMR techniques for the study of heterogeneously catalyzed reactions, such as the in situ injection technique shown in Figure C1-3. Based on the latter technique, different protocols for in situ experiments were introduced and demonstrated.[C1-6]

Until now, most of the solid catalysts investigated by the Hunger group were microporous and mesoporous solids, which were modified with Brønsted and Lewis acid sites.[C1-7, C1-8] These catalysts are important for heterogeneously catalyzed reactions at a research level or have been recently introduced as shape selective solid catalysts in chemical industry, such as for the conversion of methanol to olefins (MTO) at Brønsted acidic zeolites. For the application as catalysts in the MTO process, a large number of microporous aluminosilicates and silicoaluminophosphates were prepared and investigated. In this way, the dual-cycle mechanism of the MTO conversion at zeolite catalysts could be clarified and was utilized for improving the catalyst selectivity. For the above-mentioned investigations,[C1-7, C1-8] similar in situ solid-state NMR techniques were utilized, which will also be applied to the recent project.

As a new research topic of the past three years, zeolite catalysts modified with noble metals, such as rhodium, iridium, palladium, and platinum, came in the focus of the Hunger group. Noble metal containing zeolites are suitable catalysts, e.g., for the dehydrogenation of alkanes, the selective hydrogenation of double- and triple-bond containing organics, the hydrocracking, and the dehydroisomerization of hydrocarbons. In many of these applications, noble metal containing zeolites function as bifunctional catalysts. They have dehydrogenation/dehydrogenation properties due to the presence of well-dispersed noble metals, and they contain Brønsted acid sites, which are formed in result of the reduction of the noble metals in a hydrogen atmosphere. In most of the above-mentioned reactions, the bifunctional properties are important for the selective conversion of the reactants, such as for the hydrocracking of n-alkanes. In latter reaction, at first n-alkanes are dehydrogenated to olefins at noble metal sites. Subsequently, these olefins are cracked at Brønsted acid sites and, finally, they are hydrogenated at the noble metals. A similar synergism of different catalytic sites is utilized for ring-opening reactions of organics, which are reactions being at a research level until now.

In connection with the preparation and application of noble metal containing zeolites, these catalysts were characterized in detail by solid-state NMR spectroscopy.[C1-7] For the first time, the formation of Brønsted acid sites was quantitatively investigated for different types of introduced noble metals. Their chemical properties and accessibilities were investigated by adsorption of solid-state NMR probe molecules, such as ammonia and trimethylphosphine oxide (TMPO). As an example, Figure C1-4 shows ^{31}P MAS NMR spectra of TMPO adsorbed at rhodium, iridium, palladium, and platinum containing zeolites Na-Y with faujasite structure [C1-7]. After reduction of the noble metals on these zeolites Na-Y, the formation of 0.3 to 1.3 Brønsted acidic bridging OH groups (Si(OH)Al) per noble metal atom was observed in the small sodalite cages and large supercages of the faujasite structure. By the chemical shift of the ^{31}P MAS NMR signals of adsorbed TMPO, the interaction of this probe molecules with Si(OH)Al groups located in the sodalite cages (δ_{31P} = 55 ppm) and in the supercages (δ_{31P} = 66 ppm) could be distinguished (see Figure C1-4). Furthermore, ^{31}P MAS NMR signals at δ_{31P} = 51 ppm indicated an interaction of TMPO with accessible metal sites formed by the introduction and reduction of noble metals.

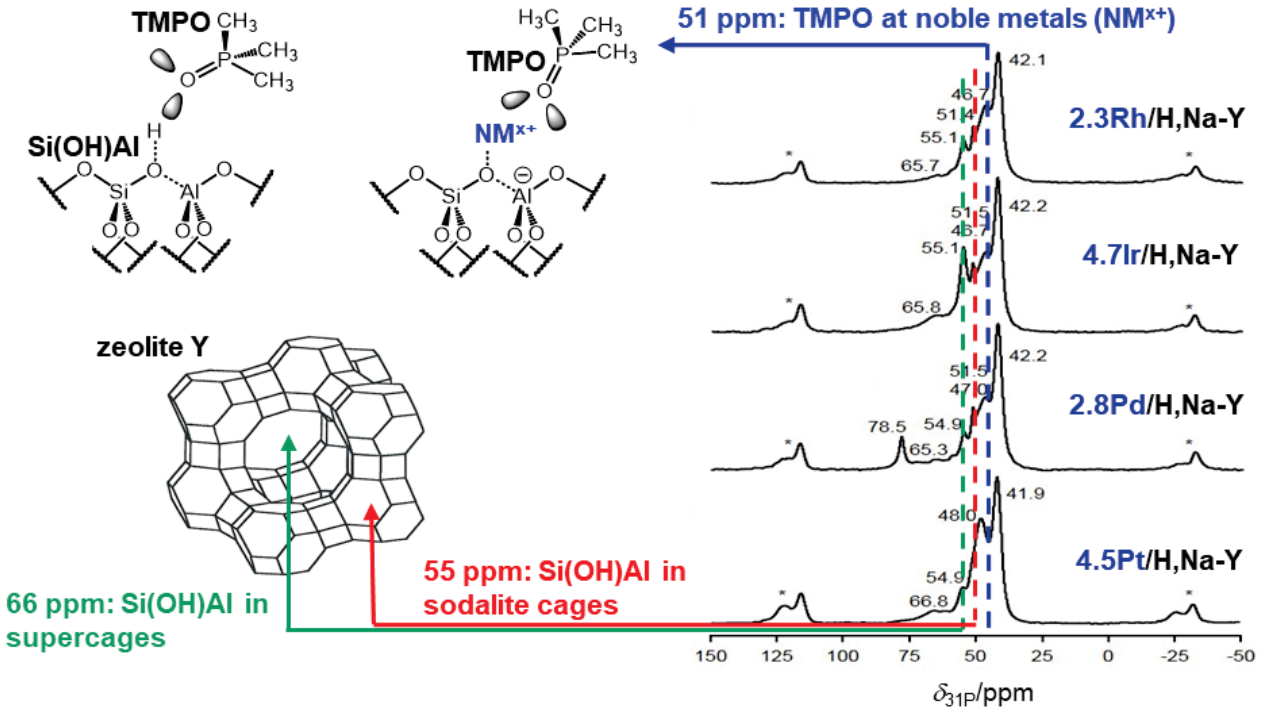

Figure C1-4. ^{31}P MAS NMR spectra of TMPO adsorbed on noble metal (Rh, Ir, Pd, and Pt) containing zeolites Na-Y (right-hand side) and assignment of the observed signals to TMPO coordinated at metal sites (δ_{31P} = 51 ppm) and physisorbed at bridging OH groups (Si(OH)Al) in supercages (δ_{31P} = 66 ppm) and small sodalite cages (δ_{31P} = 55 ppm).[C1-7]

In further studies, the hydrogenation and dehydrogenation properties of rhodium, iridium, palladium, and platinum containing zeolites Na-Y were investigated. The determination of the hydrogenation activity was performed by in situ ^{1}H MAS NMR spectroscopy under semi-batch conditions. For these experiments, the noble metal containing zeolites Y were loaded with the model reactant acrylonitrile after the reduction of the catalysts. Subsequently, these reduced and acrylonitrile loaded catalysts were transferred into MAS NMR rotors inside a glove box without contact to air and, then, inserted with the rotor into the MAS NMR probe. After reaching the required sample spinning rate and reaction temperature inside the magnetic field of the NMR spectrometer, the hydrogenation reaction was started by injecting a hydrogen flow into the spinning MAS NMR rotor filled with the acrylonitrile loaded catalyst. For this purpose, an in situ flow MAS NMR probe like shown in Figure C1-3 was utilized. As an example, Figure C1-5, left, shows the stack plot of ^{1}H MAS NMR spectra recorded during the hydrogenation of acrylonitrile (δ_{1H} = 5.9 and 6.3 ppm) to propionitrile (δ_{1H} = 1.3 and 2.5 ppm) on a zeolite catalyst as a function of time.[C1-8] By evaluating the ^{1}H MAS NMR signal intensities, reaction rates of k = 1.4 x 10^{-2} s^{-1} and 8.8 x 10^{-2} s^{-1} could be determined for the hydrogenation of acrylonitrile on zeolites 0.9Pt/Na-Y and 0.4Rh/Na-Y (both catalysts contained 0.55±0.05 metal atoms per unit cell), respectively. These results demonstrated a higher hydrogenation activity of rhodium atoms in comparison with platinum atoms dispersed on zeolite Na-Y.

Independent of the noble metal contents of the zeolite catalysts under study, the reaction rates for the acrylonitrile hydrogenation gave an activity sequence of Pd/H,Na-Y > Rh/H,Na-Y > Ir/H,Na-Y.[C1-9] For the dehydrogenation of propane on the same noble metal containing zeolites Na-Y studied under continuous flow conditions, the experimentally obtained turn-over-frequencies indicated an activity sequence of Ir/H,Na-Y > Rh/H,Na-Y > Pd/H,Na-Y. For the zeolite catalysts with high metal contents, H_2-temperature-programmed desorption (TPD) studies were performed and gave positions of the high-temperature peaks (HT) in the sequence of Pd/H,Na-Y (723 K) > Rh/H,Na-Y (713 K) > Ir/H,Na-Y (663 K). Based on these experimental data, relationships between the strength of the hydrogen adsorption at the noble metal species inside the zeolite cages and their hydrogenation and dehydrogenation properties were considered. The high desorption temperatures of the HT peaks for Pd and Rh containing zeolites Na-Y indicated strong H_2/metal interactions, which may cause a preferred hydrogen

adsorption and a preferred activation of surface hydrogen atoms, and, therefore, may cause the high hydrogenation activities of these zeolites compared with Ir/H,Na-Y zeolites. In the case of dehydrogenation reactions with hydrogen as a reaction product, the strong adsorption of hydrogen at Pd and, similarly, at Rh species in Pd/H,Na-Y and Rh/H,Na-Y zeolites, on the other hand, probably hinders the desorption of this reaction product, which leads to the lower dehydrogenation activity of these zeolite catalysts compared with Ir/H,Na-Y zeolites.

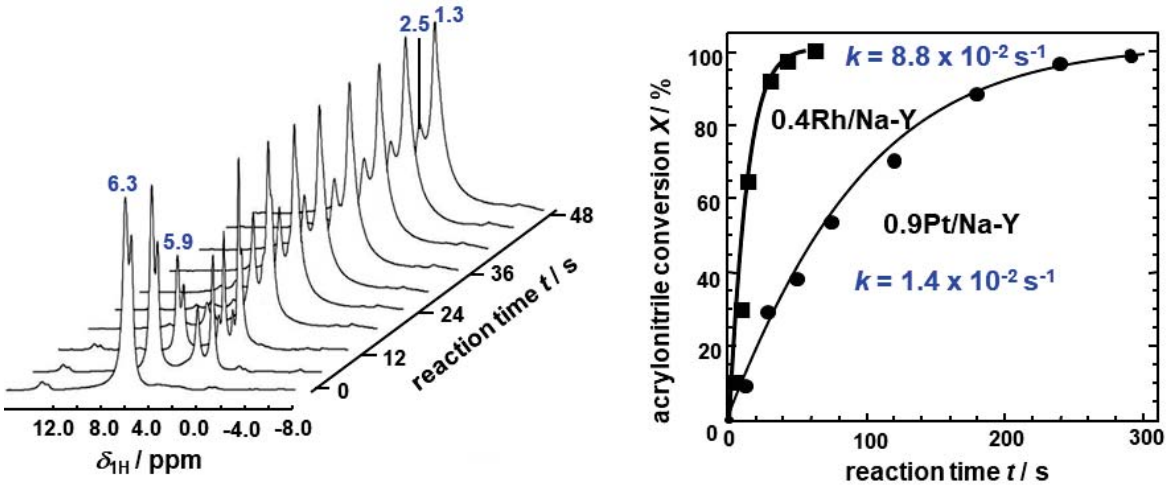

Figure C1-5. Stack plot of in situ ^{1}H MAS NMR spectra recorded during the hydrogenation of acrylonitrile (δ_{1H} = 5.9 and 6.3 ppm) to propionitrile (δ_{1H} = 1.3 and 2.5 ppm) over zeolite 0.4Rh/Na-Y at 295 K (left) and evaluation of the reaction kinetics at zeolites 0.4Rh/Na-Y and 0.9Pt/Na-Y (right).[C1-8]

A general problem of in situ solid-state NMR spectroscopy is the low detection limit of this method. Therefore, a number of research groups have recently been dealing with the development of spectroscopic techniques leading to significant NMR signal enhancements. One of these methods is the use of dynamic nuclear polarization (DNP), which is meanwhile often applied to liquid-state NMR spectroscopic studies. In DNP experiments, electron spins of paramagnetic complexes are excited by a CW-irradiation, subsequent polarization transfer is performed from the excited electron spins to neighboring nuclear spins, and, finally, this nuclear polarization is detected via an NMR spectrometer. Due to the principles of DNP, the samples under study must be loaded with paramagnetic complexes and the excitation of the electron spins must be performed at low temperature. For in situ solid-state NMR studies of catalytic systems, these methodical prerequisites may be problematic, e.g., because of the required low temperature and the introduction of additional metal sites. The Hunger group, therefore, focused on another enhancement technique of NMR signals based on parahydrogen induced polarization (PHIP). In PHIP experiments, parahydrogen with a total nuclear spin of $I = 0$ is introduced into reactants, e.g., by the hydrogenation of olefins. If the hydrogen atoms of the former parahydrogen molecules are pairwise introduced into the olefins at chemically non-equivalent positions without to lose their spin correlation, typical antiphase signals occur in the NMR spectrum. These antiphase signals can show an intensity enhancement up to a factor 10^5. Liquid-state NMR studies demonstrated that the high PHIP of ^{1}H nuclei can also be transferred to neighboring ^{13}C nuclei. For PHIP experiments in liquids, often the Wilkinson catalyst $RhCl(PPh_3)_3$ was utilized.

The Hunger group recently investigated various microporous and mesoporous materials (silica, SBA-15, zeolites DeA-Y and Na-Y), loaded with noble metals, as solid catalysts for in situ solid-state NMR investigations of the heterogeneously catalyzed hydrogenation of olefins with parahydrogen leading to the formation of PHIP.[C1-10] These experiments were carried out using an in situ flow MAS NMR probe like shown in Figure C1-3. With this probe, a continuous injection of parahydrogen into the reaction volume of the spinning MAS NMR rotor, filled with noble metal containing porous catalysts,

was performed. Utilizing this approach, series of porous support materials with pore sizes of $ø_{pore}$ = 0.7 to 4.5 nm, containing same types and numbers of noble metals, and of the same support material, containing different types of noble metals (Pt, Rh, Ir, Pd), were applied and studied as catalysts in the hydrogenation of propene with parahydrogen. The formation of hyperpolarized propane by the pairwise incorporation of parahydrogen into propene was investigated via in situ ^{1}H MAS NMR spectroscopy under continuous-flow conditions. The formation of PHIP was evaluated via the characteristic ^{1}H MAS NMR antiphase signals of propane. The aim of this work was the investigation of experimental parameters and properties of noble metal containing porous catalysts being important for the formation of PHIP. Evaluation of the observed spectra indicated a strong enhancement of the ^{1}H MAS NMR antiphase signals, especially for catalysts with large mesopores (Figure C1-6). For support materials containing numerous relaxation centers, like aluminum atoms, inside the pores, a rapid relaxation of the hyperpolarized reaction products was observed, which led to a rapid decrease of the PHIP. The above-mentioned investigations indicated that, e.g. siliceous and organic support materials with large mesopores, which are also required for the anchoring of molecular catalyst within the frame of the CRC, will be suitable materials for in situ solid-state NMR investigations of catalyst systems via PHIP.

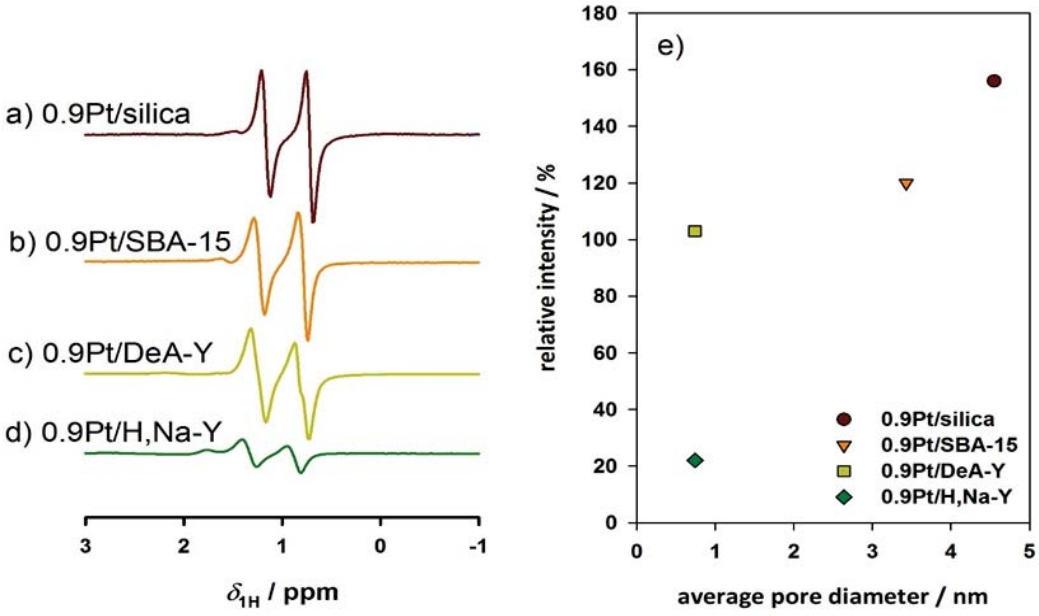

Figure C1-6. In situ ^{1}H MAS NMR antiphase signals observed during the hydrogenation of propene with parahydrogen on platinum containing (0.9 wt %) silica (a), SBA-15 (b), dealuminated zeolite DeA-Y (c), and zeolite Na-Y (d), and plot (e) of their relative intensities as a function of the pore diameters, $ø_{pores}$, of the above-mentioned porous support materials.[C1-10]

References

[C1-1] M. Dyballa, P. Becker, D. Trefz, E. Klemm, A. Fischer, H. Jacob, M. Hunger, *Catal. A: General* **2016**, *510*, 233-243.

[C1-2] S. Lang, M. Benz, U. Obenaus, R. Himmelmann, M. Scheibe, E. Klemm, J. Weitkamp, M. Hunger, *Top. Catal*., **2017**, DOI: 10.1007/s11244-017-0837-6.

[C1-3] W. Dai, C. Wang, M. Dyballa, G. Wu, N. Guan, L. Li, Z. Xie, M. Hunger, *ACS Catal.* **2015**, *5*, 317-326.

[C1-4] W. Dai, C. Wang, X. Yi, A. Zheng, L. Li, G. Wu, N. Guan, Z. Xie, M. Dyballa, M. Hunger, *Angew. Chem. Int. Ed.* **2015**, *54*, 8783-8786.

[C1-5] S. Lang, M. Benz, U. Obenaus, R. Himmelmann, M. Hunger, *ChemCatChem* **2016**, *8*, 2031-2036.
[C1-6] M. Hunger, *Prog. Nucl. Magn. Reson. Spectrosc.* **2008**, *53*, 105.
[C1-7] U. Obenaus, M. Dyballa, S. Lang, M. Scheibe, M. Hunger, *J. Phys. Chem. C* **2015**, *119*, 15254-15262.
[C1-8] H. Henning, M. Dornbach, M. Scheibe, E. Klemm, M. Hunger, *Microporous Mesoporous Mater.* **2012**, *164*, 104-110.
[C1-9] U. Obenaus, F. Neher, M. Scheibe, M. Dyballa, S. Lang, M. Hunger, *J. Phys. Chem. C* **2016**, *120*, 2284-2291.
[C1-10] U. Obenaus, S. Lang, R. Himmelmann, M. Hunger, *J. Phys. Chem. C* **2017**, *121*, 9953-9962.

3.11.4 Project plan

The general aims of this project consisting of two parts being dealt by two PhD students are (i) the development of novel solid-state NMR methods, such as solid-state NMR spectroscopy of probe molecules, for the characterization of metal centers of anchored complexes in covalent organic frameworks, mesoporous silicas, organic/inorganic hybrids and ordered mesoporous carbons, and (ii) the investigation of the mechanisms and kinetics of the ring-closing metathesis, hydrogen-autotransfer catalysis, and asymmetric catalysis as well as of the molecular transport properties of the catalyst systems under study. In the following, a summary of the work packages of these two parts (i) and (i) is given.

Part (i): Characterization of support materials and anchored metal complexes by sophisticated solid-state NMR methods, such as using novel probe molecules, performed by PhD1.

- **WP1: Characterization of the support materials before and after their modification by metal complexes.** By utilizing one- and two-dimensional solid-state NMR spectroscopy in combination with cross-polarization (CP) methods, a selective investigation of surface-near framework atoms of the support materials will be performed. In this way, surface sites acting as anchoring sites and their local structure, which are important for the modification of the support materials by metal complexes, will be identified and characterized.
- **WP2: Identification of suitable interaction centers of solid-state NMR probe molecules for the characterization of anchored metal complexes.** Investigation of the interactions of probe molecules with the surface sites of support materials and the metal sites of anchored complexes. In this way, suitable interaction centers for the characterization of the different surface sites and metals of the anchored complexes under study by probe molecules will be identified.
- **WP3: Development and application of probe molecules with suitable interaction centers and different molecular diameters.** After identification of suitable interaction centers of potential probe molecules in WP2, series of these probe molecules with different molecular diameters will be prepared and tested. By application of these molecular probes, the anchoring of metal complexes at the outer surface and inside the pores of the support materials and the accessibility of the catalytically active metal sites can be distinguished and will be investigated, respectively.
- **WP4: Development and application of two-center probe molecules for the investigation of distances between surface sites and metal sites of anchored metal complexes.** Preparation of series of probe molecules with two interaction centers of same or different nature in a well-defined distance, e.g. by modifying the length of the alkyl- or aryl-linkers between these two centers. By application of two-center probe molecules, the determination of distances between surface sites and metal sites beyond the range of dipolar interactions will be possible.

Part (ii): In situ solid-state NMR studies of intermediates, reaction mechanisms, reaction kinetics, and molecular transport properties, performed by PhD2.

- **WP5: Investigation of the interaction of model reactants with anchored metal complexes.** The adsorption and interaction of model reactants, such as diethyl diallylmalonate for the ring-closing metathesis, piperidine/benzylalcohol and aniline/benzylalcohol for the hydrogen-autotransfer catalysis, and boronic acids for the asymmetric catalysis will be investigated and compared with their adsorption state at the molecular catalysts in solution.
- **WP6: Investigation of reaction intermediates and reaction mechanisms by in situ solid-state NMR spectroscopy.** By a stepwise increase of the temperature for heterogeneously catalyzed reactions under batch conditions or by quenching of heterogeneously catalyzed reactions under stopped-flow conditions, intermediates and mechanisms of these reactions at anchored metal complexes will be investigated. For the hydrogenation of model reactants, parahydrogen will be used for reaching an improvement of the spectroscopic sensitivity under continuous-flow conditions and for obtaining novel insights into the reaction route.
- **WP7: Determination of the kinetics of reactions catalyzed by anchored metal complexes via in situ solid-state NMR spectroscopy.** For model reactants with a high NMR sensitivity in combination with heterogeneously catalyzed reactions in a temperature range available for in situ solid-state NMR spectroscopy, both selected in WP6, kinetic studies are planned. These in situ experiments will be performed under batch and semi-batch conditions.
- **WP8: Determination of the transport properties of model reactants in porous support materials modified with metal complexes.** By application of PFG NMR (pulsed-field gradient), the diffusion of model reactants and solvent molecules and the effect of the anchored metal complexes on the molecular transport inside the pores of the support materials will be determined. These experiments, together with the results of WP6 and WP7, will support the modelling of the kinetics of the heterogeneously catalyzed reactions under study.

The following Sections 3.11.4.1 to 3.11.4.8 give a more detailed insight into the investigations planned within the above-mentioned work-packages.

3.11.4.1 WP1: Characterization of the support materials before and after their modification by metal complexes

The high sensitivity of solid-state NMR spectroscopy for the local structure of solids will be utilized for the investigation and characterization of polymeric monoliths (**A1**), covalent organic frameworks **(A3, C2)**, mesoporous silicas **(A4)**, organic/inorganic hybrids **(A5)**, ordered mesoporous carbons **(A6)**, polymeric nanofoams **(A7)** and polymers **(A2, C2)** prepared as support materials within the CRC. For this purpose, modern methods of one- and two-dimensional solid-state NMR spectroscopy (e.g. double-quantum NMR) will be applied.[10, 11] For reaching a selective insight into the nature and properties of surface sites of the support materials, cross polarization (CP) experiments are planned, which are based on the excitation of abundant ^{1}H nuclei, such as protons of surface hydroxyl groups, strongly adsorbed solvent molecules or probe molecules, and a subsequent polarization transfer to dipolar coupled framework atoms. In this way, e.g. ^{13}C and ^{29}Si nuclei in the surface near region or in the local structure of surface sites will be selectively characterized. Furthermore, this approach allows the selective investigation and identification of surface sites acting as anchoring atoms for metal complexes. These investigations are important for optimizing the preparation routes of porous support materials in the **projects A3**, **A4**, **A5**, **A6** and **C2** and for their modification by a tailored anchoring of catalytically active metal complexes within the **projects B1**, **B2**, and **B3**.

3.11.4.2 WP2: Identification of suitable interaction centers of solid-state NMR probe molecules for the characterization of anchored metal complexes

Direct solid-state NMR investigations of the various metals (Ru, Mo, W, Rh), introduced by the anchoring of metal complexes, are not possible due to their low resonance frequency and low NMR sensitivity. Therefore, an indirect investigation of these metals by probe molecules is a suitable experimental approach. Requirements for these probe molecules are high chemical stability, long residence time at the surface sites and metals at near-ambient temperature, and high NMR sensitive or cheap isotopic enrichment. Possible candidates are alkyl phosphine oxides (POR_y) and alkyl phosphines (PR_y), which are already utilized for the characterization of Brønsted and Lewis acid sites of solid catalysts.[12, 13] Interaction centers of these probe molecules are, e.g., the electronegative oxygen atoms of POR_y being sensitive for surface OH groups acting as anchoring sites and the nucleophilic P atoms of PR_y probe molecules. These two types of probe molecules have the advantage of a high NMR sensitivity of the ^{31}P nuclei, but may require demanding preparation methods for the catalyst samples under study. Therefore, easily reproducible methods for the loading of the probe molecules, e.g., in solution or via the gas phase have to be developed for the specific applications within the frame of the CRC. Model reactants can also be potential probe molecules for studying their interactions with catalytically active sites. Problems could be a low chemical stability and a too short residence time at the surface sites under study in comparison with the observation time of solid-state NMR spectroscopy. WP2 is an important methodical prerequisite for the development of specifically tailored probe molecules in WP3 and WP4. The preparation of commercially not available probe molecules will be performed by one of the PhD students of the Hunger group under the guidance of the colleagues of the **projects B1**, **B2**, and **B3** by utilizing their laboratory equipment and their long-year experiences in organic synthesis.

3.11.4.3 WP3: Development and application of probe molecules with suitable interaction centers and different molecular diameters

For obtaining highly selective catalyst systems, the anchoring of the metal complexes must be performed exclusively inside the pores of the support materials. The solid-state NMR characterization of these modified support materials, therefore, will be performed using probe molecules with different molecular sizes, which are able to distinguish the spatial distribution of the anchored metal complexes, i.e. their anchoring at the outer surface of the support particles and inside the pores of these materials (see Figure C1-7). For this purpose, a series of probe molecules with suitable interaction centers and different ligand lengths will be prepared. A suitable approach could be the preparation of alkyl phosphine oxides (POR_y), alkyl aryl phosphine oxides ($POAr_xR_y$), alkyl phosphines (PR_y), and alkyl aryl phosphines (PAr_xR_y) with a systematically increased number of aryl groups and length of the alkyl chains.[13, 14] Since only few of these molecules are commercially available, most of the probe molecules with large alkyl and aryl chains must be prepared by one of the PhD students of the Hunger group under the guidance of the colleagues of the **projects B1**, **B2**, and **B3**. As for WP2, reproducible methods for the quantitative loading of these probe molecules on the modified support materials must be developed and tested.

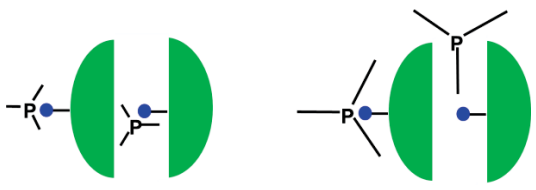

Figure C1-7. Schemes of the interaction of small-size (left-hand side) and large-size (right-hand side) probe molecules (e.g. alkylphosphines) with anchored metal sites (●) inside and outside the pores of a support material (◖◗). The ^{31}P nuclei of the adsorbed molecules are utilized as NMR probes.

3.11.4.4 WP4: Development and application of two-center probe molecules for the investigation of distances between surface sites and metal sites of anchored metal complexes

For the determination of atom-atom distances by NMR spectroscopy, often the strength of the dipolar interaction between the corresponding atoms is investigated and evaluated. However, this method is limited by the range of dipolar interactions (< 0.5 nm) and their NMR detection. Therefore, a novel experimental method for the determination of distances between surface sites and metal sites of anchored complexes will be developed, which is based on probe molecules with two interaction centers in a well-defined distance. A simultaneous interaction of the two molecular interaction centers with metal and/or surface sites of the catalysts under study will indicate that their distances coincide (see Figure C1-8). For this purpose, series of probe molecules with two interaction centers of same or different nature, connected via linkers with different length will be prepared and tested. Possible candidates are bisphosphine oxides and bisphosphines with alkyl and aryl linkers of different length. Again, only few of these molecules are commercially available and probe molecules with large linkers must be prepared by one of the PhD students of the Hunger group under the guidance of the colleagues of the **projects B2** and **B3**. As for WP2 and WP3, specific methods for the quantitative loading of these probe molecules on the modified support materials have to be developed and tested. The experimental approach of applying NMR probe molecules with two interaction centers will be a novel tool for characterizing the spatial arrangement of the active sites on solid catalysts. The atom probe tomography (APT) developed in **C3 (Schmitz)** will be used for investigating the same catalyst/substrate systems, so that the obtained results are important for a mutual cross check of the innovative methods.

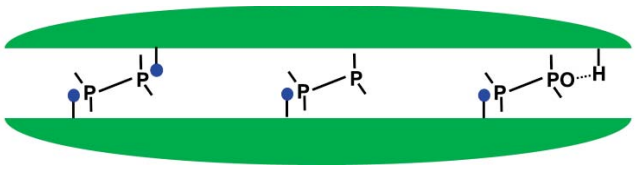

Figure C1-8. Scheme of two-center probe molecules (e.g. bisphosphine oxides, bisphosphines, and mixed phosphines) interacting with metal (●) and surface (H) sites in the pores of the support materials (◓). The ^{31}P nuclei of the adsorbed molecules are utilized as NMR probes.

3.11.4.5 WP5: Investigation of the interaction of model reactants with anchored metal complexes

These experiments will be performed in cooperation with the **projects B1,** focusing on the hydrogen-autotransfer reaction of piperidine/benzylalcohol and/or aniline/benzylalcohol at anchored ruthenium-complexes, **B2,** focusing on the ring-closing metathesis of diethyl diallyl malonate at anchored molybdenum- and tungsten-complexes, and **B3,** focusing on the asymmetric catalysis with boronic acids at anchored rhodium-complexes. For each of these combinations of model reactants and molecular catalysts, suitable methods for the reproducible preparation of NMR samples must be developed and tested. In this connection, it must be mentioned that solid-state NMR experiments require catalyst samples low solvent contents or with strongly adsorbed solvent molecules. In a second step, the model reactants at anchored metal complexes and at metal complexes in solution, like utilized in homogeneous catalysis, will be studied by solid-state NMR and liquid-state NMR, respectively, for comparing their interactions under these different conditions. The obtained results will give insights into the effect of the anchoring of metal complexes on their chemical properties. The investigations of WP5 are important prerequisites for the in situ solid-state NMR experiments planned in WP6 and WP7.

3.11.4.6 WP6: Investigation of reaction intermediates and reaction mechanisms by in situ solid-state NMR spectroscopy

After developing preparation methods for model reactants at the various catalysts in WP5, their stepwise conversion will be investigated by solid-state NMR spectroscopy under batch conditions and via stopped-flow experiments. For studies under batch conditions, the catalyst samples loaded with model reactants will be sealed in symmetric glass ampoules for spinning in MAS rotors. During these experiments, the sealed catalysts samples will be heated stepwise and, subsequently, measured by solid-state NMR at ambient temperature.[15, 16] Another experimental approach will be the in situ injection of reactants into spinning MAS rotors filled with catalysts and a stepwise quenching of the reaction after heating at reaction temperature, i.e. similar to stopped-flow experiments.[17, 18] By these two experimental approaches, the formation of intermediates and by-product will be studied. Like in WP5, these experiments will be performed in cooperation with the colleagues of the **projects B1**, **B2**, and **B3** for the same model reactants and anchored metal complexes mentioned in WP5. Especially in the case of in situ solid-state NMR experiments, model reactants must have a high NMR sensitivity, which could require their isotopic enrichment. In the case of the asymmetric catalysis with boronic acids, investigated in **project B3**, the high NMR sensitivity of ^{11}B nuclei will be utilized as a significant advantage for in situ experiments. Similarly, modification of molecular metal complexes with parafluorotriarylphosphines, such as planned in **project B1**, will allow to perform highly sensitive in situ ^{19}F and ^{31}P MAS NMR studies of reaction intermediates and reaction mechanisms. For heterogeneously catalyzed reactions containing a hydrogenation step, the insertion of parahydrogen into reactants or reaction intermediates will be investigated by in situ MAS NMR spectroscopy under continuous-flow conditions. In this case, the pairwise insertion of parahydrogen into reactants will lead to the occurrence of typical antiphase signals, which allow insight into details of the hydrogenation mechanism. Furthermore, the formation of parahydrogen induced polarization (PHIP) will be utilized as a potential method for enhancing the sensitivity of in situ solid-state NMR spectroscopy. This topic is in the focus of recent research for novel solid-state NMR spectroscopic methods applied in the field of heterogeneous catalysis.[19, 20] The results of WP6 will be important for calculations of the reactant activation and reaction intermediates performed in **project C4**.

3.11.4.7 WP7: Determination of the kinetics of reactions catalyzed by anchored metal complexes via in situ solid-state NMR spectroscopy

For model reactants with high NMR sensitivity in combination with catalytic reactions in a temperature range available for solid-state NMR spectroscopy, both selected in WP6, kinetic studies via in situ experiments are planned. These in situ solid-state NMR investigations will be performed with sealed samples under batch conditions at a reaction temperature allowing the observation of the reactant conversion in a suitable time scale. Another experimental approach will be an in situ injection of one of the key reactants into a spinning MAS rotor filled with the catalyst. The spinning MAS rotor will be heated to reaction temperature during this in situ solid-state NMR experiment under semi-batch conditions.[21, 22] Depending on the NMR sensitivity of the observed nuclei, spectra in a sequence of seconds, e.g. for in situ ^{1}H, ^{11}B, ^{19}F, and ^{31}P MAS NMR spectroscopy, or in a sequence of minute to hours, e.g. for in situ ^{13}C MAS NMR spectroscopy, will be recorded and quantitatively evaluated. Like in WP5 and WP6, these experiments are planned in cooperation with the **projects B1**, **B2**, and **B3**, i.e. focusing on the hydrogen-autotransfer reaction of piperidine/benzylalcohol or aniline/benzylalcohol at anchored ruthenium-complexes, the ring-closing metathesis of diethyl diallyl malonate at anchored molybdenum- and tungsten-complexes, and the asymmetric catalysis with boronic acids at anchored rhodium-complexes, respectively. The obtained results of the kinetic studies will deliver data for calculations of chemical reactivities performed within the **project C4**.

3.11.4.8 WP8: Determination of the transport properties of model reactants in porous support material modified with anchored metal complexes

The modelling of the heterogeneously catalyzed reactions under study requires data of the transport properties of reactants inside the pores of the modified support materials. Therefore, investigations of the diffusion parameters of model reactants and solvent molecules by ^{1}H PFG NMR spectroscopy are planned. For a selective study of the diffusion properties of specific reactants and molecules, the other mobile components must be present in their deuterated state. Furthermore, PFG NMR experiments at different temperatures will allow the determination of activation energies of the molecular transport.[23] The obtained results are important for fluid-theoretical predictions planned in **project C5** and calculations of pore diffusion processes performed by the colleagues of the **project C6**.

Chronological work plan:

	2018	2019			2020				2021				2022		
	Q3	Q4	Q1	Q2	Q3	Q4	Q1	Q2	Q3	Q4	Q1	Q2	Q3	Q4	Q1	Q2	
T1																	WP1: Characterization of the support materials before and after their modification by metal complexes (PhD1)
T2																	WP 2: Identification of suitable interaction centers of solid-state NMR probe molecules for the characterization of anchored metal complexes (PhD1)
T3																	WP 3: Development and application of probe molecules with suitable interaction centers and different molecular diameters (PhD1)
T4																	WP 4: Development and application of two-center probe molecules for investigating distances between surface sites and metal sites of anchored metal complexes (PhD1)
T5																	WP 5: Solid-state NMR spectroscopic investigation of the interaction of model reactants with anchored metal complexes (PhD2)
T6																	WP 6: Investigation of reaction intermediates and reaction mechanisms by in situ solid-state NMR spectroscopy (PhD2)
T7																	WP 7: Determination of the kinetics of reactions catalyzed by anchored metal complexes via in situ solid-state NMR spectroscopy (PhD2)
T8																	WP 8: PFG NMR studies of the transport properties of model reactants in porous support material modified with anchored metal complexes (PhD2)

3.11.4.9 Methods applied

The solid-state NMR spectroscopic characterization of porous supports in WP1 will be performed using the 400MHz solid-state NMR equipment (Bruker AVANCEIII 400WB) of the Hunger group and the liquid-state 700MHz NMR spectrometer (Bruker AVANCEIII 700NB) of the Faculty of Chemistry, which is equipped with a 2.5mm MAS NMR probe and an MAS unit. The studies of WP2 to WP4 and all in situ solid-state MAS NMR studies planned for WP5 to WP7 require specific MAS rotors (4mm MAS NMR system) and in situ MAS NMR probes (self-made flow MAS NMR probes), which exclusively exist at the above-mentioned 400MHz solid-state NMR spectrometer of the Hunger group. Also the diffusion studies of WP8 require a specific PFG NMR probe, which exclusively exists at the above-mentioned 400MHz solid-state NMR spectrometer. In the first funding period, no investment in additional NMR technique is necessary. The preparation of NMR samples, i.e. the well-defined loading of the catalyst systems with probe molecules and model reactants, will be performed in the laboratories of the Hunger group, which are equipped with vacuum lines and different self-made glove boxes for the transfer of the activated and loaded catalyst samples into the MAS NMR rotors without contact to air.

3.11.4.10 Vision

By the end of the first funding period, new solid-state NMR tools for the characterization of catalytically active metal sites via novel probe molecules will exist. These solid-state NMR probe molecules will open new possibilities for studying the chemical properties and spatial distribution of surface and metal sites on solid catalysts. The in situ solid-state NMR studies will give new insights into the mechanisms of the heterogeneously catalyzed reactions under study, i.e. the hydrogen-autotransfer catalysis, the ring-closing metathesis, and the asymmetric catalysis at anchored metal complexes. For the 2nd and 3rd funding period, the application of probe molecules with paramagnetic centers is planned. By polarization transfer from excited electron spins of paramagnetic sites to neighbouring nuclei using DNP NMR spectroscopy (DNP: Dynamic Nuclear Polarization), selective investigations of the surface near region of support materials, including adsorbed reactants, with enhanced NMR sensitivity become possible. After test measurements, e.g. at the University of Darmstadt, installation of this new NMR method at the University of Stuttgart should be considered. This approach will also open new possibilities for in situ solid-state NMR studies of low-sensitive nuclei in metal complexes, reactants, and reaction intermediates.

3.11.5 Role within the collaborative research center

For contributing to the success of the CRC, i.e. the development of highly selective catalyst systems, the Hunger group will intensively cooperate in WP1 with the colleagues of the **projects A1, A3**, **A4**, **A5**, **A6, A7** and **C2** responsible for the preparation of the three-dimensional porous supports and with the colleagues of the **projects B1**, **B2**, and **B3** performing the anchoring of the molecular catalysts inside the pores of the above-mentioned materials. Considerable research efforts will be required for the detailed investigation and characterization of the chemical properties and spatial distribution of the catalytically active metal sites within WP2 to WP4. The preparation of novel probe molecules with well-defined molecular diameters and two-center distances will be carried out under the guidance of the colleagues of the **projects B1**, **B2**, and **B3**. The study of the spatial distribution and distances of surface and metal sites will be performed in cooperation with the colleagues of **project C3** since the atom probe tomography (ATP) is a complementary method for the same purpose.

The in situ solid-state NMR studies of the interactions of model reactants with metal sites, their stepwise conversion, the study of reaction intermediates and mechanisms, and the determination of reaction kinetics in WP5 to WP7 will be performed in close cooperation with the colleagues of the **projects B1** focusing on the hydrogen-autotransfer catalysis at anchored ruthenium-complexes, **B2** focusing on the ring-closing metathesis at anchored molybdenum- and tungsten-complexes, and **B3** focusing on the asymmetric catalysis at anchored rhodium-complexes. Furthermore, the results of these in situ investigations will be important for the simulation of chemical reactivities in **project C4**. The diffusions studies carried out by ^{1}H PFG NMR spectroscopy in WP8 are important for fluid-theoretical predictions planned in **project C5** and for calculations of pore diffusion processes performed by the colleagues of **project C6**.

3.11.6 Differentiation from other funded projects

This **project C1** has no topical overlap with the following other projects of the Hunger group:

- Japanese-German project funded by the Ministry of Education, Science, Sports and Culture, Grants 25400318 and 25400319, cooperation with Prof. Dr. Kiminori Sato, Tokyo Gakugei University,Tokyo, Japan: Application of natural minerals for the decontamination of radioactive soil from the surrounding of Fukushima.

- Chinese-German project funded by the Municipal Natural Science Foundation of Tianjin, 14JCQNJC05700, cooperation with Prof. Dr. Weili Dai, Nankai University, Tianjin, P.R. China: Investigation of the mechanisms of the heterogeneously catalyzed conversion of methanol to olefins on zeolite catalysts.

References (ctd.)

[10] S. Lang, M. Benz, U. Obenaus, R. Himmelmann, M. Scheibe, E. Klemm, J. Weitkamp, M. Hunger, *Top. Catal.* **2017**, DOI: 10.1007/s11244-017-0837-6.
[11] Z. Wang, Y. Jiang, O. Lafon, J. Trebosc, K.D. Kim, C. Stampfl, A. Baiker, J.-P. Amoureux, J. Huang, *Nature Commun*. **2016**, 7, 13820.
[12] M. Hunger, *NMR Spectroscopy for the Characterization of Surface Acidity and Basicity*, in: G. Ertl, H. Knoezinger, F. Schueth, J. Weitkamp (eds.), *Handbook of Heterogeneous Catalysis*, Vol. 2, Chapter 3.2.4.4, 2nd Edition, Wiley-VCH, Weinheim, **2008**, p. 1163-1178.
[13] Y. Jiang, J. Huang, W. Dai, M. Hunger, *Solid State Nucl. Magn. Reson.* **2011**, *39*, 116-141.
[14] A. Zheng, S.-J. Huang, W.-H. Chen, P.-H. Wu, H. Zhang, H.-K. Lee, L.-C. de Menorval, F. Deng, S.-B. Liu, *J. Phys. Chem. A* **2008**, *112*, 7349-7356.
[15] W. Dai, X. Sun, B. Tang, G. Wu, L. Li, N. Guan, M. Hunger, *J. Catal.* **2014**, *314*, 10-20.
[16] W. Dai, C. Wang, X. Yi, A. Zheng, L. Li, G. Wu, N. Guan, Z. Xie, M. Dyballa, M. Hunger, *Angew. Chem. Int. Ed.* **2015**, *54*, 8783-8786.
[17] M. Hunger, J. Weitkamp, *In situ Magnetic Resonance Techniques: Nuclear Magnetic Resonance*, in: B.M. Weckhuysen (ed.), *In situ Spectroscopy of Catalysts*, American Scientific Publishers, Stevenson Ranch, California, **2004**, p. 177-218.
[18] M. Hunger, *Prog. Nucl. Magn. Reson. Spectrosc.* **2008**, *53*, 105-127.
[19] H. Henning, M. Dornbach, M. Scheibe, E. Klemm, M. Hunger, *Micropor. Mesopor. Mater.* **2012**, *164*, 104-110.
[20] U. Obenaus, S. Lang, R. Himmelmann, M. Hunger, *J. Phys. Chem. C* **2017**, *121*, 9953-9962.
[21] U. Obenaus, F. Neher, M. Scheibe, M. Dyballa, S. Lang, M. Hunger, *J. Phys. Chem. C* **2016**, *120*, 2284-2291.
[22] H. Henning, M. Dyballa, M. Scheibe, E. Klemm, M. Hunger, *Chem. Phys. Lett.* **2013**, *555*, 258-262.
[23] W. Dai, M. Scheibe, L. Li, N. Guan, M. Hunger, *J. Phys. Chem. C.* **2012**, *116*, 2469-2476.

3.11.7 Project funding

3.11.7.1 Previous funding

This project is currently not funded and no funding proposal has been submitted.

3.11.7.2 Requested funding

Funding for	2018		2019		2020		2021		2022		2018-2022	
Staff	Quantity	Sum	Quantity	Sum	Quantity	Sum	Quantity	Sum	Quantity	Sum	Quantity	Sum
PhD student, 67%	2	43,200.-	2	86,400.-	2	86,400.-	2	86,400.-	2	43,200.-	2	345,600.-
Total		43,200.-		86,400.-		86,400.-		86,400.-		43,200.-		345,600.-
Direct costs	Sum		Sum		Sum		Sum		Sum		Sum	
consumables	5,000.-		10,000.-		10,000.-		10,000.-		5,000.-		40,000.-	
Total	5,000.-		10,000.-		10,000.-		10,000.-		5,000.-		40,000.-	
Major research instrumentation	Sum		Sum		Sum		Sum		Sum		Sum	
	-		-		-		-		-		-	
Total	-		-		-		-		-		-	
Grand total	48,200.-		96,400.-		96,400.-		96,400.-		48,200.-		385,600.-	

(All figures in EUR)

3.11.7.3 Requested funding for staff

	Sequential no.	Name, academic degree, position	Field of research	Department of university or non-university institution	Project commitment in hours per week	Category	Funding source
Existing staff							
Research staff	1	M. Hunger, Dr., apl. Prof.	Solid-state NMR, Heterogeneous Catalysis	Institute of Chemical Technology	4		University
Non-research staff	2	M. Scheibe		Institute of Chemical Technology	8		University
Requested staff							
Research staff	3	N.N. M.Sc.	Solid-state NMR, Heterogeneous Catalysis	Institute of Chemical Technology		PhD	
Research staff	4	N.N. M.Sc.	Solid-state NMR, Heterogeneous Catalysis	Institute of Chemical Technology		PhD	
Research staff	5	Research assistant	Solid-state NMR, Heterogeneous Catalysis	Institute of Chemical Technology			

Job description of staff (supported through existing funds):
1
Apl. Professor, head of the research group
2
Technician, in charge of the NMR equipment and performs N_2 physisorption on porous supports (BET surface, pores volume etc.) and hydrogen chemisorption at metal sites (metal dispersion)

Job description of staff (requested funds):
3
PhD student, work packages 1 to 4
4
PhD student, work packages 5 to 8
5
Research assistants. **Justification:** Research assistants are required for the synthesis of spectroscopic probe molecules, such as alkyl aryl phosphine oxides with systematically increasing numbers of aryl groups and with alkyl chains of different length as well as of bisphosphine oxides and bisphosphines with alkyl and aryl linkers of different length. With further progress of **project C1**, the above-mentioned assistants have to support the preparation of samples for *in situ* solid-state NMR investigations of reaction intermediates and for determining reaction kinetics and molecular transport properties inside the pores of the catalyst systems under study.

After the retirement of the PI in 2021, the responsibility over these PhD students and **project C1** will be taken by Dr. Michael Dyballa (currently University of Oslo), who will start his habilitation at the University of Stuttgart in July 2018. Michael Dyballa worked as a Master and PhD student in the group of the PI between 2010 and 2015. In 2015, he moved to the Department of Chemistry of the University of Oslo, Norway. He has long-year experiences in heterogeneous catalysis and the application of NMR spectroscopy in this research field. He is author and co-author of 16 publications in international journals with peer-review system.

3.11.7.4 Requested funding of direct costs

	2018	2019	2020	2021	2022
Uni Stuttgart: existing funds from public budget	1,000.-	2,000.-	2,000.-	2,000.-	1,000.-
Sum of existing funds	1,000.-	2,000.-	2,000.-	2,000.-	1,000.-
Sum of requested funds	5,000.-	10,000.-	10,000.-	10,000.-	5,000.-

(All figures in EUR)

Consumables for financial year 2018

Chemicals, consumables, isotopic enriched materials, MAS NMR rotors and caps	EUR	5,000.-

Consumables for financial year 2019

Chemicals, consumables, isotopic enriched materials, MAS NMR rotors and caps	EUR	10,000.-

Consumables for financial year 2020

Chemicals, consumables, isotopic enriched materials, MAS NMR rotors and caps	EUR	10,000.-

Consumables for financial year 2021

Chemicals, consumables, isotopic enriched materials, MAS NMR rotors and caps	EUR	10,000.-

Consumables for financial year 2022

Chemicals, consumables, isotopic enriched materials, MAS NMR rotors and caps	EUR	5,000.-

3.11.7.5 Requested investments
none

3.12 Project C2

3.12.1 General information about Project C2

3.12.1.1 The static and dynamic electronic and geometric structure of *multiprobe* organometallic complexes in porous polymers.

3.12.1.2 Research Areas
Inorganic Molecular Chemistry - Synthesis, Characterization (301-01)
Theory and Modeling (302-03)

3.12.1.3 Principal Investigators
Ringenberg, Mark Richard, Dr., born 08.04.1984, male, American
Institut für Anorganische Chemie
Universität Stuttgart, Pfaffenwaldring 55, 70569 Stuttgart
Tel.: 0711/685-64196
E-Mail: mark.ringenberg@iac.uni-stuttgart.de
Habilitand, temporary contract, employment guaranteed for first funding period

Van Slageren, Joris, Prof. Dr., born 27.08.1973, male, Dutch
Institut für Physikalische Chemie
Universität Stuttgart, Pfaffenwaldring 55, 70569 Stuttgart
Tel.: 0711/685-64380
E-Mail: slageren@ipc.uni-stuttgart.de
Tenured Professor W3

3.12.1.4 Legal Issues
This project includes

1.	research on human subjects or human material.	no
2.	clinical trials.	no
3.	experiments involving vertebrates.	no
4.	experiments involving recombinant DNA.	no
5.	research involving human embryonic stem cells.	no
6.	research concerning the Convention on Biological Diversity.	no

3.12.2 Summary
The understanding of confinement effects in molecular heterogeneous catalysis requires that the consequences of inserting and covalently linking catalytically active organometallic species into the mesopores of a carrier material be determined. Several issues must be addressed and resolved: does the tethered catalyst point toward the middle of the pore or does it stay close to the pore wall due to an attractive interaction? What is the timescale and nature of the movements of the catalyst, i.e., its dynamics? How do the linker and the attachment to the pore wall influence the geometric and electronic structure as well as the catalytic activity of the catalyst? Many catalytically active organometallic species contain only a few spectroscopic handles, precluding detailed study of immobilized catalysts in mesoporous materials. To address these questions organometallic species were chosen for their spectroscopic richness rather than catalytic activity. These *multiprobe* complexes, based on 1,1'-bis(diphenylphosphino)ferrocene-tricarbonyliron scaffold, will be employed to assess the fundamental questions outlined above. These complexes contain many spectroscopic handles that allow for structural and electronic information to be elucidated, as well as offering several stable oxidation states and different spin-states. Using IR-, MCD-, CW- and pulsed EPR, NMR and Mössbauer spectroscopy along with DFT and molecular dynamics calculations, the static and dynamic probe molecule orientation as well as geometrical and electronic structure will be determined. We have chosen two types of mesoporous materials that will be provided to us by **projects A2** (mesoporous polymer films) and **A3** (covalent organic frameworks).

3.12.3 Research rationale

3.12.3.1 Current state of understanding and preliminary work

Over the past decades, many efforts have been spent on immobilizing homogeneous catalysts. On the one hand, the driver for these efforts was the facile separation and recovery of the expensive transition metal catalysts from the reaction mixture post reaction. Furthermore, better performance and reactivities different from what was found in homogeneous solution were also actively sought. In the latter case, catalysts have been inserted into the pores of a suitable carrier material rather than on the surface of particles, so that the pore wall may exert a positive influence on the selectivity and reactivity of the catalyst. Such effects have been exploited by nature to an extreme extent in metalloenzymes. Also in molecular heterogeneous catalysis, a number of cases of positive effects on catalytic performance compared to homogeneous conditions were reported, but in other cases this was not the case. Gaining full understanding of these observations lies at the core of this CRC. Additional relevant information on the CRC's overall aims can be found in the general part of the collaborative research center proposal. Thus, rational progress towards exploiting secondary structures around a catalytically active center is hampered to the point of preclusion by the lack of understanding of the properties of immobilized catalysts in pores. Questions such as the following remain largely unanswered: *What is the orientation of the catalyst inside the pore?* In sketches one often finds that the catalyst points toward the empty space in the center of the pore, but there is no urgent thermodynamic reason for this to be so. *What is the dynamics of the immobilized catalyst? Does it move around; if yes with which amplitude, and on what timescale?* In this project we intend to employ a dinuclear iron molecule that provides a number of independent spectroscopic handles to elucidate the situation and to find the answer to the above questions. We will use a wide range of experimental techniques in combination with electronic structure and molecular dynamics calculations.

To be able to arrive at quantitative conclusions regarding the orientation of immobilized organometallic species in mesoporous systems it is essential that these carrier materials are very well defined in terms of pore size distribution and linker position distributions. These requirements are fulfilled by both covalent organic frameworks (COFs) and mesoporous block copolymer films on gold. The former are highly crystalline materials, synthesized from molecular precursors. Here the intended linker attachment position can be chosen with atomic precision. The crystalline nature of the materials ensures highly monodisperse pore size distributions. COF research is a very active field of research (see also **project A3**). These substances can be grown as 2D sheet-like materials or as 3D covalently bound structures and pore sizes between 1-6 nm have been obtained. Immobilization of radical species, fluorescent labels and catalyst species into COFs has been achieved. Suitable COFs will therefore be provided to us by **project A3**, that will be used to immobilize our multiprobe complex.

Mesoporous polymer films have been prepared by deposition of judiciously chosen block-copolymers onto gold, glass or silicon. The structure of these films can be improved by post-deposition methods, such as solvent-vapor annealing, electric fields or shear fields. The polymer films can be nanostructured rendering them mesoporous by dissolving or chemical decomposition of one of the two blocks (see also **project A2**). Suitable polymer films will therefore be provided to us by **project A2**, that will be used to immobilize our multiprobe complex.

Mimicking the structure and reactivity of metalloenzymes without the protein environment can be difficult; however, chemists are able to use organometallic compounds and ligands that are not found in the biosphere to adopt certain enzymatic properties. Among the numerous ligand systems existing, phosphane ligands are common in transition metal chemistry because they can be easily modified to tune electronic and structural parameters by variation of their substitution patterns. Ferrocenyl based phosphanes, especially 1,1’-bis(diphenylphosphino)ferrocene (dppf), and chelating alkylphosphane ligands such as 1,n-bis(diphenylphosphino)alkanes, where n > 0, are common ligand motifs because they offer a range of bite angles, and steric/electronic control through R-groups on the phosphane donors. Even small changes in the bite angles and thus in the coordination environment can result in dramatic changes of the reactivity of transition metal catalysts. Ferrocenyl based ligands are a key class of ligands in catalysis, however, their role in stabilizing unpaired electrons and open coordination sites is a relatively new undertaking. Ferrocenyl based ligands especially containing phosphane functionality are more flexible compared to 1,n-bis-substituted alkyl phospane ligands, or most classic ligands, which have set coordination mode. Furthermore, ferrocene is a classic redox active

organometallic center, although when bound to metal centers through the phosphane donors the redox potential is often quite cathodic and is therefore often discounted in catalysis.

Bimetallic compounds and interactions between two metal centers in general are of interest because they can reveal how electrons delocalize in complex systems, often stabilizing open shell species. The importance of M-M interactions is further highlighted by the presence of metal clusters in natural enzymes, many existing as homo-bimetallic, hetero-bimetallic or even higher nuclearity clusters. Such clusters consist primarily of first row transition metals, due in part to bioavailability, and their abundance in the earth's crust. Optimization of these enzymes over millions of years of evolution has produced catalysts, many based on iron, that are capable of performing reactions often only achieved by precious metal based catalysts in the lab. Iron is fast becoming a pillar in catalysis, but is still vastly underrepresented compared to its ubiquitous presence in metalloenzymes as a cofactor essential to life. Iron complexes can occur in diverse redox (Fe^{-II} to Fe^{IV}) and spin states (high-, intermediate-, low spin). Metalloenzymes tune these redox- and spin-states through different ligands and structural variations of the protein environment, even employing CO and CN^-, redox-active noninnocent ligands, and/or metal clusters. The weak interactions present in the active site of metalloenzymes mediate the spacial and temporal delivery of incoming substrates (including electrons) as well as stereo- and regiochemistry of the reaction. Redox-active moieties in close proximity to active sites allow for rapid separation or combination of charge, a key factor for performing multi-electron transfers using base metals. Charge separation is also important in the processing of small molecules, such as H_2, N_2, O_2 or CO_2, which must overcome large kinetic barriers toward activation. [C2-1]

The Ringenberg group specializes in organometallic synthesis especially concerning first-row transition metal complexes containing redox-active noninnocent ligands.[1,4] The group performs electrochemistry and spectroscopy (including absorption (UV-Vis-near IR), vibrational (IR), and X-band CW EPR) in order to determine the often complicated electronic structure of organometallic complexes containing noninnocent ligands.[C2-2,C2-3] The lab has also developed an expertise in hybrid spectroelectrochemistry technique including low-temperature (–50 C) which is useful in generating and observing *in situ* highly reactive or metastable oxidation states of organometallic complexes. They are also active in the development of novel electrocatalyst for hydrogen evolving reactions (HER).[C2-1] The group performs calculations based on the spectroscopic results in order to develop a more holistic understanding of the organometallic species under investigation.[C2-3] There is also a long standing interest in the development and reactivity of complexes containing noninnocent redox-active ligands for use as catalysts especially for the processing of small molecues.[C2-1]

Recently, the Ringenberg group has shown that dppf can stabilize spin from metal carbonyls ($Fe(CO)_3$[C2-2,C2-3] and $Mn(CO)_3$[C2-5] by distributing an unpaired electron over two metal atoms. The stability of these radical species was enhanced through the formation of Fe-M interaction, which can occur through the distortion of the cyclopentadienyl ligands and decrease of the M-M distance (Fig. 1.a). The spectroscopic and electronic structures of the diiron complex $Fe(CO)_3$(dppf) (diFe) and similar ferrocenyl phosphino ligand complexes have recently been described.[C2-3] The diFe complex can exist in three stable and isolable oxidation states, Fe(0) (diamagnetic), Fe(I) (paramagnetic), and Fe(II) (diamagnetic). The ^{31}P-NMR spectrum is sensitive to the oxidation state at the tricarbonyliron center; additionally the α- and β-H signals on the ferrocene are sensitive to the degree of ligand distortion. Information about the geometry and electronic density at the tricarbonyliron site was determined by IR spectroscopy because the ν_{CO} vibrations are excellent reporter ligands. The paramagnetic state Fe(I) shows dynamic behavior with two possible configurations (Fig. C2-1b). The Fe(I) species can be isolated by chemical or electrochemical oxidation. The EPR spectrum of the Fe(I) state shows two distinct triplets (g = 2.05 and 2.02) in the X-band which could be assigned to two geometric configurations, trigonal-bipyramidal and square-pyramidal (Fig. C2-1a.). These two configurations were in equilibrium that was temperature controlled. Currently unpublished results show that diFe can be used to afford electrons in a HER. These results are similar to the recent work using a $CpNi(dap)^+$ complex, which also showed similar HER activity.[C2-1] The reported hydride complex, $diFeH^+$, was formed by the addition of a strong acid to diFe,[C2-3] and unpublished results show that this complex, in the presence of excess acid, shows a HER rate of 0.5 s^{-1}. The reaction is hampered by the electrostatic repulsion of the H^+ with $diFeH^+$ and the relatively high pKa of the tricarbonyliron site, a result of the strong inductive effect of the CO ligands, although this is currently under further investigation.

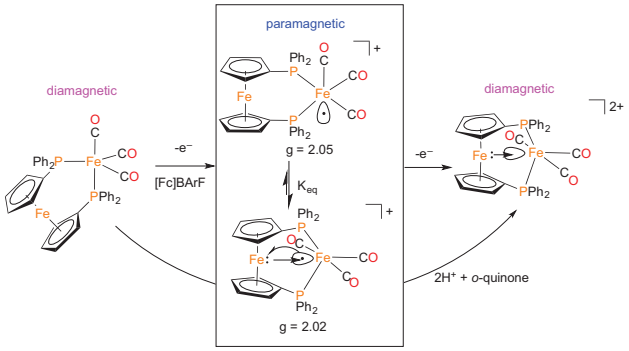

Fig. C2-1a: Oxidation states and equilibirum of diFe

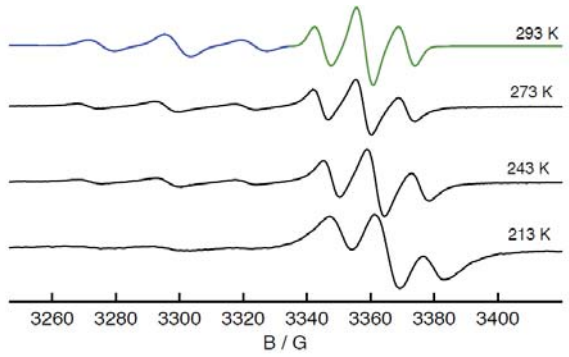

Fig. C2-1b: Variable temp. X-band EPR of $diFe^{+}$

The Van Slageren group specializes in the spectroscopic and magnetic study of paramagnetic molecules such as single-molecule magnets and other magnetic materials. They have studied mononuclear and polynuclear transition metal, lanthanide and actinide complexes, as well as magnetic nanoparticles and nanocarbon materials. They have investigated static and dynamic magnetic susceptibilities and magnetization by means of SQUID-magnetometry. They have specialized in electron paramagnetic resonance techniques especially at high frequencies, both CW and pulsed, both in the field and frequency domains. In addition, they have applied optical spectroscopic techniques including magnetic circular dichroism at temperatures down to 1.5 K and fields up to 10 T. Importantly, they have actively constructed novel and adapted existing measurement equipment to fit their needs.
Work by the Van Slageren group on mono- and dinuclear cobalt(II) and iron(II) complexes, carried out on samples obtained from the Sarkar group (FU Berlin) is especially relevant in this regard. As an example, in ref[C2-6], we have investigated the properties of a series of dinuclear iron(II) complexes with symmetric [N,O,N,O] and asymmetric [N,O,O,O] bridging ligands (Fig. C2-2a). Susceptibility measurements revealed the occurrence of a thermally induced spin-crossover transition between a high-temperature high-spin and a low-temperature low-spin form in both cases (Fig. C2-2b). Conversion to the high-spin state at low temperatures could be achieved by light irradiation of the asymmetric complex. For the symmetric complex, high-frequency EPR revealed in detail the magnetic coupling and local electronic structure of the iron(II) ions. By means of far-infrared measurements, they have demonstrated very large energy barriers toward relaxation of the magnetization.[C2-7] A second research area where the Van Slageren group is very active is that of spectroscopic studies of lanthanides, where they were the first to perform a comprehensive spectroscopic study of a lanthanide-based single molecule magnet.[C2-8] Finally, they have been very active in the field of molecular quantum bits, which may find application as building blocks of quantum computers. In this field they have set the record quantum coherence time for a solid state molecular quantum bit of 68 µs.[C2-9] This project sees the Van Slageren group develop versatile, variable temperature Mössbauer spectroscopy. Although they themselves have not previously used this technique, they have experience in interpreting Mössbauer data.[C2-10]

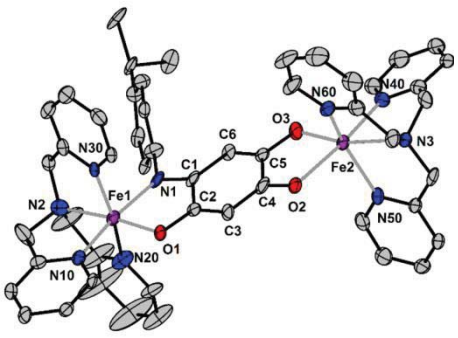

Fig. C2-2a: Dinuclear iron(II) complexes with asymmetric [N,O,O,O] bridging ligands

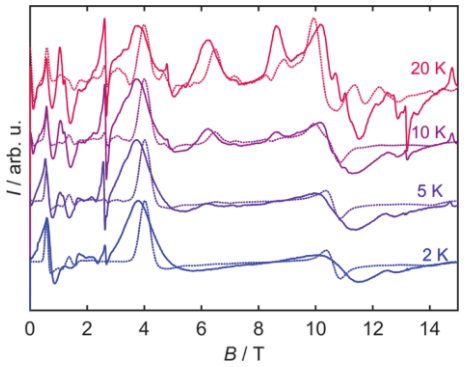

Fig. C2-2b: HFEPR spectra of the complex of Fig. C2-2a

3.12.3.2 Project-related publications by participating researchers

Ringenberg

[C2-1] C. Sondermann, M. R. Ringenberg*, *Dalton Trans.* **2017**, *46*, 5143-5146.
[C2-2] M. R. Ringenberg*, M. Schwilk, F. Wittkamp, U.-P. Apfel, W. Kaim, *Chem. Eur. J.* **2017**, *23*, 1770-1774.
[C2-3] M. R. Ringenberg*, F. Wittkamp, U.-P. Apfel, W. Kaim, *Inorg. Chem.* **2017**, *56*, 7501-7511.
[C2-4] V. K. K. Praneeth, M. R. Ringenberg, T. R. Ward, *Angew. Chemie Int. Ed.* **2012**, *51*, 10228-10234.
[C2-5] K.M. Schäfer, L. Reinders, J. Fiedler, M.R. Ringenberg*, *Inorg. Chem.* **2017**, 56, 14688-14696.

Van Slageren

[C2-6] M. van der Meer, Y. Rechkemmer, F.D. Breitgoff, R. Marx, P. Neugebauer, U. Frank, J. van Slageren*, B. Sarkar*, *Inorg. Chem.* **2016**, *55*, 11944.
[C2-7] Y. Rechkemmer F.D. Breitgoff, M. van der Meer, M. Atanasov, M. Hakl, M. Orlita, P. Neugebauer, F. Neese, B. Sarkar, J. van Slageren*, *Nat. Commun*. **2016***, 7*, 10467.
[C2-8] Y. Rechkemmer, J.E. Fischer, R. Marx, M. Dörfel, P. Neugebauer, S. Horvath, M. Gysler, T. Brock-Nannestad, W. Frey, M.F. Reid, J. van Slageren*, *J. Am. Chem. Soc.* **2015**, *137*, 13114.
[C2-9] K. Bader, D. Dengler, S. Lenz, B. Endeward, S.D. Jiang, P. Neugebauer, J. van Slageren**, *Nat. Commun.* **2014***, 5*, 5304.
[C2-10] J. van Slageren, P. Rosa, A. Caneschi, H. Casellas, Y.V. Rakitin, L. Cianchi, F. Del Giallo, G. Spina, A. Bino, A.-L. Barra, T. Guidi, S. Carretta, R. Caciuffo, *Phys. Rev. B* **2006**, *73*, 014422.

3.12.4 Project plan

Several important factors make the diFe compound especially suitable to achieve some of the major aims of this Collaborative Research Centre, especially regarding the understanding of the properties and behavior of immobilized species in mesoporous materials. It can serve as an organometallic *multiprobe* complex to help understand the effects immobilization has on both structural and dynamic characteristics of organometallic complexes. The diFe complex has many spectroscopic handles that reveal both the electronic and geometric structure at both iron ions. Structural information can be obtained from IR, NMR/EPR (oxidation state dependent), Mössbauer, as well as several hybrid or pulse techniques. Electron paramagnetic resonance will elucidate the magnetic anisotropy of paramagnetic states of the complex. Pulsed EPR measurements may be used to determine distances between electron spins and other electron spins or nuclear spins. These features render diFe especially attractive as a probe molecule to investigate immobilized catalysts in mesoporous systems. The diFe multiprobe molecule will allow us to investigate the effect of immobilization on its electronic structure, which is intimately connected to its catalytic activity. Furthermore, through pulsed EPR and ENDOR (electron-nuclear double resonance) distance measurements, we will gain information on the orientation of the $diFe^{+}$ complex in the pore and the corresponding dynamics. Voltammetry, especially cyclic-voltammetry, is a very sensitive technique to show how modification to and environment around the probe molecule diFe or other redox-active organometallic complexes (**B1**, **B2**) affects the redox potentials, and important fundamental characteristic.

The diFe system developed in the Ringenberg lab[C2-2, C2-3] will be modified according to the synthesis presented in Fig. 3.a. Currently being synthesized in the Ringenberg lab is the addition of a $–CH_2NMe_2$ group to the ferrocenyl backbone of the dppf ligand (Fig. C2-3a).[2] This ligand can be modified to an azide and the azide functionality can be transformed to a triazole via “click” chemistry with an acetylene “linker” moiety (Fig. C2-3b) similar to the methods proposed in **B1**, **B2**, and **B3.** Our system is chosen for it spectroscopic richness rather than potential as a catalytically active species. Preliminary results have shown catalytic activity of this diFe system, but this will not be primarily developed within the first funding period. However, it is of interest towards future funding periods.

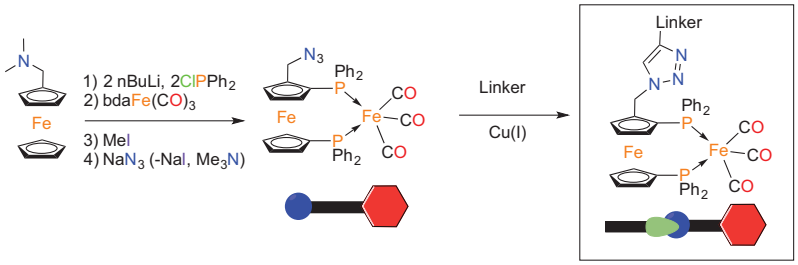

Fig. C2-3a: Synthesis of N_3-diFe and immobilization

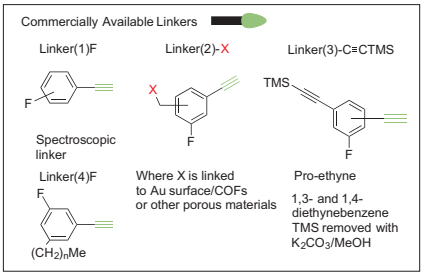

Fig. C2-3b: Various linkers to be investigated

In summary, the research goals are organized in work-packages as follows:

- **WP1: Synthesis and Characterization of Prolinker-diFe *Multiprobe* Complexes.** This WP deals with the development of suitable probe molecules to investigate the influence of immobilization on the electronic structure of the immobilized species, as well as to investigate the orientation and relevant dynamics of the probe molecule in the mesopore. This involves the introduction of spectroscopic tags in relevant places and the development of the linker chemistry.
- **WP2: Development of Methods: Mössbauer Spectroscopy and Unconventional Spectroelectrochemistry**. In this WP, we will develop variable-temperature Mössbauer spectroscopy as a sensitive tool to study immobilized iron species. Furthermore, we will develop sample holders to investigate in situ oxidized or reduced species by advanced spectroscopic methods, such as high-frequency EPR and magnetic circular dichroism spectroscopy.
- **WP3: Multiprobe Molecules in Mesoporous Block Copolymer Films**. Starting from the mesoporous block copolymer films provided to us by **project A2** (Ludwigs), we will develop and investigate hybrid diFe-polymer films. Here the focus is on elucidating the influence the presence of the pore walls on the geometric and electronic structure of the probe molecule, factors which are intimately linked to its catalytic activity. Secondly, we will focus on the electrochemistry of the immobilized species.
- **WP4: Multiprobe molecules in Covalent Organic Frameworks (COFs).** Using the COFs provided to us by **project A3** (Lotsch), we will develop and investigate hybrid diFe-COF materials. Here the focus is on the determination of the orientation of the probe molecule inside the well-defined pores by means of magnetic resonance techniques. In addition, we will again study the electrochemistry

3.12.4.1 WP1: Synthesis and Characterization of Prolinker-diFe *Multiprobe* Complexes

In this WP, we will synthesize and characterize functionalized molecules based on the (dppf)$Fe(CO)_3$ (diFe) platform. We will target systems of increasing complexity, so as to rationally develop the synthetic methodology (T1.1). The synthesized prolinker-functionalized diFe-molecules (L-diFe) will be characterized in detail spectroscopically (T1.2). Finally, we will investigate the redox chemistry of the L-diFe complexes and isolate the one-electron oxidized species L-diFe$^+$ (T1.3)[C2-2]

Task 1.1. Synthesis and characterization of prolinker-(dppf)$Fe(CO)_3$ (L-diFe) complexes. The central method to link the probe molecule to polymer and COF carrier materials is the "click" reaction between acetylene and organic azide moieties, yielding a triazole ring with high yield and specificity. We will functionalize one of the Cp-moieties on the ferrocene-part of the complex for attachment of the linker (Fig. C2-3b) Our first target system is (dppf)$Fe(CO)_3$ (diFe) functionalized with a -CH_2N_3 group (N_3CH_2-diFe). This complex is accessible through introduction of a -CH_2NMe_2-group on the Cp ring, which has already been achieved in the Ringenberg group. The NMe_2 moiety can be methylated, and the resulting trimethylammonium group can be displaced by addition of N_3^-, yielding N_3CH_2-diFe.[3] This molecule can already be reacted with acetylene-functionalized carrier materials (WP3 and WP4) to give hybrid probe-mesoporous materials. To investigate the influence of a triazole (trz) moiety close to the metal centers, we will react N_3CH_2-diFe with a prolinker molecule without the functional group that connects to the carrier material. Here we have opted for fluorine-substituted phenylacetylene as an example of such a molecule (Fig. C2-3). Thus the complex FPh-trz-CH_2-diFe is the second target molecule. The fluoride atom will aid in elucidating the dynamics of the linker in solution (T1.2). Possible

issues arise due to the potentially coordinating triazole to the $Fe(CO)_3$ site, this can be prevented by methylation of the triazole. However, we do not expect such issues in view of the steric protection of the $Fe(CO)_3$ site by the dppf-phenyl groups. To provide longer linkers, we will use diacetylene substituted benzene, where one of the acetylene groups is TMS-protected, for the click reaction with N_3CH_2-diFe. This linker molecule is commercially available. Subsequent deprotection yields a diFe complex with a longer linker (linker(3)) that is also acetylene-functionalized: C≡C-Ph-trz-CH_2-diFe. The TMS group allows for only a single click reaction to be performed at the free acetylene, and the TMS to be later removed under very mild conditions ($MeOH/K_2CO_3$), this method is preferred because it offers a mild and straightforward synthesis of the multiprobe molecule that can be immobilized via "click" chemistry to any of the compatible materials provided by other working groups. This complex can be reacted with any carrier material that has been functionalized with organic azide groups. In case the synthesis of L-diFe proves to be challenging, we will synthesize the analogous substituted ferrocene complexes L-Fc to aid in finding suitable reaction conditions for the synthesis of the target molecules.

Task 1.2 Characterization of the L-diFe complexes. The complexes prepared under T1.1 must be thoroughly characterized to assess how functionalization influences the electronic structure. This is a necessity for the investigation of the effects of immobilization in mesopores in WP3 and WP4. To this end, we will carry out a range of spectroscopic investigations. Vibrational spectroscopy (both IR and Raman) is a highly sensitive tool for investigating the electronic structure of the L-diFe complexes, especially the electron density at the tricarbonyliron center. The electron density at this center governs the amount of backbonding toward the CO-ligands, which in turn influences their vibrational frequencies. An additional advantage is that the CO stretching frequencies lie in an otherwise relatively empty region of the mid-IR-spectrum (1600-2200 cm^{-1}). We will also implement variable temperature Mössbauer spectroscopy (WP2). We will accompany these experimental studies by DFT calculations of the electronic structure (coll. Fyta/Holm, **project C6**). We will employ solution NOESY (focussing on the $^{19}F–^{31}P$ coupling) to investigate the geometric structure of the linker in solution. In addition, we will use solid state MAS-NOESY with the complex in a suitable solid matrix such as a polymer to assess the suitability of this method to study the linker confirmation in the immobilized complexes. Finally, we will characterize the redox chemistry by means of solution state cyclic voltammetry. The accompanying changes in the electronic structure will be studied by means of IR- and UV/Vis-spectroelectrochemistry.

Task 1.3 Isolation and characterization of cationic complexes L-diFe$^+$. For EPR-based methods to determine distances (WP4), it is essential that the probe molecule is paramagnetic. Unfortunately, the complexes L-diFe are diamagnetic in their native state. However, one electron chemical or electrochemical oxidation yields paramagnetic species that are excellently suited to EPR investigations, where preliminary work demonstrated the existence of a dynamic equilibrium between two redox isomers. After isolation of the chemically oxidized complexes L-diFe$^+$, variable-temperature Mössbauer spectroscopy will shed light on the oxidation state of the two iron ions and the position and its temperature dependence of the abovementioned equilibrium in the solid state. Infrared and Raman spectroscopic studies of the CO-stretching frequencies will allow careful assessment of the electron density on the carbonyl-bound iron ion. High-frequency EPR will enable precise determination of the *g*-tensor values and their temperature dependence. Importantly, we will employ pulsed EPR and ENDOR spectroscopies for detailed investigations and as preliminary work for WP3. Pulsed Q-Band (35 GHz) EPR will be used to determine the spin-lattice (T_1) and spin-spin (T_2) relaxation times. Observation of a spin echo will confirm the applicability of pulsed EPR techniques for each L-diFe$^+$ derivative. The spin relaxation times determine the maximum length of EPR pulse sequences that can be used and therefore the level of complexity of such measurements. Pulsed ENDOR will allow precise coupling to NMR-active nuclei, such as the Cp protons, but also the linker nuclei, especially for the fluorine substituted linker. Again these experimental studies will be supported by DFT calculations (coll. Fyta/Holm, **project C6**).

3.12.4.2 WP2 Development of Methods: Mössbauer Spectroscopy and Unconventional Spectroelectrochemistry

The ability to investigate the hybrid probe molecule-carrier materials and as a tool for work in further funding periods of the collaborative research center, we will develop two novel techniques. First of all, we will develop Mössbauer spectroscopy. This technique is exquisitely sensitive to small changes in the electronic structure of iron ions, allowing the investigation of the influence of immobilization of homogeneous catalysts on their electronic structures. This will aid in elucidating the origin of any observed differences in catalytic activity between homogeneous and immobilized catalysts. This

technique also has applications in determining electron and structural characteristics of organometallic species containing iron/ferrocene such as those found in **B1** and **B2**. Secondly, we will develop electrochemical cells for carrying out EPR and optical (absorption, magnetic circular dichroism, fluorescence studies) for *in situ* spectroscopic investigations on various oxidized states of the immobilized diFe multiprobe molecules. In addition, these will be useful tools in the investigation of other redox-active catalytic systems of relevance to this CRC.

Task 2.1 Development of a Mössbauer spectrometer. Mössbauer spectroscopy provides a local probe that is exquisitely suited to studying the local electronic structure of iron ions, irrespective of oxidation and spin state. Here, we will implement variable temperature Mössbauer spectroscopy, using an existing cryostat and a spectrometer (to be acquired, funding requested). The Mössbauer isomer shift is a sensitive probe of the oxidation state of the iron ion, while the quadrupole splitting is sensitive to the local electronic structure and its anisotropy. Therefore, we will develop a Mössbauer spectrometer. We will combine a commercial RCPTM MS96 3rd generation Mössbauer spectrometer (funding requested) with an existing (EPSRC-funded) Janis SVT400 helium bath cryostat. To this end we will build a cryostat stand that allows alignment in three directions. In addition, we will equip the stand with an optical rail to allow mounting of the source and detector parts of the Mössbauer spectrometer. We will test the spectrometer with standard samples, such as sodium nitroprusside, but also materials undergoing magnetic ordering such as iron oxides. In WP3 and WP4, we will apply the developed cryostat to the hybrid materials containing iron ions.

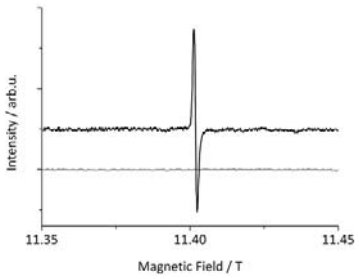

Fig. C2-4a: HFEPR spectra of a 3 nm layer of an organic radical

Fig. C2-4b: Fabry-Pérot resonator (FPR)

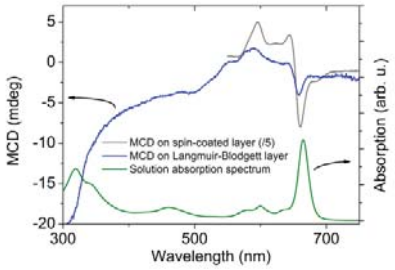

Fig. C2-4c: Monolayer sensitivity in MCD

Task 2.2 Development of in situ electrochemical cells. In order to study different redox states of the immobilized organometallic complexes (see WP Au-immobilized catalysts), we plan to develop optically transparent electrochemical cells for application to the *in situ* investigation of different oxidized states of our multiprobe molecule as well as for general application in the investigation of redox catalysis.[4] We will optimize the design for each of the spectroscopic techniques to be employed: (i) high frequency EPR, (ii) Q-band pulsed EPR, and (iii) optical measurements. In many cases the measurements must be carried out in the frozen solution state at low temperatures. Consequently, we will electrolyze of the analyte at room temperature until the desired conversion is reached followed by quench freezing the solution. We will test various cells and improve their designs in a feedback loop. We will employ an existing AMEL potentiostat for electrolysis for testing and measurements. (i) High frequency EPR. This spectrometer (DFG INST41/863) typically takes flat samples of up to 8mm diameter. The EPR measurement is a reflection measurement, where we have demonstrated a 10^7 spin sensitivity, allowing for thin layer measurements (Fig. C2-4a). This means that we can use the gold layer that the sample is deposited on as the bottom mirror of the sample holder as well as working electrode. We will test optically transparent counter electrodes made of indium tin oxide (ITO). The ITO can be patterned with UV lithographic techniques to allow deposition of a reference electrode from Ag, followed by chlorination of the silver.[5] The two parts of the cell can be separated with a suitable polymeric spacer. We will also test an alternative design, where a circular counter electrode is deposited on a photoresist, deposited onto the working electrode.[6] (ii) Q-band pulsed EPR. Such measurements are both the most challenging and potentially most rewarding measurements. We have recently developed a Fabry-Pérot resonator (FPR) for our Q-band pulsed EPR spectrometer (Fig. C2-4b). Such a resonator is convenient for flat samples and electrical connections can be provided. We can use metallic electrodes, because the skin depth is quite large at Q-band frequencies, e.g., 400 nm for gold, 5 µm for ITO. It is unclear how much the insertion of a large amount of material into the FPR will deteriorate its properties. We will carry out the relevant microwave simulations and optimize the design on the basis of the results. (iii)

Optical measurements. We will use our absorption/MCD spectrometer (DFG INST 41/864), and in cooperation with Prof. Ludwigs (**A2**) group's luminescence spectrometer. Here we will exclusively focus on designs based on ITO electrodes, as previous attempts using wire grid electrodes failed. We have demonstrated monolayer sensitivity in MCD (Fig. C2-4c).[7],[8],[9]

3.12.4.3 WP3: Multiprobe Molecules in Mesoporous Block Copolymer Films.
For this WP, **project A2** (Ludwigs) will provide us with mesoporous block copolymer films on gold, where the mesopores have been bottom-functionalized with acetylene-alkane thiolates. We will proceed to attach the R-diFe probe molecules to the azide/alkyne moieties, yielding the immobilized molecules in defined mesopores (Fig. C2-5), relevant to the overall aims of this collaborative research center. We will again characterize the topology of the hybrid materials by means of AFM and SEM. We will study the redox chemistry of the immobilized complexes by means of cyclic voltammetry as well as the flux of different substrates to the diFe site via rotating disk electrode (RDE) experiments.
Task 3.1 Immobilization of L-diFe multiprobe complexes in mesoporous polymer films on gold substrates. As an intermediate step between the functionalized probe molecules L-diFe and the pore-immobilized species, we will investigate anchoring the probe molecule on a gold surface. Prof. Ludwigs (**project A2**) will prepare self-assembled monolayers of click-amenable azide or acetylene substituted alkane thiols, on neat gold surfaces. We will then proceed to attach the probe molecules N_3CH_2-diFe and C≡C-Ph-T-CH_2-diFe to these functionalized surfaces by means of click chemistry. (Fig. C2-6a) In cooperation with **A2**, we will investigate the influence of the linker length on the performance of the click reaction and also to study the dependence of the probe molecule dynamics on the linker length (Task 3.2). We will also investigate mixed SAMs consisting of mixtures of functionalized and non-functionalized alkane thiols. We will characterize the probe-molecule-functionalized SAMs by microscopic techniques such as atomic force microscopy (AFM) and scanning electron microscopy (SEM). In a second step we will use mesoporous polystyrene polymer films on gold, rather than neat gold substrates. These films will be provided by **project A2**. Using similar strategies as for the neat gold films we will attach the L-diFe molecules to the gold substrate on the bottom of the pores. Should the absolute amount of probe molecules obtained in this way be insufficient for some of the subsequent studies (Task 3.2), we will also consider probe wall functionalization, resulting in much larger numbers of immobilized probe molecules.

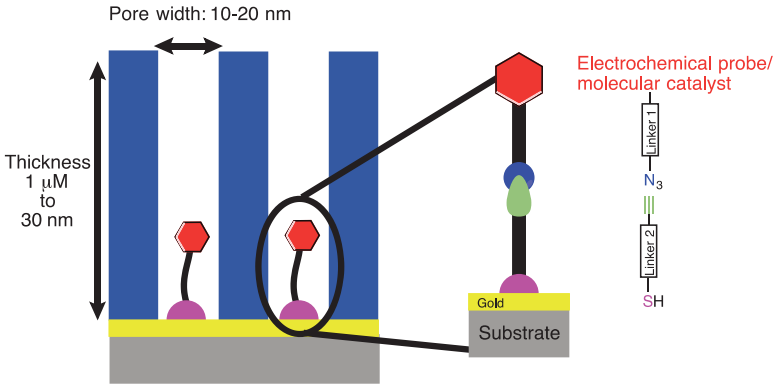

Fig. C2-5: Bottom-functionalized gold surface with mesopores imprinted block-copolymers

Task 3.2 Investigation of immobilized species. We will investigate the electronic structure of the surface, pore bottom-immobilized and possibly wall-immobilized species. We have demonstrated monolayer sensitivity for MCD spectroscopy, a technique to which ferrocene derivatives are amenable. If the substrate is transparent and the thickness of the gold layer is below the skin depth (several nm) the sample should be transparent enough to measure in transmission. Otherwise, one can measure in reflection using a thicker layer of gold as a mirror. For the wall-immobilized species, we will also attempt recording Mössbauer spectra. Paramagnetic species (see Task 3.3) can be investigated by means of high-frequency EPR, where we have also demonstrated monolayer sensitivity (see 3.1.3.1). The combination of these methods will allow elucidating the influence of immobilization on the electronic structure of the L-diFe probe molecules. DFT calculations (**project C6**) will aid in understanding the electronic structure.
Task 3.3 Electrode dynamics with immobilized species. Electrochemistry and immobilization of the probe molecules onto the surface of the electrode offer a very sensitive technique for measuring electron transfer to/from the analyte.[10] This technique has also been widely used to study electrocatalysts with high precision and in order to study these modified electrodes more effectively by employing a rotating disk electrode (RDE). RDE can be used to determine several important kinetic and physical parameters, both in the bulk and of an analyte adsorbed on the electrode. These data include:

the rates of electron transfer from the electrode to the analyte, the number of electrochemical processes, the rate of adsorption/desorption, and lastly electrochemical mechanisms. These factors make RDE an exceptionally powerful tool for understanding how diFe and other organometallic species behave on the surface of the electrode and the rate of electrochemical reactions where steady-state conditions do not apply,[11] such as a carrier material containing several redox-active moieties, decomposition/deposition of analyte onto the electrode surface, ligation of substrate or solvent, or dimerization.[12] These types of dynamic processes can be correlated to computational models (**C5**) and physical measurements (**C1**).

Immobilization of electroactive porous materials or those containing redox-active organometallic species allow for a highly sensitive method for determining the flux of substrate to/from the redox-active moiety, the information obtained from these studies can be used to enhance the diffusion modeling performed in **C5**. These electrochemical investigations have been used extensively to study reactions such hydrogen evolving reaction (HER) or hydrogen oxidation reaction (HOR). RDE method is widely employed in studies on the HOR/HER owing to its well-defined mass transport behaviors. HOR current is controlled by both the electrode kinetics and the diffusion of H_2, HER is typically assumed to be free of diffusion limitation, although this is not always the case.[13] Extending this method to studying not only hydrogen but other reactions can be key in understanding reactions that can occur at diFe or other redox active species such as those described in **B1.**

To this end we propose to use diFe as a probe molecule to study the flux of ligands (or substrates such as H_2 for HOR) outlined in Fig. C2-6b. The diFe multiprobe complex can be oxidized by two electrons forming a stable Fe(II) tricarbonyl which increases the Lewis acidity of the tricarbonyliron substantially (Fig. C2-6b). This increased Lewis acidity induces the formation of Fe-Fe bond (~20 kcal/mol) from the ferrocene iron to the tricarbonyliron. $DiFe^{2+}$ can also ligate different Lewis bases such as solvent (MeCN), ligands (PPh_3), redox moieties (ferrocene) and potentially catalytically relevant substrates (H_2). The ligation reaction changes coordination environment and thus the electronic structure for the $diFe^{2+}$. Therefore, the resulting dynamic process can only be studied by standard static electrode when the reaction is diffusion limited. However, most cases, such as those described, are not diffusion limited, and a rotating disk electrode must be employed (requested funding) used with a potentiostat (requested funding). Rotation establishes a well-defined flow pattern distribution (Fig. C2-6b), in effect the solution is pulled towards the electrode and flung outwards. This can be used to analyze flux of analyte or substrates to an electrode containing the diFe probe molecule.[14] Additionally, RDE can unequivocally show the number of electrochemical processes. Secondary reactions due to electrochemically induced chemical reactions with linker groups, substrates, or the walls of porous material can be determined with RDE studies. RDE experiments can also show how the confinement effects influence the flux of substrate to electroactive catalysts and can assist in the unambiguous determination of electrochemical mechanism.[15] Electrochemistry is also used by **B2** (Plietker) to understand how minor ligand modification can affect the electronic structure.[16]

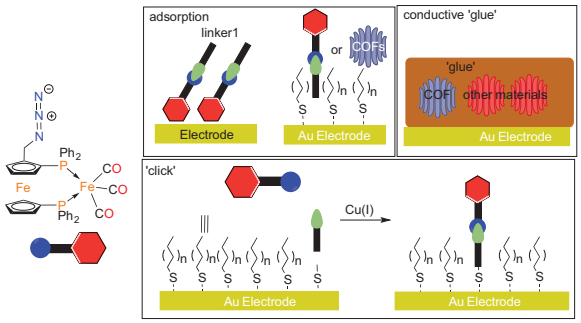

Fig. C2-6a: Immobilization methods for diFe and porous materials

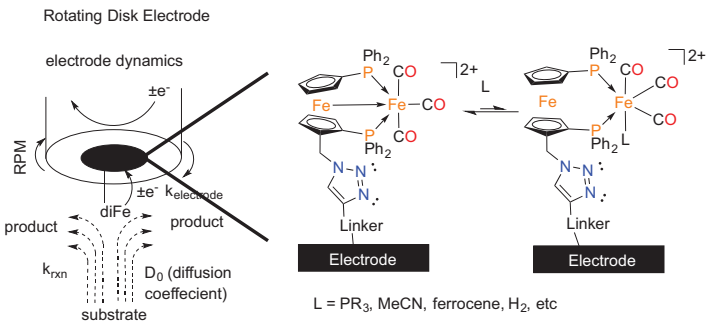

Fig. C2-6b: RDE dynamics and proposed electrocatalytic cycle for HER/HOR for diFe complex

3.12.4.4 WP 4: Multiprobe molecules in covalent organic frameworks (COFs)

In this work package, we will develop and investigate hybrid materials based on covalent organic frameworks (COFs) as carriers and the R-diFe multiprobe molecules. COFs are advantageous in that they possess extraordinarily well-defined (crystalline) structures, which will be of great help in obtaining quantitative results regarding the geometric structure of the probe molecule inside the pore. Immobilization of radical species, [17] fluorescent labels[18] and catalyst species[19] into COFs has been achieved.

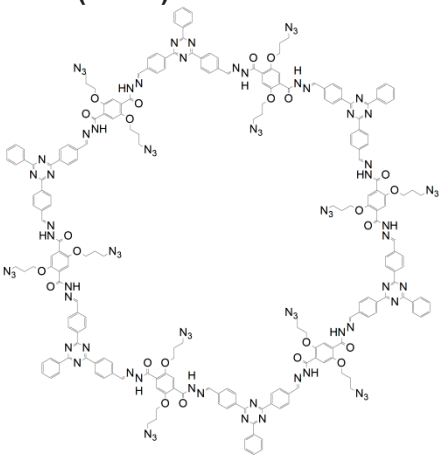

Fig. C2-7: Azide-functionalized COF.

Task 4.1 Immobilization of R-diFe in COFs. We will start with azine-linked triphenyl arene-based COFs[20] that are functionalized with acetylene groups based on the Linker(2)-diFe (Fig. C2-3b). Using click chemistry, we will insert and immobilize N_3-diFe-molecules into the pores. These COFs have relatively narrow pores of the order of 2.5 nm. We will compare benzene and triazine node moieties (N0-COF, N3-COF, respectively, Fig. C2-7), which are expected to have different effective pore wall properties. In case larger pores will be desirable, these can be obtained by exchanging the azine linker by an augmented linear building block as described in **project A3**. Different linkers, i.e. Linker-CCH or Linker-N_3, will as well be provided by **A3** with different rigidity and lengths because post-synthetic modification would be done at the building block level. These hybrid materials will also be studied by means of QM/MM computational methods already proposed between **C4** and **A3**.

Task 4.2 Investigations of diFe-COF hybrid materials. In collaboration with **project A3**, we will use scanning and transmission electron microscopy methods to characterize the morphology of both the hybrid materials. We will determine the effective surface area by gas sorption experiments. This will also reveal to what extent the pores are occluded by the incorporation of the diFe complexes. We will determine the degree of crystallinity by means of powder x-ray diffraction. The electronic structure of the diFe probe molecule inside the pore will be determined by means of IR-, Mössbauer, CV and MCD spectroscopies. As outlined above, IR-spectroscopy is especially sensitive to the charge on the carbonyl iron, Mössbauer to the oxidation state and geometry of both iron ions, and magnetic circular dichroism to the electronic structure of the complex.[21],[22] To investigate the geometry of the probe molecule in the pore, we will employ solid state MAS NMR techniques in close collaboration with **project C1**.

Task 4.3 Investigations of the redox chemistry of diFe-COF hybrid materials. We will attempt to COF-functionalized electrodes by (i) gluing the polycrystalline COF onto suitable electrode by means of conductive paste. This will allow us to study the electrochemical properties of the hybrid materials. The aim is twofold: (i) first to assess the suitability of the COFs for later stage photoelectrocatalysis (see outlook) and (ii) to generate the diFe probe molecule in its paramagnetic cationic state, such as to render it suitable for EPR-analysis. Covalent immobilization can be accomplished by edge-on attachment through dangling aldehyde groups, which can be attached through Schiff base reactions with amine or hydrazine functionalized alkylthiolates bound to the electrode.

Task 4.4 Distance measurements in COF hybrid materials. On account of their crystalline nature and monodisperse pore distributions, COF-based materials are excellently suited for the determination of the exact orientation of immobilized molecules in mesoporous carriers. The methods of choice in this regard are those based on electron paramagnetic resonance, because they allow accurate measurements of much larger distances (up to 8 nm) than possible with NMR-methods (up to 1 nm). As a paramagnetic probe we will use $diFe^+$ (Task 3.3). Additionally, we will consider inserting stable organic radicals such as TEMPO into the mesopores as an alternative to $diFe^+$. Radical functionalized COFs have been reported in literature.[17] The organic radical has the advantage that EPR lines are narrower and spin-spin relaxation times potentially longer, allowing for more sophisticated measurements. The $diFe^+$-complex has the advantage that it is more comparable to the other catalysts studied in this collaborative research center. We will first determine the spin-lattice and spin-spin relaxation times of the paramagnetic center by means of Q-Band pulsed EPR (inversion recovery and Hahn-echo sequences, respectively). Subsequently, we will carry out pulsed ENDOR (electron nuclear double resonance) measurements. These measurements should give us the dipolar coupling of the electron spin to various nuclei of interest, e.g., nitrogen of the framework or the fluorine of the linker

molecule. Additionally we will consider substituting the central 1,3,5,-substituted benzene node with deuterium atoms to serve as an additional marker. These measurements should give us a set of distances and their distributions, which will shed light on the position of the radical center inside the pore.
In addition, we will look into the following directions in which to extend this research. First of all, by using a chelating linker (e.g. bipyridine), a COF can be generated that can complex paramagnetic metal ions, such as copper(II). Immobilization of $diFe^{+}$ or another paramagnetic probe molecule will then allow carrying out electron-electron resonance measurements such as double electron-electron resonance (DEER), or relaxation induced dipolar modulation (RIDME) techniques. These techniques are very powerful especially to determine large distances in view of the much larger electron magnetic moment compared to the nuclear magnetic moment.

Chronological work plan

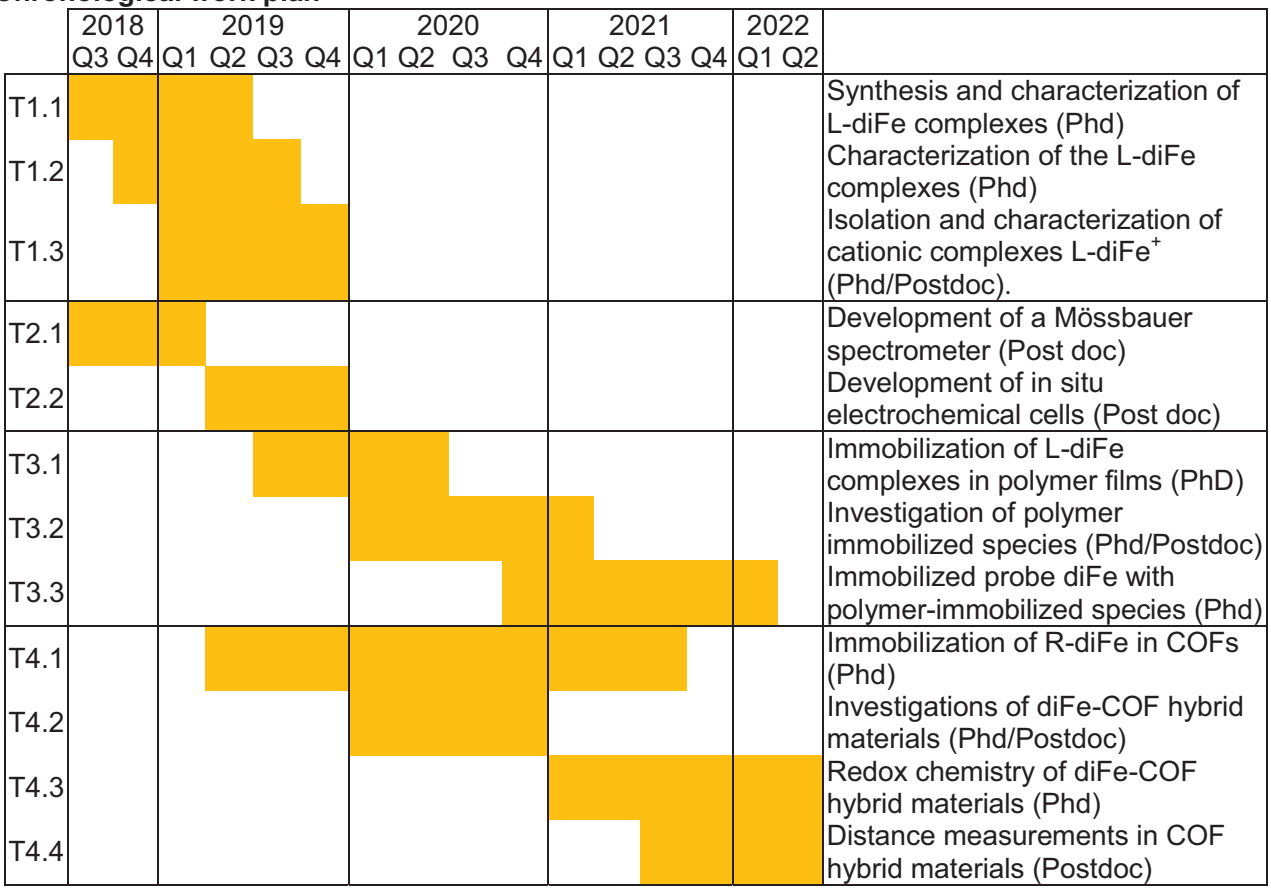

3.1.4.5 Methods applied
Infrared and Raman Spectroscopy, UV-Vis Absorption, Mössbauer, EPR (HF-EPR, X-band, Q-band, Pulse techniques), NMR (solution/solid state, NOESY/MAS-NOESY), Electrochemistry (cyclic voltammetry, liner sweep voltammetry, rotating disk electrode, X-ray Diffraction and powder diffraction, DFT (dynamic modeling, and quantum mechanical), QM/MM modeling, magnetic circular dichroism (MCD), Hybrid spectroelectrochemistry, AFM and SEM (microscopy).

3.12.4.6 Vision
Beyond the first funding period, this work can be expanded in several ways. First of all, the lessons learned from the careful and detailed investigation of the behavior of immobilized species will aid in developing new catalysts tailored so as to make maximum use of the directing effects of the mesopores. Secondly, we intend to proceed along the avenue of photocatalytic investigations with Lotsch (**project A3**) also beyond the first funding period. Using the carrier material as light harvesting materials to transfer electrons to a catalytically active species can convert of solar energy into chemical energy. The use of both COFs and earth abundant transition metals catalysts provides a robust and inexpensive means to afford such reactivity. Thirdly, we intend to develop the probe molecule

(dppf)Fe(CO)$_3$ as a catalyst. The diFeH$^+$ species shows some preliminary interesting reactivity for the reduction of ketones, this process is achiral and is quite slow (>12 h) with low yields. Chiral phosphines are excellent for chiral induction because the ferrocene group is quite large. The pore provides an increased relative pKa by increasing the local concentration of H$^+$ ions, this means that even weak acids can be used. The triazole can also act a proton relay, which further amplifies the localized concentration of H$^+$ ions even more. The synergetic effect of both the linker and porous environment facilitates in the formation of diFeH$^+$. This effect can be used to afford protonation of the diFe complex without the use of strong acids, e.g. HBF_4. The increased local concentration of additional substrates, e.g. acetophenone, results in overcoming the slow reaction rates observed in the solution chemistry. Additionally, reduction of substrates such as CO_2, which has a high kinetic barrier due to the relatively low concentration in solution, is an avenue that will be explored in later stages of this CRC project. Critical to this and future projects is understanding the electronic structure of the catalyst and materials, electrochemistry can be used to understand both qualitatively and quantitatively these effects. While voltammetry represents on of the most straightforward applications, several different hybrid methods can be developed and expanded upon based on voltammetry.

3.12.5 Role within the collaborative research center

This project represents an important role in the larger CRC project because its goal is towards the development of spectroscopic techniques that are key in understanding dynamic and static properties of immobilized organometallic species in porous environments. This allows a picture of the molecule to be generated. The present research project has a special but not isolated position in the CRC. On the one hand we do not study catalysis directly, but rather the electronic structure and motional dynamics of immobilized species. On the other hand, the project directly addresses the core question of the CRC, which is how the mesopores in carrier materials influence immobilized species in their geometric and electronic structures. Only by understanding this can rational progress toward exploiting mesopores in directing catalysis be achieved.

This **project** (**C2**) has a number of direct links to other projects within the CRC. We will be provided with tailored COF materials by **project A3** (Lotsch) and with mesoporous polymers on gold substrates by **project A2** (Ludwigs). We will work in close cooperation with the theoretical **project C6** (Fyta/Holm), which will provide DFT calculations of the electronic structure of functionalized diFe complexes and molecular dynamics simulations of the molecules inside the pores. **Project C1** (Hunger) will carry out solid-state NMR measurements on the immobilized catalyst systems provided by us. Additionally, quantum mechanical calculations (QM/MM) on diFe-COF materials will be performed with **C4** (Kästner). Beyond the present funding period, the expertise and infrastructure in Mössbauer spectroscopy and unconventional spectroelectrochemistry will benefit types of catalysis that involve iron and/or redox active species (**B1**, **B2**). Already during the present funding period, we will apply this expertise to catalysts provided to us by **project B2** (Plietker). Further development of photoelectrochemistry with **A3** (Lotsch) can be developed through understanding the electron transfer to catalytic centers.

3.12.6 Differentiation from other funded projects

Ringenberg. None of Ringenberg's current and past projects have directly dealt with porous materials or immobilization of catalysts.

1. State of Baden-Württemberg through bwHPC and the German Research Foundation (DFG) through grant no. INST 40/467-1 FUGG provide access to the Justus cluster “Calculations on Organometallic Complexes Containing Redox-Active Noninnocent Ligands”.

Van Slageren. None of Van Slageren's current and past projects have directly dealt with porous materials and/or catalysts and catalysis.

In detail Van Slageren's recent projects are the following:

1. EU (FET-OPEN 767227, 2018-2021), "Plasmon Enhanced Terahertz Electron Paramagnetic Resonance" deals with development of high-frequency EPR methods in directions not relevant for the present proposal.
2. Vector Stiftung (2016-065, 2016-2018), " Ab initio Untersuchungen von auf f-Elementen basierenden molekularen Nanomagneten" deals with ab initio calculations of f-element complexes
3. DFG (SL104/3-2, 2015 - 2018), "Improving the sensitivity of THz frequency domain magnetic resonance" deals with the improvement of EPR methods especially in the frequency domain. The current project will benefit from these developments. The developments proposed in the current project (spectroelectrochemistry) are not part of SL104/3-2.

4. DFG (SL104/5-1, 2015 - 2018) "Spektroskopische Untersuchungen an auf Lanthanoid-Ionen basierten Einzelmolekülmagneten". This project deals with spectroscopic investigations of lanthanide complexes and has thus no overlap to the present project

References

[1] J. C. Peters, M. P. Mehn, in *Activation of Small Molecules*, Wiley-VCH Verlag GmbH & Co. KGaA, **2006**, pp. 81-119.
[2] M. Madalska, P. Lönnecke, V. Ivanovski, E. Hey-Hawkins, *Organometallics* **2013**, *32*, 5852-5861.
[3] G. Ghini, L. Lascialfari, C. Vinattieri, S. Cicchi, A. Brandi, D. Berti, F. Betti, P. Baglioni, M. Mannini, *Soft Matter* **2009**, *5*, 1863-1869.
[4] W. Kaim, J. Fiedler, *Chem. Soc. Rev.* **2009**, *38*, 3373-3382.
[5] P. Learngarunsri, P. Chaiyen, T. Srikhirin, W. Veerasai, S. Dangtip, *Phys. Procedia* **2012**, *32*, 265-271.
[6] S. D. Branch, A. M. Lines, J. Lynch, J. M. Bello, W. R. Heineman, S. A. Bryan, *Anal. Chem.* **2017**, *89*, 7324-7332.
[7] J. Rozboril, Y. Rechkemmer, D. Bloos, F. Munz, C. N. Wang, P. Neugebauer, J. Cechal, J. Novak, J. van Slageren, *Dalton Trans.* **2016**, *45*, 7555-7558.
[8] S. V. Novichikhin, V. K. Imschennik, I. P. Suzdalev, Y. B. Kopylovskii, A. A. Popov, V. K. Runov, in *Applications of the Mössbauer Effect: Chemistry*, Gordon and Breach Science Publishers, USSR, **1985**, p. 1193.
[9] A. D. Pomogailo, *Catalysis by Polymer-Immobilized Metal Complexes*, CRC Press, **1999**.
[10] Z. W. Seh, J. Kibsgaard, C. F. Dickens, I. Chorkendorff, J. K. Nørskov, T. F. Jaramillo, *Science* **2017**, *355*
[11] C. C. L. McCrory, C. Uyeda, J. C. Peters, *J. Am. Chem. Soc.* **2012**, *134*, 3164-3170.
[12] M. L. Pegis, C. F. Wise, B. Koronkiewicz, J. M. Mayer, *J. Am. Chem. Soc.* **2017**, *139*, 11000-11003.
[13] J. Zheng, Y. Yan, B. Xu, *J. Electrochem. Soc.* **2015**, *162*, F1470-F1481.
[14] A. J. Bard, L. R. Faulkner, *Electrochemical Methods: Fundamentals and Applications*, Wiley, **2000**.]
[15] S. Treimer, A. Tang, D. C. Johnson, *Electroanalysis* **2002**, *14*, 165-171.
[16] D. Weickmann, W. Frey, B. Plietker, *Chem. Eur. J.* **2013**, *19*, 2741-2748.
[17] B. K. Hughes, W. A. Braunecker, D. C. Bobela, S. U. Nanayakkara, O. G. Reid, J. C. Johnson, *J. Phys. Chem. Lett.* **2016**, *7*, 3660-3665.
[18] S. Rager, M. Dogru, V. Werner, A. Gavryushin, M. Gotz, H. Engelke, D. D. Medina, P. Knochel, T. Bein, *CrystEngComm* **2017**, *19*, 4886-4891.
[19] A. V. Bavykina, A. I. Olivos-Suarez, D. Osadchii, R. Valecha, R. Franz, M. Makkee, F. Kapteijn, J. Gascon, *ACS Appl. Mater. Interfaces* **2017**, *9*, 26060-26065.
[20] V. S. yas, F. Haase, L. Stegbauer, G. Savasci, F. Podjaski, C. Ochsenfeld, B. V. Lotsch, *Nat. Commun.* **2015**, *6*, 8508.
[21] D. Nielson, D. Boone, H. Eyring, *J. Phys. Chem.* **1972**, *76*, 511-515.
[22] D. Nielson, M. Farmer, H. Eyring, *J. Phys. Chem.* **1976**, *80*, 717-721.

3.12.7 Project funding

3.12.7.1 Previous funding

This project is currently not funded and no funding proposal has been submitted.

3.12.7.2 Requested funding

Funding for	2018		2019		2020		2021		2022		2018-2022	
Staff	Quantity	Sum	Quantity	Sum	Quantity	Sum	Quantity	Sum	Quantity	Sum	Quantity	Sum
PhD student, 67%	1	21,600.-	1	43,200.-	1	43,200.-	1	43,200.-	1	21,600.-	1	172,800.-
PostDoc	1	35,000.-	1	69,900.-	1	69,900.-	1	69,900.-	1	35,000.-	1	279,700.-
Total		56,600.-		113,100.-		113,100.-		113,100.-		56,600.-		452,500.-
Direct costs	Sum		Sum		Sum		Sum		Sum		Sum	
consumables Institute of Inorganic Chemistry	8,000.-		8,000.-		8,000.-		8,000.-		4,000.-		36,000.-	
consumables Institute of Physical Chemistry	13,000.-		18,000.-		10,000.-		10,000.-		5,000.-		56,000.-	
Total	21,000.-		26,000.-		18,000.-		18,000.-		9,000.-		92,000.-	
Major research instrumentation	Sum		Sum		Sum		Sum		Sum		Sum	
Mössbauer	35,800.-		-		-		-		-		35,800.-	
Electrochemistry equipment	19,000.-		-		-		-		-		19,000.-	
Total	54,800.-		-		-		-		-		54,800.-	
Grand total	187,200.-		139,100.-		131,100.-		131,100.-		65,600.-		654,100.-	

(All figures in EUR; staff funding according to DFG form 60.12)

3.12.7.3 Requested funding for staff

	Sequential no.	Name, academic degree, position	Field of research	Department of university or non-university institution	Project commitment in hours per week	Category	Funding source
Existing staff							
Research staff	1	Mark R. Ringenberg Dr., Habilitand	Inorganic Chemistry	Institute of Inorganic Chemistry	8		University
Research staff	2	Joris van Slageren, Prof. Dr.	Physical Chemistry	Institute of Physical Chemistry	4		University
Research staff	3	Heiko Bamberger, MSc, PhD student	Physical Chemistry	Institute of Physical Chemistry	2		University
Research staff	4	Samuel Lenz, MSc, PhD student	Physical Chemistry	Institute of Physical Chemistry	2		Zeiss-foundation
Non-research staff	5	Thomas Weigend	Physical Chemistry	Institute of Physical Chemistry	2		University
Non-research staff	6	Inge Blankenship		Institute of Physical Chemistry	2		University
Requested staff							
Research staff	7	N. N.; M. Sc.	Inorganic Chemistry	Institute of Inorganic Chemistry		PhD student, 67%	
Research staff	8	NN; Dr.	Physical Chemistry	Institute of Physical Chemistry		Postdoc, 100%	
Research staff	9	Research assistant	Physical Chemistry	Institute of Physical Chemistry			

Job description of staff (supported through existing funds):

1

Mark Ringenberg will supervise all synthetic and characterization efforts (tasks **T1.1**, **T1.2**, **T1.3**, **T3.1**, **T4.1**) and lead all electrochemical work (**T1.3**, **T3.3**, **T4.3**). He will cowrite papers with Van Slageren, and the PhD student and postdoc for whom funding is requested.

2

Joris van Slageren will supervise all method development (WP2), all advanced spectroscopy (tasks **T1.3**, **T3.2**, **T4.2**, **T4.4**). He will cowrite papers with Ringenberg, and the PhD student and postdoc for whom funding is requested.

3

Heiko Bamberger will train the postdoc (requested) in MCD measurements.

4

Samuel Lenz will train the postdoc (requested) in pulsed EPR measurements.

5

Thomas Weigend is head of the mechanical workshop and will carry out and supervise all work in spectrometer setup and adaptation.

6

Secretary

Job description of staff (requested funds):

7

The PhD student to be employed on this project will carry out all syntheses and chemical characterizations of L-diFe and will under the guidance of Dr Ringenberg perform all electrochemical and UV/IR-spectroelectrochemical experiments. She/he will liaise with our collaborators from projects **A2**, **A3**, **B1**, **B2**.

8

The Postdoc to be employed on this project will set up the Mössbauer spectrometer and develop cells for nonconventional spectroelectrochemistry. He/she will perform all Mössbauer and CW EPR experiments. After initial training by experienced PhD students, he/she will carry out all MCD and pulsed EPR measurements. He/she will liaise with our collaborators from project **C1**, **C4** and **C6**. It is absolutely necessary to employ a postdoctoral researcher for this part of the project, given the breadth of the work to be carried out. This ranges from spectrometer development, to advanced spectroscopic measurements with multiple techniques at high magnetic fields and low temperatures. In addition, the postdoctoral researcher will need to interact with confidence with our theoretical and materials partners. The person to be hired on this project will therefore already have a background in advanced spectroscopy, which ensures that we can make rapid progress and achieve our objectives. A PhD student will not have any of this background, given that the type of work to be carried out is not part of any undergraduate curriculum. At most they would have carried out their MSc thesis work in the Van Slageren group, at which point they would have hands-on experience with ONE of the many techniques to be employed, but certainly not with instrumental development.

Qualification concept: The postdoc will be trained in scientific methods, including electron paramagnetic resonance spectroscopy, esp. at high frequencies up to 1 THz, pulsed EPR spectroscopy and magnetic circular dichroism spectroscopy. The postdoc will have the opportunity for training in transferable skills through the wide range of courses and seminars on offer at the University of Stuttgart. These courses span a variety of subjects including grant proposal writing, leadership, negotiation, outreach and social media and entrepreneurship. The postdoc will also be closely mentored and be given career advice by Van Slageren. The postdoc will present scientific results at international conferences increasing his visibility and providing networking opportunities. Through the Van Slageren membership of the COST Molspin Network, there will also be further possibilities for research stays abroad for learning new scientific skills. The postdoc to be appointed on this project will bring new spectroscopic expertise to a group already spectroscopically well equipped. The postdoc can profit from this environment and develop his own research line, leading to scientific independence for example through a Habilitation.

9.

Research assistants. **Justification:** We will employ undergraduate students as research assistants (HiWis). This will enable early exposure of such early career researchers to hands-on scientific research and allow the project to proceed more quickly. Tasks for research assistants will include: (participation in) the synthesis of functionalized multiprobe complexes and electrochemical

measurements (AG Ringenberg) and (participation in) magnetic resonance, Mössbauer and optical spectroscopic measurements (AG Van Slageren).

3.12.7.4 Requested funding of direct costs

	2018	2019	2020	2021	2022
IAC existing funds from Institute	0.-	0.-	0.-	0.-	0.-
IPC existing funds from Institute	2,000.-	4,000.-	4,000.-	4,000.-	2,000.-
Sum of existing funds	2,000.-	4,000.-	4,000.-	4,000.-	2,000.-
Sum of requested funds	21,000.-	26,000.-	18,000.-	18,000.-	9,000.-

(All figures in EUR)

Consumables and small equipment for financial year 2018

Ringenberg: Chemicals, solvents, metal salts	EUR	8,000.-
Van Slageren: Sample preparation materials: quartz windows, EPR sample tubes, gold-coated mirrors, solvents, specialty greases	EUR	5,000.-
Van Slageren: Mechanical, optical, sample holder parts for development Mössbauer spectrometer	EUR	8,000.-

Consumables and small equipment for financial year 2019

Ringenberg: Chemicals, solvents, metal salts	EUR	8,000.-
Van Slageren: Sample preparation materials: quartz windows, EPR sample tubes, gold-coated mirrors, solvents, specialty greases	EUR	10,000.-
Van Slageren: Materials (windows, electrodes, connectors) for spectroelectrochemical cell development	EUR	8,000.-

Consumables and small equipment for financial year 2020

Ringenberg: Chemicals, solvents, metal salts	EUR	8,000.-
Van Slageren: Sample preparation materials: quartz windows, EPR sample tubes, gold-coated mirrors, solvents, specialty greases	EUR	10,000.-

Consumables and small equipment for financial year 2021

Ringenberg: Chemicals, solvents, metal salts	EUR	8,000.-
Van Slageren: Sample preparation materials: quartz windows, EPR sample tubes, gold-coated mirrors, solvents, specialty greases	EUR	10,000.-

Consumables and small equipment for financial year 2022

Ringenberg: Chemicals, solvents, metal salts	EUR	4,000.-
Van Slageren: Sample preparation materials: quartz windows, EPR sample tubes, gold-coated mirrors, solvents, specialty greases	EUR	5,000.-

3.12.7.5 Requested funding for major research instrumentation

Equipment between 10000 and 50000 € for financial year 2019

Variable temperature Mössbauer spectrometer. We will develop Mössbauer spectroscopy as a versatile probe of the oxidation state and coordination geometry of iron ions. In this project this will enable (i) understanding the changes in local electronic structure and geometry of the multiprobe molecule diFe upon immobilization in mesoporous materials, (ii) understanding the changes in oxidation state upon (electro)chemical oxidation and reduction of the probe molecule. In addition, we are generating infrastructure and expertise for the entire collaborative research centers for future funding periods in which iron catalysis will play an important role. The Mössbauer spectrometer will be acquired from RCTPM, Olomouc, Czech and adapted to an existing helium bath cryostat (original price 38.5 k€) together with an Fe-Source (6 k€).	EUR	35,800.-
Electrochemistry. Potentiostat 204, Rotating Disk Electrode, Gold/Platinum Electrodes The Institut für Anorganische Chemie, currently has a Potentiostat 101 for the instrumental analytics laboratory and used by AK Kaim, which is compatible with the proposed rotating disk electrode (8270.50 Eur), however this instrument PG101 (6700Eur) is quite basic and far less powerful than the PG204 (7770 Eur). Additionally, this instrument is used for twice a year for ~1.5 months for teaching labs and is therefore unavailable for research. The PG204 has better signal to noise, important when studying low concentration of analytes. It is also important to have a devoted poteniostat for the project because understanding the effects to the electronic structure via linker modification and immobilization is critical throughout every step of the project. Additionally, the PG204 has the capability for expansion or “add-ons”, such as impedance measurements, pH monitoring, and electrochemical quartz crystal microbalance. While these features are not currently requested in this funding period, the ability to expand the capability of the potentiostat is desirable to address future problems that may arise. The rotating disk electrode (RDE) is key device for understanding the flux of analyte to the electrode as well as the number of electron transfers and rate of transfer from the electrode to the analyte. This feature makes it fundamentally important for the understanding of electrochemical mechanisms such coordination of ligands/solvent/substrate/ions/etc.	EUR	19,000.-

3.13 Project C3

3.13.1 General information about Project C3

3.13.1.1 High resolution tomography of mesoscopic pore structures

3.13.1.2 Research Areas
406 Materials Science
406-4 Structuring and Functionalisation

3.13.1.3 Principal Investigator
Schmitz, Guido, Prof. Dr. Dr. h.c., born 11.08.1962, male, German
Institut für Materialwissenschaft
Universität Stuttgart, Heisenbergstr. 3, 70569 Stuttgart
Tel.: 0711/685-83
E-Mail: guido.schmitz@imw.uni-stuttgart.de
Tenured professor W3

3.13.1.4 Legal Issues
This project includes

1.	research on human subjects or human material.	no
2.	clinical trials.	no
3.	experiments involving vertebrates.	no
4.	experiments involving recombinant DNA.	no
5.	research involving human embryonic stem cells.	no
6.	research concerning the Convention on Biological Diversity.	no

3.13.2 Summary
Mesoporous materials produced in the CRC (section A) will be structurally and chemically characterized in highest available resolution. Porosity, pore size and shape as well as connectivity of the pore network will be determined. After impregnation with the metal-organic catalysts produced in section B of the CRC, the spatial distribution and positioning of the active molecules with respect to inner pore surfaces will be measured. These microscopic data are required to optimize the template structures (produced in section A) and the function of the linkers (developed in section B) and also to understand the guiding function of the confinement. Since the employed template materials possess a complex microstructure, tomographic techniques of three dimensional imaging and analysis will be applied to avoid projection artifacts of conventional electron microscopy. For this, ground-breaking methodic developments are planned in atom probe tomography to open this analysis technique for the investigation of soft matter and liquids.

To bridge the relevant length scales of the complex materials, we will apply correlative microscopy comprising scanning techniques with electrons and ions, transmission electron microscopy, and atom probe tomography, in order of increasing spatial resolution. The former two can be considered as well established, although in detail challenges remain regarding sample preparation, image contrast and beam sensitivity of the samples. The latter technique of atom probe tomography, however, has been established only in the analysis of hard compact materials, such as metals, semi-conductors or ceramics. Thus, the project needs to develop dedicated cryo-preparation methods, the required dedicated hardware and new algorithmic tools of data interpretation to exploit the strengths of atom probe tomography in the analysis of soft macromolecular materials and mesoporous microstructures. Our innovative concept is filling the pore structure with suitable contrasting liquids that function as moderators for the electrical field. Liquid components will be fixed by shock-frosting. A direct cryotransfer into a dual beam scanning microscope (FIB) and subsequently into the atom probe chamber allows cutting to tiny needles that are finally field evaporated without interrupting the cryogenic cooling line.

In hard materials, the 3D reconstruction of the atomic structure is enabled by identification of the field-evaporated single atoms, correct modelling of their trajectories and evaluation of the sequence of

detection. In contrast, macromolecular materials field-desorb in molecular fragments and the strict order of evaporation becomes disturbed. Hence, sound theoretical methods that allow a prediction of the splitting into the observed molecular fractions will be developed based on ab-initio methods and approximate LCAO techniques. In the first funding period, the practical analysis will focus on porous metals, porous silica networks and polymeric monoliths. Model systems to develop the microscopic analytics for linker molecules will be self-assembling monolayers bond by thiol, silane or phosphonic acid anchor groups to metallic, SiO_2 and Al_2O_3 oxide surfaces, respectively. The latter are also preferred scaffold candidates in other projects of the CRC (especially **project A5**).

3.13.3 Research rationale

3.13.3.1 Current state of understanding and preliminary work

In current nanotechnology, three dimensional structures play an increasingly important role. Illustrative examples can be found in recent microelectronics in which the use of the third dimension e.g. in deep trench capacitors, FINFET transistors or concepts using nanowires allow a significant increase in the packaging density. To characterize such complex nanostructures, tomographic methods have recently gained importance. In order of increasing resolution, FIB tomography [1], neutron and X ray tomography [2], electron tomography [3], and atom probe tomography (APT) are the most relevant. The goal of this project is to make APT accessible to the particular aims and objectives of the CRC, and so to exploit the technique with the highest possible resolution in 3D imaging and microscopic chemical analysis with single atom sensitivity. APT has been applied successfully to hard and compact materials [4]. Now, we aim to develop experimental and theoretical procedures to investigate porous matrices and soft matter with this technique.

The method of atom probe tomography

APT follows a surprisingly transparent measurement principle [5]: Needle-shaped samples with an apex curvature radius of about 50 nm are positioned opposed to a 2D detector setup that is able to detect the impact of individual ions. The sample is cooled to about 50 K to reduce thermal atomic motion. A high voltage (10 – 20 kV) is supplied to generate an electrical field of about 50 V/nm at the tip surface. This field strength is so high that the electron density of the atomic bonds or the band structure become strongly distorted. Exceeding a certain field threshold, atoms leave the condensed material and are accelerated towards the detector. UHV conditions allow the free flight on well-predictable trajectories. By evaluating the impact positions on the detector and the order of the detection events, the original positions of the atoms inside the sample are reconstructed with an unprecedented accuracy of 0.2 to 0.5 nm. Triggering the field-desorption by short high voltage pulses or by laser flashes enables a flight of mass spectrometry that allows identification even of the isotopes of a species. In investigation of nanostructured metals, semi-conductors [6] and ceramics [7], battery materials [8] and hard biomaterials [9], the method is well established and has often delivered decisive results that led to a profound understanding of the behavior of the materials. Figure C3-1, summarizes the principle of the method and presents typical results obtained with nanostructured metallic multilayers. By contrast, only very few, though encouraging, results have been presented with organic materials [10] or porous geometries. These few examples require expansion and careful evaluation, before APT can reasonably contribute to progress in understanding of organic and hybrid materials.

In the early period of field ion microscopy and atom probe spectroscopy, the required needle-shaped samples were usually produced by electro-polishing from metallic wires which severely restricted the range of possible investigations. Recently, the preparation of samples by focused ion beam cutting has become a more flexible alternative that nowadays allows to shape sharp needles from almost any solid material. An example (Fig. C3-2) of the work in our own team is the preparation of a thin film solar cell material [13]. First a lift out of a thin lamella is performed similar to the usual practice in electron microscopy. A part of the lamella is glued to a suitable support wire and then thinned to the final tip radius less than 150 nm in diameter by azimuthal milling along the tip axis.

It is obvious that besides achieving a reproducible field desorption, the numerical reconstruction of the chemical data is a key step that controls the accuracy of the microscopic analysis. To this aim, the present state of APT uses a reconstruction scheme that was first proposed in 1995 [14] (see Fig. C3-3). It assumes a homogeneous evaporation probability of the material, in which case, the tip naturally

develops a hemispherical apex geometry. Hence, the apex radius is known at any stage of the measurement from geometric and electrostatic arguments. Furthermore, a normalized distribution of the electrical field is established around the tip that allows the reliable prediction of the ion trajectories. In consequence, the event position on the detector and the initial position at the sample surface can be linked by a straight-line projection.

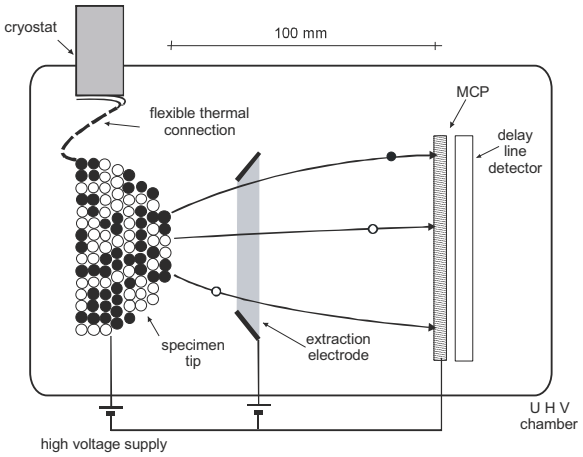

(a)

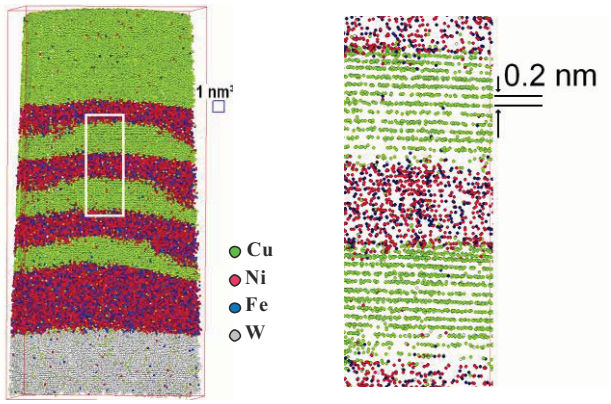

(b)

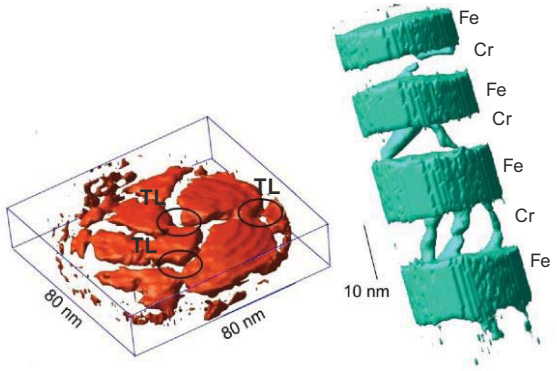

(c)

Fig. C3-1: Atom probe tomography. a) Principle of the method, b) tomographic reconstruction of a magnetic sensor consisting of Cu and Ni(Fe) layers [11]. Colored dots mark the position of the detected atoms. The magnified detail demonstrates the reconstruction of lattice planes. c) Tomograpy of nanocrystalline Fe/Cr layers. By evaluation of the local atomic density the grain structure of the sample is clarified (left). By annealing, atomic transport along the triple junctions of the grain structure is initiated which show up in isoconcentration maps as tube-shaped paths crossing the Cr layer (right). Note, the small length scale of the examples demonstrating the outstanding resolution in 3D chemical analysis [12].

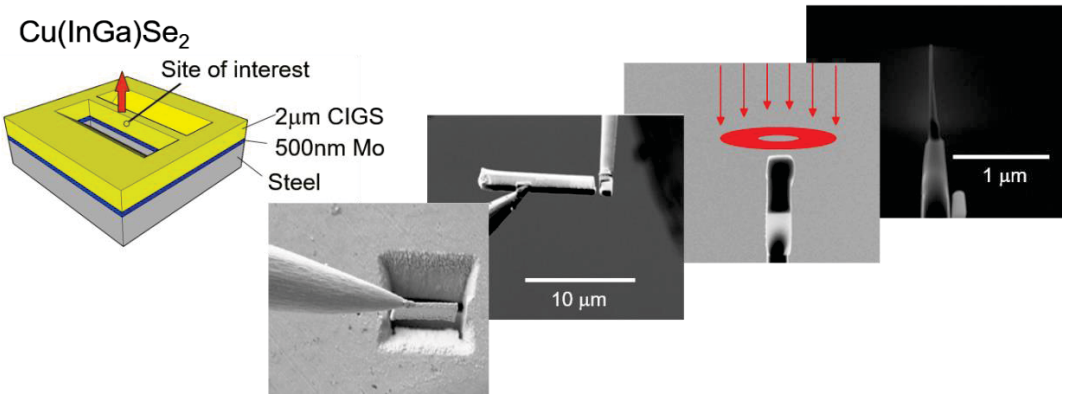

Fig. C3-2: Basic steps of FIB-based preparation of needle-shaped samples at the example of a CuInGaSe layer [13]: From left two right: Scheme of geometry, milling of two deep trenches to form a thin lamella, lift-out by using a micromanipulator, gluing to a tungsten post and thinning by axial milling on concentric circles. The final tip should have a small shaft angle and an apex radius less than 100 nm.

The stacking of the atoms in depth (along the tip axis) is reconstructed under the assumption of constant atomic density and a strict order of the events from the surface towards the depth of the volume, as illustrated in Fig. C3-3b. These straightforward assumptions, however, may not be fulfilled in realistic cases, as demonstrated in Fig. C3-4. The discrete geometry of the atomic terraces deflects the trajectories, even trajectory overlap can appear near to the zone axis directions of crystalline samples [15] (Fig. C3-4a). In the case of complex heterogeneous samples, the aberrations may become even more severe. For example, consider a precipitate of a second phase that requires a higher or a lower field strength for evaporation. Correspondingly, the sample surface develops local protrusions or indents (Fig. C3-4b). This deviation of the shape from the assumed ideal hemisphere will deflect the trajectories which leads to local magnification or demagnification and thus to an undesired distortion of the reconstructed volume. Even more severe,

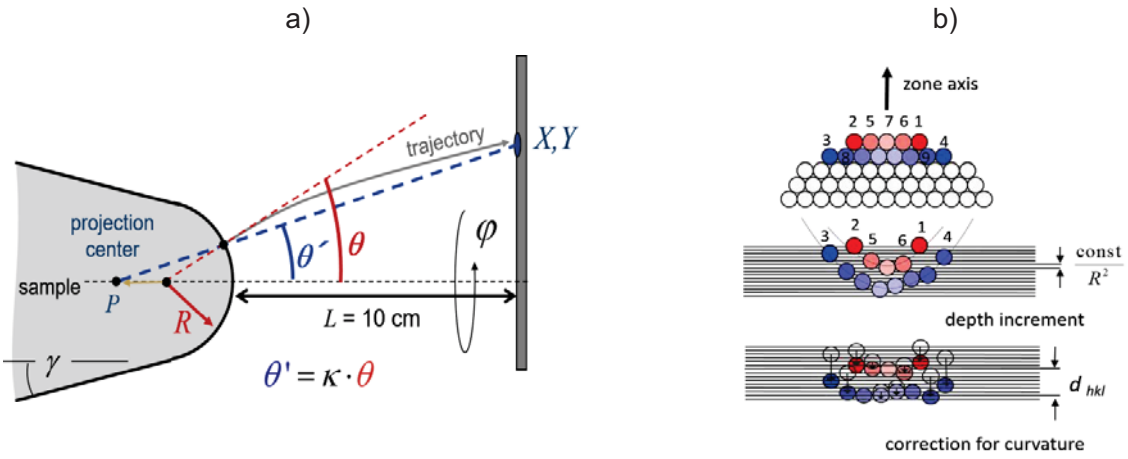

Fig. C3-3: Fundamental steps of the tomographic volume reconstruction according to Bas et al. [14]: a) approximation of the trajectories between tip and detector by a linear point projection. b) Evaluation of the sequence of events to establish a natural depth scale. Outer events are shifted somewhat more downwards to correct for the hemispherical curvature and so to reconstruct planar lattice planes.

trajectories can overlap so that the reconstructions present an apparent mixing of the atoms; hetero-phase interfaces would become unrealistically broad. As illustrated in Fig. C3-4b (right side), it is obvious that a similar mis-shaping of the surface, even more extreme, must appear with porous materials, whenever the desorption front discovers a pore. A deeply concave surface would deflect the trajectories so strongly that they cannot be appropriately treated by the present-day reconstruction algorithms.

To estimate such aberration phenomena, computational schemes have been developed that simulate the full measurement process of the atom probe [16]. These enable a comparison between the experimental and the simulated reconstructions so that at least the impact of possible artifacts can be reliably estimated. There is however, up to now, no reconstruction scheme available that could treat the trajectory deflection in a physically sound manner and could so reconstruct correct 3D atomic maps in such complex cases. Our team has significantly contributed to this field of research [17,18].

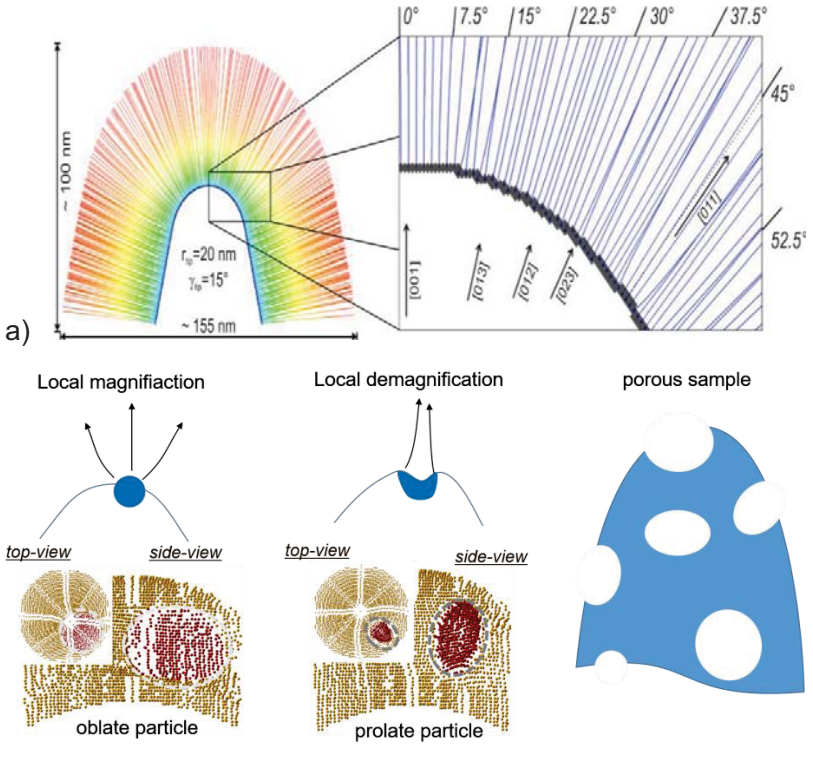

Fig. C3-4: The origin of reconstruction artifacts: trajectory aberrations by a) lattice discretization and b) deviations from ideal hemispherical geometry: From left to right, cases of a protruding particle (higher evaporation field strength, local lateral magnification leads to an oblate shape in the reconstruction), of a receding particle (lower evaporation threshold, local demagnification leads to a prolate shape), and a porous sample (Regions of receding surface are expected to be even more pronounced than in the case of heterogeneous precipitates). Simulated trajectories and reconstructions were published [15].

3.13.3.2 Own work, project-related publications by participating researchers

The team of the PI has achieved profound expertise in the application of APT and various techniques of electron microscopy to solid state reactions in nanostructure materials (see [C3-1…C3-10]). In APT, our contributions have been significant and always at the cutting edge of the method. In the early times (1996-2006), we were the first focusing on the investigation of thin films with this method. Beginning with 2007, we were one of the first teams working with laser-assisted evaporation on oxides, and recently, we focused on the theoretical understanding and simulation of the measurement process. Beside this general expertise, we carried out preparatory work dedicated to the proposed project, as described in the following.

Design of a new atom probe instrument: "Micro-TAP"

As explained further below, the innovative concept of this proposal is the development of APT to the extent that liquids and mixtures of solid and liquids can be analyzed in a controlled manner. It is obvious that this is only possible by cryo-freezing the liquid so that it can be handled as a solid material under ultra-high vacuum conditions. To achieve this challenging goal, we designed a new instrument and

already installed it in our lab space. It represents a unique combination of a dual beam scanning microscope for FIB preparation, extended by all facilities to enable a cryo-preparation, (deep quench freezer, vacuum de-icing, thin film coater, cooled shuttle transfer, cryogenic sample stage), and a new miniaturized, custom-made APT chamber that is directly linked to the scanning microscope via a magnet transfer rod and a plate valve (see Fig. C3-5). The instrument was put into operation and first preliminary proof of concepts could be performed, although still some software development is necessary to bring the instrument to daily operation. The cryo-transfer from the FIB to the atom probe proceeds in a few seconds so that a temperature of about 150 K can be warranted during all stages of treatment. Beside the possibility of investigating frozen liquids, the chamber geometry of the miniaturized APT also allows new, very efficient sample preparation and measurement techniques. The sample stage is mounted on a flexible hexapod, so it can be arbitrarily tilted and positioned towards the laser beam with nanometer accuracy. In this way, needles that are simply eroded into a planar layer (see Fig. C3-5, right-hand side) can be analyzed without a lift-out making the fixation to a dedicated support post obsolete (the required gluing would be almost impossible at cryogenic temperatures).

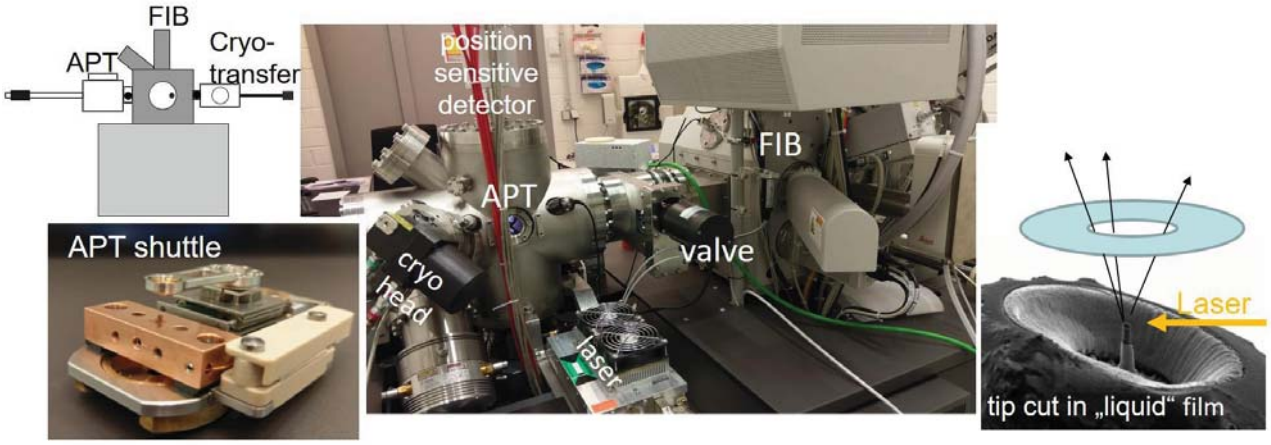

Fig. C3-5: The newly constructed Micro-TAP/FIB combination at the Chair of Materials Physics. The functional “heart” of the instrument is the “APT shuttle”, containing sample stage, cryo connection to reach 20 K, a piezo drive that controls the 20 μm extraction electrode, 20 kV high voltage supply lines and insulation (all on 4x7 cm^2 footprint).

Polymeric materials in the atom probe and focused ion beam preparation

Regarding the possibility of measurements of soft or polymeric materials with the APT, we refer on the one hand to our early experiments with self-assembling monolayers that we have previously published [C3-10]. Alkyl-thiols and perfluorinated alkyl-thiols were deposited on Au substrates. Both kinds of molecules could be field desorbed in laser-assisted APT. But surprisingly, the field evaporation of both molecules appeared in fundamentally different way. While the alcane chains desorbed in small CH_x units, the perfluorinated chains first striped off the head group and then all Fluor atoms. The Carbon backbone was finally detected as a long alcene together with the Sulphur anchor group. This fundamentally different field-desorption behavior, in spite of the fact that both chains are structurally very similar, is presently not understood.

In addition, we carried out further preparatory measurements with polyelectrolyte multilayers as a proof of concept (Fig. C3-6). By alternatively dipping electropolished Au tips into solutions of the anion polyallylamine hydrochloride (PAH) and the cation polyacrylic acid (PAA), we coated the tips by a polymeric layer of 30 to 50 nm in thickness which is dominantly stabilized by ionic interchain bonds. The investigated molecules consisted mostly of hydrocarbon backbones with a few other elements located at side groups (nitrogen, oxygen, sulphur, phosphor). For better adhesion, we used one layer of polyethylenimine (PEI) as a cationic adhesion aid in contact to the Au. Using the laser-assisted atom probe, we could prove that well-controlled field evaporation of the macromolecular material is possible and reasonable mass spectra are obtained. An example is shown in Fig. 6.

In comparison to conventional work with hard materials, the mass spectra are quite complex revealing many different fractions of hydrocarbon chains of alkyne, alkene and alkane units. Nevertheless, we could identify important regularities in the abundance of the mass peaks. With regard to the general formula C_xH_y, we typically observe groups from x=1 to x=8. In each group, the number of H atoms varies from y=x to y=2x+2. Thus, the saturated alkane always marks the end of the group, although it is not necessarily a part of the original polymer chains. Obviously, some of the detected molecular fractions are newly formed in the moment of evaporation from the available atoms at the surface under high field conditions. The ethane group with x=2 is most abundant and within each group, the peak with y=2x (the alkene) is dominant. These general rules help identifying peaks in cases of ambiguity. For example, we notice in Fig. 6 that the peaks at m/z=29 ("C_2H_5") and m/z=44 ("C_3H_8") are rather large and so obviously hurt the previously stated rules. However, a second view on the composition of the monomer units indicates that dominantly CNH_3^+ and COO^+ contribute to these peaks, respectively.

The chemical analysis of the APT is calibration free, meaning the events are directly counted and evaluated assuming identical detection efficiency for all species. (In the present instrument, this efficiency is close to 50%.) By evaluation of the hydrogen to nitrogen ratio, the stoichiometry of the polyelectrolyte layer is determined to be almost 1:1 with a very slight advantage to the anion side. Consequently, only Cl cations are observed as counter ions to a small percentage of 4%. Producing the polyelectrolyte layers at different pH values of the dipping solutions changes the iconicity of the polymers and thus the relative polymer content that is required by charge neutrality. In correspondence, we could demonstrate the change in the relative

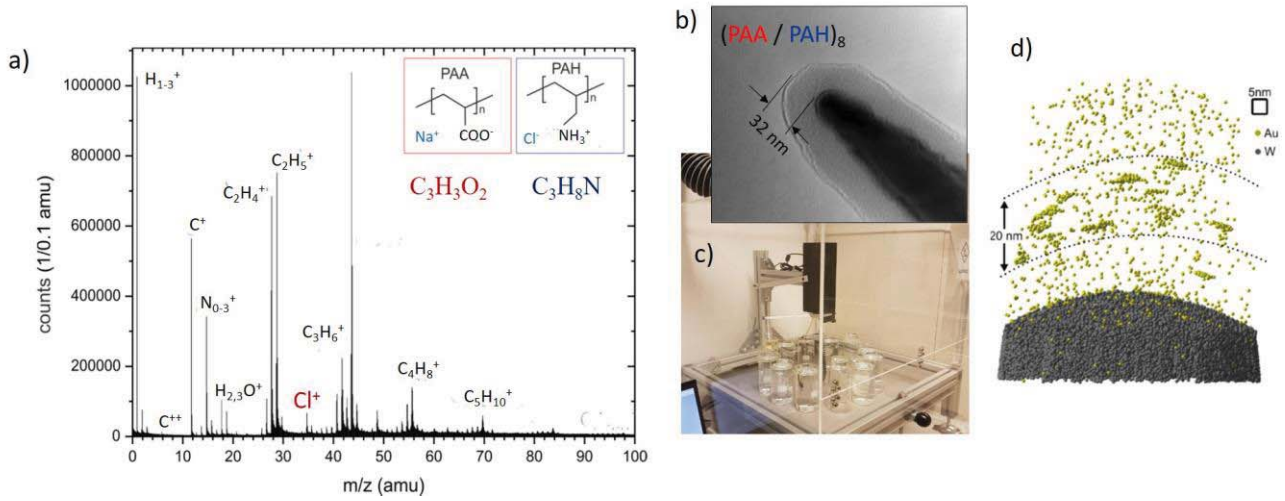

Fig. C3-6: Fig. 6: APT analysis of a PAA/PAH polyelectrolyte. a) mass spectrum, b) TEM of a coated tip, c) used dipping robot, d) APT of Au clusters embedded in polyelectrolyte layer on top of tungsten support. (Max Steimle, Univ. of Stuttgart 2017)

peak abundance and concentration of counter ions (e.g. at pH=3 the polycation PAA becomes largely decharged, consequently its gets 10 times more abundant than that of the anion PAH.) These quantitative details make clear that the calibration-free chemical analysis of the macromolecules functions to high precision. We also collected clear indication for a reasonable depth profiling by the APT: Embedding Au particles in a certain depth of the polyelectrolyte layer, we find them afterwards in the reconstruction at the expected depth (see Fig. C3-6d).

Liquid materials in the atom probe analysis

The new cryogenic sample preparation and measurement line was checked by model investigations of natural honey, scientifically a liquid mixture of water and sugars. To avoid any fixation or gluing in the cooled state, we let droplets of honey wet rough surfaces of wire shaped posts of a few micrometers in diameter. After freezing the droplets, nanometric needles were cut by the focused Ga beam and the tip then transferred into the atom probe without interrupting the cooling. Analysis of the frozen honey tip proceeded similar as the investigations of the polyelectrolyte material. (UV laser pulses, 220 fs). Exemplary data are shown in Fig. C3-7. Again, the mass spectra are quite complex, but they clearly

allow distinguishing between the dominating water and sugar parts. In comparison to the polyelectrolytes, the overall spectrum is oxygen rich and no nitrogen-containing peaks are observed. These findings are in agreement with the chemical structure of the various variants of sugars. A first volume reconstruction of such sugar analysis is presented in Fig. C3-7b. The evaporation proceeded reasonably homogeneous, so that the shown reconstruction can be indeed reliable. The observed decomposition into oxygen-rich and oxygen-poor regions on the length

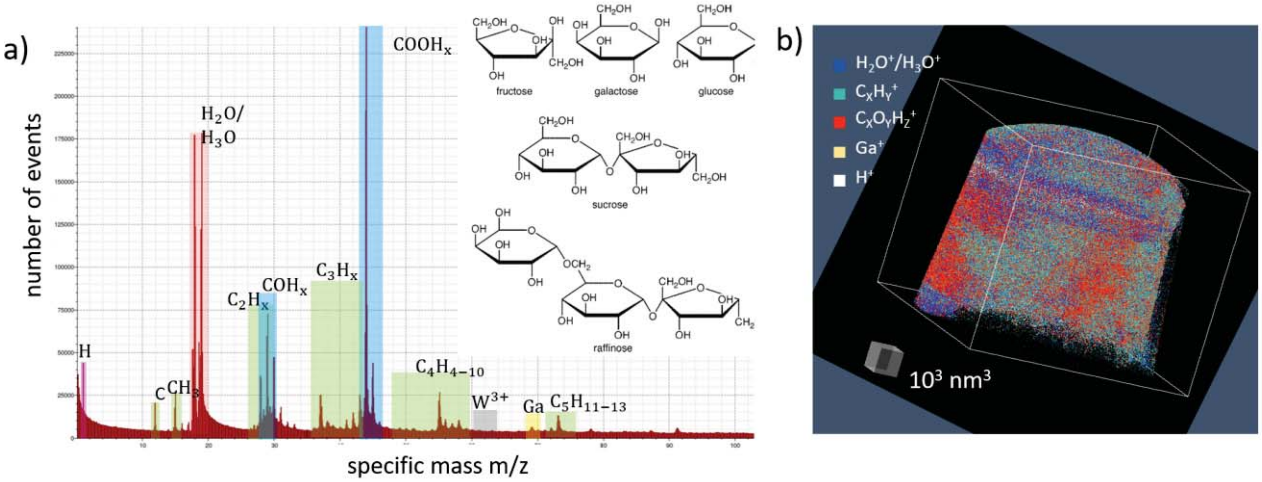

Fig. C3-7: APT analysis of natural honey: a) mass spectrum, b) volume reconstruction of a part of a nanometric tip FIB cut from frozen honey (Jonas Ott, Univ. of Stutgart 2017).
scale of about 20 nm is surprising and needs further reflection. Owing to this preliminary success, we are confident that the goal of a spatially resolved analysis of complex liquid/solid soft matter structures is available in near future.

Preliminary proofs of concept with materials of the collaboration partners

To check the possibilities of preparation of the two main materials classes considered in the CRC as templates, we checked the FIB preparation and transmission electron microscopy of porous silicate glasses (FDU-12, **project A4**) and the polyurethane monoliths (**project A1**). Both materials could be reliably prepared by the FIB technique. For example, Fig. C3-8 presents TEM micrographs of the FDU-12, decorated with a few metallic particles as well as an SEM image of the monolith and the subsequent shaping of an atom probe needle from this material.

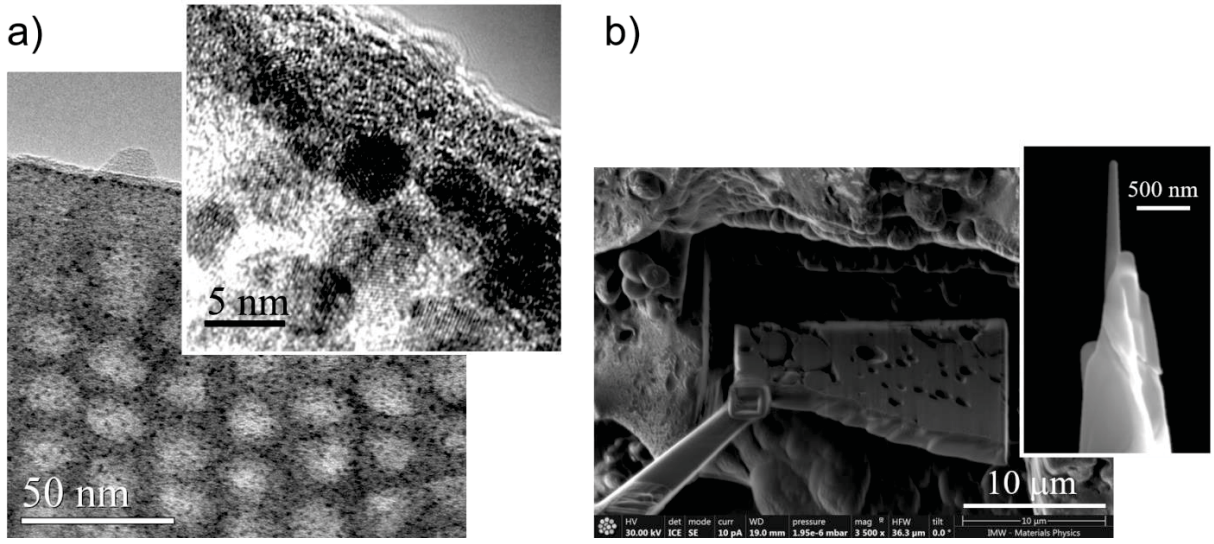

Fig. C3-8: Proofs of concept: a) FDU-12 silicate decorated with metallic particles. Expected regular arrangement in an fcc arrangement is proven. Inset shows phase contrast image of metallic clusters. b) FIB cutting of polyurethane monolith after vacuum drying. Grab out of a lamella. Inset show the finally prepared atom probe tip.

References

[1] L. Holzer and M. Cantoni, *Review of FIB-tomography* in I. Utke et al. (eds.) *Nanofabrication Using Focused Ion and Electron Beams*, Oxford 2012, p. 410-435.
[2] W. Reimers, A.R. Pyazalla, A. Schreyer, H. Clemens, *Neutron and Sychrotron radiation in Materials Science*, Wiley-VCH Weinheim 2008.
[3] J. Evans and H. Friedrich, *Advanced tomography techniques for inorganic, organic, and biological materials*. MRS Bulletin, 2016, 41, 516. (and further articles therein)
[4] Y. Amouyal and G. Schmitz, *Atom probe tomography – A cornerstone in materials characterization*, MRS Bulletin 2016, **41**, 13 (and further articles therein).
[5] D. N. Seidman, *Ann. Rev. Mat. Res.* **2007**, *37***,** 127.
[6] M. Gilbert, W. Vandervorst, S. Koelling, A.K. Kambham, *Ultramicr.* **2011**, *111*, 530.
[7] G. Sundell, M. Thuvander, H.-O. Andren, *Corros. Sci.* **2012**, *90*, 1
[8] A. Devaraj, et al., *Nature Commun*. **2015**, *6*, 8014.
[9] L.M. Gordon, L. Tran, D. Joester, *Nano* **2012**, *6*, 10667.
[10] Y. Zhang, A. C. Hillier, *Anal. Chem*. **2010**, *82*, 6139.
[11] C. B. Ene, G. Schmitz, R. Kirchheim, A. Hütten, *Acta Materialia* **2005**, *53*, 3383
[12] P. Stender, Z. Balogh, G. Schmitz, *Phys. Rev.* **2011** *B 83*, 121407(R)
[13] R. Schlesiger, C. Oberdorfer, R. Würz, G. Greiwe, P. Stender, M. Artmeier, P. Pelka, F. Spaleck, G. Schmitz, *Rev. Sci. Instrum.* **2010**, *81*, 043703.
[14] P. Bas, A. Bostel, B. Deconihout, D. Blavette, *Appl. Surf. Sci.* **1995**, *87/88*, 298.
[15] C. Oberdorfer, S. M. Eich, and G. Schmitz*, Ultramicr.* **2013**, *128*, 55.
[16] F. Vurpillot, C. Oberdorfer, *Ultramicr*. **2015**, *159*, 202.
[17] C. Oberdorfer, S. M. Eich, M. Lütkemeyer, G. Schmitz *Ultramicr*. **2015**, *159*, 184.
[18] D. Beinke, C. Oberdorfer, G. Schmitz*, Ultramicr.* **2016**, *165*, 34.

Project relevant recent publications

[C3-1] Y. Amouyal, G. Schmitz, *MRS Bulletin* **2016**, *41***,** 13.
[C3-2] H. Bouchikhaoui, P. Stender, Z. Balogh, D. Baither, A. Hütten, K. Hono, and G. Schmitz, *Acta Mater.* **2016**, *116*, 298.
[C3-3] D. Beinke, C. Oberdorfer, G. Schmitz, *Ultramicr.* **2016**, *165*, 34.
[C3-4] C. Oberdorfer, S. M. Eich, M. Lütkemeyer, G. Schmitz, *Ultramicr.* **2015**, *159*, 184.
[C3-5] F. Vogel, N.Wanderka, Z. Balogh, M. Ibrahim, P. Stender, G. Schmitz, J. Banhart, *Nat. Commun.* **2014**, *4*, 2955.
[C3-6] G. H. Greiwe, Z. Balogh, G. Schmitz, *Ultramicr.* **2014**, *141*, 51.
[C3-7] C. Oberdorfer, S. M. Eich, and G. Schmitz, *Ultramicr.* **2013**, *128*, 55.
[C3-8] J. Keller, R. Schlesiger, I. Riedel, J. Parisi, G. Schmitz, A. Avellan, T. Dalibor, *Sol. Energ. Mat. & Solar Cells* **2013**, *117*, 592.
[C3-9] M.R. Chellali, Z. Balogh, R. Schlesiger, P. Stender, H. Bouchikhaoui, L. Zheng, G. Schmitz, *Nanoletters* **2012**, *12*, 3448.
[C3-10] A. Stoffers, C. Oberdorfer, G. Schmitz*, Langmuir*, **2012**, *28*, 56.

3.13.4 Project plan

The ambitious goal of a 3D nano-analysis in atomic accuracy of the carrier materials and catalysts will be achieved by a combination of FIB cryo-preparation, FIB tomography, analytical TEM and laser-assisted APT. The correlative application of these methods covers all length scales relevant for the research collaboration: 1-5 nm: orientation and position of the active catalyst molecules, 5 to 30 nm: pore volume, 30 nm to 10 μm: connectivity and transport through the pore network. The FIB preparation, FIB tomography, and the transmission electron microscopy of solid materials are routinely performed in our team, so that we will make these techniques available to the collaboration directly from the beginning of the funding period. The cutting-edge application of atom probe tomography to porous microstructures however, requires fundamental research in innovative microscopic methods. Naturally, we will focus on these developments within the first funding period. We are confident that for the suggested procedures sufficient maturity can be achieved in time so that the atom probe tomography

will deliver important information on the mesoporous materials still in the first funding period. The proposed methodical research has to overcome two decisive obstacles:

i) The preliminary work has demonstrated that field desorption of macromolecular materials proceeds by small fragments rather than single atoms. In consequence, the atom probe mass spectra become comparably complex. Not in all cases do the observed atom groups correspond to direct fragments of the former structure. Instead, the detected small molecules are partly formed by gas-phase reaction of the available fragments under the high surface fields. The depth scaling of the tomographic reconstruction expects a natural top to bottom order of evaporation. However, since this is not assured any longer, the positioning accuracy is significantly degraded. Although we demonstrated a primitive volume reconstruction even in the case of self-assembled monolayers, the achieved accuracy has not been satisfying yet.

ii) Easy predictable ion trajectories and thus a tomographic reconstruction with the present-day methods require a smooth, hemispherical/conical shape of the specimens during all stages of the measurement. The mesoporous materials interesting the CRC obviously do not fulfill this condition, since pores that meet the surface induce strong roughening. In consequence, the field at the tip apex and thus the trajectories will be deflected. So, the established point projection that links detection position to the launching position at the sample surface is no longer valid.

In view of this situation, we formulate the following goals for the first funding period:

1. Development of methods to smoothly field-evaporate pores and inner surfaces based on liquid fillers and the application of cryo-preparation.
2. Development of numerical reconstruction schemes that are suited for the correct reconstruction of pore structures on the length scale of 1 to 100 nm.
3. Achievement of a fundamental understanding of the field desorption sequence of macromolecular materials based on measurements of selected model structures that are compared to the predictions of Density-Functional Theory.
4. Measurement of the geometry, size distribution and connectivity of the pore structure in mesoporous metals, silicate glasses, and polymeric monoliths.
5. Determination of the spatial distribution and linkage distance of metal-organic catalysts within the pore structure.

In summary, the research goals are organized in work-packages as follows, which are further detailed below:

WP 1: Preparation of required model matrix materials
WP 2: Correlative microscopy of porous metals and silica networks
WP 3: FIB tomography of polymeric monoliths
WP 4: Impregnation by liquid fillers and cryo-preparation
WP 5: Atom probe analysis of filled pore structures
WP 6: Atom probe analysis of self-assembled monolayers
WP 7: Nanoanalysis of immobilized catalyst-linker systems
WP 8: TEM characterization of CRC materials

3.13.4.1 WP 1: Preparation of mesoporous model materials (collaboration with A1 and A4)

The initial stage of the project will focus on three model scaffolds, namely porous metal layers, mesoporous silica (FDU-12) and polyurethane monoliths as examples of the important material classes considered as matrices in the CRC. The latter two will be provided by collaboration partners A4 and A1, respectively. The porous metallic matrices serve as a starting model since they allow easier and more accurate atom probe analysis in atomic resolution. They will be produced by ourselves sputtering Au-Ag alloys to a thickness of about 1 μm followed by selective dissolution of the Ag component under potentiostatic or current-less edging conditions. In a series of experiments, we will explore the variation of controlling parameters such as alloy composition, type and concentration of the solvent, applied voltage and temperature to learn how to produce different pore sizes and connectivity in a target-oriented manner. We plan to produce samples with pores of about of 5, 10, and 20 nm diameter which seems in view of present literature [19,20] readily available. In a subsequent step, we will also try to transfer the procedure to alternative CuAl and NiFe alloys to possibly produce porous matrices of Cu or Ni. These are expected to field-evaporate in the atom probe more reliably than Au because of advantageous mechanical properties.

3.13.4.2 WP 2: Correlative microscopy of porous metals and silica networks (collaboration with A4)

Silica and metallic porous matrices will be characterized by TEM and APT with respect to the size and shape of the pores as well as the density and connectivity of the porous network. To this aim, needle-shaped samples will be produced by FIB milling. On the one hand, sharp needles with a curvature radius of about 50 nm are required to perform the field desorption in the atom probe. On the other hand, we will also use the same sample geometry in the TEM. The cylindrical symmetry of the needles allows a large angle rotation, which should ideally reach the full +/- 90° range and so to achieve an accurate tomographic reconstruction by TEM as well. In our presently available hardware (CM200-FEG, self-constructed tip-sample holder), the achievable angular range amounts to +/- 70°, which already allows reasonable tomography. However, it is further planned to raise this limitation by purchasing/producing a dedicated sample holder that enables even a full rotation. Taking a series of micrographs with angle increments of $\Delta\alpha$ = 2°, one can expect to achieve a tomography with a resolution of about Δx = 3 nm [21]. Established weighted back projection algorithms [22] will be used for the numerical tomographic reconstruction of the set of 2D projections.

Our preliminary tests of TEM on mesoporous silica have shown that the usual 2D projection is sufficient to identify the pore size. However, conventional TEM did not allow a clear determination whether the pores remain isolated or form a linked network, which is an essential information required within the CRC. We propose to overcome this shortcoming by performing the described TEM-based electron tomography. Performing the electron tomography before the destructive atom probe field desorption, both electron microscopy and atom probe tomography can be applied to the same sample (correlative microscopy). Applying the basic concept of a geometric reconstruction, it is clear that the APT reconstructed pore shape will be strongly distorted. We will therefore try to improve the reconstruction scheme by realistic calculations of ion trajectories as we initiated in previous work concerning samples with heterogeneous phase distribution (see [C3-10]). Comparing these improved APT reconstructions

with the result of electron tomography, the derived algorithms will be optimized to achieve a match between TEM and APT as close as possible.

As a reliable outcome, the work package should state the minimum pore size required to detect pores in APT and TEM, respectively. The contour accuracy of both methods will be quantified and demonstrated. As the decisive advantage, APT allows in addition a local chemical analysis. So, WP2 will also determine and quantify an eventual segregation of impurities (e.g. remaining Ag atoms at the Au scaffold) and of functionalizing groups brought in purpose to the internal interfaces. Subsequently, the same will be also tried with the mesoporous silica produced in **project A4** which is one of the key templates in the CRC. We will also accept the challenge to microscopically demonstrate terminating OH groups at the inner surfaces.

3.13.4.3 WP 3: FIB tomography of polymeric monoliths (collaboration with A1)

The polymer monoliths prepared by the collaboration partners (**project A1**) reveal porosity on a broad range of lengths scales (see our preliminary investigations, sect. 3.1.3.2). To image and characterize the connectivity of the pore network on the μm scale, we will produce 3D density maps by FIB tomography. The material is eroded in thin slices by the ion beam and an SEM image is obtained from each slice. Numerically combining the stack of 2D images, a tomographic representation of the mass density is produced, that discovers the connectivity and the hierarchy of different pore sizes. Geometric calculations of the inner surface area will be compared with the result of gas adsorption/desorption experiments (**project A1**) to secure the correct imaging by the FIB tomography. For the tomographic reconstruction, a commercial software ("AVIZO") is available. Up to now however, no profound experience has been gained with this method, especially with polymeric materials. So the handling of the relevant polymeric materials in the SEM and TEM has to be explored. The main issue will be the beam sensitivity. Low beam intensities and cooling of the samples will become presumably necessary strategies. In the case of success, the methods will be made available also to the other partners in the collaboration working with polymeric materials, e.g. block-copolymers (**project A2**) and foams (**project A7**)

3.13.4.4 WP 4: Impregnation by liquid fillers and cryo-preparation

Filling the pores with suitable contrasting liquids represents the decisive innovative concept to characterize the pore network of metals, oxides and polymeric monoliths by atom probe tomography without the aforementioned distortions of the ion trajectories. After impregnation with the liquid fillers, the matrices will be shock-frosted and, as a compact solid material, cut to nanoscopic needles by a focused Ga beam.

First, the filling of the pores is necessary to achieve a continuous field distribution around the tip-shaped atom probe samples and thus to guarantee well predictable trajectories. But furthermore, it is essential for the further goals of the CRC, as active catalysts and linkers are introduced in liquid solvents and also the transport of reactants and products of the catalytic process may proceed in liquid phase. So developing, this innovative technique will not only allow the characterization of the geometric parameters of the matrices, but also the later analytical observation of the complete catalytic systems provided within the collaboration.

The work package needs first to identify and test suitable liquid fillers. On the one hand these must properly wet the materials so that impregnation of even the smallest pores is enabled. On the other hand, the liquids should reveal a pronounced mass contrast to all components of the matrices. For metallic and ceramic scaffolds, we will first experiment with water/alcohol mixtures, since water appears in atom probe mass spectra at the rather low mass to charge ratio of 17 Da (OH^+) and 18 Da (H_2O^+). This is much lighter than the specific mass of most metals, especially Cu, Ni and Au, promising a clear contrast in the time of flight mass spectrometry. The mentioned water peaks are also clearly distinguished from those of Si and O, the main components of the silicate scaffolds. So it is expected that the pore volumes could be unambiguously identified as those regions revealing a pronounced content of water at 18 Da. Aqueous liquids, however, do not wet the polymeric monoliths. For the polymeric matrices, potential filler candidates are organic liquids such as trichloro and tribromo benzene, or similar solvents with the heavier halogens offering contrast to the low mass components of

the macromolecules. Thus, in this case pores will be discovered as regions of high Cl or Br content. Finally, we address the relevant liquids for the catalytic processes planned in the **projects B1** to **B3**: e.g. Toluol, Dioxan, Dodekan, DME.

Impregnated tips will be mounted on suitable tungsten posts, shock frosted and without interrupting the cooling inserted into the dual beam microscope. The required cryo-preparation and transfer unit (Leica), as well as a cryogenic sample stage in the FIB are well-tested equipment in the chair of materials physics.

3.13.4.5 WP 5: Atom probe analysis of filled pore structures (collaboration with A1, A4)

The pore-filled matrices have to be inserted into the atom probe chamber without interrupting the cooling line and the vacuum. As described under preliminary investigations (3.1.3.2), we have already constructed an innovative instrument just for this purpose. The samples are directly transferred within a few seconds between the dual beam microscopy chamber and a miniaturized atom probe without interrupting cooling. A very flexible sample stage allows new sample preparation techniques that make gluing inside the FIB by means of metal-organic gases obsolete. Such gluing would be extremely difficult in the cooled state.

Since we have proven in our example study of honey that the handling of frozen liquid tips and the measurement of water is possible, we do not expect particular difficulties in the APT analysis of the metal and ceramic scaffolds. However, the exact evaporation field threshold of water in comparison to metals and silica is not known. It is planned to especially select scaffold material and filler to make the evaporation of all components as homogeneous as possible. The results of the reconstruction will be compared with those obtained in WP 2. We expect that the contour accuracy will be significantly improved by the filling technique.

Atom probe tomography of the polymeric monoliths has no examples in the literature. We can expect that the mass spectra are quite complex. However, we know from our work with polyelectrolytes that e.g. Cl^+ ions can be clearly distinguished from the appearing multiple hydrocarbon peaks. So it should be possible to spot reliably the geometry of the pores and their interconnection by the spatial distribution of Cl or Br in the 3D chemical maps. We expect that still a significant variation of the evaporation threshold is unavoidable. Hence, improved reconstruction algorithms must be applied which are presently under development in our team [C3-3, C3-7]. The already derived concepts of a multiscale trajectory simulation (based on a Voronoi partition) will be adopted to the particular requirement of the amorphous matrix. Instead of single atoms, the basic units of reconstruction will become small volume units, which may make the numerical concept even more efficient, as we can use a coarse-grained description.

Beside the size of the pores, it is especially important to characterize their shape to determine variation of local curvature. The latter can be assumed to be a decisive parameter in controlling the catalysis by confined geometries. Also, the density of attachment of active catalysts possibly depends on the curvature of the inner surface.

3.13.4.6 WP 6: Atom probe analysis of self-assembled monolayers (collaboration with A5, C4)

Small chain molecules attached to metal and oxide surfaces represent the second important structure on which our project will focus, as these provide a model to the linkage of the catalysts to the porous matrices. In controlled studies with well-known oligomers, the characteristic features of field desorption of such short-chained organic molecules will be determined. We will clarify the kind and order of field-desorbed fractions as a function of laser intensity, wavelength, pulse width, strength of the electrical field and the sample temperature. To obtain high spatial resolution, it would be important to identify conditions that deliver molecular fractions as small as possible. On the other hand, for chemical identification, it can be advantageous to detect larger molecular units. To check for a possible improvement by resonant evaporation, it is required to extend our current fiber-based laser system (Clark IMPULSE, 250 fs) by an additional non-collinear optical parametric amplifier. This will allow a continuous variation of the laser wavelength and application of significantly shorter pulse width (40 fs) so that the laser pulses may be adapted to specific chemical bonds. The evaporated molecular

fractions and the order of their appearance will be compared to predictions by ab-initio methods. To this aim, the colleagues in **project C4** will simulate the field desorption of the same molecules by DFT calculations, so that a detailed understanding of the conditions of field evaporation will be achieved, e.g. which role plays the polarizability of atoms and the polarity of the bonds, what is the impact of single or double bonds in a carbon chains on controlling the evaporating molecular fractions? Furthermore, we will explore in our own team to which extent approximations by a linear combination of atomic orbitals allow a reasonable understanding in the high field situation of the atom probe.

Two important methodologies will be applied for performing the APT: i) metallic tips of Au and tungsten, produced by electro-polishing, will be shaped by field evaporation. Then, by dipping into respective solutions, we will deposit self-assembled monolayers to the apex of these tips. After washing and drying, tips will be reinserted into the atom probe and the monolayer is analyzed by laser-assisted field desorption. ii) Self-assembled monolayers will be deposited on flat metallic or oxide surfaces and shock-frosted together with and without the solvent. Then, a protecting coating (e.g. Cu or Ni) will be deposited. These samples are introduced into the new FIB/microtap instrument, in which tips are cut and afterwards analyzed by laser-assisted field desorption.

We will start these experiments with conventional alkyl-thiols and perfluorinated alkyl-thiols attached to Au for which we have already previous experience [C3-10]. We will also use mixtures of both kind of molecules (alkyl and perfluorinated chains). They can be well distinguished by the presence or absence of Fluor. In this samples, phase separation between the two surface components can be proven and statistical parameters (size and number of islands of second phase in dependence on the mixing ratio) of the decomposition can be determined. Within the CRC, templates of oxide ceramics (silica and alumina: **projects A4, A5**) are of particular interest. To address these systems, we will subsequently perform the analogous investigations with molecules that contain anchor groups of silane or phosphonic acids and link best to silicate or alumina surfaces, respectively. These types of linker molecules are also investigated in **A5**. We will exchange molecules with this project to enable a direct comparison. Required oxide surfaces will be produced by direct oxidation of the base metals or by reactive sputter deposition. In a later stage, also the polymer-oxide hybrids produced in **project A5** will be used as substrate.

As an interesting problem, we would like to clarify whether the field strength to evaporate the anchor group (S or O) is related to the bonding strength to the substrate. If such correlation could be confirmed, one could possibly use field desorption experiments even as a quantitative measure for the bonding strength. Furthermore, we will extend the experiments to molecules that are still immersed in the solvent. Via shock-freezing and FIB preparation, we will try to measure the molecules within the solvent environment. This situation closely resembles a small number of confined catalysts linked to the inner surfaces while embedded in a liquid solvent. If in a later stage of the collaboration the best-suited linker molecules have become clear, we are confident to replace in our experiments the model molecules by these optimized linkers. Having understood the principles of field desorption of the proposed model structures, even a reconstruction of the molecule conformation may become possible.

3.13.4.7 WP 7: Nanoanalysis of immobilized catalyst-linker systems (collaboration with B3, B2, C1)

With the techniques explored in WP 1-6, the porous matrices will be impregnated with solutions containing the catalyst-linker systems that are developed in the projects of section B. We will focus first on the catalysts produced in **project B3** linked to silica networks. The template material containing the immobilized catalyst together with the solvent will be shock frosted, prepared to needles by FIB cutting, and afterwards analyzed by atom probe tomography. In later stages, we will extend our investigations to the polymeric monoliths in combination with the catalyst systems produced in **project B2**.

All metal-organic catalysts developed in section B of the collaboration contain different heavy metal atoms as active centers (**B1**: Ru, **B2**: Mo, W, **B3**: Rh). In terms of their atomic mass, they well contrast to the linker and the organic shells of the catalysts and also to the solvents. Thus, the position of the active catalysts within the pores can be localized, if these metallic centers are discovered by the time of flight mass spectrometry. However, due to their extremely small number, such investigation is close to the limit of statistical feasibility. We are nevertheless confident to reach significance by averaging on multiple catalyst molecules to determine at least the regular position of the catalyst centers. Primary goal is at least to distinguish between pores loaded with one or two Rh centers. The colleagues in

project B3 have agreed to also produce contrast-enhanced variants of the linker or the organic part of the catalyst by replacing hydrogen with deuterium or Fluor, so that the complexes can be definitely proven by detection of several unambiguous atoms. In order to increase the chance of success, we also plan to improve the detection efficiency of the atom probe instrument to the maximum which is nowadays possible (increase from 50% to 85% detection probability). For this, the presently used micro-channel plates have to be replaced by state of the art ones offering the best sensitive open area ratio available.

For the understanding of the catalysis, it is important to clarify the density of active molecules as a function of the pore size, of the composition and polarity of the inner surfaces. The microscopic analysis shall also clarify the effective length and conformation of the linker molecules and thus the distance of active centers to the pore walls. Achieved microscopic data will be exchanged with **project C6** to compare the experimental observations with the predictions of MD simulations on the chain conformation. The MD data will also be used to optimize and verify the reconstruction schemes used in the tomography.

The analytical data on the distribution and linkage of the catalyst molecules will be secured by comparison to the results of NMR which will explore the local neighborhood of the molecules (**project C1**). In the case of successful installation of an aberration corrected microscope at the University of Stuttgart (see WP 8), we will also undertake the endeavor trying to identify single heavy atoms by local energy loss spectroscopy in high-resolution scanning transmission electron microscopy.

3.13.4.8 WP 8: TEM characterization of CRC materials (collaboration with A1 to A7)

Separated from the key research goals of our project in approaching APT to the problems of the CRC, we will provide electron microscopy analysis to the collaboration partners by established conventional methods. These comprise lift-out FIB preparation of thin cross sections, bright and dark field as well as high resolution phase contrast imaging, also fast screening by scanning electron microscopy. Presently, the chair of materials physics operates a transmission microscope equipped with a field emission gun that offers in structural imaging a point resolution of 2.5 Å and an information limit of about 1.5 Å. The spatial resolution in chemical analysis (EDX, EELS) is limited to about 1 to 2 nm. This performance is still fine to solve many standard problems in the development of the porous template materials, but it is certainly not sufficient to analyze individual catalyst molecules within their cavities. In view of the recent development in electron microscopy, our currently operated instrument is far from state of the art. Nevertheless, presently no better instrument is available at the University of Stuttgart.

Triggered by the CRC, but also justified by other materials-oriented research projects at the University, we, therefore, started an initiative to procure a state-of-the-art aberration corrected microscope which should be operated by the faculty of chemistry in a central University laboratory. Equipped with a pre-specimen corrector, a sensitive camera system and an outstandingly stable sample stage, such modern instrument promises tomography, in the ultimate limit, even in atomic resolution and single atom analytical sensitivity. These features are decisive for the key goals of the CRC in understanding single catalytic molecules in their interaction within a confinement in the nanometer range. The instrument will be the subject of a large equipment investment application under the art. 91b scheme of the DFG. The required proposal is presently prepared under lead management by this **project C3**. The state contribution to the budget is already secured by a commitment of the university so that a successful application and an installation within the first funding period of the CRC would be rather likely.

3.13.4.9. Chronological work plan:

		2018 Q3 Q4	2019 Q1 Q2 Q3 Q4	2020 Q1 Q2 Q3 Q4	2021 Q1 Q2 Q3 Q4	2022 Q1 Q2	
WP1	PhD I						Preparation of mesoporous model materials
WP2							Correlative microscopy of porous networks
WP3							FIB tomography of polymeric monoliths
WP4							Impregnation by liquid fillers and cryo-preparation
WP5							Atom probe analysis of filled pore structures
WP6	PhD II						Atom probe analysis of self-assembled monolayers
WP7							Nanoanalysis of immobilized catalyst-linker systems
WP8							TEM characterization of CRC materials

3.13.4.10 Methods applied:

Ion beam sputter deposition; electro-deposition; electro-polishing; field-emission scanning electron microscopy (FE-SEM); transmission electron microscopy (TEM): Analytical (energy dispersive spectrometry (EDS), electron energy loss spectroscopy (EELS), high resolution phase contrast imaging (HR-TEM); dual beam microscopy (FIB): FIB tomography; FIB nano preparation; Cryo-freezing; Laser-assisted atom probe tomography (LA-APT): time of flight spectroscopy (ToF), volume reconstruction, field ion microscopy (FIM).

3.13.4.11 Vision:

Beside the direct goals pointed out for the first funding period, the suggested work should lead to a general methodology of a microscopic analysis with close to single atom sensitivity of liquid/liquid and liquid/solid interfaces, at the final end even of proteins and complex biomaterials. The methods developed and discovered in the projected first funding period will be used in the later course of the research collaboration to extensive investigations of the transport and segregation processes, surface near concentration profiles and space charge zones within the open porosity. The comparison of the experimental concentration profiles with the results of the continuum modelling in **project C5** will lead to a comprehensive understanding of the reactive transport processes.

3.13.5 Role within the collaborative research center

The proposed project addresses the real structure/microstructure of the produced scaffold materials and will provide information on the spatial distribution and arrangements of the catalysts inside the confinement. In this role, the project is essential to check the scaffold structures that are produced in section A enabling a direct feed-back that allows optimization of these structures. Knowledge of the exact spatial arrangements of the active molecules is furthermore an important prerequisite for a target-oriented simulation by the theoretical **projects C4** to **C6** and an understanding of the catalytic behavior.

Besides the general collaboration within the CRC, we have planned more intensive cooperation with projects A1, A4 and A5 that will provide polymeric and ceramic scaffold structures or linker systems. Furthermore, we will address the block copolymers produced in **A2**, first with TEM methods and later with the new APT methods. The investigation of catalysts and linkers is first started with the systems provided in **project B3** combined with silica scaffolds. **B3** will even provide molecules especially tailored to improve the mass contrast in APT. In the further course, we will extend these investigations to the catalyst molecules and linkers produced in **B2** and **B1** in polymeric scaffolds and feed-back the microscopic data to the collaboration partners.

A particular intensive collaboration is planned with **project C4** working towards a fundamental understanding of the field-evaporation sequence and the formed molecular fractions. With **C6** we will

exchange and compare data on the conformation of linker molecules. Furthermore, the results of **project C1** by NMR will be compared and combined with the information of the APT to achieve a comprehensive understanding of neighbor relations, bonding and geometries of the molecule environment.

3.13.6 Differentiation from other funded projects

The proposed project may be seen in close relation to two other DFG funded projects SCHM 1182/16 and SCHM 1182/18, as these also address atom probe tomography and the latter even concerns catalysis. However, the former project is a purely theoretical work dedicated to improved reconstruction methods for conventional APT work. It has reached its final stage. In contrast, the now proposed project is clearly a fundamental experimental work that focuses on way different materials and structures. Nevertheless, we will try to use the results of our previous theoretical work as a starting base to improve the quality of analysis. The latter project addresses the catalytic function of Pt, Pd and PdPt alloy particles on washcoat supports with macroscopic geometries in real automotive catalysts. So, it addresses conventional solid state materials and classical heterogeneous catalysis rather than the mesoporous materials and metal-organic catalysts that are the subject of this CRC.

3.13.7 Project funding

3.13.7.1 Previous funding

This project is currently not funded and no funding proposal has been submitted.

References (ctd.)

[19] A. J. Forty, *Nature* **1979**, *282*, 597.
[20] J. Erlebacher, M. J. Aziz, A. Karma, N. Dimitrov, K. Sieradzki, *Nature* **2001**, *410*, 450.
[21] P.A. Midgley, M. Weyland, *Ultramicr.* **2003**, *96*, 413.
[22] A.J. Koster et al., *J. Struct. Biol.* **1997**, *120*, 276.

3.13.7.2 Requested funding

Funding for	2018		2019		2020		2021		2022		2018-2022	
Staff	Quantity	Sum	Quantity	Sum	Quantity	Sum	Quantity	Sum	Quantity	Sum	Quantity	Sum
PhD student, 67%	2	43,200.-	2	86,400.-	2	86,400.-	2	86,400.-	2	43,200.-	2	345,600.-
Total		43,200.-		86,400.-		86,400.-		86,400.-		43,200.-		345,600.-
Direct costs	Sum		Sum		Sum		Sum		Sum		Sum	
consumables	8,000.-		16,000.-		16,000.-		16,000.-		8,000.-		64,000.-	
Total	8,000.-		16,000.-		16,000.-		16,000.-		8,000.-		64,000.-	
Major research instrument-tation	Sum		Sum		Sum		Sum		Sum		Sum	
NOPA	88,500.-		-		-		-		-		88,500.-	
autocorrelator	20,400.-		-		-		-		-		20,400.-	
Total	108,900.-		-		-		-		-		108,900.-	
Grand total	160,100.-		102,400.-		102,400.-		102,400.-		51,200.-		518,500.-	

(All figures in EUR)

3.13.7.3 Requested funding for staff

	Seq. no.	Name, academic degree, position	Field of research	Department of university	commitment h/w	Category	Funding source
Existing staff							
Research staff	1	Guido Schmitz Dr., Full Prof.	Materials Physics Nanostructured Materials	Institute of Materials Science	4		University
	2	Patrick Stender, Dr.	Materials Physics APT instrumentation	Institute of Materials Science	6		University
	3	Efi Hadjixenophontos (Dr.)	Materials Science Electron microscopy	Institute of Materials Science	4		University
	4	Sebastian Eich (Dr.)	Materials Physics Materials simulation	Institute of Materials Science	2		University
Non-research staff	5	Peter Engelhardt Mechatronics		Institute of Materials Science	4		University
Non-research staff	6	Jacqueline Schimmel		Institute of Materials Science	2		University
Requested staff							
Research staff	7	n.n., PhD student	Materials Science/Physics	Institute of Materials Science		PhD	
	8	n.n., PhD student	Materials Physics	Institute of Materials Science		PhD	
	9	Research assistant	Materials Physics	Institute of Materials Science			

Job description of staff (supported through existing funds):
1
Full Professor, Head of the Institute, PI
2
Scientific coworker (Atom probe instrumentation, FIB preparation, tomographic reconstruction)
3
Scientific coworker (General TEM and SEM investigations, WP 8)
4
Scientific coworker (Computational materials science)
5
Technician, in charge of maintenance of UHV equipment, laser security, and electrical installations
6
Secretary

Job description of staff (requested funds):
7
PhD student, WP 1-5
8
PhD student, WP 6-7
9
Research assistants. **Justification for research assistants:** It is planned to engage master students during their thesis work in tasks such as sample preparation (thin film deposition, electrolytic preparation of nanometric tips, production of mesoporous metal films) as well as electron microscopy investigations performed within WP8 and so to bring them early into contact to exciting science.

3.13.7.4 Requested funding of direct costs

	2018	2019	2020	2021	2022
Uni Stuttgart: existing funds from public budget	4,000.-	8,000.-	8000.-	8,000.-	4,000.-
Sum of existing funds	4,000.-	8,000.-	8000.-	8,000.-	4,000.-
Sum of requested funds	8,000.-	16,000.-	16,000.-	16,000.-	8,000.-

(All figures in EUR)

Consumables for financial year 2018

Ga sources, FEG emitters, gluing cartridges, TEM grids, vacuum sealing, Laser diodes	EUR	8,000.-

Consumables for financial year 2019

Ga source, FEG emitter, Gluing cartridges, TEM grids, Vacuum sealing, Laser diodes	EUR	16,000.-

Consumables for financial year 2020

Ga source, FEG emitter, Gluing cartridges, TEM grids, Vacuum sealing, Laser diodes	EUR	16,000.-

Consumables for financial year 2021

Ga source, FEG emitter, Gluing cartridges, TEM grids, Vacuum sealing, Laser diodes	EUR	16,000.-

Consumables for financial year 2022

Ga source, FEG emitter, Gluing cartridges, TEM grids, Vacuum sealing, Laser diodes	EUR	8,000.-

3.13.7.5 Requested funding for major research instrumentation

Non-collinear Optical Parametric Amplifier	88,500.- EUR
Autocorrelator for laser pulses < 50 fs	20,400.- EUR

Our available ultra-short-pulse laser system (IR, 250 fs) will be extended by a pulse and frequency shaping unit that allows continuous variation of the wave length and a further shortening of the pulses. Together with the use of secondary and tertiary harmonics, we will be able to vary the wavelength continuously between 350 and 1050 nm, and the pulse width between 40 fs and 6 ps. In WP 6 and 7, we plan to explore to which extent the kind and order of evaporated molecular fractions in APT of macromolecular materials can be controlled by matching the wave length and pulse width. The autocorrelator is required to operate and maintain the NOPA.

3.14 Project C4

3.14.1 General information about Project C4

3.14.1.1 Simulation of chemical reactivities

3.14.1.2 Research Areas
Theoretical Chemistry (303-02)

3.14.1.3 Principal Investigator
Kästner, Johannes, Prof. Dr. born 30. 01. 1978, male, Austrian
Institut für Theoretische Chemie
Universität Stuttgart, Pfaffenwaldring 55, 70569 Stuttgart
Tel.: 0711/685-64473
E-Mail: kaestner@theochem.uni-stuttgart.de
Tenured Professor W3

3.14.1.4 Legal Issues
This project includes

1.	research on human subjects or human material.	no
2.	clinical trials.	no
3.	experiments involving vertebrates.	no
4.	experiments involving recombinant DNA.	no
5.	research involving human embryonic stem cells.	no
6.	research concerning the Convention on Biological Diversity.	no

3.14.2 Summary
The catalytic processes of this collaborative research center (CRC) will be modeled theoretically on an electronic and atomistic scale. Reaction mechanisms of the catalysts synthesized in area B will be investigated by electronic structure calculations, mainly using density functional theory. These will provide rate constants for the chemical steps of the catalysis and will lead to a detailed understanding of the reactions. The steric and electrostatic influence of the pore environment on the reactions will be simulated by a combined quantum/classical treatment of the whole system of the catalytic complex, reactants and products, linkers, the solvent and the pore in a QM/MM treatment. Besides rate constants for the chemical step in the pore, these simulations will provide structural data on the active catalysts and its arrangement within the pores as well as steric requirements during substrate binding and product release. The modeling will initially be done with COF pores and subsequently it will be extended to mesoporous silica. The kinetic data can be compared to the results from solid-state NMR experiments and will serve as input for the reactive lattice-Boltzmann simulations in **project C6**. The field desorption and fragmentation of molecules in atom probe tomography will be simulated from first principles. This will facilitate the interpretation of the experimental data of **project C3**, and will augment the extension of atom probe tomography to the investigation of soft matter. Overall, the simulations performed in this project model the smallest scales of the systems investigated in this collaborative center and will contribute to our fundamental understanding of the catalytic processes, which are developed within the CRC.

3.14.3 Research rationale

3.14.3.1 Current state of understanding and preliminary work
Catalytic processes can be simulated by several different theoretical approaches. Especially in heterogeneous catalysis, where many time and length scales need to be bridged, combinations of several techniques are necessary. This is the main reason why in this CRC we combine quantum chemical methods and QM/MM techniques for the smallest scale (**project C4**) with molecular dynamics and rare-event sampling techniques (**project C5**) for the medium scales and fluid theory (**project C5**)

as well as reactive lattice-Boltzmann techniques (**project C6**) for the largest scales. This combination will provide an overall description of the catalytic processes which occur in the pores studied here.
QM/MM, the combination of quantum mechanics (QM) and force fields (molecular mechanics, MM), is established as one of *the* main techniques to study chemical reactions under the influence of the chemical environment.[1] Typically about 50 to 200 atoms of the chemically active center, especially those that are directly involved in bond breaking or formation or those that take part in electron transfer, are treated by quantum chemical methods. Often electronic density functional theory (DFT) is used. The remainder of the system, in many cases several tens of thousands of atoms, is described by classical force fields. The latter describe interactions between the species accurately, but are unable to cover the breaking and formation of chemical bonds. QM/MM techniques will be used for the greater part of the present project.
The mechanisms of the three catalytic reactions which are to be investigated in this CRC: the autotransfer reactions of **project B1**, the olefin metathesis of **project B2,** and the 1,4-addition of boronic acids to enones of **project B3**, have been theoretically investigated to varying degrees. While the electronic structure of the catalytic metal complexes used in **project B1** was characterized by DFT calculations,[2–6] details of its mechanism are still unclear. The reaction consists of three distinct steps: the dehydrogenation of an alcohol with formation of a metal hydride at the catalyst, a condensation and imine formation, which is proposed to be non-catalyzed, and a hydrogenation to form a secondary amine, see Fig. C4.1.

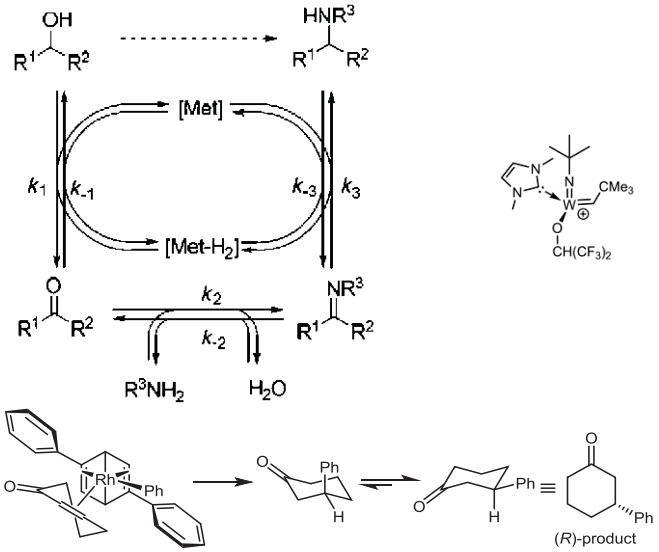

Figure C4.1: Top left: schematic representation of a catalyzed hydrogen autotransfer reaction studied in **project B1**, which leads from alcohols in a direct conversion to amines (figure from reference [4]). Top right: catalyst used in **project B2** for olefin metathesis. Bottom: enantioselective Rh-catalyzed 1,4-addition of phenylboronic acid to cyclohexenone in the presence of a chiral diene as studied in **project B3**.

Olefin metathesis using Schrock-type catalysts was simulated extensively in the literature, both the electronic structure of the catalytic complex[7, 8] as well as the reaction mechanism and possible side reactions.[9–11] The 1,4-addition of boronic acids to enones catalyzed by rhodium complexes was investigated theoretically.[12] That study suggested a mechanism, which will be the basis of our simulations. However, no studies in a confined environment have appeared to the best of our knowledge. The effect of linkers on the catalytic complexes, their spatial arrangement in pores and the effect of the pore environment on the reactivity are unknown.
Atom probe tomography is an established experimental method to analyze the chemical composition and 3D structure of materials in atomistic detail.[13] A very sharp tip of the material is subjected to high electrostatic voltage. The large curvature at the tip (small radius) leads to very high electric fields, which lead to ionization, fragmentation of molecules, and desorption. The ionized fragments are accelerated and reach a detector. The mass/charge ratio and the position are measured. Reconstruction of the trajectories provides information on the 3D structure of the initial sample. This technique will be used by the group of Prof. Schmitz in **project C3** to analyze catalytic complexes in pores. Since for many of the

materials used in this CRC the fragmentation pattern in a high field is unclear, theoretical support will aid the interpretation of the raw data.
Simulation of such processes is difficult, which is why it was rarely done in the literature. Field desorption is described phenomenologically with the image hump model, which describes the removal of a charged species from a conducting surface, or the charge exchange model, in which the removed species is charged only when reaching the top of the energy barrier.[14] Both describe the energy during the desorption of atoms from a surface only semi-quantitatively and can not describe fragmentation of molecules. Field desorption of atoms from a metal surface[15–17] and even insulators[18] was modeled by DFT in the literature. The field-fragmentation of fluorinated hydrocarbons was simulated[19] and compared to experiments[20] with limited success. The reason is the complexity of the processes, which lead to fragmentation and desorption. The strong field distorts the electronic structure, which itself can be included in the simulation in a straightforward manner by adding the operator for the electrostatic field to the Hamiltonian. However, the fragmentation and desorption are non-equilibrium processes which may require a significant amount of sampling. The problem shows some similarity to the simulation of the fragmentation of molecules in electron ionization mass spectrometry, for which successful simulations were recently reported in the literature for the first time.[21, 22] There, extensive molecular dynamics sampling and averaging was necessary, but this effort lead to excellent agreement with the experimental fragmentation patters. We will investigate how promising similar approaches are in the case of atom probe tomography.
Initial, very preliminary, calculations of molecules in strong electrostatic fields lead to the images shown in Fig. C4.2. There, linear n-hexane is subjected to an electric field of 0.03 atomic units (≈ 1.5×10^{10} V/m) along its molecular axis. The distortion of the electronic density is clearly visible.

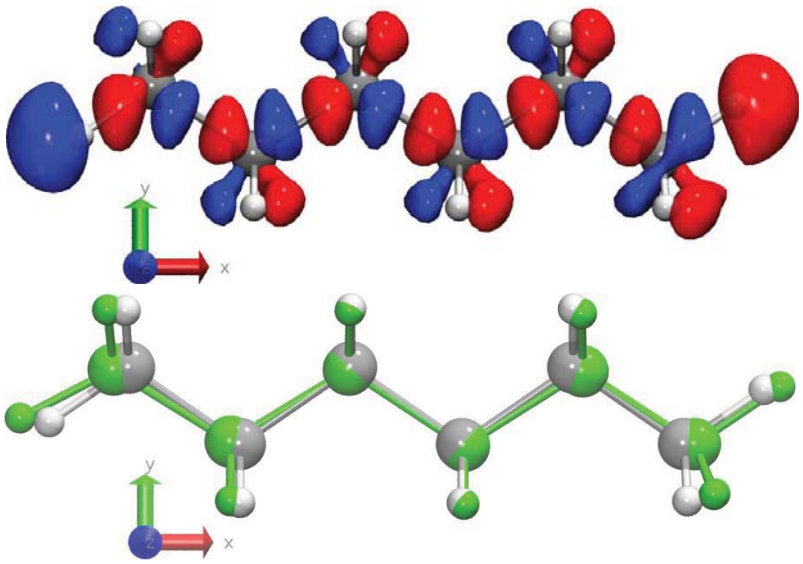

Figure C4.2: Preliminary results for an electric field in positive x-direction, which distorts the electron density of n-hexane. Top: Nuclear geometry of the equilibrium structure at zero field, electron density subject to an electric field of 0.03 at. u. compared to the zero-field density. Blue are areas with increased density, red with decreased density. The iso-surfaces are drawn at ±0.003 e/Bohr^3. Bottom: the green structure shows the distortion at higher field strength: 0.04 at. u. in x-direction, compared to the zero-field structure in gray/white. An even stronger field leads to the dissociation of H^+ or similar fragments to the right.

References

[1] H. M. Senn, W. Thiel, *Angew. Chem. Int. Ed.* **2009**, *48*, 1198–1229.
[2] E. A. B. Kantchev, *Chem. Commun*. **2011**, *47*, 10969–10971.
[3] S. Gosiewska, J. A. Raskatov, R. Shintani, T. Hayashi, J.M. Brown, *Chem. Eur. J.* **2012**, *18*, 80–84.
[4] D. Weickmann, W. Frey, B. Plietker, *Chem. Eur. J.* **2013**, *19*, 2741–2748.
[5] E. A. B. Kantchev, *Chem. Sci.* **2013**, *4*, 1864–1875.
[6] N. Sieffert, J. Boisson, S. Py, *Chem. Eur. J.* **2015**, *21*, 9753–9768.
[7] A. Poater, X. Solans-Monfort, E. Clot, C. Coperet, O. Eisenstein, *Dalton Trans.* **2006**, 3077–3087.
[8] F. Blanc, J.-M. Basset, C. Copéret, A. Sinha, Z. J. Tonzetich, R. R. Schrock, X. Solans-Monfort, E. Clot, O. Eisenstein, A. Lesage, L. Emsley, *J. Am. Chem. Soc.* **2008**, *130*, 5886–5900.
[9] A. Poater, X. Solans-Monfort, E. Clot, C. Copéret, O. Eisenstein, *J. Am. Chem. Soc.* **2007**, *129*, 8207–8216.
[10] X. Solans-Monfort, C. Copéret, O. Eisenstein, *Organometallics* **2012**, *31*, 6812–6822.
[11] X. Solans-Monfort, C. Copéret, O. Eisenstein, *Organometallics* **2015**, *34*, 1668–1680.
[12] H. Qin, X. Chen, Z. Shang, E. A. B. Kantchev, *Chem. Eur. J.* **2015**, *21*, 3079–3086.
[13] T. F. Kelly, M. K. Miller, *Rev. Sci. Instrum.* **2007**, *78*, 031101.
[14] R. Gomer, *Surf. Sci.* **1994**, *299*, 129–146.
[15] E. R. McMullen, J. P. Perdew, J. H. Rose, *Solid State Commun.* **1982**, *44*, 945–949.
[16] C. G. Sanchez, A. Y. Lozovoi, A. Alavi, *Mol. Phys.* **2004**, *102*, 1045–1055.
[17] T. Ono, T. Sasaki, J. Otsuka, K. Hirose, *Surf. Sci.* **2005**, *577*, 42–46.
[18] E. P. Silaeva, M. Karahka, H. J. Kreuzer, *Curr. Opin. Solid State Mater. Sci.* **2013**, *17*, 211–216.
[19] B. S. Nickerson, M. Karahka, H. J. Kreuzer, *Ultramicroscopy* **2015**, *159*, 173–177.
[20] A. Stoffers, C. Oberdorfer, G. Schmitz, *Langmuir* **2012**, *28*, 56–59.
[21] S. Grimme, *Angew. Chem. Int. Ed.* **2013**, *52*, 6306–6312.
[22] C. A. Bauer, S. Grimme, *J. Phys. Chem. A* **2016**, *120*, 3755–3766.
[23] G. Knizia, *J. Chem. Theory Comput.* **2013**, *9*, 4834–4843.

Preliminary work

The applicant has ample experience in the simulation of catalytic processes including the effects of the environment. Over a decade ago, he started to simulate enzymatic processes using the QM/MM approach. Already then he started to co-develop the ChemShell code,[C4-1] a flexible program suite, which couples several stand-alone quantum chemistry and force field codes. This allows for computational efficiency, since most of the computer time is spent on the quantum mechanical calculations and the flexible design of ChemShell allows to pick the quantum chemistry code which is most efficient for the specific molecular system and the desired degree of parallelization on the computer hardware.
The applicant is the lead developer of the general-purpose geometry optimization library DL-FIND,[C4-2] which is interfaced to ChemShell. It focuses on geometry optimization and transition state search algorithms in high dimensional systems, which frequently occur in large QM/MM setups. Besides a linearly scaling minimizer based on internal coordinates, the applicant developed a super-linearly converging variant of the dimer method[C4-3] to find transition states in many thousand degrees of freedom, which will be important for the present project. The transition state search is particularly efficient as the calculation of Hessian matrices is avoided. The dimer method is a surface-walking algorithm. Chain-of-states methods like nudged-elastic band and the string method are also available within DL-FIND.
To calculate free energy differences, the applicant has developed several sampling techniques. The main one is umbrella integration, which allows calculating the mean force, which traditionally is obtained in thermodynamic integration, from umbrella sampling simulations. This was extended to multidimensional free-energy surfaces with particular focus on the identification of minima and transition states without characterizing the whole surface. Free-energy barriers obtained from umbrella sampling, combined with transition state theory allow to estimate rate constants of processes which are many orders of magnitude slower than the longest time scales which can be reached by direct molecular dynamics.

To calculate rate constants at lower temperature, the applicant has developed an improved version of instanton theory to estimate the effect of atom tunneling on rate constants. This theory is regularly applied and further developed in the applicant's group in the course of his ERC Consolidator grant project. It is applicable to the large systems studied in this CRC. However, since it is unlikely that tunneling effects will play a significant role for the catalytic processes studied here, the application of instanton theory will probably not be necessary.
In the area of enzyme catalysis, the applicant's group recently unraveled the reaction mechanism of enzymes, e.g., salicylate dioxygenase[C4-4] or taurine/α-ketoglutarate-dependent dioxygenases, by means of QM/MM simulations. In all these cases, reaction mechanisms were solved and rate constants were calculated for complex reactions under explicit treatment of environmental effects. The challenge to a theoretical description is similar to that found in catalysis in pores, as it will be studied in this CRC. While the applicant initially mainly focused on enzymatic catalysis, he recently extended his scope to catalytic processes on ice surfaces as they occur in the interstellar medium.[C4-5] The same program infrastructure and the same set of methods is now to be used to simulate catalytic processes in pores.
Catalytic processes in the homogenous phase were simulated in the applicant's group several times before, often already in cooperation with partners from this new CRC initiative. In cooperation with Prof. Plietker (**project B1**), the applicant uncovered details in the carbonylation of alkyl halides using $[Fe(CO)_3(NO)]^-$ and shed light on the catalytic activity of that complex.[C4-6] With Prof. Buchmeiser (**projects B2**,**A1**) he used intrinsic bond orbitals[5] (IBOs) to explain the effect on catalysis of structural changes in Mo complexes capable of catalyzing metathesis reactions[C4-7] and calculated Tolman's electronic parameters for ligands in similar catalysts.[C4-8] Other processes in homogenous catalysis were simulated, in general in cooperation with experimental partners.[C4-9, C4-10]
The applicant is well connected with other members of this CRC. Besides the above-mentioned publications, he has co-supervised theses with S. Naumann (**project A6**), B. Plietker (**project B1**), N. Hansen (**project C5**), M. Fyta (**project C6**) and C. Holm (**project C6**).

3.14.3.2 Project-related publications by participating researchers

[C4-1] S. Metz, J. Kästner, A. A. Sokol, T. W. Keal, P. Sherwood, *WIREs Comput. Mol. Sci.* **2014**, *4*, 101–110.
[C4-2] J. Kästner, J. M. Carr, T. W. Keal, W. Thiel, A. Wander, P. Sherwood, *J. Phys. Chem. A* **2009**, *113*, 11856–11865.
[C4-3] J. Kästner, P. Sherwood, *J. Chem. Phys.* **2008**, *128*, 014106.
[C4-4] S. Roy, J. Kästner, *Angew. Chem. Int. Ed.* **2016**, *55*, 1168–1172.
[C4-5] L. Song, J. Kästner, *Phys. Chem. Chem. Phys.* **2016**, *18*, 29278–29285.
[C4-6] J. E. M. N. Klein, G. Knizia, B. Miehlich, J. Kästner, B. Plietker, *Chem. Eur. J.* **2014**, *20*, 7254–7257.
[C4-7] S. Sen, W. Frey, J. Meisner, J. Kästner, M. R. Buchmeiser, *J. Organomet. Chem.* **2015**, *799*, 223–225.
[C4-8] M. Koy, I. Elser, J. Meisner, W. Frey, K. Wurst, J. Kästner, M. R. Buchmeiser, *Chem. Eur. J.* **2017**, *23*, 15484–15490.
[C4-9] L. Nunes dos Santos Comprido, J. E. M. N. Klein, G. Knizia, J. Kästner, A. S. K. Hashmi, *Angew. Chem. Int. Ed.* ***2015****, 54*, 10336–10340.
[C4-10] D. Brodbeck, F. Broghammer, J. Meisner, J. Klepp, D. Garnier, W. Frey, J. Kästner, R. Peters, *Angew. Chem. Int. Ed*. **2017**, *56***,** 4056–4060.

3.14.4 Project plan

In summary, the research goals are organized in work-packages as follows:

- **WP1: Establishing suitable methods** for the simulation of the reaction mechanisms studied in area B is necessary for the subsequent WPs of our **project C4**. Benchmark calculations will provide a sound theoretical foundation for predictive simulations during the further course of this CRC.
- **WP2: Reaction mechanisms and rate constants** will provide the intrinsic reactivity of examples of the three types of reactions of area B. Data will be verified by NMR by **project C1** and will, together with the spectroscopic evidence from **project C2** provide input for the reactive lattice-Boltzmann simulations in **project C6** and lead to a detailed understanding of the reaction mechanisms. It will provide structural information on the size of the encounter complexes and the transition states, which will be important for the design of pore sizes and pore geometries.
- **WP3: Force field parameters for COFs** and their interactions with solvents, linkers, catalytic complexes and substrates/products are necessary for the subsequent QM/MM modeling of the catalytic processes in pores. The parameters will also be used by the other theory projects in their molecular dynamics studies.
- **WP4: Influence of the pore environment.** This is one of the main tasks of this project. COF pore geometries from **project A3** will be used to model the arrangement of the catalytic complex, substrates and products, the linker, the solvent and the pore. Barriers and reaction energies will be calculated in a QM/MM setting. This will provide rate constants of the chemical step, geometries of the active catalytic complex and information on the steric requirements. These studies will initially be performed for COF structures. The examples of catalytic complexes from all three projects in the B-area will be modeled, starting with the ruthenium-complexes of **project B1**. The interacting structures as well as the kinetics will be compared to the data from solid-state NMR experiments performed in **project C1**. The kinetic data from the chemical step together with the diffusion constants obtained in **project C5** will allow the calculation of turnover frequencies.
- **WP5: QM/MM simulations in silica pores.** Here, we will investigate the reactivities of the above-mentioned catalytic complexes in silica pores with a QM/MM approach. The force field for the surrounding of the active complex, along with the encounter structures, will be obtained from the MD simulations in **project C5**. The pore geometries found in **project A4** will be used. We will calculate reaction barriers and from those rate constants of the chemical process. Combined with the diffusion kinetics, these will result in turnover frequencies.
- **WP6: Simulation of field desorption in atom probe tomography** will provide computational support for the atom probe tomography experiments performed by Prof. Schmitz in **project C3**. We will model the behavior of molecular structures in the influence of strong electrostatic fields. Initially we will model structures for which the fragmentation patterns are well known, so that we can gain experience and calibrate our computational protocol. Then, the fragmentation patterns of novel soft substances, such as the pore materials used in this CRC, will be modeled alongside the experimental observations made in **project C3**. Knowledge about the field desorption and fragmentation will facilitate the reconstruction of the information on the material composition from the measured abundances in **project C3**.

3.14.4.1 WP 1: **Establishing suitable methods** is necessary to describe reaction mechanisms in solution and in pores adequately on a reliable theoretical basis. In order to be able to model the influence of the pore and the confined geometry on a reaction, an accurate description of the reaction itself is required. To achieve that, examples of the autotransfer reactions of **project B1**, the olefin metathesis of **project B2** and the 1,4-addition of boronic acids to α,β-unsaturated ketones in dioxane/water or THF/water mixtures of **project B3** will be simulated. The catalytic complexes including the anchor groups for the linker, i.e., triazole groups from the click reaction, will be modeled. In case of the ruthenium-catalyzed hydrogen-autotransfer reactions, the three different steps will be investigated separately. The influence of linker positions on the structural and energetic properties is to be studied.
The reactions will be described with density functional theory (DFT), with solvent effects approximated by continuum methods, as successfully used by the applicant in previous projects [C4-6, C4-9]. Reaction barriers ($\Delta^{\neq}G$) will be compared to experimental turnover rate constants. Comparison to

benchmark calculations, like single-point energies on L-CCSD(T)-F12 level, will be performed where possible (probably on smaller model complexes). These will allow for the choice of an adequate density functional to describe the individual reactions with sufficient accuracy. Besides a well-justified choice of methods, these investigations will provide information on chemical requirements of the specific reactions in their environment: steric as well as electrostatic properties during the chemical turnover can be obtained, which are relevant for the embedding of the reactions in pores that are to be studied in the following work packages. Especially in the autotransfer reactions, the different solubilities of the reactants and products in protic and aprotic solvents will provide opportunities for the immobilization in pores. These need to be well defined based on the quantum chemical simulations of this work package.

3.14.4.2 WP 2: Reaction mechanisms and rate constants of the reactions mentioned in WP 1 will be investigated. Previous mechanistic proposals will be tested by calculating reaction paths and reaction barriers. Using transition state theory, we will use these to calculate rate constants of the chemical step of the conversion. Those can be compared to experimental kinetic data measured by in situ IR, e.g. in **project B1**. Our calculated rate constants refer to the chemical conversion. These will be used in the reactive lattice-Boltzmann simulations by Prof. Holm in **project C6**. To obtain a turnover frequency, diffusion must additionally be taken into account, which will be simulated in **projects C5** and **C6**. The rate constant of the chemical step provides, however, a lower bound to the turnover frequency.
To aid the ligand design in **project B1**, we will model their ruthenium complexes with several different ligands and anchor groups for the linkers. Previously[4] a clear correlation between the stability of the HOMO and the redox potential was found, which relates to the catalytic efficiency. Similar quantities will be calculated for a larger set of ligands. The reactivity of the bare catalysts will be compared to that of the catalyst with linkers attached.
Spectroscopic data such as vibrational frequencies and NMR parameters will be calculated and compared to results of the measurements performed in **project C1** and **project C2**. In situ solid-state NMR investigations in **project C1** show which intermediates occur and provide data on their reactivity. These can be directly compared to the results of our simulations.
To gain more insight into the electron flux during such reactions, intrinsic bond orbitals[5] (IBOs) will be calculated and followed during the course of the reaction, see Fig. C4.3. These can provide hints on a possible electrostatic influence of the pore on the reaction. Furthermore, IBOs can be used to optimize ligands with respect to their electronic properties.

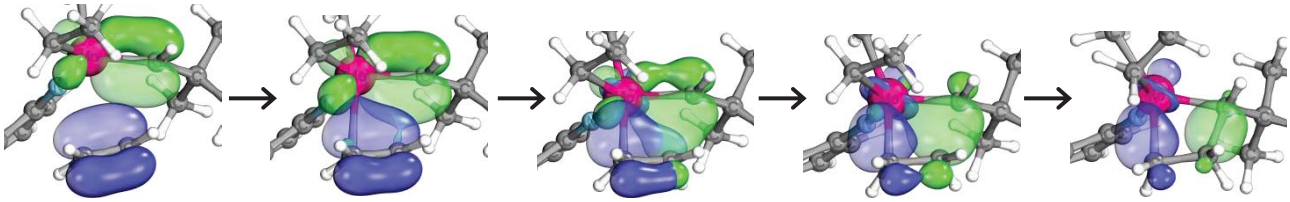

Figure C4.3: Intrinsic bond orbitals allow for the monitoring of specific orbitals during a chemical reaction, here the first step of a metathesis reaction, the association of C_2H_4 to the Mo-catalyst, as studied in **project B2**. Note how both orbitals originate as π-orbitals of the double bonds and continuously change to σ-orbitals of the new single bonds during the course of the reaction.

3.14.4.3 WP 3: Force field parameterization for COFs. In order to describe the environment of the reactive center in an efficient and accurate way, the solvent, linker and pore materials must be described by empirical atomistic force fields. Those are readily available for the usual solvents as well as for some pore materials. The first set of materials to study in this project will be the covalent organic framework (COF) pores of **project A3**. This choice is based on several reasons. The COF structures are quite well defined. The molecular connectivity is known. Thus, accurate structural models can easily be built up. However, interlayer displacements as well as layer bendings are less well characterized. They will have only a minor influence on the structural model. Apart from that, the pores are with diameters of 2–5 nm rather small and, thus, save computational power. An initial, very preliminary, force field model of a COF is shown in Fig. C4.4.

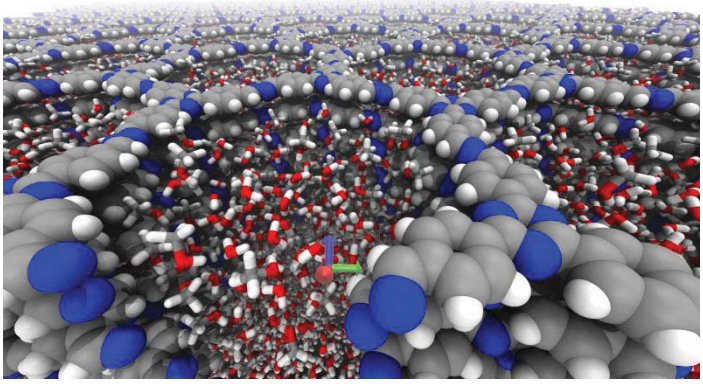

Figure C4.4: A COF structure resulting from preliminary MD simulations including a mixture of water and methanol as solvent. The pore size of this particular COF is 2.5 nm.

For COF structures, some force fields were proposed in the literature. We will base on these and adjust them to the actual COF variants designed by Prof. Lotsch in **project A3**. The linker molecules will be parameterized with special focus on the triazole rings from the click reactions. Initially, the focus lies on the hydrogen autotransfer reaction of **project B1**, where toluene is used as a solvent. Interaction of the pore with the linker and solvent needs to be parameterized, the interaction with the catalyst and the reactants will be handled by DFT in WP 4. Interactions with THF, dioxane and water will also be parameterized to allow the extension to **projects B2 and B3**. This will provide insight on the mechanical stability and stiffness of the linkers, which has an indirect influence on the positioning of the metal complexes in the pore.
Force fields for COFs can sometimes be approximated based on homology to already existing chemical building blocks. This was used to generate the preliminary data for Fig. C4.4. To obtain force fields which allow for qualitatively or even quantitatively predictive simulations their parameters need to be parameterized against DFT data and to experimental results. DFT data will mainly be used for the parametrization of internal degrees of freedom. The experimental interlayer distance is important to adjust the dispersion parameters between the layers.
The force fields developed here will be used in the QM/MM modeling in WP 4 as well as in the molecular dynamics studies in the other theory projects (**project C5** and **project C6**).

3.14.4.4 WP 4: Influence of the pore environment. The influence of the pore environment was modeled primarily via changes in the dielectric constants of the surrounding as a first approximation in the previous work packages. A more accurate investigation will be performed via QM/MM modeling of parts of the pore: the catalytic complex, the substrates, the solvent as well as the linker and the pore wall. As usual in the QM/MM approach, the chemically active part of the system (typically the catalytic complex and the substrates, generally about 100 atoms) are described by DFT (quantum mechanics, QM), the environment is described by force fields (molecular mechanics, MM). To achieve that, the functionals identified in WP 1 will be used. The QM/MM simulations will be performed for COF pores with the force fields parameterized in WP3. We plan to study examples of all three reaction types of the B area. In the case of Rh-complexes of **project B3**, the possible interactions of two Rh-complexes immobilized in close proximity will be studied. This is relevant as they are immobilized as dimers, and then activated to work as monomeric catalysts. A schematic view of catalytic complexes in a TFPT-DETH-COF (idealized geometry without interlayer displacement) is given in Fig. C4.5 to visualize the steric demands.

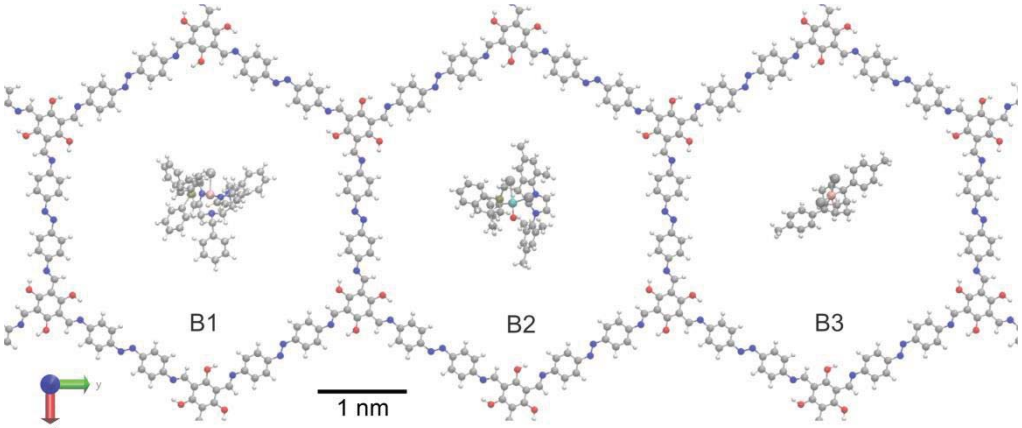

Figure C4.5: Schematic comparison of the pore sizes of an azobenzene COF in an idealized geometry with typical catalytic metal complexes used in area B. Linkers are omitted.

The PI's group has extensive experience in the QM/MM treatment of chemical reactions in soft and flexible environments, originally particularly enzymes. These techniques and the associated programs will be extended to catalysis in pores. As employed successfully in the past, our QM/MM program suite ChemShell will be used. It is interfaced to over a dozen quantum chemistry codes and three force field engines. Thus, it allows for enormous flexibility concerning the most efficient choice of QM programs, which determine the required CPU time, and force field programs, which must be chosen based on the availability of force fields for specific systems. We expect that most of the simulations will be performed with Turbomole as the QM code and DL-Poly as the MM code. Due to its flexible architecture, ChemShell can easily be adjusted to the requirements of new projects and, thus, allows for truly innovative science.
The interaction of substrates with the metal complexes modeled in a realistic environment will be compared to the results of solid-state NMR experiments performed in **project C1**. Differences in the reactivities between solution and in the pore can be directly compared to the NMR data.
Fig. C4.6 shows a schematic illustration of the multiscale modeling of the processes in a pore as they will be performed in cooperation with **projects C5** and **C6**.

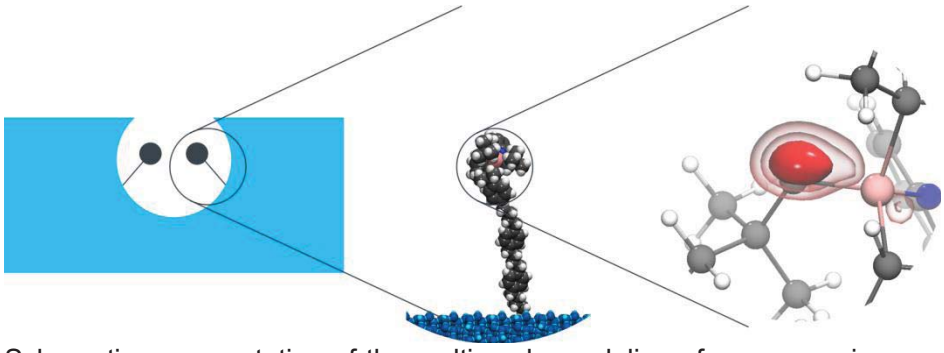

Figure C4.6: Schematic representation of the multi scale modeling of processes in a pore as it will be performed in this CRC.

3.14.4.5 WP 5: QM/MM simulations in silica pores. The force fields to describe mesoporous silica, which is synthesized in **project A4**, are developed in the group of N. Hansen in **project C5**. In WP 5 we will use those in collaboration with **project C5** to evaluate reaction barriers and reaction enthalpies of the above-mentioned catalytic processes in silica pores. These pores are significantly larger than the COF pores modeled in WP 4. The structural arrangements of the metal complexes and solvents in functionalized silica pores will be obtained from molecular dynamics simulations by **project C5**. We will then combine these with our quantum chemical models of the catalysis to obtain realistic predictions of the reactivates, which can be compared to our results from the catalytic complexes in COF structures and with the experimental turnover frequencies.

3.14.4.6 WP 6: Simulation of field desorption in atom probe tomography. In **project C3** the technique of atom probe tomography (APT) will be extended to soft matter. While this method is established in the analysis of metallic and meanwhile also hard insulating samples, the fragmentation and field desorption of macromolecular structures is not well understood. In WP 6 of this project, the fragmentation of molecules in strong electric fields (in the order of 10^{10} V/m) will be simulated. We will find out which fractions are produced in which order. This will facilitate the interpretation of APT measurements performed in **project C3**. To achieve that, strong electrostatic fields will be included in the Hamiltonian and the Kohn-Sham equations will be solved self consistently with this additional term. The necessary algorithms are available in several electronic structure codes, e.g. Turbomole. The results of very preliminary calculations are depicted in Fig. C4.2.
The simulation of the basic processes of APT is a new field with hardly any previous literature available. While the basic theoretical framework is clear, it is not known a priory how well the real measurements can actually be reproduced. We will have to find out how large the structural models have to be, how much sampling is necessary and, thus, what the necessary computational effort is. WP 6 certainly is a venturos part of the project, with potential high gain. The direct interaction with the group of Prof. Schmitz (**project C3**) will increase the chances of success. If it turns out that these simulations fail, the impact on the project as a whole will be small. A possible fallback option is to calculate bond energies in the absence of an external field and estimate the fragmentation patterns from those.
Initially, the simulations will be restricted to small model systems of organic molecules (alkane chains, possibly perfluorinated, anchored by thioles or silanes) for which the experimental fragmentation is known. Later, after some experience was gained, we will extend the simulations to organic polymers of **project A1** and / or the silicate materials studied in **project A4**.

Chronological work plan:

	2018		2019				2020				2021				2022		
	Q3	Q4	Q1	Q2	Q3	Q4	Q1	Q2	Q3	Q4	Q1	Q2	Q3	Q4	Q1	Q2	
WP 1																	Establishing methods (PhD 1)
WP 2																	Mechanisms (PhD 1)
WP 3																	Parameters COF (PhD 2)
WP 4																	Influence of COF pores (PhD 1)
WP 5																	Silica pores (PhD 2)
WP 6																	Field desorption, APT (PhD 2)

3.14.4.7 Methods applied: The simulations in this part of **project C4** will mainly be performed with quantum chemical methods. Density functional theory will be used for the majority of the reactivity studies. The choice of the basis set and functional will be based on comparison with experimental data and with benchmark calculations on the level of explicitly correlated coupled cluster theory with single and double excitations and triple excitations taken into account perturbatively (CCSD(T)-F12). All calculations will be performed with the ChemShell code, which performs geometry optimizations, transition state search, molecular dynamics and file handling. The quantum chemistry is done by standalone codes. ChemShell is interfaced to more than 10 electronic structure codes. The CCSD(T)-F12 calculations will be performed by Molpro interfaced to ChemShell, the DFT calculations by turbomole or NWchem, depending on the availability of the functionals which turn out most promising in the benchmark. Dispersion correction of at least Grimme-D3-type will be used. The same approach has been used successfully for many projects in the applicant's group.
Intrinsic bond orbitals,[5] see Fig. C4.3, will be used to monitor the rearrangement of electrons along chemical reactions. They are a chemically intuitive way of localizing orbitals, which can be used to track the change of a molecular orbital during a chemical reaction.
The QM/MM simulations will also be performed using ChemShell. For the quantum mechanical part, the same quantum chemical methods and codes as above will be used. The force field (MM) part will be handled by DL-Poly, which is included in ChemShell. For the COFs, force files in the Charmm format will be used. Initial parameters will also be chosen in homology to existing Charmm fragments (residues). Parameterization will improve the force fields, however. The DL-FIND code within

ChemShell, primarily developed in the applicant's group, provides a linear-scaling geometry optimizer based on internal coordinates, which allows for efficient minimizations of large systems. A superlinearly converging variant of the dimer methods makes it possible to locate transition states in many thousand degrees of freedom without ever calculating the full Hessian matrix. This is highly beneficial to study reaction barriers of the catalytic processes in pores, which are investigated in this CRC.
The simulation of molecular structures in high electric fields requires several components. The static electric field can be included in the Hamiltonian in a straightforward manner. Ionization will be dealt with as ad-hoc process by removing electrons. It is much more challenging to find out how much sampling is required and how large the structural models need to be. A protocol to simulate a similar process, ionization mass spectrometry, was recently proposed.[21, 22] We will investigate comparable approaches of fast, parameterized semi-empirical quantum mechanical treatment based on a tight binding scheme. These will speed up the calculations. We will endeavor to keep the accuracy high enough for predictive simulations of the fragmentation processes.
In cooperation with the other theory groups, these methods will allow a truly multi-scale simulation of the whole catalytic process including transport of substrates to the metal complex and removal of products.

3.14.4.8 Vision: By the end of the first funding period we aim, in cooperation with the other theory groups in the CRC, for a comprehensive theoretical description of the processes leading to catalysis in pores in COFs and silicate material. Together with the synthetic research in areas A and B and the measurements in C, we aim at a global understanding of the synergism between pore dimensions, their functionalization, linker lengths, the catalytic centers and their influence on the activity, productivity and selectivity. A thorough understanding which quantities need to be known accurately and which are less important to explain the catalytic processes and their efficiency (TOF and stability / TON) is expected. Based on that, the studies can be expanded to further classes of materials and possibly other catalytic processes. Ideally, the simulations require less detail for each specific combination based on what we have learned from the detailed studies in the first period. As a vision for a third funding period, we expect suggestions for improvement of material properties and new materials or functionalization.

3.14.5 Role within the collaborative research center
This project links between the experimental design and investigation of the catalytic complexes in the B-area and the measurements and simulations in area C under the influence of the pore materials, which are designed in area A. Within the simulations, C4 covers the smallest length and time scales by simulating the chemical processes during the catalysis with quantum mechanical and QM/MM methods. The differentiation within the theoretical projects is based on methods and on systems studied: quantum chemistry is used in **projects C4** and **C6**, where **C4** approaches the overall goal from the catalysis side modeling mechanisms and reactivities, while **C6** focuses on materials properties. Both use QM techniques to parameterize force fields, but for different systems. Atomistic molecular dynamics is used in all three theory-projects: in **C4** on COFs, in **C5** on silica, and in **C6** on the materials from **projects A2** and **A5**, whereas coarse grained methods are dealt with only in **C6**. Fluid theoretical methods like classical DFT are used only in **project C5**, while the lattice-Boltzmann method is used exclusively in **project C6**.
Examples of the reactions studied in **projects B1**, **B2** and **B3** will be simulated, which provides barrier heights and rate constants of the chemical steps in solution and in the pores, which can be compared to the experimental data from area B. Changes in the electronic structure, which we simulate with quantum chemistry, can be compared to the spectroscopy performed in **project C2**. WP 2 provides structural data, e.g., of the encounter complexes, which allow the steric design of pores and leads to an estimate of the actual confinement within the pores. This may lead to the re-design of ligands (bulkier or less bulky) in **projects B1**, **B2** and **B3** in order to better align in the pores. In WP 4 we use the structural analysis of bare COF structures (characterized primarily by X-ray powder diffraction, solid-state NMR and transmission electron microscopy) by **project A3** to build up our structural model. We will be able to provide data on the effective pore size of the COFs to **project A3** by simulating the interlayer displacement and possible bending of the layers. The arrangement of the catalytic complexes in the COF pores, the polarity gradient depending on the pore functionalization, and the flexibility of the linker molecules will also be provided by our WP 4. These data can directly be compared to the data obtained by solid state NMR in **project C1**.
In WP 5 we use the force field description of silica pores developed in **project C5** based on the structural data by **project A4**. Based on the arrangement of the catalytic complexes in the silica pores

identified in **project C5**, we provide data on the reactivity and on possible intermediates, which will be verified with NMR data from **project C1**. The arrangement of the catalytic complexes within the pore can be compared to the APT-results obtained in **project C3**. Different functionalization of the pore wall is expected to lead to different reactivity, which can be modeled directly.
Steric and structural data, although primarily simulated for COFs and silica materials in the first funding period, will also influence the choice of pore geometries of the other materials, like monoliths in **project A1**, and block copolymers in **project A2**.
Our DFT studies in WPs 1 and 2 will provide geometries and force fields for the catalytic metal complexes and their interactions with solvents, linkers and COF pore walls to the molecular dynamics projects **projects C5** and **C6**. The rate constants of elementary processes will be used by the reactive lattice-Boltzmann simulations in **project C6**. The force fields for silicates and their interactions with the other components will be developed by **project C5** and used by us and by **project C6**. Atomistic molecular dynamics in **C5** and coarse grained molecular dynamics in **project C6** will provide structural data on the arrangement of all components within the pore, which can be used by our simulations of reaction barriers in a QM/MM framework.
Atom probe tomography in **project C3** will be essential to obtain experimental evidence for the structural arrangement of the active components (catalytic complex, linker, substrates, products) within the pore. While this technique is well established for the analysis of metallic samples, it has recently been extended to insulating solid substances. Within this CRC, it will be further extended to soft materials, like the ones used as pore materials. It is not clear from the outset how, e.g., organic polymers respond to the field ionization and field fragmentation. This will be supported by the simulation of such organic materials in very strong electric fields in our work package WP 6. Initially, organic materials for which the fractionation pattern is known by **project C3** will be simulated in order to find out which methods to use. Later, predictive simulations are expected to facilitate the analysis of ATP raw data by **project C3** and to help to elucidate the spatial arrangements of different components within the pore.
Overall, our **project C4** links between input from the synthetic groups in area B and the materials design in A and provides mainly structural information and data on the reactivity under the influence of ligands, linkers and the pore environment.

3.14.6 Differentiation from other funded projects

Project C4 has no topical overlap with any other projects of the PI's group. The PI leads several other projects funded by the DFG and the ERC, specifically:

ERC Consolidator grant "TUNNELCHEM, Atom-Tunneling in Chemistry", 07.2015–06.2020: Deals with the calculation of tunnel effects on reaction rates in different areas of chemistry and method development to improve the available computer codes. Codes to calculate classical rate constants developed in that project will be used in the current proposal. Otherwise there is no overlap with the current proposal.

CRC-project C.6 "Minimum Free Energy Path Calculated using Umbrella Sampling Simulations" within the DFG-funded CRC 716 "Dynamic Simulation of Systems with Large Particle Numbers", 01.2015–12.2018, which deals with free-energy sampling techniques and has no overlap with the current proposal.

CRC-project C.8 "Molecular Dynamics Simulations for the Detection of Unfolding Pathways and Stable Conformations of DNA G-quadruplexes" within the DFG-funded CRC 716 "Dynamic Simulation of Systems with Large Particle Numbers", 01.2015–12.2018, which deals with application of free-energy sampling techniques to DNA structures and has no overlap with the current proposal.

Project "Interpolation of Potential Energy Surfaces using Gaussian Process Regression," 11.2017–12.2018 within the SimTech Cluster of Excellence has no overlap with the current proposal.

3.14.7 Project funding

3.14.7.1 Previous funding

This project is currently not funded and no funding proposal has been submitted.

3.14.7.2 Requested funding

Funding for	2018		2019		2020		2021		2022		2018-2022	
Staff	Quantity	Sum	Quantity	Sum	Quantity	Sum	Quantity	Sum	Quantity	Sum	Quantity	Sum
PhD student, 67%	2	43,200.-	2	86,400.-	2	86,400.-	2	86,400.-	2	43,200.-	2	345,600.-
Total		43,200.-		86,400.-		86,400.-		86,400.-		43,200.-		345,600.-
Direct costs	Sum		Sum		Sum		Sum		Sum		Sum	
consumables	800.-		1,500.-		1,500.-		1,500.-		800.-		6,100.-	
Total	800.-		1,500.-		1,500.-		1,500.-		800.--		6,100.-	
Major research instrumentation	Sum		Sum		Sum		Sum		Sum		Sum	
	-		-		-		-		-		-	
Total	-		-		-		-		-		-	
Grand total	44,000.-		87,900.-		87,900.-		87,900.-		44,000.-		351,700.-	

(All figures in EUR)

3.14.7.3 Requested funding for staff

	Sequential no.	Name, academic degree, position	Field of research	Department of university or non-university institution	Project commitment in hours per week	Category	Funding source
Existing staff							
Research staff	1	Johannes Kästner, Prof.	Theoretical Chemistry	Institute for Theoretical Chemistry	4		University
Research staff	2	Sonia Alvarez Barcia, Dr.	Theoretical Chemistry	Institute for Theoretical Chemistry	16		University
Non-Research staff	3	Ines Lombardi		Institute for Theoretical Chemistry	2		University
Requested staff							
Research staff	4	Max Markmeyer, M. Sc.	Theoretical Chemistry	Institute for Theoretical Chemistry		PhD	
Research staff	5	Robin Schuldt, M. Sc.	Theoretical Chemistry, molecular Physics	Institute for Theoretical Chemistry		PhD	
Research staff	6	Research assistant	Theoretical Chemistry, molecular Physics	Institute for Theoretical Chemistry			

Job description of staff (supported through existing funds):

1: Principal investigator for **project C4**

2: Dr. Sonia Alvarez Barcia, a postdoctoral researcher in the group of the PI, has performed the initial parameterization of the COF structures shown in Fig. C4.4. Moreover, she has ample experience in performing QM/MM simulations. She will train both students so that they are able to perform WPs 3, 4, and 5.

3: Secretary

Job description of staff (requested funds):

4: PhD student, work packages 1, 2, and 4: The quantum chemical calculations in WPs 1 and 2 will be performed by one PhD student along with the QM/MM simulations of the reactions in the COF structure. A well-trained theoretical chemist will be required to achieve these tasks.

5: PhD student, work packages 3, 5, and 6: The second PhD student will focus on WP6, the simulation of APT process for the majority of the work. This is a risky project, so a safe side project is necessary to ensure the achievement of a PhD even if major obstacles are encountered in WP 6. Thus, PhD student 2 will initially parameterize the force fields for the COFs (WP3), which is required before WP 4 can start and is too much work for student 1 additionally to WPs 1 and 2. As an additional safe side project, student 2 will perform the QM/MM modeling of catalysts in silica pores in WP5 as soon as the respective force fields are available from **project C5**. To perform the quite formidable WP 6, a well-trained physicist or chemist with experience in quantum mechanics as well as computer programming will be required.

I am fortunate to have, with Max Markmeyer and Robin Schuldt, two excellent and interested candidates available.

6: Research assistants. **Justification:** Research assistants will support the doctoral students in carrying out the research and will, vice versa, be trained as future coworkers in the group.

This project will require significant computational power. Part of that will be provided by the institute for theoretical chemistry from university core funding. Our local computer cluster is available for smaller test calculations, benchmarks, initial investigations and possible program development in WP 6. Production runs will be performed, as currently done in the PI's goup, on the bwHPC facilities, the federated support for users of high performance computing (HPC) in the state of Baden-Württemberg. Within that framework, the JUSTUS bwForCluster for Computational Chemistry located in Ulm and its successor machine will be primarily used. If more computational power is required, additional proposals to high-performance super computer centers, like the HLRS in Stuttgart, will be put forward

3.14.7.4 Requested funding of direct costs

	2018	2019	2020	2021	2022
Uni Stuttgart: existing funds from public budget	1,000.-	2,000.-	2,000.-	2,000.-	1,000.-
Sum of existing funds	1,000.-	2,000.-	2,000.-	2,000.-	1,000.-
Sum of requested funds	800.-	1,500.-	1,500.-	1,500.-	800.-

(All figures in EUR)

Consumables for financial year 2018

E.g. data storage devices, IT materials	EUR	800.-

Consumables for financial year 2019

E.g. data storage devices, IT materials	EUR	1,500.-

Consumables for financial year 2020

E.g. data storage devices, IT materials	EUR	1,500.-

Consumables for financial year 2021

E.g. data storage devices, IT materials	EUR	1,500.-

Consumables for financial year 2022

E.g. data storage devices, IT materials	EUR	800.-

3.15 Project C5

3.15.1 General information about Project C5

3.15.1.1 Atomistic and fluid-theoretical predictions of static and dynamic fluid properties in functionalized silica mesopores

3.15.1.2 Research Areas

Heat Energy Technology, Thermal Machines, Fluid Mechanics: Technical Thermodynamics (404-02)
Process Engineering, Chemical Technology: Chemical and Thermal Process Engineering (403-01)

3.15.1.3 Principal Investigators

Hansen, Niels, Jun.-Prof. Dr.-Ing. habil. born 22. 07. 1977, male, German
Institut für Technische Thermodynamik und Thermische Verfahrenstechnik
Universität Stuttgart, Pfaffenwaldring 9, 70569 Stuttgart
Tel.: 0711/685-66112
E-Mail: hansen@itt.uni-stuttgart.de
Professor W1, fixed term (employment assured for the first funding period)

Groß, Joachim, Prof. Dr.-Ing. born 12. 10. 1970, male, German
Institut für Technische Thermodynamik und Thermische Verfahrenstechnik
Universität Stuttgart, Pfaffenwaldring 9, 70569 Stuttgart
Tel.: 0711/685-66140
E-Mail: gross@itt.uni-stuttgart.de
Tenured professor W3

3.15.1.4 Legal Issues

This project includes

1.	research on human subjects or human material.	no
2.	clinical trials.	no
3.	experiments involving vertebrates.	no
4.	experiments involving recombinant DNA.	no
5.	research involving human embryonic stem cells.	no
6.	research concerning the Convention on Biological Diversity.	no

3.15.2 Summary

The properties of fluid mixtures composed of solvent, reactant and product molecules within functionalized mesoporous materials and the local composition of reacting species around the catalytically active complex anchored covalently inside the inner pore space are important factors determining the activity of catalytic reactions in confined geometries. Classical force field all-atom molecular simulations are applied in this project to determine the multicomponent phase behavior and transport properties inside mesoporous confinement. The structural models will be developed in close collaboration with the experimental groups working on synthesis and characterization. A special focus will be given to silica materials. Once established the pore models allow for a systematic investigation of the effect of pore size, shape, polarity of functional groups, type of solvent, temperature and pressure on the environment around catalytically active sites by means of atomistic molecular dynamics and Monte Carlo simulations. Observables such as diffusion coefficients measured by NMR will be used to validate the model building. The interplay of solvent molecules, reactants and products with each other and with the pore walls leads to highly non-ideal behavior that may be utilized to engineer desired properties such as specific concentration profiles in the pore and around the catalytically active site. For designing optimal mesoporous materials systematically, it is required to predict transport properties for varying geometric and chemical specifications of a mesoporous material using computationally efficient approaches. Therefore, classical (molecular) density functional theory (CDFT) models are developed to predict the transport properties in porous materials. The atomistic simulations will serve to extract averaged fluid-wall interfacial potentials that are required for modeling the system with CDFT but

provide also a basis for coarse graining simulations. This allows for the comparison of different strategies for a multiscale description up to the continuum level and the development of material design concepts that have already been established for solvent design.

3.15.3 Research rationale

3.15.3.1 Current state of understanding and preliminary work

Recent advances in designing mesoporous silica nanoparticle materials with surface-anchored functional groups have shown promising potential for applications in heterogeneous catalysis.[1] For example, by using an immobilized Rh-complex inside of SBA-15 mesopores, a rate enhancement for 1-octene hydroformulation was observed compared to the homogeneous analogue, which was explained by the suppression of the formation of inactive forms of the catalyst inside the pores.[2] Selectivity and conversion of reactions can be affected due to controlling the factors that influence the mobility of reactants and products including molecular size, shape, configuration, degree of confinement, pore topology, strength of adsorption on pore walls, and the possibility of hydrogen bonding between reactants or/and products. Experimental data alone do not provide sufficient information to quantitatively model diffusion of complex mixtures. Integral to the use and rational design of functionalized mesoporous materials is the existence of a model for predicting how pore dimension and surface functionalization influence the fluid properties under confinement. Fluids confined in mesoporous materials present a particular challenge to empirical tuning, as it is difficult to experimentally probe such properties as composition and phase behavior within the mesopores. For this reason there is interest in computational modeling studies to provide a fundamental molecular-level description of the systems. The elementary steps involved in a catalytic process taking place under confinement are illustrated in Figure C5-1. Several transport barriers and adsorption/desorption steps are taking place that are influenced in a complex manner by the fine structure of the porous material.

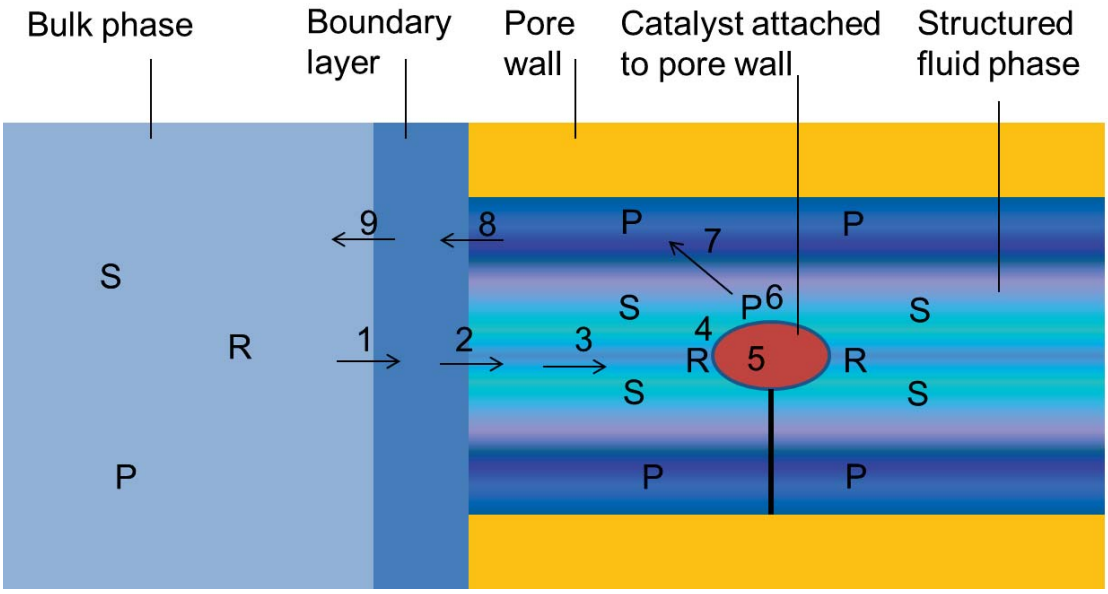

Figure C5-1. Elementary steps in molecular heterogeneous catalysis in the liquid phase consisting of solvent (S), reactant (R) and product (P) molecules. (1) Mass transport through the boundary layer separating bulk and confined phase, (2) mass transport through the pore entrance and partitioning of bulk phase, (3) diffusion within the pore, (4) adsorption at the catalytically active complex, (5) catalytic reaction, (6) product desorption from the catalytically active complex, (7) product diffusion towards the pore entrance, (8) product exit, (9) product diffusion through the boundary layer into the bulk phase.

As opposed to e.g. zeolites, the structure of mesoporous silica materials is usually amorphous, so a suitable model is one that is representative from a statistical point of view, rather than correct atom by atom. X-ray diffraction (XRD) patterns reveal the average characteristic distances as the unit cell size of the regular structure, which are expressed as distinct peaks in X-ray powder diffraction patterns, but

also information about pore diameters.[3] Agreement in the unit cell size is a fundamental requirement to model for periodic mesoporous silicas. X-ray results are usually interpreted with the aid of parametrized structural models, which give rise to a “best fit model” paradigm.[4] This indirect approach yields good qualitative and quantitative results when the behavior of the surface groups is reasonably well known and the structure arising at the interface is stable. However, with more complex systems and limited initial information on the expected structures, results can become ambiguous and several physically sound models, or several parametrizations of the same model, can be found to adequately describe the experimental data. Thus, although general features such as layer thickness are usually unambiguously described across the models, and can therefore be extracted with confidence, the detailed molecular structure of the interface is more difficult to obtain. In a recent study the fundamental importance of the direct comparison between MD simulations with X-ray reflectivity measurements was demonstrated using an ionic liquid at a neutral sapphire interface as example. This comparison enabled one to use detailed description obtained from simulation with confidence.[5] Besides X-ray diffraction other characterization methods deliver useful structural information. ^{29}Si-nuclear magnetic resonance (NMR) spectroscopy measures the distribution of silicate tetrahedra with *n* bridging oxygens (shared between two tetrahedra), labelled as Q^n (n from 0 to 4), i.e. the connectivity of the silicon atoms in the silica network. Transmission electron microscopy (TEM) pictures are of help to reveal pore shape and regularity of mesoporous materials. The degree of realism of a model can further be investigated by its ability to predict experimental data such as adsorption isotherms of probe molecules. Adsorption experiments with different adsorptives give information about the porosity, the pore size distribution, the surface area, and surface chemistry. The agreement of experimental and simulated adsorption isotherms is a key criterion in the evaluation of the developed models for mesoporous materials. Multidimensional MAS NMR experiments provide information on the spatial arrangement of solvent molecules inside the pores.[6]

Mass transport of molecular compounds through porous solids is a decisive step in molecular heterogeneous catalysis. It is a multi-scale, hierarchical phenomenon: Macrodiffusion (>μm) is influenced, in addition to parameters like grain boundaries and particle packing, by meso-scale (>10nm, <μm) factors like particle size and the connectivity of pores. More importantly, meso-scale diffusion and macro-scale diffusion are first and foremost determined directly by processes on the molecular scale (<10 nm), which depend on numerous factors like pore-size, interactions of the host with the solid surfaces and with the solvent. Due to high complexity of the latter and the fact that current analytical techniques such as MAS PFG NMR or spatially and time-resolved electron paramagnetic resonance (EPR) spectroscopy, respectively,[7,8] enable only limited insights into solvent filled pores with sufficient spatial and temporal resolution, the knowledge about the molecular origins of diffusive processes in porous materials is still restricted. Molecular dynamics therefore offers complementary information for interpreting NMR measurement of diffusion.

Molecular dynamics simulations have been used to investigate the characteristics of diffusion of a variety of alkanes in unfunctionalized silica mesopores. Even for such relatively simple systems, a complex concentration dependent diffusion behavior may be present,[9] that can be cast into the Maxwell-Stefan formulation.[10] Methodology to calculate the required thermodynamic correction factor for confined fluids has been reported recently.[11] As in simulations of bulk fluids, finite-size effects have to be considered carefully if comparison to experiment is intended.[12] Moreover, when fixing the positions of the pore wall atoms, proper thermostatting of the confined fluid has to be carried out to avoid artefacts.[13] Simulations of water dynamics in MCM-41 have been interpreted with the core-shell model in which the first water monolayer is immobile on diffusive time scales while the core water exhibits essentially bulk behavior.[14] MD simulation have also been used to interpret NMR measurements of partly and fully filled MCM-41 pores.[15] In inhomogeneous and anisotropic media mass transport is described by an anisotropic diffusion tensor that depends on the position in the pore. Diffusion parallel to the pore axis might differ from diffusion normal to the pore axis. A proper description of these effects requires the position dependent free-energy profiles of the various species.[16] Functionalized mesopores such as MCM-41 have been studied using molecular dynamics simulations with the aim to determine the spatial distribution of two co-adsorbed molecules like N_2 and CO_2. The strong effect of aminophenyl surface groups on the selectivity and the importance of calculating cross-term diffusion was demonstrated. Insights from these simulations allow for the design of tailor made surface groups.[17,18,19]

A substantial number of simulation studies appeared over the last 25 years with the aim to provide a molecular-level description of physical processes underlying the reversed-phase liquid chromatography (RPLC), in particular (i) the structure and dynamics of the bonded phase and its interface with the mobile phase, (ii) the interactions of analytes with the bonded phase, and (iii) the retention mechanism for different analytes.[20] By simulations it was shown, for example, that retention into octyl (C8) phases is best described as an adsorption process, while for octadecyl (C18) phases both adsorption and partition play a role for nonpolar analytes, whereas adsorption is always the major mechanism for analyte molecules with polar groups that lead to an amphiphilic character. A recent MD study investigated the surface diffusion of four typical aromatic hydrocarbon analytes in RPLC through molecular dynamics simulations in a slit-pore RPLC model consisting of a silica-supported end-capped, C18 stationary phase and a 70/30 (v/v) water/acetonitrile mobile phase. The results show that the lateral (surface-parallel) diffusive mobility of the analytes goes through a maximum in the acetonitrile ditch, an acetonitrile-rich border layer around the terminal part of the bonded-phase chains.[21] The latter study illustrates the state of the art in model building and simulation methodology that is ideally suited as a starting point for the investigations planned in this project.

In the context of the present proposal, the catalytically active site is to be modelled for two different scenarios. First, a classical force field description is required to be used to study all non-reactive processes in which the linker and the active site attached to it may have an influence on the transport properties of reactants and products as well as their distribution radial to the pore axis. The reaction itself may be incorporated in the framework of reaction ensemble simulations which have been used successfully to study confined reactive systems.[22,23] Second, a QM/MM model will be used in **project C4** to study the reactive events using a QM-description of the active site. The chemical structures of the catalytic complexes relevant for this proposal usually contain groups that are not included in the common force fields. While there are a broad range of options to model metal ion-containing system using classical force fields,[24] the first classical description may rely on the functional form typically used in biomolecular force fields. Attempts to parametrize a force field for Ru catalytic complexes in this way based on quantum chemical calculations are described by Ahmadi et al.[25]

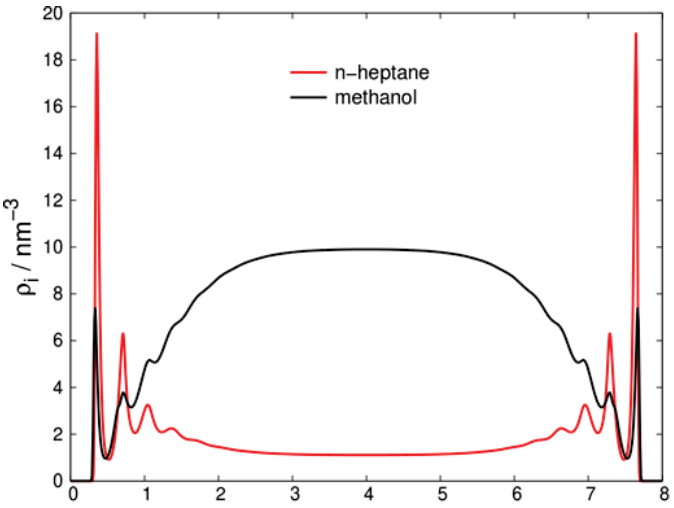

Figure C5-2. Density profiles of a binary mixture of *n*-heptane and methanol in a graphene-like slit-shaped 8 nm pore, obtained by classical density functional theory. The corresponding bulk phase properties are T = 40°C, p = 8 bar and $x_{heptane}$ = 0.1.

According to Rosenfeld's Entropy Scaling principle,[26] transport properties are functions solely of the residual entropy. Entropy scaling has developed as a powerful framework for correlating and predicting viscosities, thermal conductivity, and self-diffusion coefficients. In an ongoing project, our group has made progress in predicting transport diffusion coefficients from self-diffusion coefficients. Entropy scaling was initially proposed only for simple fluids in the liquid phase. In recent time, however, it was seen that the method also holds for complex fluids exhibiting hydrogen-bonding interactions or substances of high molecular mass. A first study demonstrates the suitability for estimating transport properties in mesopores. It is thereby required to calculate the local entropy density for highly heterogeneous (confined) mixtures. Classical density functional theory is suitable for predicting properties of mixtures under these confined conditions.

Classical DFT is furthermore valuable for predicting the local density of each substance in a mixture within confined mesoporous conditions,[C5-13] see Figure C5-2. The local densities of all species are very important quantities, because the reaction kinetics severely depends on the local composition around an active site. In the first funding period, we do not intend to model reactions, however, the local composition of reactants is a measure for the kinetics. The local densities from DFT are compared to local densities determined from molecular simulations in order to verify the approach. Catalysis in

mesoporous materials inevitably requires a suitable trade-off between, on the one hand, diffusional transport resistance of reactants and products to and from the active site, respectively, and, on the other hand, favorable local densities of reactants at the active site. Classical DFT is particularly suited to optimize mesoporous materials, in terms of pore size and chemical specifications of the surface, for a particular application. The systematic optimization of material properties has to be the objective for subsequent funding periods.

It can be concluded that methodological advances in obtaining computational models of mesoporous materials, in calculating adsorption and diffusion of various molecules in such materials as well as in applying fluid-theoretical approaches to porous materials have reached a level that allows for combining these methods with the goal to study reactive systems in confined media. However, in contrast to studies investigating reactions in ordered microporous materials such as zeolites or metal-organic frameworks, computational studies that have showcased their potential as a useful tool in the rational design of mesoporous environments are very rare. This proposal is an important step towards a consistent multi-scale description with the ultimate goal to gain understanding how structurally defined pore geometry interacts with functional surface groups in order to guide the catalytic process towards higher activity, productivity and selectivity.

In a preliminary project a model system was designed to study confinement effects on the ring-closing metathesis reaction of 9-decen-1-yl 10-undecenoate to oxacycloicos-11-ene-2-one over a ruthenium catalyst, following the preliminary experimental work described in **project B2**. A cylindrical silica mesopore with diameter of 9.2 nm and length of 9.46 nm, functionalized with epoxy groups on the inner surface and modified with trimethylsilyl groups on the outer surface was constructed, according to the methodology reported by Talarek and coworkers,[27] see Figure C5-3. To enable fast generation of various model systems within this project an efficient python implementation of the pore construction procedure was implemented. The force field parameters for the Si, O, and H atoms of the silica surface were taken from Gulmen and Thompson.[28,29] A ruthenium complex bearing an N-heterocyclic carbene ligand, attached to the pore surface via a linker was used to represent the immobilized catalyst. A recently proposed AMBER-compatible force field description for N-heterocyclic carbenes was used,[30] in combination with automatically parametrized force field descriptions of the linker, reactant and product, using the ANTECHAMBER routines of the AMBER program package.[31] The ruthenium center was modeled using parameters reported by Ahmadi et al.[25] The system is coupled to a bulk reservoir containing reactant and product and solvent molecules at specified conditions. Preliminary simulations concerned validation of the various molecular models and benchmark calculations on the hardware architecture to be used in this project.

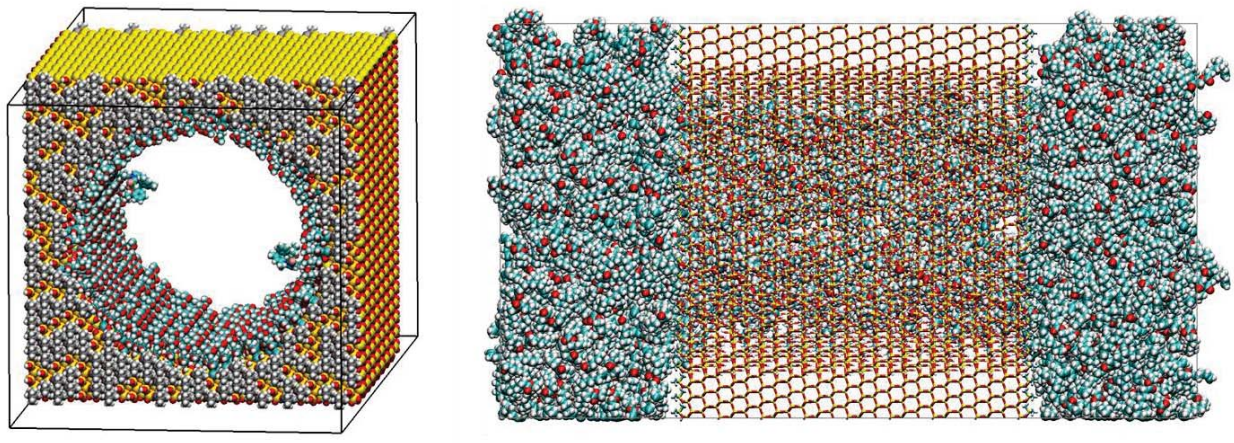

a) b)

Figure C5-3. a) Front view on the nearly cylindrical silica mesopore of 9.46 nm diameter, carved into a silica block. The inner surface is functionalized with epoxy groups. The outer surface is occupied by trimethylsilyl groups. Two catalytically active complexes are anchored to the inner surface; b) Side view of the studied model system, containing an equimolar mixture of reactant and product molecules.

References

[1] E. L. Margelefsky, R. K. Zeidan, M. E. Davis, *Chem. Soc. Rev.* **2008**, *37*, 1118-1126.
[2] F. Marras, J. Wang, M.-O. Coppens, J. N. H. Reek, *Chem. Commun.* **2010**, *46*, 6587-6589.
[3] Y. Ishii, Y. Nishiwaki, A. Al-zubaidi, S. Kawasaki, *J. Phys. Chem. C* **2013**, *117*, 18120-18130.
[4] C. Schumacher, J. Gonzalez, P. A. Wright, N. Seaton, *J. Phys. Chem. B* **2006**, *110*, 319-333.
[5] Z. Brkljača, M. Klimczak, Z. Miličević, M. Weisser, N. Taccardi, P. Wasserscheid, D. M. Smith, A. Magerl, A.-S. Smith, *J. Phys. Chem. Lett.* **2015**, *6*, 549-555.
[6] J. B. Mietner, F. J. Brieler, Y. J. Lee, M. Fröba, *Angew. Chem. Int. Ed.* **2017**, *56*, 12348-12351.
[7] J. Kärger, R. Valiullin, *Chem. Soc. Rev.* **2013**, *42*, 4172-4197.
[8] M. Wessig, M. Spitzbarth, M. Drescher, R. Winter, S. Polarz, *Phys. Chem. Chem. Phys.* **2015**, *17*, 15976-15988.
[9] R. Krishna, J. M. van Baten, *Microporous. Mesoporous Mater.* **2011**, *138*, 228-234.
[10] R. Krishna, J. M. van Baten, *Microporous Mesoporous Mater.* **2009**, *64*, 3159-3178.
[11] J. Collell, G. Galliero, *J. Chem. Phys.* **2014**, *140*, 194702.
[12] P. Simonnin, B. Noetinger, C. Nieto-Draghi, V. Marry, B. Rotenberg, *J. Chem. Theory Comput.* **2017**, *13*, 2881-2889.
[13] S. De Luca, B. D. Todd, J. S. Hansen, P. J. Daivis, *J. Chem. Phys.* **2014**, *140*, 054502.
[14] I. C. Bourg, C. I. Steefel, *J. Phys. Chem. C* **2012**, *116*, 11556-11564.
[15] A. Pajzderska, M. A. Gonzalez, J. Mielcarek, J. Wąsicki, *J. Phys. Chem. C* **2014**, *118*, 23701-23710.
[16] A. Ghysels, R. M. Venable, R. W. Pastor, G. Hummer, *J. Chem. Theory Comput.* **2017**, *13*, 2962-2976.
[17] J. J. Williams, A. D. Wiersum, N. A. Seaton, T. Düren, *J. Phys. Chem. C* **2010**, *114*, 18538-18547.
[19] Y. Zhu, J. Zhou, J. Hu, H. Liu, *Catal. Today* **2012**, *194*, 53-59.
[18] J. J. Williams, N. A. Seaton, T. Düren, *J. Phys. Chem. C* **2011**, *115*, 10651-10660.
[20] R. K. Lindsey, J. K. Rafferty, B. L. Eggimann, J. I. Siepmann, M. R. Schure, *J. Chromatogr. A* **2013**, *1287*, 60-82.
[21] J. Rybka, A. Höltzel, U. Tallarek, *J. Phys. Chem. C* **2017**, *121*, 17907-17920.
[22] A. Poursaeidesfahani, R. Hens, A. Rahbari, M. Ramdin, D. Dubbeldam, T. J. H. Vlugt, *J. Chem. Theory Comput.* **2017**, *13*, 4452-4466.
[23] R. G. Mullen, E. J. Maginn, *J. Chem. Theory Comput.* **2017**, *113*, 4054-4062.
[24] P. Li, K. M. Merz Jr., *Chem. Rev.* **2017**, *117*, 1564-1686.
[25] A. Ahmadi, C. McBride, J. J. Freire, A. Kajetanowicz, J. Czaban, K. Grela, *J. Phys. Chem. A* **2011**, *115*, 12017-12024.
[26] Y. Rosenfeld. *Phys. Rev. A* **1977**, *15*, 2545-2549.
[27] S. M. Melnikov, A. Höltzel, A. Seidel-Morgenstern, U. Tallarek, *Angew. Chem. Int. Ed.* **2012**, *51*, 6251-6254.
[28] T. S. Gulmen, W. H. Thompson, *MRS Proc.* **2005**, *899*, 0899-N06-05.
[29] T. S. Gulmen, W. H. Thompson, *Langmuir* **2006**, *22*, 10919-10923.
[30] S. Gehrke, O. Hollóczki, *Phys. Chem. Chem. Phys.* **2016**, *18*, 22070-22080.
[31] J. Wang, W. Wang, P. A. Kollman, D. A. Case, *J. Mol. Graphics Modell.* **2006**, *25*, 247-260.

3.15.3.2 Own work, project-related publications by participating researchers

The applicants have experience in force field-based simulations and fluid-theoretical methods. The work of N. Hansen over the last years was focused on classical MD simulations of complex condensed phase systems. The work of J. Groß is focused on fluid theories, recently with emphasis on interfacial properties and on transport properties as well as force field development for molecular simulations. The combination of the complementary expertise of N. Hansen and J. Groß enables a systematic study of thermodynamic properties relevant for catalytic systems in confined media.

During his dissertation N. Hansen developed a multi-scale model for describing the zeolite-catalyzed alkylation of benzene with ethene. This project involved the entire set of methods from highly accurate coupled cluster (CCSD(T)) calculations over classical MC and MD simulations to study adsorption and diffusion processes, towards continuum approaches to describe coupled diffusion and reaction in

catalyst pellets.[C5-1] He has also experience with simulating reactive systems in confined media by means of reactive Monte Carlo simulations. Using the example of the propene metathesis in zeolites it was shown that the confined environment may increase the conversion significantly. A large change in selectivity between the bulk phase and the pore phase was observed. Pressure and temperature have strong influence on both conversion and selectivity.[C5-2] Experience with quantum chemical calculations and the elucidation of reaction mechanisms including the calculation of rate-coefficients was gained in several projects involving the N_2O decomposition over zeolite Fe-ZSM-5, alkane cracking over zeolite H-ZSM-5 and benzene alkylation.[C5-3] N. Hansen also has a track record in the study of complex condensed phase systems such as proteins in solution or host-guest complexes.[C5-4] One of his focal areas are free-energy calculations.[C5-5] N. Hansen is one of the current developers of the GROMOS biomolecular simulation package where he is mainly involved in the implementation and testing of structure refinement methods. He is well connected with other members of the CRC through joint projects with M. Buchmeiser (**A1,B2**), S. Laschat (**B3**) and T. Sottmann (**A7**) as well as through co-supervision of theses with J. Kästner (**C4**) and C. Holm (**C6**).

Joachim Groß is performing research in molecular thermodynamics and thermal separation processes. He develops engineering models, such as the PC-SAFT (perturbed-chain statistical associating fluid theory) equation of state,[C5-6] which is widely used, both in academia and in industry. His focus has shifted to interfacial properties of vapor-liquid mixtures and liquid-liquid systems, as well as fluids in confined porous materials.[C5-7] Joachim Groß, together with a colleague from the RWTH, proposed a method (CoMT-CAMD, Continuous Molecular Targeting Computer Aided Molecular Design) for the simultaneous design of processes and solvents. As a requirement for a meaningful design of solvents, he began researching transport properties, such as viscosity, thermal conductivity, and diffusion coefficients, where he developed predictive methods based on Entropy Scaling.[C5-8] He is author of a textbook on non-equilibrium thermodynamics.[C5-9] Moreover, as a research line of its own right, he is engaged in developing a transferable force field (TAMie Transferable Anisotropic Mie force field) for molecular simulations with emphasis on predicting phase equilibria and thermodynamic properties of mixtures.[C5-10]

References

[C5-1] N. Hansen, F. J. Keil, *Soft Mater.* **2012**, *10*, 179-201.
[C5-2] N. Hansen, S. Jakobtorweihen, F. J. Keil, *J. Chem. Phys.* **2005**, *122*, 164705.
[C5-3] N. Hansen, T. Kerber, J. Sauer, A. T. Bell, F. J. Keil, *J. Am. Chem. Soc.* **2010**, *132*, 11525-11538.
[C5-4] J. Gebhardt, N. Hansen, *Fluid Phase Equilib.* **2016**, *422*, 1-17.
[C5-5] J. Smiatek, N. Hansen, J. Kästner, Free energy calculation methods and rare event sampling techniques for biomolecular simulations, in "Simulating Enzyme Reactivity", Eds: I. Tuñón und V. Moliner, RSC Cambridge, 2017.
[C5-6] J. Gross, G. Sadowski, *Ind. Eng. Chem. Res.* **2001**, *40*, 1244-1260.
[C5-7] E. Sauer, J. Gross, *Ind. Eng. Chem. Res.* **2017**, *56*, 4119-4135.
[C5-8] O. Lötgering-Lin, J. Gross, *Ind. Eng. Chem. Res.* **2015**, *54*, 7942-7952.
[C5-9] S. Kjelstrup, D. Bedeaux, E. Johannessen, J. Gross, Non-Equilibrium Thermodynamics for Engineers, 2nd Ed., World Scientific Publishing, Singapore, 2017.
[C5-10] A. Hemmen, J. Gross, *J. Phys. Chem. B* **2015**, *119*, 11695-11707.

3.15.4 Project plan

The primary material for the initial phase of this project is mesoporous silica because it is readily available for both experimental (**project A4**) and theoretical investigations. The initial reaction to be investigated is the H_2-autotransfer catalysis over (N,N,N,N)(P)Ru-complexes studied in **project B1**, because solvent, reactants and products and linker molecules are relatively easily accessible for a force field description. Once established, the workflow will be transferred to other materials in particular covalent organic frameworks, which are synthesized in **project A3**, and catalytic reactions, in particular those planned in **project B3**. The project is divided into five work packages, which are supervised by both PIs. In the detailed description of the work packages, the respective PI taking the main responsibility is indicated.

In summary, the research goals are organized in work-packages as follows:

- **WP1: Construction of atomic resolution structural models for mesoporous silica** This will serve as model system for the subsequent work packages. The model building will be carried out in close collaboration with **projects A4 (Traa)** and **C1**.
- **WP2: Choice of suitable force field parameters and parametrization** This WP deals with validation of force field parameters based on thermodynamic bulk phase properties as well as spatial information obtained in **projects A4** as well as diffusion coefficients measured in **C1**.
- **WP3: Investigation of static and dynamic properties** This is one of the main tasks of this project. The spatial and temporal behavior of the fluid mixtures consisting of reactants, products and solvent molecules will be studied at atomistic resolution using molecular dynamics and Monte Carlo simulations. These simulations provide the basis for the QM/MM simulations carried out in **project C4 (Kästner)** and provide diffusion coefficients to be used in the lattice-Boltzmann simulations carried out in **project C6 (Holm/Fyta)**. Moreover, averaged interfacial potentials will be extracted that are used in WP for a fluid-theoretical treatment of the pore system.
- **WP4: Description of the system with fluid-theoretical methods** A coarse grained description of the system based on averaged fluid-wall potentials extracted from atomistic simulations will be conducted using classical density functional theory.
- **WP5: Description and prediction of diffusion coefficients in mesoporous materials** This WP aims at developing a method for the diffusional transport in mesoporous material based on entropy scaling and classical DFT.

3.15.4.1 WP1 (N. Hansen): Construction of an atomic resolution structural model for mesoporous silica

In close collaboration with **project A4** (Traa) atomic resolution structural models for mesoporous silica will be developed. At the beginning we focus on structures that are well known from the literature such as SBA15, SBA16 or PHTS. The atomistic models are generated following routes described in the literature.[32,33,34] The obtained models are then validated against those structures synthesized in **project A4** (Traa) in terms of structural parameters that are independent of or only weakly dependent on the nonbonded force field terms used in subsequent work packages. These properties include the connectivity, the nature of the inner pore surface, i.e. free or geminal silanol groups, siloxane bridges or hydrogen-bonded silanol groups, as well as X-ray diffraction patterns. The latter can be calculated using available software.[35,36] For silica mesopores suitable force field parameters are available from the literature. The same holds for simple probe molecules such as Ar, Kr, N_2 or CO_2. Therefore, grand canonical Monte Carlo simulations can be used to calculate adsorption isotherms, isosteric heat of adsorption and Henry coefficients for a set of probe molecules which can be compared to experiment to validate further the pore volume and shape of the structural models employed. The nature of functional groups on the surface as well as of the triazol linkers will be worked out in cooperation with **project B1** and **A4** (Traa). Once established, this workflow will be applied to the materials prepared by the liquid crystal route used in **project A4** (Gießelmann). The spatial distribution of the catalysts in the pore will be determined in **project C3**. The procedures used in this work package will be applied for different starting materials several times over the funding period, as indicated in the chronological work plan.

3.15.4.2 WP2: (N. Hansen, J. Groß): Choice of suitable force field parameters and parametrization

For silica mesopores suitable force field parameters are available from the literature.[29] This also holds for solvents such as toluene or dioxane, reactants such as benzyl alcohol or aniline and products such as water. However, for these systems it needs to be verified, that thermodynamic properties of multicomponent mixtures are correctly represented. The triazole groups included in the linker concept of **project B1** have to be parametrized in this work package in collaboration with **project C6** (Fyta). The same holds for the (N,N,N,N)(P)Ru-complex for which a molecular mechanical description is developed in cooperation with **project C4** using quantum chemical calculations. The interplay between all components is then investigated by means of Monte Carlo and molecular dynamics simulations and compared to experimental data from other projects and from the literature. In order to study the

influence of confinement on the fluid phase behavior of the complex mixture of solvent, reactants and products, the force field will be validated based on thermodynamic properties of the bulk phase. For example the binary mixture toluene/water shows an azeotrope at reaction conditions. In confined environment this phase behavior might differ substantially. The validation of fluid phase behavior in the pore includes diffusion measurements by NMR in **project C1,** fluxes of substrate to/from an organometallic species determined in **project C2,** as well as adsorption measurements performed in **project A4**. The final validated structural model and force field will then be used in QM/MM simulations performed in **project C4**. Moreover, the force field parameters may be transferred to study the SiO_2 materials produced in **project A5**. The procedures used in this work package will be applied for different starting materials several times over the funding period, as indicated in the chronological work plan.

3.15.4.3 WP 3: (N. Hansen): Investigation of static and dynamic properties

This is the central work package of the project. Once established, the pore models allow for a systematic investigation of the effects of pore size, shape, and polarity of functional groups, type of solvents as well as temperature and pressure and thus enable one to study a variety of confinement effects.

1. Confinement by size:
a) Reactivity, chemo- and stereoselectivity can be strongly altered compared to the parent catalyst in solution through additional steric constraints acting on the catalyst through the pore walls and the distribution of solvent molecules, reactants and products in the pore.
b) Side reactions (e.g. polymerization) can be suppressed through variation of the pore diameter such that the formation of bulky oligomers is prevented. In general the reaction pathway may change due to geometric restraints acting on reactants.

To study these effects, the distribution of reactants and products, and the local concentration of reactants around the active site are systematically investigated as function of the pore size.

2. Confinement by geometry:
a) The geometry of pores, e.g. cylindrical vs. slit-shape, vs. spherical vs. beaker-shape will have an influence on mass transport and molecular distributions.

Various pore shapes will be generated keeping all other model parameters unchanged. The influence on molecular distributions and diffusion coefficients will be investigated.

3. Confinement by polarity:
a) By altering the polarity of the porous support, the surface functional groups, the solvent and the catalyst, the concentration profiles around the active site can be tuned. For example the removal of by-products can be enhanced through incorporation of functional groups.[37]

b) Use of static electric fields to stabilize the transition state.[38] The pore and the attached functional groups may be tuned to control the approaching reactants with respect to the field stimulus.

To study these confinement effect concentration profiles and diffusion coefficients of reactants and products within the pore will be calculated for the scenarios outlined above. The polarity of the silica material can be changed by introducing aluminum sites. The results are compared to experimental measurements performed in **projects C1, C2** and **C3**.

A further aspect is the detailed investigation of pore entrance effects, i.e. the estimation of transport barriers. For this purpose enhanced sampling free-energy techniques such as forward flux sampling (FFS)[39] or umbrella sampling (US)[40] combined with replica exchange will be used. FFS is an unbiased method, relying on multiple trajectories initiated along a reaction coordinate which continuously connects the inner pore space with the bulk phase without any further requirements. US is a biased method which allows to estimate efficiently the free energy difference between the bulk phase and the interior of the pore, but, in contrast to FFS, does not deliver kinetic information. Once established the

analysis methods developed for mesoporous silica materials are applied to covalent organic frameworks from **project A3** for which the model building is done in **project C4**.

3.15.4.4 WP4 (J. Groß): Description of the system with fluid-theoretical methods.

For the systematic design (beyond screening techniques) of porous materials, predictive models are required that allow to predict the local density distribution of solvents, reactants and products in the mesoporous material. The classical density functional theory is in particular suitable for this purpose due to the availability of reliable Helmholtz energy functionals. This WP aims at predicting the local density of all species in the mesopore. The model development critically depends on results from WP1 and WP2. From the simulations of WP1 and WP2, averaged interfacial potentials will be extracted that represent the porous structure in the CDFT calculations. As a meaningful first application, we calculate the nitrogen adsorption experiments, conducted in **project A4** (Traa), for characterizing the pore volume and pore diameter. The nitrogen measurements show an adsoprtion/desorption hysteresis, which is a valuable feature for assessing both, the Helmholtz energy functional used in the CDFT calculations and the chemical properties assigned for the pore surface (WP1).[41] A second application is meant for assessing the potential of CDFT for optimizing the porous environment. Based on the simulations performed in WP1 and WP2 for the H_2-autotransfer catalysis (**B1**) the pore geometry and polarity will be tuned by CDFT calculations such that the water can be efficiently removed from the active site.

3.15.4.5 WP5 (J. Groß): Description and prediction of diffusion coefficients in mesoporous materials.

This project aims at predicting transport properties along a mesopore. A predictive model is a necessity for systematically designing mesoporous materials for a certain chemical reaction, because the material design has to reflect an optimal trade-off between pore diffusion and pore reaction kinetics. The transport in confined geometries is clearly different from a diffusion process in bulk phases. We develop a method for the diffusional transport in porous materials based on entropy scaling and classical DFT. In view of scarce experimental data for porous materials, the model development critically relies on results from WP3 as well as the coarse grained simulation performed in **project C6**. The results of WP3 are the reference for developing predictive models for transport properties, such as transport diffusion coefficients, based on an entropy scaling approach. We note, however, that the actual material design framework will be established in a subsequent funding period.

Chronological work plan:

	2018	2019			2020				2021				2022	
	Q3	Q4	Q1	Q2	Q3	Q4	Q1	Q2	Q3	Q4	Q1	Q2	Q3	Q4	Q1	Q2	
T1																	WP1: Construction of atomic resolution structural models for mesoporous silica
T2																	WP 2: Choice of suitable force field parameters and parametrization
T3																	WP 3: Investigation of static and dynamic properties
T4																	WP 4: Description of the system with fluid-theoretical methods
T5																	WP 5: Description and prediction of diffusion coefficients in mesoporous materials

3.15.4.6 Methods applied

The project relies on both, molecular simulations (Monte Carlo and molecular dynamics) using classical force fields and fluid theoretical approaches, i.e. the classical density functional theory. The choice of the force field for the molecular simulations will be based on comparison with experimental data and on quantum chemical calculations carried out in **project C4**. The molecular dynamics simulations will be performed with the GROMACS code[42] patched to the free-energy library PLUMED.[43] Scripts to run forward flux sampling (FFS) simulations are already available in the research group of N. Hansen. The Monte Carlo simulations will be carried out with one of the open-source codes available in the scientific community such as RASPA, Cassandra, or DL_MONTE. Classical DFT calculations are performed using in-house codes that are in active development in the research group of J. Groß. Other methods reported in the literature may be beneficial for this project. This includes for example quantum-guided molecular mechanics (Q2MM), an automated force field parametrization method that generates accurate, reaction-specific transition state force fields by fitting the functional form of an arbitrary force field using only electronic structure calculations by minimization of an objective function. Using these force fields, the stereoselectivity of a reaction can be calculated by summation over the Boltzmann-averaged relative energies of the conformations leading to the different stereoisomers.[44]

3.15.4.7 Vision

The model building, which is the focus of the first funding period, relies on the insights obtained in many sub-projects. In subsequent funding periods this information flow will be reverted, i.e. predictions from multiscale simulations are expected to serve as basis for optimization of catalytic processes, which provide in turn continuous feedback to refine the models. In the third funding period the developed models should be applied for rational materials design.

3.15.5 Role within the collaborative research center

This project links between the experimental design of porous materials in the A-area and the measurements and simulations in area C. A close collaboration will be established with **project A4** (Traa, Gießelmann) as mesoporous silica materials will be the main focus of **C5**. Structural data of the catalyst within the pore can be compared to the results of atom probe tomography experiments performed in **project C3** (Schmitz). Within the simulation **projects C5** has three bridging functions. First it provides a force field description of a silica model system to be studied by QM/MM techniques in **C4**. Second it will provide transport coefficients to be used in lattice-Boltzmann simulations carried out in **C6**. Third, averaged interface potentials are extracted for a coarse-grained description by means of classical DFT simulations calculated within this project but also in **C6** for other materials. The work carried out in this project will also provide important information such as concentration profiles and transport properties over flat (2D) SiO_2-based materials studied in **project A5**.

The differentiation within the theoretical projects is based on methods and on systems studied: quantum chemistry is used in **projects C4** and **C6**, where **C4** approaches the overall goal from the catalysis side, modeling mechanisms and reactivities, while **C6** focuses on materials properties. Both use QM techniques to parametrize force fields, but for different systems. Classical all-atom molecular dynamics is used by all three theory-projects: in **C4** on COFs, in **C5** on silica and, in a later stage, also on COFs but with a different focus compared to **C4**, and in **C6** on the materials from **A2**, **A3** and **A5**, whereas coarse-grained methods are only dealt with in **C6**. Fluid theoretical methods like classical DFT are used only in **project C5**, while the lattice-Boltzmann method is used exclusively in **project C6**.

3.15.6 Differentiation from other funded projects

The work described in **project C5** is not subject or partly subject of any other research by the applicants.

3.15.7 Project funding

3.15.7.1 Previous funding

This project is currently not funded and no funding proposal has been submitted.

References (ctd.)

[32] B. Coasne, F. Di Renzo, A. Galarneau, R. J. M. Pellenq, *Langmuir* **2008**, *24*, 7285-7293.
[33] S. M. Melnikov, A. Höltzel, A. Seidel-Morgenstern, U. Tallarek, *Anal. Chem.* **2011**, *83*, 2569-2575.
[34] C. D. Williams, K. P. Travis, N. A. Burton, J. H. Harding, *Micropor. Mesopor. Mater.* **2016**, *228*, 215-223.
[35] www.iza-structure.org/IZA-SC_Software.htm.
[36] ww1.iucr.org/sincris-top/logiciel.
[37] C.-H. Tsai, H.T. Chen, S. M. Althaus, K. Mao, T. Kobayashi, M. Pruski, V. S.-Y. Lin, *ACS Catal.* **2011**, *1*, 729-732.
[38] A. C. Aragones, N. L. Haworth, N. Darwish, S. Ciampi, N. J. Bloomfield, G. G. Wallace, I. Diez-Perez, M. L. Coote, *Nature* **2016**, *531*, 88-91.
[39] R. J. Allen, C. Valeriani, P. R. ten Wolde, *J. Phys.: Condens. Mater.* **2009**, *21*, 463102.
[40] G. M. Torrie, J. P. Valleau, *J. Comput. Phys.* **1977**, *23*, 187-199.
[41] K. Miyasaka, A. V. Neimark, O. Terasaki, *J. Phys. Chem. C* **2009**, *113*, 791-794.
[42] M. J. Abraham, T. Murtola , R. Schulz , S. Páll , J. C. Smith , B. Hess , E. Lindahl , *SoftwareX* **2015**, *1-2*, 19-25.
[43] G. A. Tribello, M. Bonomi , D. Branduardi , C. Camilloni , G. Bussi , *Comput. Phys. Commun.* **2014**, *185*, 604-613.
[44] E. Hansen, A. R. Rosales, B. Tutkowski, P.-O. Norrby, O. Wiest, *Acc. Chem. Res.* **2016**, *49*, 996-1005.

3.15.7.2 Requested funding

Funding for	2018		2019		2020		2021		2022		2018-2022	
Staff	Quantity	Sum	Quantity	Sum	Quantity	Sum	Quantity	Sum	Quantity	Sum	Quantity	Sum
PhD student,100%	1	32,300.-	1	64,500.-	1	64,500.-	1	64,500.-	1	32,300.-	1	258,100.-
Total		32,300.-		64,500.-		64,500.-		64,500.-		32,300.-		258,100.-
Direct costs	Sum		Sum		Sum		Sum		Sum		Sum	
consumables	800.-		1,500.-		1,500.-		1,500.-		800.-		6,100.-	
Total	800.-		1,500.-		1,500.-		1,500.-		800.-		6,100.-	
Major research instrumentation	Sum		Sum		Sum		Sum		Sum		Sum	
	-		-		-		-		-		-	
Total	-		-		-		-		-		-	
Grand total	33,100.-		66,000.-		66,000.-		66,000.-		33,100.-		264,200.-	

(All figures in EUR)

3.15.7.3 Requested funding for staff

	Sequential no.	Name, academic degree, position	Field of research	Department of university or non-university institution	Project commitment in hours per week	Category	Funding source
Existing staff							
Research staff	1	Niels Hansen, Jun.-Prof.	Molecular Simulation, Free-energy calculations	Institute of Thermodynamics and Thermal Process Eng.	8		University
Research staff	2	Joachim Groß, Prof.	Thermodynamics, Fluid Theories, Molecular Simulation	Institute of Thermodynamics and Thermal Process Eng.	4		University
Non-research staff	3	Agnes Schmidtgen		Institute of Thermodynamics and Thermal Process Eng.	2		University
Requested staff							
Research staff	4	N. N.; M. Sc.	Fluid theories, Molecular simulation	Institute of Thermodynamics and Thermal Process Eng		PhD	
Research staff	5	Research assistant	Fluid theories, Molecular simulation	Institute of Thermodynamics and Thermal Process Eng			

Job description of staff (supported through existing funds):
1
Principal investigator for **project C5**, in particular work packages 1,2,3
2
Principal investigator for **project C5**, in particular work packages 2,4,5
3
Secretary

Job description of staff (requested funds):
4
PhD student, work packages 1-5
5
Research assistants. **Justification:** The research assistants support the doctoral student in data analysis, routine simulations, literature research and preparation of figures.

This project will require significant computer power. Part of it will be provided by the Institute of Thermodynamics and Thermal Process Engineering from university core funding. Our local computer cluster is available for smaller test calculations, benchmarks, initial investigations and possible program development. Production runs will be performed, as currently done in other projects of the PIs, on the bwHPC facilities, the federated support for users of high performance computing (HPC) in the state of Baden-Württemberg. Within that framework, the BinAC bwForCluster in Tübingen and the ForHLR machines will be used. If more computational power is required, additional proposals to high-performance super computer centers, such as the HLRS in Stuttgart, will be put forward.

3.15.7.4 Requested funding of direct costs

	2018	2019	2020	2021	2022
Uni Stuttgart: existing funds from public budget	2,000.-	4,000.-	4000.-	4,000.-	2,000.-
Sum of existing funds	2,000.-	4,000.-	4000.-	4,000.-	2,000.-
Sum of requested funds	800.-	1,500.-	1,500.-	1,500.-	800.-

(All figures in EUR)

Consumables for financial year 2018

data storage devices, IT materials	EUR	800.-

Consumables for financial year 2019

data storage devices, IT materials	EUR	1,500.-

Consumables for financial year 2020

data storage devices, IT materials	EUR	1,500.-

Consumables for financial year 2021

data storage devices, IT materials	EUR	1,500.-

Consumables for financial year 2022

data storage devices, IT materials	EUR	800.-

3.15.7.5 Requested funding for major research instrumentation
none

3.16 Project C6

3.16.1 General information about Project C6

3.16.1.1 A multi-scale simulation approach for optimizing molecular heterogeneous catalysis in confined geometries

3.16.1.2 Research Areas
Statistical Physics, Soft Matter, Biological Physics, Nonlinear Dynamics (310-01), Condensed Matter Physics (307-02)

3.16.1.3 Principal Investigator
Holm, Christian, Prof. Dr., born 03.05.1960, male, German
Institut für Computerphysik
Universität Stuttgart, Allmandring 3, 70569 Stuttgart Tel.: 0711/685-63701
E-mail: christian.holm@icp.uni-stuttgart.de
Tenured professor (W3)

Fyta, Maria, JP Dr., born 25.08.1976, female, Greek
Institut für Computerphysik
Universität Stuttgart, Allmandring 3, 70569 Stuttgart Tel.: 0711/685-63935
E-mail: mfyta@icp.uni-stuttgart.de
Professor W1, fixed term (employment assured for the first funding period)

3.16.1.4 Legal Issues
This project includes

1.	research on human subjects or human material.	no
2.	clinical trials.	no
3.	experiments involving vertebrates.	no
4.	experiments involving recombinant DNA.	no
5.	research involving human embryonic stem cells.	no
6.	research concerning the Convention on Biological Diversity.	no

3.16.2 Summary
The role of structural and conformational details, as well as the dynamics and transport properties of the starting material (reactants) and products with immobilized catalysts within confined geometries are at the core of this project. We will use computational tools within a bottom-up approach in order to unravel the most important factors affecting molecular heterogeneous catalysis in nanometer-sized pores. For this, we will work simultaneously on the small scale, investigating specific intermolecular interactions, as well as on larger coarser scales, quantifying the transport of reactants and products in and out of confined spaces. On the small scale, we will use quantum-mechanical calculations within the density-functional-theory approach. This part will focus on structural properties of materials, such as the tunable block copolymer templates **A2**, the crystalline porous polymers (COFs) in **A3**, or the organic/inorganic hybrids **A5** synthesized in **Area A**. For these materials, different functional groups and linkers for the catalyst will be studied. The linker length and density on the pore surface, as well as the conformational variability and structuring of the solvent in polar/apolar solvents will be evaluated with atomistic and coarse-grained molecular dynamics approaches. At a larger scale, the transport properties of the reactant into a pore and that of the catalytic product out of the pore will be investigated in detail using a non-equilibrium coarse-grained approach, either with an extended multicomponent reactive lattice-Boltzmann fluid using appropriate diffusion constants and catalytic rates as input parameters, or with a hybrid particle/lattice Boltzmann algorithm. Confinement effects due to variations in the pore geometry will be accounted for as well. The main goal of this project is, together with the other theory projects, **C4** and **C5**, to assist a better design of optimum conditions and materials for increasing the turnover frequencies of catalytic reactions related to the catalysts from **Area B** in confined geometries.

3.16.3 Research rationale

3.16.3.1 Current state of understanding and preliminary work

Computational modeling can provide insight into time and length scales not easily accessible by experimental means. Depending on the numerical method used, different properties can be probed. For a catalytic reaction, simulations can provide a link between the molecular process of the catalysis and the engineering of macroscopic catalytic systems.[1] In this respect, each numerical method starting from very accurate quantum-mechanical (QM) schemes and density functional theory (DFT), QM/MM and atomistic Molecular Dynamics (MD) up to coarse-grained, kinetic/mesoscopic schemes and computational fluid dynamics can serve as a corner stone in a comprehensive understanding of a catalytic process. At the lowest scales and the molecular level, electronic-structure calculations based on first-principles quantum-mechanical approaches unravel the making and breaking of chemical bonds. At the largest mesoscopic scale, statistical simulations account for the interplay between all elementary processes involved in the catalytic cycle. At the macroscopic scale, continuum theories can yield the effect of heat and mass transfer.

Numerical studies have, among others, also focused on molecular heterogeneous catalysts, which are used in industry for the production of key compounds, such as hydrogen, sulfuric acid, nitric acid, polymers, etc.[2]. Computational modelling can be used to screen for potentially active catalytic materials before synthesizing the most promising candidates in the lab, thereby improving the efficiency of catalyst discovery. Within this CRC, such catalysts are ruthenium or rhodium complexes[3, 4] as well as metal N-heterocyclic carbene complexes based on Mo and W.[5] Catalytic reactions are generally characterized by the complex interaction of various physical and chemical processes and need to be treated with care. A long-standing goal in the field of molecular heterogeneous catalysis has been to predict, from first principles, the effects of catalyst composition and structure on the rates of catalyzed reactions, as well as the distribution of products (e.g. enantiomers) formed from a specified set of reactants. QM calculations on catalytic processes have provided insights into why and how changes in the composition and structure of catalytically active sites affect their activity and selectivity for targeted reactions.[6, 7] DFT simulations are especially suited to predict catalytic properties of materials and to design more efficient and cheaper catalysts for gas-phase reactions. However, in many important electrochemical processes, the surfaces are in contact with a liquid phase. Reactions and processes at liquid/solid interfaces pose additional challenges compared to gas-phase reactions.[8] A possible way to tackle these challenges, while still at the QM level, is to turn to *ab initio* MD. The strength of this method is its ability to follow the changes of the nuclei positions as well as the dynamic change of the electronic structure. The limitations are, however, that only small length scales and short simulations times can be achieved.[9] *Ab initio* MD simulations have been used to study a number of problems ranging from homogeneous and molecular heterogeneous catalytic systems[10] to reactions in solution, biocatalysis and materials surface chemistry.[11, 12]

In order to extend these length and time scales, one needs to resort to classical MD simulations. Such schemes have been applied for many years in molecular heterogeneous catalysis to compute reaction rates and reaction mechanisms, in spite of activation barriers that are much higher than thermal energies.[13] However, when diffusion is not of the same or lower order as the reaction rates, MD cannot provide reliable results, as it cannot model very long time scales,[9] and also typically does not model the reaction itself. Typical aspects having a direct impact on the reaction rates that MD modeling is able to handle are information on the explicit molecular environment around the catalytic center,[14] diffusion, selectivity,[15] the influence of solvent[16] and related conformational changes.[17] Such simulations combined with experiments have led to a general understanding of catalytic mechanisms.[16] For example, theoretical activities related to Ruthenium-catalyzed olefin metathesis have been shown to compare well with experimental results.[18] Through this comparison, the modeling scheme can be evaluated and further applied to other catalytic systems.

Ab initio and classical MD can be combined with metadynamics[19] to provide free energy landscapes of molecular heterogeneous catalytic reactions, minimum energy reaction pathways, energy barriers and evaluate possible rate-limiting steps, which might impede sustained catalytic activity. On top of these dynamic approaches, stochastic schemes, such as the kinetic Monte Carlo can become very efficient in evaluating the surface kinetics[20] description of the involved elementary steps, typically comprising absorption and desorption processes of reactants and reaction intermediates, as well as surface

diffusion and surface reactions. When aiming at a material-specific modeling that is at best of predictive quality, the computation of the corresponding kinetic parameters is at the realm of electronic structure theories that explicitly treat the electronic degrees of freedom and thus the quantum-mechanical nature of the chemical bond. At larger scales, computational fluid dynamics and kinetic modeling are methods of choice[21, 22] due to the prohibitive computational cost of using QM or MD on these scales. Especially the lattice-Boltzmann (LB) method, an efficient mesoscopic fluid solver,[23] can be applied to model chemical reactions and the involved mass transport.[24, 25]

At even larger scales, the mass transport induced by the solvent plays a dominant role in reactive flows. The advection of reactants towards the pore, the diffusion of reaction intermediates, and even entry events across multiple pores are examples of physical mechanisms that occur over mesoscopic length scales. These crucial mechanisms require different simulation approaches in order to cover the necessary time scales. The Lattice-Boltzmann (LB) method is widely used for simulating hydrodynamic interactions across complex geometries at mesoscopic length scales. The simulation space is divided into lattice nodes, which hold phase space distributions of particle populations. In this kinetic model, the distributions are propagated via local collisions, which ultimately lead to hydrodynamic flow that satisfies the Navier-Stokes equations. Although the LB method is widely used to model a single component solvent, the framework can be generalized to treat dilute solutes. Additionally, chemical reactions can be modeled in the LB framework by allowing a species exchange between the populations of the different components.[26-29] Catalytic sites can be modeled as lattice nodes, which allow for this exchange.[26, 30–33]

LB can be used as a stand-alone hydrodynamics solver coupled to various representations of solutes. On one end of the spectrum, a colloid can be modeled from LB boundary nodes,[34] a particle-based representation can interact with the LB layer via point-like coupling.[35] At the other end, a continuum representation can be used by coupling convection-diffusion equations to the LB layer.[36] In the latter approach, chemical reactions on a catalytic surface may be modeled through a solute flux normal to the boundary. The product flux can be constructed in a way to depend upon the local reactant concentration. To reduce the granularity of this continuum representation, event-based reactions can be catalyzed via a Monte-Carlo scheme.[37] This allows to sample effects from fluctuations, and reduces to the continuum description after sufficient averaging.[37] Tuning the pore geometries, as a function of transport properties of the reactants and products will depend on the reaction details. The different LB approaches can provide the required degrees of freedom in order to correctly model the reaction at a certain coarse-grained level.

For a catalytic reaction, it is often necessary to provide supported catalysts. However, the design of supported catalysts is still a challenge and often involves a trial-and-error process. Recently, DFT has shown its potential to provide new insight into the atomic-scale mechanisms of molecular heterogeneous catalysis, helping to interpret the large amount of experimental data gathered during the last decades.[38] DFT calculations can provide reactivity trends for the chemistry at transition-metal surfaces and have enabled in silico design of molecular heterogeneous catalysts.[39] Similar calculations on metal oxides reveal their unique electronic and structural properties that render them highly favorable for applications in molecular heterogeneous catalysis.[40] Different surface configurations of the materials involved in the catalysis impose different activation pathways, evaluated through activation energies, reaction energies, transition state structures, and charge analysis results. Similar effects of geometrical micro-irregularities in narrow porous catalyst membranes of a millimeter size have been underlined through LB schemes indicating an appreciable effect on the effective reaction efficiency in the molecular heterogeneous catalysis taking place in the channels.[41] At this level, a mapping of the chemical reactions and mass transport inside the complex nano-scale architecture of porous catalyst membranes can be directly compared to experiments.[42] In the end, the success of a catalytic reaction or at least reaching a high rate in catalytic reactions especially in confined media is influenced by a variety of factors ranging from the medium properties, the solvent, the reactant and catalyst characteristics, confinement effects, etc. This project aims to use a number of numerical schemes at different time and length scales in order to evaluate and optimize these factors together with the experiments.

References

[1] O. Deutschmann, *Modeling and simulation of heterogeneous catalytic reactions: from the molecular process to the technical system*, John Wiley & Sons, **2013**.
[2] C. N. Satterfield, *Heterogeneous catalysis in industrial practice*, New York, NY (United States); McGraw Hill Book Co., **1991**.
[3] D. Weickmann, W. Frey, B. Plietker, *Chem. Eur. J.* **2013**, *19*, 2741–2748.
[4] S. Helbig, S. Sauer, N. Cramer, S. Laschat, A. Baro, W. Frey, *Adv. Synth. Catal.* **2007**, *349*, 2331–2337.
[5] R. Schowner, W. Frey, M. R. Buchmeiser*, J. Am. Chem. Soc.* **2015**, *137*, 6188–6191.
[6] A. T. Bell, M. Head-Gordon, *Annu. Rev. Chem. Biomol. Eng.* **2011**, *2*, 453–477.
[7] J. Greeley, J. K. Nørskov, M. Mavrikakis, *Annu. Rev. Phys. Chem.* **2002**, *53*, 319–348.
[8] J. K. Nørskov, T. Bligaard, J. Rossmeisl, C. H. Christensen, *Nat. Chem.* **2009**, *1*, 37–46.
[9] R. A. Van Santen, M. Neurock, *Molecular heterogeneous catalysis: a conceptual and computational approach*, John Wiley & Sons, **2009**.
[10] M. Boero, M. Parrinello, K. Terakura, *J. Am. Chem. Soc.* **1998**, *120*, 2746–2752.
[11] D. Marx, J. Hutter, Grotendorst, J., Ed **2000**, 301–449.
[12] B. L. Trout, *Adv. Chem. Eng.* **2001**, *28*, 353–397.
[13] A. Jansen in *Fundamental Aspects of Heterogeneous Catalysis Studied by Particle Beams*, Springer, **1991**, pp. 133–144.
[14] M. Gilson, T. Straatsma, J. McCammon, D. Ripoll, C. Faerman, P. Axelsen, I. Silman, J. Sussman, et al., *Science* **1994**, 1276–1276.
[15] G. Sastre, A. Chica, A. Corma*, J. Catal.* **2000**, *195*, 227–236.
[16] M. Karplus, J. Kuriyan, *Proc. Natl. Acad. Sci. United States Am.* **2005**, *102*, 6679–6685.
[17] G. Papoyan, K.-j. Gu, J. Wiorkiewicz-Kuczera, K. Kuczera, K. Bowman-James, *J. Am. Chem. Soc.* **1996**, *118*, 1354–1364.
[18] O. M. Aagaard, R. J. Meier, F. Buda, *J. Am. Chem. Soc.* **1998**, *120*, 7174–7182.
[19] M. Ghoussoub, S. Yadav, K. K. Ghuman, G. A. Ozin, C. V. Singh, **2016**.
[20] K. Reuter, Model. Heterog. Catal. React. From Mol. Process. to Tech. Syst. **2011**, *1*.
[21] V. M. Janardhanan, O. Deutschmann in *Modeling and Simulation of Heterogeneous Catalytic Reactions*, Wiley-VCH, **2011**, pp. 251–282.
[22] M. Stamatakis, *J. Phys. Condens. Matter* **2014**, *27*, 013001.
[23] S. Succi, *The lattice Boltzmann equation: for fluid dynamics and beyond*, Oxford University Press, **2001**.
[24] S. Succi, O. Filippova, G. Smith, E. Kaxiras*, Comput. Sci. Eng.* **2001**, *3*, 26–37.
[25] A. Gabrielli, S. Succi, E. Kaxiras, *Comput. Phys. Commun.* **2002**, *147*, 516–521.
[26] S. Bartlett, *Computation* **2017**, *5*, 37.
[27] S. Ayodele, F. Varnik, D. Raabe, *Phys. Rev. E* **2011**, *83*, 016702.
[28] S. Ayodele, D. Raabe, F. Varnik, *Commun. Comput. Phys.* **2013**, *13*, 741–756.
[29] R. Blaak, P. M. Sloot, *Comput. Phys. Commun.* **2000**, *129*, 256–266.
[30] Q. Kang, D. Zhang, S. Chen, X. He, *Phys. Rev. E* **2002**, *65*, 036318.
[31] Q. Kang, D. Zhang, S. Chen, *J. Geophys. Res. Solid Earth* **2003**, *108*.
[32] Q. Kang, P. C. Lichtner, D. Zhang, *J. Geophys. Res. Solid Earth* **2006**, *111*.
[33] J. Kang, N. I. Prasianakis, J. Mantzaras, *Phys. Rev. E* **2014**, *89*, 063310.
[34] C. K. Aidun, Y. Lu, E.-J. Ding*, J. Fluid Mech.* **1998**, *373*, 287–311.
[35] P. Ahlrichs, B. Dünweg, *J. Chem. Phys.* **1999**, *111*, 8225–8239.
[36] F. Capuani, I. Pagonabarraga, D. Frenkel, *J. Chem. Phys.* **2004**, *121*, 973–986.
[37] S. K. Mishra, A. De, *Comput. Fluids* **2013**, *71*, 91–97.
[38] J. K. Nørskov, M. Scheffler, H. Toulhoat, *MRS Bull.* **2006**, *31*, 669–674.
[39] J. K. Nørskov, F. Abild-Pedersen, F. Studt, T. Bligaard, *Proc. Natl. Acad. Sci.* **2011**, *108*, 937–943.
[40] M. Ghoussoub, PhD thesis, University of Toronto (Canada), **2016**.
[41] S. Succi, G. Smith, E. Kaxiras*, J. Stat. Phys.* **2002**, *107*, 343–366.
[42] G. Falcucci, S. Succi, A. Montessori, S. Melchionna, P. Prestininzi, C. Barroo, D. C. Bell, M. M. Biener, J. Biener, B. Zugic, et al., *Microfluid. Nanofluidics* **2016**, *20*, 1–13.

3.16.3.2 Own Work, Project-related publications by participating researchers

The applicants have a long experience with molecular simulations at different length and time scales and have been working on systems ranging from electronic transport in graphene sheets to ionic transport through nanopores. M. Fyta has a broad experience on smaller scales probed with quantum-mechanical and atomistic computational schemes, but also multi-scale computational schemes. C. Holm has his main expertise in coarse-grained charged soft matter systems, development of novel methods for the statics and dynamics of charged systems, and recently also non-equilibrium systems like catalytically driven self-propelled particles.

Specifically, M. Fyta's work lies at the interface of Condensed Matter Physics, Biophysics, and Materials Science. She has been performing computer simulation methods ranging from classical (Monte-Carlo schemes within empirical potential approaches, Molecular Dynamics), semi-empirical (parametrized tight-binding schemes), quantum mechanical (implementations of the density functional theory also in conjunction with non-equilibrium Greens functions for quantum transport), and multi-scale methodologies (coupled Langevin molecular-dynamics and lattice-Boltzmann method for modeling molecular motion in a fluid solvent) to investigate diverse systems. Among others and relevant to this project, these cover N-heterocyclic carbene-metal complexes,[C6-1] the absorption of self-assembled monolayers (SAMs) on metallic surfaces,[C6-2] translocation of polymers through nanopores and functionalized electrodes for DNA sensing,[C6-3] ionic solutions and force field development for coarse-grained large scale simulations,[C6-4] solvent effects,[C6-5] etc.

C. Holm is an established researcher in the field of magnetic and charged soft matter physics. In his group, the code ESPResSo[C6-6] was developed, a software package for simulations of soft matter systems that is used worldwide by numerous research groups. ESPResSo has a fast (GPU) implementation of the LB method. The LB model employed by ESPResSo boasts thermodynamically consistent fluctuations. These play a crucial role in reproducing correct nanoscale dynamics. A finite differences solver for the convection-diffusion equation, which can couple with the LB layer has also been implemented in the GPU LB code (for historical reasons this is called the electrokinetics (EK) LB, though the solutes need not to be charged). Moreover, ESPResSo can also model diffusiophoretically driven particles with full hydrodynamic interactions (HIs). This includes the diffusion and advection of individual solvated chemical species and a catalytic reaction scheme that operates locally on these species and models a catalytic reaction with a user-set reaction rate. We will refer to this model as the Lattice-Boltzmann plus Catalytic Reaction (LB-EK-CR) model. Recently, a moving boundary implementation of the method was used to investigate the electrophoretic mobility of charged particles.[C6-7] C. Holm has ample experience with coarse-grained and all-atom simulations of electrolyte flow and charged macromolecules in confinement, transport phenomena in confined geometries,[C6-8] and coarse-graining strategies for studying dynamical properties.[C6-9] Using the reaction-ensemble methods also charged interfaces with pH-dependent surface charges were investigated. Chemical reactions also played a role in the work on the theory of self-electrophoresis of catalytically driven particles.[C6-10] This existing work will provide a significant head start into implementing different flavors of catalytic surface reactions.

Both PIs have successfully collaborated with other principal investigators of this proposed CRC in the past on other projects. Together with J. Kästner they worked in the CRC 716, of which C. Holm is the spokesperson. They have co-supervised doctoral theses with J. Kästner (**C4**), N. Hansen (**C5**), and J. Groß (**C5**).

[C6-1] A. Natterer, B. Adhikari, M. Fyta, *J. Organomet. Chem.* **2016**, *815*, 8–15.
[C6-2] B. Adhikari, S. Meng, M. Fyta, *Nanoscale* **2016**, *8*, 8966–8975.
[C6-3] G. Sivaraman, R. G. Amorim, R. H. Scheicher, M. Fyta, *Nanotechnology* **2016**, *27*, 414002.
[C6-4] C. W. Hsu, M. Fyta, G. Lakatos, S. Melchionna, E. Kaxiras, *J. Chem. Phys.* **2012**, *137*, 105102.
[C6-5] T. Kobayashi, J. E. Reid, S. Shimizu, M. Fyta, J. Smiatek, *Phys. Chem. Chem. Phys.* **2017**, *19*, 18924–18937.
[C6-6] H. J. Limbach, A. Arnold, B. A. Mann, C. Holm, *Comput. Phys. Commun.* **2006**, *174*, 704–727.
[C6-7] M. Kuron, G. Rempfer, F. Schornbaum, M. Bauer, C. Godenschwager, C. Holm, J. de Graaf, *J. Chem. Phys.* **2016**, *145*, 214102.
[C6-8] S. Kesselheim, W. Müller, C. Holm, *Phys. Rev. Lett.* **2014**, *112*, 018101.
[C6-9] F. Weik, S. Kesselheim, C. Holm, *J. Chem. Phys.* **2016**, *145*, 194106.
[C6-10] A. T. Brown, W. C. K. Poon, C. Holm, J. de Graaf, *Soft Matter* **2017**, *13*, 1200–1222.

3.16.4 Project plan

In summary, the research goals are organized in work-packages (**WPs**) as follows:

- **WP1: Surface functionalization, materials' properties, and short linkers** will be investigated at a more detailed level using quantum-mechanical calculations. The focus will lie on certain material classes from **Area A**, which include those involving the growth of self-assembled layers on the tunable block copolymer templates in **A2** and on the organic/inorganic hybrids in **A5 (A7)**.
- **WP2: Linker length and density, solvent effects** will be accounted for by investigating the influence of these parameters on conformational aspects of the linkers on the pore surfaces. The linker details (length and chemical specificity), as well as the choice of the solvent will be investigated together with the synthesis **projects A2** and **A5** and the researchers from **B1- B3**.
- **WP3: Force-field parameterization** will be essential for describing the interactions between the different components (pore, surface functionalization, linkers, solvent, and catalysts) in an atomistic or coarse-grained approach as described in **WP4 - WP8**. Available classical force fields from the literature need to be supplemented with additional parameters and in some cases functional forms in order to be able to perform the simulations planned in this project.
- **WP4: Influence of the catalyst** on conformational aspects of the catalytic system will be assessed by attaching the catalysts from **B1-B3** on the linkers and materials from **WP1- WP2**.
- **WP5: Development of a multispecies reactive lattice Boltzmann algorithm (LB-EK-CR) with explicitly diffusing particles and implementation into ESPResSo**. In this work package, we will extend the algorithm of Capuani *et al.* to include several diffusive species. We will also include reactive flux boundaries, and implement everything into the GPU LB of ESPResSo.
- **WP6: Inclusion of thermal fluctuations into the diffusion-advection and the reaction scheme**. Here, we will extend the LB-EK-CR algorithm by adding thermal fluctuations to the diffusion advection dynamics of chemical species and the catalytic reaction scheme. These can be important for nanoscale thermal systems.
- **WP7: Set up of a pore system with inlet-outlet flow in various geometries.** We will perform extensive parameter studies with our thermal and deterministic LB-EK-CR algorithm to study the full catalytic cycle under non-equilibrium conditions in various geometries. The rates will be obtained from simulations in **C4**, the diffusion constants will be taken from the simulations of **C5**, and the experimental values come from **B1** and **C2**.
- **WP8: Construction of coarse-grained catalytic particle model coupled to a LB fluid.** Here, we will start to develop a refined coarse-grained model to study the dynamics of the catalytic reactions. All particles will be modelled explicitly except the background fluid that is modelled with the LB algorithm. The reactions are handled through a MC algorithm in the reaction ensemble.

Overall, we will work on various scales, where M. Fyta leads and coordinates mainly **WP1**-**WP4**, and C. Holm leads and coordinates mainly **WP5**-**WP8.** Our bottom-up approach is expected to unravel the factors that would be essential for molecular heterocatalysis in confined pores. Starting from the absorption of functional groups on surfaces and the influence of a solvent on the linker conformations, we will move up the scales to reach to the diffusion of catalysis products out of the pore. A sketch of this approach is given in Fig.C6-1.

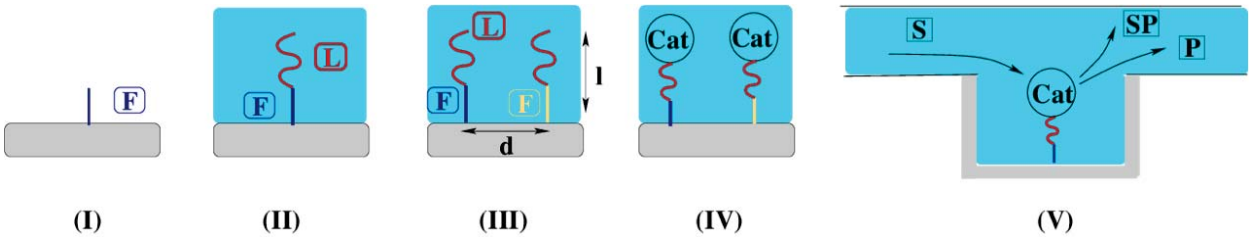

Figure C6-1: The bottom-up approach followed in this sub-project using quantum-mechanical, atomistic, coarse-grained, and mesoscopic simulations is depicted. The material surface is shown in gray, the different functional groups on these surfaces are in blue and yellow (F), while in red (L) are the linkers. Using first principles approaches the attachment of the functional groups in (I) will be studied. This will be followed in (II) by *ab initio* and classical Molecular Dynamics (MD) on the attachment of a linker group, while the influence of the linker length l and the intra-linker distance d at step (III) will be studied with classical MD. The attachment of the catalyst (Cat) on a linker at step (IV) will be analyzed through atomistic and coarse-grained MD. In all steps after (I), the influence of the solvent (light blue background) will be accounted for through an implicit and later an explicit scheme. At the largest scale (V), the mass transport of the reactant (S) into the pore, the reaction with the catalyst, and the further transport of products (P) and side-products (SP) out of the pore will be modeled.

3.16.4.1 WP1 (M. Fyta): Surface functionalization, materials' properties, and short linkers

A first step towards the goal of this CRC is the investigation of the modified surfaces used for the pores. Here, we will focus on a class of materials from the **A-Area**, which will be functionalized with self-assembled monolayers (SAMs) on top of which the linkers and the catalyst will be eventually attached. The materials of interest in this project are the tunable block copolymer templates from **A2** and the organic/inorganic hybrid materials from **A5 (A7)**. We will obtain their properties through quantum-mechanical calculations within the density functional theory (DFT) approach. For example, for the hybrid materials, the influence of the type of transition metals on these properties as evaluated through our results would be very relevant for the materials synthesis. Based on these types of simulations, we will gain information on the stability and absorption of the SAMs on the oxides **A5**, and the structural properties of the tunable templates in **A2**. Towards the end of **WP1**, we will also address the interaction and absorption energies between the oxide films such as ZnO on flat nano-foams in order to assist the characterization of the materials in **A7**. The nucleation of the oxide films on the nano-foams will be studied in detail in the second funding period. In view of the collaboration with **A2**, we will first focus on the surfaces functionalized with azide and alkyne head groups and at a second step move to the OH-modified pore surfaces.

In this part (see Fig. C6-1 (II-III)), we will begin with surfaces on which a single molecule is attached. For the oxides in **A5**, the experimentally relevant structures will be studied. These are inorganic materials such as SiO_2, TiO_2, ZNO, Al_2O_3, etc. on which the docking of OH-, COOH-, and N_3- groups will be analyzed. All calculations for this part will be done in vacuum. These will be supplemented by additional simulations with a background dielectric medium resembling an implicit solvent. *Ab initio* MD calculations will be performed on top of these for including some conformational aspects of the functional groups, as well. In this way, the influence of a solvent will be taken into account at a first approximation. An explicit solvent will be added at a next level (**WP2**). The outcome of **WP1** in terms of the stability of the structures will assist the characterization of the materials as planned in **Area C**. From the modeling's point of view, the details on the local structure/conformation will be important for

attaching the linkers relevant to the experiments. In this **WP**, the shortest linkers will be taken in agreement with **B1**-**B3**.

3.16.4.2 WP2 (M. Fyta): Linker length and density, solvent effects

This part (see Fig. C6-1 (I-II)) will focus on the structuring of different solvents around the linker-material system studied in **WP1**. The main goal is to study the influence of the solvent on the conformational arrangement/ orientation and variability of the linkers on the pore materials. We will search for specific solvent effects, layering, chiral hydration shells, distinct solvation shells or polar/apolar regions for different surface functionalizations and linker lengths. The materials and functional groups from **WP1,** and the linker types and lengths suggested in **B1**-**B3** will be considered. We will begin the study without the linkers and will perform a careful scan of polar/apolar surfaces in combination with a polar/apolar solvent. The polarity of the surfaces will be modeled by attaching the anchor groups from **WP1**, but also including alkyl-, fluorite-, and silane-groups. At a first approximation, the solvent will be modeled as a dielectric medium for which we will vary the dielectric constant. From these calculations we will get an estimate of the interplay between the material polarity and the solvent polarity. Having understood this interplay, explicit solvents in classical atomistic simulations within the force field approach will be used to refine the results. At this level, the exact details of the solvent will become important and need to be taken care of through classical MD, as the system sizes become too large to be treated with DFT.

For the solvent, water, mixture of water with toluene, dioxane, and tetrahydrofuran (THF) will be taken. Depending on the catalysis conditions and the input from **B1**-**B3**, additional solvents will be investigated. We aim to unravel specific structuring and hydration shells around the catalytic centers. From a theoretical point of view, it is also interesting to analyze the expected deviations for the various materials and linker chemistry. For this, all results will be compared with the case of water, which is taken as a reference. The interplay between linker chemistry and the solvent properties is expected to be of importance for the projects in **Area B** and the choice of the linker. This choice will be based on the conformational details of the linker with respect to the surface. As an example, we will begin this study with the linker molecules suggested in **B1**. These have three different lengths and rigidity (aryl-, biaryl- and triaryl-linker, as well as propyl-, pentyl- and heptyl-linker) and will be attached on the functionalized surfaces from **A2** as modeled in **WP1**. In addition to the chemistry and length of the linkers, their density on the pore material will also be evaluated. For this, more than one linker will be attached on the functional groups of the surfaces and their separation will be varied. Again, conformational aspects of the linkers and their interactions will be evaluated in order to shed light into the relation between pore polarity and solvent polarity with the packing of the linkers. The results will be an input to the materials **projects A2**, **A5** and be compared to the high-resolution tomography **project C3,** and are expected to give hints on particular chemical transformations in the pore. Specifically, for the azide/alkyne functionalized surfaces from **A2**, we will begin with ferrocene as a test molecule. This will be attached on the functional groups of the template. After establishing an understanding on the dynamics of the test molecule, we will add a linker and finally vary the length of the linker and evaluate conformational changes and molecular arrangements on the material, as well as the influence of the solvent. For this, a close collaboration with **projects C4** and **C5** is foreseen.

3.16.4.3 WP3 (M. Fyta): Force-field parameterization

Based on DFT calculations on the interactions between functional groups and surfaces, functional groups and linkers, linkers and catalyst, catalyst with solvent, linkers with solvent, solvent with surface, we need to enlarge the parameter space for the relevant classical force fields found in the literature. The aim of this work package is to develop force fields for the materials/groups/linkers for which no relevant or insufficient interactions can be found in the literature. In order to pursue this part two single molecular groups will be taken each time, e.g. surface atoms with functionalizing group, functionalizing group with part of the linker molecule, etc. For these, the energetic contributions from varying distances, angles, etc. will be evaluated, fitted to analytic formulas and parametrized. In this way, also an efficient coarse-graining similar to some of our previous work[C6-4] will be done. This will allow larger scale simulations in certain cases, e.g. the copolymer materials of **A2** or when increasing the linker length (**WP2**). The DFT calculations will be done both in vacuum and using a dielectric medium to roughly

capture some solvent effects. Depending on the input from the experimental projects in this CRC, as well as the simulation details (accuracy and computational cost vs. system size/time), we will decide on the fly on the degree of the coarse-graining that will be applied for the generation of the force-fields. The force fields developed here will be used in the atomistic and coarse MD modeling in **WP2** (in case the linkers will be too long to be efficiently modelled with atomistic MD), **WP3**, the LB simulations in **WP5**-**WP8**, as well as in the QM/MM and MD studies in the other theory **projects** (**C4** and **C6**). **WP3** will involve many benchmark simulations.

3.16.4.4 WP4 (M. Fyta): Influence of the catalyst

This part (see Fig. C6-1 (IV)) will include classical and coarse-grained MD simulations, as the system sizes will be prohibitive for modeling with QM simulations. At a first step, the catalysts from **B1**-**B3** will be attached to the shortest linkers in order to look into the arrangement and the conformational aspects of the catalysis-systems. The changes on the solvent/linker interactions by also attaching a catalyst on the short linkers will be evaluated. For longer linkers, some degree of coarse-graining will be needed as performed through the parameterization in **WP3**. In this way, not the full chemical specificity of the linkers needs to be taken into account. Evaluating this arrangement (whether the linkers are standing upright, tilted or closer to the surface) and the relevant conformational details is expected to have a strong impact on the efficiency of the catalytic reaction. A possible different (than expected) orientation/arrangement of the linker will impose unwanted conformational variability of the catalyst prohibiting its activity. The results of **WP4** will be compared to the catalytic systems from **B1**-**B3**. Close collaboration with the characterization projects **C1**-**C2** is foreseen for this part and the conformational results will be directly compared to those from **C3**.

This **WP** will begin with the less complex catalyst from **B1** and the modified surfaces from **A2** as a test case. An important question to be tackled here is related to the packing of the linker-catalyst molecules on top of the surfaces. We aim to understand what kind of packing of the linker-catalyst on the surface will provide good conditions for the molecular heterogeneous catalysis. The interplay between solvent/linker/catalyst through our modeling approaches should provide a clear picture on the important factors, which can be chosen properly in order to optimize the catalytic reactions. The catalysts from **B2** and **B3** will be taken once the simplest test case mentioned above has been evaluated. At the very end of this **WP** and towards the second phase of this CRC, instead of planar materials we will model a well with polar surfaces functionalized with OH-groups in collaboration with **A2**. This will more effectively include the role of the confinement. Along these lines, at a later stage, curvature will also be imposed on the templates in order to model cavities.

3.16.4.5 WP5 (C. Holm): Development of a multispecies reactive LB with explicitly diffusing particles and implementation into ESPResSo

In this work package, we will extend the algorithm of Capuani *et al.*[36] in order to use it for the modelling of all catalytic reactions happening in **B1**-**B3**. This means on the one hand to include multiple diffusive species, since the Capuani method was intended to work for charged species only. On the other hand, we will also include multiple reactive flux boundaries, meaning that we will include LB boundary nodes that can drive catalytic reactions, which is the discrete analog of the continuum flux boundaries.[43] This will allow for variable reaction rates at catalytic boundary nodes. We will also implement a three-step catalytic reaction as used within the CRC in **B1**. This will simply mean that other side products can react with a different rate at the provided catalytic sites. In addition, we will implement generic particle-wall interactions in order to be able to tune the wall properties from hydrophilic to hydrophobic (polar/apolar) walls. We will also include an excluded volume term for our diffusive species in order to cope with the expected higher densities at larger reaction rates or in the case of high reactant density. Several mechanisms exist here in the literature, e.g.[44], and we have to test which is the most appropriate one. All different species can interact with different potentials with each other and with the wall. In such a way we can tune one species to behave like water, and model through realistic reaction rates and diffusion constants quite accurately the different reactants, products, and side products. This means that we can start immediately with the model building, and use in the beginning sensible parameters for the reactants and products, and later refine the model, once the reaction rates and

diffusion constants are better known from the other theory **projects C4** and **C5**, and experimental measurements in **B1** and **C1**.

When the implementation is finished, we will have to check its validity for a simple pore geometry. We plan to use here an infinite cylindrical pore. We will first test the implementation against continuum equations describing the diffusive transport of multiple species from reactive sites of variable reactivity. We will then study equilibrium density profiles resulting from the continuum equations against the ones obtained for our algorithm.

3.16.4.6 WP6 (C.Holm): Inclusion of thermal fluctuations into the diffusion-advection and the reaction scheme

In this work package, we will extend our LB-EK-CR algorithm by including thermal fluctuations. Our LB algorithm is already equipped with a multi-relaxation time (MRT) algorithm including a thermodynamically consistent thermalization.[45, 46] To date, the EK extension modeling the diffusion-advection dynamics of chemical species and the catalytic reaction scheme use a deterministic mean-field description and does not include thermal fluctuations.

Since the investigated reactions take place in confined geometries with sizes of 10 – 15 nm, the magnitude of thermal fluctuations in the system is significant. Due to the non-linear nature of the advective dynamics and the reactions, the effect of these fluctuation can not be expected to simply average out — we therefore cannot neglect thermal fluctuations. We plan to include thermal fluctuations into the EK-CR extension for the LB algorithm by adding stochastic random flux contributions into the propagation scheme obeying the fluctuation-dissipation relation for the Nernst-Planck equation. After completion, we will be able to assess the relevance of these fluctuations by comparing previous deterministic results with the ones obtained by including thermal fluctuations.

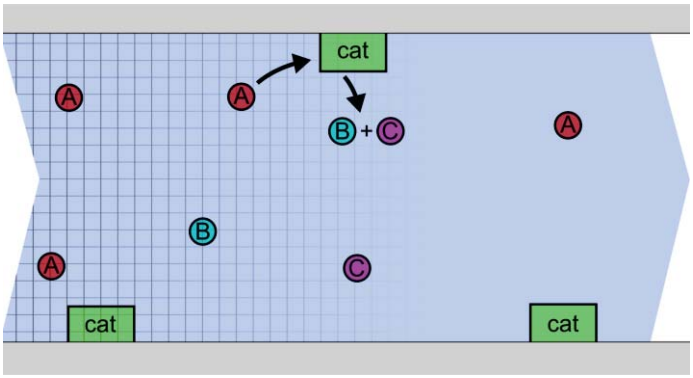

Figure C6-2: Sketch of a cylindrical pore with different catalytic sites present. The pressure driven or diffusive flow with a certain reactant (A) concentration produces catalytic reactions when the reactant is close to the catalytic sites. The products (B, C) will have to be transported away yielding a certain turnover rate. The interactions of species (A, B, C) with each other and with the pore wall can be adjusted.

3.16.4.7 WP7 (C.Holm): Set up of a pore system with inlet-outlet flow in various geometries.

After having achieved the necessary methodological advances, we will perform extensive parameter studies first for the infinite cylindrical pore as sketched in Fig. C6-2. The model can be equipped with parameters for the experimentally investigated systems of this CRC. The values for the diffusion coefficients of the species will be taken from **C5**, the reaction rates for the catalytic reactions will come from **C4**, while the force-field parameters developed in **projects C4**, **C5** and our **WP2** will serve as input for the interaction parameters in the model developed here. The results on the diffusion processes will be compared to relevant experimental studies in **C1**, **B1**, and **C2**.

In a second step, we will study the diffusive transport of a potentially pressure driven flow through a multi-pore system with inlet and outlet flow. Here, the geometric set-up can look like Fig. C6-1 (V), where the reactant has to diffuse into pores of variable geometry. We will start out with a slit pore and will later model it like a finite cylinder in order to be closer to the geometries investigated in the **projects A1**, **A2**, **A3** and **A6**. The reactant needs to diffuse from the flow into the confined finite pore where the catalysis happens. We will investigate the transport properties of the substrates and products into and out of the pore. Especially the kinetics, the potentially non-linear correlations of in-flux and out-flux of all species will be investigated as a function of different interactions. These can be the interactions of the reactant with the catalyst, but also all involved products with each other and the wall. Here, we envision the appearance of excluded volume interactions to become relevant and will investigate those closely. Since, one of the products of the catalysis in **B1** is water that has to be transported away, we will especially investigate the effects of hydrophilic walls. Also, the position and the number of involved catalysts per pore will be investigated. A relevant outcome of these investigations will be the dependence of the turnover rates on the used parameters, i.e. one can specifically look for optima while tuning the ratios of diffusion constants of reactant, products, and intermediate products, as well as the influence of variable reaction rates in multi-step reactions.

3.16.4.8 WP8 (C.Holm): Construction of coarse-grained catalytic particle model coupled to a LB fluid

In this work package we will start to develop a microscopically more accurate, but still coarse-grained model to study the dynamics of the catalytic reactions, starting with the catalytic cycle used in **B1**. We will use the lattice Boltzmann method to model the background fluid flow, but model the dispersed reactants, products, and side-products as coarse-grained particles, as well as the catalyst, the spacers and the linkers to the material surfaces. The particles will be coupled via a frictional coupling to the LB fluid,[35] and extended particles with rotational degrees of freedom can be coupled via the raspberry model.[47, 48] The particle representation will allow us to model the interactions of the reactants and the products with each other, the walls and the catalysts, as well as any other involved particle species such as linkers and spacers more specifically. Effective interactions for all particles can be derived from the detailed studies performed in **WP1**-**WP4**. The catalytic reactions will be dealt with by employing a Monte Carlo procedure using the reaction ensemble. We have already experience with this approach, since we employed the reaction ensemble for the study of the association-dissociation equilibrium of weakly charged groups.[49, 50] Moreover, since we can assemble the catalyst from several CG beads, we can make it shape asymmetric, and we can also mimic the occurrence of specific catalytic sites for each reaction. We will again investigate the influence of the non-equilibrium situations created by the catalytic process, study the turnover rates for various geometries and flow conditions. The reaction rates can be again taken from the experiments and theory **projects B1**, **C1**, and **C2**. Since we are more sensitive to chemical and physical details, we can address more detailed questions. Specifically, for the catalysts from **B3** we will look into identifying chiral solvation shells. For any interactions not found in the literature, we will turn to **WP3** to develop the missing force field parameters or get them – if applicable - from **C4** or **C5**.

3.16.4.9 Chronological work plan:

A rough sketch of the time allocated for each **WP** is given in Table 1. In all **WPs**, the time included for tests and benchmarks is included.

	2018		2019				2020				2021				2022		
	Q3	Q4	Q1	Q2	Q3	Q4	Q1	Q2	Q3	Q4	Q1	Q2	Q3	Q4	Q1	Q2	
T1																	WP 1: Surface functionalization, materials' properties, and short linkers
T2																	WP 2: Linker length and density, solvent effects
T3																	WP 3: Force-field parameterization
T4																	WP 4: Influence of the catalyst
T5																	WP 5: Development of a multispecies reactive LB with explicitly diffusing particles and implementation into ESPResSo
T6																	WP 6: Inclusion of thermal fluctuations into the diffusion-advection and the reaction scheme
T7																	WP 7: Set up of a pore system with inlet-outlet flow in various geometries
T8																	WP 8: Construction of coarse-grained catalytic particle model coupled to a LB fluid

3.16.4.10 Methods applied

This project will apply a number of computational methods at different length and time scales in order to address the questions arising from the **WPs** described above. At the lower scale, quantum-mechanical calculations within the DFT approach will be used and complemented with *ab initio* MD (AIMD) techniques. For addressing the conformational questions of the functionalization of the pores and the various linkers, classical MD will be applied for which the force fields will be either taken from the literature, developed within this project (**WP2**) or taken from the parameterization in **C4**, **C5**. These projects will also provide with the diffusion rates for the LB calculations on the mass transport in and out of the pores. For all methods, initial benchmarking and continuous tests will provide information whether these schemes are sufficient or another level of approximation is needed.

(i) Quantum-mechanical scheme: The QM method used in this project is based on density functional theory (DFT)[51] and can provide information on ground-state properties for relatively small system sizes (up to 10^3 particles) due to the high computational demand. We will use a number of relevant computational codes such as SIESTA,[52] VASP,[53] Turbomole.[54] A valence triple-ζ polarized basis set, def2-TZVP[55], is employed for all the calculations. For heavy elements, e.g. Au atoms, a minimum basis set will be used for computational efficiency. Different pseudopotentials will model the core electrons.[56-58] Regarding the exchange-correlation functionals, approximations beyond the local density approximation (LDA)[59] will be relevant. At a lower level a generalized gradient approximation (GGA)[60] will be used. For better implementing dispersion forces, van der Waals functionals such as the VDW-D2[61] scheme will be used based on the Perdew-Burke-Ernzerhof ansatz (PBE).[62] These VDW-DW functionals have been efficiently used for modeling hydrogen bonds or π - π-interactions and compared to high-level *ab initio* calculations.[63] The influence of the solvent will be modeled implicitly through the COSMO solver.[64]

(ii) *Ab initio* Molecular Dynamics (AIMD): MD at the QM level will also be applied in this project in order to evaluate conformational aspects and the influence of the solvent at a QM level. For the simulations the Car-Parinello MD (CPMD) method will be used[65] implemented in the code CP2K.[66] At a first approach, the revised PBE (revPBE) functional[62] will be taken. At this level, any dispersion corrections will again be applied through the Grimme-ansatz.[67] The explicit solvent will

be modeled on the classical level. The molecular conformations will be evaluated with this scheme for different solvents. The systems calculated with AIMD will span sizes up to a few hundreds of atoms and time scales up to a few tenths of picoseconds depending on the exact numerical details used.

(iii) Classical Molecular Dynamics: in order to extend the system sizes and scales, classical force fields will be taken and together with Newton's second law describe the motion of the atoms or molecules involved in the simulations. The codes GROMACS[68] and LAMMPS[69] will be used. Depending on the system, the force fields (FF) used will be the OPLS-AA,[70] the generalized AMBER (GAFF) and the DREIDING force field.[71] Depending on the exact FF, water models such as SPC/E[72] and TIP4P[73] will be chosen. For the materials and some of the linkers, the interactions will be modeled through reactive bond order potentials (ReaxFF)[74] and simpler pair-potentials. For the latter and the case of oxides, potentials can be found in the literature,[75, 76] but need to be tested in the current framework. For gold, the embedded atom method (EAM) will be taken.[77] Since, not all interactions involved in the complex systems studied here will be found in the literature, own parameterization will be carried out as discussed in **WP3** involving extensive benchmarking.

(iv) Reactive Lattice-Boltzmann: simulations including the microfluidic environment and its influence on mass transport will be carried out on a continuum level using an extended LB scheme. The LB algorithm will model the viscous flow of the overall fluid, while the transport of the miscible species taking part in the reaction will be modeled using a finite volume diffusion-advection scheme coupled to the fluid flow.[36] Chemical reactions at catalytic surfaces are modeled through fluxes of reactants into the surface and fluxes of products out of it. The magnitude of these fluxes depends on the local fluid composition and will be chosen such that it reproduces the reaction rates obtained from the more detailed MD and QM simulations. We previously applied this model successfully to chemically propelled micro-particles — another system where the correct modeling of the interdependency of mass transport and catalytic reactions is critical. Partial implementations of these algorithms are available as part of our in-house open-source simulation package ESPResSo and take advantage of GPU accelerated computations. What is missing is the consistent inclusion of fluctuations into the diffusion-advection scheme and into the reactions, which is part of **WP 6**.

3.16.4.11 Vision

This project aims to fill the gap between the experimental design of materials in **Area A** and the investigation of catalytic complexes of **Area B**. Together with the other modeling **projects** (**C4**, **C5**), **C6** covers a variety of length scales in order to unravel the influence of the microscopic properties, such as the linker density on the pore surface on the catalytic selectivity. The aim is to reveal a link between the polarities of the functionalized materials and the solvent, the linker length, and the molecular conformations in the confined space of the pore. Furthermore, we hope to understand the complicated relationship of the diffusion of the reactant into and of the catalysis products out of these pores. The mass transport calculations will be performed on the most active catalyst systems from **B1**-**B3** presently on a coarse-grained level. For the future, we plan to extend the investigation on the nano-foams from **A7**. We will also try to input more and more microscopic details into our model in order to put forward quantitative predictions, or at least be able to quantitatively match available experimental data. In the further funding periods we will address additionally the heat flux that is generated during catalysis using a lattice version of Fourier's law. Catalysis is a non-equilibrium phenomenon, and one needs to understand the different dynamic contribution to the whole catalytic process. Using inputs from **projects C4** and **C5**, the goal is to evaluate the most important factors influencing molecular heterogeneous catalysis in confined pores and assist the two other **Areas A** and **B** in shaping the design of the pores, the location of the catalysts, and necessary other parameters for optimizing the turnover frequency and the efficiency of the catalysis.

3.16.5 Role within the collaborative research center

This project together with the other theoretical **projects C4** (Kästner), **C5** (Groß/Hansen) aims to link the materials designed in the Area **A** with the catalytic complexes of the Area **B** in order to investigate the role of confinement on static and dynamic processes. **C6** aims to unravel the important factors that will eventually guide molecular heterogeneous catalysis within confined pores. The materials and catalysts involved in this CRC require a large modeling effort, which is to be handled by the three theoretical **projects C4**-**C6**.

The differentiation within the theoretical projects is based on methods and on systems studied: quantum chemistry is used in **projects C4** and **C6**, where **C4** approaches the overall goal from the catalysis side modeling mechanisms and reactivities, while **C6** focuses on materials properties. Both use QM techniques to parametrize force fields, but for different systems. Classical all-atom molecular dynamics is used by all three theory-projects: in **C4** on COFs, in **C5** on silica, and in **C6** on the materials from **A1**, **A2**, **A3**, **A5**, whereas coarse-grained methods are only dealt with in **C6**. Fluid theoretical methods like classical DFT are used only in **project C5**, while the lattice-Boltzmann method is used exclusively in **project C6**. Fluid theoretical methods like classical DFT are used only in **project C5**, while the lattice-Boltzmann method is used exclusively in **project C6**.

The properties of the materials synthesized in **Area A**, especially the self-assembled monolayers of **A2** and **A5 (A7)** will be modeled here with electronic structure DFT. A close collaboration with these projects is anticipated, as the properties calculated here will assist the materials' design. The transport of the reactants and products will be extensively studied in cooperation with the characterization **projects C1**, **C2** that will provide diffusion constants and catalytic reaction rates, and also experimental data on approximate conversion rates. The arrangements of the catalytic systems on the materials will be evaluated in collaboration with **C3**. The mass transport modeling will be very relevant for **projects A3, B1**- **B3**. The parameterization of interactions needed for the simulations is demanding and time consuming, and will be divided among all three modeling **projects C4** - **C6**. There we will work closely together, by not only exchanging results, but also disseminating knowledge and experience on different methodologies. Our studies in the framework of these **WPs** are very relevant to Areas **A** and **B** for the optimization of the conditions for the catalysis.

3.16.6 Differentiation from other funded projects

The work described in C6 is currently not funded by any funding agency and no relevant funding proposal has been submitted or is under revision.

3.16.7 Project funding

3.16.7.1 Previous funding

This project is currently not funded and no funding proposal has been submitted.

References (ctd.)

[43] P. Kreissl, C. Holm, J. de Graaf, *J. Chem. Phys.* **2016**, *144*, 204902.
[44] D. Antypov, M. C. Barbosa, C. Holm, *Phys. Rev. E* **2005**, *71*, 061106.
[45] B. Dünweg, A. J. C. Ladd in *Advanced Computer Simulation Approaches for Soft Matter Sciences III*, Advances in Polymer Science, Springer-Verlag Berlin, Berlin, Germany, **2009**, pp. 89–166.
[46] B. Dünweg, U. D. Schiller, A. J. C. Ladd, *Comput. Phys. Commun.* **2009**, *180*, 605–608.
[47] L. P. Fischer, T. Peter, C. Holm, J. de Graaf, *J. Chem. Phys.* **2015**, *143*, 084107.
[48] J. de Graaf, T. Peter, L. P. Fischer, C. Holm, *J. Chem. Phys.* **2015**, *143*, 084108.
[49] J. Landsgesell, C. Holm, J. Smiatek, *J. Chem. Theory Comput.* **2017**, *13*, 852–862.
[50] J. Landsgesell, C. Holm, J. Smiatek, *Eur. Phys. J. Special Top.* **2017**, *226*, 725–736.
[51] W. Kohn, L. J. Sham, *Phys. Rev.* **1965**, *140*, A1133.
[52] J. M. Soler, E. Artacho, J. D. Gale, A. García, J. Junquera, P. Ordejón, D. Sánchez-Portal, *J. Phys. Condens. Matter* **2002**, *14*, 2745.
[53] G. Sun, J. Kürti, P. Rajczy, M. Kertesz, J. Hafner, G. Kresse, *J. Mol. Struct.: THEOCHEM* **2003**, *624*, 37–45.
[54] R. Ahlrichs, M. Bär, M. Häser, H. Horn, C. Kölmel, *Chem. Phys. Lett.* **1989**, *162*, 165–169.
[55] F. Weigend, R. Ahlrichs, *Phys. Chem. Chem. Phys.* **2005**, *7*, 3297–3305.
[56] N. Troullier, J. L. Martins, *Phys. Rev. B* **1991**, *43*, 8861–8869.
[57] D. Vanderbilt, *Phys. Rev. B* **1990**, *41*, 7892–7895.
[58] D. R. Hamann, M. Schlüter, C. Chiang, *Phys. Rev. Lett.* **1979**, *43*, 1494–1497.
[59] J. P. Perdew, A. Zunger, *Phys. Rev. B* **1981**, *23*, 5048.
[60] J. P. Perdew, K. Burke, M. Ernzerhof, *Phys. Rev. Lett.* **1996**, *77*, 3865.
[61] K. Lee, É. D. Murray, L. Kong, B. I. Lundqvist, D. C. Langreth, *Phys. Rev. B* **2010**, *82*, 081101.
[62] Y. Zhang, W. Yang, *Phys. Rev. Lett.* **1998**, *80*, 890–890.
[63] J. Klimeš, A. Michaelides, *J. Chem. Phys.* **2012**, *137*, 120901.
[64] A. Klamt, G. Schüürmann, *J. Chem. Soc. Perkin Trans.* 2 **1993**, 799–805.
[65] R. Car, M. Parrinello, *Phys. Rev. Lett.* **1985**, *55*, 2471.
[66] J. VandeVondele, M. Krack, F. Mohamed, M. Parrinello, T. Chassaing, J. Hutter, *Comput. Phys. Commun.* **2005**, *167*, 103–128.
[67] S. Grimme, J. Antony, S. Ehrlich, H. Krieg, *J. Chem. Phys.* **2010**, *132*, 154104.
[68] S. Pronk, S. Páll, R. Schulz, P. Larsson, P. Bjelkmar, R. Apostolov, M. R. Shirts, J. C. Smith, P. M. Kasson, D. van der Spoel, et al., *Bioinformatics* **2013**, *29*, 845–854.
[69] S. J. Plimpton, *J. Comput. Phys.* **1995**, *117*, 1–19.
[70] W. L. Jorgensen, D. S. Maxwell, J. Tirado-Rives*, J. Am. Chem. Soc.* **1996**, *118*, 11225–11236.
[71] S. L. Mayo, B. D. Olafson, W. A. Goddard, *J. Phys. Chem.* **1990**, *94*, 8897–8909.
[72] H. Berendsen, J. Grigera, T. Straatsma, *J. Chem. Phys.* **1987**, *91*, 6269.
[73] W. L. Jorgensen, J. Chandrasekhar, J. D. Madura, R. W. Impey, M. L. Klein, *J. Chem. Phys.* **1983**, *79*, 926–935.
[74] A. C. Van Duin, S. Dasgupta, F. Lorant, W. A. Goddard, *J. Phys. Chem. A* **2001**, *105*, 9396–9409.
[75] V. Swamy, J. D. Gale, *Phys. Rev. B* **2000**, *62*, 5406.
[76] P. Erhart, N. Juslin, O. Goy, K. Nordlund, R. Müller, K. Albe, *J. Phys. Condens. Matter* **2006**, *18*, 6585.
[77] S. Foiles, M. Baskes, M. S. Daw, *Phys. Rev. B* **1986**, *33*, 7983.

3.16.7.2 Requested funding

Funding for	2018		2019		2020		2021		2022		2018-2022	
Staff	Quantity	Sum	Quantity	Sum	Quantity	Sum	Quantity	Sum	Quantity	Sum	Quantity	Sum
PhD student, 67%	2	43,200.-	2	86,400.-	2	86,400.-	2	86,400.-	2	43,200.-	2	339,200.-
Total		43,200.-		86,400.-		86,400.-		86,400.-		43,200.-		339,200.-
Direct costs	Sum		Sum		Sum		Sum		Sum		Sum	
consumables	800.-		1,500.-		1,500.-		1,500.-		800.-		6,100.-	
Total	800.-		1,500.-		1,500.-		1,500.-		800.--		6,100.-	
Major research instrumentation	Sum		Sum		Sum		Sum		Sum		Sum	
	-		-		-		-		-		-	
Total	-		-		-		-		-		-	
Grand total	44,000.-		87,900.-		87,900.-		87,900.-		44,000.-		351,700.-	

(All figures in EUR)

3.16.7.3 Requested funding for staff

	Sequential no.	Name, academic degree, position	Field of research	Department of university or non-university institution	Project commitment in hours per week	Category	Funding source
Existing staff							
Research staff	1	Christian Holm, Prof. Dr.	Soft-Matter, Computational Physics	Institute for Computational Physics	4		University
	2	Maria Fyta, Jun.Prof. Dr.	Condensed Matter Physics	Institute for Computational Physics	8		University
Non-research staff	3	Frank Huber		Institute for Computational Physics	4		University
	4	Henriette Patzelt		Institute for Computational Physics	4		
Requested staff							
Research staff	5	N. N., M. Sc.	Computational Physics	Institute for Computational Physics		PhD	
Research staff	6	N. N., M. Sc.	Computational Physics	Institute for Computational Physics		PhD	
Research staff	7	Research assistant	Computational Physics	Institute for Computational Physics			

Job description of staff (supported through existing funds):
1
Full Professor, Head of the Institute, leads and coordinates mainly **WP5**-**WP8**
2
Junior professor, leads and coordinates mainly **WP1**-**WP4**
3
Technician, permanent staff, in charge of computer equipment
4
Secretary, permanent staff, secretarial assistance

Job description of staff (requested funds):
5
PhD student, should carry out the research planned in **WP5**-**WP8**
6
PhD student, should carry out the research planned in **WP1**-**WP4**
7
Research assistants. **Justification:** The research assistant supports the doctoral researchers, for example, in code documentation, simulations, and visualization, etc., and will help in preparing the initial structures for the DFT simulations and with the benchmarks and test of the methods.

Based on the workload, and the various levels of modeling using different schemes, this project has to be carried out by two PhD students. One PhD student should focus on the *ab initio* scale and atomistic simulations, while the other Ph.D. student should focus on the coarse-grained MD and the LB-EK-CR scheme. However, since the understanding of the smaller scale should be vertically transferred into the models on the larger scale, they will also have to frequently interact, for example in the development of the necessary interaction parameters, and the used coarse-graining strategies. The complementary background of the PI is here very helpful, since M. Fyta brings in the knowledge of the *ab initio* modeling and the force-field development for the all-atom simulations, while C. Holm has extensive background on coarse-graining strategies and the LB method. The PIs will supervise the two PhD students together.

The use of the numerical methods mentioned in the work packages can be realized only with the availability of sufficient computational power. Locally at the Institute for Computational Physics (ICP), we can make use of around 50 computers that are all equipped with Nvidia Kepler Maxwell, and Pascal GPUs and powerful Intel Sandy Bridge, Haswell, and Kaby Lake Central Processing Units (CPUs), as well as a 47-node compute cluster with Nvidia Kepler GPUs, coupled to Intel Haswell CPUs. All cluster nodes are connected over a 4x Quadruple Data Rate (QDR) Infiniband network. This cluster will be relevant for benchmark calculations, testing, and small simulations for the development of classical force fields (**WP2**), but also for all the GPU supported applications done with ESPResSo. The other production runs will mostly be done on the high performance computing (HPC) centers in the state of Baden-Württemberg. The groups of the applicants are already using these computational facilities, such as the JUSTUS bwForCluster for Computational Chemistry located in Ulm and its successor machine, as well as the ForHLRI/II facilities at the Karlsruhe Institute of Technology (KIT). It is anticipated that the related computational power will suffice for the purposes of this project.

3.16.7.4 Requested funding of direct costs

	2018	2019	2020	2021	2022
Uni Stuttgart: existing funds from public budget	2,000.-	4,000.-	4,000.-	4,000.-	2,000.-
Sum of existing funds	2,000.-	4,000.-	4,000.-	4,000.-	2,000.-
Sum of requested funds	800.--	1,500.-	1,500.-	1,500.-	800.-

(All figures in EUR)

Equipment up to EUR 10,000, software and consumables for 2018

Consumables for financial year 2018

Data storage devices, IT materials	EUR	800.-

Consumables for financial year 2019

Data storage devices, IT materials	EUR	1,500.-

Consumables for financial year 2020

Data storage devices, IT materials	EUR	1,500.-

Consumables for financial year 2021

Data storage devices, IT materials	EUR	1,500.-

Consumables for financial year 2022

Data storage devices, IT materials	EUR	800.-

3.16.7.5 Requested funding for major research instrumentation

None.

3.17 Project S1

3.17.1 General Information about Project S1

3.17.1.1 X-ray absorption spectroscopy of molecular heterogenous catalysts in mesoporous materials

3.17.1.2 Research Areas
302-02 Physikalische Chemie von Festkörpern und Oberflächen, Materialcharakterisierung

3.17.1.3 Principal Investigator
Plietker, Bernd J., Prof. Dr. born 22. 01. 1971, male, Germany
Professor für Organische Chemie, Institut für Organische Chemie
Universität Stuttgart, Pfaffenwaldring 55, 70569 Stuttgart
Tel.: 0711/685-64283
E-Mail: bernd.plietker@oc.uni-stuttgart.de
Tenured Profdessor W3

Bauer, Matthias, Prof. Dr. born 16.08.1977, male, Germany
Professor für Anorganische Chemie, Department Chemie
Universität Paderborn, Warburger Str. 100, 33098 Paderborn
Tel.: 05251-605614
E-Mail: matthias.bauer@upb.de
Tenured Professor W3

3.17.1.4 Legal Issues
This project includes

1.	research on human subjects or human material.	no
2.	clinical trials	no
3.	experiments involving vertebrates.	no
4.	experiments involving recombinant DNA.	no
5.	research involving human embryonic stem cells.	no
6.	research concerning the Convention on Biological Diversity.	no

3.17.2 Summary
The structure of molecular catalysts in solution is highly flexible and able to adopt different coordination modes depending on external stimulus (solvent, temperature, ligand dissociation and association through coordination of starting material or dissociation of product(s), etc.). The ligand field created around the metal center defines the electronic ground state configuration of metal complexes. By immobilizing metal complexes inside mesoporous materials it is expected that the complex coordination chemistry is influenced both by pore size and geometry. Steric constraints generated inside the mesopores will thus alter the coordination chemistry at the metal and, as a consequence, the catalytic activity of the supported catalyst. In this project, X-ray spectroscopy using hard X-rays will be used to measure these influences on heterogeneous molecular catalysts inside different mesoporous materials. It will also allow analyzing the electronic structure of the catalytic center in solution. X-rays analysis will comprise of XANES (X-ray absorption near edge structure), EXAFS (Extended X-ray absorption fine structure), HERFD-XANES (high energy resolution fluorescence-detected XANES), vtc-XES (valence-to-core X-ray emission spectroscopy) and ctc-XES (core-to-core X-ray emission spectroscopy) measurements. These methods provide information about the oxidation state (XANES), local structural parameters around an X-ray absorbing metal center (EXAFS), the LUMO (HERF-XANES) and HOMO (vtc-XES) states of the complexes under investigation and their spin state (ctc-XES) *without* the need for any translational symmetry, i.e. crystallinity, and fully *independent* of the state of aggregation, which means that they can be applied to amorphous solids, solutions and interphases. Using this hard X-ray bunch of methods in combination with theoretical calculations, all relevant information to understand the structure and working principle of molecular heterogeneous catalysts in **projects B1** – **B3** *in situ* as well as *in operando* can be obtained.

3.17.3 Research rationale

3.17.3.1 Current state of understanding and preliminary work

Excitation of electrons located close the atom nucleus by high-energy photons can be used to determine the local electronic structure of a given material. Depending on the kind of electrons that are excited one has to differentiate between K- (excitation of 1s electrons to valence bound states at the metal), L- (excitation of 2s electrons) and M-edge (excitation of 3s electrons). Within **project** S1 mainly the K-edge is of interest, which can be divided into the *pre-edge region* (comprising the pre-edge and rising edge transitions) and the *near-edge region* (comprising the intense edge transition). The use of hard X-rays allows to obtain XANES (X-ray absorption near-edge structure), EXAFS (Extended X-ray absorption fine structure), HERFD-XANES (High energy resolution fluorescence detected XANES), vtc-XES (valence-to-core X-ray emission spectroscopy) und ctc-XES (core-to-core X-ray emission spectroscopy) spectra fully *independent* of the state of aggregation, which means that they can be applied to amorphous solids, solutions and interphases.[1-2] Figure S1-1 summarizes all methods and the underlying processes. Starting with the XANES region, lots of structural and electronic information content is found in the *pre-edge* signal of transition metals.[3] It basically contains information about the lowest unoccupied (LUMO) states of metal catalysts. These LUMO states unambiguously reflect the geometric (coordination symmetry) and electronic (oxidation state) structure.

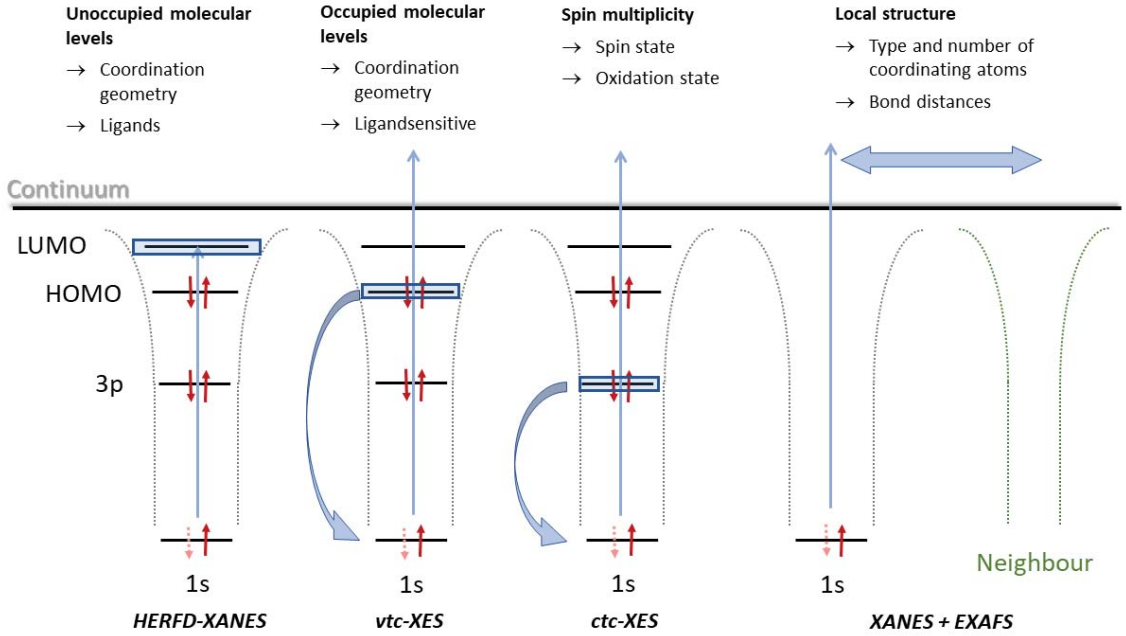

Figure S1-1. Hard X-ray methods and the underlying processes for the example of K-edge spectroscopy.

However, extracting LUMO information from conventional transition metal K-edge XANES spectra is complicated by the core–hole lifetime broadening of the 1s electron hole, which smears out features in the prepeak spectrum. Already in the mid 80ies of the last century, Eisenberger[4] showed that the lifetime broadening in the XANES region could be reduced by detecting the X-ray absorption spectrum using the intensity of the emitted X-ray fluorescence in a narrow energy bandwidth.

This technique was called high-energy-resolution fluorescence detected XANES (HERFD-XANES). In a pioneering study, this technique was applied by de Groot to investigate iron in zeolites catalysts.[5] The benefit of recording a high resolution XANES spectra becomes most obvious if pre-peaks of the first transition metal row are considered, which are more often than not due to quadrupole transitions to unoccupied 3d states, and thus of low intensity. Therefore, with HERFD-XANES, the LUMO structure at a central atom in catalysts can be probed, giving a precise measure of the symmetry dependent arrangement of molecular orbitals and their occupancy. It thus presents a semi-quantitative extension of the 'fingerprinting approach' of conventional XANES analysis concerning the oxidation state and coordination geometry. Over the last years, the Bauer group published several studies on the high

potential of x-ray spectroscopy for the investigation of molecular orbital levels in transition metal catalysts. They all prove the sensitivity of HERFD-XANES to changes in the inner[S1-2,S1-2,S1-3], and even in the outer coordination sphere[S-4] of a metal complex.
The EXFAS region, following the XANES part in an X-ray absorption spectrum, is defined by oscillations of the X-ray absorption coefficient, which are caused by the coordinating atoms and further local environment of the X-ray absorbing atom.[2,S1-5,S1-6] Therefore, structural parameters of the local environment, including type and number of neighbor atoms, and their distance to the central atom, can be precisely determined. However, a severe limitation of EXAFS spectroscopy exists concerning the sensitivity for different light atom ligands coordinating a central metal. Due to their similar atomic order, and thus very similar scattering factors, oxygen, nitrogen and carbon can hardly be distinguished, and hydride ligands can not be detected at all.
Vtc-XES[6,7,S1-1,S1-6,S1-7] is able to overcome these limitations, while still using hard X-rays. In this technique, the 1s electron is non-resonantly excited into the continuum far off the threshold energy, and the following radiative HOMO→1s relaxation of a valence electron is detected. These valence electrons originate from the highest occupied molecular orbitals (HOMO). In a complex, these are formed by interaction of the metal nd valence orbitals with ligand orbitals. Consequently, vtc-XES is highly sensitive to the ligands coordinating to a metal center, since the character of the valence orbitals changes the most for different chemical species. Very recently, the possibility to investigate hydride species with vtc-XES in combination with HERFD-XANES was elaborated in a cooperation by the *Plietker and the Bauer group* (vide infra).[S1-1]
Although ctc-XES, corresponding to the 3p→1s relaxation channel is also of value for investigations into catalytic systems, one of the rare applications to investigate the electronic state of a catalyst was carried out for the Hieber anion.[S1-6] ctc-XES is sensitive to the spin multiplicity and thus offers the chance to determine the spin state of a catalyst or the metal centered oxidation state by count of unpaired d-electrons.[8]

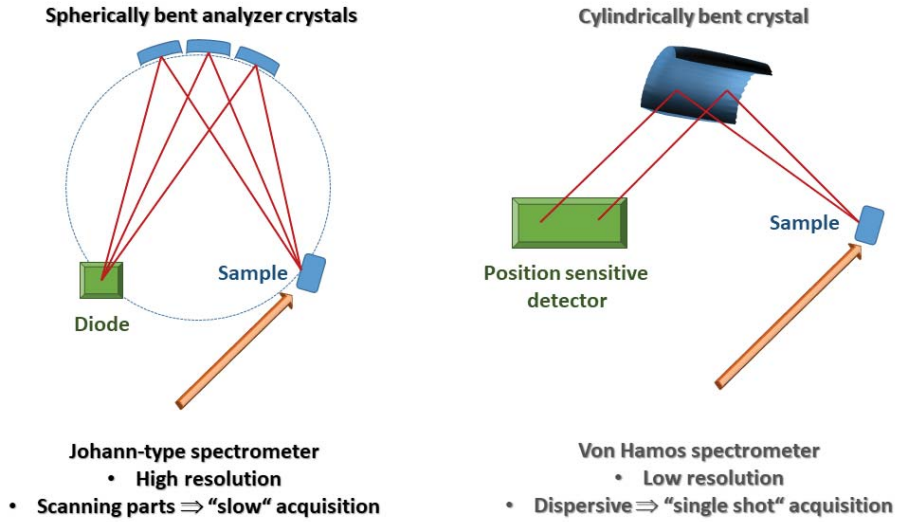

Figure S1-2. Two spectrometer types for the acquisition of HERFD-XANES, vtc-XES and ctc-XES.

Typically, XANES and EXAFS are conducted at dedicated XAS beam lines in transmission or fluorescence geometry, while HERFD-XANES, vtc-XES and ctc-XES require either a scanning Johann or a dispersive von Hamos spectrometer as depicted in figure S1-2. The first one uses a focusing spherical analyzer crystals and a point detector. To record HERFD-XANES spectra the intensity of a single fluorescence channel, selected with the analyzer crystals, is monitored with a resolution smaller than the lifetime broadening, while sweeping the incident energy of the double crystal monochromator. In contrast, to record XES spectra, the incident energy is fixed at a constant value off resonance beyond the edge position and the analyzer crystals are swept over the desired emission energy range.
Using a dispersive von Hamos spectrometer avoids any scanning movements by applying cylindrically bent dispersive crystals and a position sensitive two-dimensional detector. With such a spectrometer, the emission spectrum can be obtained in a dispersive way, which can reduce the acquisition time significantly. However, with such a spectrometer, the energy resolution is slightly reduced compared to a Johann one.

All methods are crucially depending on theoretical input for spectra analysis, either as starting points for simulation for the EXAFS fitting procedure, or as input for calculation of the different spectra types. Here however, different methods are usually to extract as much information as possible from the spectral data. For example, DFT is well-established vtc-XES.[7,S1-1,S1-6,S1-7] XANES spectra are predicted with good accuracy by TD-DFT methods only for the pre-edge signals. The fine structure of the rising edge caused by quasi-continuum states are intrinsically problematic to localized DFT methods. Here plane augmented wave approaches are superior.[S1-3] Both in Stuttgart and Paderborn expert for sophisticated methods are available if problems arise beyond the typical DFT users level.

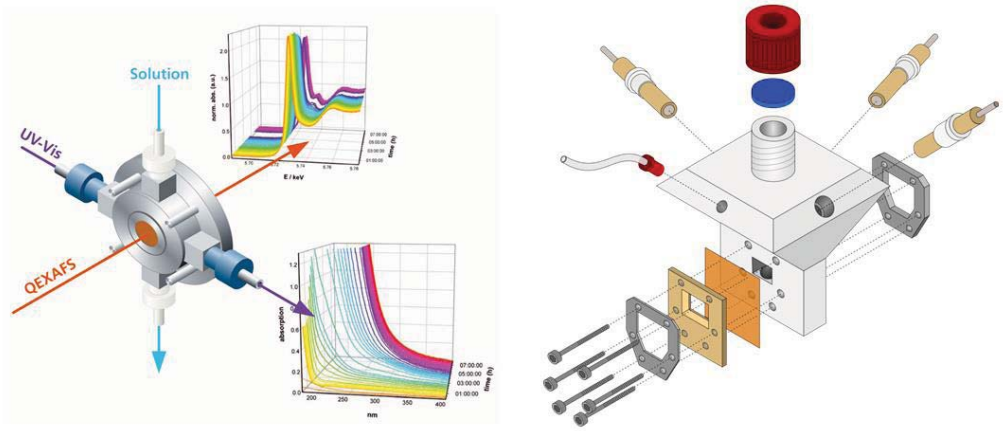

Figure S1-3. Measurement cell for combined X-ray and UV/Vis experiments (left) and X-ray spectro-electrochemical cell (right).

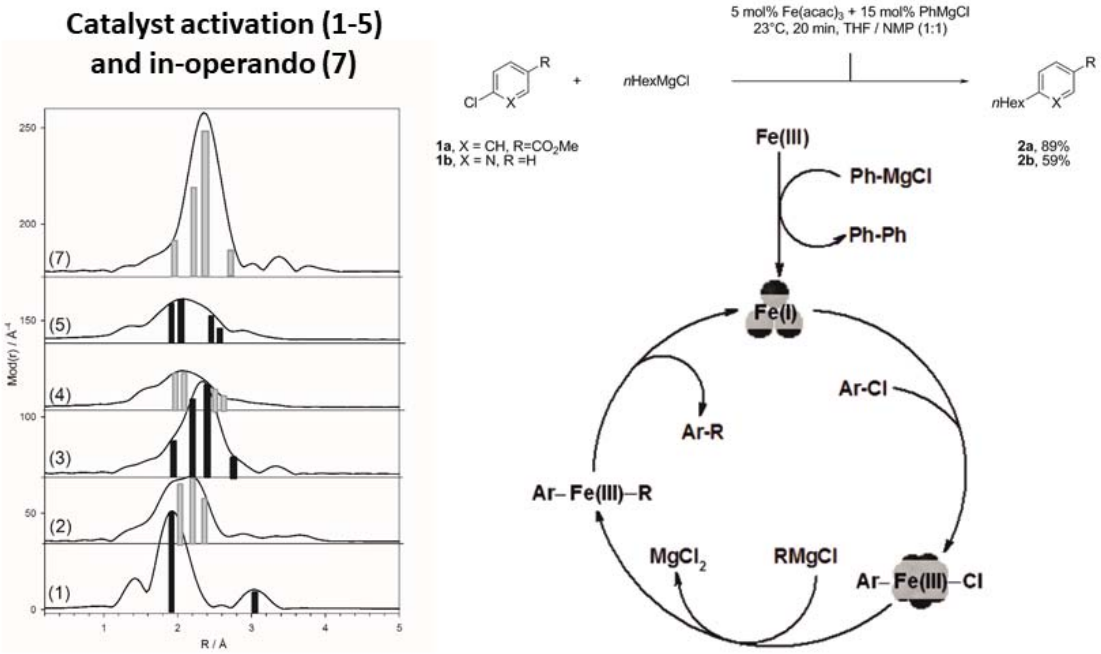

Figure S1-4: In-situ and in-operando EXAFS investigation of a homogeneous iron-catalyzed cross-coupling reaction.[S1-8]

Although the combination of these hard X-ray methods provide already a rich view on transition metal catalysts, the combination with other spectroscopic techniques might be advantages, e.g. to follow kinetics by vibrational spectroscopy or to gain complementary information by optical absorption spectroscopy. Following this idea, the Bauer group combines hard X-ray spectroscopy with other techniques in a multi-dimensional spectroscopic set-up. Although this set-up was only used with XANES and EXAFS so far, its implementation into HERFD-XANES, vtc- and ctc-XES experiments is straightforward and waiting only for its initiation by interesting problems that require such measurements. Two modi operandi are possible, one using a pump in combination with reaction vessel

and measurement cell equipped with fiber optics (Figure S1-3), the other with a Schlenk measurement tube using dip probes for Raman and UV/Vis. Similarly, a X-ray spectro-electrochemical cell has been designed which allows the investigation of redox-products and the X-ray spectroscopic signatures of the molecular catalysts (Figure S1-3).
An *example from the Bauer-group* for the investigation of transformations of a pre-catalyst during the activation is given in figure S1-4.
Here iron-catalyzed cross coupling reactions were investigated. In the figure changes in the Fourier transformed EXAFS functions are obvious as the pre-catalyst $Fe(acac)_3$ is stepwise activated by the addition of 1-4 equivalents Grignard compound PhMgCl. The activation proceeds via different degrees of iron aggregation (dimer → nanoparticles → trinuclear cluster). The stabilizing ligands could be rationalized, however, with conventional XAS, final identification could not be achieved. All these results were backed by simultaneously recorded UV/Vis and Raman data.[S1-8] In a second step, the reaction mechanism was investigated by operando XAS. Analysis of the XANES data showed an increase in the oxidation state from Fe(I) to Fe(III), accompanied by an increasing agglomeration of the iron centers, which is also shown in figure S1-4. Such experiments can of course be carried out as well on heterogeneous molecular complexes to understand the changes in course of catalytic reactions.
Despite such sophisticated applications of XAS, it can also be used to check the stability of transition metal complexes in solution or disordered materials. Figure S1-5 demonstrates this usage with the example of iron-NHC photosensitizers applied in photocatalytic proton reduction. Noble metal photosensitizers typically suffer from photodegradation, while the iron complex shown in this figure is proved via XANES fingerprinting to be fully long-term stable under catalytic conditions.[S1-9] Since immobilized catalysts might undergo structural transformations as well, this example demonstrates a simple but highly important tool to check for structural integrity.

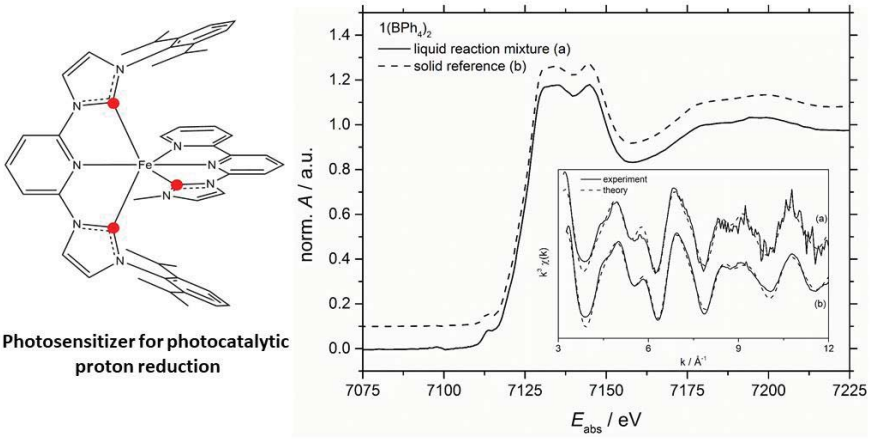

Figure S1-5: Proof for the long-term stability of a iron-NHC photosensitizer complex by XANES.[S1-9]

An example from the *Bauer-group* for the high potential of HERFD-XANES and vtc-XES is given with the investigation of a Fe-based hydrosilylation catalyst that was developed in the *Plietker-group*. The main aim of this study was to establish both methods for the detection of hydride ligands and to investigate the fate of such ligands during catalytic reactions. Both the HERFD-XANES and vtc-XES spectra show characteristic signals for the Fe-H motif in comparison to the spectra of reference complexes without hydride ligands.[S1-1] By combination with (TD-)DFT methods, the molecular origin of these hydride signals could be further determined, which allows now the application of both methods for in-situ studies on similar catalysts.

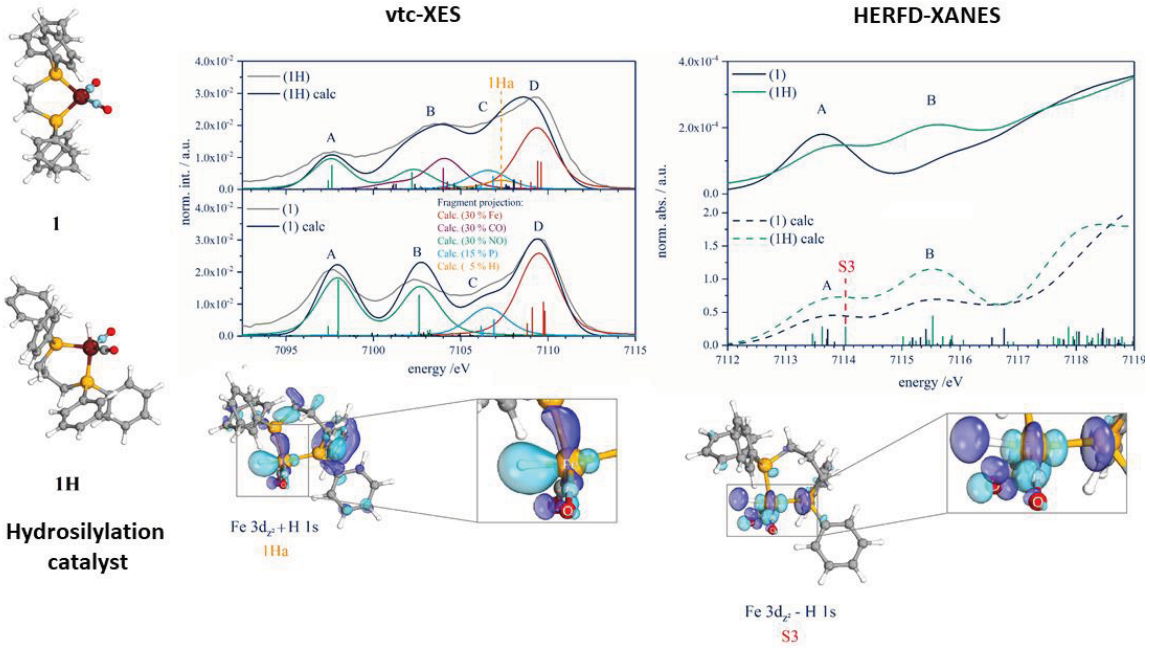

Figure S1-6: Identification and investigation of Fe-H bonds in catalysts by vtc-XES and HERFD-XANES in combination with (TD-)DFT calculations.[S1-1]

References

[1] M. Bauer, *Phys. Chem. Chem. Phys.* **2014,** *16*, 13827-13837.
[2] M. Bauer, H. Bertagnolli, X-Ray Absorption Spectroscopy – the Method and Its Applications. In *Methods in Physical Chemistry*, Wiley-VCH Verlag GmbH & Co. KGaA: **2012**; 231-269.
[3] A. M. Beale, B. M. Weckhuysen, B. M., *Phys. Chem. Chem. Phys.* **2010,** *12*, 5562-5574.
[4] P. Eisenberger, P. M. Platzman, H. Winick, *Phys. Rev. Lett.* **1976,** *36*, 623-626.
[5] W. M. Heijboer, P. Glatzel, K. R. Sawant, R. F. Lobo, U. Bergmann, R. A. Barrea, D. C. Koningsberger, B. M. Weckhuysen, F. M. F. de Groot, *J. Phys. Chem. B* **2004,** *108*, 10002-10011.
[6] M. A. Beckwith, M. Roemelt, M.-N. I. Collomb, C. DuBoc, T.-C. Weng, U. Bergmann, P. Glatzel, F. Neese, S. DeBeer, *Inorg. Chem.* **2011,** *50*, 8397-8409.
[7] C. J. Pollock, S. DeBeer, *J. Am. Chem. Soc.* **2011,** *133*, 5594-5601.
[8] P. Glatzel, U. Bergmann, *Coord. Chem. Rev.* **2005,** *249*, 65-95.

3.17.3.2 Project-related publications by participating researchers

[S1-1] I. Burkhardt, M. Holzwarth, **B. Plietker**, **M. Bauer**, *Inorg. Chem.* **2017**, 56, 13300-13310.
[S1-2] A. J. Atkins, M. Bauer, C. R. Jacob, *Phys. Chem. Chem. Phys.* **2015,** *17*, 13937-13948.
[S1-3] N. Vollmers, P. Müller, A. Hoffmann, S. Herres-Pawlis, M. Rohrmüller, W. G. Schmidt, U. Gerstmann, M. Bauer, *Inorg. Chem.* **2016,** *55*, 11694-11706.
[S1-4] A. Atkins, A. J.; Jacob, C. R.; Bauer, M., *Chem. Eur. J.* **2012,** *18* , 7021-7025.
[S1-5] M. Bauer, R. Schoch, L. Shao, B. Zhang, A. Knop-Gericke, M. Willinger, R. Schlögl, D. Teschner, *J. Phys. Chem. C* **2012,** *116* (42), 22375-22385.
[S1-6] J. E. M. N. Klein, B. Miehlich, M. S. Holzwarth, **M. Bauer**, M. Milek, M. M. Khusniyarov, G. Knizia, H.-J. Werner, **B. Plietker**, *Angew. Chem. Int. Ed.* **2014**, *53*, 1790 - 1794.
[S1-7] M.-U. Delgado-Jaime, S. DeBeer , M. Bauer, *Chem. Eur. J.* **2013,** *19*, 15888-15897.
[S1-8] R. Schoch, W. Desens, T. Werner, M. Bauer, *Chem. Eur. J.* **2013,** *19*, 15816-15821.
[S1-9] P. Zimmer, P. Müller, L. Burkhardt, R. Schepper, A. Neuba, J. Steube, F. Dietrich, U. Flörke, S. Mangold, M. Gerhards, M. Bauer, *Eur. J. Inorg. Chem.* **2017,** 1504-1509.

3.17.4 Project plan

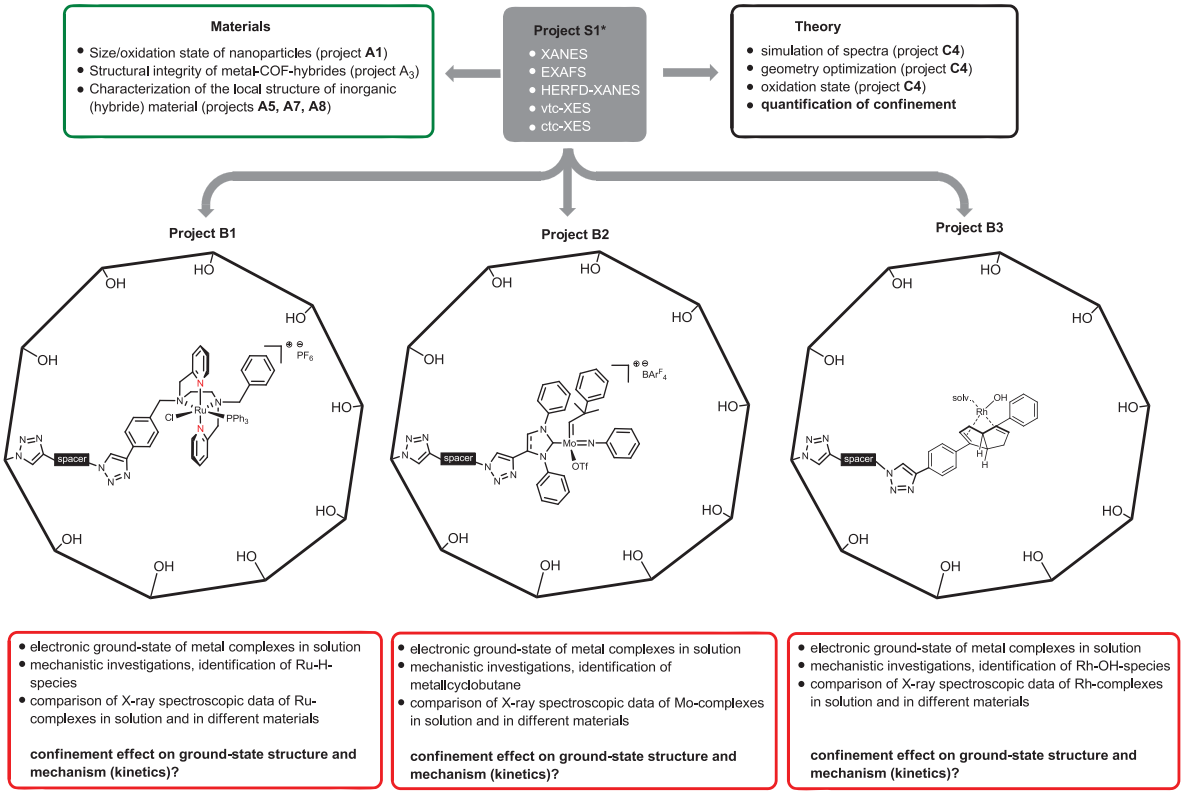

Figure S1-7. X-ray spectroscopy for *in situ* and *in operando* spectroscopy of as a central spectroscopic tool.

The X-ray spectroscopic methods presented above are a powerful tool to investigate the nature of the catalyst complex in a specific environment (in solution as well as inside a mesoporous material). The excitation of the 1s-electrons of a specific metal complex generates data that do not only allow to describe the electronic ground-state structure of the complex in solution but allows to compare the results with the data of the same complex inside a pore. Hence, through this method one can specifically determine the influence of pore-size and structure onto the electronic ground-state structure independent on the bulk material used. Moreover, in operando measurements are possible allowing the direct detection of potential catalytic intermediates.

- **WP1: X-ray spectroscopic investigation of homogenous Ru-catalyzed H_2-autotransfer catalysis.** Spectroscopic investigation of the (N,N,N,N)(P)Ru-complex in solution, in operando spectroscopic investigation of the H_2-autotransfer catalysis, identification of *Ru-H-species*.
- **WP2: Characterization of (N,N,N,N)(P)Ru-complexes inside mesoporous materials.** Characterization of Ru-complex immobilized inside the pores of different mesoporous materials. Ground-state structure investigation, comparative study using different spacers.
- **WP3: *In operando* spectroscopic investigation of H_2-autotransfer catalysis using heterogenized Ru-complexes.**
- **WP4: X-ray spectroscopic investigation of homogenous Mo-catalyzed ring-closing metathesis.** Spectroscopic investigation of cationic Mo-metathesis catalysts in solution, in operando measurement to determine the structure of the *metallacyclobutane* intermediate.
- **WP5: Characterization of immobilized Mo-carbene complexes.** Characterization of Mo-complexes inside various mesoporous materials. Ground-state structure investigation, comparative study using different spacers.
- **WP6: *In operando* spectroscopic investigation of ring closing metathesis using heterogenized Mo-complexes.**
- **WP7: X-ray spectroscopic investigation of homogenous Rh-catalyzed asymmetric 1,4-addition.** Spectroscopic investigation of the mononuclear diene-Ru-complex in solution, in operando spectroscopic investigation of the 1,4-addition, identification of *Rh-OH-species*.
- **WP8: Characterization of diene-Rh-complexes inside mesoporous materials.** Characterization of the mononuclear Rh-diene-complexes inside the pores of different mesoporous materials. Ground-state structure investigation, comparative study using different spacers.

3.17.4.1 WP1: X-ray spectroscopic investigation of homogenous Ru-catalyzed H_2-autotransfer catalysis.

As pointed out in **project B1** (WP2-B) understanding the mechanism of the H_2-autotransfer catalysis, kinetic analysis of the different transformations and identification of potential catalytic intermediates are a premium prerequisite in understanding or extracting potential confinement effects. This project will support the mechanistic studies both through in situ and in operande X-ray spectroscopy. Applying the bundle of spectroscopic methods (vide supra) allows to

- Analyze the electronic ground-state structure of the (N,N,N,N)(P)Ru-catalyst in solution (correlation with data obtained experimentally in **project C1**, interpretation of the data in collaboration with **project C4**)
- Get inside into the HOMO-LUMO-gap (interpretation of the data in collaboration with **project C4**, correlate the data with experimentally determined redox potentials in **project B1**)
- Identify potential catalytic intermediates using vtc-XES in combination with HERFD-XANES
- Perform kinetic investigation while identifying intermediates (multidimensional spectroscopy)

The experimental data will be analyzed through DFT-calculation in collaboration with **project C4**. The kinetic data will be used in **projects C6** to simulate the diffusion processes within the pore. The detailed analysis of the ground-state structure of the (N,N,N,N)(P)Ru-complex in solution serves as a reference to extract potential confinement effects.

3.17.4.2 WP2: Characterization of (N,N,N,N)(P)Ru-complexes inside mesoporous materials.

As described in **project B1** a set of (N,N,N,N)(P)Ru-complexes will be immobilized into the pores of inorganic (**project A4**) as well as organic materials (**projects A1**, **A2**, **A3**, and **A6**). Following the work-flow described in **project B1** the initial set of four catalyst plus material hybrides will be analyzed by X-ray spectroscopy for a given pore diameter of 5 – 10 nm. It is the goal to analyze potential interactions between pore wall and catalytic center, which will probable effect the electronic ground-state structure of the Ru-complex. Different from the spectroscopic methods in **projects C1** – **C3** X-ray spectroscopy allows a direct investigation of the nature of the Ru-species inside the pore. The experimental data will

be interpreted using DFT-calculations (**project C4**). Comparison of these data will lead to a first identification of potential influences. In combination with NMR-spectroscopic measurements (^{1}H, ^{31}P, ^{19}F, **project C1**) and Mössbauer-spectroscopy (investigation of the absorption of γ-rays through an Fe-nucleus as a molecular probe, **project C2**) a detailed picture of the influence of pore wall distance and pore structure on the configuration-electronics of the Ru-complex in a given pore. Correlation of these results with spacer length and orientation of the catalyst within the pore (**project C3**) will, together with the theoretical analysis of catalyst mobility within the pore (**project C5**) lead to a good picture of the electronics of a specific Mo-catalyst inside a specific pore.

3.17.4.3 WP3: *In operando* spectroscopic investigation of H_2-autotransfer catalysis using heterogenized Ru-complexes.

Recording X-ray spectroscopic data of the immobilized Ru-complexes during H_2-autotransfer catalysis in different mesoporous materials and comparison of these data with the data obtained from the same reaction under homogenous catalysis conditions (WP1) will allow to quantify the confinement effects on

- Structure of catalytic intermediates, elucidation of mechanistic steps.
- Kinetics of dehydrogenation, condensation and hydrogenation.

The data will be aligned with the data obtained through in operando NMR-spectroscopy (**project** C1). Through detailed analysis of the kinetic data, the influence of the pore size, geometry and polarity on the rate-limiting step within this catalytic reaction sequence will be apparent.

3.17.4.4 WP4: X-ray spectroscopic investigation of homogenous Mo-catalyzed ring-closing olefin metathesis.

Similar to WP1, the detailed knowledge on catalytic intermediates is an important prerequisite for understanding potential confinement effects. With regard to olefin metathesis (**project B2**), the control of *E*- or *Z*-configuration of the newly generated C-C-double bond in the product relies solely on the diastereoselective course of the [2+2]-cycloaddition between a metal-carbene and an olefinic starting material. A good level of control of the reactive conformation of the starting materials relative to each other prior to the cycloaddition is necessary in order to achieve good levels of chemo- and stereoselectivity in the desired products. In order to delineate any effects, which ever, on such chemo- and stereoselectivity by the pore walls in mesoporous materials, a detailed spectroscopic investigation of the reaction mechanism in terms of reactivity of *syn*- and *anti*-isomers and approach of the olefin in homogenous catalysis is inevitable. For these purposes, the in-silico studies performed in **project C4** will be accompanied by X-ray spectroscopic investigations (this project) and NMR-studies (**project C1**). Through multidimensional spectroscopy (UV- or IR-spectroscopy coupled to EXAFS) different olefin adducts to Mo/W imido/oxo alkylidene NHCs might be detectable in case unsymmetrical dienes, e.g., α-allyl-ω-methallyl derivatives, are used.

3.17.4.5 WP5: Characterization of immobilized Mo-carbene complexes.

The different Mo-carbene complexes that are immobilized on both organic and inorganic materials will be analyzed through X-ray spectroscopy, too. The influence of pore size, geometry and polarity on the electronic-ground state of the immobilized complex relative to the homogenous catalyst will be measured and correlated with DFT-calculations (**project C4**). Correlation of these results with spacer length and orientation of the catalyst within the pore (**project C3**) will, together with the theoretical analysis of catalyst mobility within the pore (**project C5**) lead to a good picture of the electronics of a specific Mo-catalyst inside a specific pore.

3.17.4.6 WP6: *In operando* spectroscopic investigation of ring closing metathesis (RCM) using heterogenized Mo-complexes.

As outlined in **project B2**, RCM is envisioned to be favored over oligomerization through confinement by space and polarity inside mesoporous materials. In addition, the diastereoselective course of the [2+2]-cycloaddition might be influenced by the confinement effects inside the porous materials. Comparative X-ray spectroscopic analysis of the olefin adducts in solution and inside the mesopores will be used to identify potential confinement effects. The experimental results will be analyzed using DFT-methods (**project C2**, *vide supra*)s in order to quantify these confinement effects.

3.17.4.7 WP7: X-ray spectroscopic investigation of homogenous Rh-catalyzed asymmetric 1,4-addition.

The Rh-catalyzed asymmetric 1,4-addition (**project B3**) is usually performed using binuclear Rh-complexes possessing two bridging chloride ligands. The current mechanistic understanding bases on a chloride-hydroxide exchange through salt metathesis and dissociation of the binuclear Rh-complex into mononuclear R-OH-complexes, which are the proposed catalytically active species. The Laschat-group was able to isolate a mono-nuclear Rh-complex, however, these compounds are unstable and decompose quickly. Application of the X-ray spectroscopic tools to analyze the effect of hydroxide ion on the dissociation of the binuclear pre-catalyst structure will provide fundamental insights into the structure and electronics of potential Rh-OH-species in solution. Moreover, mechanistic investigations and kinetic measurements will help to rationalize the effect of base, water, and structure of the boronic acid employed in this transformation. These results will be aligned with the NMR-spectroscopic investigations (**project C1**) and quantumchemical analysis of the mechanism (**project C4**).

3.17.4.8 WP8: Characterization of diene-Rh-complexes inside mesoporous materials.

Project B3 presents two different strategies for immobilizing Rh-diene-complexes inside mesoporous materials. The most fundamental strategy relies on the use of a heteroleptic binuclear Rh-complex in which only one of the two diene-ligands are “clickable”. Treatment of this material with hydroxide-solution is proposed to generate the reactive mononuclear Rh-OH-complex in situ. The second strategy relies on the development of mononuclear Rh-diene-Cl-complexes, in which a sacrificial ligand is proposed to improve the chemical stability of the mono-nuclear complexes. Activation of these complexes after fixation inside the mesoporous material through ligand dissociation sets the stage for the catalytic transformation. X-ray spectroscopic analysis will be used to identify and characterize the primary immobilized complexes, which depending on the activation strategy would lead to identical mono-nuclear Rh-OH-complexes.

Apart from these important investigations on the activation step, the influence of an achiral porous material on a chiral, enantiopure Rh-complex will be investigated through X-ray spectroscopic analysis of the electronic-ground states in different materials and pore sizes/geometries.

3.17.4.9 WP9: *In operando* spectroscopic investigation of asymmetric 1,4-addition using heterogenized Rh-complexes.

As for WP6 a comparative X-ray spectroscopic analysis of the 1,4-addition both in solution and inside the mesopores will be performed to evaluate the influence of the pore wall onto the stereoselective course of the C-C-bond formation.

3.17.4.10 Methods applied and Equipment to be used

Full instrumentation to perform the above mentioned experiments is accessable at the University of Paderborn. The instrumentation in detail:

- **von Hamos spectrometer (own design) with two detectors at beamline P64 (PETRA III, Hamburg)**
- **Measurement cells for homogeneous and heterogeneous reactions under defined atmospheres**
- UV/Vis spectrometer (Ocean optics) with fibre optics for implementation into X-ray experiments
- Raman spectrometer (Ocean optics) with dip probe into X-ray experiments
- IR spectrometer (Bruker Vertex 70) with dip probe into X-ray experiments
- Time correlated single photon counting spectrometer (Horriba)
- Spectro-electrochmistry (UV/Vis, IR)
- From 2019: *in-house* XAS/XES spectrometer for static measurements
- Full standard methods for preparational work (glove box, MPLC, 700 MHz NMR, MS, GC)

At beamline P64 (PETRA III) currently a von Hamos spectrometer is available as property of the Bauer group. Due to the design of the beam line, the collection of conventional XANES and EXAFS in parallel to HERFD-XANES and in row (without changing the set-up) with vtc- and ctc-XES is possible. Current developments of the Bauer group at this beam line focus on the implementation of optical pump- X-ray probe experiments for photo-induced reactions. Laser and liquid jet hardware is already and will be

installed till mid 2018. Due to the development efforts of the University of Paderborn at PETRA III, frequent access is guaranteed independent of the regular application processes at beam line P64 in Hamburg. Other beam lines that are used on a regular proposal basis are Hamburg (Germany: P64, P65), Viligen (Switzerland: SuperXAS, microXAS), Grenoble (France: ID16, ID26, BM23) and Oxford (UK: B18).

Chronological work plan:

	2018	2019			2020				2021				2022		
	Q3	Q4	Q1	Q2	Q3	Q4	Q1	Q2	Q3	Q4	Q1	Q2	Q3	Q4	Q1	Q2	
T1																	WP1: X-ray spectroscopic investigation of homogenous Ru-catalyzed H_2-autotransfer catalysis.
T2																	WP2: Characterization of (N,N,N,N)(P)Ru-complexes inside mesoporous materials.
T3																	WP3: *In operando* spectroscopic investigation of H_2-autotransfer catalysis using heterogenized Ru-complexes.
T4																	WP4: X-ray spectroscopic investigation of homogenous Mo-catalyzed ring-closing metathesis.
T5																	WP5: Characterization of immobilized Mo-carbene complexes.
T6																	WP6: *In operando* spectroscopic investigation of ring closing metathesis using heterogenized Mo-complexes.
T7																	WP7: X-ray spectroscopic investigation of homogenous Rh-catalyzed asymmetric 1,4-addition.
T8																	WP8: Characterization of diene-Rh-complexes inside mesoporous materials.
T9																	WP9: *In operando* spectroscopic investigation of asymmetric 1,4-addition using heterogenized Rh-complexes.

3.17.5 Role within the collaborative research center

Project S1 is a central service project and supports the different collaborations between section A, B, and C through application of different methods for X-ray spectroscopy. This method is the only spectroscopic tool that allows to investigate both the resting state of the catalyst independent on the material (**projects B1** – **B3**), in which the catalyst is immobilized, and to deliver mechanistic data on catalytic intermediates. The method is complementary to the advanced NMR- (b **C1**) and Mössbauer-spectroscopy (**project C3**) as it is based on excitement of 1s electrons and does not rely on nuclear spins. X-ray spectroscopy is a missing link in this collaborative research center as it allows the selectivele detection and abalysis of the active catalyst inside the pore. No spectroscopic probe molecule is required. Furthermore, the method allows analyzing the structure of the material, oxidation state of metal cations within the material (**projects A5**, **A7**), structural integrity of the material (catalyst on pore wall or oriented into the pore) (all B-projects).

3.17.6 Delineation from other funded projects

No funding proposal has been submitted or is under revision.

3.17.7 Project funding

3.17.7.1 Previous funding

This project is currently not funded and no funding proposal has been submitted.

3.17.7.2 Requested funding

Funding for	2018		2019		2020		2021		2022		2018-2022	
Staff	Quantity	Sum	Quantity	Sum	Quantity	Sum	Quantity	Sum	Quantity	Sum	Quantity	Sum
PhD student, 67%	1	21,600.-	1	43,200.-	1	43,200.-	1	43,200.-	1	21,600.-	1	172,800.-
Total		21,600.-		43,200.-		43,200.-		43,200.-		21,600.-		172,800.-
Direct costs	Sum		Sum		Sum		Sum		Sum		Sum	
consumables	8,000.-		16,000.-		16,000.-		16,000.-		8,000.-		64,000.-	
Total	8,000.-		16,000.-		16,000.-		16,000.-		8,000.-		64,000.-	
Major research instrumentation	Sum		Sum		Sum		Sum		Sum		Sum	
GC-MS			-		-		-		-		-	
Total			-		-		-					
Grand total	29,600.-		59,200.-		59,200.-		59,200.-		29,600.-		236,800.-	

(All figures in EUR)

3.17.7.3 Requested funding for staff

	Sequential no.	Name, academic degree, position	Field of research	Department of university or non-university institution	Project commitment in hours per week	Category	Funding source
Existing staff							
Research staff	1	B. J. Plietker, Dr., Prof.	Organic chemistry, Catalysis, Organometallic Chemistry	Institute of Organic Chemistry	6		University
	2	M. Bauer, Dr., Prof.	Organometallic Chemistry, Physical Inorganic Chemistry	Inorganic Chemistry, University of Paderborn	6		University
Requested staff							
Research staff	3	n.n. M.Sc.	Organic chemistry, Catalysis, Organometallic Chemistry	Institute of Organic Chemistry		PhD	
Research staff	4	Research assistant	Organic chemistry, Catalysis, Organometallic Chemistry	Institute of Organic Chemistry			

Job description of staff (supported through existing funds):
1
Professor
2
Professor
Job description of staff (requested funds):
3
PhD student for WPs 1-8, working on collaborations and refinement of the measurement techniques.
4
Research assistant. **Justification:** The research assistants will perform spectroscopic measurements and help with data analysis, repetitive work and sample preparation.

3.17.7.4 Requested funding of direct costs

	2018	2019	2020	2021	2022
Uni Stuttgart: existing funds from public budget	1,000.-	2,000.-	2,000.-	2,000.-	1,000.-
Sum of existing funds	1,000.-	2,000.-	2,000.-	2,000.-	1,000.-
Sum of requested funds	8,000.-	16,000.-	16,000.-	16,000.-	8,000.-

(All figures in EUR)

Consumables for financial year 2018

Chemicals, consumables, monomers, solvents, silica for columns, gases (Ar), NMR solvents	EUR	8,000.-

Consumables for financial year 2019

Chemicals, consumables, monomers, solvents, silica for columns, gases (Ar), NMR solvents	EUR	16,000.-

Consumables for financial year 2020

Chemicals, consumables, monomers, solvents, silica for columns, gases (Ar), NMR solvents	EUR	16,000.-

Consumables for financial year 2021

Chemicals, consumables, monomers, solvents, silica for columns, gases (Ar), NMR solvents	EUR	16,000.-

Consumables for financial year 2022

Chemicals, consumables, monomers, solvents, silica for columns, gases (Ar), NMR solvents	EUR	8,000.-

3.17.7.5 Requested funding for major research instrumentation
-none-

3.18 Central administrative project Z1

3.18.1 General information about project Z

3.18.1.1 Title: Central Tasks of the Collaborative Research Centre

3.18.1.2 Project leaders

Michael Buchmeiser, Prof. Dr., 08. 03. 1967, male, Austrian
Lehrstuhl für Makromolekulare Stoffe und Faserchemie, Institut für Polymerchemie, Universität Stuttgart,
Pfaffenwaldring 55, D-70569 Stuttgart
0711-685-64075
michael.buchmeiser@ipoc.uni-stuttgart.de
Tenured Professor W3

Bernd Plietker, Prof. Dr., 22. 01. 1971, male, German
Institut für Organische Chemie, Universität Stuttgart
Pfaffenwaldring 55, D-70569 Stuttgart
0711-685-64283
bernd.plietker@oc.uni-stuttgart.de
Tenured Professor W3

3.18.1.3 Legal issues

This project includes

1.	research on human subjects or human material.	no
2.	clinical trials	no
3.	experiments involving vertebrates.	no
4.	experiments involving recombinant DNA.	no
5.	research involving human embryonic stem cells.	no
6.	research concerning the Convention on Biological Diversity.	no

3.18.2 Summary

Z1 is the central project for the CRC 1333 and comprises of the management and promotion of the central activities of the CRC. The CRC Office is responsible for the coordination and administration of the CRC. **Z1** is run by the CRC Speaker, Prof. Dr. Michael R. Buchmeiser, and the Deputy Speaker, Prof. Dr. Bernd Plietker and is allocated at the Institute of Polymer Chemistry, Chair of Macromolecular Compounds and Fiber Chemistry. The Office is operated by one scientific coworker, Dr. Elisabeth Rüthlein, who serves as chief operating officer. She coordinates all central tasks such as colloquia, seminars and summer schools, all future applications (phase 2, phase 3 of the CRC) as well as the conception of the homepage with regard to contents. In view of the following tasks, the office plays a key role in the CRC:

- Management of DFG contacts, contacts to the University's Central Administration, contacts to the subprojects, contacts to the Cluster of Excellence *SimTech*.
- Contact to foreign institutions for student exchange measures.
- Financial administration, in particular management of the general and global capital, lump sums, travel costs and costs for guests and visiting scientists.
- Organization of General Meetings, CRC-colloquia, CRC-status seminars and summer schools.
- Coordination of research, coordination and compilation of reports and proposals.
- Time scheduling.
- Assistance to visiting scientists.
- Public Relations, CRC-homepage.
- Data Management.

In view of the complexity of some of these tasks (e.g., data management) and the necessity to coordinate different scientific disciplines (chemists, materials scientists, physicists and engineers) it is inevitable to have a scientist running the above-outlined duties as chief operating officer.

3.18.3 Role within the collaborative research center

This project is the central project of the CRC 1333 and coordinates all projects, joint science and joint actions as outlined in detail.

3.18.4 Differentiation from other funded projects

The work described in Z1 is *not* subject or partly subject of any other research project.

3.18.5 Project funding

3.18.5.1 Previous funding

This project is currently not funded and no funding proposal has been submitted.

3.18.5.2 Existing funds

Existing Staff	Sequential no.	Name, academic degree, position	Field of research	Department of university or non-university institution	Project commitment in hours per week	Funding source
Research staff	1	M. R. Buchmeiser, Dr., Full Prof.	Polymer Science, Catalysis, Organometallic Chemistry	Institute of Polymer Chemistry	5	University of Stuttgart
	2	B. Plietker	Synthetic Organic Chemistry, Catalysis	Institute of Organic Chemistry	5	University of Stuttgart
Non-research staff	3	R. Stiehle	-	Institute of Polymer Chemistry	2	University of Stuttgart

Job description of staff (supported through existing funds):
1
Full Professor, Chair Holder and Head of the Institute, speaker of the CRC 1333, coordination of the CRC, responsible contact person to the DFG.
2
Professor of Organic Chemistry, Deputy Speaker of the CRC 1333, co-coordination of the CRC
3
Secretary, Administrative work

	2018	2019	2010	2021	2022
existing funds from the University of Stuttgart	3,000.-	6,000.-	6,000.-	6,000.-	3,000.-
Sum of existing funds for direct costs	3,000.-	6,000.-	6,000.-	6,000.-	3,000.-
Sum of requested funds for direct costs	55,600.-	111,200.-	111,200.-	111,200.-	55,600.-

(All figures in EUR)

3.18.5.3 Requested funding

Funding for	2018		2019		2010		2021		2022		2018-2022	
Staff	Quantity	Sum	Quantity	Sum	Quantity	Sum	Quantity	Sum	Quantity	Sum	Quantity	Sum
Ph.D., 100%	1	32,300.-	1	64,500.-	1	64,500.-	1	64,500.-	1	32,300.-	1	258,100.-
Research assistants*)	17	59,500.-	17	119,000.-	17	119,000.-	17	119,000.-	17	59,500.-	17	476,000.-
Total		91,800.-		183,500.-		183,500.-		183,500.-		91,800.-		734,100.-
Direct costs	Sum		Sum		Sum		Sum		Sum		Sum	
Travel		30,800.-		61,600.-		61,600.-		61,600.-		30,800.-		246,400.-
Guests		20,000.-		40,000.-		40,000.-		40,000.-		20,000.-		160,000.-
Literature		4,800.-		9,600.-		9,600.-		9,600.-		4,800.-		38,400.-
Total		55,600.-		111,200.-		111,200.-		111,200.-		55,600.-		444,800.-
Global funds	Sum		Sum		Sum		Sum		Sum		Sum	
Coordination measures		5,000.-		10,000.-		10,000.-		10,000.-		5,000.-		40,000.-
Workshops, colloquia		15,000.-		30,000.-		30,000.-		30,000.-		15,000.-		120,000.-
Equality measures		15,000.-		30,000.-		30,000.-		30,000.-		15,000.-		120,000.-
Lump sum funds		50,000.-		100,000.-		100,000.-		100,000.-		50,000.-		400,000.-
Total		85,000.-		170,000.-		170,000.-		170,000.-		85,000.-		680,000.-
Grand total		**232,400.-**		**464,700.-**		**464,700.-**		**464,700.-**		**232,400.-**		**1,858,900.-**

(All figures in EUR). *) individual justifications for the research assistant scan be found in **projects A1**, **A2**, **A4**-**A7**, **B1**-**B3**, **C1**-**C6**, **Z1**, **S1**.

Justification for research assistant in Z1: These will aid the chief operating officer in fulfilling the multiple CRC-specific tasks. In particular, this concerns the following duties: help in the organization of general meetings, CRC-colloquia, CRC-status seminars and summer schools, help in compilation of reports and proposals (data formatting and editing), assistance to visiting scientists, help in compiling, formatting and editing of data for public relations and for the CRC-homepage.

3.18.5.4 Requested funding for staff

	Sequential no.	Name, academic degree, position	Field of research	Department of university or non-university institution	Project commitment in hours per week	Category	Funding source
Requested staff							
Non-research staff	4	Dr. E. Rüthlein	-	Institute of Polymer Chemistry	39.5	chief operating officer	

Job description of staff (requested funds):
4
chief operating officer

3.18.5.5 Requested funding for direct costs

Requested funding for coordination for the financial year 2018

Scientific coworker, 100%, Management of DFG contacts, contacts to the University's Central Administration, contacts to the subprojects, contacts to the Cluster of Excellence *SimTech*, contact to foreign institutions for student exchange measures, financial administration, in particular management of the general and global capital, lump sums, travel costs and costs for guests and visiting scientists, organization of general meetings, CRC-colloquia, CRC-status seminars and summer schools, coordination of research, time scheduling, coordination and compilation of reports and proposals, assistance to visiting scientists, public relations, CRC-homepage, data management	EUR	32,300.-

Requested funding for coordination for the financial year 2019

Scientific coworker, 100%, Management of DFG contacts, contacts to the University's Central Administration, contacts to the subprojects, contacts to the Cluster of Excellence *SimTech*, contact to foreign institutions for student exchange measures, financial administration, in particular management of the general and global capital, lump sums, travel costs and costs for guests and visiting scientists, organization of general meetings, CRC-colloquia, CRC-status seminars and summer schools, coordination of research, time scheduling, coordination and compilation of reports and proposals, assistance to visiting scientists, public relations, CRC-homepage, data management	EUR	64,500.-

Requested funding for coordination for the financial year 2020

Scientific coworker, 100%, Management of DFG contacts, contacts to the University's Central Administration, contacts to the subprojects, contacts to the Cluster of Excellence *SimTech*, contact to foreign institutions for student exchange measures, financial administration, in particular management of the general and global capital, lump sums, travel costs and costs for guests and visiting scientists, organization of general meetings, CRC-colloquia, CRC-status seminars and summer schools, coordination of research, time scheduling, coordination and compilation of reports and proposals, assistance to visiting scientists, public relations, CRC-homepage, data management	EUR	64,500.-

Requested funding for coordination for the financial year 2021

Scientific coworker, 100%, Management of DFG contacts, contacts to the University's Central Administration, contacts to the subprojects, contacts to the Cluster of Excellence *SimTech*, contact to foreign institutions for student exchange measures, financial administration, in particular management of the general and global capital, lump sums, travel costs and costs for guests and visiting scientists, organization of general meetings, CRC-colloquia, CRC-status seminars and summer schools, coordination of research, time scheduling, coordination and compilation of reports and proposals, assistance to visiting scientists, public relations, CRC-homepage, data management	EUR	64,500.-

Requested funding for coordination for the financial year 2022

Scientific coworker, 100%, Management of DFG contacts, contacts to the University's Central Administration, contacts to the subprojects, contacts to the Cluster of Excellence *SimTech*, contact to foreign institutions for student exchange measures, financial administration, in particular management of the general and global capital, lump sums, travel costs and costs for guests and visiting scientists, organization of general meetings, CRC-colloquia, CRC-status seminars and summer schools, coordination of research, time scheduling, coordination and compilation of reports and proposals, assistance to visiting scientists, public relations, CRC-homepage, data management	EUR	32,300.-

Requested funding for research assistants 2018

project	**Hours per year for each project**	**Sum (EUR)**
A1, A2, A4 – A7, B1 – B3, C1 – C6, S1, Z1	240	59,500.-

Calculation base: 14,58 Euro/h.

Requested funding for research assistants 2019

project	**Hours per year for each project**	**Sum (EUR)**
A1, A2, A4 – A7, B1 – B3, C1 – C6, S1, Z1	480	119,000.-

Calculation base: 14,58 Euro/h.

Requested funding for research assistants 2020

project	**Hours per year for each project**	**Sum (EUR)**
A1, A2, A4 – A7, B1 – B3, C1 – C6, S1, Z1	480	119,000.-

Calculation base: 14,58 Euro/h.

Requested funding for research assistants 2021

project	**Hours per year for each project**	**Sum (EUR)**
A1, A2, A4 – A7, B1 – B3, C1 – C6, S1, Z1	480	119,000.-

Calculation base: 14,58 Euro/h.

Requested funding for research assistants 2022

project	Hours per year for each project	Sum (EUR)
A1, A2, A4 – A7, B1 – B3, C1 – C6, S1, Z1	240	59,500.-

Calculation base: 14,58 Euro/h.

Individual justifications for the research assistant can be found in **projects A1**, **A2**, **A4**-**A7**, **B1**-**B3**, **C1**-**C6**, **Z1**, **S1**.

Requested funding for direct costs for the financial year 2018

Travel: participation in both national and international meetings, schools and conferences. We ask for EUR 2,200.- per year and scientific coworker funded by the CRC, i.e. per PhD and PostDoc, respectively.	EUR	30,800.-
Guests: The visiting scientists program serves the exchange nationally- and internationally-renown scientists working in the areas of the CRC 1333. Funding will be used to cover the costs for both short- and long-terms visit od these scientists. Visiting scientists will also give individual lectures as well as lecture series (block form) on topics relevant to this CRC. Funding shall also be used for any potential joint supervision of PhD students. We ask for EUR 2,500 per project and year.	EUR	20,000.-
Literature: funding shall be used to purchase special literature such as books or literature not available via the resources provided by the University of Stuttgart. We ask for EUR 600.- per year and research project.	EUR	4,800.-

Requested funding for direct costs for the financial year 2019

Travel: participation in both national and international meetings, schools and conferences. We ask for EUR 2,200.- per year and scientific coworker funded by the CRC, i.e. per PhD and PostDoc, respectively.	EUR	61,600.-
Guests: The visiting scientists program serves the exchange nationally- and internationally-renown scientists working in the areas of the CRC 1333. Funding will be used to cover the costs for both short- and long-terms visit od these scientists. Visiting scientists will also give individual lectures as well as lecture series (block form) on topics relevant to this CRC. Funding shall also be used for any potential joint supervision of PhD students. We ask for EUR 2,500 per project and year.	EUR	40,000.-
Literature: funding shall be used to purchase special literature such as books or literature not available via the resources provided by the University of Stuttgart. We ask for EUR 600.- per year and research project.	EUR	9,600.-

Requested funding for direct costs for the financial year 2020

Travel: participation in both national and international meetings, schools and conferences. We ask for EUR 2,200.- per year and scientific coworker funded by the CRC, i.e. per PhD and PostDoc, respectively.	EUR	61,600.-
Guests: The visiting scientists program serves the exchange nationally- and internationally-renown scientists working in the areas of the CRC 1333. Funding will be used to cover the costs for both short- and long-terms visit od these scientists. Visiting scientists will also give individual lectures as well as lecture series (block form) on topics relevant to this CRC. Funding shall also be used for any potential joint supervision of PhD students. We ask for EUR 2,500 per project and year.	EUR	40,000.-
Literature: funding shall be used to purchase special literature such as books or literature not available via the resources provided by the University of Stuttgart. We ask for EUR 600.- per year and research project.	EUR	9,600.-

Requested funding for direct costs for the financial year 2021

Travel: participation in both national and international meetings, schools and conferences. We ask for EUR 2,200.- per year and scientific coworker funded by the CRC, i.e. per PhD and PostDoc, respectively.	EUR	61,600.-
Guests: The visiting scientists program serves the exchange nationally- and internationally-renown scientists working in the areas of the CRC 1333. Funding will be used to cover the costs for both short- and long-terms visit od these scientists. Visiting scientists will also give individual lectures as well as lecture series (block form) on topics relevant to this CRC. Funding shall also be used for any potential joint supervision of PhD students. We ask for EUR 2,500 per project and year.	EUR	40,000.-
Literature: funding shall be used to purchase special literature such as books or literature not available via the resources provided by the University of Stuttgart. We ask for EUR 600.- per year and research project.	EUR	9,600.-

Requested funding for direct costs for the financial year 2022

Travel: participation in both national and international meetings, schools and conferences. We ask for EUR 2,2000.- per year and scientific coworker funded by the CRC, i.e. per PhD and PostDoc, respectively.	EUR	30,800.-
Guests: The visiting scientists program serves the exchange nationally- and internationally-renown scientists working in the areas of the CRC 1333. Funding will be used to cover the costs for both short- and long-terms visit od these scientists. Visiting scientists will also give individual lectures as well as lecture series (block form) on topics relevant to this CRC. Funding shall also be used for any potential joint supervision of PhD students. We ask for EUR 2,500 per project and year.	EUR	20,000.-
Literature: funding shall be used to purchase special literature such as books or literature not available via the resources provided by the University of Stuttgart. We ask for EUR 600.- per year and research project.	EUR	4,800.-

3.18.5.6 Requested global funds

Requested global funds for the financial year 2018

Coordination measures: Consumables, data storage devices for the management (EUR 5000,-), copy costs (EUR 2,500.-), costs for public relations and internet (EUR 2,500.-)	EUR	5,000.-
Project specific workshops and colloquia: The CRC 1333 will organize workshops on various specific topics. We expect to have up to 4 one-day workshops (EUR 5,000.- each) including a workshop with our international collaborators. Complementary, we will organize 1 two-day status seminar per year (EUR 5,000.-) and a summer school (EUR 5,000.-) with total costs per year of EUR 30,000.-.	EUR	15,000.-
Equality measures: As outlined above, 50% of the funding will be pooled to supported gender and equality measures organized centrally by the University of Stuttgart. Apart from that, funding for the invitation of renowned international scientists for lectures and discussions is asked for. For traveling, lodging and appropriate announcement and implementation we estimate costs of EUR 8,000.- per year. Additionally, the budget dedicated solely to childcare is estimated to be 7,000.- per year.	EUR	15,000.-
Allowances: A lump sum of 100,000.- EUR per year enables for flexible support for new emerging developments of scientific, methodological and technical nature. The lump sum also includes support for publication of scientific and technical results and patents.	EUR	50,000.-

Requested global funds for the financial year 2019

Coordination measures: Consumables, data storage devices for the management (EUR 5000,-), copy costs (EUR 2,500.-), costs for public relations and internet (EUR 2,500.-)	EUR	10,000.-
Project specific workshops and colloquia: The CRC 1333 will organize workshops on various specific topics. We expect to have up to 4 one-day workshops (EUR 5,000.- each) including a workshop with our international collaborators. Complementary, we will organize 1 two-day status seminar per year (EUR 5,000.-) and a summer school (EUR 5,000.-) with total costs per year of EUR 30,000.-.	EUR	30,000.-
Equality measures: As outlined above, 50% of the funding will be pooled to supported gender and equality measures organized centrally by the University of Stuttgart. Apart from that, funding for the invitation of renowned international scientists for lectures and discussions is asked for. For traveling, lodging and appropriate announcement and implementation we estimate costs of EUR 8,000.- per year. Additionally, the budget dedicated solely to childcare is estimated to be 7,000.- per year.	EUR	30,000.-
Allowances: A lump sum of 100,000.- EUR per year enables for flexible support for new emerging developments of scientific, methodological and technical nature. The lump sum also includes support for publication of scientific and technical results and patents.	EUR	100,000.-

Requested global funds for the financial year 2020

Coordination measures: Consumables, data storage devices for the management (EUR 5000,-), copy costs (EUR 2,500.-), costs for public relations and internet (EUR 2,500.-)	EUR	10,000.-
Project specific workshops and colloquia: The CRC 1333 will organize workshops on various specific topics. We expect to have up to 4 one-day workshops (EUR 5,000.- each) including a workshop with our international collaborators. Complementary, we will organize 1 two-day status seminar per year (EUR 5,000.-) and a summer school (EUR 5,000.-) with total costs per year of EUR 30,000.-.	EUR	30,000.-
Equality measures: As outlined above, 50% of the funding will be pooled to supported gender and equality measures organized centrally by the University of Stuttgart. Apart from that, funding for the invitation of renowned international scientists for lectures and discussions is asked for. For traveling, lodging and appropriate announcement and implementation we estimate costs of EUR 8,000.- per year. Additionally, the budget dedicated solely to childcare is estimated to be 7,000.- per year.	EUR	30,000.-

Allowances: A lump sum of 100,000.- EUR per year enables for flexible support for new emerging developments of scientific, methodological and technical nature. The lump sum also includes support for publication of scientific and technical results and patents.	EUR	100,000.-

Requested global funds for the financial year 2021

Coordination measures: Consumables, data storage devices for the management (EUR 5000,-), copy costs (EUR 2,500.-), costs for public relations and internet (EUR 2,500.-)	EUR	10,000.-
Project specific workshops and colloquia: The CRC 1333 will organize workshops on various specific topics. We expect to have up to 4 one-day workshops (EUR 5,000.- each) including a workshop with our international collaborators. Complementary, we will organize 1 two-day status seminar per year (EUR 5,000.-) and a summer school (EUR 5,000.-) with total costs per year of EUR 30,000.-.	EUR	30,000.-
Equality measures: As outlined above, 50% of the funding will be pooled to supported gender and equality measures organized centrally by the University of Stuttgart. Apart from that, funding for the invitation of renowned international scientists for lectures and discussions is asked for. For traveling, lodging and appropriate announcement and implementation we estimate costs of EUR 8,000.- per year. Additionally, the budget dedicated solely to childcare is estimated to be 7,000.- per year.	EUR	30,000.-
Allowances: A lump sum of 100,000.- EUR per year enables for flexible support for new emerging developments of scientific, methodological and technical nature. The lump sum also includes support for publication of scientific and technical results and patents.	EUR	100,000.-

Requested global funds for the financial year 2022

Coordination measures: Consumables, data storage devices for the management (EUR 5000,-), copy costs (EUR 2,500.-), costs for public relations and internet (EUR 2,500.-)	EUR	5,000.-
Project specific workshops and colloquia: The CRC 1333 will organize workshops on various specific topics. We expect to have up to 4 one-day workshops (EUR 5,000.- each) including a workshop with our international collaborators. Complementary, we will organize 1 two-day status seminar per year (EUR 5,000.-) and a summer school (EUR 5,000.-) with total costs per year of EUR 30,000.-.	EUR	15,000.-
Equality measures: As outlined above, 50% of the funding will be pooled to supported gender and equality measures organized centrally by the University of Stuttgart. Apart from that, funding for the invitation of renowned international scientists for lectures and discussions is asked for. For traveling, lodging and appropriate announcement and implementation we estimate costs of EUR 8,000.- per year. Additionally, the budget dedicated solely to childcare is estimated to be 7,000.- per year.	EUR	15,000.-
Allowances: A lump sum of 100,000.- EUR per year enables for flexible support for new emerging developments of scientific, methodological and technical nature. The lump sum also includes support for publication of scientific and technical results/patents	EUR	50,000.-

4 Bylaws of the Collaborative Research Centre
Satzung der Universität Stuttgart für den Sonderforschungsbereich 1333 „Molecular Heterogeneous Catalysis in Confined Geometries “

Vom …
Aufgrund der §§ 40 Abs. 4, 19 Abs. 1 Satz 2 Nr. 10 des Landeshochschulgesetzes (LHG) hat der Senat der Universität Stuttgart nach vorheriger Abstimmung mit der Deutschen Forschungsgemeinschaft (DFG) am … die nachfolgende Satzung der Universität Stuttgart für den Sonderforschungsbereich 1333 „Molecular Heterogeneous Catalysis in Confined Geometries“ beschlossen.

§ 1 Rechtsform, Name, Sprecherhochschule und Aufgaben des Sonderforschungsbereichs

(1) Der Sonderforschungsbereich 1333 „Molecular Heterogeneous Catalysis in Confined Geometries“ ist eine zentrale wissenschaftliche Einrichtung und ein interdisziplinärer Forschungsschwerpunkt der Universität Stuttgart gemäß § 40 Abs. 4 LHG.

(2) In dem Sonderforschungsbereich (CRC) werden miteinander zusammenhängende Forschungsvorhaben auf den Gebieten der Chemie, der Physik, der Technischen Chemie, der Materialwissenschaften sowie der Simulation bearbeitet. Er gliedert sich in Projektbereiche und Teilprojekte.

(3) Des Weiteren setzt sich der Forschungsverbund zur Aufgabe, die Interaktion mit anderen Forschungseinrichtungen, den wissenschaftlichen Nachwuchs, die internationale Zusammenarbeit sowie die Chancengleichheit zu fördern.

§ 2 Mitgliedschaft

(1) Ordentliche Mitglieder des Sonderforschungsbereiches sind die Teilprojektleiterinnen und Teilprojektleiter der bewilligten CRC 1333-Teilprojekte.

(2) Korrespondierendes Mitglied des Sonderforschungsbereichs kann auf Antrag jede Person werden, die der Universität Stuttgart oder sonstigen Forschungseinrichtungen angehört und in dem Forschungsgebiet des Sonderforschungsbereichs die Befähigung zu eigenständiger wissenschaftlicher Tätigkeit (i. d. R nach Abschluss der Promotion) nachgewiesen hat. Die korrespondierende Mitgliedschaft ist nicht an eine Förderung im Rahmen des Sonderforschungsbereiches geknüpft.

(3) Wissenschaftlerinnen und Wissenschaftler können die ordentliche Mitgliedschaft sowie die korrespondierende Mitgliedschaft beim Vorstand des Sonderforschungsbereiches beantragen. Über diesen Antrag entscheidet der Vorstand des CRC.

(4) Die ordentliche wie auch die korrespondierende Mitgliedschaft enden, wenn das Mitglied seinen Austritt aus dem Sonderforschungsbereich bei der Sprecherin bzw. dem Sprecher schriftlich anzeigt.

(5) Über den Verlust bzw. die Aberkennung der ordentlichen Mitgliedschaft wie auch der korrespondierenden Mitgliedschaft entscheidet der Vorstand mit absoluter Mehrheit.

§ 3 Rechte und Pflichten der Mitglieder

(1) Die ordentliche Mitgliedschaft im Sonderforschungsbereich berechtigt prinzipiell zur Vorlage eines Projektentwurfs bei dem für die Vorbereitung des Gesamtfinanzierungsantrages zuständigen Gremium des Sonderforschungsbereiches (Vorstand).

(2) Die ordentlichen Mitglieder sind zur Zusammenarbeit, gegenseitigen Beratung und Unterstützung verpflichtet. Gemeinsame Einrichtungen sowie die Mittel des Sonderforschungsbereiches können von allen Mitgliedern im Rahmen der vorhandenen Möglichkeiten in Anspruch genommen werden.

(3) Die ordentlichen Mitglieder sind verpflichtet, an der konzeptionellen und organisatorischen Arbeit, der Nachwuchsförderung, der Gleichstellung sowie an der Verwaltung des CRC nach Maßgabe dieser Satzung mitzuwirken.

(4) In Veröffentlichungen, die auf die Forschungsarbeiten des CRC zurückgehen, muss auf die Förderung durch die DFG hingewiesen werden.

(5) Jede Teilprojektleitung ist verpflichtet, nach Abschluss einer Förderperiode bzw. bei Beendigung des Teilprojektes einen Bericht über die Arbeiten im Projekt und einen Finanzbericht über die Fördermittelverwendung entsprechend der Richtlinien der DFG und der Universität Stuttgart vorzulegen. Das Ende der Mitgliedschaft berührt diese Pflicht nicht.

(6) Scheidet eine Teilprojektleiterin oder ein Teilprojektleiter aus dem Sonderforschungsbereich aus, können die dem Sonderforschungsbereich für das betroffene Teilprojekt bewilligten Geräte und Finanzmittel während der Laufzeit des CRC prinzipiell nicht an den neuen Ort mitgenommen werden; eine anderweitige Lösung (z.B. Mitnahme von Geräten) bedarf der Zustimmung des Vorstands des CRC sowie der Kanzlerin oder des Kanzlers der Universität Stuttgart. Eine Standortänderung von Geräten über 10.000 Euro während der Laufzeit des CRC ist der DFG mitzuteilen.

§ 4 Organisatorischer Aufbau (Organe) des Sonderforschungsbereichs

(1) Der CRC hat folgende Organe:
1. Mitgliederversammlung,
2. Vorstand,
3. Sprecherin bzw. Sprecher,
4. Geschäftsführung.

(2) Teilprojektleiterinnen oder Teilprojektleiter sollen diejenigen Wissenschaftlerinnen und Wissenschaftler sein, die das Forschungsvorhaben maßgeblich konzipiert haben.

§ 5 Zusammensetzung und Aufgaben der Mitgliederversammlung

(1) Die Mitgliederversammlung besteht aus den ordentlichen Mitgliedern.

(2) Die Mitgliederversammlung hat folgende Aufgaben:
1. Vorschläge zur Beschlussfassung über diese Satzung und ihre Änderung,
2. Verabschiedung des Gesamtfinanzierungsantrags für die weiteren Förderphasen,
3. Wahl der Sprecherin oder des Sprechers, der Stellvertretung und der übrigen Vorstandsmitglieder.

(3) Folgende Aufgaben überträgt die Mitgliederversammlung auf den Vorstand:
1. Entwicklung des wissenschaftlichen Programms und seine Koordination,
2. Vorbereitung des Gesamtfinanzierungsantrags, interne Vorprüfung der Teilprojektanträge sowie Beschluss über Änderungen finanzieller Aspekte von Teilprojektanträgen,
3. Entscheidung über die Einbeziehung neuer Teilprojekte während des Förderzeitraums,
4. Programmändernde Finanzierungsmaßnahmen während des laufenden Förderungszeitraums (z.B. inhaltlich begründete Beendigung oder Anfinanzierung eines neuen Teilprojektes),

5. Beratung über die Beantragung und Beschaffung von durch mehrere Teilprojekte genutzten Geräten,
6. Vorbereitung und Organisation wissenschaftlicher Veranstaltungen des CRC.

(4) Bei der Wahl der Sprecherin oder des Sprechers und der Vorstandsmitglieder sowie bei Vorschlägen zu Änderungen dieser Satzung entscheidet die Mitgliederversammlung mit absoluter Mehrheit der Mitglieder. In allen anderen Fällen entscheidet die Mitgliederversammlung mit einfacher Mehrheit der Anwesenden. Die Mitgliederversammlung ist beschlussfähig, wenn mindestens die Hälfte der Mitglieder anwesend ist.

(5) Die Mitgliederversammlung wird mit einer Ladungsfrist von mindestens sieben Tagen elektronisch oder schriftlich durch die Sprecherin oder den Sprecher des CRC einberufen; die Tagesordnung wird mit der Einladung an alle Mitglieder versandt. Eine Mitgliederversammlung ist außerdem auf Antrag von drei ordentlichen Mitgliedern des CRC mit o.g. Frist einzuberufen. Dieser Antrag ist an die Sprecherin oder den Sprecher zu stellen.

§ 6 Zusammensetzung, Amtszeit und Aufgaben des Vorstands

(1) Der Vorstand setzt sich aus der Sprecherin oder dem Sprecher, der Stellvertretung sowie drei weiteren Mitgliedern und der Geschäftsführung zusammen. Er entscheidet mit einfacher Mehrheit. Er ist beschlussfähig, wenn mindestens die Hälfte der Vorstandsmitglieder anwesend ist. Bei Stimmengleichheit entscheidet die Stimme der Sprecherin oder des Sprechers.

(2) Die weiteren Mitglieder des Vorstands werden durch die Mitgliederversammlung für eine Amtszeit von vier Jahren mit einfacher Mehrheit der Anwesenden gewählt. Die Mitgliederversammlung kann diese weiteren Mitglieder jederzeit in toto oder einzeln mit absoluter Mehrheit abwählen. Die Abwahl der Sprecherin oder des Sprechers ist nur wirksam, wenn zugleich eine neue Sprecherin oder ein neuer Sprecher gewählt wird.

(3) Neben den ggf. von der Mitgliederversammlung übertragenen Aufgaben (§ 5 Abs. 3) trägt der Vorstand für folgende Aufgaben Verantwortung:
1. Personalfragen,
2. Mitwirkung bei der Einstellung und Entlassung von Mitarbeitenden (durch die Hochschule oder beteiligte Einrichtungen), die aus Mitteln des CRC bezahlt werden (nach Rücksprache mit dem betroffenen Teilprojektleitenden),
3. Konzeption und Organisation von Maßnahmen zur Förderung des wissenschaftlichen Nachwuchses und der Chancengleichheit,
4. Aufnahme von Mitgliedern und Entscheidung über die Beendigung der Mitgliedschaft,
5. alle Fragen, die nach dieser Satzung nicht in die Zuständigkeit eines anderen Organs fallen.

§ 7 Aufgaben und Amtszeit der Sprecherin oder des Sprechers

(1) Zur Sprecherin oder zum Sprecher und der Stellvertretung kann gewählt werden, wer eine Professur der Universität Stuttgart inne hat, in einem hauptamtlichen, senatsfähigen Dienst- oder Arbeitsverhältnis steht und ordentliches Mitglied des CRC ist. Die Sprecherin bzw. der Sprecher hat die Leitung des Verwaltungsprojektes inne, muss jedoch kein wissenschaftliches Projekt leiten.

(2) Die Sprecherin oder der Sprecher ist Vorsitzende oder Vorsitzender von Vorstand und Mitgliederversammlung und vertritt den Sonderforschungsbereich nach außen (z.B. gegenüber der Hochschulleitung/-verwaltung, der DFG).

(3) Zu den Aufgaben des Sprecheramtes gehört

1. die Einberufung von Vorstandssitzungen und Mitgliederversammlungen,
2. die Information der Mitglieder,
3. Entscheidungen über Umdispositionsanträge größeren Umfangs,
4. Kommunikation und Information über die Tätigkeiten des CRC nach innen und nach außen,
5. Abstimmung mit und Aufsicht über die Geschäftsführung,
6. Beratungen mit der Hochschulleitung und Beratung mit der Leitung der Fakultäten über Fragen der Grundausstattung sowie Berufungsfragen.

(4) Die Amtszeit beträgt vier Jahre. Eine Wiederwahl ist beliebig oft möglich.

§ 8 Aufgaben der Geschäftsführung

(1) Die Berufung und Abberufung der Geschäftsführung erfolgt auf Vorschlag der Sprecherin oder des Sprechers durch die Mitglieder des Vorstands. Die Entscheidung erfolgt mit einfacher Mehrheit. Kommt keine Mehrheit zustande, entscheidet die Stimme der Sprecherin oder des Sprechers. Die Berufung erfolgt auf unbefristete Zeit. Die Geschäftsführung besteht aus einer Person. Die Geschäftsführung kann zu ihrer Unterstützung eine Geschäftsstelle einrichten. Der Geschäftsführung untergeordnet werden das Verwaltungsprojekt (Zentrale Aufgaben des CRC) sowie das Teilprojekt Öffentlichkeitsarbeit.

(2) Die Geschäftsführerin oder der Geschäftsführer unterstützen den Vorstand und die Sprecherin oder den Sprecher bei der Erfüllung der Aufgaben des Sonderforschungsbereichs. Ihr oder ihm obliegen für den Vorstand und die Sprecherin oder den Sprecher folgenden Aufgaben:

1. Konzeption, Ausarbeitung und Organisation von Maßnahmen zur Förderung des wissenschaftlichen Nachwuchses,
2. die Führung der laufenden Geschäfte einschließlich der laufenden Mittelverwaltung und -abrechnung sowie die Entscheidung über Dispositionsanträge kleineren Umfangs,
3. die Information der Mitglieder und Mitarbeiterinnen und Mitarbeiter,
4. Öffentlichkeitsarbeit,
5. Repräsentationspflichten, die nicht Aufgaben der Sprecherin oder des Sprechers nach § 7 Abs. 2 dieser Satzung sind,
6. Konzeption und Organisation von Gastwissenschaftler- und Austauschprogrammen,
7. Beratung über die Beantragung und Beschaffung von durch mehrere Teilprojekte genutzten Geräten,
8. Vorbereitung und Organisation wissenschaftlicher Veranstaltungen des CRC.

(3) Die Geschäftsführerin oder der Geschäftsführer kann aus den pauschalen Projektmitteln (zentral verwaltete Mittel) teil- oder vollfinanziert werden. Über die Finanzierung entscheidet die Sprecherin oder der Sprecher des CRC.

§ 9 Verfahren zur Vergabe zentral verwalteter Mittel sowie von DFG-Programm-pauschalen-Mitteln

(1) Der Vorstand des CRC entscheidet über die Budgetierung/Aufteilung der zentral verwalteten Mittel sowie der DFG-Programmpauschalen-Mittel. Er legt die jeweiligen Mittelbeträge (Budgetobergrenzen) für die unterschiedlichen Ausgabenpositionen fest. Für die zentral verwalteten Mittel sind insbesondere die nachfolgenden Ausgabenpositionen vorgesehen:
1. Budget für Anschubfinanzierungen,
2. Budget für Publikationen,
3. Budget für spezifische Öffentlichkeitsarbeit.

(2) Für die DFG-Programmpauschalen-Mittel sind insbesondere die nachfolgenden Ausgabenpositionen vorgesehen:

1. Budget für Mitarbeit von Nichtprojektfinanzierten-Personen,
2. Budget für Zulagen für besondere wissenschaftliche Leistungen,
3. Budget für Professionalisierung des Forschungsmanagements,
4. Budget für die Vergabe an die Teilprojekte.

(3) In Übereinstimmung mit den DFG-Verwendungsrichtlinien für Sonderforschungsbereiche können vom Vorstand weitere Ausgabenpositionen für beide Mittelarten ergänzt werden.
(4) Im Rahmen der jeweiligen Budgetobergrenzen entscheidet die Sprecherin oder der Sprecher des CRC in Abstimmung mit der Geschäftsführung des CRC über die Mittelverwendung.

§ 10 Verfahrensordnung
Soweit in dieser Satzung nichts Anderes geregelt ist, gilt die Verfahrensordnung der Universität Stuttgart vom 18. Dezember 2006 (Amtliche Bekanntmachungen der Universität Stuttgart Nr. 179 vom 27. Dezember 2006) in der jeweils geltenden Fassung.

§ 11 Inkrafttreten
Diese Satzung tritt am Tag nach ihrer Bekanntmachung in den Amtlichen Bekanntmachungen der Universität Stuttgart in Kraft.

Stuttgart, den 20. 12. 2017

5 Declaration on working space for the Collaborative Research Centre

Is the existing office and/or lab space sufficient to accommodate the Collaborative Research Centre at the time of submitting the proposal?	yes
Will there be sufficient office and/or lab space to accommodate the Collaborative Research Centre including any planned extensions in the financial years…	
… 2018	yes
… 2019	yes
… 2020	yes
… 2021	yes
… 2022	yes
If the answer to one of the above questions is “no”:	
Will additional office and/or laboratory space be acquired by…	
… re-allocation of existing rooms?	n.a.
… new construction or remodeling?	n.a.
… renting?	n.a.
Will these measures be funded through…	
… the university budget?	n.a.
… other funds?	n.a.
If working groups participating in the Collaborative Research Centre are planned to be moved into newly built or remodeled rooms, please state the time of the relocation:	
none	n.a.

Stuttgart, 20. 12. 2017

Dr. Ulrich Engler (stellvertretender Kanzler)

6 Declaration on lists of publications

We hereby declare that the lists of publications included in this proposal and in the attached research profiles of the principal investigators were compiled in accordance with DFG rules on publication lists.

Stuttgart, 20. 12. 2017

Prof. Dr. Michael R. Buchmeiser (Spokesperson of CRC)

Stuttgart, 20. 12. 2017

Prof. Dr.-Ing. W. Ressel (Rector of applicant university)

Appendix

Appendix I: Cooperations Stuttgart

Prof. Dr. J. Bill
Prof. Dr. T. Sottmann, University of Stuttgart: Synthesis of nanoporous polymeric and organic/inorganic materials
Prof. Dr. Peter A. van Aken, MPI-FKF, Stuttgart: TEM characterization of hybrid materials
Dr. Marko Burghard, MPI-FKF, Stuttgart: Electrical properties of mineralized single viruses

Prof. Dr. M. R. Buchmeiser:
Jun.-Prof. Dr. N. Hansen, University of Stuttgart: calculations on Ru-alkylidene NHC complexes in mesoporous systems
Prof. Dr.-Ing. Dr. e.h. Dr. h.c. W. Sobek, Prof. Dr.-Ing. Dr. h.c. O. Sawodny, University of Stuttgart, CRC 1244
Prof. Dr.-Ing. E. Klemm, ITC, University of Stuttgart: Bio-based acrylonitrile

Jun. Prof. Dr. M. Fyta
Prof. Dr. M. Dressel, University of Stuttgart: nano-confinement of water in crystals
Prof. Dr. A. Weidenkaff, University of Stuttgart: perowskite-based membranes
Prof. Dr. S. Schmauder, University of Stuttgart: copper alloys

Prof. Dr. F. Gießelmann
Prof. Dr. Peer Fischer, MPI-IS, Stuttgart: soft robotics

Jun. Prof. Dr.-Ing. N. Hansen
Prof. Dr. M. R. Buchmeiser, University of Stuttgart: calculations on Ru-alkylidene NHC complexes in mesoporous systems
Prof. Dr. S. Laschat, University of Stuttgart: Investigation of linker flexibility
Prof. Dr. J. Pleiss, University of Stuttgart: Thermodynamic activity-based interpretation of enzyme kinetics
Prof. Dr. R. Ghosh, University of Stuttgart: Experimental and theoretical investigation of protein stability

apl. Prof. Dr. M. Hunger:
Prof. Dr.-Ing. E. Klemm, ITC, University of Stuttgart, Stuttgart, Germany: Development of solid catalysts for the dehydration of lactic acid to acrylic acid

Prof. Dr. Kästner:
Dr. S. Naumann, University of Stuttgart:: dual catalysis for lactone polymerization

Prof. Dr. S. Laschat
Prof. Dr. Andreas Köhn, University of Stuttgart: theoretical calculations of catalytic reactions

Prof. Dr. Bettina Lotsch
Prof. Dr. Joachim Maier, MPI-FKF Stuttgart: Electrochemical characterization of Li solid electrolytes
Prof. Dr. Klaus Kern, MPI-FKF Stuttgart: STM characterization of 2D frameworks on surfaces

Prof. Dr. S. Ludwigs
Prof. S. Laschat, Prof. F. Giesselmann: electronic and electrochemical measurements of liquid crystals
Prof. J. Maier, MPI Stuttgart: impedance spectroscopy of ionic polymers
Prof. J. van Slageren & Prof. J. Schulze, University of Stuttgart: polymer spintronics
Prof. H. Steeb, University of Stuttgart: mechanical properties of adaptive polymers
Prof. M. Berroth, University of Stuttgart: electro-optic modulators
Dr. H. Klauk, MPI Stuttgart: organic field-effect transistors

Dr. S. Naumann
Prof. Dr. Christian Bonten, University of Stuttgart: latent NHC-based polymerization processes for polyamide production
apl. Prof. Dr. T. Sottmann, University of Stuttgart: block-copolymers in microemulsion
Prof. Dr. Kästner, University of Stuttgart: dual catalysis for lactone polymerization

Prof. Dr. B. Plietker
Prof. Dr. W. Kaim, University of Stuttgart: spectroelectrochemical investigations on Ru- and Fe-complexes
Prof. Dr.-Ing. E. Klemm, University of Stuttgart: Ru-catalyzed reduction of CO_2
Prof. Dr. J. Kästner, University of Stuttgart: DFT-analysis of Ru- and Fe-catalyzed transformations
Prof. Dr. A. Köhn, University of Stuttgart: CASSCF-analysis of photochemically activated Fe-NO-complexes
Prof. Dr. B. Hauer, University of Stuttgart: Hem-catalyzed carbene transfer reactions

Dr. Mark Ringenberg
Prof. Dr. René Peters, University of Stuttgart, Electrochemistry and spectroscopy of gold complexes containing ferrocene based ligands

PD Dr. Yvonne Traa
Jörg Maier, Prof. Dr. Günter Scheffknecht, Universität Stuttgart: Hydrogenation of biocoals and similar biomass reactants
Prof. Dr. Cosima Stubenrauch, Universität Stuttgart: Immobilization of Pd nanoparticles synthesized in microemulsions on mesoporous silica FDU-12

Prof. Dr. G. Schmitz
Dr. H. Klauk, MPI Stuttgart, Germany: APT of SAM in microelectronics
Dr. F. von Wrochem, Fa. Sony Stuttgart: Measurement of Work function of SAM layers by field emission

apl. Prof. Dr. T. Sottmann
Prof. J. Bill, University of Stuttgart: synthesis of nanoporous polymeric and organic/inorganic materials
Prof. C. Stubenrauch, University of Stuttgart: gelled lyotropic liquid crystalline phases and microemulsions
Dr. S. Naumann, University of Stuttgart: Block-copolymers in microemulsion

Appendix II: Joint publications

P. Zhang, M. Perfetti, M. Kern, P. P. Halmen, L. Ungur, S. Lenz, **M. R. Ringenberg**, W. Frey, H. Stoll, G. Rauhut, **J. van Slageren**, *Chem. Sci*. **2017**, DOI:10.1039/C7SC04873D.
J. Kirres, K. Schmitt, I. Wurzbach, **F. Giesselmann**, **S. Ludwigs**, **M. Ringenberg**, A. Ruff, A. Baro, **S. Laschat**, *Org. Chem. Frontiers* **2017**, *4*, 790-803.
J. C. Haenle, K. Bruchlos, **S. Ludwigs**, A. Köhn, **S. Laschat**, *ChemPlusChem* **2017**, *82*, 1197 –1210.
J. E. M. N. Klein, G. Knizia, B. Miehlich, **J. Kästner, B. Plietker**, *Chem. Eur. J*. **2014**, *20*, 7254.
J. E. M. N. Klein, B. Miehlich, **J. Kästner**, **B. Plietker** *Dalton Trans*. **2013**, *42*, 7519.
Chapter “Free energy calculation methods and rare event sampling techniques for biomolecular simulations” **J, Kästner**, J. Smiatek, **N. Hansen** in “Simulating Enzyme Reactivity”, Eds: Iñaki Tuñón und Vicente Moliner, RSC Cambridge, 2016. Print ISBN: 978-1-78262-429-5, DOI (chapter): 10.1039/9781782626831-00185.
P. Staffeld, M. Kaller, S. J. Beardsworth, K. Tremel, **S. Ludwigs, S. Laschat, F. Giesselmann**, *J. Mater. Chem. C* **2013**, *1*, 892.
S. Sen, R. Schowner, D.A. Imbrich, W. Frey, **M. Hunger, M. Buchmeiser**, *Chem. Eur. J.* **2015**, *21*, 13778-13787.
M. Dyballa, U. Obenaus, S. Lang, B. Gehring, **Y. Traa**, H. Koller, **M. Hunge**r, *Microporous & Mesoporous Mater.* **2015**, *212*, 110-116.
G. Naefe, M.-A. López-Martínez, **Y. Traa**, M. Dyballa, **M. Hunger**, Th. Hirth, E. Klemm, *J. Catal.* **2015**, *329*, 413-424.

R.A. Rakoczy, M. Breuninger, **M. Hunger**, **Y. Traa**, J. Weitkamp, *Chem. Eng. Technol.* **2002**, *25*, 273-275.
A. Raichle, S. Moser, **Y. Traa, M. Hunger**, J. Weitkamp, *Catal. Commun.* **2001**, *2*, 23-29.
A. Raichle, M. Ramin, D. Singer, **M. Hunger, Y. Traa**, J. Weitkamp, *Catal. Commun.* **2001**, *2*, 69-74.
G. Bauer, A. Lange, N. Gribova, **C. Holm**, **J. Gross**, *Molec. Simul*. **2015**, *41*, 1153-1158.
S. Sen, W. Frey, J. Meisner, **J. Kästner**, **M. R. Buchmeiser**, *J. Organomet. Chem.* **2015**, *799-800*, 223-225.
G. Bauer, N. Gribova, A. Lange, **C. Holm**, **J. Gross**, *Molec. Phys*., **2017**, *115*, 1031-1040.
E. Roduner, Ch. Jensen, **J. van Slageren**, R. A. Rakozy, O. Larlus, **M. Hunger**, *Angew. Chem. Int. Ed.* **2014**, *53*, 4318-4321**.**
T. Wöhrle, S. J. Beardsworth, C. Schilling, A. Baro, **F. Giesselmann, S. Laschat,** *Soft Matter* **2016,** *12***,** 3730–3736.
T. Wöhrle, I. Wurzbach, J. Kirres, A. Kostidou, N. Kapernaum, J. Litterscheidt, J. C. Haenle, P. Staffeld, A. Baro, **F. Giesselmann**, **S. Laschat**, *Chem. Rev.* **2016**, *116*, 1139–1241..
E. Wuckert, M. D. Harjung, N. Kapernaum, C. Mueller, W. Frey, A. Baro, **F. Giesselmann**, **S. Laschat**, *Phys. Chem. Chem. Phys.* 2015, *17*, 8382–8392.
M. Butschies, M. Mansueto, J. H. Haenle, C. Schneck, S. Tussetschläger, **F. Giesselmann, S. Laschat**, *Liq. Cryst.* **2014**, *41*, 821–838.
P. Staffeld, M. Kaller, S. J. Beardsworth, K. Tremel, **S. Ludwigs**, **S. Laschat, F. Giesselmann**, *J. Mater. Chem. C* **2013**, *1*, 892–901.
E. Roduner, W. Kaim, B. Sarkar, V. B. Urlacher, J. Pleiss, R. Gläser, W.-D. Einicke, G. A. Sprenger, U. Beifuß, E. Klemm, C. Liebner, H. Hieronymus, S.-F. Hsu, **B. Plietker, S. Laschat**, *ChemCatChem* **2013**, *5*, 82–112.
M. Kaller, S. J. Beardsworth, P. Staffeld, S. Tussetschläger, **F. Gießelmann, S. Laschat**, *Liq. Cryst.* **2012**, *39*, 607–618.
M. Mansueto, J. H. Porada, **S. Laschat**, C. Stubenrauch, **F. Giesselmann**, *Synthesis* **2011**, *18*, 3032–3036.
M. Kaller, P. Staffeld, R. Haug, W. Frey, **F. Giesselmann**, **S. Laschat**, *Liq. Cryst.* **2011**, *38*, 531–553.
E. Wuckert, C. Hägele, **F. Giesselmann**, A. Baro, **S. Laschat**, *Beilstein J. Org. Chem.* **2009**, *5*, No. 57.
G. F. Starkulla, E. Kapatsina, A. Baro, **F. Giesselmann**, S. Tussetschläger, M. Kaller, **S. Laschat**, *Beilstein J. Org. Chem.* **2009**, *5*, No. 63.
M. Kaller, S. Tussetschläger, P. Fischer, C. Deck, A. Baro, **F. Giesselmann, S. Laschat**, *Chem. Eur. J.***2009**, *15*, 9530–9542.
S. Sauer, S. Saliba, S. Tussetschläger, A. Baro, W. Frey, **F. Giesselmann, S. Laschat**, W. Kantlehner, *Liq. Cryst.* **2009**, *36*, 275–299.
C. Hägele, E. Wuckert, **S. Laschat, F. Giesselmann**, *ChemPhysChem* **2009**, *10*, 1291–1298.
A. Schreivogel, U. Dawin, A. Baro, **F. Giesselmann, S. Laschat**, *J. Phys. Org. Chem.* **2009**, *22*, 484–494.
S. Sauer, N. Steinke, A. Baro, **S. Laschat, F. Giesselmann**, W. Kantlehner, *Chem. Mater.* **2008**, *20*, 1909–1915.
S. Laschat, A. Baro, N. Steinke, **F. Giesselmann**, C. Hägele, G. Scalia, R. Judele, E. Kapatsina, A. Schreivogel, S. Sauer, M. Tosoni, *Angew. Chem.* **2007**, *119*, 4916-4973. *Angew. Chem. Int. Ed.* **2007**, *46*, 4832 –4887.
N. Steinke, W. Frey, A. Baro, **S. Laschat**, C. Drees, M. Nimtz, C. Hägele, **F. Giesselmann**, *Chem. Eur. J.* **2006**, *12*, 1026–1035.
E. Wuckert, **S. Laschat**, A. Baro, C. Hägele, **F. Giesselmann**, H. Luftmann, *Liq. Cryst.* **2006**, *33*, 103–107.
E. Wuckert, M. Dix, **S. Laschat**, A. Baro, J. L. Schulte, C. Hägele, **F. Giesselmann**, *Liq. Cryst.* **2004**, *31*, 1305–1309.
A. Schultz, **S. Laschat**, A. Saipa, **F. Gießelmann,** M. Nimtz, J. L. Schulte, A. Baro, B. Miehlich, *Adv. Funct. Mater.* **2003**, *14*, 163–168.

Appendix III: Joint Master and PhD Students

J. Karwounopoulos, Bachelorarbeit 2017, Cobetreuung J. Kästner, S. Naumann
S. Jobst, Diplomarbeit 2012, Cobetreuung S. Ludwigs mit J. Bill.
I. Wurzbach, Doktorarbeit seit 2015, Erstbetreuer F. Gießelmann, Zweitbetreuer S. Ludwigs
J. Baz, Doktorarbeit seit 2015, Erstbetreuer N. Hansen, Zweitbetreuer J. Kästner
D. Markthaler Doktorarbeit seit 2014, Erstbetreuer N. Hansen, Zweitbetreuer J. Kästner
M.U. Bohner, Doktorarbeit 2014, Erstbetreuer J. Kästner, Zweitbetreuer C. Holm
A. Hemmen, Doktorarbeit 2015, Erstbetreuer J. Groß, Zweitbetreuer J. Kästner
G. Sivaraman, Doktorarbeit 2017 Cobetreuung, M. Fyta, J. Kästner, J. Groß
L. Michalek, Masterarbeit 2016, Erstbetreuer G. Schmitz, Zweitbetreuer M. R. Buchmeiser
E. Choi, Masterarbeit 2016, Cobetreuung J. Bill mit S. Ludwigs
H. Bilgili, Doktorarbeit, Cobetreuung Prof. J. Groß, Jun. Prof. N. Hansen, Dr. T. Sottmann
J. Zeman, Doktorarbeit seit 2015, Erstbetreuer C. Holm, Zweitbetreuer J. Kästner

Appendix IV: Joint projects

EU-Projekt “FASTCARD” M. Hunger, Y. Traa, Projekt-Nr. NMP4-LA-2013-604277, „FAST industrialisation by Catalysts Research and Development“, Laufzeit: 2014 bis 2017

DFG Gemeinschaftsprojekt "Ionic Liquid Crystals“, S. Laschat (LA 907/17-1) F. Gießelmann (GI 243/8-1), Laufzeit 2014 – 2017

International Max-Planck-Research School „Condensed Matter Science“ (IMPRS CMS), J. Bill, F. Gießelmann (Board Member), S. Laschat, S. Lotsch, S. Ludwigs, G. Schmitz, J. van Slageren, Laufzeit: 2014 – 2020

A1	Prof. Dr. Michael Buchmeiser	Monolithic polymeric supports with uniform pore diameter and tailored functional groups
A2	Prof. Dr. Sabine Ludwigs	Tunable block copolymer templates for spatially controlled immobilization of molecular catalysts
A3	Prof. Dr. Bettina Lotsch	Covalent organic frameworks as tailored substrates with molecularly defined pores for molecular heterogeneous catalysis
A4	PD Dr. Yvonne Traa Prof. Dr. Frank Gießelmann	Controlled synthesis of mesoporous silica materials
A5	apl. Prof. Dr. Joachim Bill	Organic/inorganic hybrid materials with tunable pore size as catalyst supports
A6	Dr. Stefan Naumann	Carbon materials with tailored, selectively functionalized mesopores using organocatalytically derived polyethers
A7	apl. Prof. Dr. Thomas Sottmann	Nanoporous host materials with adjustable pore size, geometry and distribution: synthesis, functionalization and characterization
B1	Prof. Dr. Bernd Plietker	„Inner-pore“-tethered tetraaza-ruthenium-complexes for the directed hydrogen-autotransfer catalysis
B2	Prof. Dr. Michael Buchmeiser	Immobilized molybdenum imido, tungsten imido- and tungsten oxo alkylidene N-heterocyclic carbene complexes for olefin metathesis
B3	Prof. Dr. Sabine Laschat	Asymmetric catalysis with supported chiral olefin-rhodium complexes in defined porous networks
C1	apl. Prof. Michael Hunger	Solid-state NMR methods for the study of the properties and spatial distribution of organo-metallic compounds anchored in porous solids
C2	Prof. Dr. Joris Van Slageren Dr. Mark Ringenberg	The static and dynamic electronic and geometric structure of catalysts in porous polymers
C3	Prof. Dr. Dr. h.c. Guido Schmitz	High resolution tomography of mesoscopic pore structures
C4	Prof. Dr. Johannes Kästner	Simulation of chemical reactivities
C5	Prof. Dr. Joachim Groß Jun. Prof. Dr. Niels Hansen	Atomistic and fluid-theoretical predictions of static and dynamic fluid properties in functionalized mesopores
C6	Prof. Dr. Christian Holm Jun. Prof. Dr. Maria Fyta	A multi-scale simulation approach for optimizing molecular heterogeneous catalysis in confined geometries
S1	Prof. Dr. Bernd Plietker Prof. Dr. Matthias Bauer	Service project
Z1	Prof. Dr. Michael Buchmeiser Prof. Dr. Bernd Plietker	CRC central planning